

**ALLUVIAL SAPPHIRES AND DIAMONDS
OF THE NEW ENGLAND GEM FIELDS,
NEW SOUTH WALES,
AUSTRALIA**

by

Robert Raymond Coenraads

Honours Degree of Bachelor of Arts, Macquarie University, Sydney, 1978.

Master of Science, University of British Columbia, Vancouver, 1982.

Diploma in Gemmology, Gemmological Association of Australia, 1990.

**A Thesis Submitted in Fulfillment
of the Requirements for the Degree of
Doctor of Philosophy**

**School of Earth Sciences
Macquarie University**

June, 1991

TABLE OF CONTENTS

Table of Contents	ii
Summary	vi
Certificate	vii
Acknowledgements	viii
List of Colour Plates.....	ix
List of Plates.....	x
List of Figures	xi
List of Tables.....	xvii

Chapter 1

Sapphire and Diamond Exploration in the New England Gem Fields, New

South Wales, Australia.....	1
1.1 Aims	1
1.2 Introduction	3
1.2.1 Corundum deposits of metamorphic association.....	3
1.2.2 Corundum deposits of igneous association	3
1.2.3 Australian sapphire deposits.....	5
1.2.4 Volcanism in the Central Province.....	5
1.3 The alluvial sapphire and diamond mining industry in eastern Australia.....	7
1.3.1 Development of the industry in Australia	7
1.3.2 Sapphire mining and processing.....	7
1.3.3 Sapphire exploration methodology.....	9
1.3.4 Sapphire sorting and grading.....	11
1.3.5 Gemstone processing.....	11
1.3.6 Gemstone enhancement.....	12

Chapter 2

The Nature and Origin of Corundum associated with Volcanic Provinces	16
2.1 Introduction	16
2.2 Properties of corundum	16
2.3 Form of sapphires from the Central Volcanic Province.....	17
2.4 Surface features of rubies and sapphires from volcanic provinces	20
2.4.1 Negative crystal impressions	20
2.4.2 Surface etch features.....	24
2.4.3 Healed fracture surfaces and damage resulting from transport in an alluvial environment.....	30
2.4.4 Discussion.....	30
2.5 Inclusions in sapphires and zircons from the Central Volcanic Province.....	31

2.6 U-Pb dating of the zircon inclusions in Central Volcanic Province sapphires.....	39
2.7 Sapphire-bearing rocks in the Central Province volcanic sequence	45
2.8 Conclusions	46
Chapter 3	
Key Areas for Alluvial Diamond and Sapphire Exploration in the New England Gemfields, New South Wales	47
3.1 Introduction	47
3.2 Central Province volcanism.....	47
3.2.1 Structural control of Central Province volcanism	49
3.2.2 Timing of Central Province volcanism.....	49
3.3 Sapphire and diamond occurrences in the Central Volcanic Province.....	50
3.3.1 Quaternary alluvium.	50
3.3.2 Tertiary deep leads.	50
3.4 Identification of exploration targets for diamond and sapphire	52
3.4.1 Analysis of sub-volcanic topography	52
3.5 Geologic and geomorphic evolution of the Central Volcanic Province.....	58
Chapter 4	
Delineation of Alluvial and Deep Lead Exploration Targets: Case Studies.....	60
4.1 Introduction	60
4.2 Diamond prospectivity in the palaeo-Gwydir River system	60
4.3 Kings Plains and Reddestone type alluvial sapphire deposits.....	63
4.4 Braemar type deep-lead sapphire deposits	68
4.4.1 Sapphire-bearing palaeodrainage systems near Braemar	80
4.4.2 Extent of the Eocene/Oligocene sapphire-bearing sediments below basalt near Braemar	82
4.4.3 Implications of the Braemar deposit in the search for similar deposits in the zone-of-overlap between the East and West Central Provinces	84
4.4.4 Conclusions and exploration-mining problems.....	85
Chapter 5	
Heavy Mineral Suites within the Central Province, New South Wales.....	88
5.1 Introduction	88
5.2 Preparation of heavy mineral concentrates	88
5.3 Heavy minerals present in the Central Volcanic Province.....	90
5.4 Comparison between heavy mineral suites from collection sites within the Central Volcanic Province.	92

5.5 Ilmenite mantled rutile crystals from the Uralla district	97
5.5.1 Occurrence.....	97
5.5.2 Description of the ilmenite-rutile crystals.	97
5.5.3 Comparisons with ilmenite-rutile crystals and ilmenite found elsewhere	101
5.6 Garnets from Horse Gully in the New England gemfields.	107
5.6.1 Occurrence.....	107
5.6.2 Features and properties of the gem garnets	107
5.7 Implications for genesis of heavy mineral placer deposits.....	111
5.8 Conclusions and interpretation.....	112

Chapter 6

Evaluation of Sapphire Source Rocks and Potential Source Structures in the

Central Volcanic Province.	115
6.1 Introduction	115
6.2 Evaluation of the natural lagoons of the Central Volcanic Province -Are they sapphire-producing maars ?	115
6.3 Detailed work at Kings Plains and Dunvegan lagoons	119
6.4 Sapphire-source rock evaluation in the Central Volcanic Province.....	132
6.4.1. Watershed analysis of the Central Volcanic Province.	133
6.4.2 Definition of specific catchment areas for sapphire exploration.	133
6.4.3 Source rock evaluation program.....	133
6.4.4 Chemical features of the Mount Buckley lavas.....	143
6.5 Comparison between volcanics of the sapphire-bearing East and sapphire-barren West Central Province.....	148
6.6 Comparison between the Central Province and other volcanic provinces in northeastern Australia and southeast Asia.....	149
6.7 Conclusions	149

Chapter 7

Summary and Conclusions.....	151
7.1 Origin of corundum associated with volcanic provinces	151
7.1.1 Aims and achievement of aims	151
7.1.2 Inclusion studies	151
7.1.3 Surface features	152
7.2 Division of the New England gem fields into three exploration regions	153
7.2.1 Diamond-bearing deep leads of the West Central Volcanic Province.....	153

7.2.2 Holocene alluvial sapphire deposits of the East Central Volcanic Province.....	154
7.2.3 Braemar-type deep lead deposits in the zone-of-overlap	154
7.3 Heavy mineral suites in the New England gem fields.....	155
7.3.1 Sapphire associates of the East Central Volcanic Province	155
7.3.2 Ilmenite-mantled rutile crystals of the Uralla area	155
7.3.3 Pyrope-almandine garnets from Horse Gully	155
7.4 Investigation of sapphire source rocks and potential source structures in the Central Volcanic Province	156
References	158
Appendix 1	
Pre-Volcanic Tertiary Landscape and Drainage of the New England Region, New South Wales	173
Appendix 2	
Description of Water Bores drilled in the New England Region, New South Wales	225
Appendix 3	
Geophysical Assessment	230
Appendix 4	
Drilling Programme.....	260
Appendix 5	
Mt Buckley Basalt Flows; Thin Section Descriptions	271
Appendix 6	
Material published during Doctor of Philosophy Candidature	274

Summary

The Central Volcanic Province in northern New South Wales, also known as the New England Gem Field, is one of Australia's most important sapphire producing areas. Large-scale mechanized mining and restoration techniques are the most effective means of recovering this resource from beneath valuable farm land.

The alluvial sapphires are shown to be derived from the 32-38 million year old alkaline basaltic volcanic rocks comprising the eastern portion of the Central Province via uranium-lead dating of zircon inclusions within the sapphires. Corundum, zircon and other exotic minerals crystallized in coarse aggregates when high proportions of incompatible elements and volatiles were present in early melt fractions. These unusual crystallization products were subsequently transported to the surface by voluminous basaltic magmas. Surface dissolution or etch features on the corundum occurred in the melt environment en route to the surface.

In the East Central Province the post-eruptive fluvial history was vital in controlling the concentration of economic sapphire deposits from lower grade source rocks. The sapphire-bearing placer deposits occur as "shoestring" type accumulations occupying channels within basalt-filled valleys. The highest grades generally correspond to areas where channels are deepest. Minimal evidence of abrasion due to fluvial transport, coupled with the spatial variability in the character of the corundum, and the differences in proportions of heavy minerals in placer deposits, collectively indicate minimal amount of fluvial transport, reworking or mixing. Within these low energy systems the heavy minerals have moved vertically downwards and become concentrated with time. Such observations indicate that the corundum is derived from local multiple sources.

Highly prospective diamond-bearing "deep leads" associated with the palaeo-Gwydir River have been traced under the 19-23 million year old basalts of the West Central Province via reconstruction of the pre-volcanic topography. The palaeotopographic reconstruction indicates at least 3 separate systems of diamond bearing alluvials and therefore, local, multiple sources for the diamonds.

The Central Volcanic Province has been divided into three prospective alluvial target regions. These comprise a western region with Tertiary deep-lead diamond deposits, a central belt with Eocene-Oligocene deep-lead sapphire deposits, and an eastern division with Holocene sapphire deposits.

CERTIFICATE

I certify that the work presented in this thesis is original unless otherwise referenced and has not been submitted for a higher degree at any other university or institution.

.

Robert R. Coenraads

Acknowledgements

I would like to thank Mr. Tom Nunan of T.J & P.V. Nunan Pty Ltd, Mr. Bruce Hyman of Jingellic Minerals N.L., Mr. Peter Kennewell of Cluff Resources Pacific Limited, and Mr. Colin and Mrs. Joan Rynne of Braemar for allowing publication of information concerning their exploration and mining areas. Dr. Steve Webster of the Department of Minerals and Energy and Mr. Zoltan Beldi of Geo-Instruments Pty Ltd are thanked for generously supplying the geophysical instrumentation, Prof. Don Emerson for the geophysical measurements of the drill core and Dr. Stephen Bannister, Dr. Graeme Chapman and Miss Sue Froud for their assistance with the geophysical field programme. Funding for the geophysical and drilling programme was provided by T.J & P.V. Nunan Pty. Ltd. and Jingellic Minerals N.L. Sapphires, rubies and other heavy minerals for inclusion and surface feature studies were generously supplied by T.J. & P.V. Nunan Pty Ltd, Colin and Joan Rynne, John MacCormack, S.A.P. Mining Co, Bo Ploi and Nakorn Gems, Thailand; garnets from Horse Gully were provided by John Joris of Joris Gemstone Traders Pty. Ltd, Sydney and faceted by Henk van der Graaf; and ilmenite mantled rutile crystals were provided by Simon Paige. I would like to thank the Australian Museum for providing funds for the ion probe analyses, and Dr W. Compston, Dr F. L. Sutherland and Dr P. D. Kinny for their interest and support of this project. I would also like to thank Mr. Jim Stroud and his team at the Department of Minerals and Energy, Armidale Office, for providing the 1:25,000 scale geologic maps that were essential for this study. Many individuals have contributed generously to this project by offering suggestions, advice and critical reviews of manuscripts. It is therefore a pleasure to thank Dr Jane Barron, Dr. Larry Barron, Dr. Bill Birch, Mr. Bob Brown, Dr. Graeme Chapman, Mr Terry Coldham, Dr. Peter Flood, Prof. Brenda Franklin, Dr. A.L. Jacques, Mr. David Jones, Dr. John Lusk, Prof. Cliff Ollier, Mr. Simon Pecover, Mr. Ross Pogson, Dr. A.J. Stoltz, Dr. F. Lin Sutherland, Mr. Pongsak Vichit, Prof. J.F.G. Wilkinson, and Prof. Ken Williams. John Coenraads' patient assistance with manuscript typing and fieldwork, and the assistance of Mr David Barnes, Dr. Günther Bischoff, Dr. Ron Oldfield, Mr Jack Thompson with photography are gratefully acknowledged.

I would like especially to thank Simon Pecover for his initial encouragement to undertake a research project in sapphires, John Lusk for supervising my project, and Lin Sutherland and Günther Bischoff for their untiring support during the project. Their continuing enthusiasm, inspiration and friendship during the project has been greatly appreciated.

My sincere appreciation is extended to many individuals and families who offered hospitality and friendship of during my fieldwork in the New England Area. Special mention is due to Tony and Lucia Boomgaard, Bruce Mair, Tom and Pat Nunan, Cliff and Jeannetta Ollier, Alan and Elizabeth Uebergang, Joyce Willows, Ralph and Pam Paige, Col and Joan Rynne, and Len and Lou Stewart.

LIST OF COLOUR PLATES

Colour Plate 1. Partially resorbed sapphire "dog tooth" crystal from the New England gem fields, New South Wales.....	xviii
Colour Plate 2. Heavily included sapphire "barrel" crystal from the New England gem fields, New South Wales.....	xviii
Colour Plate 3. "Dog tooth" and "barrel" sapphire crystals from the New England gem fields, New South Wales.....	xix
Colour Plate 4. Inclusions in sapphire from the New England gem fields.....	xix
Colour Plate 5. Landsat Image No. 095-081 (Australian Centre for Remote Sensing) showing the Maybole volcanic centre in the New England gemfields, New South Wales, together with the lineament interpretation.....	xx
Colour Plate 6. Parcel of "fancy" sapphires from the New England gem fields, New South Wales collected by T.J. & P.V. Nunan Pty. Ltd. over several years.....	xx
Colour Plate 7. Quarry at Braemar (circa 1987). Sapphire-bearing fluvio-lacustrine sediments are exposed in the southwest face below a protective capping of 23 million year old basalt.....	xxi
Colour Plate 8. Highly ferruginous volcanic rock intruding hydraulically fractured Devonian-Carboniferous metasilstone at Braemar in the New England gemfields, New South Wales.....	xxi
Colour Plate 9. Small sapphire recovery plant of Mr. Col Rynne at Braemar, New South Wales.....	xxii
Colour Plate 10. Sapphire recovery plant of T.J. & P.V. Nunan Pty. Ltd. at Reddestone Creek in the New England gemfields, New South Wales.....	xxii
Colour Plate 11. Alluvial plains of Back Plains Creek in the New England gemfields, New South Wales, showing the layout of a well designed exploration programme of T.J. & P.V. Nunan Pty. Ltd.....	xxiii
Colour Plate 12. Sapphire mining operation of T.J. & P.V. Nunan Pty. Ltd. on the Kings Plains Creek Eastern Feeder, low angle aerial photograph, looking west.....	xxiii

LIST OF PLATES

- Plate 1. 1. Negative crystal socket in blue sapphire. 2. Negative crystal in blue-purple sapphire. 3. Negative crystal socket in purple ruby, all from the Ruby Well Mine, Chanthaburi-Trat. 4. Sapphire from Reddestone Creek, No. 2 plant, New England. Flat topped triangular hillocks and detail showing relief of hillocks and their irregular, eroded appearance, note damage to top edge of the hillock due to fluvial transport..... 23
- Plate 2. 1. Blue sapphire from Reddestone Creek, No. 1 plant, New England, surface perpendicular to the c-axis, showing oriented flat, shallow hexagonal etch depressions with central hillocks. 2. Blue sapphire from SAP mine, Bo Ploi, hexagonal etch depressions with a central hillock. 3. Pink-purple ruby, Ruby Well mine, Chanthaburi-Trat, showing early stages of formation of triangular and hexagonal hillocks. 4. Deep prominent etch sculpturing on a pink-purple ruby, Ruby Well mine, Chanthaburi-Trat, showing detail of etch channels..... 25
- Plate 3. Blue sapphires from 1. New England gem fields. "Shark-skin like" etch channels. 2. SAP mine, Bo Ploi. "Intaglio-like" surface due to extensive etching showing structural control of "intaglio" pattern and microlamination due to successive layer dissolution. 3. Braemar, New England. Etch pattern resembling trigonal prismatic "stacked bricks" on a surface oriented at a low angle to the c-axis. 4. Braemar, New England. Triangular pyramidal depressions resulting from etching of a surface at an intermediate angle to the c-axis..... 26
- Plate 4. Blue sapphires from Braemar, New England. 1. Etch surface at a low angle to the c-axis resembling trigonal prismatic "bricks". 2. Chatter marks or sub-parallel curved grooves attributed to mechanical stress. 3. Sapphire traversed by numerous fractures. 4. Fracture radiating from an inclusion in sapphire..... 27
- Plate 5. Blue sapphires 1. Ruby Well mine, Chanthaburi-Trat showing surface covered with triangular hillocks. Detail of triangular hillocks, some chipped due to fluvial damage. 2. Reddestone Creek No. 1 plant; specimen showing a "bladed" surface texture. Crystallographic control as the raised "blades" form two sides of triangular pyramidal shaped pit. 3. SAP mine, Bo Ploi. Rebroken healed fracture surfaces reveal a "fingerprint-like" pattern of exposed, formerly fluid filled, tubes. 4. Reddestone Creek, No. 1 plant, New England. Conchoidal fracturing on the edge of this sapphire is evidence of damage in the fluvial environment. 5. Ruby Well mine, Chanthaburi-Trat. Protruding hillock broken off at its base leaving a clean fracture surface is evidence of damage in the fluvial environment..... 28

LIST OF FIGURES

Figure 1-1. Location of the Central Province in northeastern New South Wales. Inset shows Mesozoic-Cenozoic volcanic provinces which form a discontinuous band within or adjacent to the eastern Australian highlands.....	2
Figure 1-2. Operations flowchart for a typical large scale sapphire mine.....	10
Figure 2-1. Ruby and sapphire crystal forms belonging to the rhombohedral division of the trigonal system.....	18
Figure 2-2. Sapphire-anorthoclase xenolith from basalt, Mt Leura, Hoy Province, Queensland.....	19
Figure 2-3. Sapphire crystal from the Central Province, N.S.W., showing a negative crystal shape in its faces.....	21
Figure 2-4. Sapphire crystal from the Central Province, N.S.W., showing uneven chemical resorption.....	21
Figure 2-5. Scenario explaining uneven chemical resorption such as seen on the sapphire crystal shown in Figure 4.....	22
Figure 2-6. Compositional ranges of feldspar inclusions in sapphires and zircons from the Central Volcanic Province.....	33
Figure 2-7. Backscatter photographs of a euhedral feldspar inclusion in a sapphire from Braemar.....	34
Figure 2-8. Spinel inclusions in New England sapphires plotted within the spinel family prisms.....	35
Figure 2-9. Gahnospinel (sample nos. 1-17) and hercynite (nos. 18-24) inclusions in sapphire from the Central Volcanic Province.....	36
Figure 2-10. Niobium-rutile (sample nos. 1-3) and columbite (nos. 4-13) inclusions in sapphire from the Central Volcanic Province.....	37
Figure 2-11. Melt inclusions in sapphire (nos. 1-15) and zircon (18-24) from the Central Volcanic Province.....	38

Figure 2-12. Euhedral zircon crystals included in sapphire, transmitted light photomicrographs.....	40
Figure 2-13. Zircon inclusion 28/11, showing the sputter-hole excavated by the ion-beam.....	42
Figure 3-1. Structural elements of the Central Province, New South Wales, determined by landsat lineament analysis.....	48
Figure 3-2. Drainage pattern of the Central Province and location of heavy mineral collection sites listed in Table 5-1.....	51
Figure 3-3. Illustration of the Technique by which sub-basaltic topography is determined.....	53
Figure 3-4. Present-day and palaeodrainage patterns in the Central Province, New South Wales.....	54
Figure 3-5. Progressive stages in the development of relief inversion by lateral stream formation.....	56
Figure 3-6. Stages in the development of stream piracy illustrated by two examples in the Central Province.....	57
Figure 4-1. Central Province, New South Wales divided into broad zones indicating suitability for sapphire or diamond exploration.....	61
Figure 4-2. Diamond-bearing palaeodrainage and distribution of historic mines of the Copeton Field.....	62
Figure 4-3. Economic Holocene sapphire deposits of the Kings Plains palaeochannel.....	64
Figure 4-4. Economic Holocene sapphire deposits of the Reddestone Channel.....	65
Figure 4-5. The development of economic sapphire deposits through stream concentration.....	67
Figure 4-6. Reddestone Creek sapphire deposit and sapphire concentrations in river gravels.....	69

Figure 4-7. Kings Plains Creek sapphire deposits and sapphire concentrations in river gravels.....	69
Figure 4-8. Location of the Braemar sapphire deposit in the zone-of-overlap between the East and West Central Provinces.....	71
Figure 4-9. Location of the Braemar sapphire deposit in relation to the geology of the Elsmore-Swan Brook area.....	72
Figure 4-10. Reconstruction of the surface geology at Braemar.....	73
Figure 4-11. Stratigraphy of the old quarry (south-west face) at Braemar (circa 1986).	74
Figure 4-12. Stratigraphic and intrusive relationships evident in costeans A to D at Braemar.....	75
Figure 4-13. Stratigraphic and intrusive relationships evident in costeans E to J at Braemar.....	76
Figure 4-14. Breccia dyke intruding Devonian-Carboniferous metasiltstone, exposed in costean B at Braemar.....	77
Figure 4-15. Distribution of Eocene/Oligocene deep lead sapphire deposits and Holocene sapphire-bearing alluvium at Braemar.....	78
Figure 4-16. Proposed extent of Eocene/Oligocene sapphire-bearing sediments at Braemar beneath a capping of 23.2 Ma. basalt	79
Figure 4-17. Positions of the Braemar and Swan Brook palaeochannels as determined by basement palaeotopographic analysis on the Elsmore 1:25,000 sheet.....	81
Figure 4-18. Cross sections, AB and CD, of the Braemar palaeochannel looking north.....	83
Figure 4-19. Inversion of the palaeo-Swan Brook by lateral streams, Swan Brook and Kings Creek and potential deep lead sapphire deposits.....	86
Figure 5-1. Central Province spinel plotted within the spinel family prisms.....	91
Figure 5-2. Central Province chromium-spinel compositions.....	93

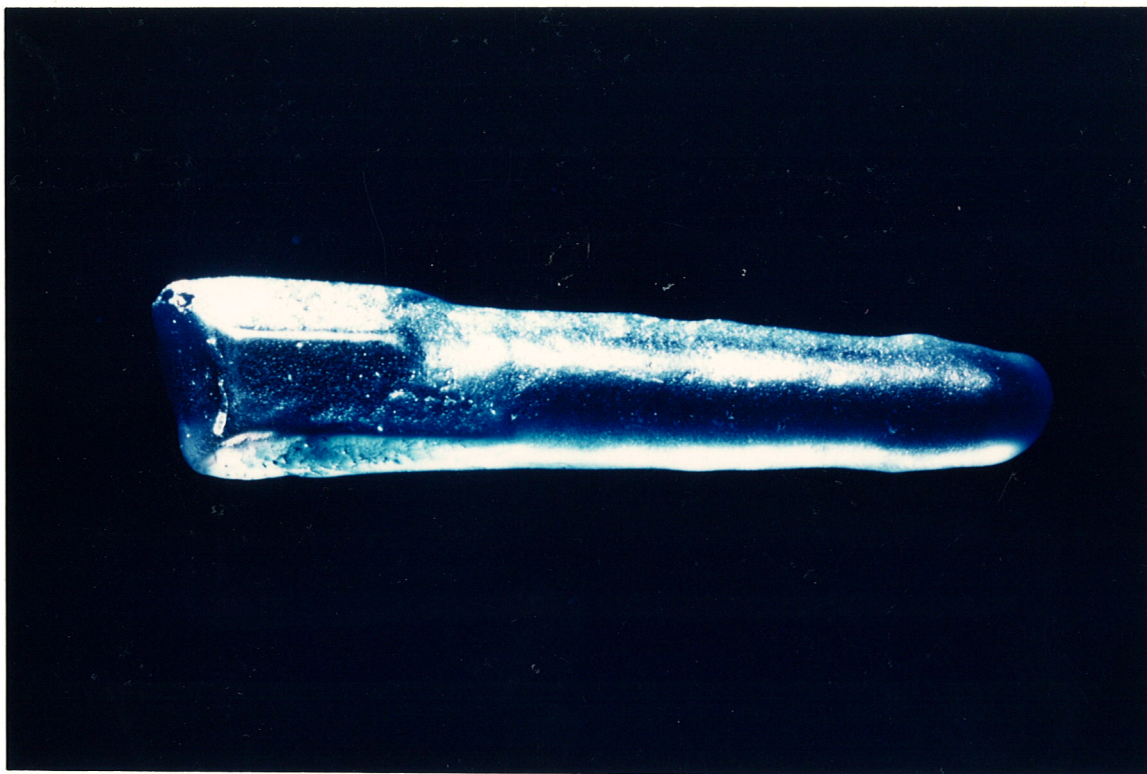
Figure 5-3. Central Province pleonaste compositions.....	94
Figure 5-4. Central Province titanium-magnetite compositions.....	95
Figure 5-5. Central Province ilmenite compositions.....	96
Figure 5-6. Geology of the Uralla district, New SouthWales and location of the ilmenite coated rutile crystals.....	98
Figure 5-7. Ilmenite mantled rutile crystals from the Rocky River Goldfield near Uralla.....	99
Figure 5-8. Transmitted light photomicrographs of sections cut through ilmenite mantled rutile crystals.....	100
Figure 5-9. Summary of microprobe results across 4 ilmenite mantled rutile crystals cut perpendicular to the C-axis.....	102
Figure 5-10. Summary of the main elemental oxide ranges in the Uralla ilmenite compared to those in literature sources.....	105
Figure 5-11. Location of Horse Gully in the New England Gemfields, New South Wales.....	108
Figure 5-12. Relationship between refractive index, specific gravity and end member composition for the Horse Gully Garnets.....	110
Figure 6-1. Location of the natural lagoons of the Central Province, N.S.W.....	116
Figure 6-2. Kings Plains Lagoon, aerial photograph.....	117
Figure 6-3. Dunvegan Lagoon, aerial photograph.....	118
Figure 6-4. Clarevaulx and Dunvegan Lagoons, aerial photograph.....	118
Figure 6-5. John Ryall Lagoon, aerial photograph.....	118
Figure 6-6. Barley Field Lagoon, aerial photograph.....	118
Figure 6-7. Basement topography in the vicinity of Kings Plains Lagoon.....	118

Figure 6-8. Basement topography in the vicinity of Clarevaulx and Dunvegan Lagoons.....	121
Figure 6-9. Basement topography in the vicinity of John Ryall Lagoon.....	122
Figure 6-10. Basement topography in the vicinity of Barley Field Lagoon.....	123
Figure 6-11. Basement topography in the vicinity of Inverell Racecourse.....	124
Figure 6-12. Cross sections through; A; Kings Plains Lagoon. B; Dunvegan Lagoon. C; Clarevaulx Lagoon. D; John Ryall Lagoon. E; Barley Field Lagoon. F; Sheep Station Creek in the vicinity of Inverell Racecourse.....	125
Figure 6-13. Kings Plains Lagoon geophysical survey area, elevation.....	127
Figure 6-14. Dunvegan Lagoon geophysical survey area, elevation.....	128
Figure 6-15. Model explaining the development of the lagoons in the Central Province.....	130
Figure 6-16. Surface configuration of Kings Plains, Dunvegan, Clarevaulx, John Ryall and Barley Field Lagoons.....	131
Figure 6-17. Watershed analysis for the Central Volcanic Province in northeastern New South Wales.....	134
Figure 6-18. Central Province watershed analysis and location of Mt Buckley study area.....	135
Figure 6-19. Location of basalt sample localities at Mount Buckley.....	136
Figure 6-20. Total alkalis versus silica plot for the Central Province and Mt Buckley analyses.....	141
Figure 6-21. C.I.P.W. normative plagioclase versus differentiation index for the Central Province and Mt Buckley analyses.....	141
Figure 6-22. C.I.P.W. nepheline or hypersthene versus normative plagioclase for the Central Province and Mt Buckley basalt analyses.....	142

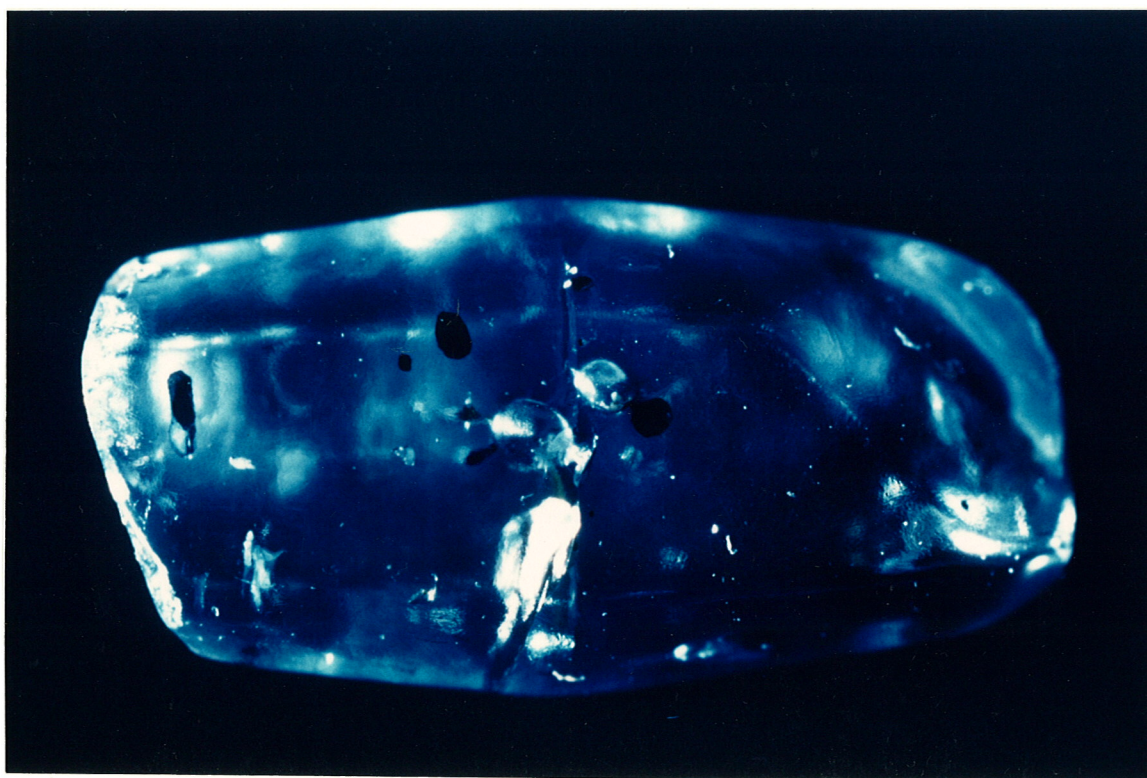
Figure 6-23. C.I.P.W. nepheline or hypersthene versus normative plagioclase for the Mt Buckley basalt analyses.....	143
Figure 6-24. Na ₂ O versus K ₂ O plot for the Central Volcanic Province and Mt Buckley basalt analyses.....	144
Figure 6-25. C.I.P.W. nepheline or hypersthene versus flow number for Mt Buckley flows.....	145
Figure 6-26. Major elements versus flow number at Mt Buckley.....	146
Figure 6-27. Trace elements versus flow number at Mt Buckley.....	147
Figure 6-28. Total alkalis versus silica plot, compositional fields of the Central Volcanic Province, northeastern Australian corundum-bearing provinces and the corundum-bearing and corundum-less southeast Asian volcanic provinces.....	144

LIST OF TABLES

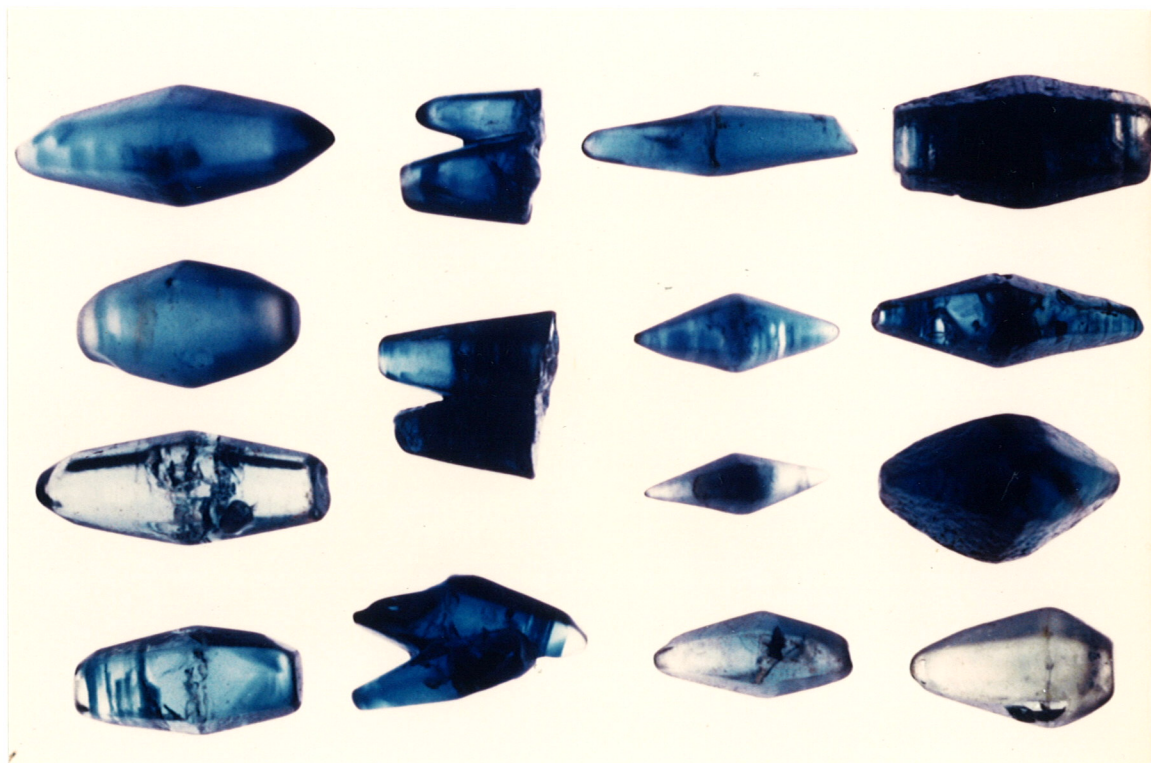
Table 1-1. Age data available for the Central Province.....	6
Table 1-2. History of the east Australian sapphire and diamond industry.....	8
Table 2-1. Properties of Corundum.....	13
Table 2-2. Inclusion suite for Central Volcanic Province Sapphires.....	32
Table 2-3. Inclusion suite for Central Volcanic Province Zircons.....	32
Table 2-4. U-Pb ages of zircon inclusions in sapphire.....	43
Table 5-1. Heavy mineral suites from soil and placer collection sites within the Central Province.....	89
Table 5-2. Weight percent oxide content for the Central Province heavy mineral suite.....	89
Table 5-3. Main elemental oxide ranges in the Uralla ilmenite compared to those in literature sources.....	103
Table 5-4. Composition and gemmological properties of the Horse Gully Garnets.....	109
Table 6-1. Location, chemical analyses and CIPW norms for the Mt Buckley basalts..	139



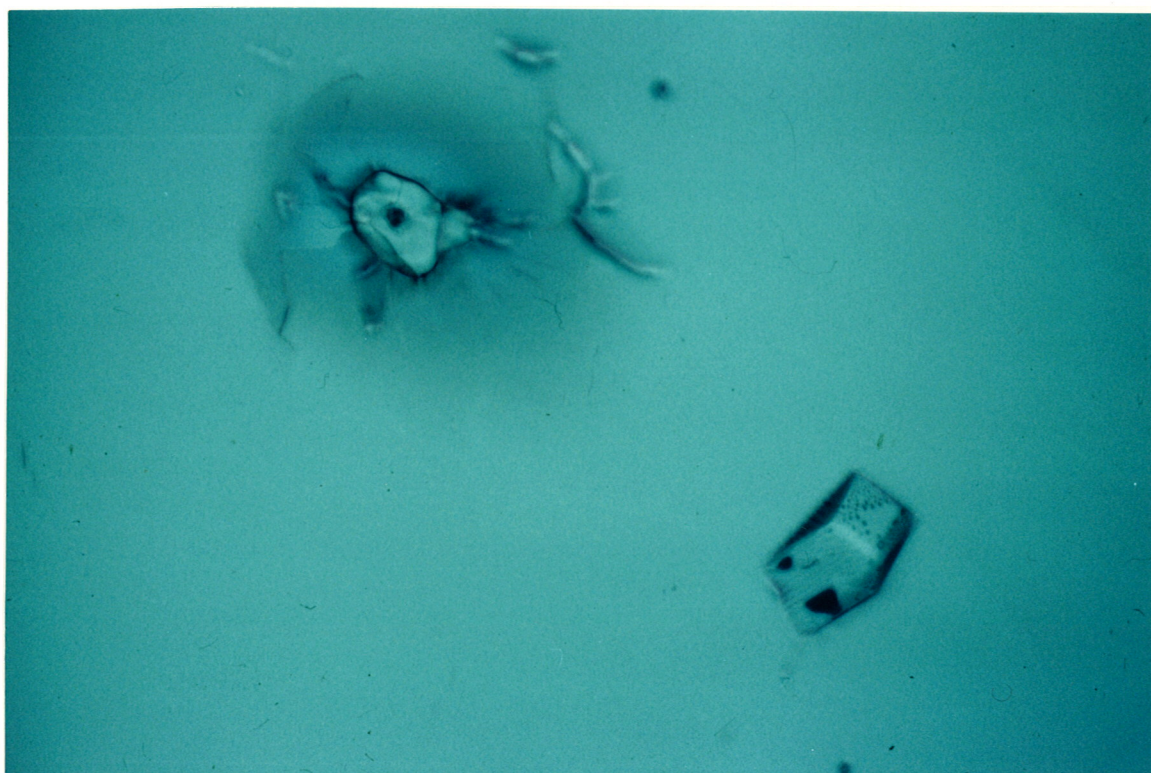
Colour Plate 1. Sapphire "dog tooth" crystal from the New England gem fields, New South Wales. One end of the 20mm crystal shows markedly greater chemical resorption than the other. Figure 2-5 shows a possible scenario to explain its appearance. (Collection of T. J. Nunan, photograph by D. Barnes).



Colour Plate 2. Sapphire "barrel" crystal from the New England gem fields, New South Wales. The opaque black euhedral inclusions are probably columbite. (Collection of T. J. Nunan, photograph by D. Barnes).



Colour Plate 3. "Dog tooth" and "barrel" sapphire crystals from the New England gem fields, New South Wales. (Collection of T. J. Nunan, photograph by D. Barnes).



Colour Plate 4. Inclusions in sapphire from the New England gem fields, New South Wales. The inclusion on the right is a zircon (28/11) with a U-Pb age of 33.7 ± 2.1 million years, the inclusion on the left is a thorium silicate containing 80% ThO_2 . A smoky halo around the thorium silicate inclusion indicates radiation damage of the host sapphire. Sample from test drilling of Dunvegan Lagoon by T.J. & P.V. Nunan Pty. Ltd. Base of photo is 0.22mm.



Colour Plate 5. Landsat Image No. 095-081 (Australian Centre for Remote Sensing) showing the Maybole volcanic centre in the New England gemfields, New South Wales, together with the lineament interpretation. The centre is marked by a series of concentric ring fractures about a point where the major lineament sets appear to intersect.



Colour Plate 6. Parcel of "fancy" sapphires from the New England gem fields, New South Wales collected by T.J. & P.V. Nunan Pty. Ltd. over several years. By far the majority of sapphires mined in the New England gem fields are of blue or green-blue colour.



Colour Plate 7. Quarry at Braemar (circa 1987). Sapphire-bearing fluvio-lacustrine sediments are exposed in the southwest face below a protective capping of 23 million year old basalt. The location of the quarry is shown in Figures 4-9 and 4-10.



Colour Plate 8. Highly ferruginous volcanic rock intruding hydraulically fractured Devonian-Carboniferous metasiltstone at Braemar in the New England gemfields, New South Wales. (Photograph by R. McIver).



Colour Plate 9. Small sapphire recovery plant of Mr. Col Rynne at Braemar. Alluvial material is washed into a rotating trommel then passes over pulsating jigs which trap the heavy material.



Colour Plate 10. Sapphire recovery plant of T.J. & P.V. Nunan Pty. Ltd. at Reddestone Creek in the New England gemfields, New South Wales. Alluvial gravels dumped by truck in the feed box pass into rotating scrubbers which assist breakdown of clay material, then through a series of trommels which size the material and pass each fraction onto a separate pulsating jig.



Colour Plate 11. Alluvial plains of Back Plains Creek in the New England gemfields, New South Wales, showing the layout of a well designed exploration programme of T.J. & P.V. Nunan Pty. Ltd. Piles of dirt indicate the position of large-diameter bucket drill holes. (Photograph by J. Thompson).



Colour Plate 12. Sapphire mining operation of T.J. & P.V. Nunan Pty. Ltd. on the Kings Plains Creek Eastern Feeder, looking west. In such a professional operation, the mine face moves (from right to left) along the alluvial placer deposit, behind which the farmland is restored, in several stages, to its original condition. (Photograph by J. Thompson).

Chapter 1

SAPPHIRE AND DIAMOND EXPLORATION IN THE NEW ENGLAND GEM FIELDS, NEW SOUTH WALES, AUSTRALIA.

1.1 Aims

The principal aims of this study are to examine the occurrence and origin of Australian sapphires which are found associated with Tertiary Central Volcanic Province of eastern Australia (the New England Gemfields), (Figure 1-1). This province was chosen for study because it is Australia's principal producer of sapphire.

Sapphires occurring in the Central Province are principally extracted from unconsolidated Quaternary alluvial placer deposits. Sapphires and diamonds also occur in basalt covered Tertiary deep lead placer deposits. The successful exploration for new deposits, together with the effective mining of existing deposits requires an integrated understanding of geological, geomorphic and hydrologic factors which contributed to the concentration of the sapphires from their host rocks into economically workable alluvial deposits. The present study therefore attempts to explain the distribution of Quaternary alluvial sapphire, Tertiary deep lead concentrations of diamond and sapphire, and associated heavy minerals in the Central Province in terms of these factors. The Reddestone Creek and Kings Plains sapphire-bearing placers; the Braemar deep-lead sapphire deposit, and the Copeton deep-lead diamond deposits of the New England Gemfields are used as case studies with this aim in mind. The model developed for the Central Volcanic Province and its exploration implications may be used in other volcanic provinces to assist in the development of a systematic exploration programme for commercial sapphire concentrations.

A study of the characteristics of the sapphires themselves, such as their surface morphology and inclusion suite, aims to positively link their formation with that of the associated Central Volcanic Province.

The following chapters will deal with the characteristics of sapphires of volcanic origin, as well as aspects of the Central Volcanic Province, including controls on its emplacement, timing of emplacement, the volcanic rocks which make up the province, eruptive mechanisms, the pre-emplacement surface, pre and post volcanic drainage systems and heavy mineral assemblages associated with the province.

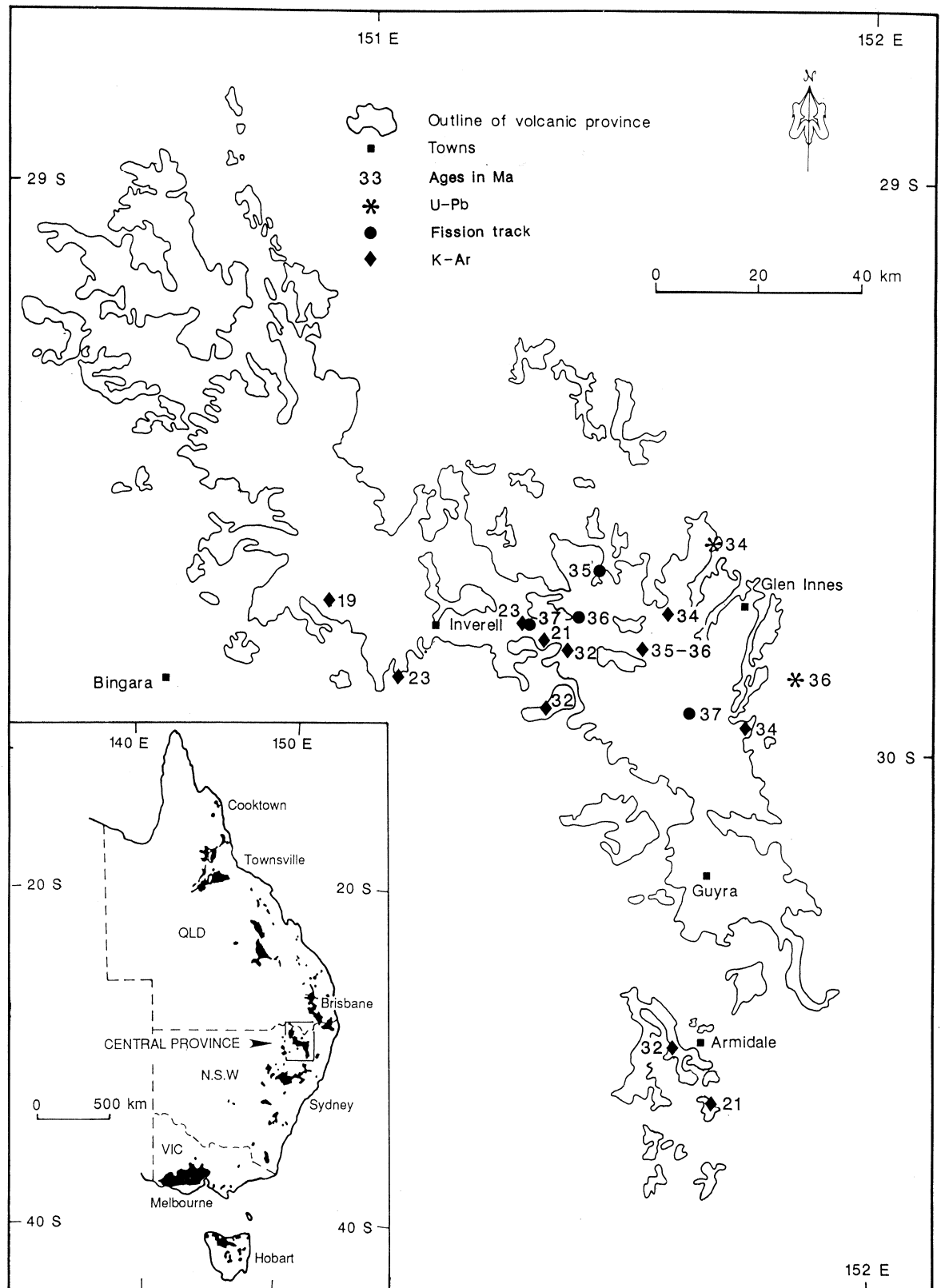


Figure 1-1. Location of the Central Province in northeastern New South Wales. The inset shows Mesozoic-Cenozoic volcanic provinces which form a discontinuous band within or adjacent to the eastern Australian highlands. Available ages, listed in Table 1, have been rounded to the nearest Ma and plotted.

1.2 Introduction

Gem quality corundum occurs in both igneous and metamorphic rocks, however, it is most commonly found and mined from concentrations in alluvial systems draining these source terrains. Corundum is concentrated by the processes of weathering and erosion into alluvial deposits by virtue of its high specific gravity. It is not broken down owing to its high hardness and lack of cleavage and occurs together with other resistant, heavy minerals such as zircon, garnet, spinel and ilmenite.

1.2.1 Corundum deposits of metamorphic association.

Corundum may occur as an accessory mineral in metamorphic rocks, such as metamorphosed limestones and dolomites, mica schists, gneisses and amphibolites. Gemfields associated with metamorphic terrains include Mogok (worlds finest ruby) in Burma (Iyer, 1953; Webster, 1975), Hunza valley (ruby) in Pakistan, Ratnapura and Elahera (many colours and star stones) in Sri Lanka (Munasinghe & Dissanayake, 1981; Zwaan, 1982; Gunawardene & Rupasinghe, 1986; Heilmann & Henn, 1986), Umba Valley and in the western Uluguru mountains near Morogoro (all colours) in Tanzania (Hanni, 1987), the Chimwadzulu hill in southern Malawi (Webster, 1975), Jagdalak (ruby) in Afganistan (Webster, 1975), and India (star ruby).

1.2.2 Corundum deposits of igneous association

A large number of important sapphire and ruby gemfields throughout the world are associated with igneous rocks. These are predominantly volcanic terrains of alkaline type, and also pegmatites.

Gem fields associated with alkaline basaltic volcanism include New England (sapphire) and Anakie (worlds best green and golden yellow sapphire) in Australia (MacNevin, 1972; Broughton, 1979; Coenraads, 1990); Pailin (sapphire) in Cambodia (Jobbins and Berange, 1981); Chanthaburi-Trad (ruby and sapphire), Denchai, Bo Ploi (sapphire) and Khorat Plateau in Thailand (Vichit et al, 1979; Barr and MacDonald, 1981; Keller, 1982; Yaemniyom, 1982; Gunawardene and Chawla, 1984; Vitchit, 1987); Bokeo Plateau, Xuan Loc Plateau, Cardamones Massif, Solovens Plateau and Kassens Plateau in Kampuchea (Lacombe, 1969-70); Haut Chalong Plateau, Pleiku Plateau, Darlac Plateau and Djiring Plateau in South Vietnam; Kouang Tcheoci Wan, Fujian Province and Hainan Island in Southern China (Keller and Keller, 1986; Keller and Wang, 1986); Mercaderes Rio Mayo area in Colombia (Keller et al, 1985); Gimi Valley near Jemaa and Kaduna Province in Nigeria (Wright, 1969; Kiefert and Schmetzer, 1987). Sapphires may be found in matrix in basic dykes of alkaline affinity at Yogo Gulch near Utica, Montana, U.S.A. (Brownlow and Komorowski, 1988), and at Loch Roag on the Isle of Lewis, Scotland (Jackson, 1984).

Gemfields associated with pegmatites include Soomjam Village in the Pader District, Kashmir (Webster, 1975; Atkinson and Kothavala, 1983) and Barauta, Zimbabwe (Sweeney, 1971).

Striking similarities between the gemfields of volcanic association can be seen.

- (a) They are associated with extrusive basaltic lava fields or eroded remnants, or also laterites.
- (b) In most cases, crater lakes, cones, cone remnants or plugs can be found.
- (c) Alkaline basalt types appear to be always present.
- (d) Ultramafic xenoliths (predominantly mantle lherzolites) are commonly reported.
- (e) In a number of the fields, older basalt flows are tholeiitic with younger flows being increasingly alkaline.
- (f) The corundum and associated megacrysts are corroded implying disequilibrium with the carrier magma.
- (g) In-situ corundum megacrysts are rarely seen within the basalts, apart from rare mafic dykes (such as Loch Roag, Jackson, 1984).
- (h) Different areas within a gem-producing terrain may yield different coloured stones, with characteristics changing in distances under 10 kilometres; this implies multiple sources.
- (i) Crystal inclusions found in sapphire include; apatite, columbite, rutile, pyrrhotite, boehmite, zircon, hercynite (Fe spinel), gahnospinel (Fe, Zn spinel), almandine, pyrope, hotchetelite (U, Ti pyrochlore), alkali-feldspar and plagioclase.
- (j) Sapphires are characteristically associated with zircon, spinel and ilmenite in placer deposits. Occasionally they may also be associated with olivine, clinopyroxene, garnet, magnetite or feldspar.

1.2.3 Australian sapphire deposits

Sapphires have long been recognized in areas of basaltic volcanism (Dunstan, 1902), being found, in varying quantity and quality, in streams and rivers draining many Cenozoic-Mesozoic "lava field" provinces in eastern Australia, (Spencer, 1983). The two lava field provinces which contain known economic concentrations of sapphire are the Central Province in northern New South Wales (the New England gem field) and the Hoyt Province in central Queensland (the Anakie gem field). Recent exploration suggests that the other provinces in central Queensland (the Lava Plains gem field) also contain potential deposits (S.R. Pecover, pers comm.).

1.2.4 Volcanism in the Central Province

The Central Volcanic Province, in northeastern New South Wales is one of a number of Mesozoic-Cenozoic intraplate volcanic provinces which form a discontinuous belt stretching over a distance of 4400 kilometers and up to 300 kilometers wide, within or adjacent to the Eastern Australian Highlands (Johnson, 1989). The locations of east Australian volcanic provinces are shown in Figure 1-1.

The Central Volcanic Province, comprising Tertiary basaltic volcanics, intrusives and minor sediments, locally overlies and intrudes Devonian to Triassic volcanics, metasediments and plutonics of the Woolomin-Texas Block of the New England Fold Belt (Leitch, 1974). It extends from Armidale in the south, through Glen Innes and Inverell, to the Queensland border in the north (Figure 1-1).

The basaltic rocks of the Central Province yield potassium-argon ages of 19 to 38 Ma (Cooper et al, 1963; McDougall & Wilkinson, 1967; Wellman & McDougall, 1974; Smith, 1988; C.D. Ollier, pers. comm. 1989; Coenraads et al, 1990; Sutherland & Raynor, unpubl. data) and from 2 to 49 Ma based on reset zircon fission track ages (Hollis & Sutherland, 1985; Sutherland & Hollis, unpubl. data). The ages available for the Central Province are shown on Figure 1-1 and are listed in Table 1-1.

The lavas are predominantly alkaline to strongly alkaline. They include alkali olivine basalts, basanites, hawaiites and nepheline hawaiites (Wilkinson, 1962; Wilkinson, 1966; Binns, 1969; Binns et al, 1970; Duggan, 1972; Wilkinson, 1973; Wilkinson & Duggan, 1973; Street, 1974; McKay, 1975; McQueen, 1975; Barron, 1987; Coenraads, in prep). Tholeiites occur in the vicinity of Inverell (Duggan, 1972; Wilkinson & Duggan, 1973). Breccias and volcanoclastic rocks have been reported by various workers (Lishmund & Oakes, 1983; Sutherland, 1985; Temby, 1986 and Barron, 1987) and occur throughout the Inverell-Glen Innes region at or near the base of the volcanic pile (Brown & Pecover, 1986a,b; Pecover & Brown, 1986; Brown, 1987; Pecover, 1987; Pecover and Coenraads, 1989). Some of the volcanoclastic rocks are known to contain sapphire (Pecover and Coenraads, 1989).

Table 1-1: Comparative ages from the Central Province, New England, N.S.W.

Age (Ma)	Description	Map Sheet	Grid Ref.	Method	Reference
22.6 ± 2.0*	Copeton Rd, Inverell (flow)	Inverell 1:250,000	404304	K-Ar	Wellman & McDougall, 1974
19.0 ± 1.0*	11 km W of Inverell (flow)	Inverell 1:250,000	393308	K-Ar	McDougall & Wilkinson, 1967
21.2 ± 1.0*	Dangersleigh Rd, Armidale (flow)	Dorrigo 1:250,000	471215	K-Ar	McDougall & Wilkinson, 1967
34.3 ± 1.5*	42.5 km N of Guyra	Grafton 1:250,000	478299	K-Ar	McDougall & Wilkinson, 1967
32.2 ± 1.2*	1.5 km S of Armidale Airport	Dorrigo 1:250,000	463219	K-Ar	Wellman, 1971
33.8 ± 0.7*	11.4 km W of Glen Innes (flow)	Grafton 1:250,000	465319	K-Ar	Wellman, 1971
35 - 36*	Spring Mountain (flow)	Grafton 1:250,000	461303	K-Ar	Cooper et al., 1963
20.6 ± 0.2	Newstead Rd (flow)	Elsmore 1:25,000	389001	K-Ar	Smith, 1988
31.9 ± 0.3	Newstead South (flow)	Elsmore 1:25,000	422004	K-Ar	Smith, 1988
32.3 ± 0.2	Tingha-Guyra Rd (flow)	Indiana 1:25,000	402889	K-Ar	Smith, 1988
23.2 ± 0.5	Braemar quarry (upper flow)	Inverell 1:100,000	349033	K-Ar	C.D. Ollier pers. comm., 1989
37.0 ± 1.5 ¹	Braemar quarry (alluvials)	Inverell 1:100,000	350034	Fission Track	Hollis & Sutherland, 1985
35.9 ± 1.6 ¹	Horse Gully (alluvials)	Inverell 1:100,000	415135	Fission Track	Hollis & Sutherland, 1985
34.7 ± 1.7 ¹	Kings Plains (alluvials)	Inverell 1:100,000	492155	Fission Track	Sutherland & Hollis unpubl. data
37.1 ± 1.9	Yolanda (diatreme)	Glen Innes 1:100,000	700825	Fission Track	Sutherland & Hollis unpubl. data
35.9 ± 1.9	Yarrow River (30/26)	Glen Innes 1:100,000	908887	U-Pb	this paper
33.7 ± 2.1	Dunvegan Lagoon (28/11)	Glen Innes 1:100,000	728212	U-Pb	this paper

* Recalculated age using new IUGS constants (after Dalrymple, 1979). ¹ pooled age from a composite range of ages.

The structural control and timing of Central Province volcanism has been described by Coenraads (1988, 1990) and the province may be divided into western and eastern parts on this basis. Sapphires are found in variable quantities in almost every gully, creek and river draining the East Central Province and some of the alluvial deposits are currently being mined by large scale, mechanized operations (Nunan, 1989).

1.3 The alluvial sapphire and diamond mining industry in eastern Australia.

1.3.1 Development of the industry in Australia

The existing gem industry in Australia has developed mainly around sapphire, opal, some imported diamond and other semi-precious stones. The first reported occurrence of sapphires was in 1853 when the Reverend W.B. Clarke found sapphire associated with alluvial tin in the vicinity of Inverell (MacNevin, 1972). Early sapphire mining took place in the Anakie and New England fields from the 1890's to the 1920's with most of the production going to Czarist Russia and Germany. It was not until the 1960's, however, that commercial mechanized mining began to take place on a large scale due to an increase in demand for rough sapphires throughout Asia.

Diamonds were first recovered as a result of gold or tin mining operations in Tertiary deep leads, or in recent alluvial deposits derived from them. The Bingara and Copeton diamond fields were exploited from 1872 and 1883 respectively, however there has been little production since 1922. The total production recorded from these fields is 202,000 carats, although actual production probably exceeded this amount (MacNevin, 1977). The history and development of the sapphire and diamond industry in eastern Australia is summarized in Table 1-2.

In recent years Australia has been a major producer of sapphire, supplying between 65 and 70 percent of the total world sapphire production (Spencer 1983). The New England field contributes in excess of 50 percent of Australia's sapphire production which, although not well documented, is probably in excess of 5 million carats annually (T.J. Nunan Pty Ltd, unpublished data, 1989).

1.3.2 Sapphire mining and processing.

The types of operation found today vary from single prospectors, working in creeks and rivers with picks, shovels and sieves, through to large mechanized operations employing about 30 people and capable of processing 60 cubic yards of unconsolidated alluvium per hour. Although the prospector's pick and shovel are being replaced by bulldozers, backhoes and small processing plants (see Colour Plate 9), the principle of gemstone separation is essentially the same; the gemstone-bearing alluvial gravels or "wash" is excavated, cleaned, sized and the heavy minerals removed by gravity separation. The larger mechanized operations, such as those run by T.J. & P.V. Nunan Pty Ltd,

Table 1-2.**HISTORY OF THE EAST AUSTRALIAN SAPPHIRE & DIAMOND INDUSTRY**

- 1853 Reverend W.B. Clarke reported sapphires and other gems associated with stream tin in the vicinity of Green Swamp, now known as Inverell. Alluvial gold was still the greatest attraction until the 1860's when it began to run out.
- 1870 Joseph Wills started the tin rush, he wrote of "four or five places of sapphire". Tingha and other mining villages, including Stannifer, Kimberley, Wrighton, Stanborough, Elsmore and Gilgai grew up around Inverell; miners also uncovered other minerals and gemstones including diamond and sapphire.
- 1872 Exploitation of the Bingara diamond fields begins.
- 1873 Archibald John Richardson found sapphire near the town of Anakie in Queensland.
- 1880 The Anakie sapphire field became established with most of the early production going to Tsarist Russia via German buyers. Price approx. A\$2 per oz.
- 1883 Exploitation of the Boggy Camp (Copeton) diamond fields by small partnerships begins.
- 1890's Activity on the diamond fields increases as larger companies amalgamate claims. This activity was probably caused by disruption to the S. African diamond production during the Boer War (Inverell Times newspaper 31/12/75). From 1905 onwards output from the fields declined.
- 1900 One thousand miners employed at Anakie. Germany entered the market and imported an increasing proportion of the production. Price approx. A\$20 per oz.
- 1919 Commercial sapphire mining commences in the New England District, 1150 carats were obtained near the town of Sapphire. Mining however comes to a complete standstill due to the effects of the First World War and the collapse of imperialist Russia.
- 1960's Sapphire mining recommenced in response to an increase in demand for rough sapphire throughout Asia. This came about because of deteriorating political conditions in Burma and the Cambodia - Thailand border area which have been a source of sapphires for centuries.
- 1970 Height of the sapphire boom in the New England field with over 100 sapphire plants operating in the district.
- 1987 Renewed exploration interest when a new, non-alluvial, economic source for sapphires is proposed by the Department of Mineral Resources, May 1987. Government policy is emplaced to encourage processing of rough sapphires in Australia rather than export to traditional Asian markets.

(Nunan, 1989), are by far the most significant contributors of sapphire to the market place. A typical large-scale operational procedure is described below and illustrated in the flowchart, Figure 1-2.

Mining large areas of alluvium is carried out via overburden stripping and an advancing trench (Colour Plate 12). A backhoe digs the trench and loads the loose alluvial gravels into trucks for transport to the processing plant (Colour Plate 10). The trench is backfilled and restored as the mining operation advances. The gravels are dumped into a feed box at the upper end of the plant and, with the assistance of high pressure water jets, are gravity fed into huge rotating mesh cylinders called trommels. The trommels size the material by allowing it to pass over progressively coarser meshes. The sized fractions pass onto a series of pulsating jigs which effectively trap heavy minerals of a certain size in trays or "hutches" which are emptied by hand once or twice a day. The pulsating action causes liquefaction of the gravel allowing the heavy grains to sink rapidly. The undersize "heavies" pass through a screen at the base of the hutches and the "lights" are washed over the top. A log washer may be included in the circuit if the alluvial material is clay-rich and therefore difficult to break down. Recovery rates of sapphire are of the order of 90% or better (T.J. Nunan Pty Ltd, unpublished data, 1989).

1.3.3 Sapphire exploration methodology

Bulk sampling of a drainage system is commonly used to determine sapphire grades in the alluvium. Sapphire is usually associated with other heavy minerals such as spinel, zircon and ilmenite which yield a visible "blacksand". This is usually a good sign of potential economic grades. Exploration drilling is performed on a grid pattern (see Colour Plate 11) using a large diameter drill rig (diameter approximately 1 metre) which allows a reasonably large sample of the alluvial gravels to be processed. In a thorough exploration programme at least 0.5 to 1 loose cubic yards of sample are processed to yield a data point at each sample locality (J. McPhee pers. comm., 1987). The advantages of this method are that the depth and location of the ancient stream are determined together with the thickness and type of alluvial gravel and its expected potential in grams of sapphire per cubic metre. The colour, quality, size, etc. of the sapphire can also be assessed. In essence, a well planned exploration drilling programme will indicate the value of the ground and the expected returns prior to mining. Economic grades are dependant on a number of variables, including; current sapphire prices; type and efficiency of plant; quality, quantity and size of sapphire in the wash and; depth, thickness and lateral extent of the wash. Under economic conditions prevalent in 1988, material with grades as low as 5 grams per loose cubic yard could be worked profitably by a highly efficient mechanized operation (T. Nunan pers. comm. 1988).

When the data from the alluvial sampling have been plotted on a map, the highest sapphire grades commonly conform reasonably to an ancient drainage axis. The exploration drilling data for Reddestone Creek and Kings Plains Creek, discussed in

Sapphire Plant Flow Diagram

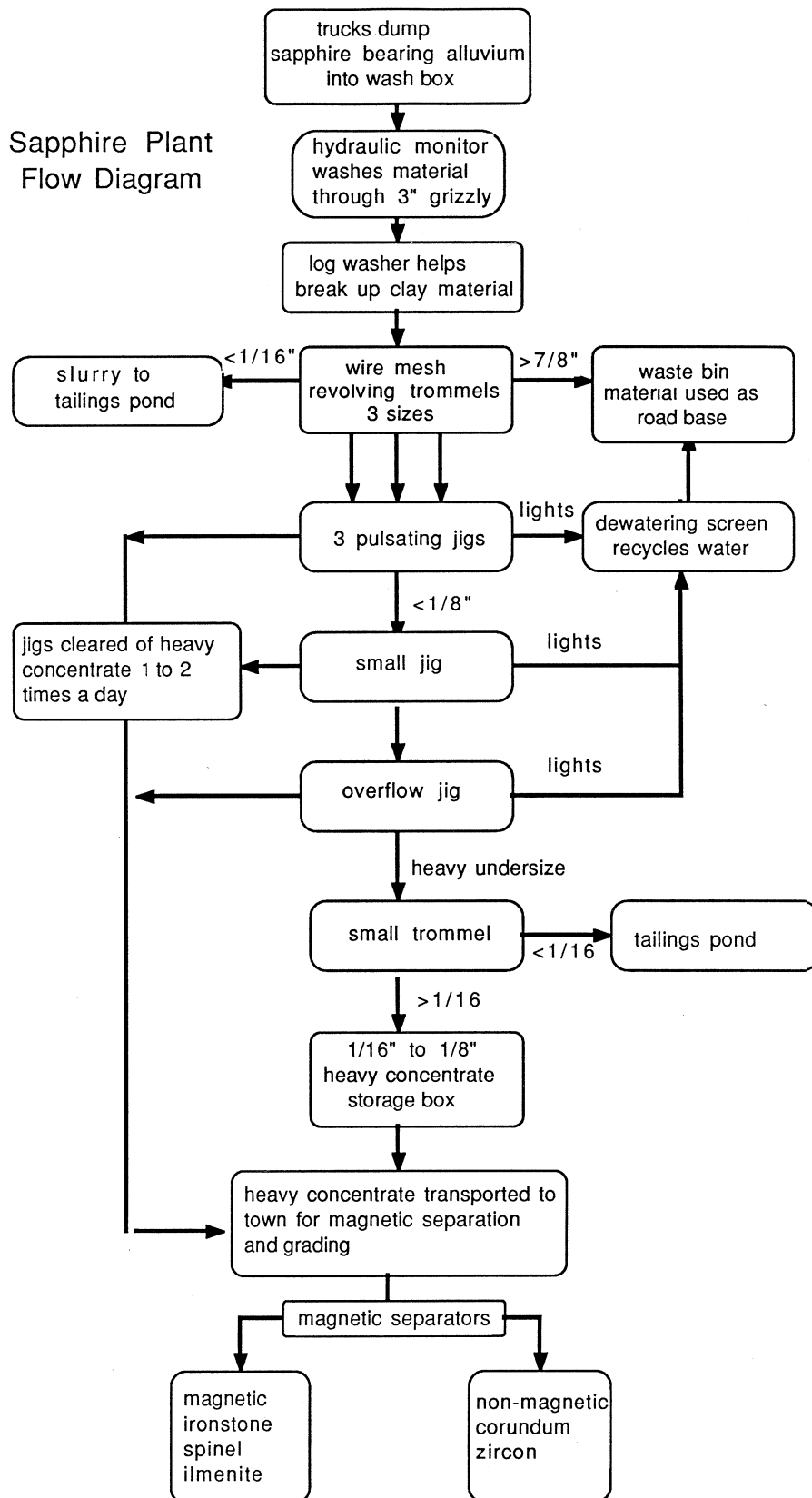


Figure 1-2. Operations flowchart for a typical large scale sapphire mine such as shown in Colour Plate 12.

Chapter 6, illustrate this point. High grades are followed upstream until an economic cutoff is reached, that is, beyond which fluvial concentration has been insufficient to create economic grades. High grades are followed downstream, away from the source region, until dilution of the gem gravels also renders the grades unworkable.

Systematic exploration for sapphires has only recently been applied in Australia due to the small size of the companies and partnerships involved in the industry. Furthermore, there had been little input of geological or geophysical expertise in sapphire exploration, prior to the directive issued by Department of Minerals and Energy at their seminar on Tertiary volcanics and sapphires in the New England district in May, 1987.

It had been recognized that exploration should be directed at defining sapphire/ruby bearing drainage systems associated with Cenozoic lava field provinces (Spencer 1983). What was poorly understood, however, is why only certain areas are rich enough to be worked economically, and why, within those areas, certain streams carry large concentrations whereas others are uneconomic.

1.3.4 Sapphire sorting and grading

The heavy mineral concentrate from the processing plant consists of spinel, ilmenite, zircon and corundum together with ironstone pisolites. This is dried and passed through magnetic separators which remove the magnetic ironstone, spinel and ilmenite. The non-magnetic residue is passed onto a team of skilled sorters and graders. Sorting and grading is normally carried out on mirrors using natural lighting. Mirrors reflect incoming light back through the stone allowing the rapid assesment of colour, clarity and the presence of flaws, without the need to pick up each stone. Zircons are removed, as are parti-coloured and other coloured sapphires (called "fancies", see Colour Plate 6). The remaining blue sapphires are graded into 3 or 4 grades (depending on the requirements of the buyer), with the sapphires in the highest grade being the best blue colour, transparent and free of flaws and inclusions.

1.3.5 Gemstone processing

Thailand is the major processor of all coloured gemstones and recent Thai statistics indicated that between 70 and 80 percent of all sapphires imported into Thailand originated from Australia (PA Technology, 1987). Australian sapphire processing technology uses machinery to set faceting angles, whereas Thailand sapphire faceting is done "by eye". The major advantage of southeast Asian processing is the large quantity of low-cost, efficient labour. Comparing average 1987 Thai and Australian working rates and salaries, the cost of cutting a stone in Australia is 16 to 18 times greater (PA technology 1987). This labour force is particularly important for the sorting and heat treatment of large numbers of gemstones.

1.3.6 Gemstone enhancement

It is an accepted practice to improve the quality of a sapphire or ruby permanently through heat treatment. Thailand has accumulated extensive practical experience in the heat treatment of sapphire and over 95% of rubies and sapphires exported from Asia are heat treated. Treatments include the removal or precipitation of fine rutile needles (silk) and the enhancement or reduction of the intensity of the blue colour by influencing the oxidation state of the trace amount of iron present. The furnace conditions necessary to achieve improvement in stones with various "problems" are outlined in Table 2-1 (Nassau, 1984).

Processes to remove fine epigenetic rutile inclusions or "silk" via rapid cooling, or oxidative heating to lighten blue colour are used by the Thais, mainly on Australian and Thai stones.

Table 2-1: PROPERTIES OF CORUNDUM

Composition:	Aluminium oxide (Al ₂ O ₃) plus traces of the metallic oxides iron (Fe) and titanium (Ti) in sapphire and chromium (Cr) in ruby		
Crystal System:	Trigonal system		
Habit:	Ruby; prismatic, flat to tabular, generally with large basal pinacoids. Sapphire; bipyramidal stepped tapering or barrel shaped crystals		
Cleavage:	None		
Parting:	Along the junction plane surfaces between the twin lamellae. 1. Lamellae parallel to the basal pinacoid:- basal planes are smooth prism and rhombohedron faces are horizontally striated 2. Lamellae parallel to a face of the primitive rhombohedron:- striations are present on the basal pinacoid,prism and rhombohedron faces		
Fracture:	Conchoidal		
Hardness:	9 on Moh's scale		
Specific Gravity:	3.80 to 4.05 (ruby) 3.99 to 4.01 (sapphire)		
Zoning:	Straight colour zoning is common in natural stones, parallel to the prism and pyramid faces and the basal plane		
Dichroism:	Strong, the colour is darker and purer when viewed along the optic axis Red stone deep red/ pale yellowish red Blue stone deep blue/ pale greenish blue Green stone green/yellowish green Violet stone violet red/ yellowish red Yellow stone yellow/ pale yellow (difficult to see) Orange stone yellow-brown or orange/ colourless		
Lustre:	Vitreous		
Optical Properties:	Refractive Index:	sapphire	1.760 - 1.774
		ruby	1.760 - 1.778
	Birefringence:	0.008 to 0.009.	
	Optic Character:	uniaxial negative,	
Dispersion:	0.018 (low)		

Table 2-1. PROPERTIES OF CORUNDUM (continued)

<p>Spectra: Ruby (Chromium)</p> <p>Spectra: Sapphire (Iron 3+)</p>	<p>Emission doublet at 694.2 nm and 692.8 nm, weaker lines at 668.0 nm and 659.2 nm, broad absorption of yellow, green and violet, Additional lines may be seen at 476.5 nm, 475.0 nm and 468.5 nm. Lines more intense in synthetic ruby</p> <p>Lines are seen at 471.0 nm, 460.0 nm and 450.0 nm and the lines at 460.0 nm and 450.0 nm may seem to merge and become a broad band. (full strength in green sapphire and in varying strength in blue and yellow sapphire proportional to iron content)</p> <p>Volcanic sapphires (e.g. Australian, Thai) show all three lines strongly</p> <p>Metamorphic sapphires (e.g. Sri Lankan) show only the 450.0 nm line, usually very faintly.</p> <p>Some Sri Lankan may also show a fluorescent line at 693.5 nm.</p> <p>Fancy coloured sapphires show mixture of the ruby and sapphire spectra</p> <p>Synthetic yellow sapphire (Ni), no iron absorption bands, and synthetic blue sapphire, no lines, or weak and vague.</p>
Chelsea Filter:	<p>Ruby (natural and synthetic) shows as a strong fluorescent red</p> <p>Blue sapphire shows as blackish green.</p>
<p>Ultra-Violet Light and X-rays:</p> <p>Ruby:</p> <p>Sapphire: Blue Green Yellow Orange Colourless Violet</p>	<p>Variable fluorescence, dampened by iron (typical of volcanic corundum)</p> <p>Burma - L.W. strong red, S.W. strong red and x-rays strong red. Sri Lanka - L.W. strong orange red, S.W. moderate orange-red Thailand - L.W. weak red, S.W. weak red or inert short-wave.</p> <p>most blues - L.W. inert, S.W. inert (some weak greenish white). Sri Lanka - L.W. weak red to orange, S.W. patchy dull greenish-white - L.W. inert, S.W. inert Australian - L.W. inert, S.W. inert Sri Lanka - L.W. apricot, S.W. weak orange-yellow, x-rays apricot - L.W. strong orange-red, S.W. inert. some - L.W. light red-orange in long-wave, S.W. inert - L.W. strong red, S.W. weak light red (Alexandrite type)</p>
Sheen: (Asterism)	<p>A six pointed star (three-rays) may be seen on the basal plane due to growth of fine rutile needles oriented in three directions 120° apart, at right angles to the c-axis, and parallel to each pair of prism faces. A rare twelve pointed star (six-rays) occasionally forms when the needles line up with both the first and second order prism faces. Colour varies from grey, bronze or black to a good blue or red.</p>
Other Properties:	<p>Specimens may phosphoresce when heated in a dark room. When rubbed with cloth or leather, the mineral acquires a positive charge which is retained for a considerable time</p>

Table 2-1. PROPERTIES OF CORUNDUM (continued)

<p>Inclusions:</p> <p>volcanic sapphires</p> <p>metamorphic</p>	<p>Australia, Thailand, Cambodia</p> <p>Crystal inclusions; apatite, columbite, rutile, pyrrhotite, boehmite, zircon, hercynite (Fe spinel), gahnospinel (Fe, Zn spinel), almandine, pyrope, hotchelite (U, Ti pyrochlore), alkali-feldspar and plagioclase. stress haloes around solid and negative inclusions lattice damage around radioactive inclusions. Silk; fine oriented epigenetic rutile. Healed or partially healed fractures ("liquid feathers" or "fingerprints")</p> <p>Sri Lanka</p> <p>Crystal inclusions; apatite, pyrite, pyrrhotite, mica, zircon negative crystals and 2 phase inclusions stress haloes around solid and negative inclusions Silk; fine and coarse rutile. Healed or partially healed fractures ("liquid feathers" or "fingerprints")</p> <p>Burma</p> <p>Crystal inclusions; rounded, resorbed crystals, coarse network of short rutile needles Silk, in patches Roiled swirls of colour Cracks, and wavy folded over feathers with long hoses (sapphire)</p> <p>Kashmir</p> <p>Crystal inclusions; tourmaline Silk, very fine and misty giving velvety look</p> <p>Africa (Umba Valley)</p> <p>Crystal inclusions; ciliated rutile ("eyelash"), tiny apatite in clusters ("snow flakes"), Edge traces. Cracks common</p>
<p>Enhancement:</p>	<p>Heat Treatment (Nassau, 1984)</p> <ol style="list-style-type: none"> 1. Removal of silk to increase transparency. Heating to 1600°C to bring rutile into solid solution followed by rapid cooling. 2. Enhancement of asterism. Sustained heating at 1300°C with very slow cooling encourages the precipitation of fine rutile. 3. Diminish the blue colour by changing the iron from Fe²⁺ to Fe³⁺ by heating to 1600°C in oxidizing conditions. Used also to produce a purer red or pink by diminishing the blue colour in purplish Thai rubies 4. Enhance the blue colour by changing the trace iron from Fe³⁺ to Fe²⁺ by heating at 1600°C in reducing conditions. Used to darken pale blue Sri Lankan sapphires. <p>Heat Treatment with Diffusion</p> <ol style="list-style-type: none"> 5. Coating with oxides of Al, Ti, and Fe and heating at 1800°C in reducing conditions for several days results in diffusion into the surface producing a thin blue layer. Other oxides may be used for a red (Cr) or orange (Ni) layer. This layer would be removed if the stone were re-polished therefore this process is not accepted by the gemmological community.

Chapter 2

THE NATURE AND ORIGIN OF CORUNDUM ASSOCIATED WITH VOLCANIC PROVINCES

2.1 Introduction

One aim of this study was to determine the origin of corundum associated with volcanic provinces ("volcanic corundum") based on the surface morphology of the corundum crystals and the nature of their inclusions. Some 255 inclusion bearing corundums were collected from streams and rivers draining the Central Volcanic Province, New South Wales (The New England Gemfields) to provide data for the project. A key result was the age relationship between the corundums and associated volcanic rocks.

The reported failure of experimental attempts to grow corundum from a corundum-bearing basaltic composition, (Green *et al.* 1978), and more significantly, the abundance of incompatible elements such as U, Th, Zr, Nb and Ta in inclusion minerals, indicate that the crystallization process is not simple. Corundum and the other minerals found as its inclusions (zircon, columbite, thorite, uranium pyrochlore, alkali feldspar etc.) could not have crystallized from most basaltic compositions. A more complex process must occur in which crystallization takes place when there are high proportions of incompatible elements and volatiles in an early melt fraction.

2.2 Properties of corundum

In gemstone form corundum is called **sapphire** if it is blue. The term **ruby** is reserved for reds and pinks; **padparadscha** for a pink-orange colour, and the term "**wattle**" is sometimes given to green and yellow parti-coloured stones. All other colours are called sapphire, with the particular colour as a prefix, and are also known as "fancies". Pure alumina is transparent and colourless and is known as leuco-sapphire, however, most natural stones contain trace amounts of elements which cause the variety of allochromatic colours ranging through blue, green, yellow, pink, and mauve. Nassau (1984) stated that the blue colour of sapphire is due to the interaction between iron (Fe^{2+}) and titanium (Ti^{2+}), with the appearance of the colour depending not only on the relative amounts of each present but also on their valence states. This is controlled by the oxidizing-reducing conditions during formation and possibly subsequent heating events. The red colour in rubies is due to chromium (Cr). A clear, transparent and faultless ruby of uniform deep red colour is the most valuable precious stone known. In sapphire, a fine "cornflower" blue is the most sought after, with paler blues, blackish or green blues being less valuable. In more recent times, fine golden stones have become popular. Stones displaying strong colour zoning are often called **parti-coloured** sapphires and are common, particularly in Australian material.

Corundum crystallizes in the rhombohedral division of the trigonal system, however because of equal development of the trigonal prisms and bipyramids, the crystals have a hexagonal appearance. Ruby and sapphire often display quite distinct crystal forms. Crystals of ruby typically display short six-sided prisms and large basal pinacoids, with only minor rhombohedral and bipyramidal development between the pinacoid and prism faces. The result is a flat to tabular prismatic habit shown in Figure 2-1a. Crystals of sapphire show a more pronounced development of the bipyramidal faces with only minor prismatic and pinacoid development, such as shown in Figure 2-1c,d. Frequent repetition or oscillation between different pyramid forms result in horizontal striations at right angles to the c-axis giving the crystals a stepped tapering appearance (Fig 2-1d) or barrel shaped appearance (Fig 2-1c, Colour Plates 2 & 3). Terms used to describe sapphire crystals include "dogs tooth" or "monkeys tooth" (Fig 1d, Colour Plates 1 & 3).

The properties of corundum are summarised in Table 2-1, (Bauer, 1968; Crowningshield, 1983 Nassau, 1984; Gemmological Association of Australia, Gem Material Constants, 1986; Coenraads, 1990):

2.3 Form of sapphires from the Central Volcanic Province

The large scale mining operations of T.J.& P.V.Nunan Pty.Ltd. allow the viewing of a very large number of sapphires as well as low value corundum making up the daily mine run. The stones are predominantly well formed crystals or fragments showing crystal faces. Pointed crystal-terminations, or "dogs teeth" and flat hexagonal prisms known locally as "flats" are common, indicating that crystals are often broken along the basal {0001} parting plane. Large whole crystals are rare but sections bounded by crystal faces and parting planes with diameters of 3 to 4 cm indicate that some crystals grew to at least 12 cm in length. Sharp crystal edges are not seen, crystal edges are slightly rounded and crystal faces are often smooth and glossy due to chemical corrosion (see Colour Plate 1). Zoning is common, both parallel to the prism and pyramid faces forming concentric colour bands, and parallel to the basal plane. Zoned crystals with greenish or yellowish cores ("pipes") and blue rims may be seen. Red and pink pipes have been reported (T. Coldham, pers. comm., 1989)

Sapphires are rarely seen intergrown with other minerals such as anorthoclase, spinel and zircon, however limited evidence suggests that they probably grew in coarse crystallized aggregates. Some examples follow:

1. A sample of sapphire intergrown with anorthoclase is known from the Hoy Province, Queensland, and is held by the Australian Museum (Figure 2-2). An anorthoclase xenolith containing corundum has been reported from Ruddons Point, U.K. by Upton et al (1983). A sapphire intergrown with pleonaste spinel was found in Reddestone Creek in the Central Volcanic Province. It was registered in the New South Wales Geological Survey collection but is now missing. A greenish blue sapphire intergrown with an

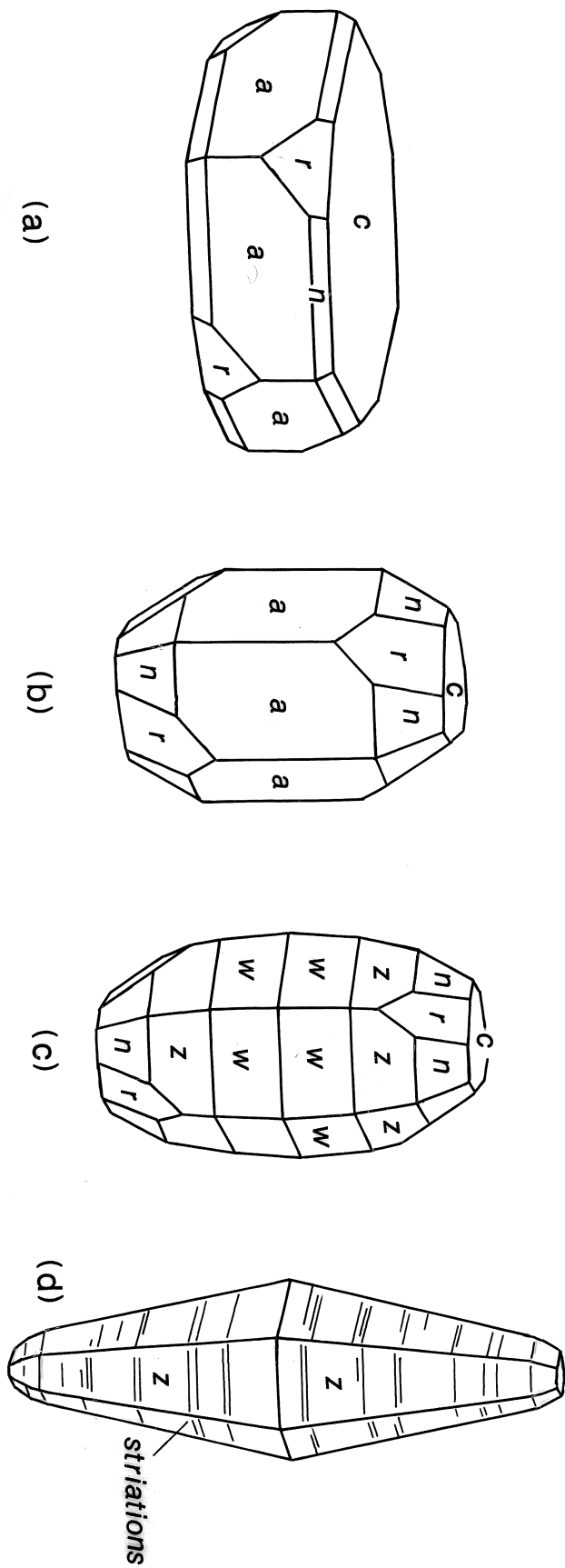


Figure 2-1. Ruby and sapphire crystal forms belonging to the rhombohedral division of the trigonal system. Ruby crystals typically display short six-sided prisms and large basal pinacoids, with only minor rhombohedral and bipyramidal development between the pinacoid and prism faces (a). Sapphire crystals show a more pronounced development of the bipyramidal faces with only minor prismatic and pinacoid development (c and d).

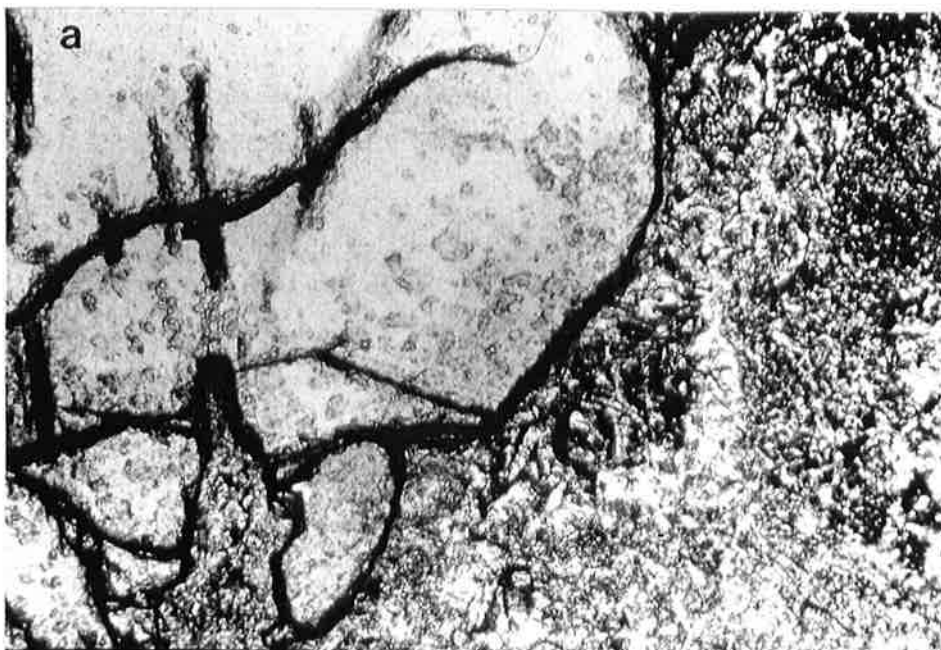


Figure 2-2. Sapphire-anorthoclase xenolith from basalt, Mt Leura, Hoy Province, Queensland. Specimen D44379 is held at the Australian Museum. The corundum is the clear, high relief grain in the upper left of photomicrograph (a). The anorthoclase, occupying the rest of the field of view is cloudy due to incipient alteration. Under crossed polars, photomicrograph (b), the corundum shows first order grey birefringence and twinning lamellae. Examples such as these together with external crystal morphological evidence suggest that sapphires may have grown as part of a coarse mineral assemblage. The base of each photo is 3.75 mm. Photographs by R.E. Pogson.

octahedral iron-rich spinel crystal and a red zircon from Khao Wua, Thailand was reported by Vichit (1987).

2. Sapphire crystals from the Central Volcanic Province occasionally show negative crystal shapes in their faces as shown in Figure 2-3. These suggest growth against other crystals even if only other sapphires.
3. Some sapphires from the Central Volcanic Province show evidence of markedly uneven chemical resorption indicating that they have been partially protected at some stage, possibly by being partially included in another mineral or aggregate of minerals. Such an example is shown in Figure 2-4 and Colour Plate 1, and Figure 2-5 shows a possible scenario explaining its morphology.

2.4 Surface features of rubies and sapphires from volcanic provinces

The surface features of a large number of stones from placer deposits associated with volcanic provinces in both eastern Australia and Thailand were examined.

Australian sapphires were collected from Reddestone Creek No 1 plant (29°41'30"S, 151°38'50"E), No 2 plant (29°43'00"S, 151°38'20"E), and Kings Plains Creek (29°41'00"S, 151°27'50"E) near Glen Innes, New South Wales; and Braemar (29°47'20"S, 151°17'30"E), near Inverell, New South Wales. Thai sapphires were collected from the SAP Mining Co, near Bo Phloi, Kanchanaburi region (14°20'30"N, 99°29'30"E); and the Elem Mine near Ban Khlang, Chanthaburi-Trat region (12°36'10"N, 102°18'10"E). Thai Rubies were collected from the Elem Mine and the Ruby Well Mine, near, Noen Chali, Chanthaburi-Trat region, (12°32'0"N, 102°30'10"E).

Samples were examined with a binocular microscope, then selected specimens were cleaned for 5 to 10 minutes in an ultrasonic bath of water or hydrogen peroxide, mounted on scanning electron microscope stubs and gold coated. Photographs were taken with a JEOL JSM 840 scanning electron microscope.

The observed features may be broadly grouped as; negative crystal impressions, surface resorption or etch features, including chatter marks, and surface damage consistent with transport in the alluvial environment.

2.4.1 Negative crystal impressions

Plates 1-1, 1-2 and 1-3 show sharp edged, deep, geometric shaped holes, or crystal impressions of the order of 0.5 - 1.0 mm across on sapphire and ruby crystal faces. The angles between the impression faces in 1-1 and 1-2 are 120°. The negative crystal shape in Plate 1-3 is particularly interesting in that it appears to show tetragonal symmetry, thus precluding the possibility of it having been a fluid filled negative crystal cavity. These impressions developed as the corundum grew as part of a coarsely crystallized aggregate

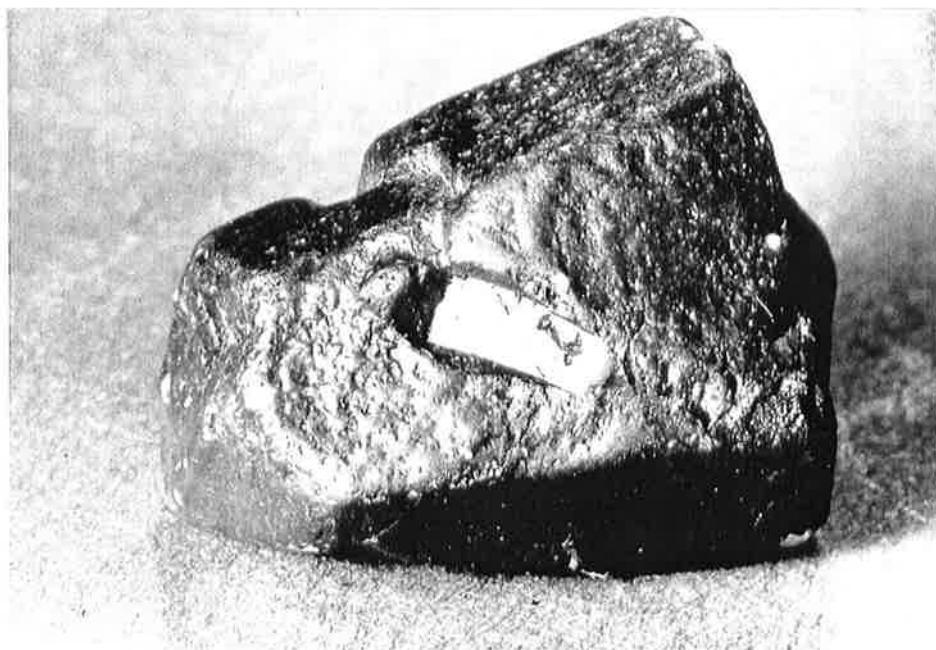
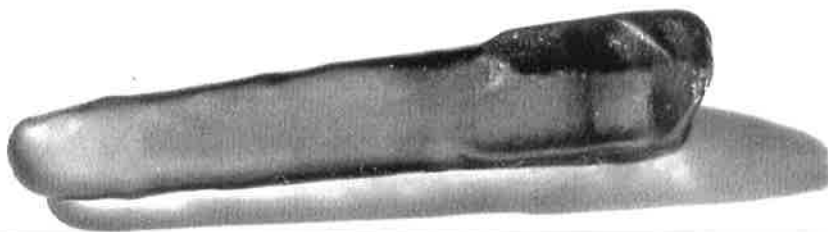


Figure 2-3. Sapphire crystal from the Central Province, N.S.W., showing a negative crystal shape in its faces. The sapphire is 20 mm in length. (Collection of T. J. Nunan, photograph by D. Barnes).

a



b



Figure 2-4. Sapphire crystal from the Central Province, N.S.W., showing uneven chemical resorption. One end of the 20mm crystal shows markedly greater chemical resorption than the other. Figure 2-5 shows a possible scenario to explain its appearance. See also Colour Plate 1. (Collection of T. J. Nunan).
(a and b are different views of the same crystal).

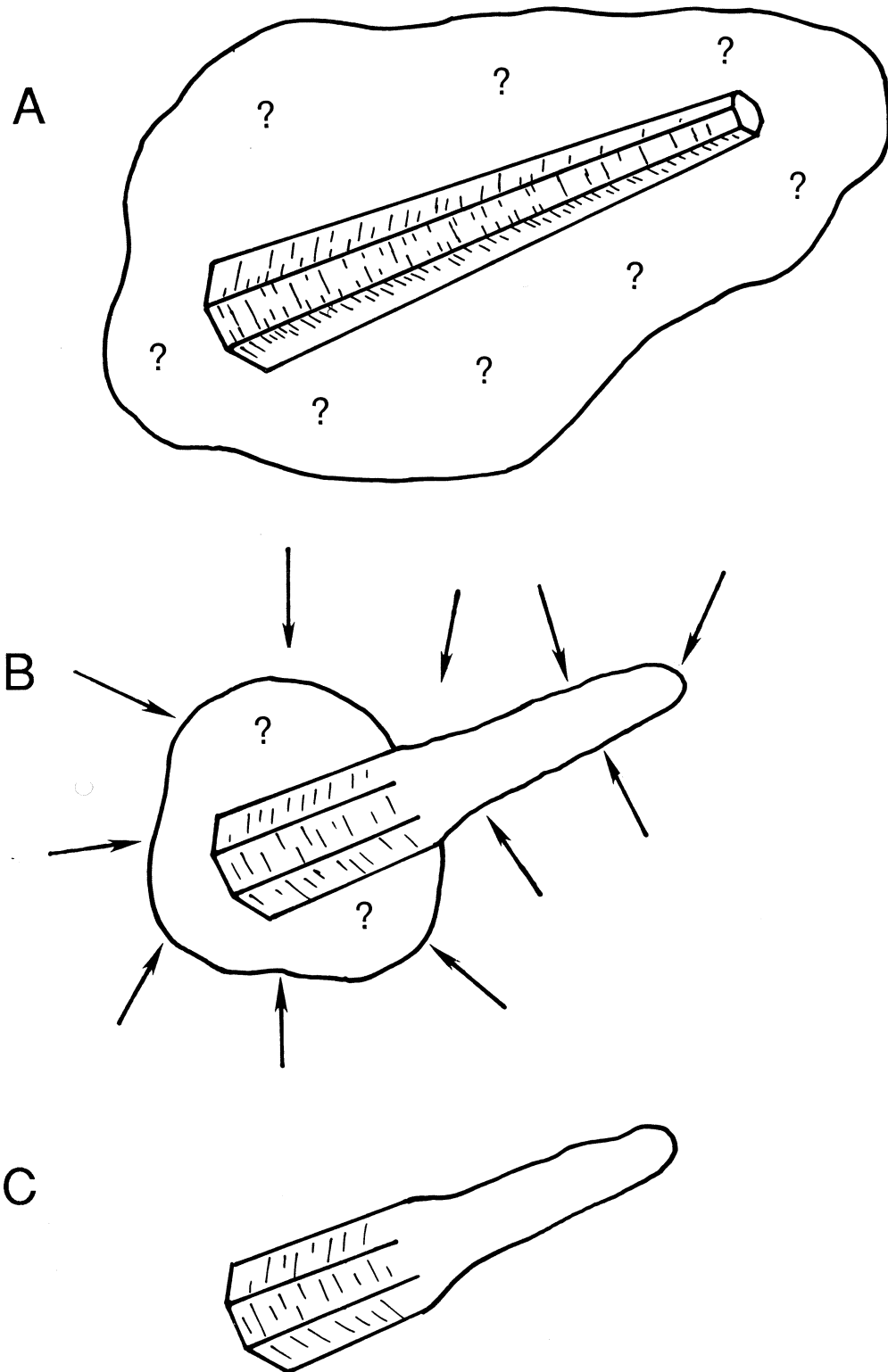


Figure 2-5. Scenario explaining uneven chemical resorption such as seen on the sapphire crystal shown in Figure 2-4.

- a) The sapphire crystal is originally intergrown with another mineral or minerals.
- b) The sapphire crystal is partially exposed. This portion of the crystal is subject to chemical corrosion due to disequilibrium with the carrier magma during its ascent to the surface. Note that alluvial abrasion cannot be evoked to explain the same scenario due to the fragility of the specimen.
- c) The sapphire crystal is liberated from its host toward the end of its journey.

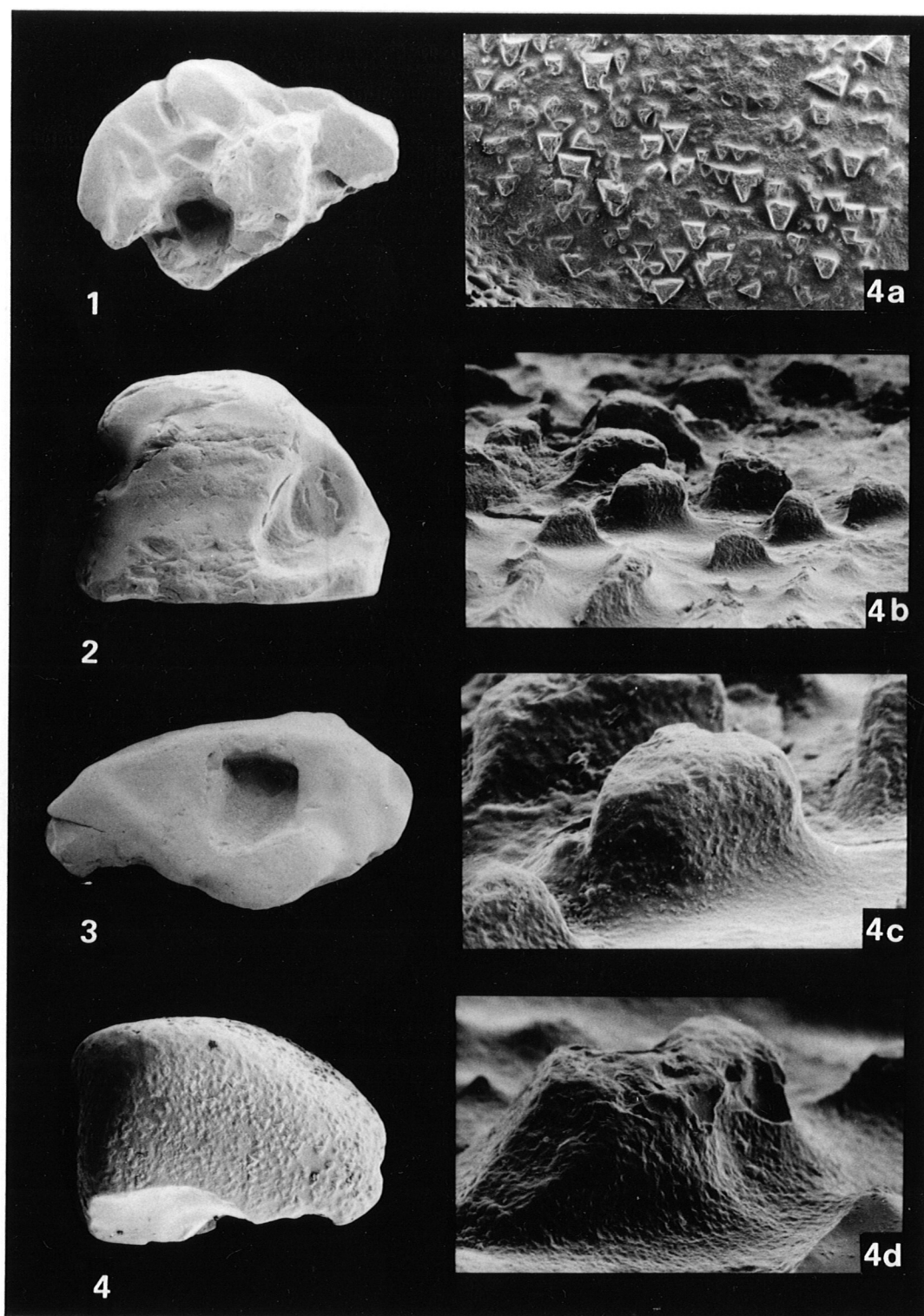


Plate 1. 1. Negative crystal socket in blue sapphire, X18. 2. Negative crystal in blue-purple sapphire, X14. 3. Negative crystal socket in purple ruby, X14, all from the Ruby Well Mine, Chanthaburi-Trat. 4. Sapphire from Reddestone Creek, No. 2 plant, New England, X25; a) detail showing flat topped triangular hillocks, X66; b) detail showing relief of hillocks and their irregular, eroded appearance, X330; c) detail of one hillock showing gradual rise from the floor into the hillock wall, X935; d) detail of one hillock showing pock marked, etched surface, note damage to top edge of the hillock due to fluvial transport, X1210.

with minerals such as anorthoclase and zircon (Coenraads et al, 1990) and spinel (Vichit, 1987).

2.4.2 Surface etch features

The above Plates, as well as Plates 1-4, 2-4a, 3-1a, 4-3a, 5-1a and 5-2a show the corundum to be sub-rounded to rounded in appearance. This rounding, although once attributed to alluvial wear, is clearly the result of resorption by magmas responsible for carrying the corundum to the surface. The grains in Plates 1-4 and 5-1a show the surface to be covered with flat topped triangular hillocks of the order of 15-20 μm which reflect the internal trigonal crystal symmetry. The only exception is where the bottom of the grain in Plate 1-4 has broken away along a conchoidal fracture surface. A further enlarged view of the sapphires' surface in Plate 1-4b shows the relief of the triangular hillocks and their irregularity in detail. They stand like sculptured "monoliths" on the surface of the sapphire, roughly equidimensional and have a relief of about 20 μm . Plates 1-4c and 1-4d show the gradual rise of the surface from the floor in between the hillocks into their walls, and the surface in detail, which is covered with sub-geometrically regular to rounded pock marks or shallow dishes about 1 μm in diameter. These features give the hillocks a distinctly eroded appearance.

The hillocks are most likely of similar origin to the pyramidal or drop shaped hillocks on rounded surfaces of diamonds (Orlov, 1977, p.93) and also reproduced in etching experiments (Patel and Agarwal, 1966).

Plates 2-1a and 2-1b show relief on a face perpendicular to the c-axis $\{0001\}$ of a sapphire crystal. The etching is variable in distinct bands. Plate 2-1b shows detail of the etching as oriented flat shallow hexagonal depressions of the order of 4-10 μm in diameter with a hexagonal shaped remnant hillock centrally positioned in each.

The probable sequence of formation of the etch features is illustrated in Plate 2-1c where all stages are present on the one crystal, and where each form merges into another across the surface. In the bottom centre of the photograph, below the large chip displaying conchoidal fracture, the surface is covered by sub-triangular to rounded hillocks described earlier. In the right of the photograph can be seen what may be the early stages of formation of such a surface. Here an originally flat surface has been etched to produce a number of hexagonal depressions, each with a centrally placed hillock. In the left of the photograph the surface has a spongy or porous appearance, probably as a result of extensive etching. Plates 2-3a and 2-3b show detail of the early stages of formation of hexagonal and triangular hillocks on a Thai ruby. Crystal terminations ranging up to 50 μm are surrounded by a moat into which the outer wall gradually slopes. In some cases preferential alignment of etching has led to the formation of ridges as seen in Plate 2-3b. The hillocks are similar in appearance to the hexagonal etch marks (of the order of 10-20 μm) seen on a Thai sapphire (Plate 2-2 and also Plate 2-1b, described above), only in this case, the outer walls of the moats are roughly sculptured as opposed to being smoothly

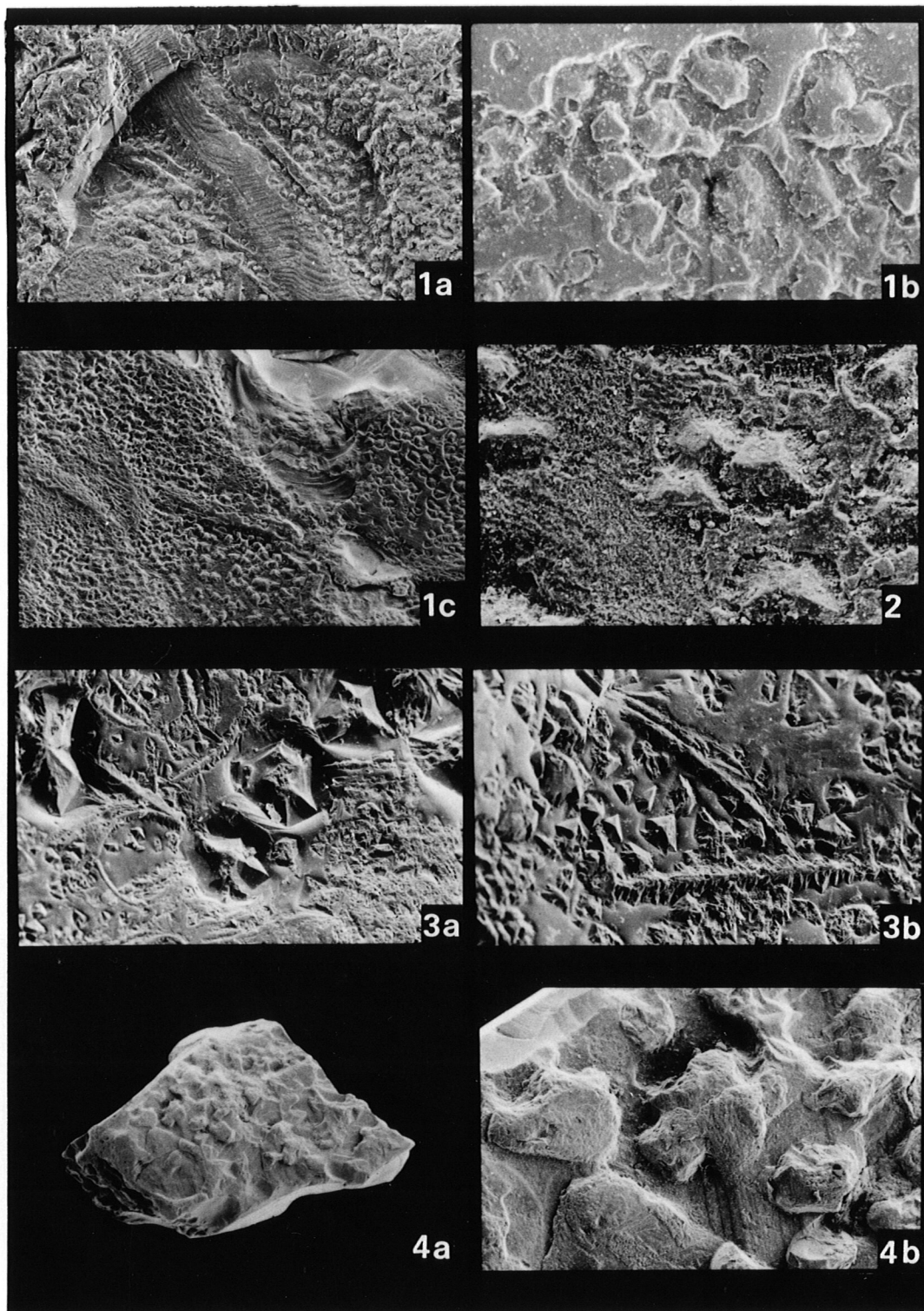


Plate 2. 1. Blue sapphire from Reddestone Creek, No. 1 plant, New England, surface perpendicular to the c-axis; a) oriented flat, shallow hexagonal etch depressions with central hillocks, X358 ; b) detail of hexagonal depressions, X2200; c) stages of formation of etch features, right-early stage of originally flat surface breaking down into etch depressions with central hillock, bottom centre-edges of depressions removed leaving only sub-triangular to rounded hillocks, left-more extensive etching gives surface a spongy appearance, X237. 2. Blue sapphire from SAP mine, Bo Ploi, hexagonal etch depressions with a central hillock, X1100. 3. Pink-purple ruby, Ruby Well mine, Chanthaburi-Trat, showing early stages of formation of triangular and hexagonal hillocks; a) X330; b) X660. 4. Deep prominent etch sculpturing on a pink-purple ruby, Ruby Well mine, Chanthaburi-Trat; a) complete specimen, X28; b) detail of etch channels, X138.

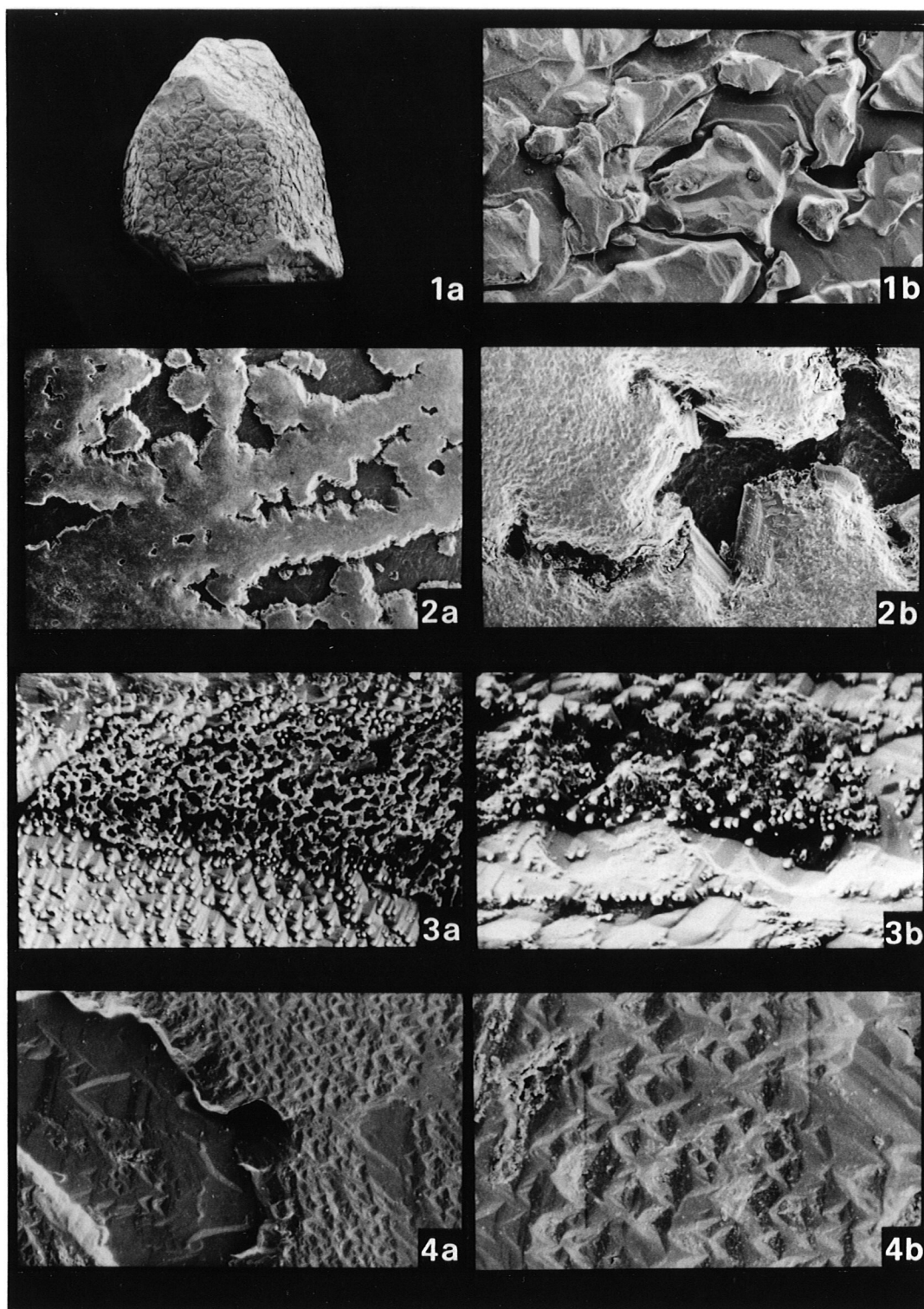


Plate 3. Blue sapphires from 1. New England gem fields; a) complete specimen, X7; b) detail of "shark-skin like" etch channels, X66. 2. SAP mine, Bo Ploi; a) "intaglio-like" surface due to extensive etching, X61; b) detail of a) showing structural control of "intaglio" pattern and microlamination due to successive layer dissolution, X440. 3. Braemar, New England; a) etch pattern resembling trigonal prismatic "stacked bricks" on a surface oriented at a low angle to the c-axis, X825; b) detail of surface, X2200. 4. Braemar, New England; a) triangular pyramidal depressions resulting from etching of a surface at an intermediate angle to the c-axis, X825; b) detail of pyramidal depressions, X2200.

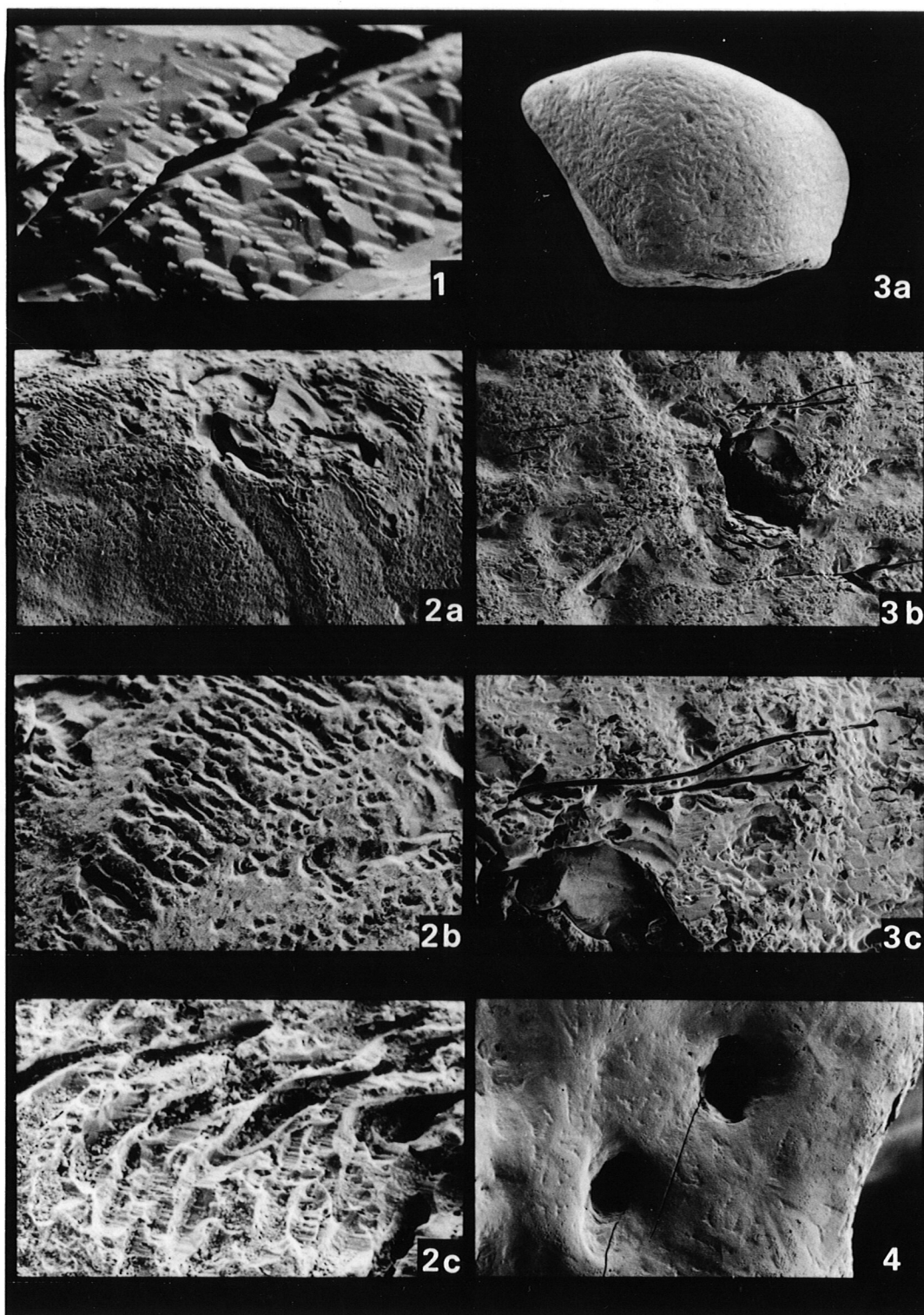


Plate 4. Blue sapphires from Braemar, New England. 1. detail of etch surface at a low angle to the c-axis resembling trigonal prismatic "bricks", X3300. 2. Chatter marks or sub-parallel curved grooves attributed to mechanical stress; a) X358; b) detail of chatter marks X1375; c) further detail, finely striated faces within chatter marks indicate that they have been enhanced by dissolution, X2365. 3. Sapphire traversed by numerous fractures; a) complete specimen, X18; b) detail of fractures, X193; c) detail of b), X495. 4. Fracture radiating from an inclusion in sapphire, X110.

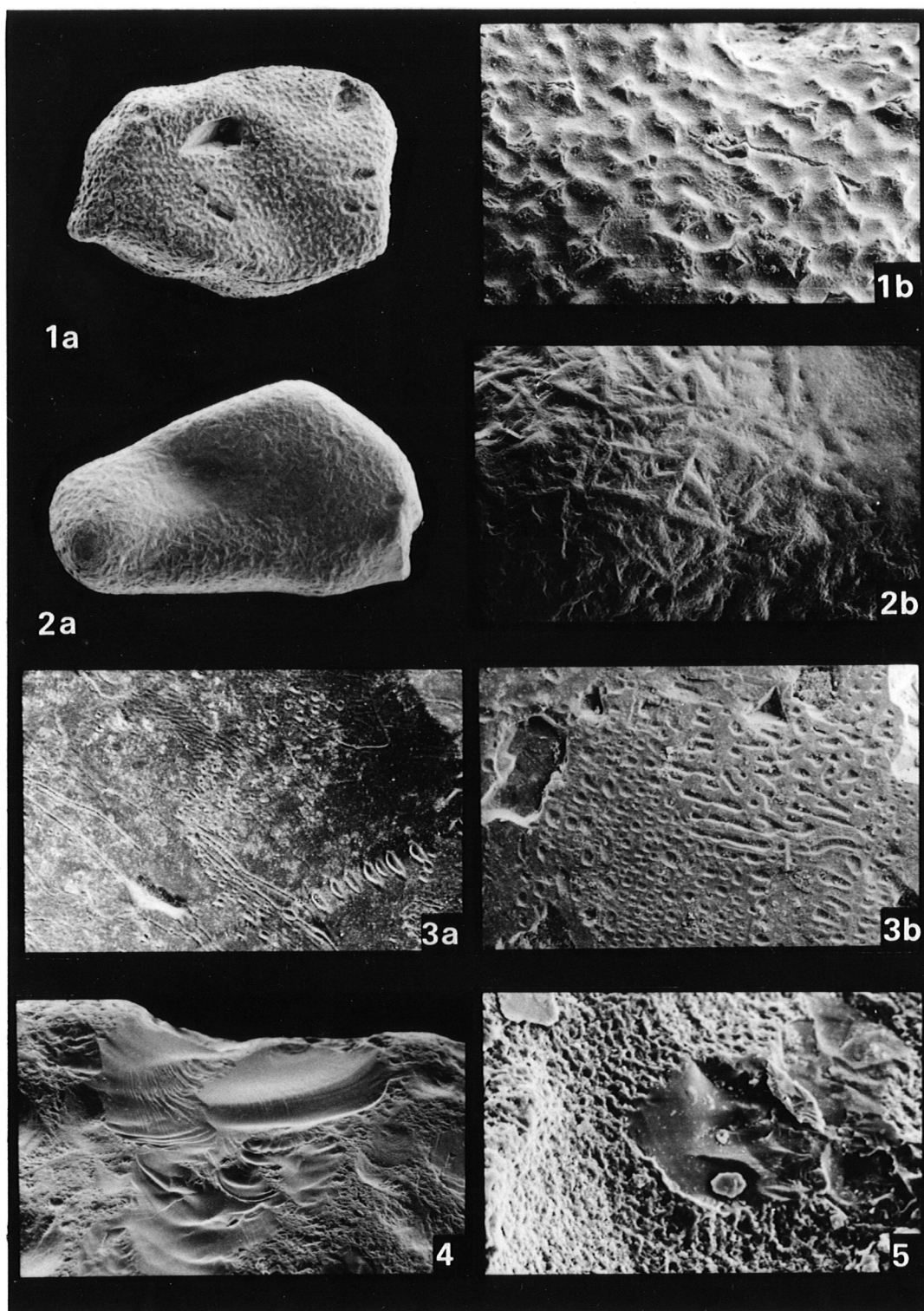


Plate 5. Blue sapphires 1. Ruby Well mine, Chanthaburi-Trat showing surface covered with triangular hillocks; a) complete specimen, X30; b) detail of triangular hillocks, some chipped due to fluvial damage, X165. 2. Reddestone Creek No. 1 plant; a) complete specimen showing a "bladed" surface texture, X24; b) detail shows crystallographic control as the raised "blades" form two sides of triangular pyramidal shaped pits, X110. 3. SAP mine, Bo Ploi. Rebroken healed fracture surfaces reveal a "fingerprint-like" pattern of exposed, formerly fluid filled, tubes; a) X440; b) X550. 4. Reddestone Creek, No. 1 plant, New England. Conchoidal fracturing on the edge of this sapphire is evidence of damage in the fluvial environment, X138. 5. Ruby Well mine, Chanthaburi-Trat. Protruding hillock broken off at its base leaving a clean fracture surface is evidence of damage in the fluvial environment, X2200.

sloping. The reason for the development of a crystal termination centrally within an etch pit is not clear, although it could be a response by the crystal to minimize its surface free energy when it was in contact with the hostile carrier magma.

As the dissolution process proceeds, etch features appear to grow and interfere with one another producing deep and prominent sculpturing ("shark skin" appearance) such as seen on the surface of the Thai ruby (Plates 2-4a and 2-4b) and Australian sapphire (Plates 3-1a and 3-1b). Orlov (1977, p.98) found similar features on the octahedral faces of diamond resulting from continued dissolution which caused the etch trigons to grow larger and crowd in on one another. Such extensive dissolution also seems to have been responsible for the "intaglio-like" surface produced on the sapphire in Plate 3-2a. The outer surface has been removed in places to a depth of about 15 μm , to a lower level which appears to be more resistant and only lightly etched. Detail in Plate 3-2b reveals a fine microlamination which has been emphasised by the dissolution as a series of steps of the order of 1 μm in size. Such microlamination is also observed in diamond (Orlov, 1977, p.87) and has been attributed to successive layer dissolution.

On surfaces which appear to be at a lower angle to the c-axis of the corundum crystal (see Plates 3-3a, 3-3b and 4-1), the etch patterns are quite different, and resemble inclined stacks of elongated, triangular shaped bricks. These structures clearly reflect the internal crystal structure of the corundum. Plate 3-3a shows two surfaces; in the lower part of the photograph, a surface roughly parallel to the c-axis displays triangular prisms whilst in the upper part of the photograph a surface perpendicular to the c-axis, partially covered by lichen, shows typical triangular hillocks described earlier. Plate 3-4a and the detail in Plate 3-4b, show triangular depressions of the order of 1-2 μm across, with the depression walls forming a negative triangular pyramid. Such features appear to be the result of etching on a surface at an intermediate angle to the c-axis.

The surface features of most grains studied, even those with an apparently random "blade-like" texture such as seen in Plate 5-2a, could be ultimately explained in terms of surface etching. Under magnification (Plate 5-2b), a crystallographic control of the features is revealed. In Plate 5-2b the raised "blades" are seen to form the sides of triangular shaped pits.

Chatter marks are occasionally present and are shown in Plates 4-2a, 4-2b and 4-2c. These features are attributed to some form of mechanical stress leading to the formation of a series of parallel or curved marks on the surface of the grain. Detail in Plate 4-2c shows that the marks may be of 1-2 μm in width and as deep or deeper. The finely striated faces within the curved chatter mark grooves show a pattern, not unlike that described in Plates 3-3a, 3-3b and 4-1. This suggests that the grooves have been enhanced by dissolution and implies that the corundum displaying chatter marks has been subject to stresses prior to, or possibly during transport to the surface.

2.4.3 Healed fracture surfaces and damage resulting from transport in an alluvial environment

Plates 4-3a, 4-3b and 4-3c show narrow (1-2 μm) but deep fractures which traverse the stone irregularly or in a semi-oriented manner. These start and end abruptly and probably represent healed or partially healed stress fractures. They are described by Orlov (1977, p.53) as planar dislocation growth defects originating from a defect centre such as an impurity or inclusion in the interior of the crystal and radiating to the faces. Such may be the case in Plate 4-4. It is logical that such planes of weakness would be likely sites for breakage in the alluvial environment. Plates 5-3a and 5-3b show such rebroken healed fracture surfaces revealing a "fingerprint-like" pattern of tubes of about 1-2 μm in size. Such fingerprints are commonly photographed within gem rubies and sapphires using light microscopes (Gübelin and Koivula, 1986, p.340).

Damage in the alluvial environment results from impact during transport. This is seen as conchoidal fracturing particularly around the more exposed edges of crystals as shown in Plate 5-4, or as chipping on protruding hillocks (Plates 1-4d and 5-1b). In Plate 5-5, an impact has completely broken off a protruding hillock leaving a smooth fracture surface.

2.4.4 Discussion

Surface features on rubies and sapphires from volcanic provinces may give an insight into the history of such crystals from the time of their growth to their eventual recovery by mining.

1. Negative crystal impressions suggest that the corundum grew as part of coarsely crystallized aggregates together with minerals such as anorthoclase, zircon and spinel.
2. Surface resorption or etching and layer dissolution features clearly result from reaction with the magmas responsible for carrying the corundum to the surface. These features include, triangular and hexagonal hillocks and depressions on faces perpendicular to the c-axis, and stacks of triangular prisms on surfaces parallel to the c-axis of the corundum crystal. Chatter marks imply that the corundum has been subject to stresses prior to, or possibly during transport to the surface.
3. Surface damage including impact marks displaying conchoidal fracture, broken off protrusions and exposed healed fracture surfaces indicate the degree of reworking in the alluvial environment. The grain surface features generally indicate a minimal amount damage due to fluvial transport. This observation, when considered in conjunction with the spatial variability in the physical characteristics of corundum in a given placer deposit

(Coenraads, 1990), indicates minimal degree of downstream reworking and mixing, and suggests that the corundum sources are local to the placer deposits.

2.5 Inclusions in sapphires and zircons from the Central Volcanic Province

Inclusions may shed light on the origin of sapphires and zircons. However, in order to do so the inclusions must be syngenetic, that is, they must have grown contemporaneously under the same pressure-temperature conditions and compositional regime as their host. Gübelin and Koivula (1986) defined criteria for inclusions to be identified as syngenetic with their host. They noted that inclusions should be euhedral and unbroken, and show no evidence of surface etching, corrosion or oxidation which would indicate an earlier period of crystallization or derivation from the wall rocks. Inclusions should also be independent from any cracks, fractures or epigenetic (later) mineralisation within the host. Trapped melt droplets are another type of inclusion perhaps capable of more directly revealing the environment in which sapphires and zircons grew. These will have smooth surface and spherical to highly irregular shapes. Contraction bubbles may be visible where inclusions are sufficiently transparent and light in colour.

Samples of sapphire and zircon from the Central Volcanic Province were examined in a high-refractive index medium (glycerine) using a binocular microscope. Those found to contain inclusions were mounted in resin disks, ground down to the inclusion level, polished and photographed. Inclusions which had been exposed by this process were analysed using an electron microprobe and their identities deduced. Compositional ranges determined for the inclusions are listed in Tables 2-2 and 2-3.

Inclusions identified in New England sapphires during this study include zircon, hercynite, gahnspinel, columbite, niobium-rutile, ilmenite, thorite, alkali feldspar, plagioclase, pyrrhotite, pyrrhotite-pentlandite intergrowth, and iron-rich melt inclusions (see Table 2-2). Uranium pyrochlore (Gübelin and Koivula, 1986), hornblende and mica (Coldham, 1985) have also been found in Australian sapphires.

Inclusions identified in New England zircons during this study include zircon, zirconia?, ilmenite, alkali feldspar and iron-rich melt inclusions (see Table 2-3).

2.5.1 Discussion of inclusion compositional ranges

Alkali feldspar inclusion compositions are plotted on the ternary diagram shown in Fig. 2-6. Compositional ranges are essentially the same for both sapphires (circles) and zircons (triangles). Of the 10 inclusions analysed, two were large enough to show compositional variation, one inclusion (19/19-1; No. 5 on Fig. 2-6) in zircon and the other in sapphire (5/10; No. 1 on Fig. 2-6). Backscatter photographs of the inclusion in sapphire (Figure 2-7) show an irregular shaped core of alkali feldspar mantled by plagioclase. The boundary between the zones is sharp and non conformable with the outer euhedral crystal faces. The plagioclase appears to be a later overgrowth.

Table 2-2. Inclusion suite for Central Volcanic Province Sapphires.

wt% oxide	Herzynite	Gahnspinel	Columbite	Nb-rutile rutile solid soln.	Ilmenite/ rutile solid soln.	Thortite	Melt inclusions 1	Melt inclusions 2	Alkali feldspar	Plagioclase	wt% element	Pyrrhotite	Pyrrpentlandite
SiO ₂	0.0-0.09	0.0-0.17	0.0	0.0-0.07	0.70-2.19	14.15	0.76-5.65	22.16-33.8	61.94-65.65	52.56-54.81	Si	0.01-0.17	0.00
TiO ₂	0.13-1.05	0.0-0.26	0.82-10.88	46.20-48.98	59.05-63.07	0.0	0.02-0.95	0.0-0.48	0.0-0.04	0.0	Ti	0.0-0.03	0.01
Al ₂ O ₃	47.76-58.11	56.20-59.55	0.06-1.16	1.16-3.65	0.45-2.70	0.40	4.72-13.71	20.39-30.55	19.36-23.71	28.85-29.81	Al	0.38-0.48	0.03
Cr ₂ O ₃	0.0	0.0	0.0	0.0-0.06	0.0-1.06	0.0	0.0-2.18	0.0-0.52	0.0	0.0	Cr	0.0	0.00
FeO total	30.39-55.57	24.50-28.63	13.16-17.44	9.75-11.90	22.5-32.05	0.47	60.73-76.00	17.82-43.54	0.0-0.26	0.0-0.09	Fe	55.91-58.57	42.81
MnO	0.49-0.85	0.60-0.84	2.19-4.31	0.07-0.36	0.23-0.41	0.0	0.0-0.24	0.0	0.0-0.25	0.0-0.25	Mn	0.0-0.01	0.00
MgO	0.08-6.09	0.18-2.14	0.40-0.97	0.08-0.13	0.69-0.97	0.0	0.03-0.31	0.05-0.42	0.0-0.03	0.0	Mg	0.0-0.01	0.02
NiO	0.0	0.0	0.0-0.05	0.0	0.0	0.0	0.0	0.0	0.0	0.0	Ni	0.72-1.15	17.46
ZnO	0.0-0.01	10.62-16.36	0.0	0.0-0.21	0.0	0.0	0.0	0.0	0.0	0.0	Zn	0.0	0.00
CaO	0.0-0.13	0.0	0.0-0.09	0.0	0.0-0.38	0.0	0.01-0.49	0.07-0.20	0.0-0.59	10.45-11.19	Ca	0.0-0.38	0.01
Na ₂ O	0.0	0.0-0.12	0.0	0.0	0.0-0.03	0.09	0.0-0.09	0.0	1.61-6.10	5.15-5.78	Na	0.0-0.01	0.00
K ₂ O	0.0-0.06	0.0-0.06	0.0-0.05	0.0-0.05	0.0-0.05	0.0	0.0-0.07	0.04-0.16	2.76-9.7	0.48-0.78	K	0.0-0.01	0.01
ZrO ₂	0.0	0.0	0.0-3.97	1.88	0.0	1.3	0.0-0.28	0.0	-	-	Zr	-	-
ThO	-	-	-	-	-	87.87	-	-	-	-	Th	-	-
Nb ₂ O ₅	-	-	63.58-77.39	-	0.0-1.41	-	-	-	-	-	S	36.92	39.64*
Ta ₂ O ₅	-	-	1.68-4.69	-	0.0	-	-	-	-	-			
No. inclusions	7	17	10	3	2	1	11	6	4	1		3	1

Table 2-3. Inclusion suite for Central Volcanic Province Zircon.

wt% oxide	Zirconia	Ilmenite/ rutile solid soln	Melt inclusion 1	Melt inclusion 2	alkali feldspar	No. inclusions
SiO ₂	0.48	3.01-7.73	1.17-2.16	6.94-37.73	55.01-68.17	1
TiO ₂	11.73	48.00-72.16	0.0-0.78	0.0-2.28	0.0-0.19	4
Al ₂ O ₃	0.33	2.81-5.08	0.46-9.64	8.74-28.52	20.09-23.62	6
Cr ₂ O ₃	0.16	0.47-1.00	0.0-1.41	0.18-0.92	0.0-0.11	11
FeO total	1.64	16.41-28.92	60.61-68.70	11.97-52.50	0.04-3.80	
MnO	0.01	0.0-0.08	0.0-0.05	0.0-0.19	0.0-0.22	
MgO	0.0	0.16-0.72	0.03-0.15	0.0-0.51	0.0-0.50	
NiO	0.0	0.0	0.0	0.0	-	
ZnO	0.0	0.0	0.0	0.0	-	
CaO	0.07	0.28-0.53	0.0-0.11	0.06-1.26	0.0-1.76	
Na ₂ O	0.0	0.0-0.18	0.0	0.0-0.37	0.99-11.92	
K ₂ O	0.05	0.03-0.08	0.0-0.01	0.0-0.13	0.73-3.12	
ZrO ₂	84.62	0.64-1.00	0.0	0.0-1.34	0.49-3.40	
No. inclusions	1	4	6	11	6	

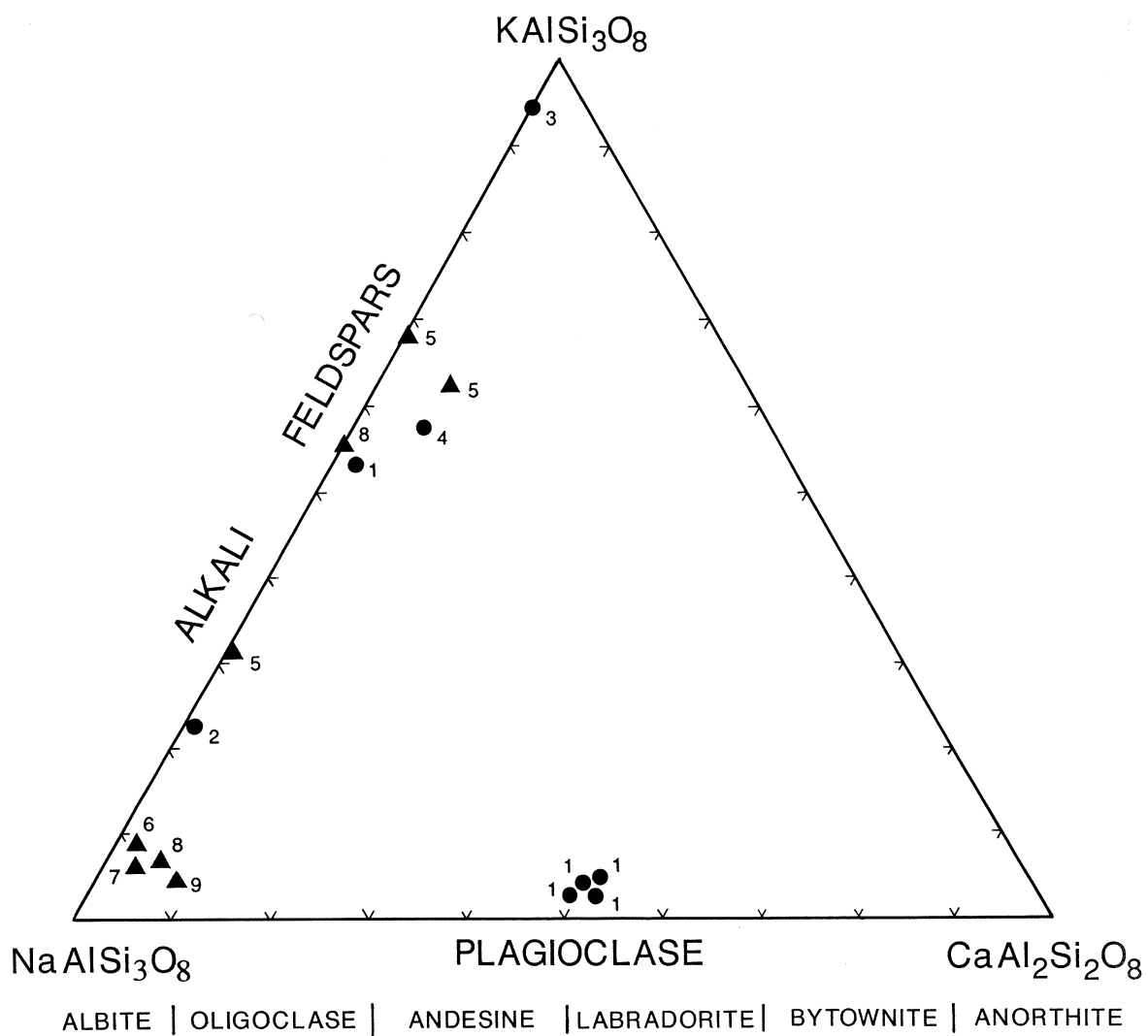


Figure 2-6. Compositional ranges of feldspar inclusions in sapphires (circles) and zircons (triangles) from the Central Volcanic Province. The compositional ranges show extensive overlap.

Spinel inclusions in sapphire plot in two distinct fields within the magnetite and ilvospinel prisms shown in Figure 2-8:

a) Hercynite group (circles):- Inclusions in this group extend from the hercynite field towards the pleonaste field. There is no Cr_2O_3 or ZnO present and MgO is low (0.1-6%).

b) Gahnospinel group (squares):- Inclusions form a tight group and are richer in ZnO (10-16%) and Al_2O_3 and poorer in FeO (24-28%) and MgO (0.1-2%) than the hercynites.

The compositional fields for the inclusion spinels do not overlap those for the spinels and magnetites associated with sapphires in alluvial heavy mineral concentrates (compare Table 2-2 with Table 5-2; and Fig. 2-8 with Fig. 5-1).

Ilmenites included in both sapphire and zircon also have low MgO content (<1%, Tables 2-2 & 2-3) compared to those found in the heavy mineral concentrates (Table 5-2 and Fig 5-5).

Common in both sapphire and zircon are opaque to brownish-red, translucent, subequant to amoeboid shaped inclusions. These may neck down into thin tubes or dumbbell shapes with no apparent relationship to the crystallographic structure of the host. These are interpreted to be primary melt inclusions. They are soft, do not polish well, and give low totals (70-85 weight %). They are composed predominantly of iron (60-75% FeO in sapphire; 45-70% FeO in zircon, melt inclusions 1, Tables 2-2 & 2-3), or a mixture of FeO , Al_2O_3 and SiO_2 (melt inclusions 2, Tables 2-2 & 2-3)

Spinel, niobite and melt inclusions were found in sufficient numbers to permit arbitrary arrangement into listings of oxides, in ascending or descending order for a given oxide. The following relationship between major and minor oxides for respective minerals are apparent:

a) Hercynite (Fig. 2-9):- Increasing FeO (total) corresponds to decreasing Al_2O_3 and weakly increasing TiO_2 .

b) Gahnospinel (Fig.2-9):- Increasing FeO (total) corresponds to decreasing ZnO and increasing MgO .

c) Columbite and niobium-rutile (Fig. 2-10):- Inclusions appear to form two distinct groups on this figure although this observation is based on only 13 inclusions.

d) Melt inclusions (Fig 2-11):- Increasing FeO (total) corresponds to decreasing Al_2O_3 , decreasing SiO_2 and, for those included in zircon, decreasing CaO and increasing Na_2O .

This diagram suggests that with more analyses a continuum may exist between the two melt inclusion groups. It is proposed that these melt inclusions should be re-analysed using a high resolution analysis technique, but this task was beyond the scope of the present study.

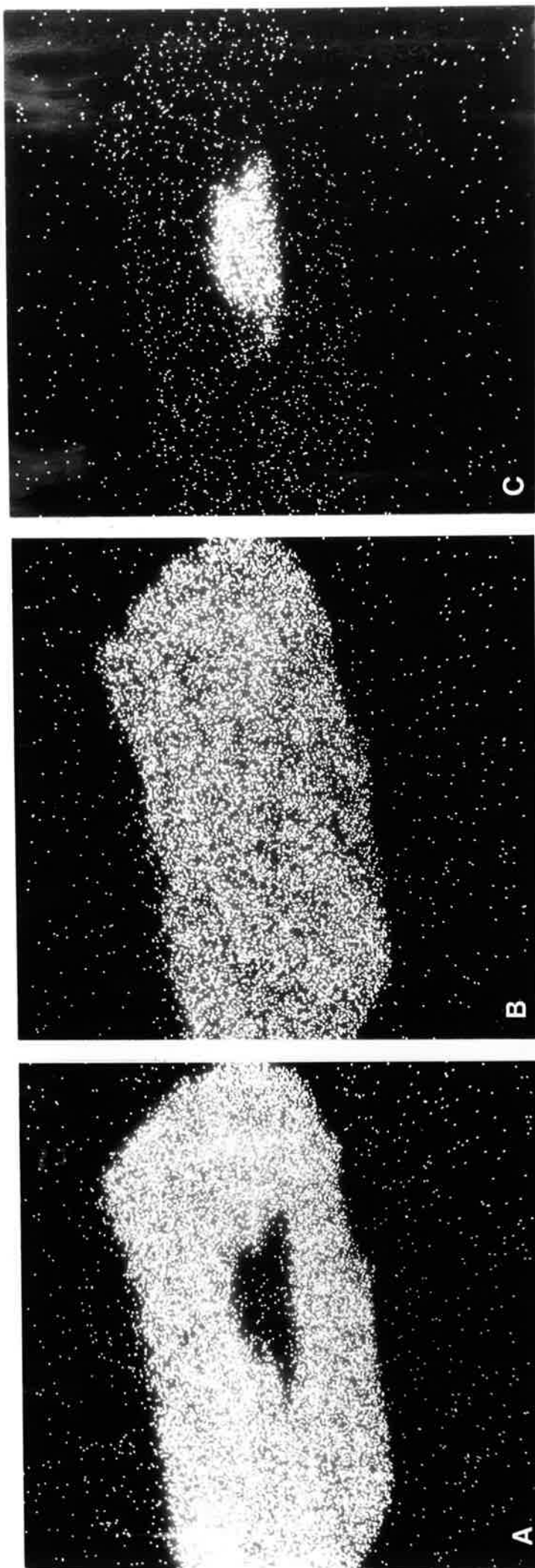


Figure 2-7. Backscatter photographs of a euhedral feldspar inclusion in a sapphire from Braemar (5/10); a) Ca distribution; b) Na distribution; c) K distribution; magnification 200X. The inclusion is Ca-rich with a distinct but irregularly shaped K-rich core. Na distribution is uniform. The composition change from core to rim is abrupt.

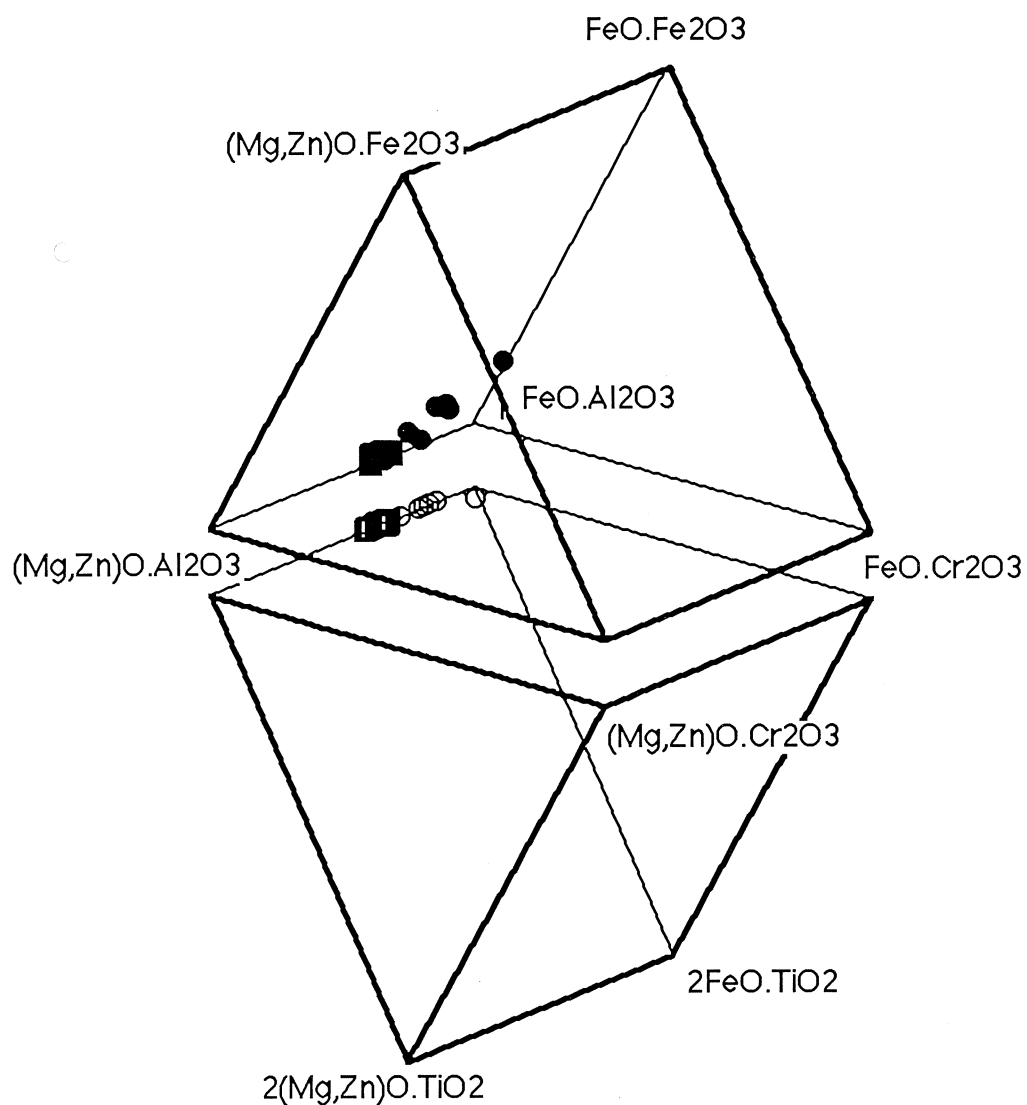


Figure 2-8. Spinel inclusions in New England sapphires. Two distinct fields, hercynite (circles) and gahnospinel (squares), are visible within the spinel family prisms (computer program courtesy of K.L.Williams, Department of Geology and Geophysics, University of Sydney).

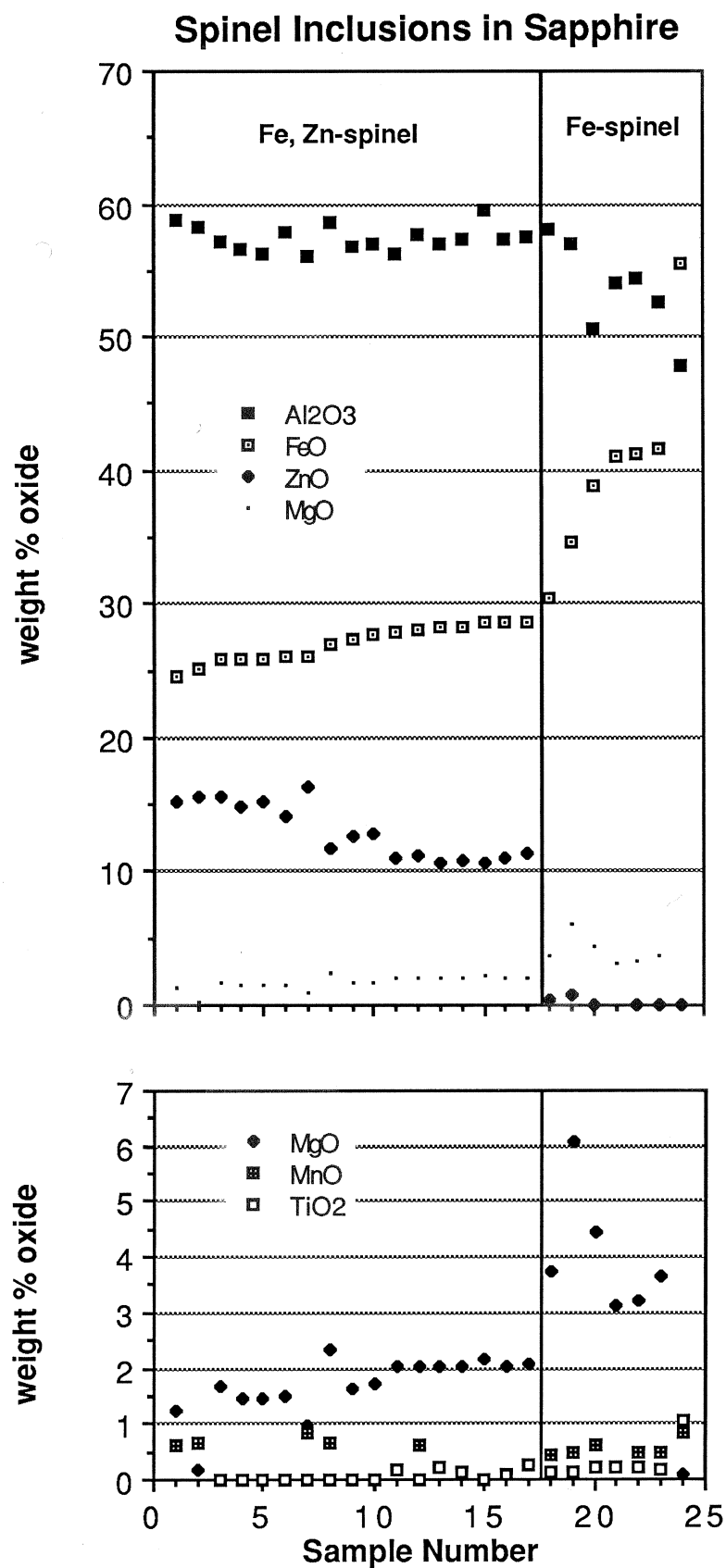


Figure 2-9. Gahnospinel (sample nos. 1-17) and hercynite (nos. 18-24) inclusions in sapphire from the Central Volcanic Province. Compositions are arranged in ascending order of percentage FeO .

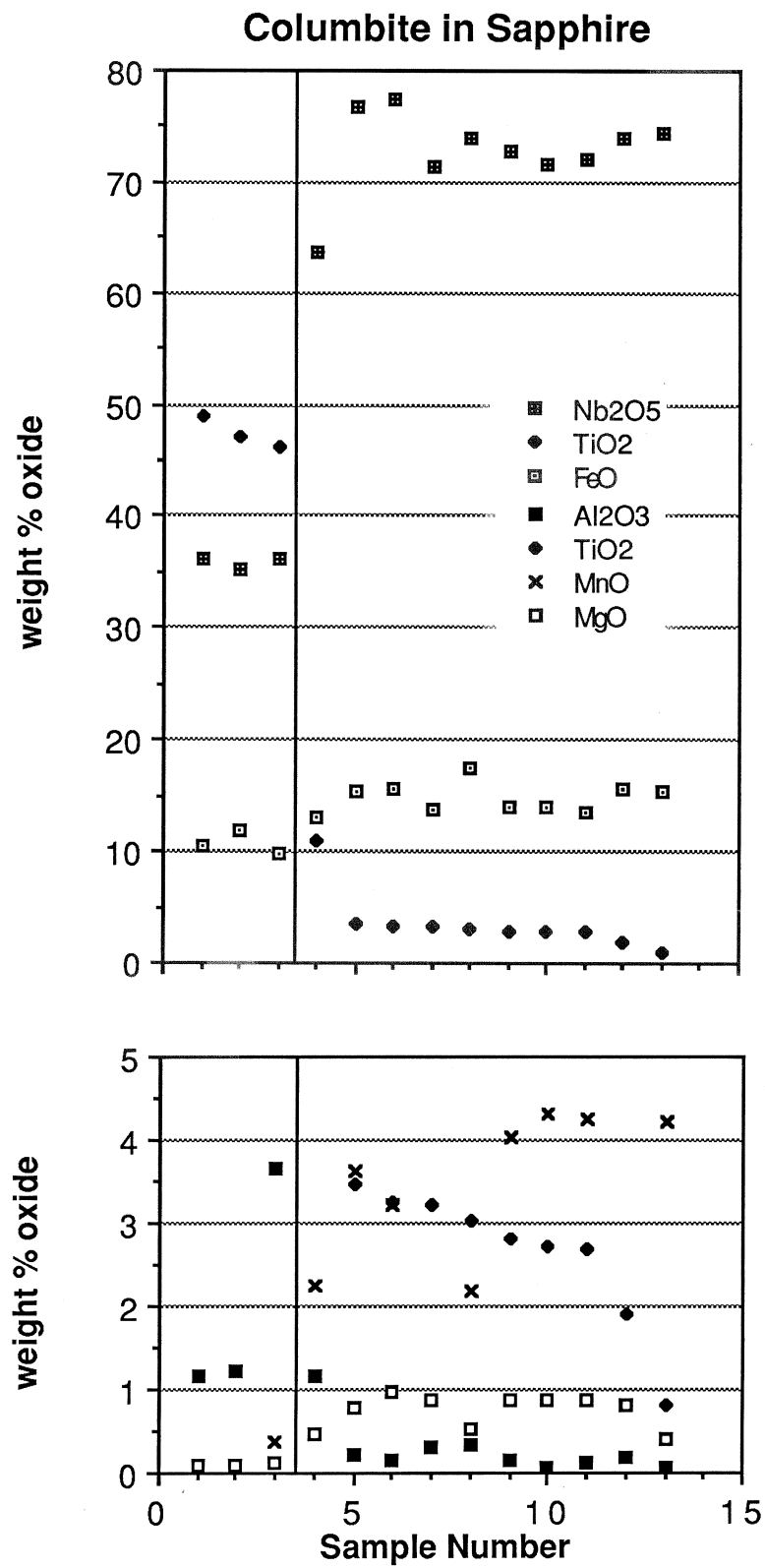


Figure 2-10. Niobium-rutile (sample nos. 1-3) and columbite (nos. 4-13) inclusions in sapphire from the Central Volcanic Province. Compositions are arranged in descending order of percentage TiO₂.

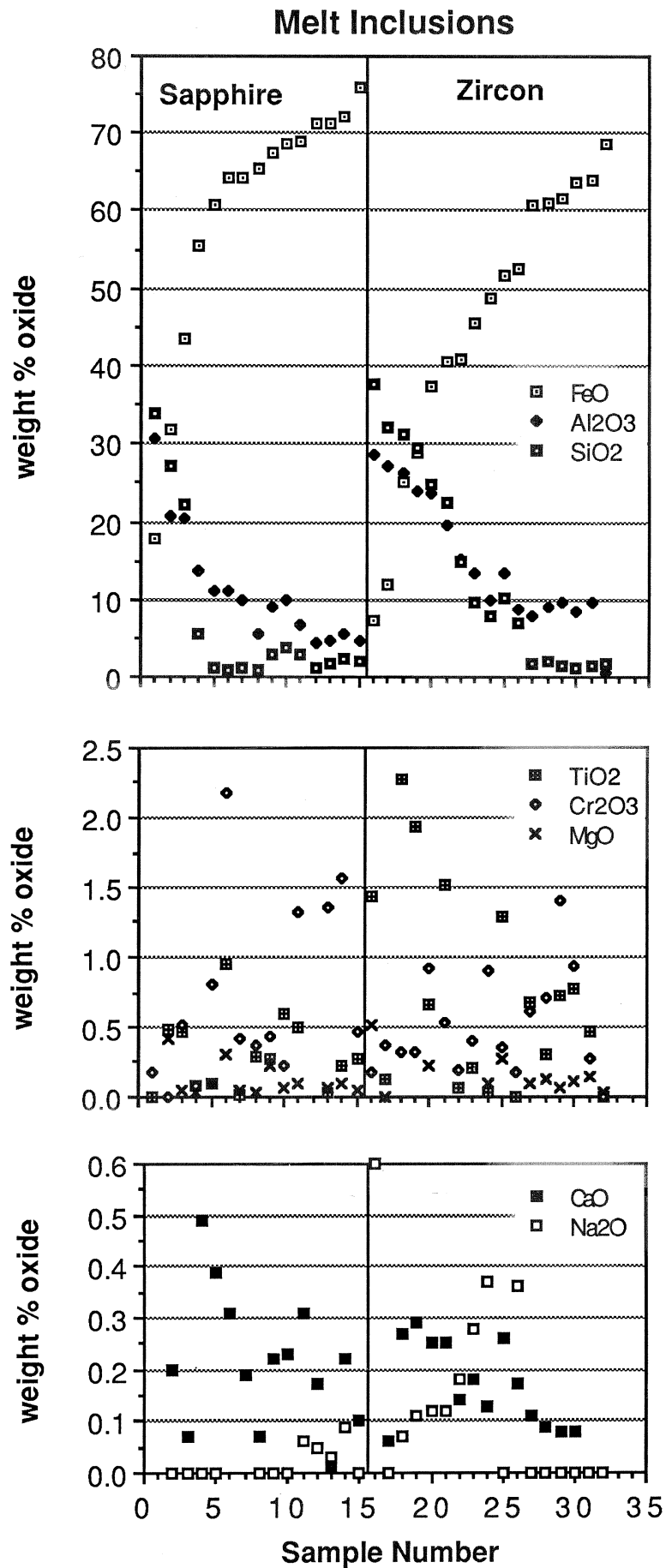


Figure 2-11. Melt inclusions in sapphire (nos. 1-15) and zircon (18-24) from the Central Volcanic Province. Compositions are arranged in ascending order of percentage FeO.

2.5.2 Conclusions

1. Syngenetic inclusions such as zircon, uranium pyrochlore, thorite, columbite, alkali feldspar and gahnospinel (Gübelin and Koivula, 1986; Coenraads et al, 1990.) as well as abundant carbon dioxide filled fluid inclusions (R. Wilkins, pers. comm. 1989) indicate that the sapphires must have grown in an environment rich in incompatible elements (eg. U, Th, Nb, Ta, Zr), alkalis (Na, K) and volatiles. Abundant iron rich melt inclusions and crystal inclusions of iron-spinel and iron -sulphides indicate a parent melt rich in iron and poor in silica and magnesium.
2. Compositional ranges for melt inclusions in sapphire and zircon show extensive overlap. This, coupled with the similarity between other common inclusions (alkali feldspar, ilmenite and zircon), suggests that sapphire and zircon grew under similar, if not identical pressure-temperature conditions and compositional regimes.
3. Inclusion minerals such as alkali feldspar, iron-spinel and zircon are also represented in rare xenoliths; thus all of these minerals appear to have formed cogenetically from an exotic melt enriched in incompatible elements.
4. Compositional ranges for the inclusion spinels and ilmenites are distinct from those similar mineral species encountered in the sapphire and zircon bearing alluvial concentrates. This implies that the sapphires and zircons, together with their exotic inclusion suite, formed prior to the crystallisation of the abundant spinels and ilmenites (comparatively richer in MgO) that occur as xenocrysts in the Central Province volcanic rocks.

2.6 U-Pb dating of the zircon inclusions in Central Volcanic Province sapphires

2.6.1 Introduction

Four small, transparent, euhedral zircon inclusions were identified during 1988 using the electron microprobe at Macquarie University. They are shown in Figure 2-12, and Colour Plate 4.

Zircons contain trace amounts of U isotopes taken into the lattice at the time of crystallization. By measuring the amount of breakdown to daughter Pb isotopes and knowing the rates at which this occurs, the zircons can be dated. It is clear that such inclusions are extremely valuable as a means of providing the age of formation of the host sapphires. However, it is only recently that U-Pb dating of such samples has become possible with the development of the Sensitive High Mass Resolution Ion MicroProbe (SHRIMP) at the Australian National University, which permits *in situ* isotopic analysis on a microscopic scale.

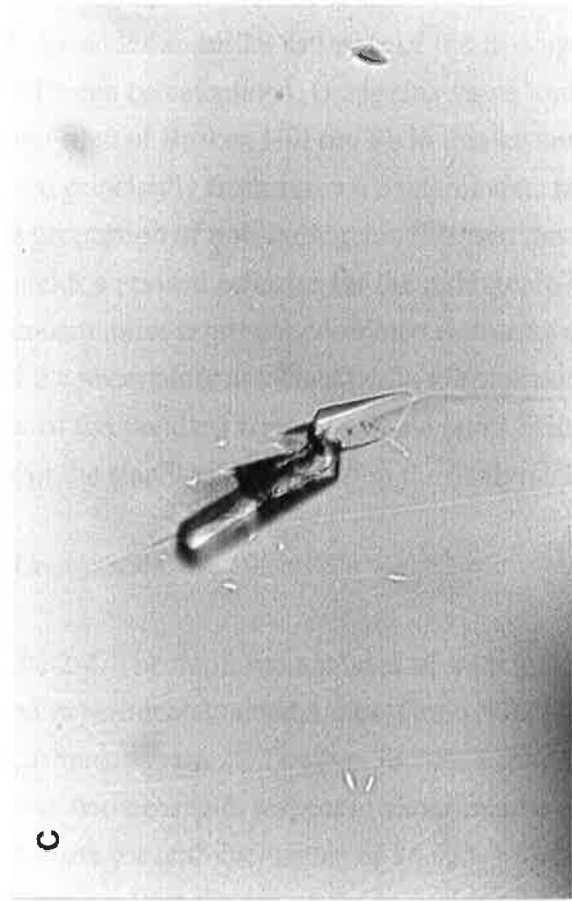
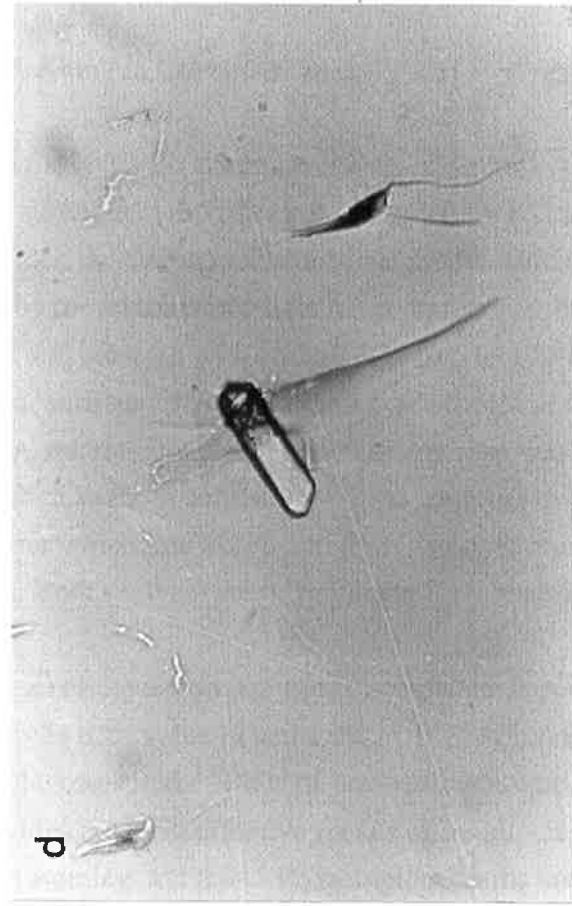
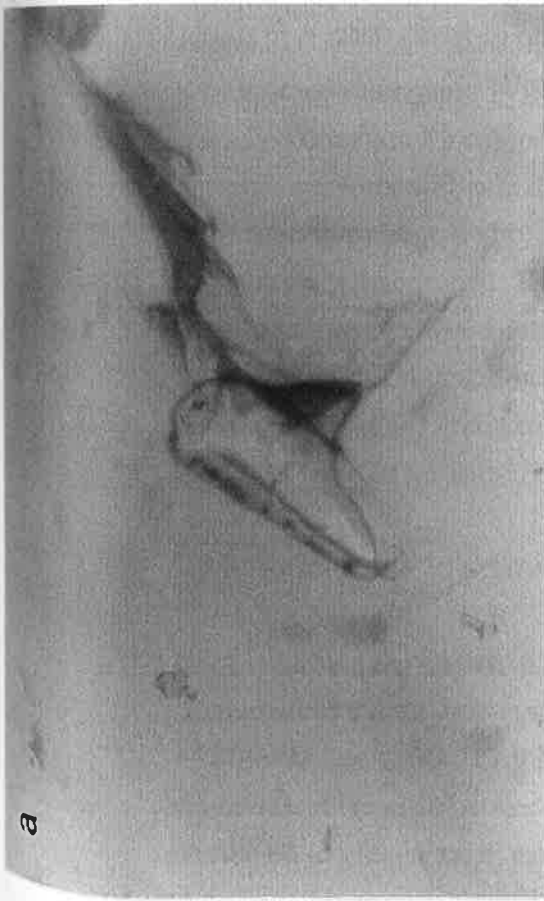
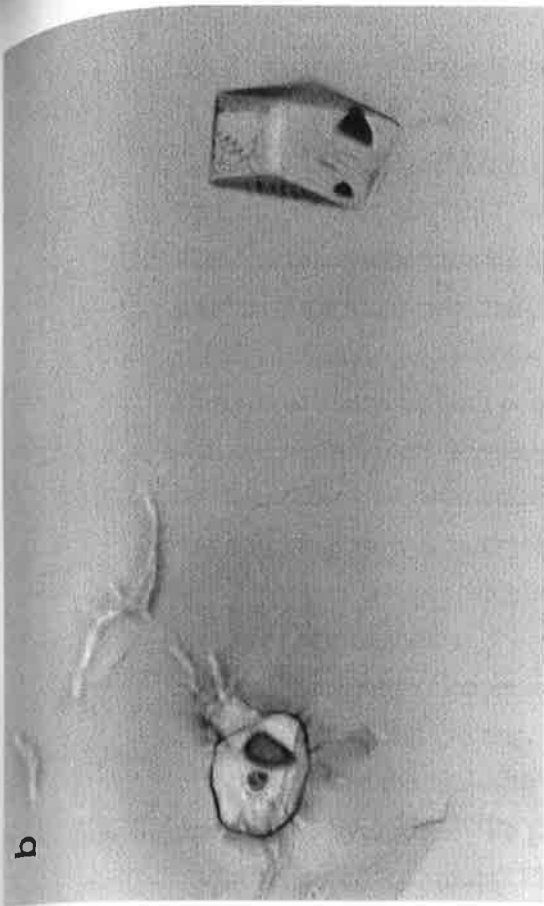


Figure 2-12. Euhedral zircon crystals included in sapphire, transmitted light photomicrographs. The base of each photo is 0.22mm. a) Inclusion 30/26 panned from the Yarrow River, GR:908887, Glen Innes 1:100,000 sheet. b) Inclusion 28/11 from alluvium obtained during test drilling of Dunvegan Lagoon by T.J. & P.V. Nunan Pty Ltd, GR:728212, Glen Innes 1:100,000 sheet. The inclusion on the right is the dated zircon, the inclusion on the left is a thorium silicate containing 60% ThO₂. Note the dark halo around this inclusion presumably due to radiation damage of the host sapphire (see also Colour Plate 4). c) Inclusion 13/1 obtained by the mining operation of T.J. & P.V. Nunan Pty Ltd. Locality unknown, either Kings Plains Creek or Reddestone Creek. d) Inclusion 13/2, another inclusion in the same host as 13/1.

2.6.2 Analytical methods (by P. Kinny in Coenraads et al, 1990)

The SHRIMP technique for U-Th-Pb isotopic analysis of zircons was first described by Compston *et al.* (1984) with subsequent modifications outlined by Kinny *et al.* (1988). The electron probe mounts in which the zircon inclusions in sapphire were identified, were modified for ion probe analysis by the addition of a hole to accommodate the laboratory standard zircon, then repolished and recoated with carbon. The two largest inclusions were chosen for analysis, both being of sufficient size to accommodate the 25 μm analytical spot without overlap onto the sapphire matrix (Fig. 2-13) which in any case was found to contain no detectable lead or uranium. Each analysis consisted of three counting cycles of the Pb, Th, and U species of interest, after which raw Pb/Pb and Pb/U isotopic ratios, and total U and Th contents were calculated. Both analyses were "duplicated" by resumed excavation of the same sputter-holes.

The young (Cenozoic) ages of the zircon inclusions necessitated special treatment of the data. For young zircons, there is little value in using the $^{207}\text{Pb}/^{206}\text{Pb}$ ratio as a measure of age, because the majority of the measured ^{207}Pb is of non-radiogenic origin. For this reason, however, the ^{207}Pb provides the most effective means of monitoring the contribution of "common" Pb. Assuming that the U-Pb isotopic systems are concordant and undisturbed, the measured $^{206}\text{Pb}/^{238}\text{U}$ ratio, normalised to that of the laboratory standard zircon SL3 ($^{206}\text{Pb}/^{238}\text{U}=0.0928$), provides an initial estimate of the true age, from which the expected radiogenic $^{207}\text{Pb}/^{206}\text{Pb}$ can be calculated. Using this value together with a modelled common Pb composition (that of Broken Hill ore Pb in this instance, because the detectable common Pb was derived principally from surface contaminants rather than intrinsic non-radiogenic Pb), the proportion of non-radiogenic ^{206}Pb in the total ^{206}Pb can be accurately determined. This yields a revised estimate for the radiogenic $^{206}\text{Pb}/^{238}\text{U}$, and a corresponding age. The quoted uncertainties represent combined estimates of the errors associated with ion-counting and the uncertainty associated with normalization of the measured $^{206}\text{Pb}/^{238}\text{U}$ ratio to that of the standard zircon SL3, the latter being based upon the reproducibility of measurements of the standard zircon during the analytical session.

2.6.3 Results

Results are shown in Table 2-4. The duplicate analyses of both inclusions are each in agreement to within their assigned experimental uncertainties. Grain 30/26 gave a mean $^{206}\text{Pb}/^{238}\text{U}$ age of 35.9 ± 1.9 Ma, whereas grain 28/11 gave 33.7 ± 2.1 Ma. Since there is no significant difference between these two ages with respect to experimental error, they may be combined to yield a mean age estimate for both inclusions of 34.9 ± 1.4 Ma (2σ). Strictly speaking, this is only a minimum estimate for the age of the inclusions, because of the possibility that at some stage of their history an unknown amount of the radiogenic Pb accumulated in the zircons may have been lost. However, we would argue against such a

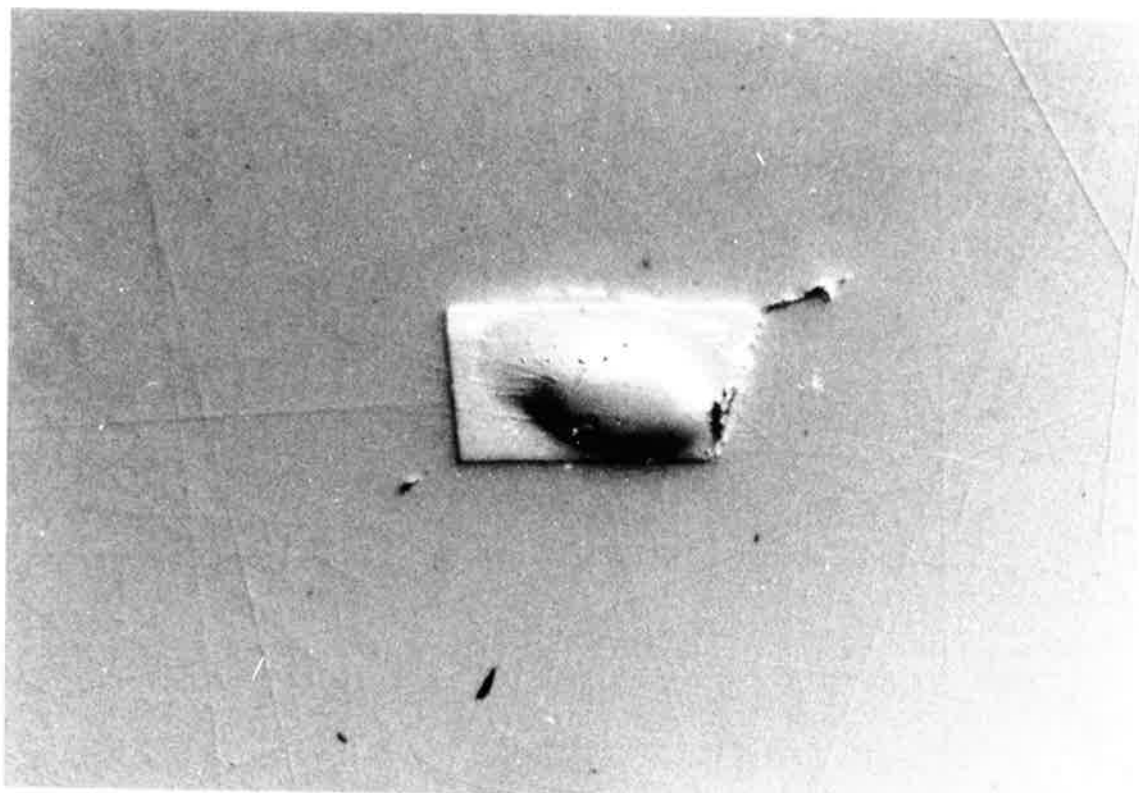


Figure 2-13. Zircon inclusion 28/11, showing the sputter-hole excavated by the ion-beam. The hole is approximately 25 μ m across.

Table 2-4. U-Pb ages of zircon inclusions in sapphire.

Spot	$^{206}\text{Pb}/^{238}\text{U} \pm 2\sigma$	AGE $\pm 2\sigma$	U	Th	Pb*	Th/U	%com. ^{206}Pb
30/26.1	0.00562 ± 42	36.1 ± 2.7	984	850	6	0.864	10.4
30/26.2	0.00553 ± 42	35.6 ± 2.7	968	832	6	0.859	5.4
28/11.1	0.00543 ± 48	34.9 ± 3.1	457	178	2	0.388	21.8
28/11.2	0.00508 ± 44	32.7 ± 2.9	449	171	2	0.380	12.3

$^{206}\text{Pb}/^{238}\text{U}$ refers to radiogenic ^{206}Pb . Pb* refers to the total radiogenic Pb. Values for U, Th and Pb* are in parts per million. %com. ^{206}Pb is the percentage of non-radiogenic ^{206}Pb in the total.

possibility for two reasons. Firstly, the young apparent age of the inclusions implies that up to the present time only minor damage would have been caused to the zircon structures by the *in situ* disintegration of U atoms (the principal cause of Pb loss from zircons), and secondly, being wholly enclosed within inert sapphire megacrysts the zircon inclusions would have been protected throughout their history from interaction with permeating fluids.

Another consideration is that Pb might not have accumulated in the zircons at all prior to the time of eruption of the host basalt, owing to the high temperature of the source regions, in which case they could be much older than their indicated age. The effective "blocking temperature" for Pb in zircon has never been established. However, Rudnick and Williams (1987) reported the preservation of Proterozoic zircon ages in lower crustal xenoliths incorporated into a Cenozoic basalt cinder cone in north Queensland, and Kinny et al. (1989) reported analyses of kimberlitic zircons from Botswana which were erupted in the Permian but which nevertheless preserved Archaean ages. Both examples suggest that if these zircons and their host sapphires were in fact ancient xenocrysts incorporated into the basaltic magmas, it is likely that the old U-Pb ages would be preserved.

On the basis of this evidence it was concluded that the true age of both inclusions, and hence of the sapphires themselves, is 35 Ma.

2.6.4 Discussion

The 35 Ma age of the zircon inclusions in the sapphires lies within the range of K-Ar ages for the basalts of the East Central Volcanic Province and within the range of zircon fission track ages for the area (Figure 1-1, Table 1-1) thus suggesting a genetic link. It is believed that the sapphires formed in some process associated with the basaltic magma generation or evolution. The surface morphology of the stones and their inclusion suite indicate, however, that this process is not simple. This is reinforced by the presence of reaction rims of spinel on some corundum crystals (Stephenson, 1976), by the reported failure of experimental attempts to grow corundum from a corundum-bearing basaltic composition under different pressure, temperature and hydrous conditions (Green *et al.* 1978), and by the anomalously high abundances of incompatible elements such as U, Th, Zr, Nb and Ta in the inclusion minerals (Gübelin and Koivula, 1986; Coenraads, 1990).

Crystallization may be taking place as partial melting of the mantle occurs and such a process might involve generation of more evolved magmas at depth, crystallization of mineral assemblages including the sapphires and their inclusion minerals from these magmas rich in volatiles and incompatible elements, and finally the disintegration and partial resorption of the rock types during transport to the surface in later magmas. Such minerals may crystallize from liquids whose composition represents very tiny amounts of upper mantle partial melting. As such, these crystallisation products could then be expected to be out of equilibrium with basalts produced by larger proportions of melting.

Irving and Price (1981) describe a fractionation model which allows the generation of evolved magmas (phonolites) at upper mantle depth, via the fractional crystallization of kaersutitic amphibole, olivine, iron-titanium spinel, aluminous clinopyroxene, mica and apatite. Their model is supported by the observation of lherzolite-bearing phonolitic lavas from Bokkos (Nigeria), Phonolite Hill (Australia) and Heldburg (East Germany). The crystallization products of such magmas may accumulate in pockets or fissures, or as plating on conduit walls (Irving, 1980), until such time as partial melting has generated sufficient magma to carry them to the surface.

Upton et al (1983) suggested that the megacrysts (eg. anorthoclase, sanidine, clinopyroxene, kaersutite, Ti-biotite, Ti-magnetite, Mg-ilmenite, apatite, zircon and corundum) found in upper Palaeozoic alkali basalts of the British Isles are the result of the disintegration of such rock types. Evidence in the form of megacryst surface morphology and the occasional observation of corundum-bearing xenoliths discussed earlier support their suggestion.

The growth zoning, CO₂-rich fluid inclusions and high inclusion homogenization temperatures (greater than 685°C) observed in Queensland sapphires led Stephenson (1976) and Irving (1986) to assign a high temperature and pressure magmatic origin to their formation. They were presumed to result from fractionation of basanitic magmas, at least within the deep crust.

2.7 Sapphire-bearing rocks in the Central Province volcanic sequence

The conclusion drawn by Thompson et al (1986) for the British Tertiary Volcanic Province and the observations of Pecover (1987) suggest that the following sequence of events may have occurred in the Central Volcanic Province :- Magma movements "ream out" conduits containing crystallization products of the highly evolved magmas or products of metasomatizing fluids, carry the evolved megacryst assemblage upwards along fracture sets and erupt explosively onto the surface. Thompson et al (1986) suggested that once the initial magmas ream out the magmatic plumbing system then the remaining batches of liquid would be able to rise without significant interruption. The implications of this model are that the volcanoclastics, or products of initial explosive volcanism, occurring towards the base of the volcanic pile are likely to contain the most abundant sapphires.

Lacombe (1969-70) noted that in the Bokeo Plateau region of Kampuchea, zircons, corundum, garnet, titanomagnetite, spinel and anorthoclase megacrysts, although present in the majority of basalts, are most abundant in the products of explosive eruptions and their weathering products. Similarly, Barr and MacDonald (1981) noted for the Chanthaburi-Trat area of Thailand that megacrysts of aluminous clinopyroxene, ilmenite, garnet, zircon and spinel are abundant in the pyroclastic debris in the vicinity of vents.

Variation in the fine details of such a process, such as the time elapsed between initial partial melting and megacryst formation, and their final transportation to the

surface, may determine the amount of sapphires in a particular source rock and possibly their size and quality. When combined with the necessary geomorphological conditions for the development of a sapphire deposit, the above-mentioned process of megacryst formation may determine whether or not a particular volcanic province has economic potential.

2.8 Conclusions

An ion microprobe age of 34.9 ± 1.4 Ma for syngenetic zircon inclusions in New England sapphires shows that the minerals originated during Cainozoic volcanism in this area. The corundum probably crystallized from strongly evolved magmas held in the deep crust or upper mantle and was carried up in profuse abundance during the volatile-rich, explosive eruptions.

Surface features on rubies and sapphires from volcanic provinces also indicate the history of such crystals.

1. Negative crystal impressions suggest that the corundum grew in coarsely crystalline aggregates along with minerals such as anorthoclase, zircon and spinel.
2. Surface resorption or etching and layer dissolution features clearly result from reaction with the magmas responsible for carrying the corundum to the surface.
3. Etched chatter marks imply that the corundum has been subject to stresses prior to, or possibly whilst in transit to the surface.
4. Surface damage, including impact marks displaying conchoidal fracture, broken off protrusions and exposed healed fracture surfaces, result from reworking in the alluvial environment. Such damage is usually minimal indicating the crystals to be near source.

Chapter 3

KEY AREAS FOR ALLUVIAL DIAMOND AND SAPPHIRE EXPLORATION IN THE NEW ENGLAND GEMFIELDS, NEW SOUTH WALES

3.1 Introduction

The aim of this chapter is to define key areas for diamond and sapphire exploration within the New England Gemfields of eastern Australia through an understanding of the geologic and geomorphic processes that operated within the Tertiary Central Volcanic Province. This chapter describes the structural control and timing of volcanism in the Central Province. These, combined with geomorphic factors, have determined the distribution of Quaternary alluvial sapphire and Tertiary deep lead concentrations of diamond and sapphire.

The palaeo-Hobbs and the palaeo-Gwydir diamond-bearing deep lead Tertiary systems, the Reddestone Creek and Kings Plains Creek sapphire-bearing placers, and the Braemar deep-lead sapphire deposit are presented as case studies in Chapter 4.

3.2 Central Province volcanism

3.2.1 Structural control of Central Province volcanism

The elongated shape of the Central Volcanic Province implies that volcanism was localized by preferred planes of weakness in the earth's crust. These were probably of the order of 100 to 200 kilometres in length. A Landsat lineament analysis and analysis of physiographic features in the Central Province were carried out to evaluate these relationships.

The lineament analysis was confined to the Woolomin-Texas structural block which is bounded by the Peel Fault to the west (Fig. 3-1), and by the Demon Fault to the east (just outside the eastern border of Fig. 3-1). The analysis covered portions of the Inverell, Manilla, Grafton and Dorrigo-Coffs Harbour 1:250,000 Geological Sheets (New South Wales Government Department of Minerals and Energy) and utilized Landsat images 090-080F, 096-081 and 095-081 (Australian Centre for Remote Sensing) which cover the area of interest with considerable overlap. All visible lineaments were highlighted on plastic overlays (Colour Plate 5) at 1:250,000 scale and the data presented in the form of a rose diagram (inset Fig. 3-1) constructed by summing the lineament lengths (in kilometres) corresponding to their respective azimuths (in degrees from north).

Analysis of physiographic features was carried out at 1:100,000 scale, using the Inverell, Glen Innes, Guyra, Bundarra, Armidale, Yallaro and Bingara topographic sheets

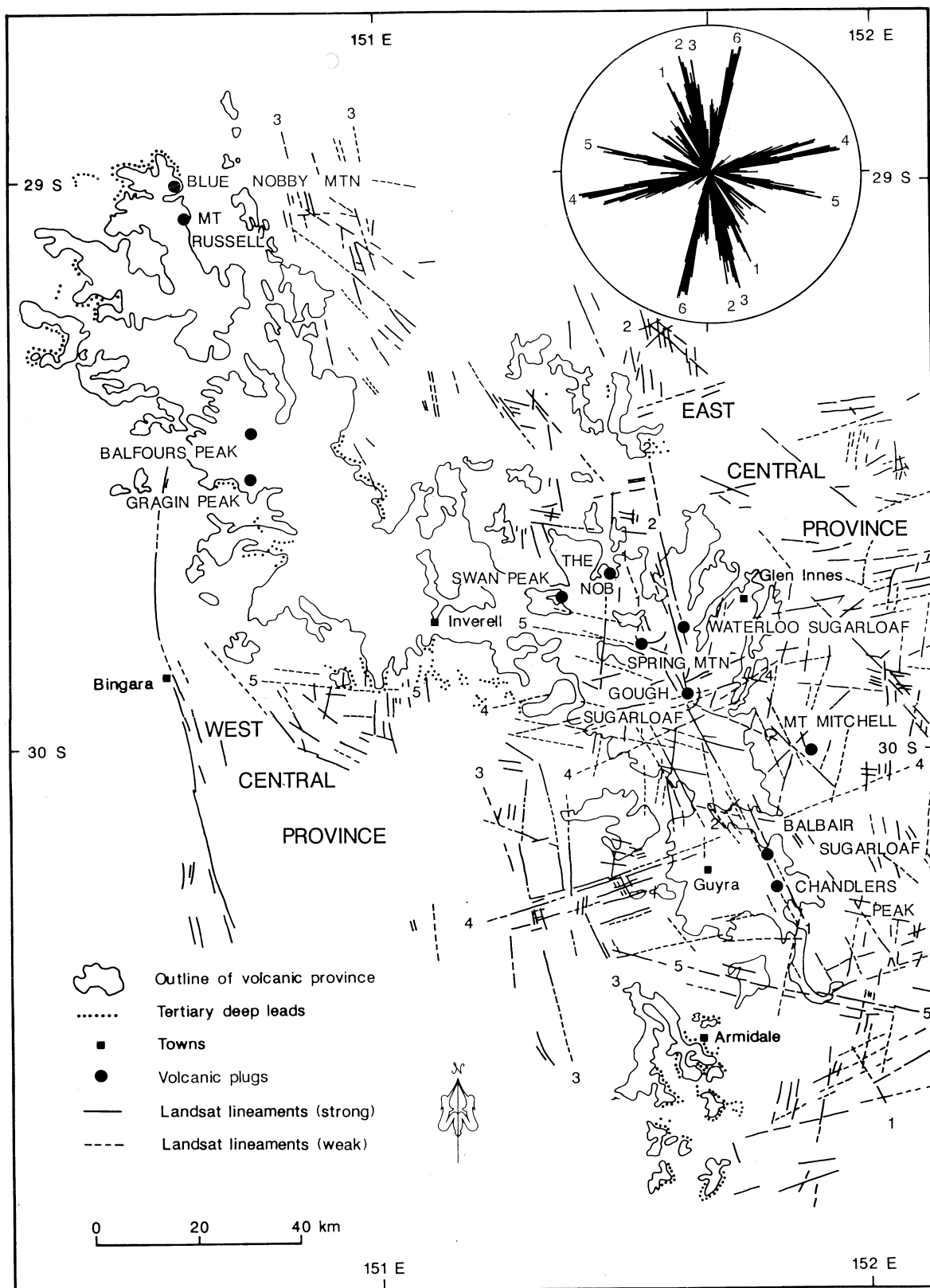


Figure 3-1. Structural elements of the Central Province, New South Wales, determined by landsat lineament analysis (see also Colour Plate 5) and topographic trend analysis. The rose diagram shows total length of landsat lineaments at respective azimuths for the map area. The SSE-NNW peak is sub-parallel to the Peel and Demon faults as well as the long axis of the Central Province.

(New South Wales Government Department of Lands). Map sheets were joined and colored in order to strongly enhance prominent ridge and valley trends as well as areas of high ground.

The major trends determined from the observed physiographic features were complimented by the Landsat interpretation. The rose diagram indicates four major groups of lineament development. The most significant are the NNW-SSE trending structural elements, (numbered 1, 2 and 3 on Fig. 3-1), which correspond to prominent long, straight ridges and areas of maximum basalt thickness. These coincide with the long axis of the Central Volcanic Province and are sub-parallel to the Peel and Demon fault traces. They will be referred to as "axial lineament trends".

The NNW-SSE trends appear to have acted as the loci for emplacement of volcanic centres and plugs located along the length of the lava field. Six named centres lie along lineament trends numbered 1 and 2 on Figure 3-1, and four named volcanic plugs lie parallel to the landsat lineament trend numbered 3. Landsat lineaments were not visible on this portion of the volcanic province itself owing to the higher landuse on the fertile volcanic soils.

A series of radial and ring fractures centered near the Gough Sugarloaf plug are clearly visible on the Landsat images (Fig. 3-1; Colour Plate 5). This structure, described as the Maybole Volcano by Pecover (1987), appears to be the most significant volcanic centre in the Province. It is located at the intersection of the four prevalent lineament sets and coincides with a maximum thickness of basalt. The Maybole Volcano is also the centre of a large radial drainage system.

A number of other important structural trend directions are evident within and around the Central Volcanic Province (Fig. 3-1). These cluster around 0°-20°, 60°-80 and 95°-110° and are reflected mainly as lineament-controlled drainage (Coenraads, 1988).

3.2.2 Timing of Central Province volcanism

The locations of age determination sites in the Central Volcanic Province are shown in Figure 1-1 and are listed in Table 1-1. The ages of volcanism associated with axial lineament trends 1 and 2 differ from those associated with, and west of, axial trend 3. Accordingly, an older East Central Province (32 - 38 Ma) and a younger West Central Province (19 - 23 Ma) can be delineated. Lineament trend 3 indicates that there is a structural link between the West Central Province and the volcanics to the south and west of Armidale, some of which have a similar age (20.7 Ma).

The results of this study show a correlation between the lineament maximum at 150° - 180° and the axis of elongation of the Central Volcanic Province. Volcanism in the Central Province has thus been controlled by NNW/SSE trending crustal fractures.

3.3 Sapphire and diamond occurrences in the Central Volcanic Province Quaternary alluvium and Tertiary deep leads.

3.3.1 Quaternary alluvium.

Figure 3-2 highlights the major rivers and creeks associated with the Central Volcanic Province. The most obvious feature is the radial pattern of drainage centered on the Ben Lomond-Maybole area. It has an approximate radius of 50 kilometres. Sapphires, together with zircon, spinel and/or ilmenite, may be found in Quaternary gravels in most gullies, creeks, and rivers draining the 32 - 38 Ma East Central Province.

Creeks and rivers flowing westward and north-westward, such as the Gwydir, Copes, Swan Brook, Middle and the Macintyre, appear to have been diverted from their original flow direction by the 19 - 23 Ma volcanic activity to the west and northeast of Inverell. Swan Brook, Middle Creek and the Macintyre have been deflected to the north in the vicinity of Inverell, and Copes Creek and the Gwydir deflected to the west (Fig. 3-2).

The 19 - 23 Ma West Central Province created its own radiating drainage network. Croppa, Gourmana, Mosquito, Reedy, Kelly's, Sheep Station and Myall Creeks flow westerly from the volcanic high ground. Oatleys and Bannockburn creeks flow northward, and Auburn Vale Creek flows to the south. Numerous small creeks drain to the east and southeast from the volcanic high ground, but the radial pattern is not fully developed due to the pre-existing high ground of the East Central Province.

Sapphires have not been reported in the streams draining the basalts of the West Central Province.

3.3.2 Tertiary deep leads.

The volcanics of the West Central Province overlie and protect alluvial sediments forming "deep leads" which have been recognized for their diamond bearing potential since 1872, (MacNevin, 1977). Cassiterite, gold, zircon, garnet, sapphire, tourmaline, and topaz are also found in the deep leads. The deep leads outcrop extensively around Armidale, in the Copeton-Gilgai-Stannifer area (south east of Inverell) and also to the north west of Inverell extending to the Queensland border (Fig. 3-1).

The possibility of two periods of volcanism, separated by a period of drainage development and alluvial deposition, was noted last century. Anderson (1888 p.156) observed boulders of basalt in deep lead alluvium which "could not have been derived from the Tertiary basalt overlying in the wash but must have come from an older bed of basalt". Using the relative heights of the bases of Tertiary deep lead channels in the Copeton, Inverell and Gragin areas, Cotton (1914) showed that the Tertiary land surface fell away to the north and west. It is likely, therefore, that the deep lead zircon and sapphire were derived from the older volcanics of the East Central Province.

3.4 Identification of exploration targets for diamond and sapphire

3.4.1 Analysis of sub-volcanic topography

3.4.1.1 Objective: Deep lead alluvials, worked for diamonds, gold and tin, have long been recognized as channel deposits with the richest grades of heavy minerals being found along the palaeochannel axes. Many attempts have been made to map the location of the palaeochannels (Anderson, 1888; Stonier, 1895; Curran, 1897; Pittman, 1897; Cotton, 1914; Gibbons & Pogson, 1963). The palaeotopographic analysis presented here makes use of large scale topographic maps, borehole data and recently available, detailed geologic maps.

The present study shows the precise location of the diamond-bearing palaeodrainage beneath the basalts of the West Central Province and also highlights likely source areas for the alluvial diamonds.

The development of post-volcanic drainage controls the location and grade of alluvial sapphire deposits derived from non-economic source rocks. Comparison of pre- and post-volcanic drainage patterns makes it possible to gain an insight into the mechanisms involved in this process and to predict areas where these mechanisms have been most effective.

3.4.1.2 Method: Analysis of the sub-basaltic topography was carried out at a scale of 1:25,000 over most of the Central Volcanic Province (see Appendix 1). The geological boundaries between Central Province volcanics and older basement rocks were overlain on the topography. Elevations for each mapped boundary were plotted and then contoured as shown in Figure 3-3. The interpretation is conservative, that is to say, in areas of basalt cover the basement surface is interpreted to dip gently and smoothly underneath. The least amount of basalt cover required was interpreted in areas of poor control.

In order to improve the analysis, data from some 430 water bores (New South Wales Government Department of Water Resources; see Appendix 2) were also plotted on the 1:25,000 sheets. The logs are poorly described but serve to distinguish between basalt and basement rocks, or at least indicate a minimum depth of basalt in a given borehole. The bore data generally supported the basement topographic analysis and, in many cases, indicated that the basalt filled valleys are steeper and deeper than are given by the conservative analysis. After contouring the pre-volcanic topography for each 1:25,000 sheet, the information was linked to the surrounding sheets and the whole reduced to 1:100,000 scale. At this scale the pre-basaltic drainage was compared with the present drainage pattern.

3.4.1.3 Results and discussion: Figure 3-4 shows the pre-volcanic and present day drainage patterns in the Central Volcanic Province. The lavas flowed into the

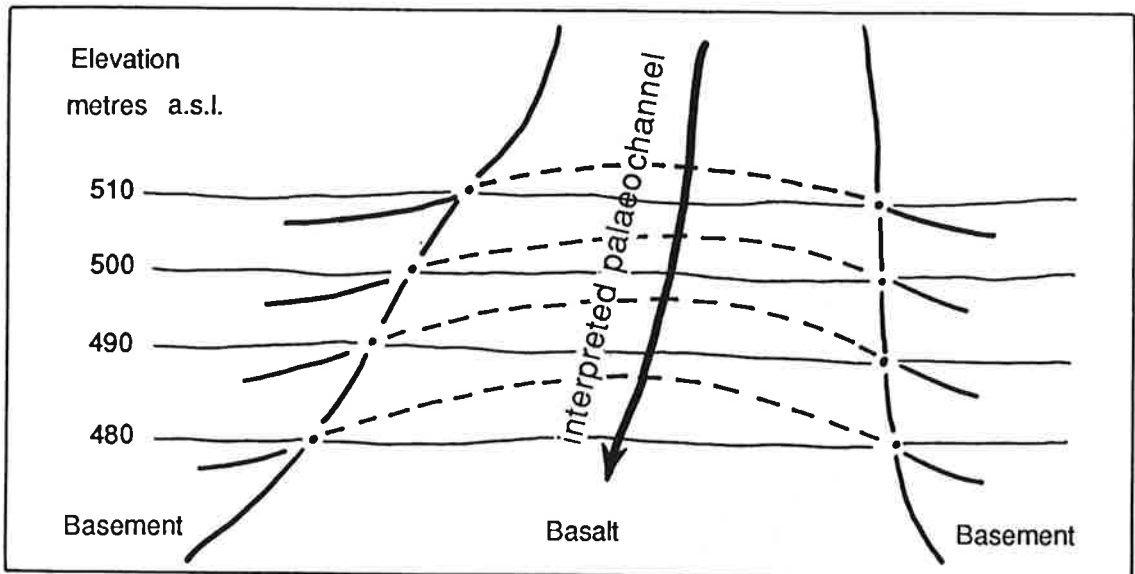


Figure 3-3. Illustration of the Technique by which sub-basaltic topography is determined. The thin lines are topographic contours which yield elevation data points where they intersect basalt-basement contacts. The thick lines are the interpreted basement contours based on these data, and are dashed where the surface is obscured by basalt or sediments. The interpretation is conservative, that is, the basement surface is interpreted to dip smoothly and shallowly beneath the basalt unless otherwise constrained by borehole data.

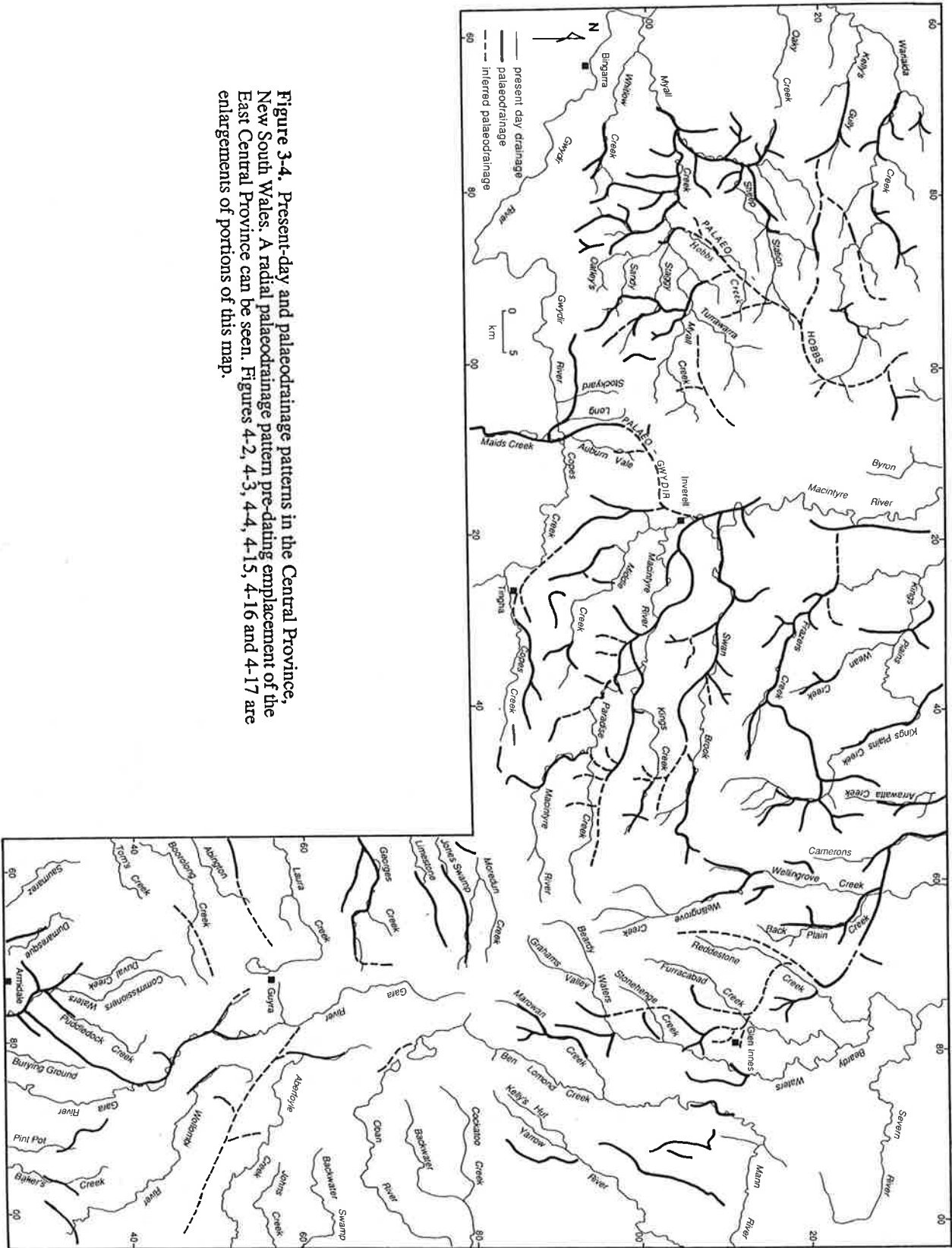


Figure 3-4. Present-day and palaeodrainage patterns in the Central Province, New South Wales. A radial palaeodrainage pattern pre-dating emplacement of the East Central Province can be seen. Figures 4-2, 4-3, 4-4, 4-15, 4-16 and 4-17 are enlargements of portions of this map.

palaeovalleys and progressively filled them. The areas of basement rocks exposed today are generally of equal or higher elevation than the immediately adjacent volcanic rocks. These acted as highs around which the lava initially flowed. In some cases, it is clear that the basement was covered and has now been exhumed. Very little basement rock is visible through the thickest and highest part of the volcanic pile along the East Axial Lineament between Glen Innes in the north and Guyra in the south. In this area the pre-basaltic drainage cannot be determined. A radial and annular pattern, controlled solely by the volcanic pile, has developed. The headwaters of the Macintyre River, Paradise Creek, Wellingrove Creek, Furracabad Creek, Stonehenge Creek, Ben Lomond Creek, Gara River and Moredun Creek are radially arranged. Beardy Waters and Grahams Valley Creek form an annular system around the Maybole Structure (Pecover, 1987).

The palaeodrainages in the East Central Province (Fig. 3-4) indicate that a radial drainage pattern was present at the onset of Central Province volcanism. This may imply pre-volcanic doming, such as was reported by Wellman (1988) for the large shield volcanos, or uplift along the Great Divide, or perhaps even an earlier eroded centre. This doming or uplift may have been responsible for opening the NNW-SSE trending axial fractures sub-parallel to the pre-existing fabric of the New England Fold Belt, which acted as the loci for Central Province volcanism.

The lavas of the West Central Province have acted similarly to those in the East, filling pre-existing valleys. Again, however, it is difficult to determine the exact position of the palaeochannels in areas where the volcanic pile is thickest, that is, to the north-west of Inverell along the West Axial Trend (Fig. 3-4). As the pre-volcanic surface was buried by basalts, the drainage was severely or entirely disrupted. Streams were reset in different positions and with different local base levels. Unlike in the East, some of the major palaeorivers in the West Central Province such as the Gwydir, Hobbs and Macintyre, have been markedly altered and even reversed in direction from their original north-easterly and north-westerly trending channels. Today, some of these palaeochannels are crosscut by numerous westerly flowing streams, including Warialda, Sheep Station, Hobbs, Myall, Staggy and Sandy Creeks (Fig. 3-4).

Based on the sub-volcanic topographic mapping, the following drainage features were developed on the post-volcanic landscape of the Central Province:

1. *Streams following their original pre-basaltic course:* These streams have remained in their original valleys even after infilling by basalt. The valleys are thus generally flat floored resulting in streams which are underfit, low energy and meander over their floodplains. Kings Plains and Reddestone Creeks are examples (Fig. 3-5A & 3-6A). This configuration is extremely important for the concentration of economic sapphire deposits.

2. *Lateral and twin lateral streams:* These streams flow alongside and parallel to the original basalt filled valleys. They flow along the contact between the basalt flows and

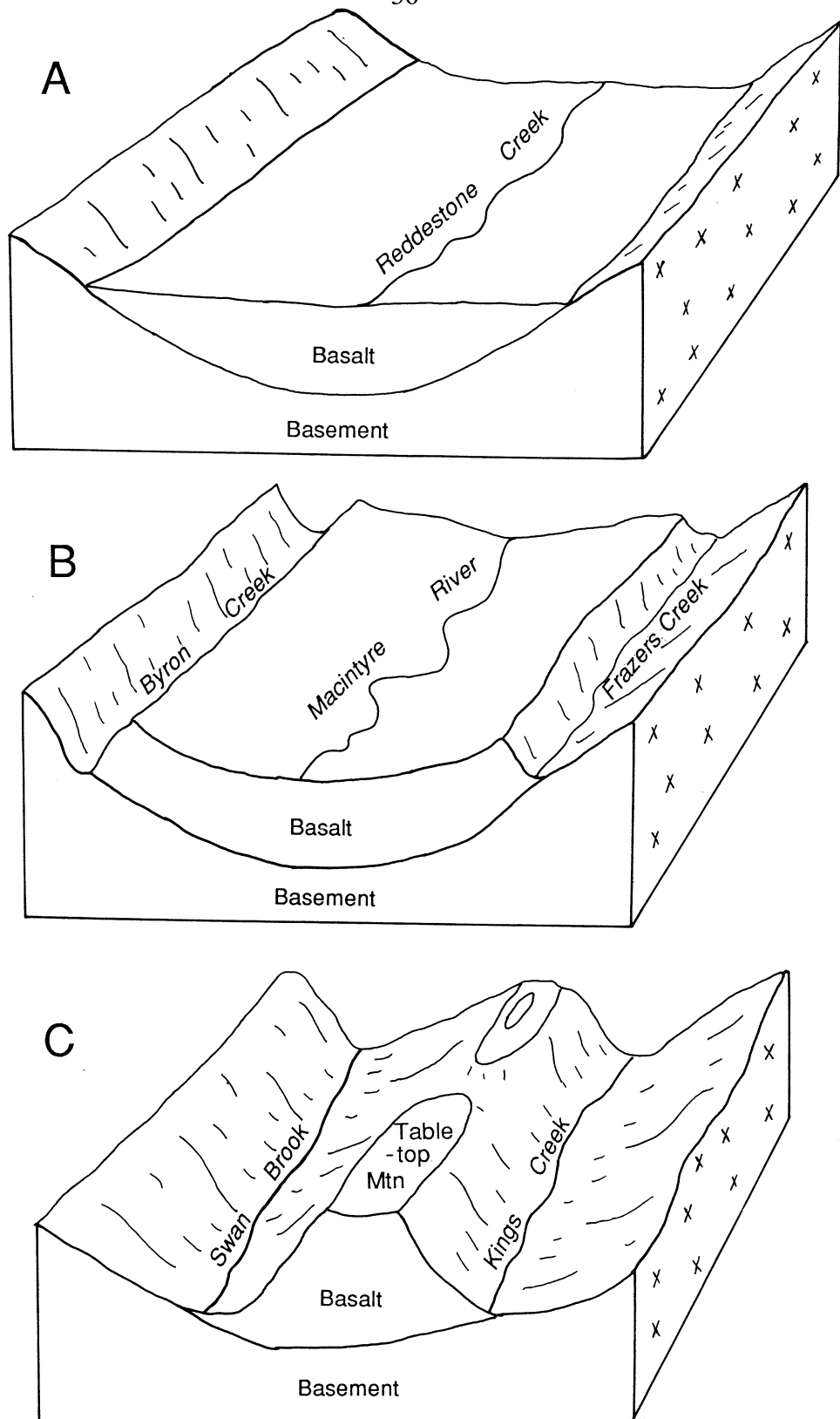


Figure 3-5. Progressive stages in the development of relief inversion by lateral stream formation. Stage A shows an underfit stream meandering in a basalt filled channel. Kings Plains and Reddestone creeks are examples. In stage B, the lateral streams have become well entrenched along the plane of weakness between the basalt flows and adjacent basement. Examples are Frazers and Byron Creeks flanking the Macintyre palaeovalley. By stage C relief inversion is complete. The original palaeochannel is marked by a line of flat-topped, or slightly concave upward, hills, and is flanked by parallel twin lateral streams. Tabletop mountain flanked by Swan Brook and Kings Creek is such an example.

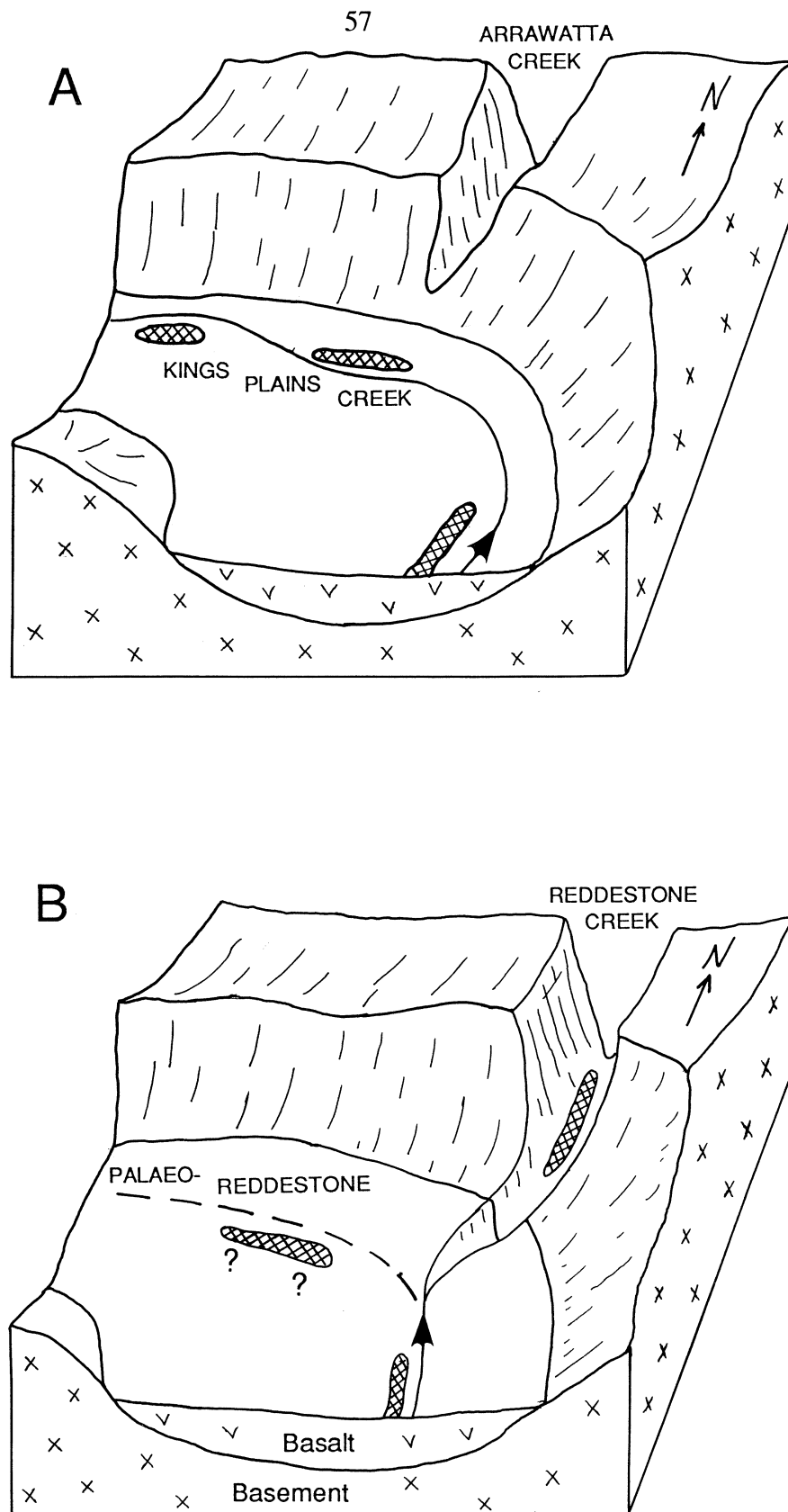


Figure 3-6. Stages in the development of stream piracy illustrated by two examples in the Central Province. In diagram A, Arrawatta Creek has not yet captured the flow of Kings Plains Creek. In diagram B, however, Reddestone Creek has been diverted from its original broad valley into a steep narrow gully flowing to the northeast. Proven or inferred sapphire deposits are represented by the cross hatched areas.

the basement rocks where there is a convenient plane of weakness (Fig. 3-5B). Once fixed in this position, continued downcutting may isolate the original basalt filled valley as a flat topped or slightly concave upwards mesa. This relief inversion by lateral stream activity is illustrated by portions of Swan Brook, Kings Creek and Paradise Creek (Fig. 3-5C).

3. *Cross cutting and pirate streams:* The process of stream piracy is illustrated in Figure 3-6 using Kings Plains and Reddestone creeks as examples. Kings Plains Creek is sketched in part A at the point where its broad basalt filled valley swings round to the west. Arrawatta Creek has not yet captured its flow. Reddestone Creek, however, (Fig. 3-6 part B), has been diverted from its original broad valley into a steep narrow gully flowing to the northeast.

4. *Reverse direction streams:* The palaeo-Gwydir and palaeo-Hobbs Rivers once flowed to the north and northeast under what is now the thickest and highest part of the West Central Province volcanic pile. These courses have since been disrupted and even reversed in flow directions in places due to volcanic activity and/or uplift. The palaeo-Gwydir (Fig. 3-4) once flowed northward and then eastward, to finally join the Macintyre River in the vicinity of Inverell. That course was blocked and today the Gwydir River flows westward. Auburn Vale Creek flows southward (a reversal) into the present Gwydir River.

3.5 Geologic and geomorphic evolution of the Central Volcanic Province.

The geological and geomorphic evolution of the Central Volcanic Province is summarized as follows:-

a/ Pre-volcanic doming, and/or uplift along the Great Divide altered the pre-volcanic topographic surface producing high ground and radial drainage centred on the East Central Province. This was accompanied by block faulting and the opening of deeply penetrating NNW trending fractures sub-parallel to the pre-existing fabric of the New England Fold Belt.

b/ Injection of breccias and explosive eruption of pyroclastic material took place prior to 36 Ma, forming a blanket of volcanic debris, (some sapphire-bearing), on the pre-basaltic topography.

c/ Explosive volcanic eruption continued, as well as basalt extrusion, with a general decrease in the amount of explosive activity with time. Early basaltic lavas flowed down valley systems and may be found directly on basement rocks in places.

d/ Major effusive basaltic eruptions took place along the Eastern Axial and Wellingrove lineaments and parallel fracture sets at about 32 - 36 Ma. This produced a "lava field" with an overall SSE-NNW elongation.

e/ Erosion and reworking, particularly of the less resistant volcaniclastic rocks, took place over some 10 million years and this material was deposited around the edges of the East Central Province. Alluvial concentration of tin, tourmaline, topaz and gold (from the granites), diamonds (from local intrusives and breccias) and sapphire and zircon (from the volcaniclastics and basalts) took place.

f/ The next phase of volcanism, also controlled by SSE/NNW trending planes of weakness, occurred further to the west. Basaltic eruptions grading from tholeiitic through to alkaline occurred at about 19-23 Ma and formed the West Central Province, which also includes volcanics south and west of Armidale. The basalts flowed out and covered the Tertiary alluvium, and thus formed the deep leads that have been periodically exploited for diamonds. To the east of the East Central Province these alluvials have long since been removed due to the westward migration of the Great Escarpment and the lack of a protective basalt cap. Pockets remain however to the northwest, west and south.

g/ The development of the West Central Province deflected the west and northwesterly flowing drainage system radiating from the Maybole high and developed a radial drainage pattern centered on the Delungra-Mount Russell areas.

Chapter 4

DELINEATION OF ALLUVIAL AND DEEP LEAD EXPLORATION TARGETS: CASE STUDIES.

4.1 Introduction

The Central Province has been divided into three prospective target regions for sapphires and diamonds (Fig. 4-1) based on the detailed palaeotopographic reconstruction technique described in the previous chapter. These regions comprise a western region with a potential for "palaeo-Gwydir type" alluvial diamond deposits, a central belt with "Braemar type" sapphire deposits, and an eastern division with "Kings Plains- Reddestone type" alluvial sapphire deposits.

Case studies of these "type" deposits of diamond or sapphire in the Central Province will be described in this chapter.

4.2 Diamond prospectivity in the palaeo-Gwydir River system

The Palaeo-Gwydir River system was buried by 19-23 Ma volcanism of the West Central Province. Prospectivity for diamond-bearing deep lead alluvium is considered to be favorable in two major palaeodrainage systems that extend northward from the present Gwydir River in the vicinity of Copeton Dam. These are described below as the palaeo-Hobbs and palaeo-Gwydir systems and are shown in Figure 4-2.

Palaeo-Hobbs: A tributary of the palaeo-Hobbs heads northward from a palaeosaddle near Copeton Dam (GR:962922 Copeton Dam 1:25,000, Fig. 4-2). Basalt at the base of the channel at this position indicates an original elevation for the palaeoriver of 650 m asl. It can be traced for 20 kilometres heading in a north to northwesterly direction, over which distance the elevation of the channel falls to 480 m asl (GR:900080 Delungra 1:25,000, Fig. 4-2). At this location the channel joins the palaeo-Hobbs and the palaeoaxis heads in a north northeasterly direction where it eventually becomes obscured by extensive basalt cover.

The palaeochannel is presently cut by westerly flowing streams, including Sandy, Hughies, Staggy, Myall and Spring creeks, which dissect the palaeovalley walls. This is particularly obvious in the western palaeovalley wall where downcutting is of the order of 100 m.

The Staggy Creek (GR:955975 Gum Flat 1:25,000, Fig. 4-2) and Wonderland (GR:968954, Fig. 4-2) diamond bearing leads form part of the NNW trending palaeo-Hobbs system. They are not part of the same system as the leads occurring at a lower elevation in the vicinity of Copeton Dam, but are from a separate source as was first suggested by Stonier (1895).

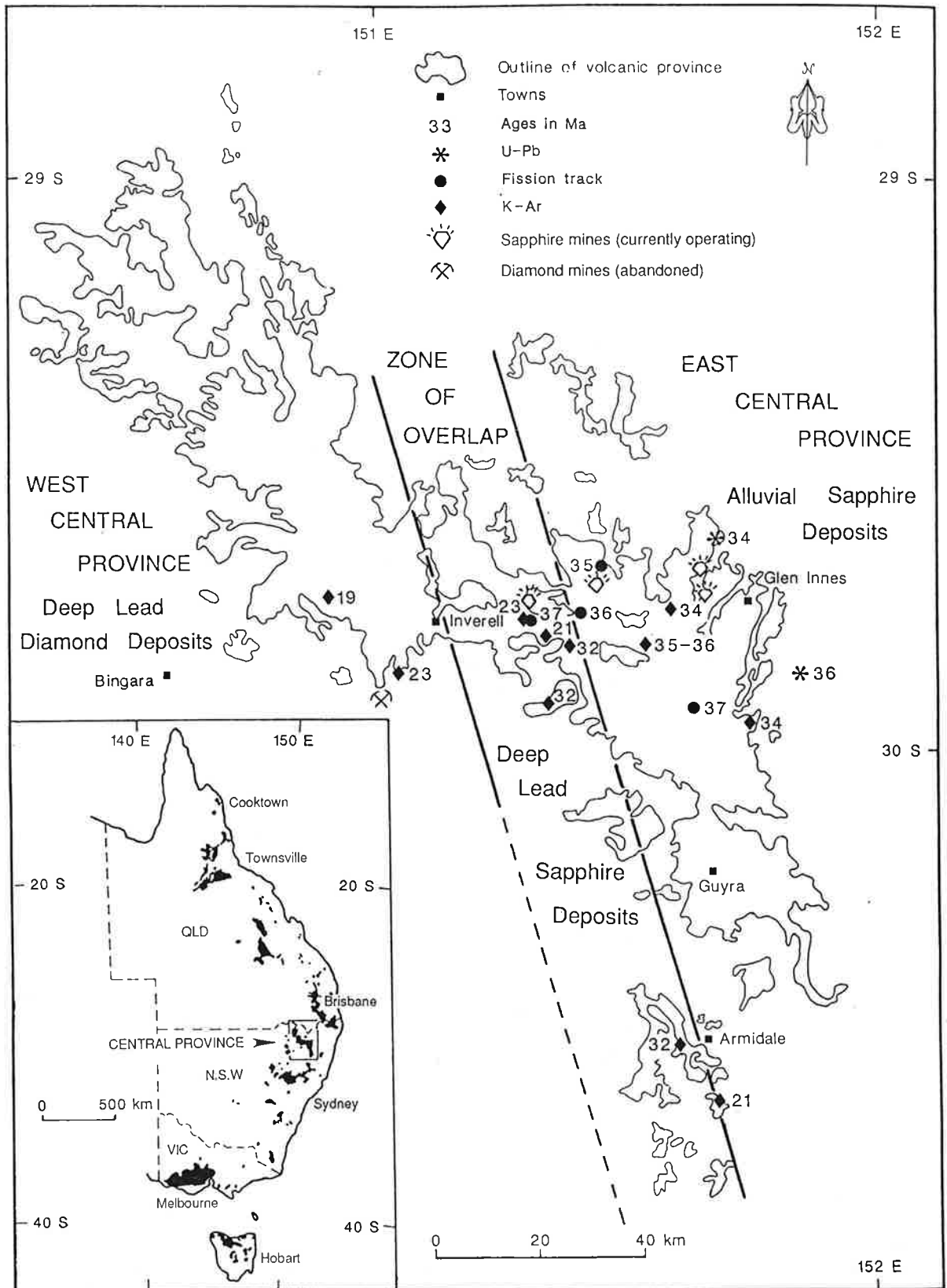


Figure 4-1. Location of the Central Province in northeastern New South Wales. The inset shows Mesozoic-Cenozoic volcanic provinces which form a discontinuous band within or adjacent to the eastern Australian highlands. The province is divided into broad zones indicating suitability for sapphire or diamond exploration.

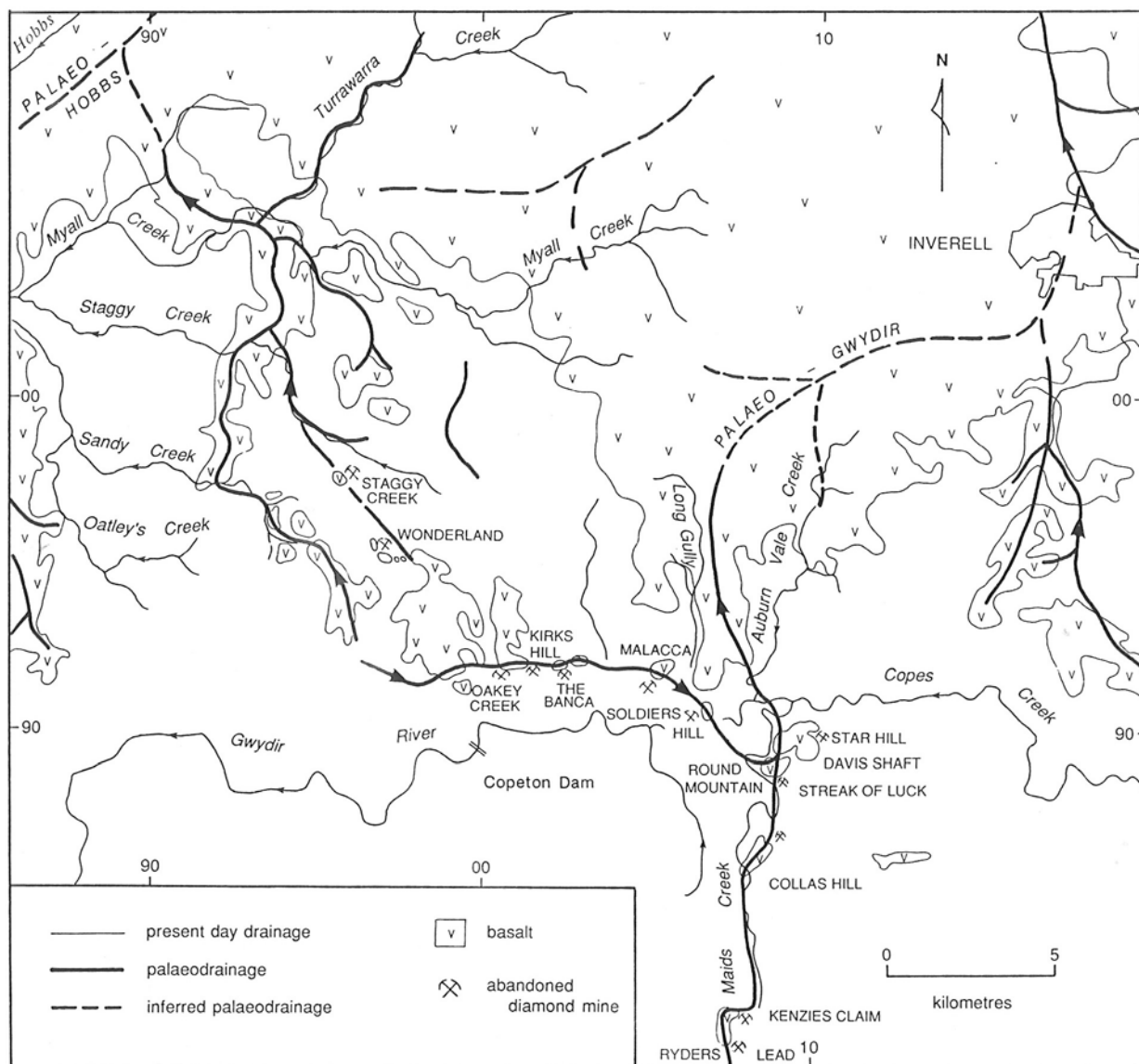


Figure 4-2. Diamond-bearing palaeodrainage and distribution of historic mines of the Copeton Field. The diamond-bearing alluvium is associated with the palaeoaxes and protected by basalts of the West Central Province. It is clear from the palaeodrainage pattern that diamonds are derived from multiple sources.

Palaeo-Gwydir: The elevations of the deep leads fall from the south, and from the west, to a point where two tributaries of the palaeo-Gwydir join, near Round Mountain (GR:087890 Tingha 1:25,000, Fig. 4-2). Progressing from the west (Fig. 4-2), Oaky Creek & Kirks Hill (GR:010920 Copeton Dam 1:25,000), The Banca (GR:022919) and Stockyard Hill (GR:043927) are at 620 m, Malacca (GR:052918) is at 600 m and Soldiers Hill (GR:067906) is at 590 m. Moving from the south, Ryders Lead (GR:075804 Tingha 1:25,000) is at 700 m, Kenzies Claim (GR:085860) is at 680 m and Collas Hill (GR:085860) is at 620 m. Stonier (1895) first recognized this channel and his ideas were verified by Cotton (1914) on the basis of numerous aneroid elevation readings. The palaeo-Gwydir leaves the Copeton Dam area in the vicinity of Auburn Vale Creek (GR:081918). At this point alluvium is exposed below the basalt fill and the channel base is at 580-590 m. asl. The channel can be traced heading northwards for approximately 8 kilometres, but becomes obscured beyond that point by extensive basalt cover. It is likely that it flowed to the NE to join the palaeo-Macintyre as was suggested by Cotton (1915), or perhaps flowed to the NW around a basement high (GR:060040 Gum Flat 1:25,000, Fig. 4-2). Today Auburn Vale and Long Gully creeks flow southward forming "twin laterals" on either side of the basalt filled valley.

The present palaeotopographic reconstruction indicates that the Gwydir River has been diverted, at least once, by the volcanic activity of the West Central Province. It also indicates at least 3 separate systems of diamond bearing alluvials and, therefore, local, multiple sources for the diamonds. MacNevin (1977 p.27) also states that "the great variety, both in size and character of the diamonds from different part of the leads" is consistent with multiple sources. Local sources for the diamonds were noted by Cotton (1914) at Oaky Creek (GR:010920, Fig. 4-2) and have been described as lamprophyric dykes intruding shattered granitic basement (Cluff Resources Pacific Limited, Annual Report, 1989). Cluff Resources Pacific Limited are currently evaluating the economic prospectivity of a lamprophyric pipe complex with associated blast breccias in the Round Mountain - Star Hill area (GR:100900, Fig. 4-2).

4.3 Kings Plains and Reddestone type alluvial sapphire deposits.

Two major sapphire deposits are situated in the Kings Plains and Reddestone Creeks of the East Central Province (Figs 4-3 and 4-4). These Holocene alluvial deposits are currently being worked by T.J. & P.V. Nunan Pty Ltd using mechanized mining methods. Each mine processes approximately 1000 tonnes of alluvium per day, yielding 1 tonne of heavy mineral concentrate containing about 10 kilograms of corundum (Nunan, 1989). The heavy minerals associated with the sapphire in the alluvial gravels are pleonaste, ilmenite, chrome-spinel, titanium-magnetite, corundum, zircon and minor chrysoberyl. There is a clear association between these deposits which have developed

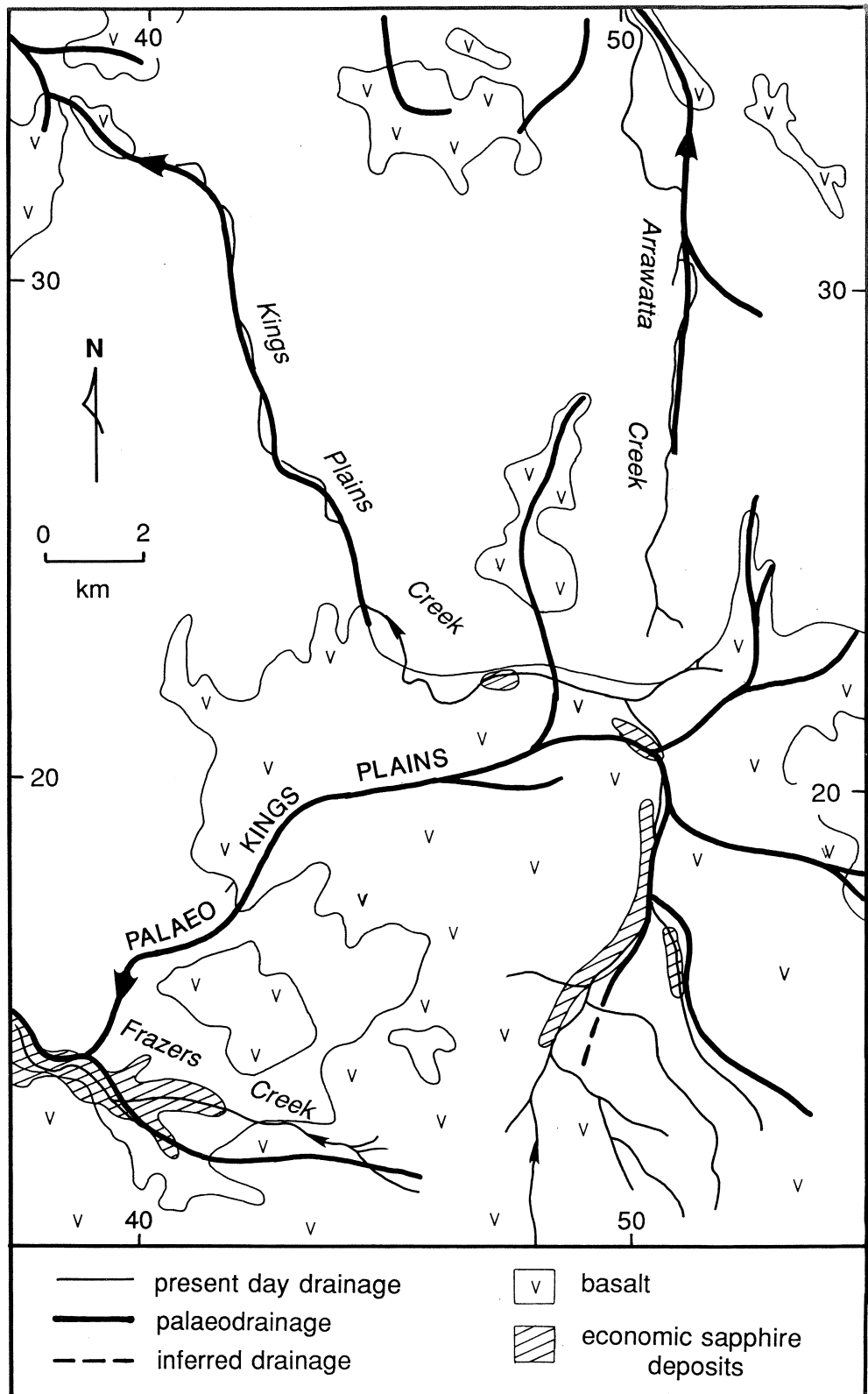


Figure 4-3. Economic Holocene sapphire deposits of the Kings Plains palaeochannel. When Arrawatta Creek captures Kings Plains Creek, the sapphire deposits downstream from that point will no longer be associated with an active channel.

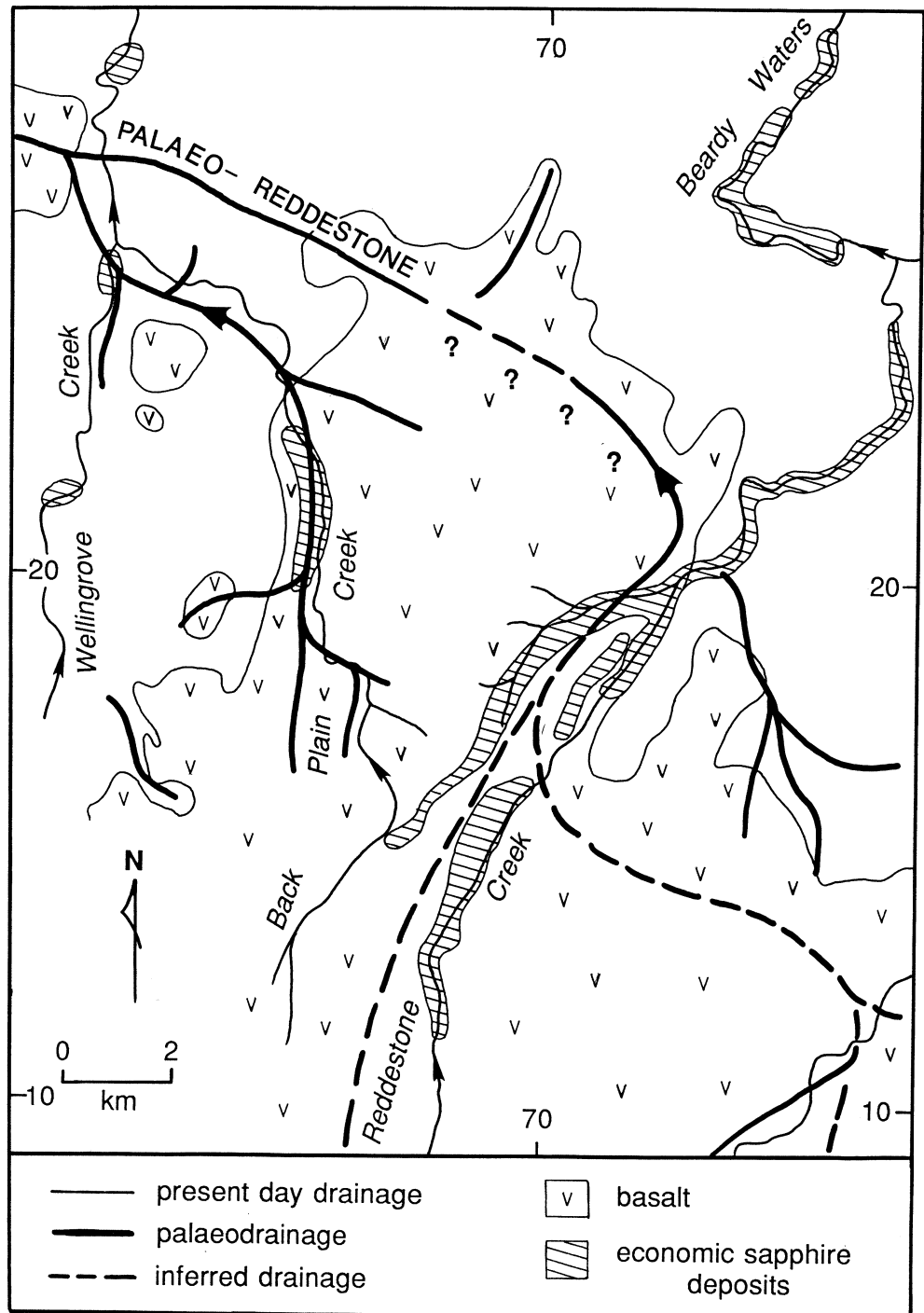


Figure 4-4. Economic Holocene sapphire deposits of the Reddestone Channel. Sapphires are associated with the present Reddestone Creek, both above and below the point of capture. Question marks indicate potential sapphire deposits associated with the now abandoned portion of the Reddestone palaeochannel

since the filling of the palaeovalleys with basalt, and the present drainage. However the locations of the sapphire deposits do not relate in detail to the position of the present low energy streams which meander across the alluvial floodplain.

Stream energies in the fluvial system must have been high enough to remove most weathered material, such as clays, downstream, but at the same time, not sufficiently high to disperse the heavy minerals of interest. In an ideally balanced system the heavy minerals tend to move vertically downwards, rather than downstream, and become concentrated with time. This is evident at a Public Fossicking Area (formerly a mining area) located at grid reference 630188 on the Glen Innes 1:25,000 sheet. Here, in a small valley, sapphires and zircons may be found in alluvium trapped in crevasses, and between boulders on Permian granodiorite. No basaltic and/or volcanoclastic source rocks remain in the present catchment area.

Concentration of sapphires is clearly favored by transporting weathering products of source rocks into smaller volumes or areas. The longer the process continues, the more effective will be the concentration of heavy resistant minerals. In contrast, a diverging, radially distributed drainage system will lead to a dispersion of the sought after gems. Both scenarios are illustrated in Figure 4-5.

The palaeotopography, palaeodrainage and present-day drainage at Kings Plains and Reddestone Creeks are shown in Figures 4-3 and 4-4. The present Kings Plains Creek flows within the palaeochannel until it is captured and diverted northward (GR:456220, Fig. 4-3). Borderline economic sapphire deposits, associated with Kings Plains Creek, exist to this point. When Arrawatta Creek eventually captures Kings Plains Creek (at GR:505215), the downstream deposits will no longer show any obvious association with the Kings Plains Creek. It is these types of abandoned channel deposits, which may otherwise be difficult to find, that are highlighted by palaeotopographic reconstruction.

Within the Reddestone palaeovalley, the present day creek has been captured and diverted northeastward (at GR:730204, Fig. 4-4). Economic sapphire deposits are associated with the present creek above and below this point.

The present study indicates that the Kings Plains palaeovalley should be explored further downstream from where the present Kings Plains Creek has been captured (at GR:456220). A comparison between Figures 4-3 and 4-4 indicates that there is the potential for sapphire deposits to be discovered along the now-abandoned palaeovalley, which continues northwestward from the point of capture of the present Reddestone Creek. Such channels may contain economic deposits if the original drainage existed for sufficient time to allow concentration to take place. The area is currently held under exploration licence by T.J. & P.V. Nunan Pty Ltd with a view to testing this prediction.

Detailed maps of the sapphire deposits are shown in Figures 4-6 and 4-7. The data were collected by T.J. & P.V. Nunan Pty Ltd, using one metre diameter bucket drills to penetrate the alluvium through to weathered bedrock (as shown in Colour Plate 11). Any gravels encountered, (generally just above the bedrock) were tested for their heavy mineral content. Data points are shown as dots, and contour lines indicate the depth to bedrock in

**DRAINAGE SYSTEM CONCENTRATION VERSUS DRAINAGE
SYSTEM DISPERSION AS THE KEY TO THE DEVELOPMENT
OF ECONOMIC SAPPHIRE DEPOSITS**

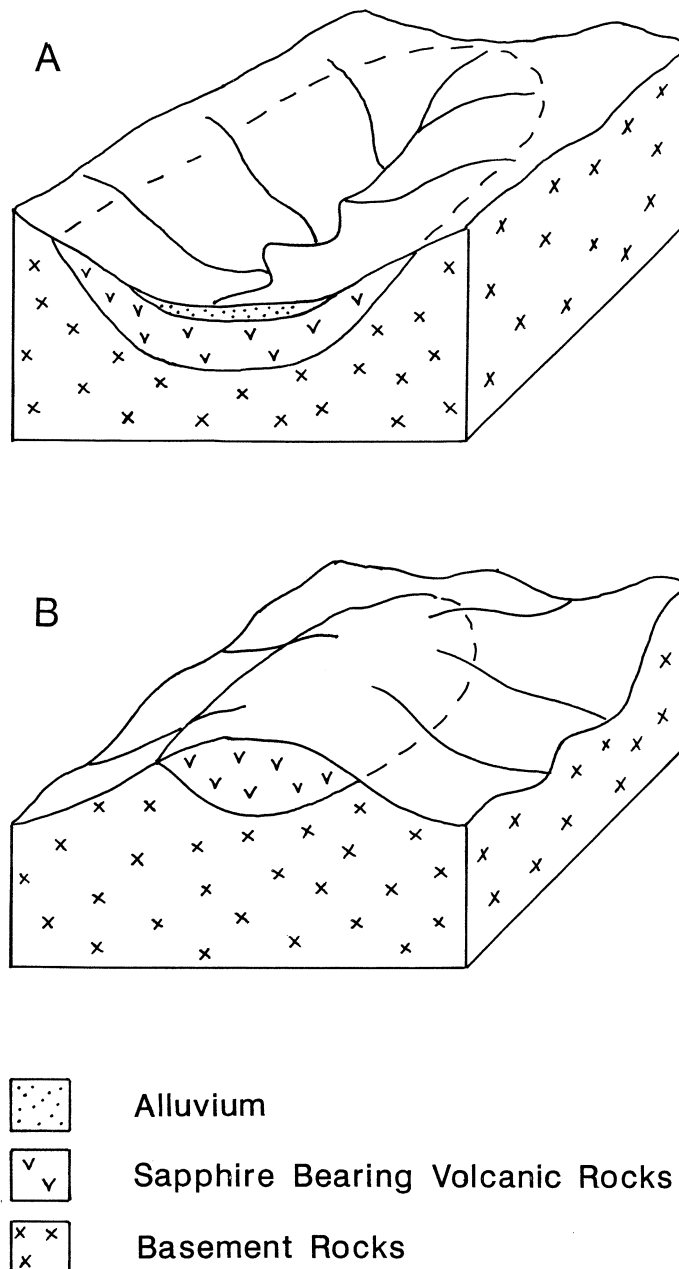


Figure 4-5. The development of economic sapphire deposits through stream concentration. In model A, streams concentrate material derived from a wide area of sapphire-bearing source rocks into a smaller area. In model B material derived from source rocks is dispersed over a larger area which will not promote the formation of economic deposits.

metres below the floodplain. The hatched areas indicate the position of sapphire bearing gravels, with concentrations of greater than 15 gm/m³ at Reddestone Creek (Fig. 4-6) and concentrations of greater than 50 gm/m³ at Kings Plains Creek (Fig. 4-7). Additional stipple indicates grades higher than 100 gm/m³ rising to an excess of 500 gm/m³ in some holes.

The maps indicate that the sapphire-bearing 'shoestrings' roughly coincide with the axis of the bedrock valley and that highest sapphire concentrations occur in deeper pockets or traps in the bedrock.

The bedrock is generally weathered basalt, or in some areas in Kings Plains, weathered silicic volcanics. Gravels generally lie on the weathered rock and include weathered basalt fragments, hard white nodules (cavity fillings of secondary mineralization from the basalt) and ironstone in a clay matrix. Quartz is noticeable where silicic volcanics form part of the channel. The sapphire-bearing "wash" occurs typically at a depth of about 4 to 9 metres, and is around 0.5 - 1 metre thick. The "wash" is overlain by fine sediments of the present floodplain.

The Reddestone and Kings Plains deposits postdate the majority of the basaltic activity (32-38 Ma), but weathered basalt overlies portions of the wash in the Western Feeder at Kings Plains (T. Nunan, pers.comm.) and at Braemar, where a K-Ar age of 23 Ma. was obtained for the overlying basalt (C.D. Ollier, pers comm.). Clays overlying the deposits at Reddestone Creek contain vertebrate fossils (Horton and Connah, 1981) which indicate a minimum age of 5000 years.

4.4 Braemar type deep-lead sapphire deposits

Potential sapphire deposits have been delineated in the Braemar palaeochannel and its tributaries up-palaeostream from the Braemar sapphire mine, in which sapphires are recovered along with other heavy minerals, with the highest concentration occurring at the base of the channel. "Braemar-type" deep lead deposits considered in this study had approximately 10 million years in which to form, and required the presence of a younger basalt capping (19-23 Ma) for their preservation.

Potential sapphire-bearing alluvials are also delineated along the topographically inverted palaeo-Swan Brook. The extent of these "deep lead" deposits to the east of Braemar, in palaeochannels that drained the sapphire-bearing East Central Province, is related to the easternmost incursions of the lavas of the West Central Province.

The Braemar sapphire deposit is located along the Gwydir Highway 18.5 kilometres east of Inverell, New South Wales (Figs. 4-8, 4-9 and 4-10). The sapphire-bearing material, exposed in Mr. Col Rynnes quarry on the side of a hill, has a tuffaceous/brecciated appearance and is overlain by a flow-basalt (Fig. 4-11; Colour Plate 7). Braemar was recognized by the New South Wales Government Department of Minerals and Energy geologists as being particularly important because of its non-

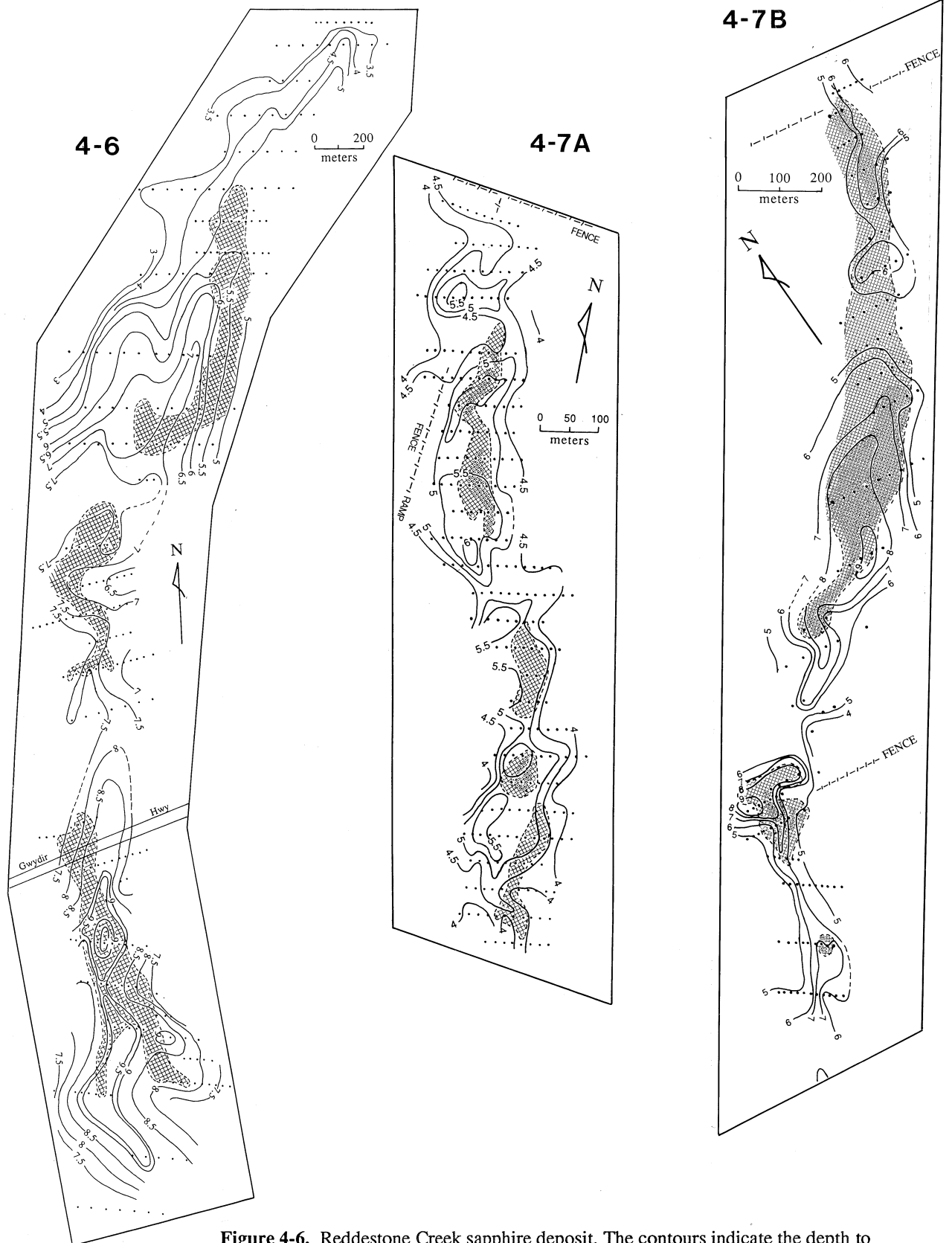


Figure 4-6. Reddestone Creek sapphire deposit. The contours indicate the depth to the weathered basalt below the Reddestone Creek floodplain. The hatched areas indicate sapphire concentrations in river gravels overlying the basalt of greater than 15 grams per cubic metre.

Figure 4-7. Kings Plains Creek sapphire deposits, showing A, the Western Feeder and B, the Eastern Feeder. The contours indicate the depth to weathered bedrock below the Kings Plain floodplain. The hatched areas indicate sapphire concentrations of greater than 50 grams per cubic metre. The areas with additional stipple contain greater than 100 grams per cubic metre with some holes yielding in excess of 500 grams per cubic metre. Note the association of the richer patches with deeper areas in the stream channel. The location of these deposits is shown in Figure 3-2.

conventional setting (being on a hillside), and thereby presenting new opportunities for sapphire exploration in the New England region, and also in many of the other eastern Australian volcanic provinces. A seminar entitled "Tertiary Volcanics and Sapphires in the New England District" was held by the New South Wales Department of Minerals and Energy on the 1st May 1987 to promote research and exploration.

Since an initial model for Braemar was proposed by Lishmund and Oakes, (1983), in which the deposit was considered to be tuffs and breccias formed around a diatrema, a significant amount of further work has been carried out in the area. The sapphire-bearing sediments at Braemar were first considered to be palaeochannel deposits by Temby (1986) owing to their appearance and the discovery of cassiterite, derived from the Permian basement, in heavy mineral concentrates. Drilling by Brown and Pecover (1986) confirmed that the sediments lie in deep basement channels.

The physical processes involved in the concentration of sapphire and other heavy minerals as placer deposits in the Braemar palaeochannel appear to be similar to those which formed the major sapphire deposits at Kings Plains and Reddestone creeks (Coenraads, 1990). Braemar is unique, however, in that it is situated in an area in which the younger (19-23 Ma.) volcanics of the West Central Province overlap onto the older (32-38 Ma.) volcanics of the East Central Province (Fig. 4-8). The sapphire-bearing, intrabasaltic sediments contain minerals which are derived from the older volcanic rocks, as demonstrated by Hollis & Sutherland, (1985) from a fission track age of 37 Ma. for a zircon from Braemar. The sediments are overlain by a basalt flow dated at 23 Ma. (C.D. Ollier, pers. comm.) and must therefore have an age of between 23 and 37 Ma.. McMinn (1989) reached a similar conclusion, dating the sediments as Eocene/Oligocene on the basis of palynology.

At least two generations of sapphire-bearing alluvial deposits exist at Braemar (Temby, 1986; Pecover & Coenraads, 1989) (Figs. 4-10, 4-12 and 4-13). The oldest economic deposits lie in a palaeochannel exposed in a quarry (Fig. 4-11; Colour Plate 7), and are worked intermittently by Mr. Col Rynne. The deposits are Eocene/Oligocene in age, and are clay-rich, white and grey, fluvio-lacustrine and tuffaceous sediments with the highest grades of sapphires occurring at the base of the channel amongst weathered basalt boulders which range in size up to half a metre. These earlier sapphire-bearing alluvials have been preserved by a capping of basalt. The youngest deposits at Braemar are Holocene alluvial gravels which are situated in Schumachers Gully and its tributaries (Figs. 4-15 and 4-16). They have undergone at least two cycles of reworking and deposition and, as a result, are the richest deposits with the highest proportion of gem-quality sapphire (C. Rynne, pers. comm.).

Zircon, ilmenite and chrome-spinel are associated with the sapphire at Braemar (Temby, 1986; Slansky, 1987; Coenraads, 1990). Cassiterite is also found in small quantities where Permian basement rocks have been reworked (Temby, 1986; Slansky, 1987) and two diamonds have been reported (J. Rynne, pers. comm.). Chrome-spinel and

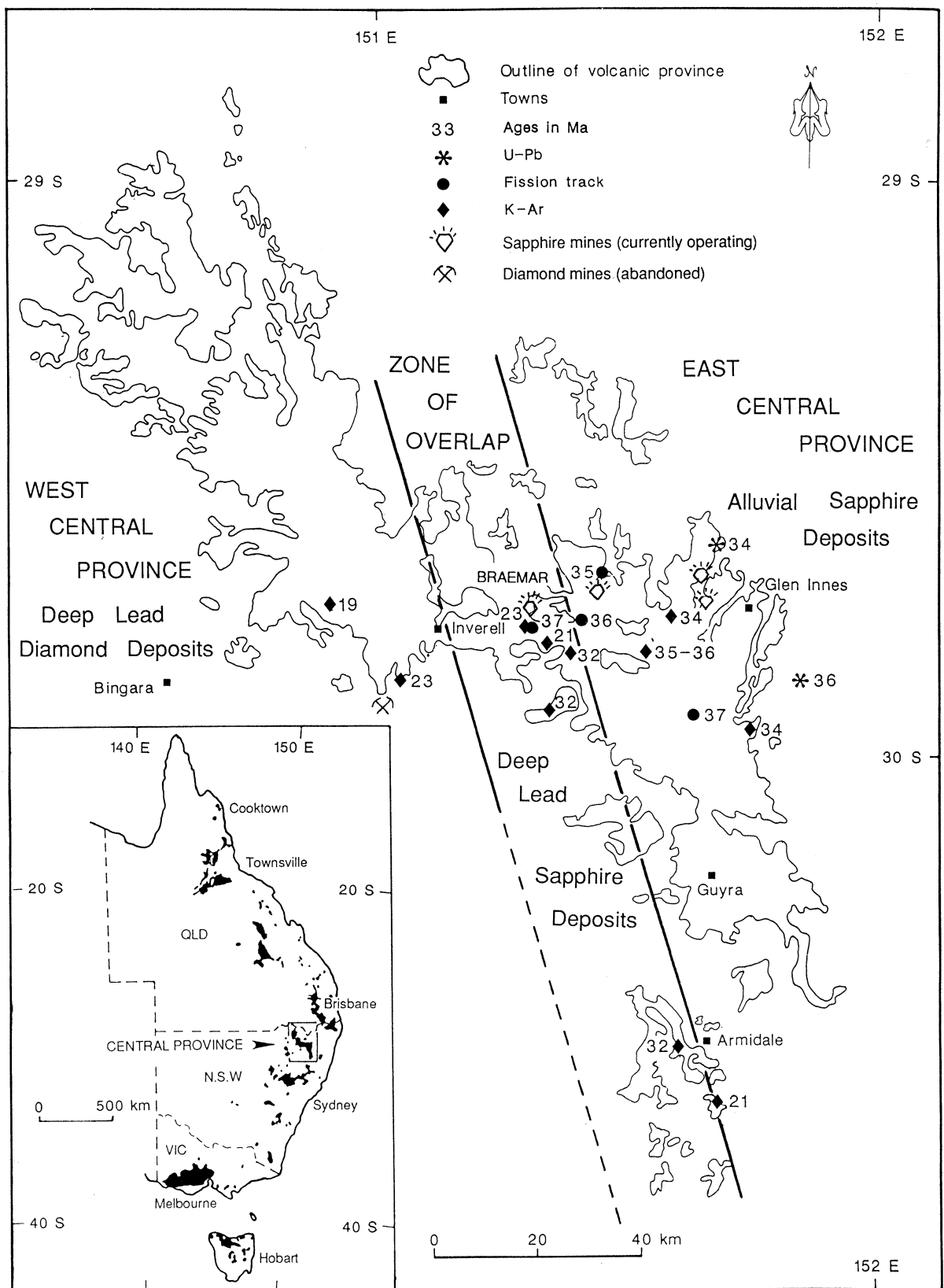
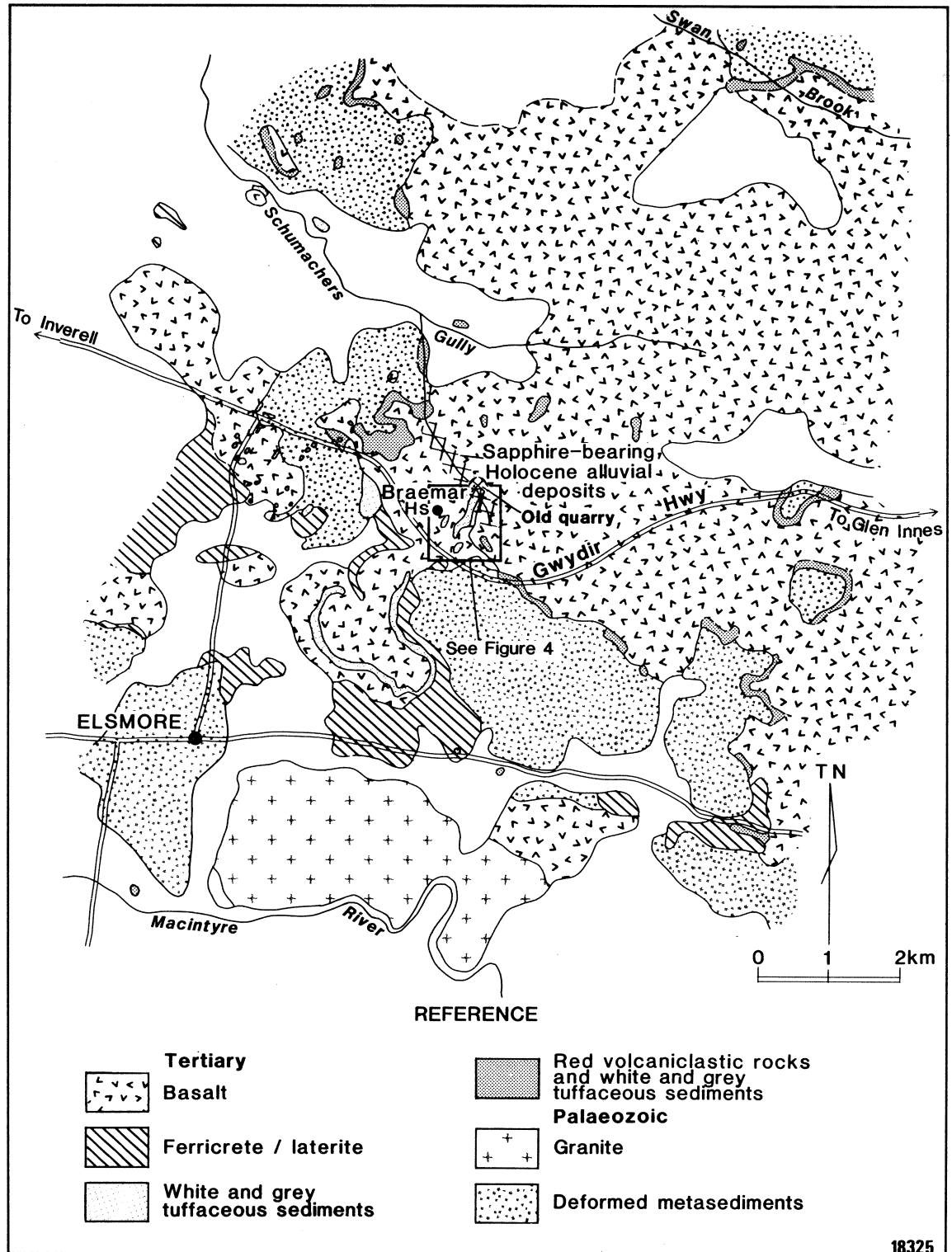


Figure 4-8. Location of the Braemar sapphire deposit in the zone-of-overlap between the East and West Central Provinces. Locations of age data for the Central Province are shown (sources of data listed in Coenraads et al, 1990).



18325

Figure 4-9. Location of the Braemar sapphire deposit in relation to the geology of the Elsmore-Swan Brook area (modified after Brown & Pecover, 1986). Detailed geology at Braemar is shown in Figure 4-10.

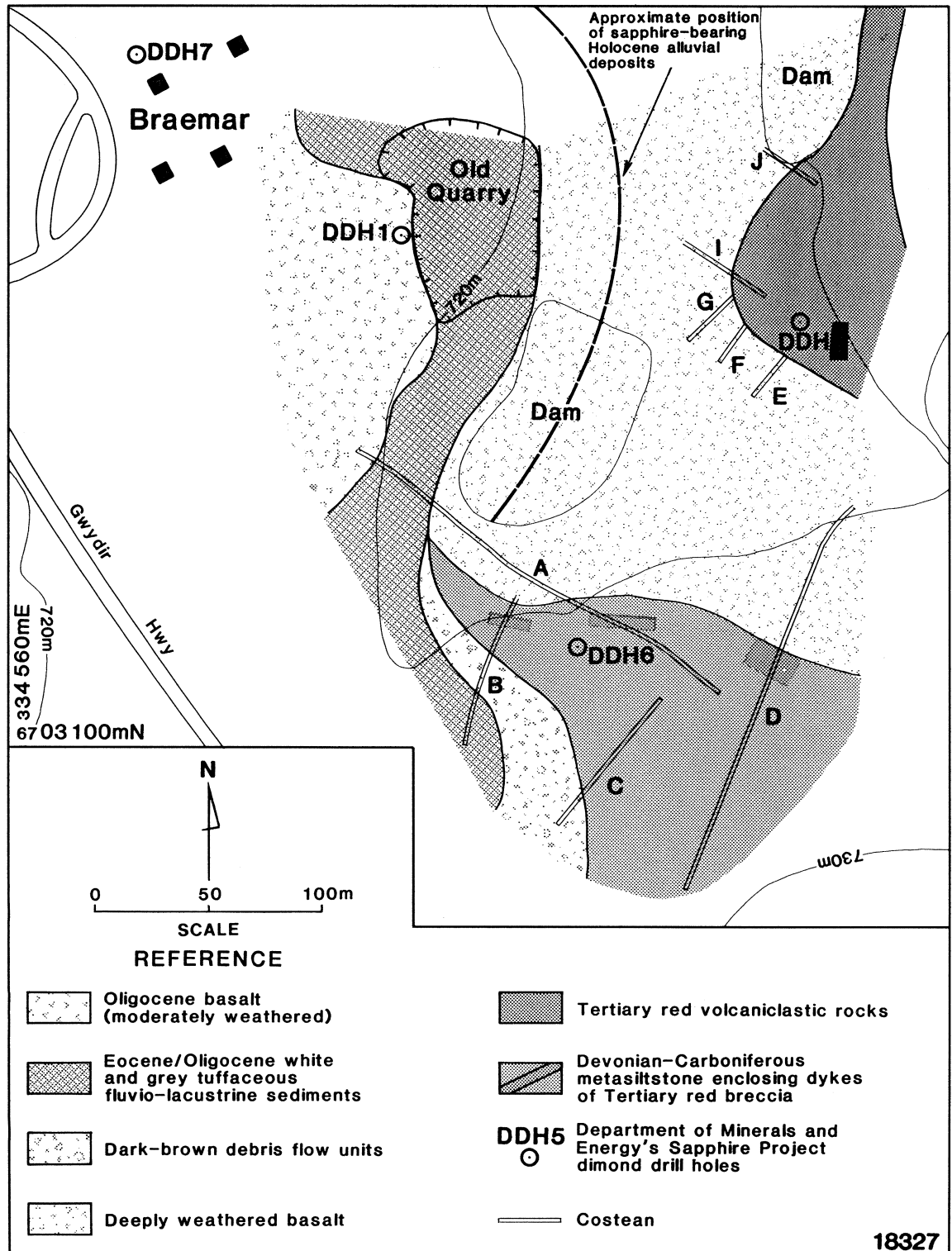


Figure 4-10. Reconstruction of the surface geology at Braemar based on isolated surface outcrops, Department of Minerals and Energy's diamond drill holes DDH 1, 5, 6 & 7, costeans A to J, and the old quarry (after Pecover and Coenraads, 1989).

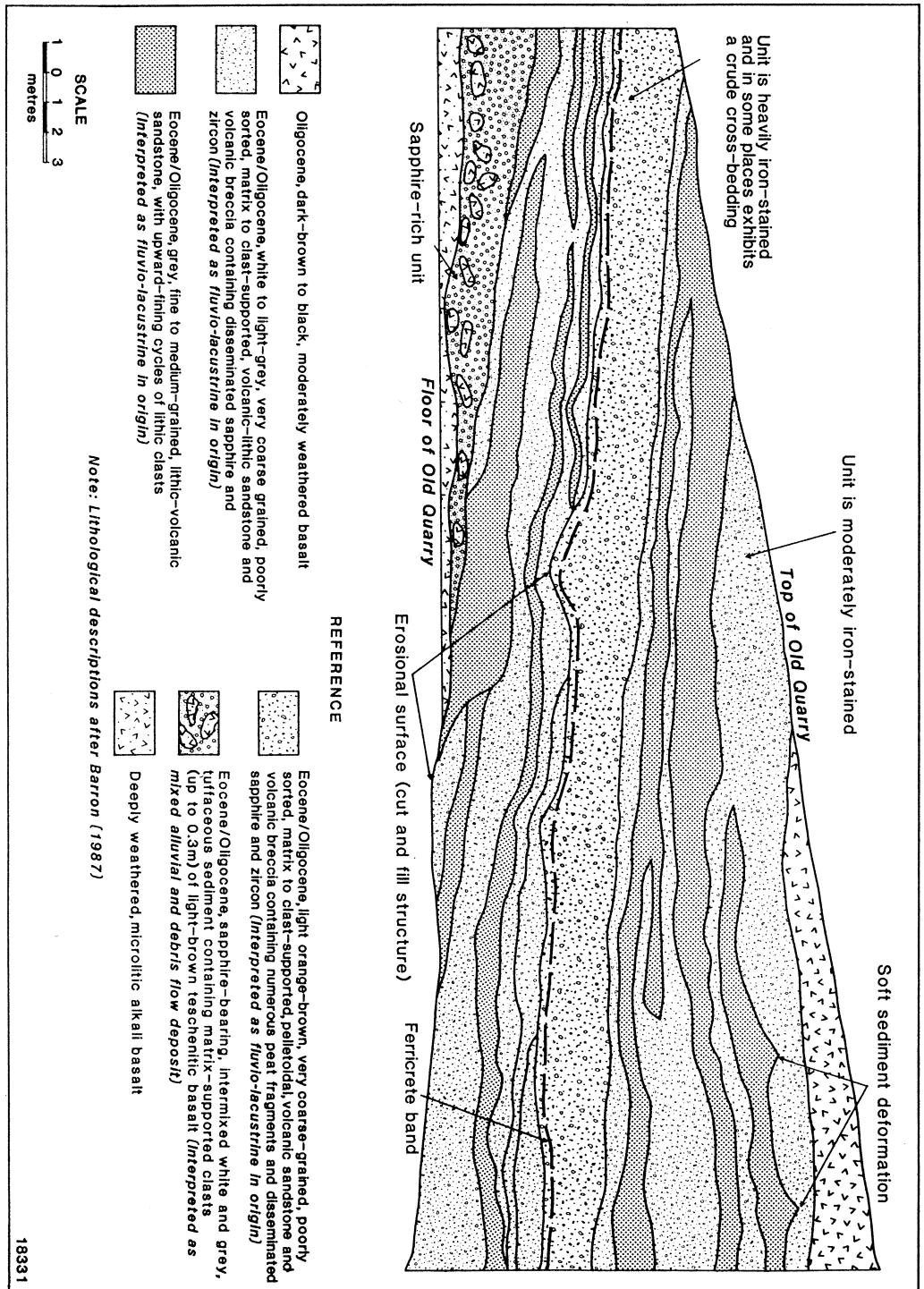


Figure 4-11. Stratigraphy of the old quarry (south-west face) at Braemar (circa 1986). See Figures 4-9 and 4-10 for location of the old quarry (after Pecover and Coenrads, 1989). See also Colour Plate 7.

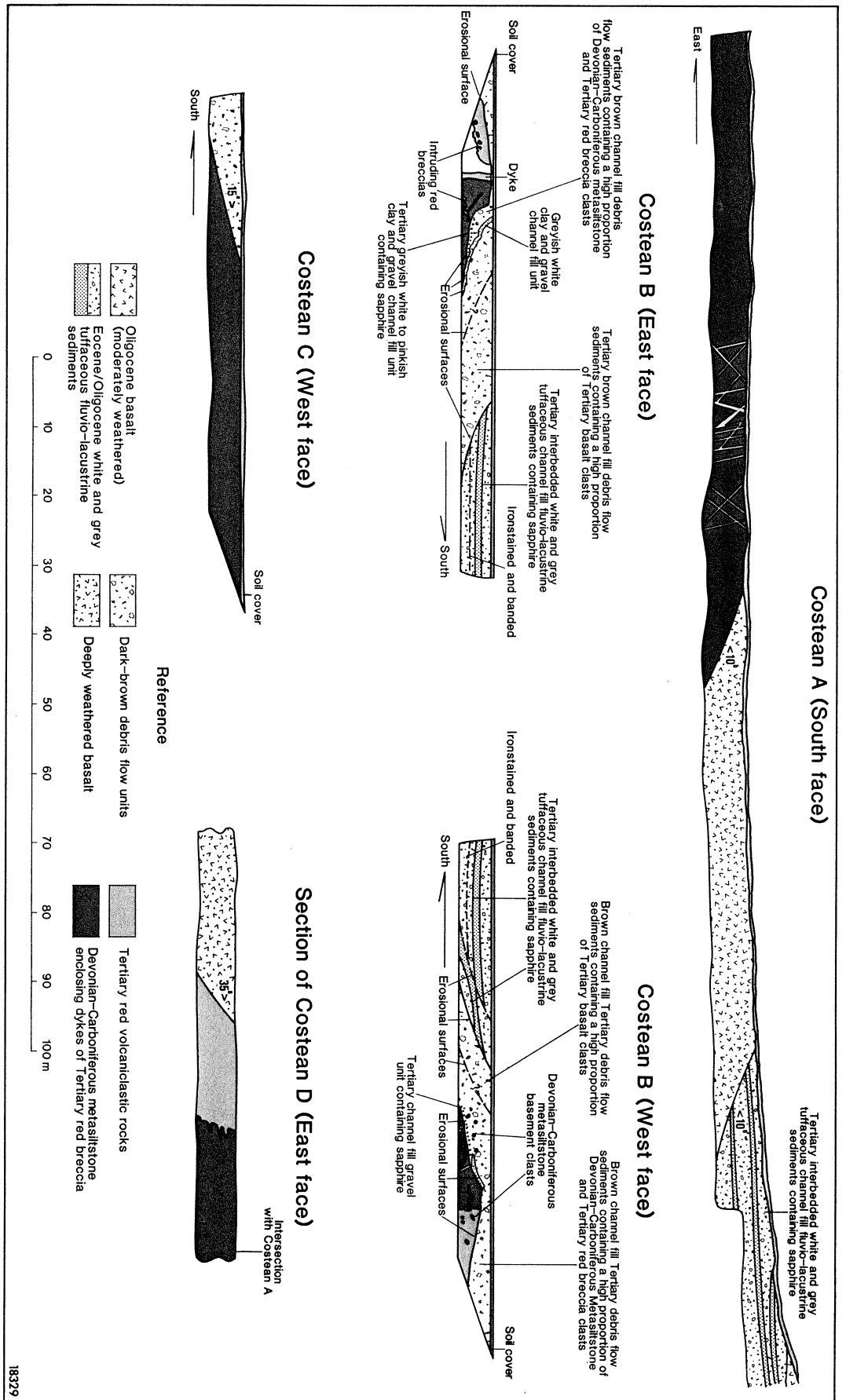


Figure 4-12. Stratigraphic and intrusive relationships evident in costeans A to D. Figure 4-14 shows detail of the dyke exposed in costean B (south-east face). See Figure 4-10 for location of costeans.

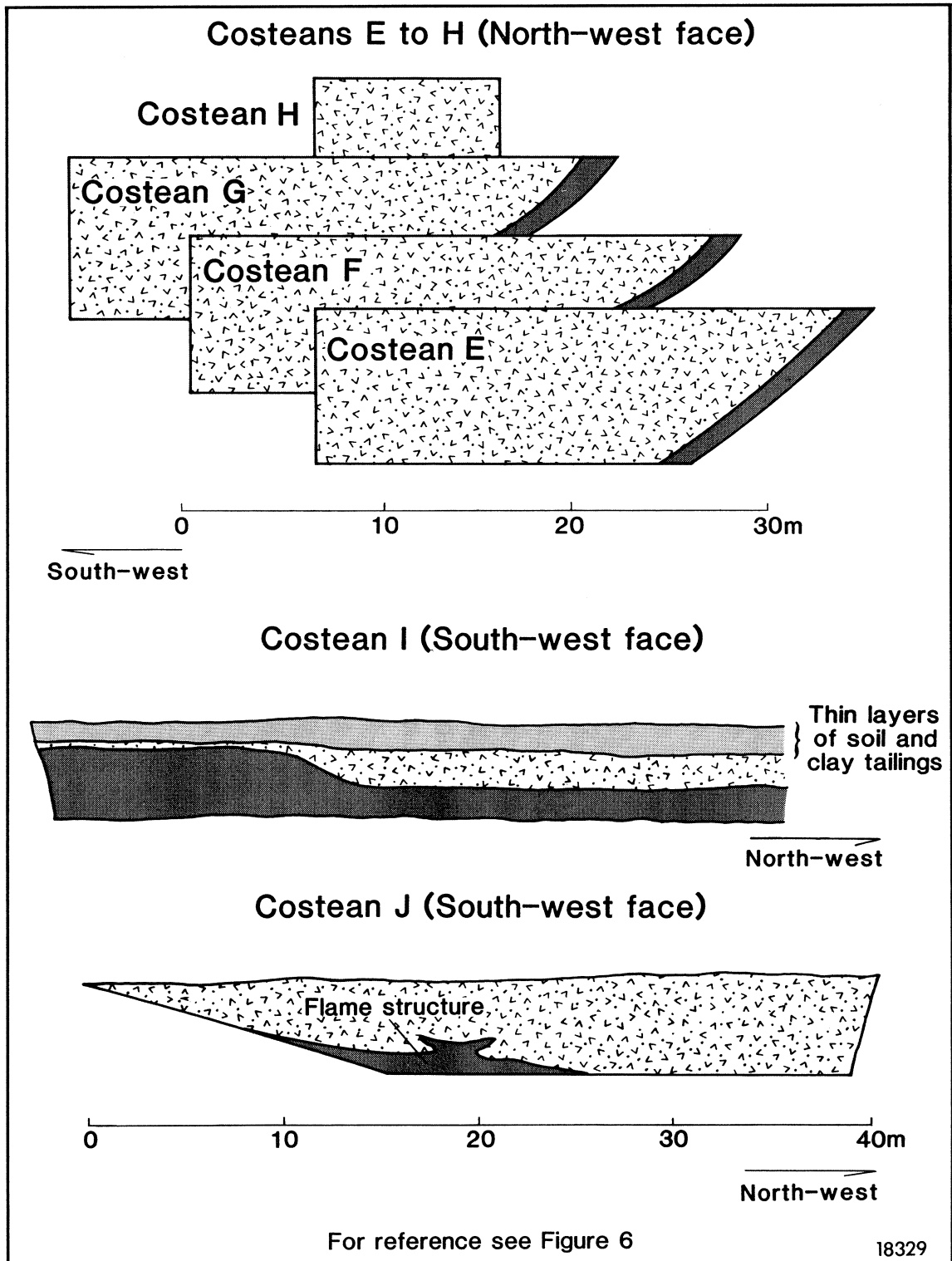


Figure 4-13. Stratigraphic and intrusive relationships evident in costeans E to J.
See Figure 4-10 for location of costeans.

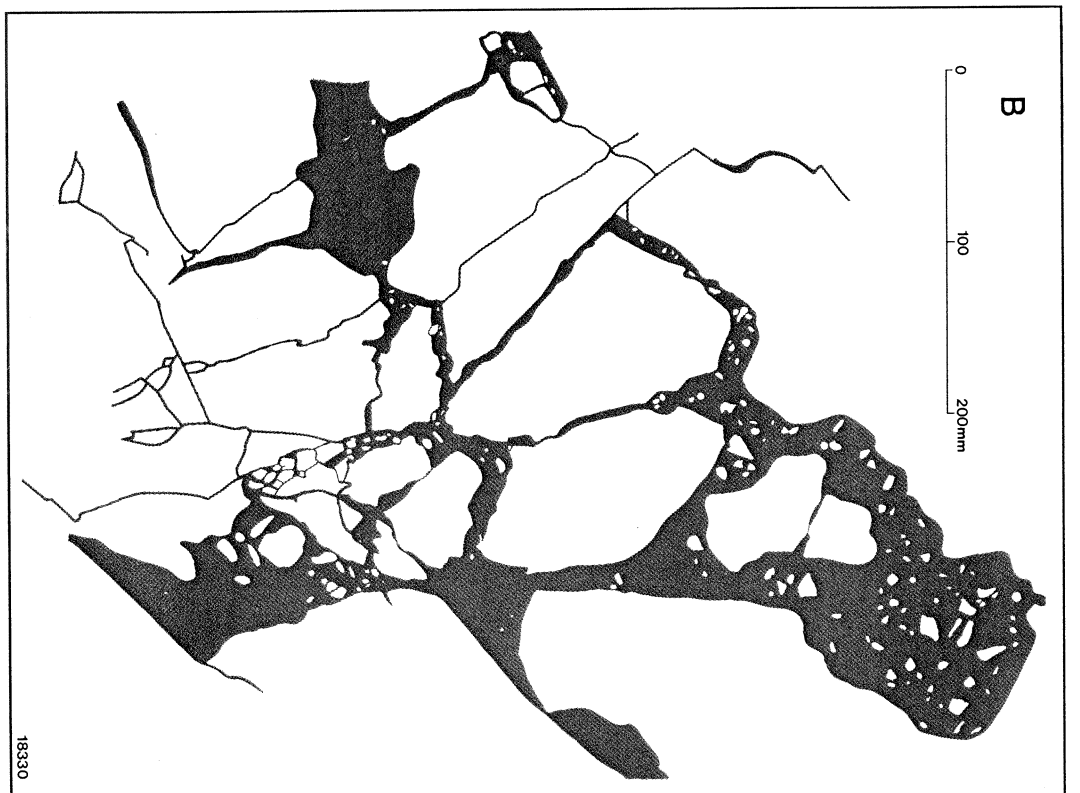
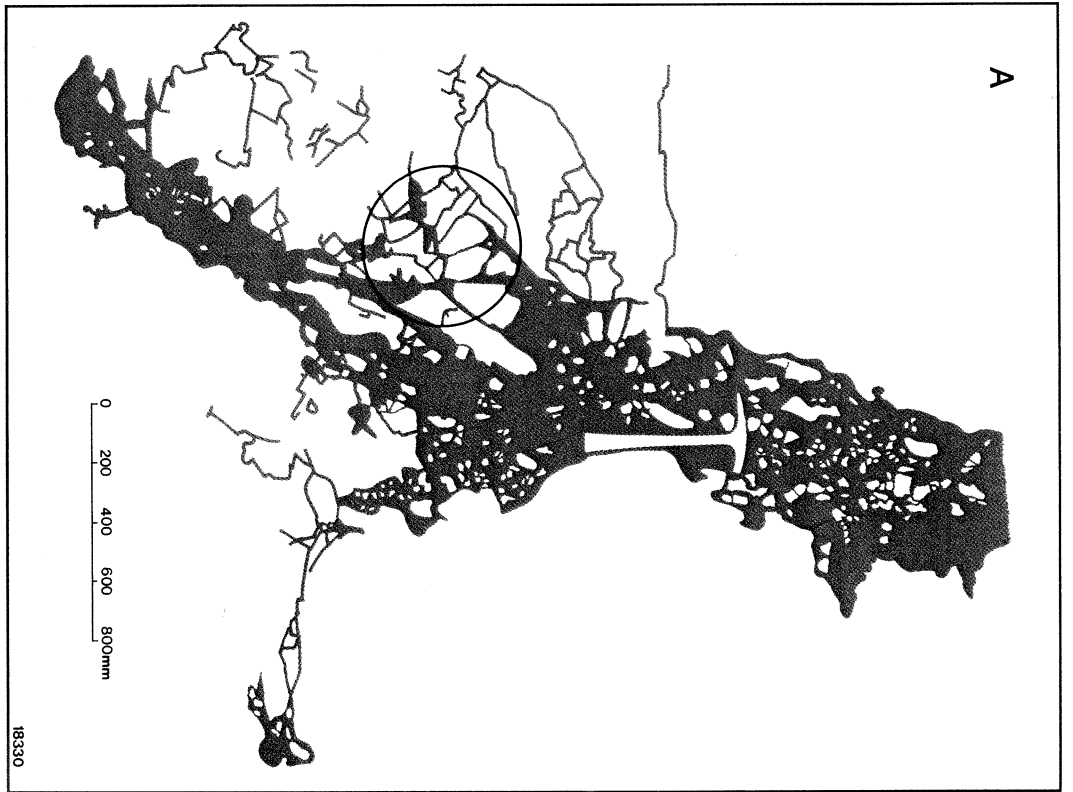


Figure 4-14. Part A, breccia dyke exposed in costean B (south-east face) comprising red, fine grained, highly ferruginous volcanic rock intruding light-coloured Devonian-Carboniferous metasilstone. Part B, blow-up section of dyke wallrock (circled in part A) showing jig-saw fit of hydraulically fractured metasilstone intruded by red, fine grained volcanic rock. See Colour Plate 8. Concentrates of the dyke material yielded chrome-spinel, ilmenite and pleonaste. See Figure 4-12 for location of dyke.

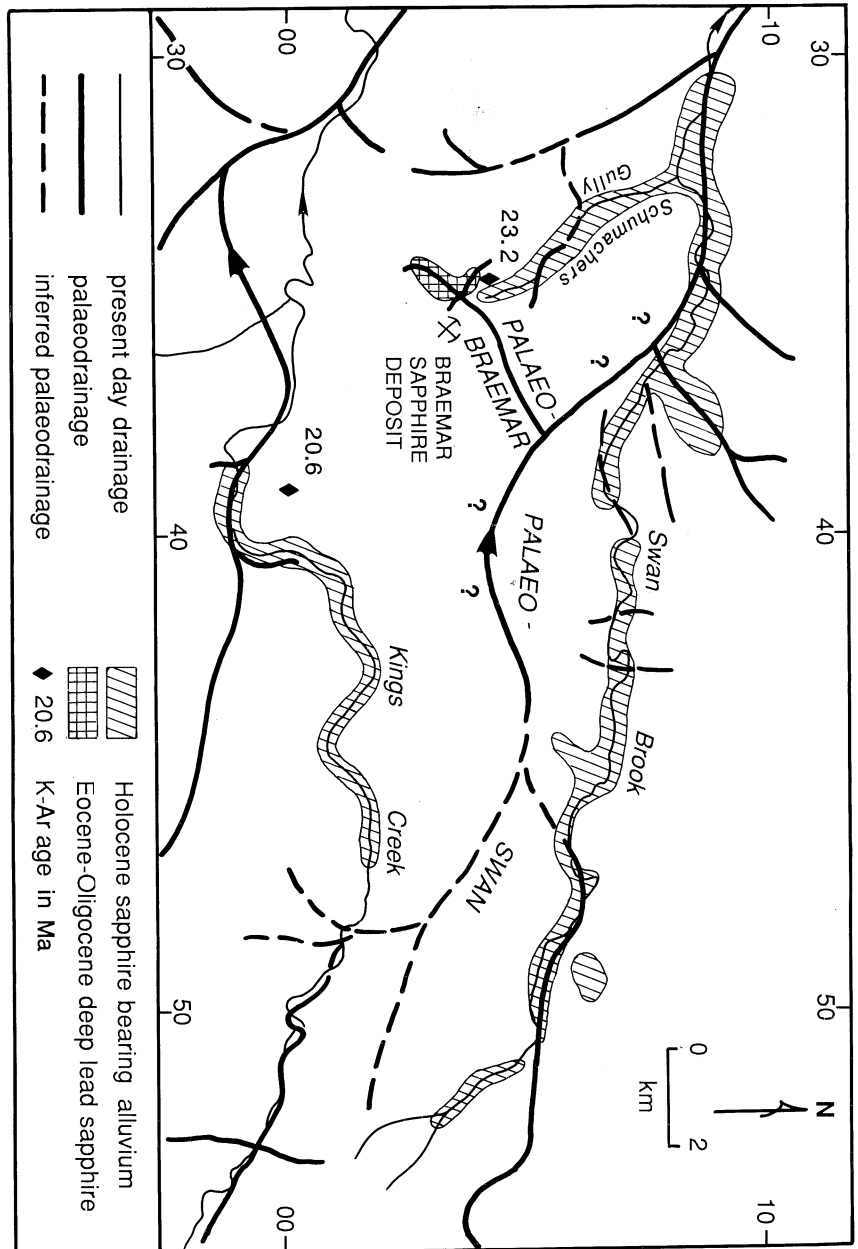


Figure 4-15. Distribution of Eocene/Oligocene deep lead sapphire deposits and Holocene sapphire-bearing alluvium. The Braemar deposit is associated with the Braemar palaeochannel and the nearby Holocene deposits in Schumachers Gully are reworked from them. The potential for further deep lead deposits associated with the palaeo Swan Brook (now a table-top ridge) is highlighted by question marks. Such deposits may be responsible for shedding sapphire into the soils flanking the ridge and the lateral streams, Swan Brook and Kings Creek. Location of K-Ar ages are also shown.

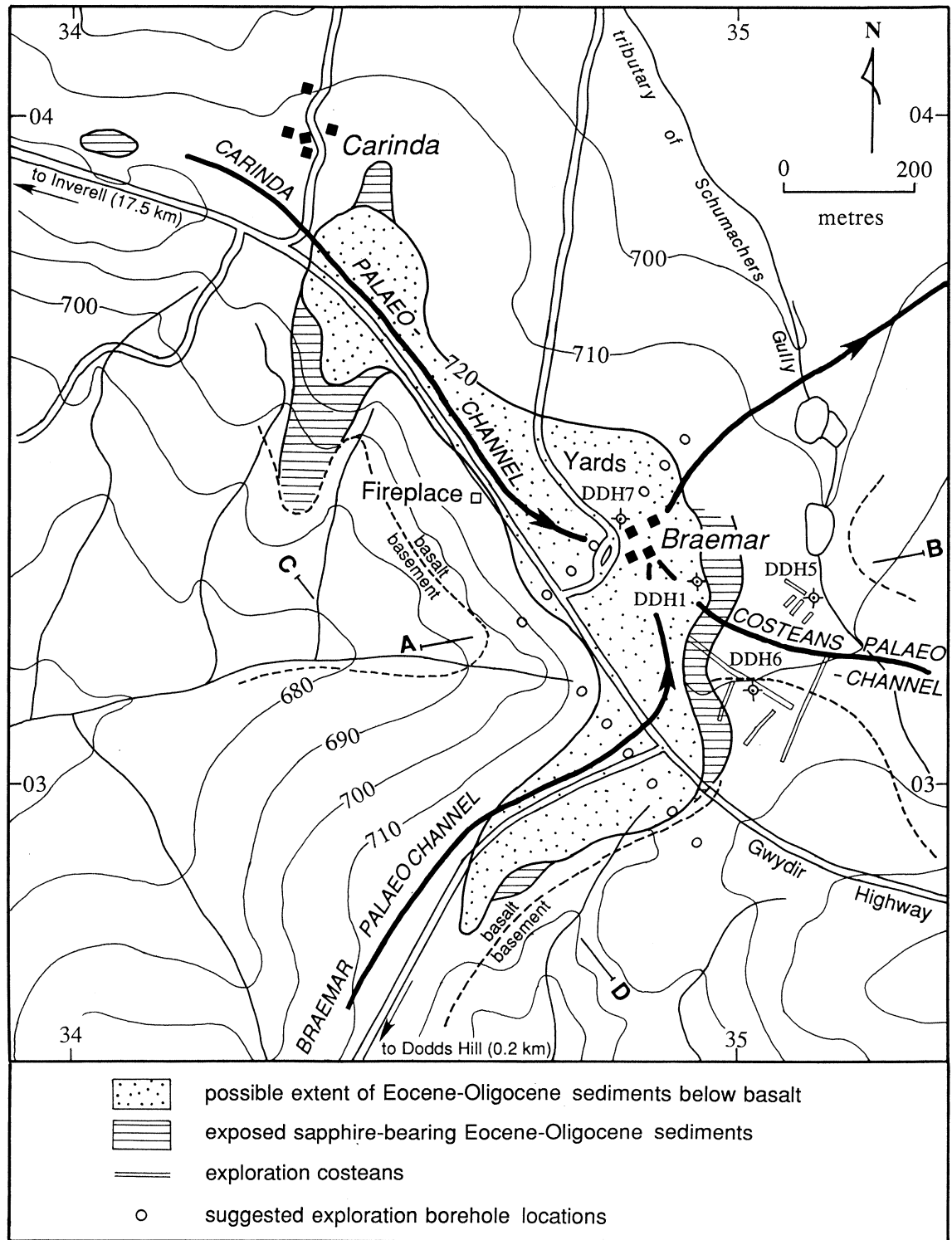


Figure 4-16. Eocene/Oligocene sapphire-bearing sediments at Braemar. Their proposed extent beneath a capping of 23.2 Ma. basalt is indicated as the stippled area bounded approximately by the 720 m elevation contour. The positions of the Braemar, Carinda and Costeans palaeochannels are shown, and two lines of exploration bore holes, one incorporating DDH 7, are proposed to test the extent of the deposits in these palaeochannels. The location of DDH 1, 5, 6 and 7; the exploration costeans; Braemar and Carinda homesteads; and the locations of sections AB and CD are also shown.

ilmeneite have also been recovered from the intrusive red breccias at Braemar (Fig. 4-14; Colour Plate 8).

Braemar is the only mine known to the author where sapphires are recovered from below basalt, although, further west in the Copeton and Bingara areas, diamond-bearing deep leads have been worked sporadically since 1872.

The aims of this section are as follows:

1. To use a palaeotopographic reconstruction technique, based on the elevation of the basalt-basement contact and available drill hole data, to determine the course of the palaeochannel in which the Braemar sapphire deposit is situated.
2. To define the extent of the Eocene/Oligocene sapphire-bearing sediments lying below 23 Ma. basalt in the Braemar palaeochannel and its tributaries.
3. To define other palaeochannels in the area of influence of the 19-23 Ma. basaltic lavas likely to have undergone a similar series of events and hence also likely to contain deep lead sapphire.

4.4.1 Sapphire-bearing palaeodrainage systems near Braemar

The palaeotopography of the Braemar area was mapped using the elevation of the basalt-basement contact based on detailed geologic mapping by Temby (1986), Brown & Pecover (1986), Brown (1987), Stroud (1989) and Pecover & Coenraads (1990). The positions of the palaeochannels can thus be better constrained, particularly in the Braemar area, than the position inferred by Temby (1986) based on the regional distribution and grainsize of outcropping sub-basaltic sediments

The sapphire-bearing Eocene/Oligocene fluvio-lacustrine sediments are situated in a basalt-filled, northeasterly trending tributary of the palaeo-Swan Brook, referred to as the "Braemar palaeochannel" (Figs. 4-15 and 4-17). A tongue of basalt extending towards Dodds Hill, south of Braemar (Figs. 4-16 and 4-17), is apparently an upstream continuation of the Braemar palaeochannel. Two smaller tributaries join the Braemar palaeochannel in the vicinity of Braemar Homestead (Fig. 4-16); the larger of the two trends southeasterly from Carinda Homestead (the Carinda Branch) and the smaller, trending westerly (the Costeans Branch), has been exposed in the exploration costeans mapped by Pecover and Coenraads (1989) (Figs 4-12 & 4-13). Diamond drill holes DDH 1 and DDH 7 at Braemar (Brown & Pecover, 1986) indicate that this channel is filled with at least 60 m of flow-basalt. Fig. 4-18 shows cross sections, AB and CD, of the Braemar palaeochannel. Section AB incorporates the data from drill hole DDH 1 (Brown & Pecover, 1986). The locations of the sections are shown on Fig. 4-16. The present day

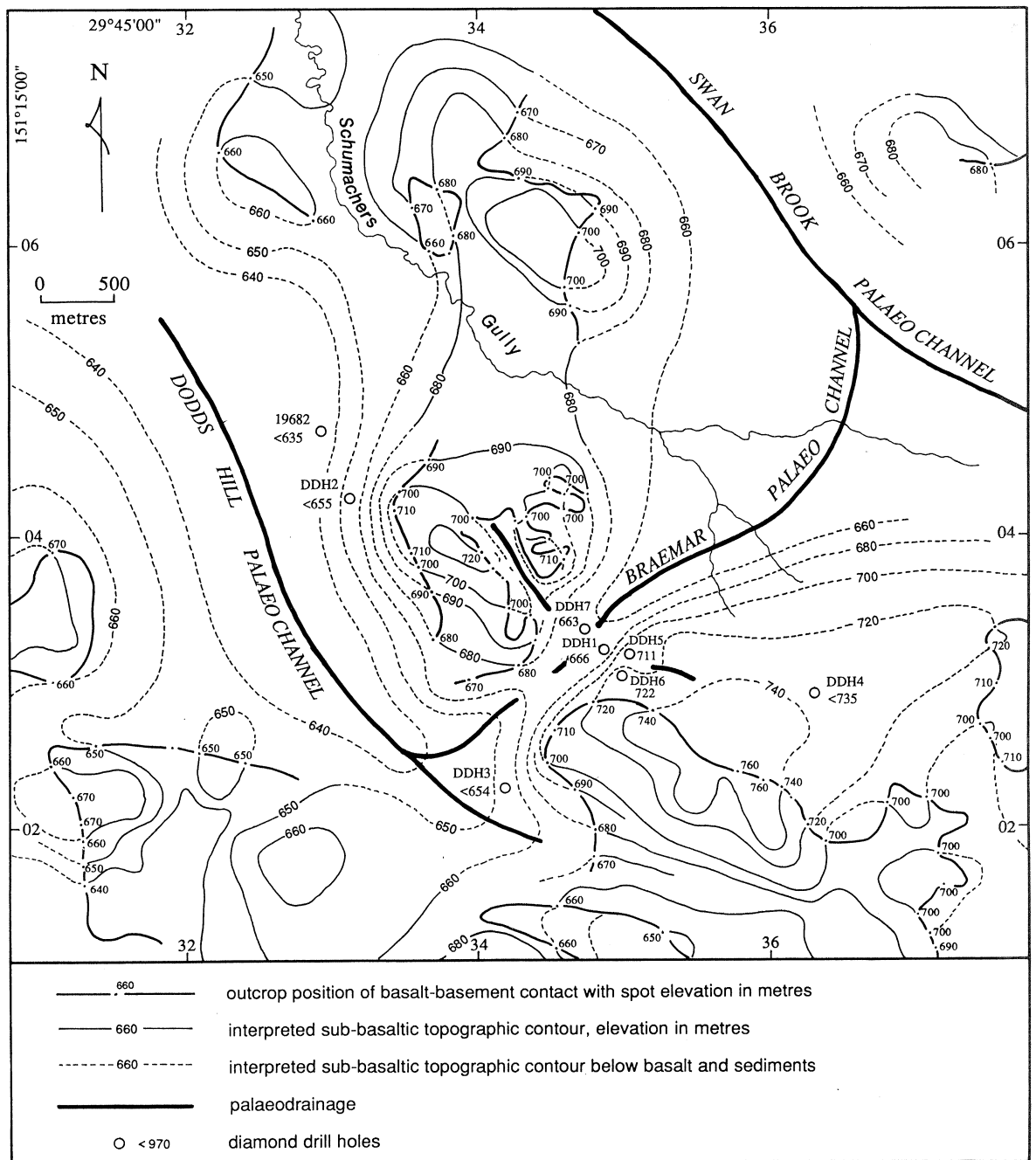


Figure 4-17. Positions of the Braemar and Swan Brook palaeochannels as determined by basement palaeotopographic analysis on the Elsmore 1:25,000 sheet. The two tributary palaeochannels join the palaeo-Braemar in the vicinity of diamond drill holes DDH1 and DDH7, shown in detail in Fig. 4-16. The contours indicate the interpreted topographic surface prior to the 32-38 Ma. basaltic eruptions.

topography (Fig. 4-16) and the sections, indicate that lateral stream activity, post dating the 19-23 Ma. basalt flows, has begun to invert the topography.

Diamond drill holes DDH 2 at McCarthys Knob and DDH 3 at Dodds Hill (Brown & Pecover, 1986) support the presence of another palaeochannel that heads in a northwesterly direction from Dodds Hill (Figs. 4-15 & 4-17) and eventually joins the palaeo-Swan Brook. DDH 2 & 3 did not reach basement rocks, but penetrated some 45 metres of white and grey, tuffaceous and fluvio-lacustrine channel fill sediments similar to those exposed in the Braemar quarry. The accumulation of such a major sedimentary sequence is thought to be due to a damming of the westerly flowing palaeochannels by faulting associated with the Severn Thrust (Temby, 1986). Alternatively, the damming may have occurred as a result of uplift and volcanism of the West Central Province which also appears to have been responsible for the deflection of the major westerly flowing rivers such as the Gwydir and Macintyre (Coenraads, 1990). Local evidence for the damming of streams by lava flows is reported by Smith (1989).

The present-day Schumachers Gully and its tributaries flow at right angles to the former flow direction of the Braemar palaeochannel (Fig. 4-16). They flow to the northwest across rocks and sediment filling the Braemar palaeochannel and then onto late Palaeozoic metasedimentary basement. The Holocene alluvials, which have been mined for sapphires in the tributaries of Schumachers Gully, are apparently reworked mainly from the Eocene/Oligocene sediments associated with the Braemar palaeochannel (Pecover and Coenraads, 1989).

4.4.2 Extent of the Eocene/Oligocene sapphire-bearing sediments below basalt near Braemar

The Eocene/Oligocene sapphire-bearing sediments at Braemar are associated with the Braemar palaeochannel and were preserved by a protective capping of 23 Ma. basalt. Locally the base of the young basalt appears to be at about 720 m above sea level. White and grey, tuffaceous and fluvio-lacustrine sapphire-bearing sediments are exposed below the basalt at this level in the quarry at Braemar (Pecover & Coenraads, 1989) (Fig. 4-11; Colour Plate 7). Similar material outcrops close to this level, south of the Gwydir Highway and near Carinda (Fig. 4-16) and has been mapped by Brown & Pecover, (1986). Based on this level, the 23 Ma. basalt cap is interpreted to extend up-palaeostream in both the Braemar palaeo-channel and the Carinda tributary. It is predicted that sapphire-bearing sediments exist beneath a thin basalt cover within the stippled area in Fig. 4-16. White and grey volcanoclastic sediments have also been mapped by Brown & Pecover (1986) at about 690 to 710 m along the sides of the palaeochannel heading northwest from Dodds Hill, in the vicinity of Dodds Hill and also south of the Gwydir Highway in the vicinity of McCarthys Nob.

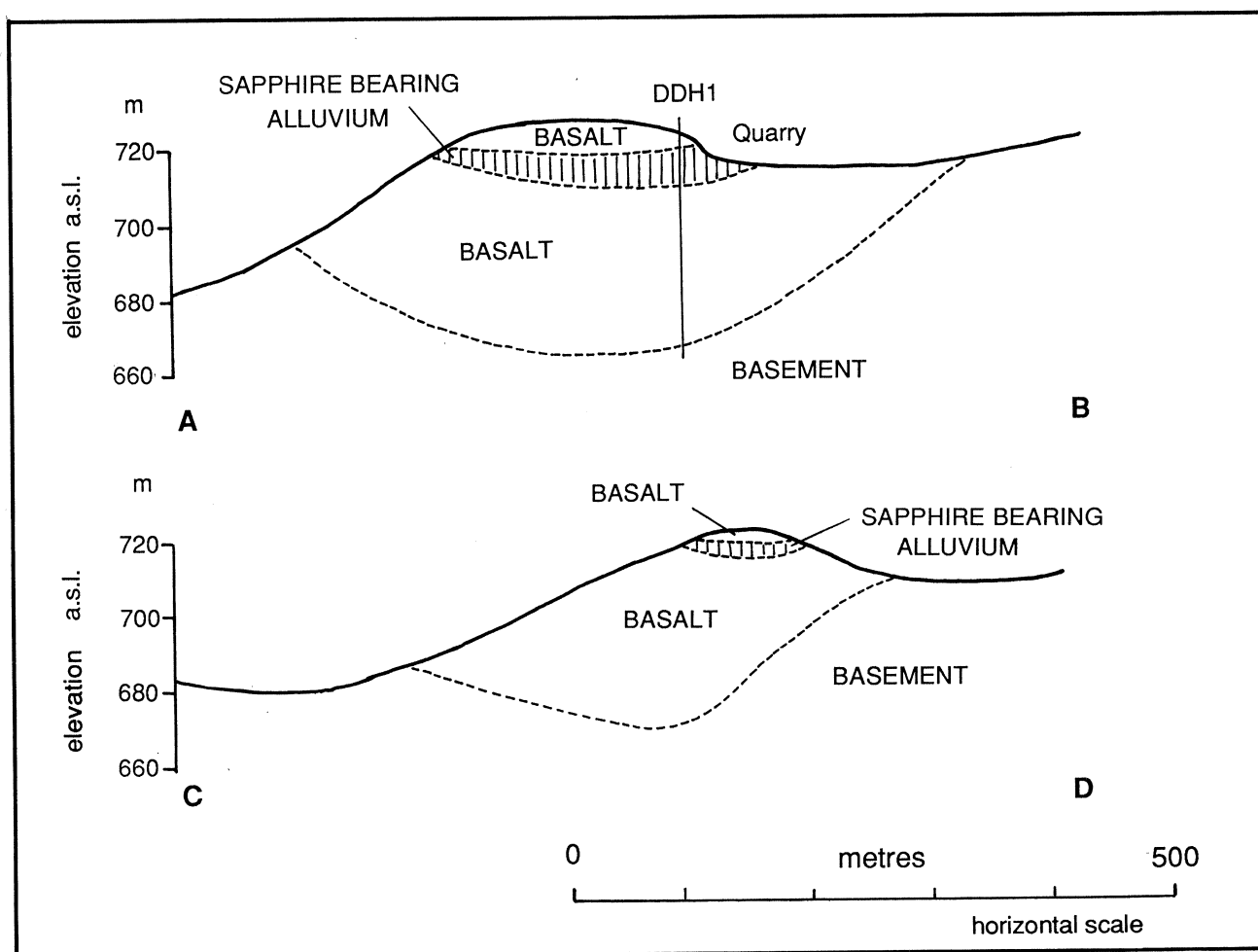


Figure 4-18. Cross sections, AB and CD, of the Braemar palaeochannel looking north. The assumed extent of the Eocene/Oligocene sapphire-bearing sediments beneath the 23.2 Ma. basalt cap is shown. The Braemar Quarry and DDH 1 are shown on section AB. The location of the sections are shown on Fig. 4-16.

Diamond drill holes DDH 2 and DDH 3 indicate the sediment in the Dodds Hill Palaeochannel (Fig. 4-15) to be more than 5 times thicker than that in the Braemar palaeochannel. Hence the axial deposits, with presumably the highest sapphire concentrations, are predicted to be deep and therefore difficult to test and extract. The exploration licence (E.L.2987) for this area was held by Hooker Resources Pty. Ltd. (Pithers, 1988) and at the time of preparation of this thesis, their findings were confidential.

In the downstream direction along the Braemar palaeochannel, in the vicinity of Schumachers Gully and its tributaries, the basalt cap is absent. It is unknown however, whether the young basalt is again present as the terrain rises at, and beyond, the intersection of the Braemar palaeochannel with the palaeo-Swan Brook.

4.4.3 Implications of the Braemar deposit in the search for similar deposits in the zone-of-overlap between the East and West Central Provinces

The sapphire-bearing Eocene/Oligocene sediments at Braemar are associated with the basalt-filled Braemar palaeochannel which is a tributary of the palaeo-Swan Brook. Similar sediments also exist immediately to the south of Braemar in the Dodds Hill palaeochannel which also joins the Swan Brook palaeochannel. The deposits are protected by a capping of younger basalt, and demonstrate that similar deposits may exist elsewhere in the zone-of-overlap between the East Central Province and the West Central Province. Owing to the limited number of ages available for the Central Volcanic Province, the extent of the zone-of-overlap can only be approximately defined by the lines shown on Fig. 4-8. The existence of similar "Braemar-type" deep leads further to the east is dependent on the presence of younger basalts further east of Braemar in the Swan Brook and other palaeochannels.

The ages of the volcanic rocks in the vicinity of Braemar are shown in Figs. 4-8 and 4-15. An age of 20.6 Ma. (Smith, 1988) at grid reference GR:389001 on the Elsmore 1:25,000 topographic sheet (Fig. 4-15) demonstrates that young basalt, and hence the potential for deep lead "Braemar-type" deposits, extends eastward at least as far as this location. Such deposits, if present, would exist on or close to the axis of the relief-inverted palaeochannels, such as the flat-topped basalt ridge running along the axis of the topographically inverted palaeo-Swan Brook (indicated by question marks on Fig. 4-15). Therefore, the Windy Ridge near Bellview (GR:440050 Elsmore 1:25,000), Bald Hills near Golden Grove (GR:470050 Elsmore 1:25,000) and possibly Table Top Mountain (GR:503022 Elsmore 1:25,000) are worthy of more detailed investigation.

If "Braemar-type" sapphire-bearing deep leads exist in these areas, then the presence of sapphire in the present-day lateral streams, Swan Brook and Kings (Newstead) Creek (Fig. 4-15), may well be explained in part by the exhumation of such deep lead deposits. This process is shown schematically in Fig. 4-19. This hypothesis may also

explain the occurrence of sapphires in soils (Mr. Doug Erry, of Golden Grove property, pers. comm.) below a certain level on hillsides on the southern side of Swan Brook which form the northern flank of the topographically inverted palaeo-Swan Brook.

4.4.4 Conclusions and exploration-mining problems

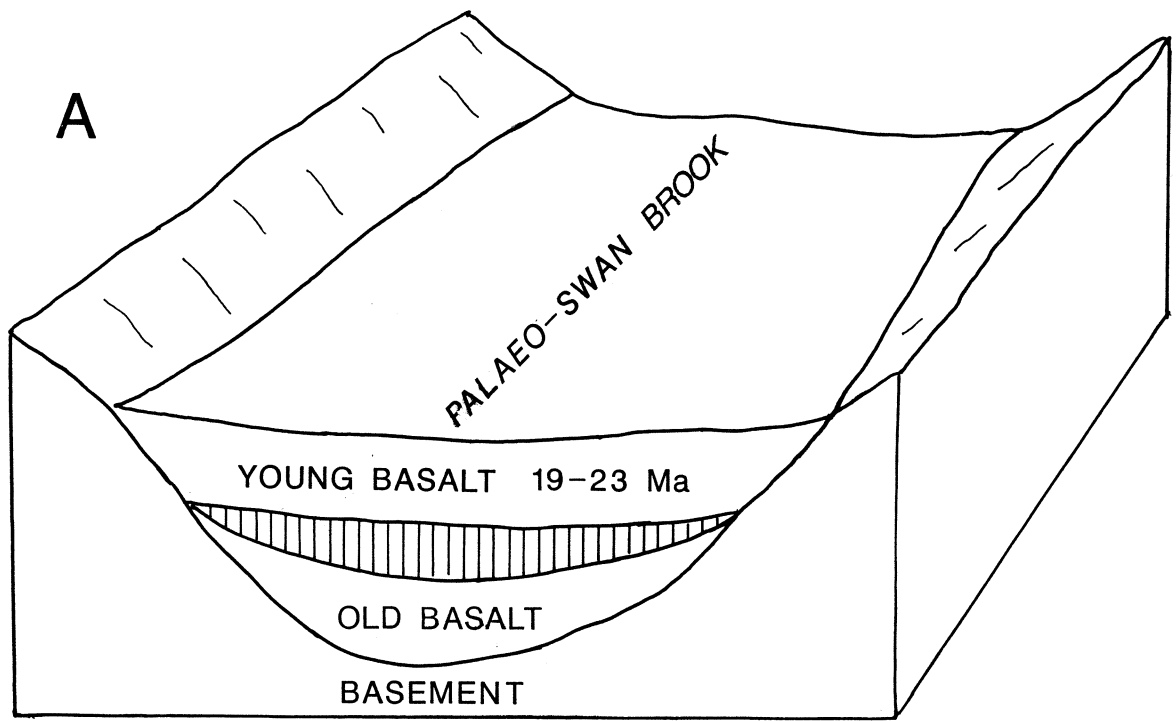
Potential sapphire-bearing deposits within the zone-of-overlap between the 32-38 Ma. East- and the 19-23 Ma. West Central Volcanic Provinces have been delineated in the Braemar palaeochannel and its tributaries, up-palaeostream from the Braemar sapphire mine. Potential sapphire-bearing alluvials are also delineated along the topographically inverted palaeo-Swan Brook.

Deep lead deposits within the zone-of-overlap would be poorly exposed and may be situated at a level well above the present day alluvials, as is the case at Braemar. The only clue to their presence may be trails of sapphires and associated heavy minerals in soils and recent alluvials downslope from the deposits.

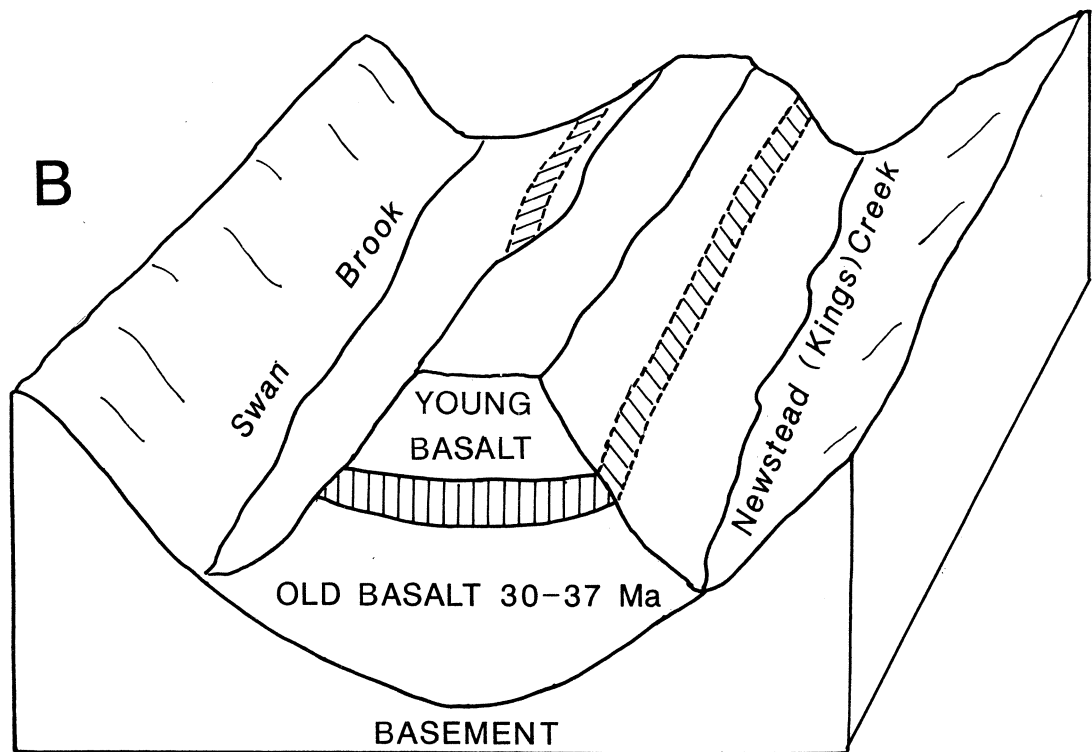
The "Braemar-type" deep lead deposits require a capping of younger basalt for their preservation. Hence, in any exploration program for deep leads, the first step is to determine of the presence or absence of young basalts. This could be assessed by K-Ar dating basalts along the relief inverted palaeochannels, such as along the palaeo-Swan Brook at the sites mentioned earlier. If K-Ar dating were to yield young ages (19-23 Ma), then deep leads may exist below these basalts. An attempt to distinguish between the older and younger basalts, based on their chemistry, is not considered as useful an exploration tool as K-Ar dating. Coenraads (in prep), using all available analyses for the Central Province, found the compositional ranges of major and minor elements for basalts of the West Central Province to largely overlap those of the East Central Province. The only exception being the tholeiites found by Duggan (1972) in the vicinity of Inverell.

Once the extent of potential cover rocks has been established, the presence and position of any palaeochannel axes may be identified using a palaeotopographic reconstruction, such as that carried out at Braemar. In the vicinity of Braemar it was possible to determine the course of the palaeochannel axes to an accuracy of $\pm 200\text{m}$, or to within $\pm 50\text{m}$ in areas of high drill hole control. The position of such palaeoaxes could subsequently be appraised by geophysical techniques relying on detectable property differences between the basement rocks of the palaeovalleys and the material filling them. Gravity surveying has been tried in this regard, yielding an accuracy of the order of $\pm 50\text{m}$ in other basalt filled palaeovalleys of the Central Province (Coenraads, 1989). It must be noted however, that the course of potential sapphire-bearing intrabasaltic channels may not conform exactly to the oldest palaeochannel axis, especially in wide valleys.

Ultimately, the presence of sapphire-bearing deep lead sediments and their economic potential must be verified by costeaning or drilling which may prove to be the economic restraint on exploration for this type of deposit. The more expensive exploration and mining program must be supported by the commodity price. At Braemar, two lines of



(not to scale)



(not to scale)

Figure 4-19. Block diagrams A and B:- Part A shows the inversion of the palaeo-Swan Brook by lateral streams, Swan Brook and Kings Creek and part B shows potential deep lead sapphire deposits, sandwiched between the older and younger basalt flows, exposed in a similar fashion to those in the Braemar palaeochannel.

holes are proposed (Fig. 4-16), comprising a maximum of 12 holes spaced at 50 m to a depth of between 5 and 20 m, to test Eocene/Oligocene sediments below a capping of hard basalt, and to determine the position of potentially sapphire rich placer deposits. Exploration holes would have to be drilled in excess of 45 m in the Dodds Hill palaeochannel.

An efficient mechanized mining operation can profitably recover grades as low as 5 grams per cubic metre (Mr. T.J. Nunan pers. comm.), from Holocene placer deposits, if the quality of stone is high. However these deposits are mined at depths of 4 to 9 metres from below soft alluvium using backhoe excavators and from areas whose grades have been proved by large diameter-bucket drilling (Coenraads, 1990). In the case of deep lead sapphire deposits, both hard basalt and excessive depth would preclude the use of cheaper large-diameter bucket drills and necessitate diamond drilling yielding a much smaller sample that cannot be used to estimate grade or quality.

Chapter 5

HEAVY MINERAL SUITES WITHIN THE CENTRAL PROVINCE, NEW SOUTH WALES

5.1 Introduction

Twelve suites of heavy mineral concentrates were analyzed, from sapphire placer deposits and from in-situ soils in close proximity. The aim of this part of the study was to shed light on the provenance of the heavy minerals and determine their behaviour during weathering and subsequent concentration in alluvial deposits.

The sampling sites for heavy minerals were chosen to test for differences in mineral constitution and composition within and between drainage catchments. Sampling (Fig. 3-2 & Table 5-1) was undertaken within the catchments of Reddestone Creek (5 sites), Kings Plains Creek (1 site), Yarrow River (2 sites), Schumachers Gully/Swan Brook (2 sites) and Dumaresq Creek/Gara River (2 sites). The locations of the sample sites are shown in Figure 3-2. Samples were collected at or near the tops of hills from thin soils directly overlying weathered basalt (*in situ* sites) and from river gravels (placer sites).

5.2 Preparation of heavy mineral concentrates

Soil samples of 5-10 kg were concentrated by sieving and panning. Gravels from creeks and rivers were likewise concentrated or taken from the mining operations of T.J.& P.V. Nunan Pty Ltd. Each concentrate was examined under a binocular microscope and blue sapphires, together with red, orange or colorless zircons, bright-green clinopyroxene and yellow-green olivine, were identified visually. Minerals chosen for detailed investigation were those with the potential for isomorphous substitution, being those most likely to show discernable differences between collection sites. These "black" minerals were difficult to identify visually, but were abundant in both the soil and placer sites. Representative samples from each concentrate were selected, mounted in plastic discs, polished and analyzed using an electron microprobe. At least two analyses were carried out on each mineral grain to check for homogeneity and the presence of zoning. Only if the analyses were sufficiently similar, was the average taken and used for data comparison. The majority of the mineral grains analyzed proved to be homogeneous, with the exception of a large number of ilmenites from the Reddestone and King Plains catchments which showed irregular variation across individual grains.

5.3 Heavy minerals present in the Central Volcanic Province.

The minerals in the concentrates and their compositional ranges are listed in Tables 5-1 & 5-2. The problem of interpreting the large number of mineral analyses was

Table 5-1. Heavy Mineral Suites from Soil and Places Collection Sites within the Central Province

Sample YAR	BRA	KPL	RE1	RE2	DUN	PAB	HIL	KNO	UNE	SWA	BRE
Placer Yarrow R.	Placer Schumachers Ck.	Placer Kings Plains Ck.	Placer Reddestone Ck.	Placer Reddestone Ck.	Basalt soil Reddestone Ck.	Basalt soil Reddestone Ck.	Basalt soil Reddestone Ck.	Basalt soil Dumaresq Ck.	Basalt soil Dumaresq Ck.	Basalt soil Yarrow R.	In situ breccia Schumachers Ck.
Corundum	Corundum	Corundum Chrysoberyl ^{1,3}	Corundum Chrysoberyl ^{1,3}	Corundum	Corundum	Corundum	Corundum ¹	Pleonaste	Pleonaste Cr spinel ¹	Cr spinel ¹	Corundum ²
	Cr spinel	Pleonaste Cr spinel ¹	Pleonaste Cr spinel ¹	Pleonaste Cr spinel ¹	Pleonaste	Pleonaste	Pleonaste	Pleonaste Cr spinel ¹	Pleonaste Cr spinel ¹	Pleonaste ¹ Cr spinel ¹	Pleonaste ¹ Cr spinel ¹
Ilmenite	Ilmenite	Magnetite Ti magnetite Ilmenite	Magnetite Ti magnetite Ilmenite	Ti magnetite Ilmenite	Ilmenite	Magnetite Ti magnetite	Ti magnetite	Ti magnetite	Ti magnetite Ilmenite ¹	Ilmenite	Ilmenite ¹ Zircon ²
Zircon	Zircon	Zircon	Zircon	Zircon	Zircon	Ilmenite	Olivine	Olivine	Olivine Enstatite Clinopyroxene		
	Enstatite ¹ Clinopyroxene ¹										
Glen Innes 1:100,000 GR:908888	Inverell 1:100,000 GR:350033	Inverell 1:100,000 GR:512152	Glen Innes 1:100,000 GR:690150	Glen Innes 1:100,000 GR:682123	Glen Innes 1:100,000 GR:727212	Glen Innes 1:100,000 GR:670148	Glen Innes 1:100,000 GR:667140	Dorrigo 1:250,000 GR:471215	Dorrigo 1:250,000 GR:468226	Glen Innes 1:100,000 GR:869871	Inverell 1:100,000 GR:350031

Abbreviations correspond to locations shown in Figure 3-2

¹ Rate

² R.H. Constable, pers. commun.

³ S. Lishmund, pers. commun.

⁴ T.J. Numan, pers. commun.

Table 5-2. Weight Percent Oxide Content for the Central Province Heavy Mineral Suite

	Corundum	Chrysoberyl	Pleonaste	Cr spinel	Magnetite	Ti mag- netite	Ilmenite	Zircon	Olivine	Orthopyroxene	Clinopyroxene	Amphibole
SiO ₂	0.0	0.0	0.0-0.21	0.0-0.17	0.29-1.45	0.0-0.93	0.0-0.22	32.7-34.1	40.9-41.0	54.6-55.6	48.0-52.7	43.0
TiO ₂	0.0-0.09	0.02-0.07	0.28-1.40	0.0-0.32	0.32-6.5	9.8-22.0	40.6-58.6	0.0	0.0	0.11-0.15	0.36-1.9	4.1
Al ₂ O ₃	99.8-101.5	77.8-80.53	56.4-65.2	42.0-60.0	3.4-4.2	3.6-11.3	0.0-2.0	0.0-0.05	0.0	4.7-5.12	3.0-9.6	11.5
Cr ₂ O ₃	0.0-0.01	0.0-0.09	0.0-0.58	8.0-27.2	0.0-0.02	0.0-0.06	0.0-0.13	0.0-0.13	0.0	0.29-0.60	0.0-1.0	0.0
FeO _{total}	0.61-1.12	1.84-4.2	15.2-27.5	10.1-14.0	82.8-87.3	65.8-80.0	29.5-56.4	0.12-0.37	10.7-11.6	6.5-6.8	2.5-8.8	16.5
MnO	0.0-0.01	0.0-0.01	0.01-0.19	0.11-0.26	0.36-0.45	0.18-0.54	0.16-0.97	0.0	0.16-0.17	0.04-0.15	0.13-0.15	0.2
MgO	0.0	0.0	13.3-20.7	17.6-21.0	0.15-1.19	0.6-5.7	0.62-7.4	0.0	49.0-49.5	14.5-15.9	32.3-33.0	10.5
NiO	0.0		0.0-0.22	0.14-0.45	0.0	0.0	0.0	0.0	0.31-0.39	0.0	0.0	0.0
ZnO			0.0-0.25	0.0-0.32			0.0-0.13			0.0-0.08		8.2
CaO	0.0-0.04		0.0-0.10	0.0-0.07	0.0	0.0-0.23	0.0-0.11	0.0	0.06-0.11	17.7-22.2	0.78-1.4	3.4
Na ₂ O	0.0		0.0-0.06	0.0-0.01	0.0	0.0-0.30	0.0-0.09	0.0-0.16	0.0	0.35-2.21	0.12-0.13	1.5
K ₂ O	0.0		0.0-0.06	0.0-0.03	0.0-0.01	0.0-0.03	0.0-0.05	0.1	0.0		0.0-0.03	
ZrO ₂												
BeO ¹												
ThO												
SrO												
No. analyses	4	7	139	38	4	59	158	4	3	2	25	1

¹ BeO by difference

approached by, firstly, characterizing the minerals for the entire volcanic province, and then, secondly, checking for subtle differences between individual sites.

The minerals studied were subhedral to rounded. Sapphires and zircons are often glossy in appearance and spinels and ilmenites are usually pitted and dull. Detailed scanning electron microscopic examination of the grain surfaces revealed little evidence of abrasion due to fluvial transport, and indicated that pitting and etching are the result of surface biodegradation, which was particularly pronounced on spinels (Bischoff and Coenraads, in prep.). Rounded and glossy mineral surfaces are attributed to disequilibrium and resorption in the carrier magmas (Coenraads et al, 1990).

The spinel-group plots in four parts of the magnetite and ulvospinel prisms shown in Figure 5-1. Their compositional features are:

- 1) Chromium-spinel group: These trend from the spinel field towards the chromite-picrochromite field. Cr_2O_3 ranges from 8 to 23 percent with FeO enrichment and MgO depletion corresponding to Cr_2O_3 enrichment. One sample from the breccia dyke at Braemar contains 39.3 percent Cr_2O_3 .
- 2) Pleonaste Group: These lie along the spinel-hercynite join from 52 to 78 percent end member spinel, and are essentially chrome free ($\text{Cr}_2\text{O}_3 < 0.52\%$).
- 3) Titanium Magnetite-Ulvospinel Group: These trend towards magnetite in the magnetite prism and plot near the ulvospinel end member in the lower prism. They have low Al_2O_3 (1-8%), MgO (0.5-6%) and are chrome free ($< 0.06\%$). Plots nearer the ulvospinel corner have slightly higher Al_2O_3 and MgO contents.
- 4) Magnetite Group: The few magnetites found plot close to the magnetite end member and have lower TiO_2 than the titanium-magnetites (maximum 6.5%).

The ilmenites for the Central Volcanic Province contain up to 8 percent MgO, and MgO is highest in those ilmenites with high TiO_2 and low FeO.

Rutile crystals with ilmenite rims have been found in heavy mineral concentrations from the Uralla area (Coenraads et al, in prep). Gem quality pyrope-almandine series garnets have been obtained from Horse Gully in the New England Gemfields (Coenraads and van der Graaf, 1991). These apparently localized and uncommon heavy minerals are described in sections 5.5 and 5.6

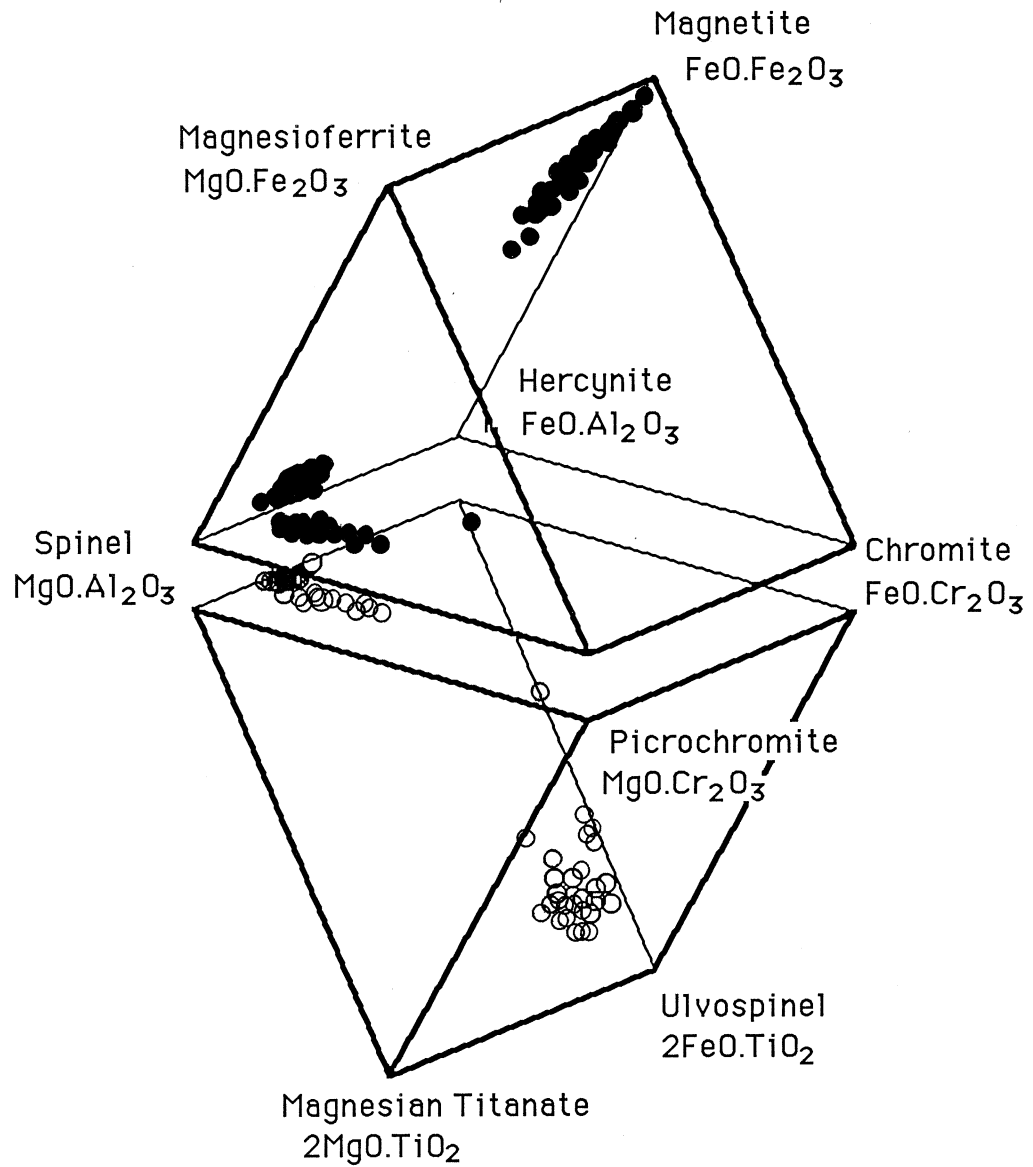


Figure 5-1. Central Province spinel. The fields of pleonaste, chromium-spinel, and titanium-magnetite/magnetite are clearly visible within the spinel family prisms (computer program courtesy of K.L. Williams, Department of Geology and Geophysics, University of Sydney).

5.4 Comparison between heavy mineral suites from collection sites within the Central Volcanic Province.

To enable detection of subtle differences between individual collection sites, each mineral species from a particular site was plotted alongside similar species from the other sites (Figs 5-2 to 5-5). The data for each site is arbitrarily arranged in ascending or descending order for a particular major oxide so that the relationship between the major oxides and minor oxides can be seen at a glance.

The figures indicate appreciable variations in weight percent oxide abundance as well as some systematic relationships between oxides as follows:-

1. *Chromium-spinel* ; (Fig. 5-2) decreasing Al_2O_3 corresponds to increasing Cr_2O_3 and MnO, decreasing MgO, and weakly decreasing NiO.
2. *Pleonaste* ; (Fig. 5-3) increasing FeO (total) corresponds to increasing TiO_2 , and decreasing Al_2O_3 and MgO.
3. *Titanium-magnetite*; (Fig. 5-4) increasing FeO (total) corresponds to decreasing Al_2O_3 , MgO and TiO_2 .
4. *Ilmenite* ; (Fig. 5-5) increasing FeO corresponds to decreasing MgO and TiO_2 .

The breccia dyke at Braemar (Fig. 4-14) described by Pecover and Coenraads, (1989) yielded 22 chromium spinels (including one grain with 39.3% Cr_2O_3), five ilmenites and one pleonaste. The minerals from the dyke showed a slight core to rim zoning with enrichment in FeO (2.77% in pleonaste, up to 0.37% in Cr-spinel, and 1.46% in the ilmenite). The chromium-spinels also showed an outward enrichment in Cr_2O_3 (up to 0.77%) and both the chrome spinels and pleonaste, a depletion in Al_2O_3 (1.56% in the pleonaste and up to 1.47% in the chrome spinels). The breccia dyke and various basalt flows are believed to be responsible for contributing to the alluvial heavy mineral deposits worked for sapphire at Braemar.

Each mineral species shows a remarkable similarity, both in ranges for given oxides and in relationships between oxides, for the sample sites. There are no significant differences between mineral compositions from the various drainage systems. However, some sites differ in the presence or absence of certain mineral species, and/or in the relative mineral abundances. Corundum and zircon appear to be common associates.

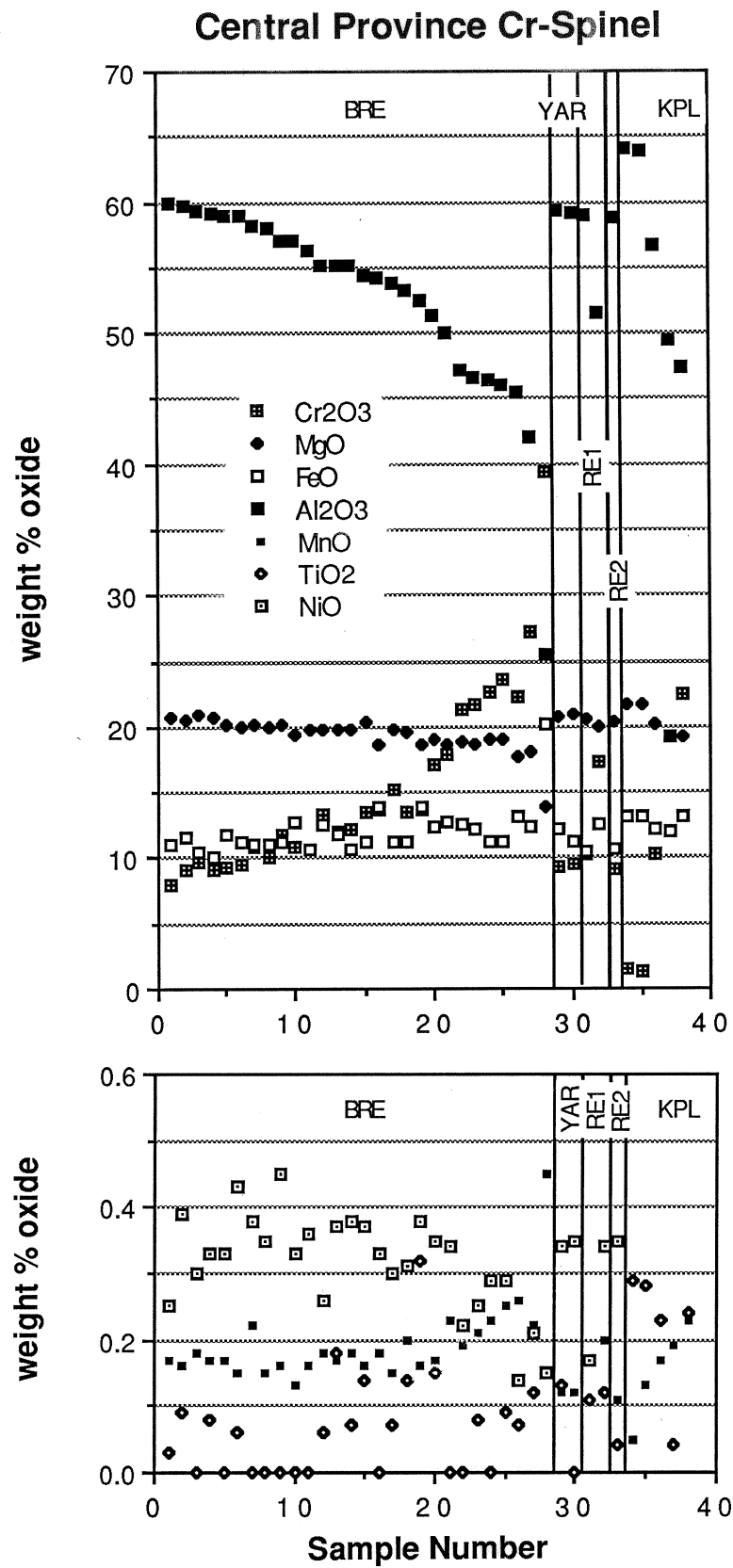


Figure 5-2. Central Province chromium-spinel. Compositions are plotted for each site and are arranged in descending order of percentage Al₂O₃.

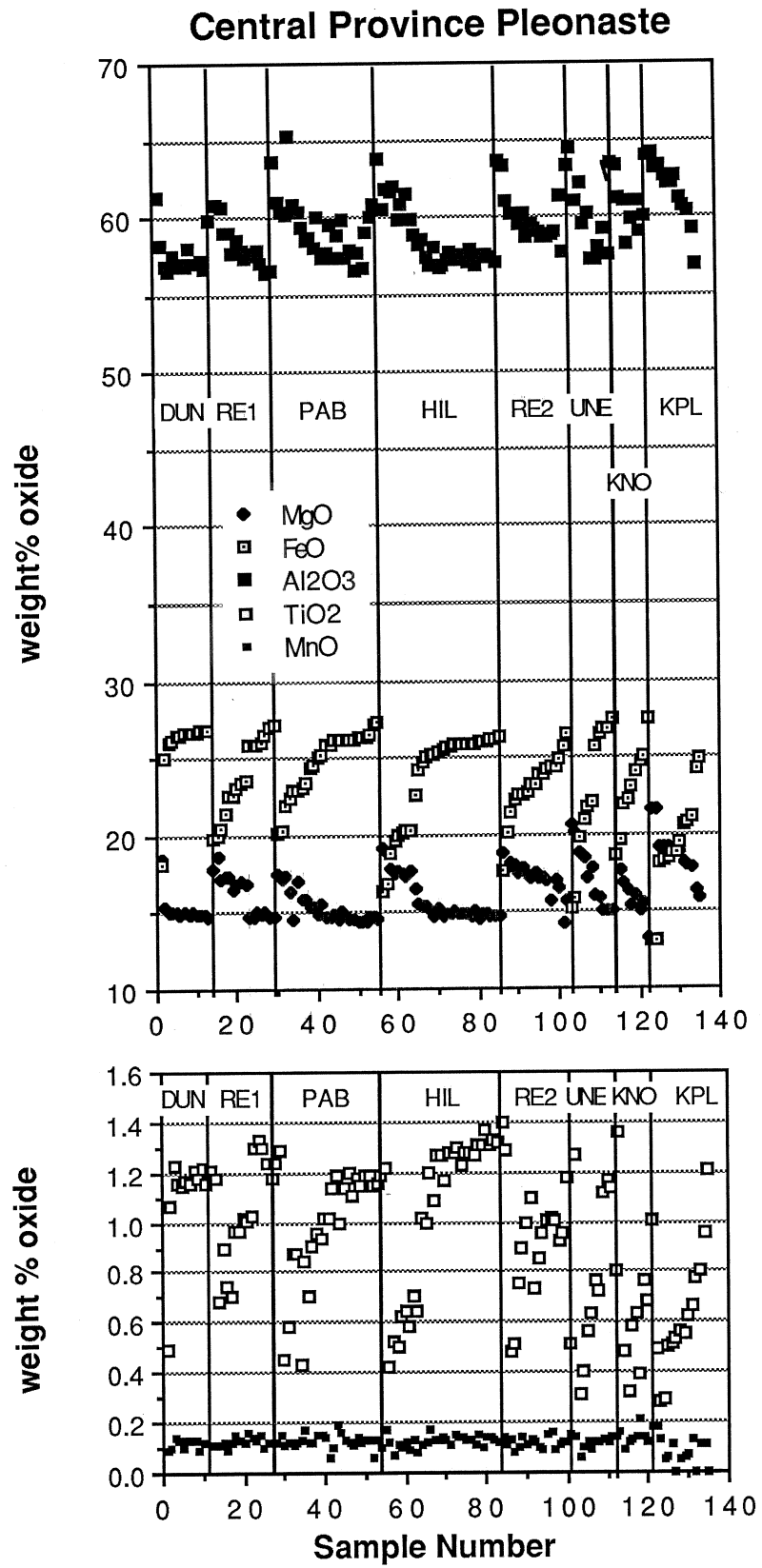


Figure 5-3. Central Province pleonaste. Compositions are plotted for each site and are arranged in ascending order of percentage FeO.

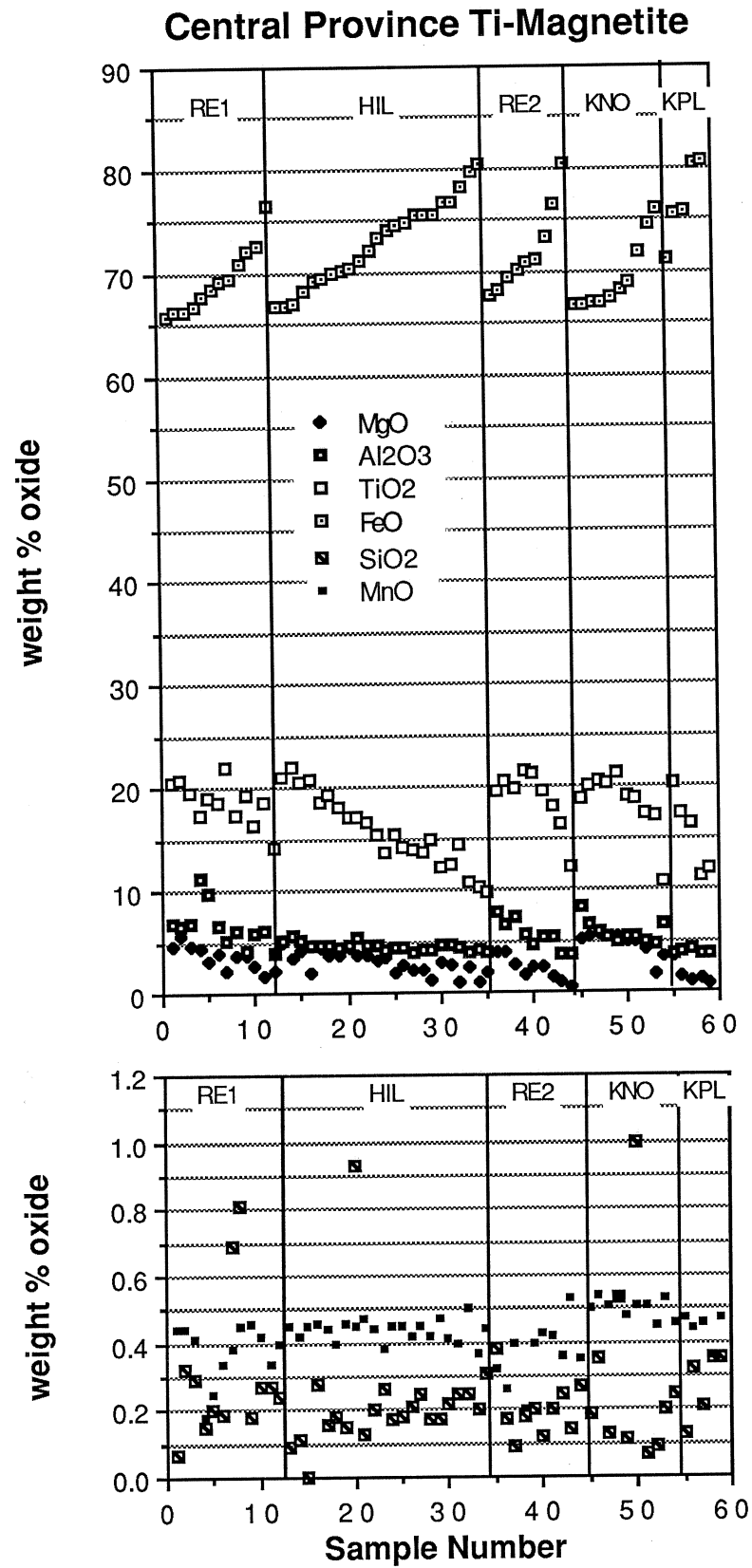


Figure 5-4. Central Province titanium-magnetite. Compositions are plotted for each site and are arranged in ascending order of percentage FeO.

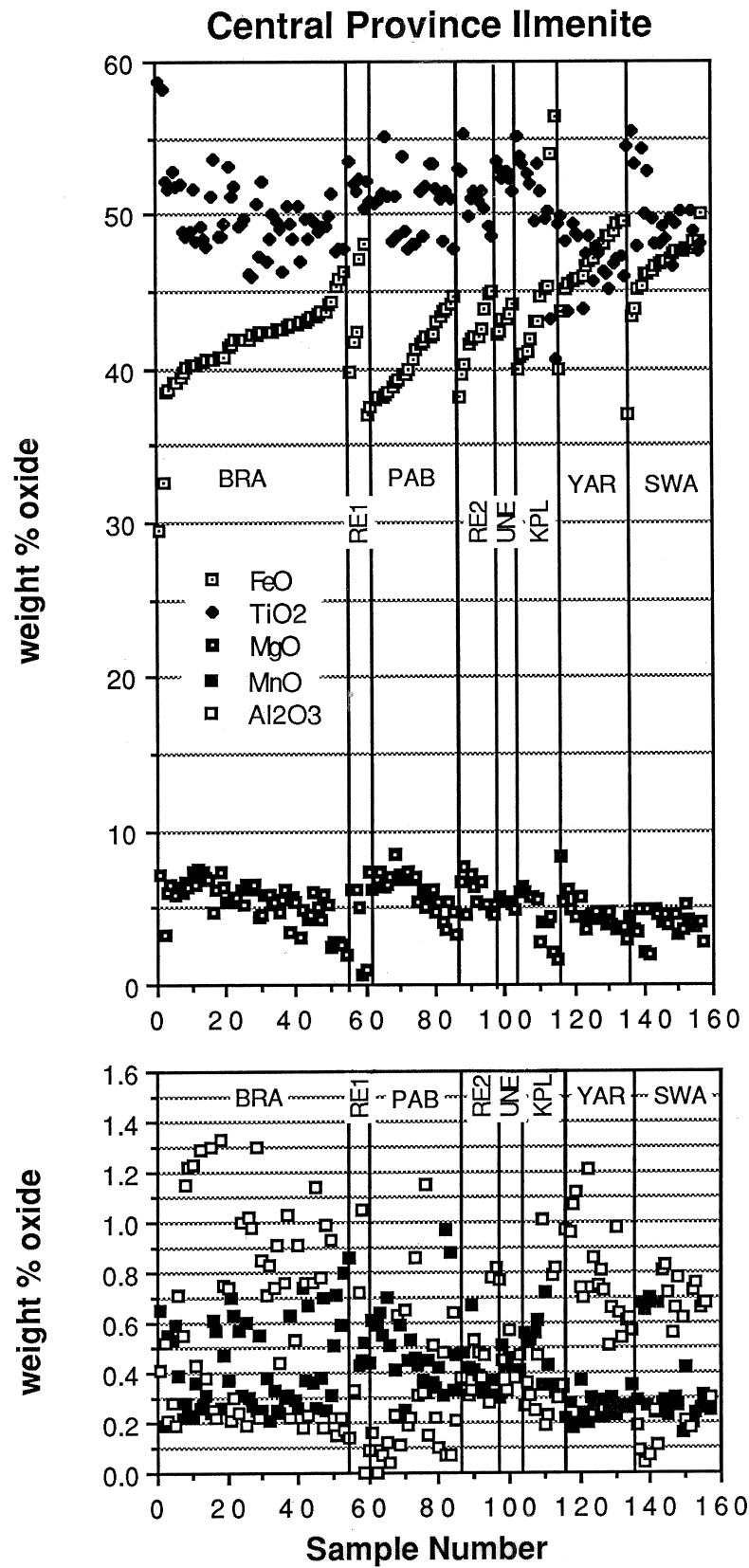


Figure 5-5. Central Province ilmenite. Compositions are plotted for each site and are arranged in ascending order of percentage FeO.

5.5 Ilmenite mantled rutile crystals from the Uralla district

5.5.1 Occurrence.

Ilmenite-mantled rutile crystals of enigmatic origin occur in Late Tertiary conglomeratic arkoses and Quaternary alluvium west of Uralla, New South Wales (Figure 5-6).

The dense, dull-black mantled crystals ranging from 0.5 to 4 cm in length are found within all types of arkose (Tca on map, Figure 5-6) and are always concentrated, by virtue of their specific gravity, with other heavy minerals within conglomerate bands. They also occur in the Rocky Creek, Kentucky Creek and the upper Rocky River drainages, being profusely abundant in areas where concentration of heavy components in gravel is high. (Qa, on map, Figure 5-6). Other heavy minerals found with them include zircon, spinel, ironstone pisoliths, tourmaline and rare corundum and diamond.

The mantled crystals were briefly described by David (1886) as "Titaniferous Iron" comprising part of the heavy mineral assemblage found in Recent alluvium along with zircon, spinel and quartz. He also reported that "nodules of titaniferous iron are abundant at Wallaby Gully, where a pebble of that mineral has been found 2 inches in diameter" (GR 509108 9136-I-N Balala 1:25000).

The ilmenite-rutile crystals have not been found to occur in any igneous rocks, or metamorphic rocks which outcrop in the Uralla area. Nor have they been found to occur in covering basalt soils or Tertiary deep-lead deposits (Coenraads et al, in prep). Their source is therefore problematic.

These crystals are of interest because of their restricted occurrence and their physical resemblance to crystals known from kimberlite pipes (Mitchell, 1979).

5.5.2 Description of the ilmenite-rutile crystals.

The crystals are shown in Figure 5-7. They are stumpy to cylindrical in shape and are always rounded. This is probably due to magmatic corrosion with only minor modification due to transport. A core of rutile is exposed below the mantle of ilmenite if the specimen has been broken or is cut. In thin slices the rutile is a deep translucent red.

Four crystals were selected for detailed study. Polished blocks were prepared for electron microprobe analysis and thin sections were cut parallel to, and perpendicular to, the long axis of the cylinder, (photomicrographs shown in Figure 5-8). Uniform extinction parallel to the long axis of the cylinder (Figure 5-8d), indicates that the rutile cores are single tetragonal crystals with the C-axis parallel to the direction of elongation of the cylinder. In reflected light the ilmenite mantle comprises a number of subgrains. Figure 5-8c shows the interface between the rutile core and ilmenite mantle. Blades of ilmenite interlock with those of rutile thereby creating a large surface area of contact. The ilmenite appears to be replacing the rutile crystals and its planes of penetration appear to be

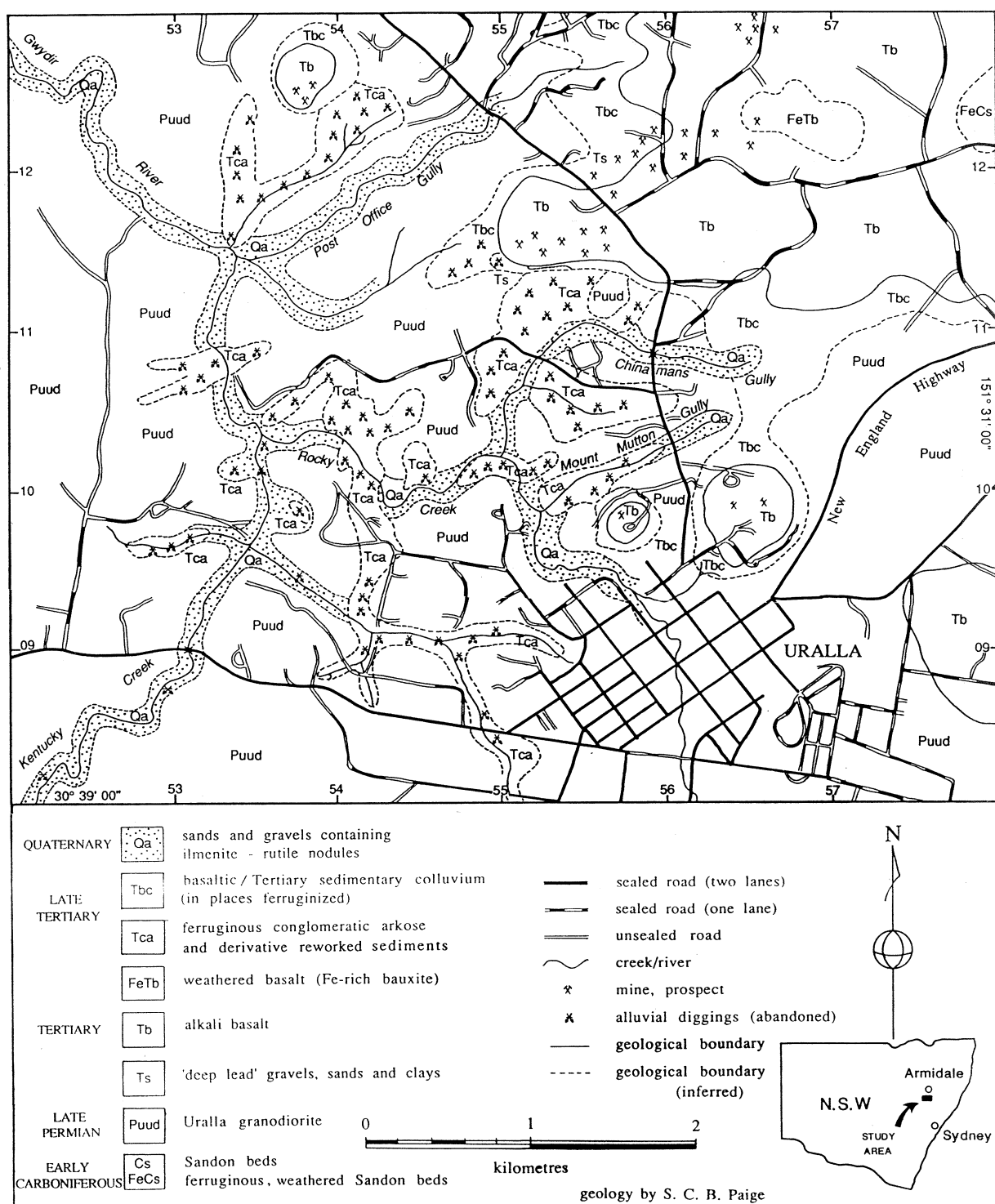


Figure 5-6. Geology of the Uralla district, New South Wales. The ilmenite coated rutile crystals have been found in late Tertiary ferruginous arkose (Tca) and Quaternary sands and gravels (Qa).



Figure 5-7. Ilmenite mantled rutile crystals from the Rocky River Goldfield near Uralla. These specimens were collected by S.C.B. Paige and examples are held by the Australian Museum (specimen number D48733). They range in size from 0.5 to 4 cm. (photograph by S. Ranson, hands of J. Thomas).

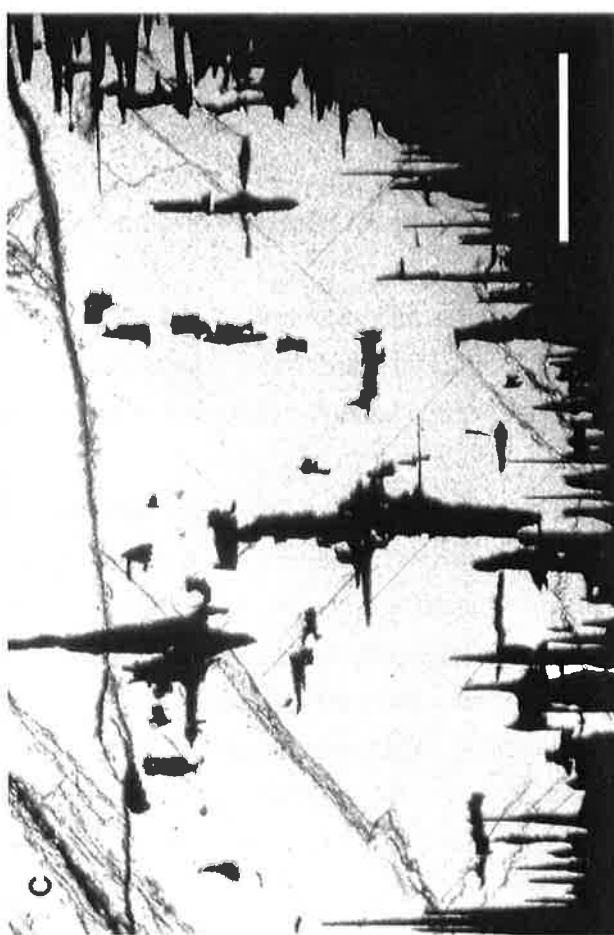
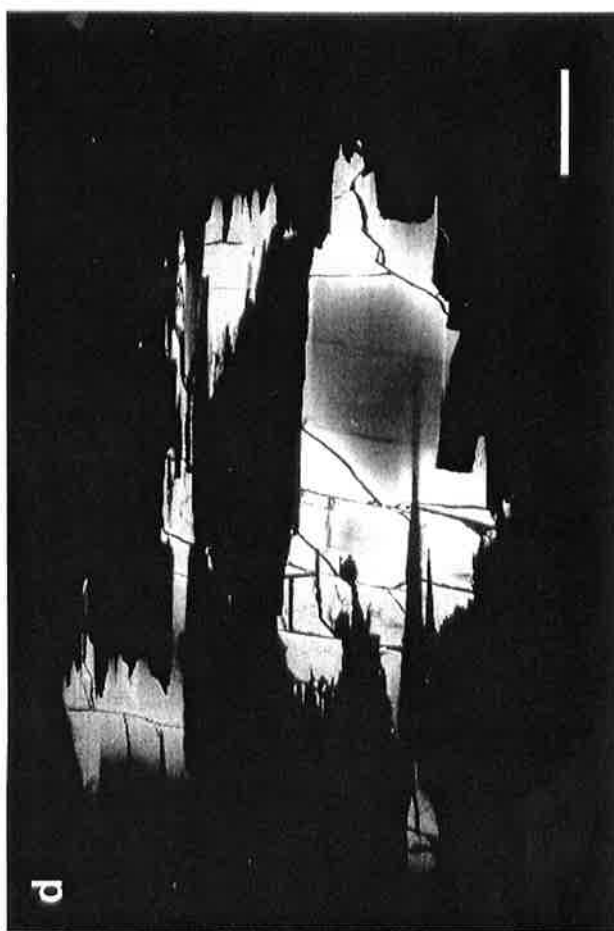
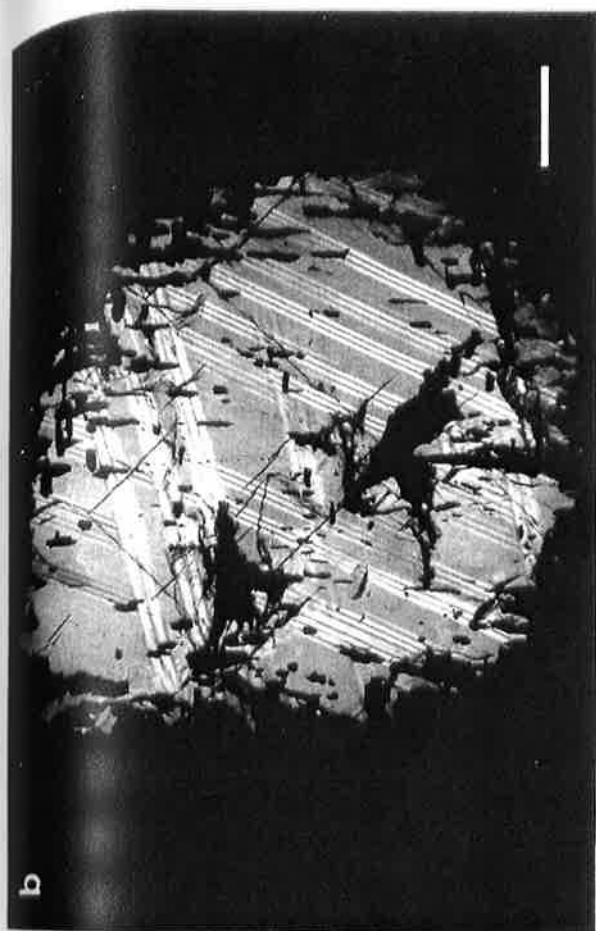


Figure 5-8. Transmitted light photomicrographs of sections cut through ilmenite mantled rutile crystals: a) Section normal to the C-axis. Interlocking blades indicate replacement of rutile by ilmenite along the {100} direction of rutile crystal. Also visible are orthogonal {110} cleavages which post date the ilmenite replacement; b) Same section as photo a, with crossed-polars, zoning or twinning is visible in the rutile; c) Enlargement of a section normal to the c-axis, clearly visible is the ilmenite replacement along two orthogonal planes and the cleavage postdating the replacement; d) Section cut through an ilmenite mantled rutile crystal parallel to the C-axis. Uniform extinction indicates the rutile is a single crystal. Ilmenite replacement of the rutile occurs parallel to {100}. The scale bar on all photos is 1 mm.

controlled by the rutile crystal structure. The planes are exactly 90° apart and are penetrating at right angles to the prism faces, that is, in the (100) direction. Also apparent in Figure 5-8c are the good (110) cleavage planes which are free of ilmenite replacement, so possibly opened during the thin sectioning procedure. In Figure 5-8d the dark ilmenite blades are parallel to the C-axis of the rutile crystal, confirming replacement along the {100} planes.

Electron microprobe results: Analyses approximately 1 mm apart, were performed on the polished sections (cut normal to the c-axis) in transect lines running from rim to core and then out to the opposite rim. Initially the full spectrum of each representative mineral was examined using Macquarie University's Link 1000 Energy Dispersive Analytical System and analyses of the elements detected were carried out using the Siemens wavelength dispersive system.

Four analyses near each desired location were averaged for plotting, and the bars in Figure 5-9 indicate the calculated standard deviations.

The rutile cores contain 0.34 to 0.44% FeO(total), but there is no discernable variation in FeO across the cores indicating them to be homogeneous crystals.

The variation in ilmenite compositions are 50.5-55.7% TiO_2 , 40.3-45.0% FeO, 1.9-3.0% MnO and 0.3-1.4% MgO. In individual samples TiO_2 increases and FeO decreases by about 1% from the outside to the inside of the rim. Mn shows no variation. In some ilmenite rims MgO increases towards the core, with the highest values recorded within the ilmenite replacement blades within the rutile core (1.4%, not shown on Figure 5-9).

A detailed transect of 11 data points, 0.3mm apart, was made across one section of the ilmenite rim in grain 3 (Figure 5-9). The overall fall in TiO_2 and a rise in FeO from the rutile-ilmenite contact to the outer edge is neither smooth nor gradational. However the changes between successive points generally lie within the error bars.

5.5.3 Comparisons with ilmenite-rutile crystals and ilmenite found elsewhere

The main elemental oxide contents of the Uralla ilmenite relative to published ilmenite compositions from many different rock associations is presented in Table 5-3 and summarized in Fig. 5-10. This highlights their somewhat unusual composition and helps to suggest potential sources.

Discrete crystals of rutile commonly mantled by magnesian ilmenite are found in heavy mineral concentrates from some kimberlites, such as at Somerset Island, Canada (Mitchell, 1979). The rutile is homogeneous but the ilmenite may be compositionally zoned with increased Mg, Cr and Mn towards the edges. Dawson (1980) proposed that fragmented eclogite xenoliths are the probable source of the rutiles prior to their mantling with kimberlitic ilmenite. Samples from the Wesselton Pipe, South Africa (Mitchell, 1973) show that the ilmenite is a replacement of the rutile. Kimberlitic ilmenites are well known

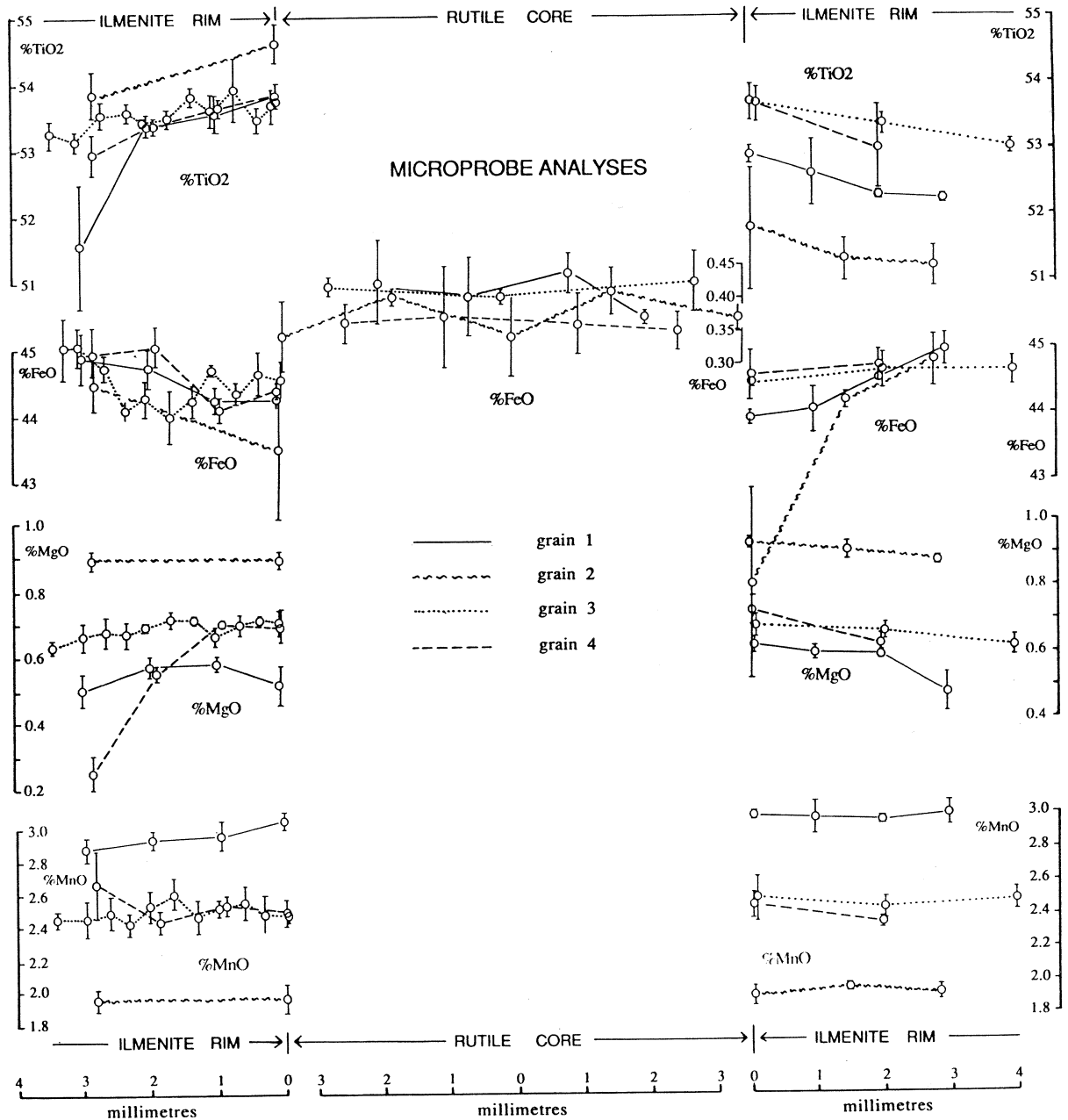


Figure 5-9. Summary of microprobe results; Oxide weight percents of TiO₂, FeO, MgO and MnO shown for transects across 4 ilmenite mantled rutile crystals cut perpendicular to the C-axis. For each transect, the edge data points in the rutile core are immediately adjacent to the inside data points taken in the ilmenite mantle. The points represent the average of four analyses and the error bars indicate the standard deviation of the data. A real decrease in percentage TiO₂ and increase in percentage FeO of the order 1% can be seen in moving from the inside to the outside edge of the ilmenite mantle. The MnO values appear to be constant across the ilmenite mantle. The percentage MgO tends to decrease in moving from the inside to the outside edge of the ilmenite mantle.

TABLE 5-3: COMPARATIVE ILMENITE ANALYSES

A. URALLA SITE & EXTRUSIVES (groundmass/late stage crystallizations)

Suite & Analysis	mantles on rutile, Uralla ¹	silicic/salic volcanics ^{2,3}	alkali basalts ⁴ S. Highlands N.S.W	coarse phases of leucities, Aust ^{5,6}	cavity fillings, basalts, Aust ^{7,8}
TiO ₂	50.47-55.71	37.60-51.60	49.40-53.60	50.04-52.40	51.94-53.04
FeO total	40.26-45.02	44.20-54.70	40.50-47.80	42.00-44.77	41.18-43.26
MnO	1.09-3.02	0.46-2.17		0.64-1.02	0.61-2.04
MgO	0.25-1.35	0.10-3.79	0.12-5.52	0.83-4.10	2.26-3.72
Al ₂ O ₃	0.00	0.00-0.36		0.05-1.00	0.00-0.19
Cr ₂ O ₃	0.00	0.00-0.21	0.00-0.15	0.00-0.06	0.00-0.04
CaO	0.00	0.00-0.06	0.00-0.88	0.00-0.19	0.00-0.10
SiO ₂			0.00-0.83	0.03-0.32	0.00-0.64
V ₂ O ₃		0.00-1.80			

B. UPPER CRUSTAL INTRUSIONS

Suite & Analyses	granites & pegmatites ⁹	syenites-foyaite ¹⁰	gabbros ^{11,12} troctolites	high Mg-tholeiite complex, S. Africa ¹³	ultramafic-14 mafic complex
TiO ₂	43.25-46.38	45.43-50.85	47.92-49.71	49.52-56.98	49.90-52.20
FeO total	45.54-48.52	41.38-50.87	44.73-48.52	33.19-48.11	42.79-47.19
MnO	0.30-5.63	0.70-7.80	0.85-2.88	0.40-1.35	0.05-0.10
MgO	0.03-1.10	0.05-1.60	1.00-2.50	0.28-10.22	0.09-2.90
Al ₂ O ₃	0.55-1.70	0.00-1.06	0.03-0.88		0.10-0.30
Cr ₂ O ₃	0.00-0.20	0.00-0.01	0.00-0.12	0.04-1.08	0.00
CaO	0.02-1.15	0.01-0.06	0.00		0.05-0.13
SiO ₂	0.10-1.49	0.19-0.28	0.00-0.08		0.20-0.70
V ₂ O ₃	0.00-0.10	0.00-0.12	0.00-0.07		0.01-0.05

C. METAMORPHIC SUITES

Suite & Analyses	nodules(+rutile) greenstones W.A. ¹⁵	granulite India ¹⁶	biotite rock (+rutile) ¹⁷	rim on rutile ¹⁸ granulite, Tas.	rim on rutile ¹⁹ gnt granulite Qld	gnt quartz ²⁰ W.A.	medium grade ²¹ greenstone W.A.
TiO ₂	50.13-50.20	48.90	51.03	57.64	46.30	51.57	52.00
FeO tot.	48.04-51.60	48.45	43.14	29.89	46.14	44.96	44.00
MnO	0.54-1.49	0.35	2.90	0.31	0.53	2.91	3.00
MgO	0.00-trace	0.56	0.08	12.34	5.34	0.34	<0.12
Al ₂ O ₃		0.54		0.59	0.91		
Cr ₂ O ₃				0.52	0.13		
CaO		0.65		0.19	0.28	0.06	
SiO ₂	0.00-0.95	0.11	0.19			0.07	
V ₂ O ₃							

D. MEGACRYST SUITES; BASALTIC ROCKS

Suite & Analyses	alluvial grains Braemar, NSW ²²	alluvial grains Yarrow Riv. NSW ²³	alkali basalts ²⁴ S.E. Queensland	alkali basalts ²⁵ Nebo Queensland	lamprophyre ²⁶ Mt. Woolloomo NSW
TiO ₂	45.96-53.64	45.17-55.40	46.77-51.50	49.54-52.56	44.47
FeO total	38.41-46.36	36.98-50.06	42.69-50.39	41.11-44.32	48.61
MnO	0.21-0.86	0.16-0.70	0.14-0.45	0.24-0.49	0.15
MgO	1.90-7.41	1.99-8.25	2.04-4.24	4.21-6.17	5.32
Al ₂ O ₃	0.14-1.67	0.04-1.99	0.21-0.84	0.21-0.51	1.53
Cr ₂ O ₃	0.00-0.03	0.00-0.08		0.00-0.13	
CaO	0.00-0.10	0.00-0.06	0.00-0.02	0.00-0.15	0.23
SiO ₂	0.00-0.09	0.00-0.12	0.00-0.02		0.68

E. MEGACRYST SUITES; KIMBERLITES, CARBONATITES, ALNOITES, LAMPROITES

Suite & Analyses	kimberlites global ^{27,28}	carbonatites global ²⁹	kimberlitic rocks W. Australia ³⁰	alnoites malaita ³¹	lamproite Zambia ³²	kimberlitic nodule ³³
TiO ₂	41.40-58.45	46.90-51.85	46.35-53.59	49.20-52.10	49.74	41.48
FeO total	20.64-49.64	41.80-45.59	33.20-46.29	31.90-35.80	43.34	55.05
MnO	0.00-1.99	2.60-4.59	0.17-4.34	0.17-0.24	1.02	0.07
MgO	3.90-23.10	0.10-5.10	1.28-9.54	5.23-7.13	2.37	1.60
Al ₂ O ₃	0.03-0.84	0.00-0.07	0.19-0.83	0.17-0.83	0.02	0.32
Cr ₂ O ₃	0.02-3.37	0.00-0.28	0.23-0.79	0.02-0.03	0.15	0.14
CaO	0.00-0.30	0.00-0.13			0.17	
SiO ₂	0.00-0.05		0.00-0.35			
NiO	0.04-0.30				0.05	

F. MANTLE INCLUSIONS

Suite & Analyses	gnt pyroxenites Brigooda, Qld ³⁴	apatite-rich rock East Aust ³⁵	pyroxenites Lesotho ³⁶	in diamond Africa-USSR ³⁷	in diamond Brazil ³⁷
TiO ₂	48.67-50.89	51.00-51.20	53.10-54.60	52.10-55.60	50.50-51.90
FeO total	37.60-42.56	41.00-42.70	26.10-27.80	29.50-36.50	47.40-48.20
MnO	0.00-0.27	0.57-0.76	0.22-0.48	0.27-0.30	0.64-0.68
MgO	6.17-9.15	5.59-6.20	13.49-15.04	9.10-13.00	0.11-0.14
Al ₂ O ₃	1.33-1.78	0.20-0.31	0.70-1.16	0.22-0.78	0.21-0.36
Cr ₂ O ₃	0.00-0.03		2.17-2.83	0.01-2.50	0.01-0.04
CaO	0.00-0.06	0.07-0.20	trace	0.00-0.04	0.01-0.07
SiO ₂	0.30-0.36	0.03-0.10	0.14-0.17	0.01-0.04	0.12-0.16
NiO			0.12-0.19	0.00-0.30	

Footnotes to accompany Table 5-3.

1 This paper. 2 Carmichael (1967, p.140-2, Tab.2-4, analy.1-29). 3 Haggerty (1976, p.Hg258, analy.9-18). 4 Wass (1973, p.430, table III, analy.1-17; p.434, Tab.IV). 5 Cundari (1973, p.478, Tab.VI, analy. BQ-PEGM, BEH-C, BEH-D). 6 Birch (1979, p.379, Tab.6, analy.CLOG-44, CLOG-45, CLOF-53). 7 Birch et al. (1982). 8 F.L.Sutherland & D.F.Hendry, unpublished data. 9 Haggerty (1976, p.Hg258 & 260, analy.1, 3-4, 6-8, 45). 10 Haggerty (1976, p.Hg259, analy.21-27). 11 Deer et al (1975, p.29, table 5, analy.3-4). 12 Haggerty (1976, p.Hg260, analy.41-44, 46-47). 13 Cawthorne et al. (1988, p.149, Tab.1A, 21/1-15, 16/1-10, NGL/9,11, 54, 56, 62, 110). 14 Haggerty (1976, p.Hg260, analy.48-54). 15 Simpson (1951, p.651, Tab.33, analy.1-6). 16 Deer et al. (1975, p.29, Tab.5, analy.5). 17 Rumble (1976, p.R4, table R2, analy.1). 18 This paper. 19 Sutherland (1980, v.2, Tab.6e, analy.1D). 20 Jaques et al. (1989, p.133, Tab.7.6, analy.7), 21 Cassidy et al. (1988, p.1055, Tab.3, analy.1) 22 Coenraads (1990, p.1205, Fig.19, 55 analy.). 23 Coenraads (1990, p.1205, Fig.19, 45 analy.). 24 Hollis et al. (1983, p.191, analy. Bal.149, Nan.II, Mt.Mit). 25 Sutherland (1980, v.2, Tab.5g, analy.1-7). 26 Jaques & Perkin (1984, p.35, analy.5). 27 Haggerty (1976, analy.1-15). 28 Dawson (1980, Tab.11, p.78, 302 analy.). 29 Haggerty (1976, p.Hg258, analy.13,15-18). 30 Atkinson et al. (1984, p.208, Tabs.1&2, 6 analy.). 31 Neal & Davidson (1989, p.1980, Tab.5, 12 analy.). 32 Scott Smith et al. (1989, p.196-7, Tab.11.3, analy.P6/2). 33 Clarke & MacKay (1990, p.231, Tab.1). 34 F.L.Sutherland, A.D.Robertson & J.D.Hollis unpublished data. 35 Wass et al. (1980, p.338-9, Tab.1, analy.K41, K3, K13A1). 36 Harte et al. (1987, pp.187-188, Tabs.3&4, 4 analy.). 37 Moore (1987, p.248, Tab.1, 3 analy.). Oxides are in weight percent. For comparison purposes all iron is presented as FeO and oxides are listed in decreasing order of abundance for the Uralla samples.

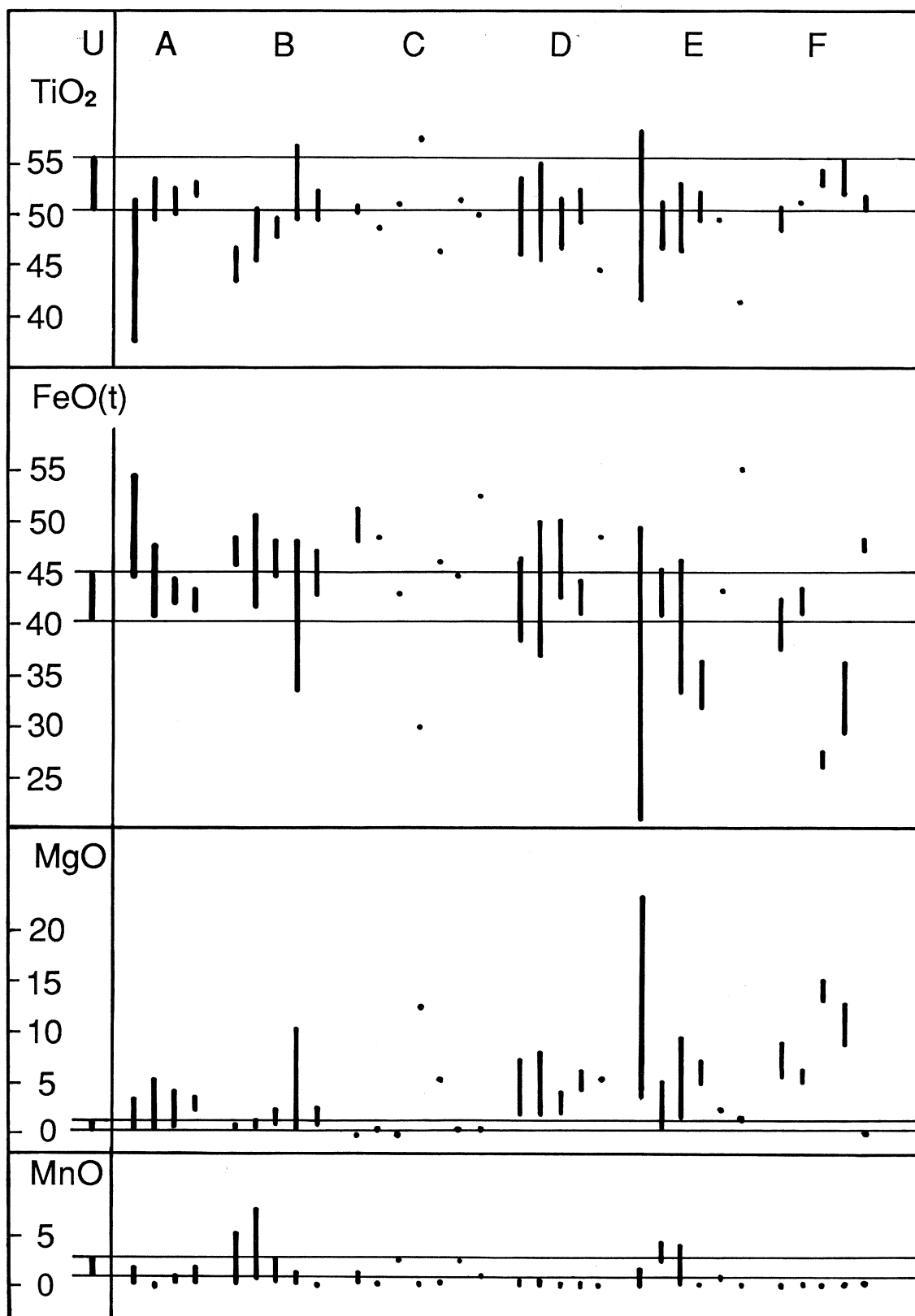


Figure 5-10. Summary of the main elemental oxide ranges in the Uralla ilmenite compared to those in literature sources (from Table 5-3). The order of associations follow those as listed under the main categories in the Table (A-F). The Uralla ilmenite is designated U and the limits for each elemental oxide are carried through to show bands of intersection with the other ranges.

for high MgO, (see Table 5-3E), with enrichment towards the edges because of magmatic reaction with the more magnesian kimberlitic melt.

The Uralla rutiles, unlike cores of rutile in kimberlite, show reaction relationships for a magma rich Fe but poor in Mg. Rutiles with replacement rims of ilmenite occur in granulitic xenoliths from Australian basalts but these ilmenite rims are also more magnesium-rich. The Uralla ilmenite compositions are compared with those from many different rock associations, as well as those derived from the volcanic rocks of the adjacent Central Province, in Table 5-3 and Fig 5-10. The Uralla ilmenites differ from the Central Province and kimberlitic ilmenites, being significantly higher in MnO, lower in MgO and having no Cr₂O₃.

In general there is too much MnO and/or too little MgO in the Uralla ilmenites to match typical ilmenites in alkali basalts, high Mg-tholeiite and mafic-ultramafic suites, including highly undersaturated melts from deep sources such as kimberlites, carbonatites, picritic monchiquites, alnoites and lamproites, or those in mantle xenoliths and xenocrysts. A rare exception is ilmenite inclusions in diamonds from Brazil, though low Mg ilmenites are not found in most other diamond suites. The contrast in size is a marked point of difference between the Brazilian and Uralla ilmenites which makes a related source unlikely. Ilmenite attributed to immiscibility processes in kimberlite melts at crustal levels (Clarke and MacKay, 1990) also differs from the Uralla compositions.

Uralla ilmenites are more akin to those found in silic igneous rocks. Comparison of their compositions with those of silicic volcanics show only a partial overlap as the latter are mostly lower in TiO₂ and higher in FeO. Ilmenites from the intrusive equivalents, granites and pegmatites are distinctly lower in TiO₂, and those from less silicic intrusions (syenite-monzonite-diorite-foyaite) barely overlap the Uralla range.

Metamorphic rocks rarely show ilmenite compositions within the Uralla range. One is a crustal xenolith of ilmenite-garnet-amphibole-plagioclase-quartz granulite from Western Australia and another crustal xenolith comes from low grade metamorphism of mafic-ultramafic rocks (see Table 5-3). However the latter are not typical of the great majority of ilmenites found in various grades of metamorphism of these rocks (Cassidy et al, 1988).

Low MgO in the Uralla ilmenite might suggest a relatively low pressure origin, as most high pressure ilmenites show high MgO contents. However, the amount of Mg entering the mineral is regarded more as a function of melt composition rather than a reflection of a depth or pressure effect (Haggerty, 1976).

5.6 Garnets from Horse Gully in the New England gemfields.

5.6.1 Occurrence

Deep red to purplish, gem quality garnets occur in sapphire bearing river gravels at Horse Gully in the New England Gemfields. The garnets were recovered by Arrawatta Sapphires Pty Ltd (J. Joris; Joris Gemstone Traders Pty Ltd, pers. comm.) within their Horse Gully mining areas near the abandoned township of Sapphire, 27 kilometres northeast of Inverell (Figure 5-11).

The garnets appear to be derived from a local source situated within the catchment area of Horse Gully.

5.6.2 Features and properties of the gem garnets

The garnets range in size up to 15 mm, are irregular and rounded in shape, and show a chipped and crazed water-worn surface. Some of the stones display a slight colour shift from a red or purplish hue in natural light to an orange red or almost pink in incandescent light. Seven garnets were polished to facilitate refractive index measurements, to provide a window into the stone for viewing inclusions, and to provide a surface for microprobe analyses.

Three microprobe analyses of each garnet proved each to be homogeneous in composition with any differences being less than one percent. The average composition of each garnet and its gemmological properties are listed in Table 5-4. They are members of the pyrope-almandine intermediate series ranging in composition from pyrope 55% - almandine 34% to pyrope 39% - almandine 49%. The stones with the highest end-member pyrope content (highest magnesium and lowest iron) display a most attractive mauve-purple to pinkish hue. The garnets have a specific gravity of 3.837 to 3.958 and a refractive index of 1.755 to 1.772. The relationship between these properties and the chemical composition is clearly shown in Figure 5-12. A higher pyrope content and a lower almandine content correspond to a lower specific gravity and refractive index, fewer inclusions and generally a lighter, more purplish colour.

The stones all show anomalous double refraction under the polariscope which is very strong in some cases (indicating a high degree of internal strain). The garnets are inert under both short wave and long wave ultraviolet light. Inclusions include, short to long, fine, oriented needles, which are probably rutile; short, colourless, oriented, cylindrical inclusions; and colourless crystals ranging from subrounded in shape to well formed hexagonal prisms. The latter are suspected to be apatite (Gübelin and Koivula, 1986), and a handsome trail of such crystals were found in garnet HG6 (Coenraads and van der Graaf, 1991).

The spectroscope revealed characteristic Fe²⁺ bands at 573 nm, 520 nm and 504 nm with another weak band at 460 nm (stones HG2, HG5 and HG7). In stones HG1

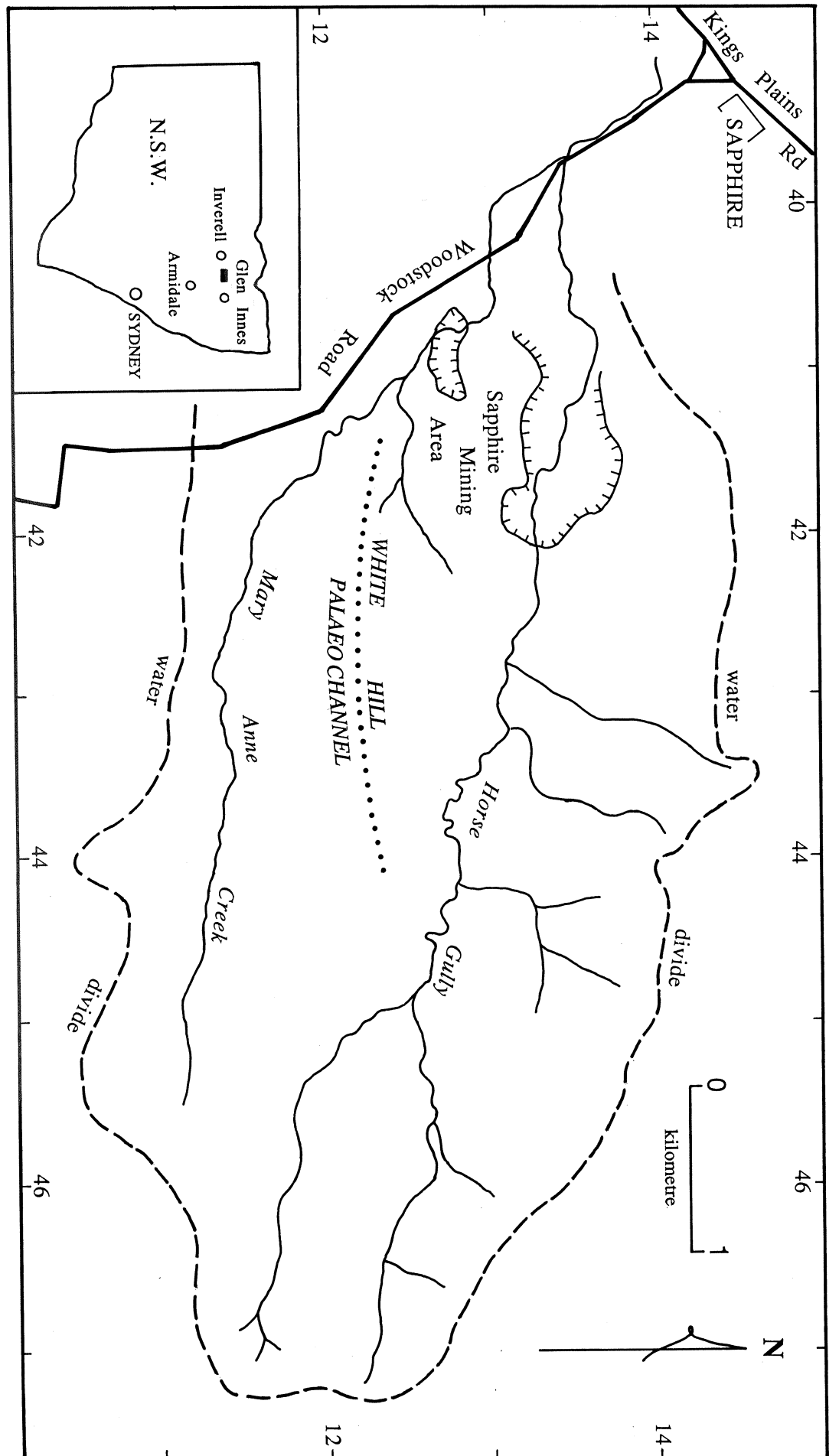


Figure 5-11. Location of Horse Gully in the New England Gemfields, New South Wales. The garnets were recovered from the mining areas of Arrawatta Sapphires Pty Ltd. The catchment area of Horse Gully and Mary Anne Creek is bounded by the water divide, shown dashed. The position of White Hill palaeochannel, now basalt filled, is indicated as a series of dots.

Table 5-4. Composition and gemmological properties of the Horse Gully Garnets.

	HG1	HG2	HG3	HG4	HG5	HG6	HG7
SiO ₂	38.94	39.30	39.99	39.23	40.09	39.89	40.26
TiO ₂	0.00	0.00	0.00	0.00	0.00	0.00	0.00
Al ₂ O ₃	22.38	22.65	22.94	22.66	23.04	22.86	22.90
Cr ₂ O ₃	0.00	0.00	0.00	0.00	0.00	0.00	0.00
FeO	23.89	21.10	18.50	21.41	17.46	18.81	18.31
MnO	0.55	1.05	0.86	1.02	0.54	0.75	0.70
MgO	10.44	11.84	14.00	11.76	15.09	13.96	14.04
CaO	3.79	4.05	3.71	3.93	3.78	3.74	3.80
Na ₂ O	0.00	0.00	0.00	0.00	0.00	0.00	0.00
K ₂ O	0.00	0.00	0.00	0.00	0.00	0.00	0.00
Total	99.99	99.99	100.00	100.01	100.00	100.01	100.01
Si	2.97	2.96	2.97	2.96	2.96	2.97	2.98
Al	2.01	2.01	2.01	2.02	2.01	2.00	2.00
Fe total	1.52	1.33	1.15	1.35	1.08	1.17	1.13
Mn	0.04	0.07	0.05	0.07	0.03	0.05	0.04
Mg	1.19	1.33	1.55	1.32	1.66	1.55	1.55
Ca	0.31	0.33	0.30	0.32	0.30	0.30	0.30
Total Cations	8.03	8.03	8.03	8.03	8.04	8.03	8.02
PYROPE	39.4	44.2	51.5	43.9	55.1	51.4	51.6
ALMANDINE	49.2	42.7	36.9	43.4	33.9	37.2	36.9
GROSSULAR	10.3	10.9	9.8	10.6	9.9	9.9	10
SPESSARTITE	1.2	2.2	1.8	2.2	1.1	1.6	1.5
Specific Gravity	3.958	3.919	3.87	3.908	3.837	3.856	3.858
Refractive Index	1.772	1.767	1.759	1.768	1.755	1.759	1.758
Colour							
natural	red	red	purplish/red	purplish/red	reddish/purple	red	reddish/purple
incandescent	red	red	red	red	orangy/pink	orangy/red	orangy/red

HORSE GULLY GARNET

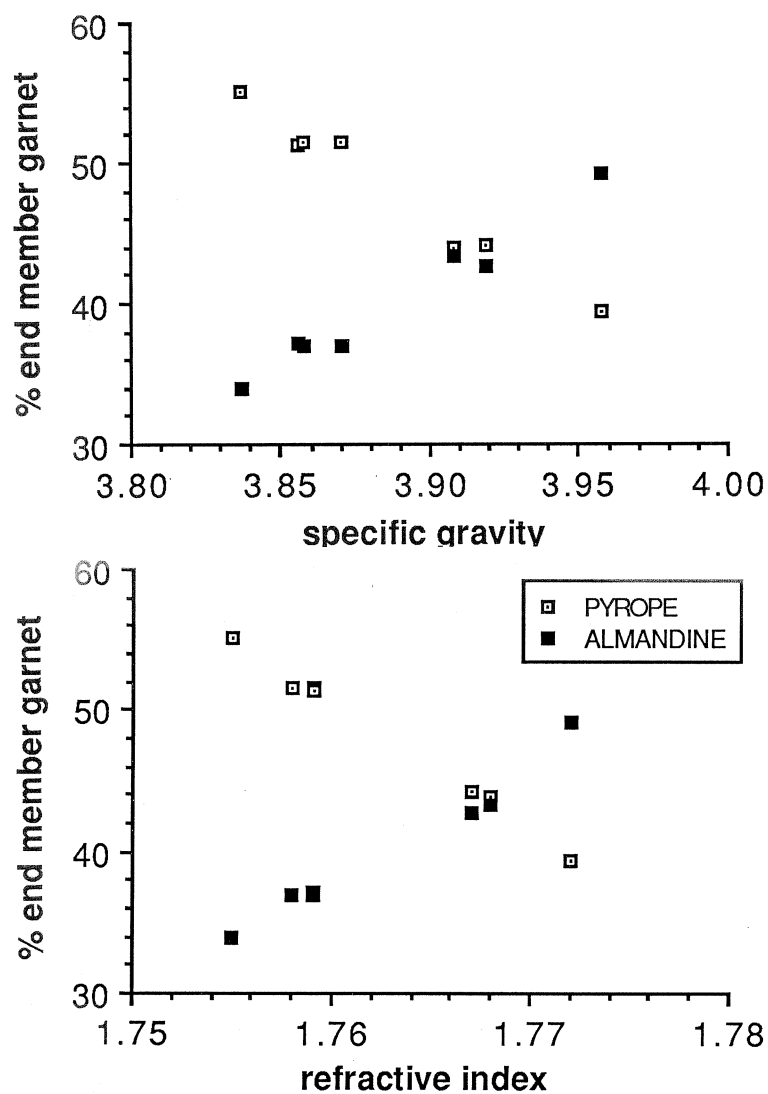


Figure 5-12. Relationship between refractive index, specific gravity and end member composition for the Horse Gully Garnets. It is clear that, a higher pyrope content and a lower almandine content correspond to a lower specific gravity and refractive index.

&HG2, the 504 nm and 520 nm bands merge to form a broad absorption band and stones HG1, HG2 & HG4 show a cutoff at the violet end of the spectrum. Based on their gemmological properties, the garnets would be classified as belonging to the pyrope-almandine intermediate series with HG5 being of sufficiently purple hue and light in colour to be called rhodolite.

5.7 Implications for genesis of heavy mineral placer deposits.

The mineral suite comprising pleonaste, chrome-spinel, titanium-magnetite/ulvospinel and ilmenite is well represented in both placer and basaltic soil concentrates. These all occur as accessory minerals or as megacrysts in the Central Province volcanic rocks (Binns, 1969 and Binns et al., 1970). Sapphire and zircon are also usually present, and a genetic link between these two minerals and the volcanic rocks has been established by U-Pb dating of zircon inclusions contained in sapphire (Coenraads et al, 1990). Ages of 34 Ma (at site DUN) and 36 Ma (at YAR) lie within the K-Ar age range for basalts of the Central Volcanic Province.

Small systematic differences in major and minor oxide content of the heavy opaque oxides in placer and soil samples from several drainage systems are not found to be statistically significant. In spite of this, subtle visual differences in the nature of the heavy mineral concentrates and in the colour, shape and size of the sapphires have been reported by miners and sorters. For example, as mining proceeds along the length of a deposit stones may vary from being predominantly parti-coloured in a particular area, to predominantly blue with a blue cross-table, or to predominantly darker blue with a green cross-table. Shape may vary from predominantly equant crystal fragments to slender pointed hexagonal pyramids (dogs teeth). Sapphires recovered from one area of Kings Plains were reported to be extensively internally fractured and jagged in appearance (K.J. Walker, pers. comm.). Corundum recovered from Furracabad Creek, in the catchment adjacent to Reddestone Creek, is largely black (T.J. Nunan, pers comm.). The ratio of zircon to sapphire has also been observed to vary from place to place (K.J. Walker, pers. comm.). These differences occur within the order of kilometres

Weathering of basalts and their volcanoclastic associates liberates all of the heavy minerals found in *in situ* basalt soils and in placer deposits. The less resistant silicates (olivine, orthopyroxene, clinopyroxene and amphibole) break down leaving the resistant heavy minerals which are concentrated into placer deposits by fluvial action. Differences in proportions of heavy minerals in placer deposits are obviously influenced by hydraulic and comminution factors. However, it is likely that they reflect net differences in the proportions of heavy minerals shed from various local basalt flows and/or nearby volcanoclastics. For instance, the breccia dyke (BRE) at Braemar is believed to have contributed partly to nearby placer deposits (Pecover and Coenraads, 1989). This, coupled with the spatial variability in the character the sapphires and grain surface features which

indicate minimal amounts of fluvial transport, suggests local multiple sources and minimal downstream reworking and mixing.

The concentration of sapphire to yield important deposits, such as those at Reddestone and Kings Plains creeks, results from favorable hydrologic conditions, including appropriate palaeostream energy and gradient, combined with the availability of suitable source rocks within the catchment.

5.8 Conclusions and interpretation.

The analysis of heavy mineral concentrates from different catchment areas in the Central Volcanic Province has led to a number of interesting findings. These are:

1) The only ubiquitous associate of sapphire is zircon. It is likely that both formed under similar conditions based on ages of zircon inclusions in sapphires (34-36 Ma) and related ages of older basalts from the Central Province (32-38 Ma). Abundant quantities of spinel or ilmenite are not necessarily indicators for sapphires or zircons, but do indicate that fluvial concentration has been successful.

2) In situ soils from basalts and their volcanoclastic associates yield suites of heavy minerals that contain various combinations of sapphire, zircon, pleonaste, chrome-spinel, titanium magnetite-ulvospinel and ilmenite. Less resistant heavy minerals (olivine, pyroxene, and amphibole) were found only in basaltic soils and immature alluvials.

3) From all the in situ soil sites visited, only one small zircon was recovered by the author (UNE). One large sapphire was found by a property owner (HIL) and small quantities of sapphire and zircon were reported to have been recovered from the red breccias at Braemar. This scarcity of sapphire and zircon demonstrates the enormous amount of concentration required to produce the economic placer deposits.

4) Placer concentrations of heavy minerals typically contain most members of the suite, although proportions of individual minerals can vary appreciably. This variability is believed to largely reflect mineralogical variation in local alkali basaltic and volcanoclastic sources for the placer concentrations. Visual characteristics of the sapphires also change locally.

5) The abundances of major and minor oxides in pleonaste, chrome-spinel, titanium-magnetite and ilmenite in both soils and placer deposits, within and between drainage systems, are remarkably uniform. Subtle differences are not significantly clear to be of use in exploring for sapphire deposits in the Central Province.

6) The gem quality pyrope-almandine garnets from the New England gemfields are very local, being found with sapphires only in Horse Gully. For this reason they are probably not derived from the widely distributed sapphire bearing volcanic rocks of the Central Province. They may be derived from a small isolated diatreme-like intrusion similar to those which produce gem quality garnets at Ruby Hill near Bingara, N.S.W. (Lovering, 1964), at Brigooda and Ballogie, near Proston, Queensland (Hollis et al, 1983; Sutherland et al, 1990) and Bogie River, north Queensland (Jones, 1983). However, the Horse Gully garnets show significantly lower CaO and MgO and higher FeO than these garnets.

The Horse Gully garnet source is located within the 18 km² catchment area of Horse Gully and Mary Ann Creek (Figure 5-11). Possibly it remains hidden by basalt that also fills the, now extinct, White Hill palaeochannel presently being exhumed by Horse Gully and Mary Ann Creek. The position of the palaeochannel is indicated as a series of dots on Figure 5-11.

The Horse Gully garnets are quite different to the spessartine-almandine garnets found in the diamond-bearing Tertiary deep leads at Copeton (D. Jones pers. comm.), and also different to the garnets derived from acid to intermediate igneous sources as these contain little CaO (0.5-1.5%) and MgO (1-6%) (W. Birch pers. comm.). It is thus most likely that the Horse Gully garnets are derived from a mafic source.

7) The source of the ilmenite mantled rutile crystals has not yet been identified. The crystals are found, concentrated by virtue of their size and weight, within conglomerate bands in arkoses of possible late Tertiary to Quaternary age. They also occur in high concentration in the modern streams draining the arkoses; however, they are seen to be fragmented within a short distance downstream. All this implies a proximal source.

Other heavy minerals associated with the arkoses include zircon, spinel, gold and sapphire, but areas of high concentration of a particular mineral, such as zircon, do not always correspond directly to areas of high ilmenite-rutile crystal concentration.

No metamorphic rocks (Sandon Beds and Dummy Creek Group) exist in the areas of highest concentration of the crystals so are unlikely to be the original source. Panned concentrates of numerous samples of sub-basaltic Tertiary gravels, chiefly from mullock heaps around shafts and from rare outcrops, contained no ilmenite-rutile crystals. Panned soil samples from around basalt outcrops produced no crystals and none were seen in hand-specimens of a wide variety of basalts from numerous locations around Uralla.

Owing to the restricted distribution of the crystals, the host rock possibly had a restricted outcrop area, thus excluding the Uralla granodiorite, and it must be local because of the immaturity of the arkoses and the inability of the crystals to withstand fluvial transportation. The chemical comparisons, discussed above, also indicate that the source rock is unlikely to be mafic or ultramafic in composition. Possibly the host rock was easily weathered and hence difficult to recognize, or has been covered by younger deposits.

The summary of the main elemental oxide contents of the Uralla ilmenite relative to ilmenite compositions in the literature (Figure 5-10) highlights their somewhat unusual composition and helps to suggest potential sources. The Uralla TiO_2 , $\text{FeO}(\text{total})$, MgO and MnO contents only intersect four of the thirty two ranges listed from the literature (salic volcanics, syenites-foyaïtes, coarse phase leucitites and the quartz granulite xenolith).

One possible source is a magmatic precipitate from a magnesium poor, iron and titanium enriched melt. If there is a link with the abundant near-source zircon crystals in the district, then these minerals would represent late-stage or cavity crystallizations from fractionated felsic magmas in subvolcanic chambers or conduits before eruption. This would be compatible with ilmenite compositions overlapping those of salic volcanics. Zircons from the Rocky River give mid to late-Tertiary ages of formation and eruption (red to orange crystals, 27 to 3 Ma; F.L. Sutherland and P.D. Kinny, unpubl. data). This relates these zircons to the Tertiary volcanic activity in the area. Such an association for these minerals could account for their apparent absence from the sub-basaltic Tertiary sediments.

Another possible source may be a coarse grained metamorphic or vein rock related to the obscured Uralla Granodiorite contact in the area. The least likely association is as an indicator for diamond source rocks.

The present study of the evolution of the Central Volcanic Province and its drainage patterns has provided valuable insight into the occurrence and mechanisms of concentration and distribution of diamond and sapphire deposits. Diamond bearing deep leads occur below the lavas of the West Central Province and sapphire bearing alluvial and deep lead deposits are associated with the East Central Province. In particular, the present study allows the prediction of possible extensions to known deposits and identifies potentially favorable areas for future exploration.

The absence of less resistant minerals and relative abundance of sapphires and zircons in the placer deposits indicate a high degree of concentration. Variability in the mineral species, and character the sapphires within short distances, however, suggests local sources. Grain surface features also indicate minimal amounts of fluvial transport. This, combined with the low gradient and low energy drainage systems suggests that reworking occurs largely in a vertical sense. The fine or light material is "winnowed out" leaving a heavy residue. A rich upstream source, in contrast, would yield a constant suite of minerals of uniform appearance downstream with more evidence of fluvial abrasion.

These observations are of vital importance in exploring for new sapphire deposits. They demonstrate that a search for elusive rich sources is inappropriate. Rather, the exploration effort should be directed towards gaining a thorough understanding of the geomorphic processes involved in the development of economic placer deposits from low-grade source rocks.

Chapter 6

EVALUATION OF SAPPHIRE SOURCE ROCKS AND POTENTIAL SOURCE STRUCTURES IN THE CENTRAL VOLCANIC PROVINCE.

6.1 Introduction

This chapter examines the natural lagoons found on the lavas of the Central Volcanic Province. These enigmatic features have been described as maar volcanoes by Pecover (1987) who also proposed that they are possible sources of sapphire-bearing volcanoclastic rocks. They thus represent potentially important economic targets.

Sapphire source-rock compositions were studied and compared with those from sapphire-bearing and sapphire-barren provinces. If definitive differences exist, these could be used as indicators in sapphire exploration programs both for new gem fields and for high grade areas within existing gem fields.

6.2 Evaluation of the natural lagoons of the Central Volcanic Province -Are they sapphire-producing maars ?

Lagoons of the Central Volcanic Province are roughly circular to amoeboidal in shape and range from less than 100 metres to several hundreds of metres in diameter. They are usually flat swampy areas or lakes surrounded by a bank up to several metres high. The sediment in the lagoons is a grey clay and the rims or banks consist of ironstone pisoles, either cemented or loose, within a red clay matrix. The rims are altered to the extent that no relict primary textures are observable. In all the lagoons examined, basalt is present in portions of the rims where it occurs as flows or discrete pebbles, cobbles and boulders within the clay and pisolitic material. These are usually the steepest and highest parts of the rims.

Maars are described by Ollier (1967) and Ollier & Joyce (1976). Typical maars in Victoria are circular depressions usually containing lakes or swamps. They are "explosion craters extending below the general ground level and surrounded by a low rim of pyroclastics, including some country rock. The pyroclastic rim is steep on the inside and very gentle on the outside, merging into the surrounding plain. The craters are 500 m to 2 km across with walls up to about 20 metres high, or higher in exceptional cases such as Bullenmerri. Ash is often asymmetrically distributed by wind, with high walls on the east side and low or no walls at all on the west" (Ollier & Joyce, 1976). They are occasionally filled with sediment and have flat crater floors. However, the maars of Victoria show internal structure in the form of characteristic bedded pyroclastic material in their rims and do not have associated ferricrete.

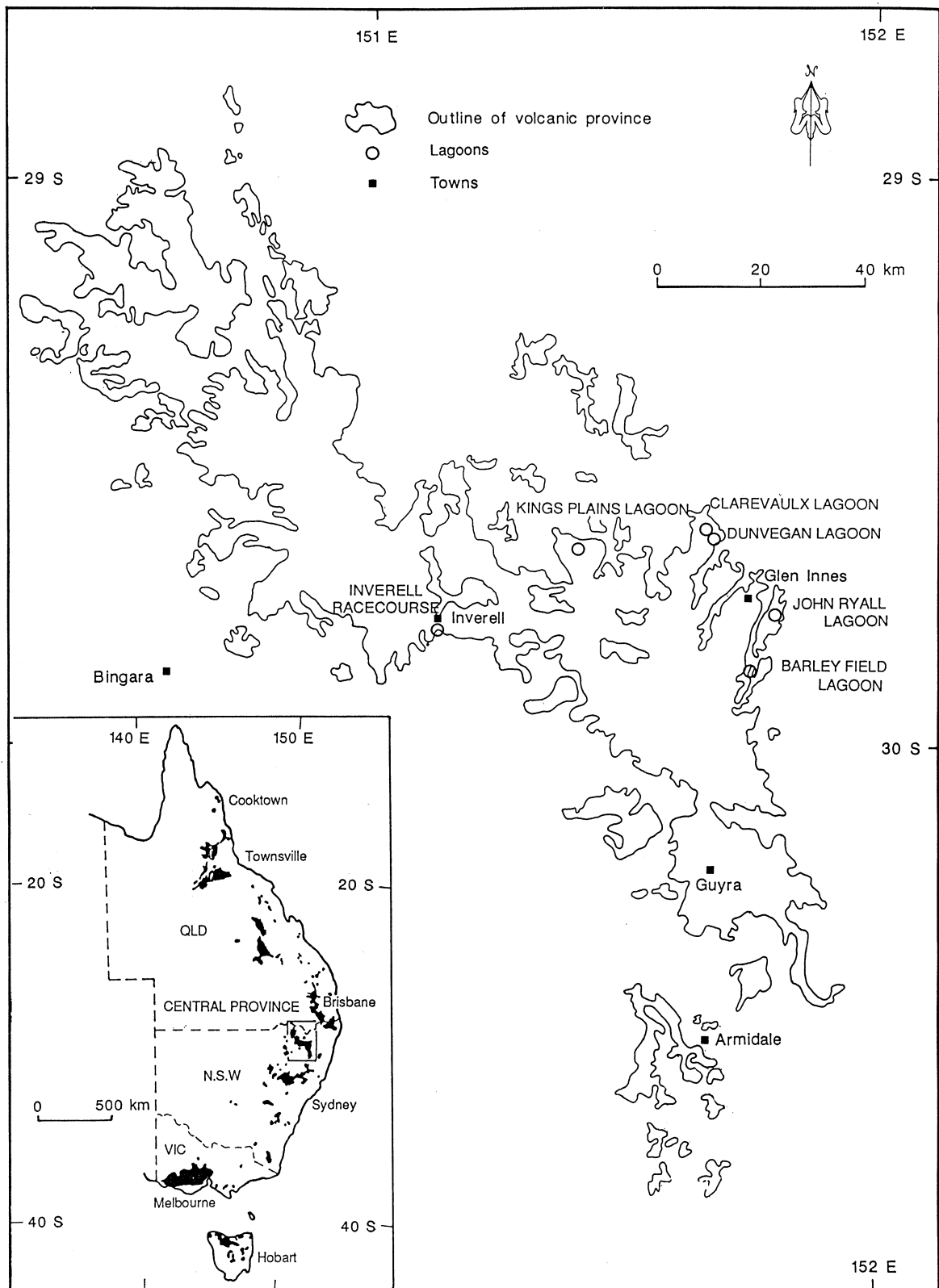


Figure 6-1. Lagoons of the Central Province, N.S.W. The locations of the natural lagoons studied are shown in relation to the outline of the Central Province. The inset shows the position of the Central Province relative to the other eastern Australian Mesozoic-Cainozoic volcanic provinces.



Figure 6-2. Kings Plains Lagoon. The area of this photograph is shown in Fig. 6-7.



Figure 6-3. Dunvegan Lagoon. The area of this photograph is shown in Fig. 6-8.



Figure 6-4. Clarevaulx and Dunvegan Lagoons. The area of this photograph is shown in Fig. 6-8.



Figure 6-5. John Ryall Lagoon. The area of this photograph is shown in Fig. 6-9.



Figure 6-6. Barley Field Lagoon. The area of this photograph is shown in Fig. 6-10.

Six natural lagoons in the Central Volcanic Province were chosen for the investigation. Their locations are shown in Fig. 6-1 and tabulated in Appendix 3. Figures 6-2, 6-3, 6-4, 6-5 and 6-6 are aerial photographs of the lagoons:

Dunvegan Lagoon and Kings Plains Lagoon, have been examined geophysically (Appendix 3) and bulk tested in order to ascertain their economic potential. Kings Plains Lagoon has been drilled extensively (Lishmund, 1987; Coenraads, 1988b). The relationship of these features to the underlying valley fill lava flows and Permian basement topography has also been examined at a scale of 1:25,000.

The geology in the vicinity of the lagoons appears in Figures 6-7, 6-8, 6-9, 6-10 & 6-11. The present edge of the basalt flows is shown as a solid thick line and areas of exposed pre-volcanic basement rocks can be seen. The contours indicate the interpreted pre-volcanic topography; solid contours are used where the basement is exposed and dashed contours indicate the interpreted basement below the basalt. The topography has been determined by plotting a series of elevations for the mapped boundaries between the Central Province volcanics and the older basement rocks. The data points have been contoured conservatively, that is, in areas of basalt cover the basement is interpreted to dip gently and smoothly underneath and the least amount of basalt cover was inferred in areas of poor control.

The cross sections (see Figure 6-12) show the relationship of the lagoons to the present surface topography, to the valley flow basalts, and to the Permian basement channels. The interpreted Permian basement is shown dotted, and indicates that the channel axis is roughly below the surface lagoonal feature in every case and that there is at least 10 metres of valley flow basalt below each feature. Drilling at Kings Plains found the valley axis to be under the feature at a depth of 46 metres. At least two lava flows, separated by a woody horizon, were seen in holes KP3, KP4 and KP1.

Gravity data at Dunvegan support a similar model of a basalt filled channel with its axis beneath the centre of the feature. The gravity data indicate that the axis of the channel is trending towards Clarevaux lagoon.

At Dunvegan sub-economic to marginally economic concentrations of sapphire were found by bulk testing in the rim, on the flanks of the rim, and below the lacustrine clay within the lagoon. No sapphires, however, were recovered during the investigation of Kings Plains Lagoon. It is noteworthy that abundant spinel and the occasional sapphire may be easily "specked" by eye from around the edges of Dunvegan Lagoon, whereas spinel is not seen around the edges of the Kings Plains feature, nor on the rims of John Ryall Lagoon and Barley Field Lagoon.

6.3 Detailed work at Kings Plains and Dunvegan lagoons

The following points describe chronologically the exploration work carried out at Kings Plains and Dunvegan lagoons.

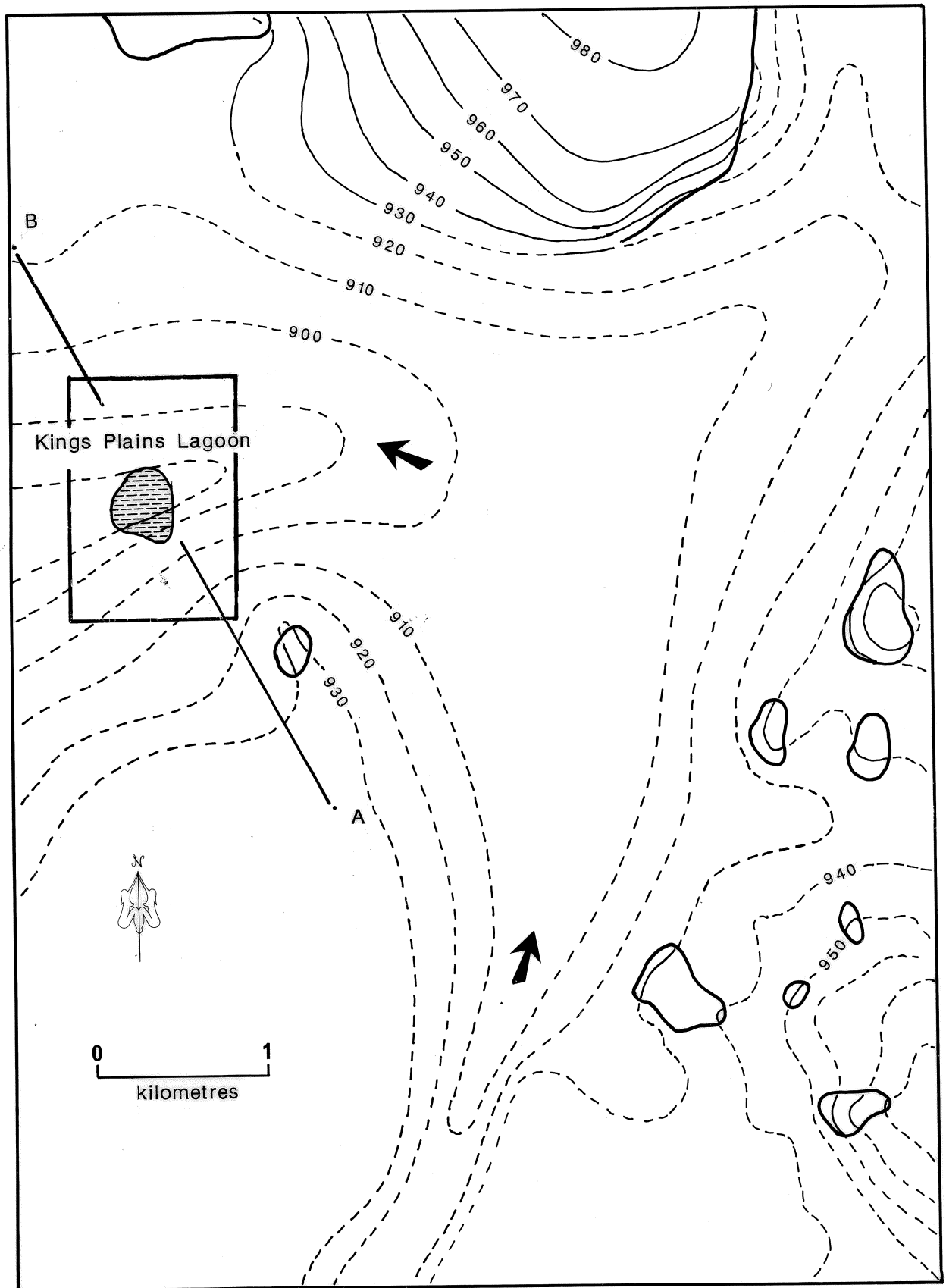


Figure 6-7. Basement topography in the vicinity of Kings Plains Lagoon. Contours are in metres and shown dashed below the basalt. The edge of the basalt is shown as a solid line. The position and direction of pre-basaltic drainage is emphasized by solid arrows. The location of cross section AB and the area of the photograph, Fig. 6-2, are also shown.

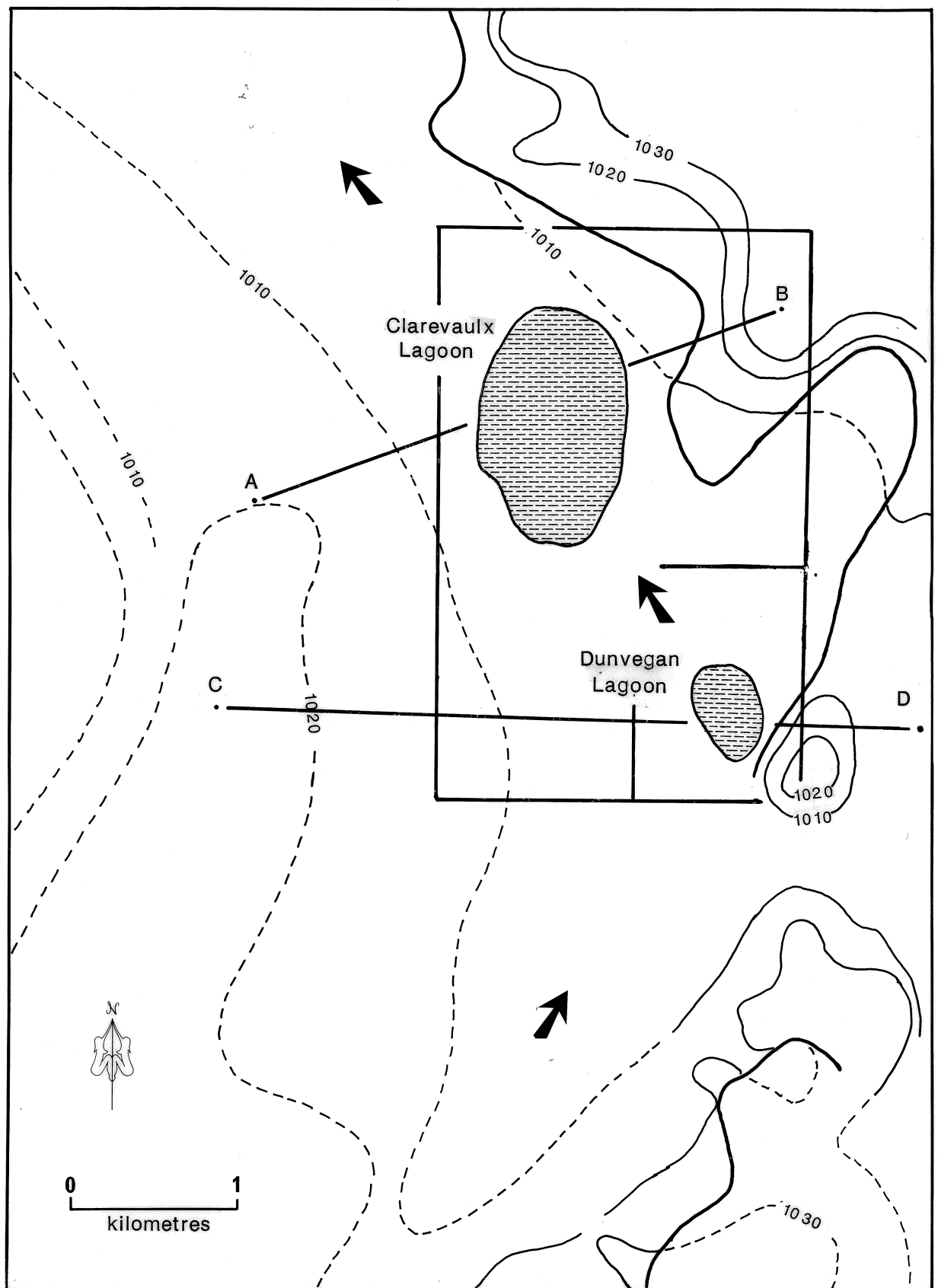


Figure 6-8. Basement topography in the vicinity of Clarevaulx and Dunvegan Lagoons. Contours are in metres and shown dashed below the basalt. The edge of the basalt is shown as a solid line. The position and direction of pre-basaltic drainage is emphasized by solid arrows. The locations of cross sections AB & CD and the area of the photographs, Figs 6-3 & 6-4, are also shown.

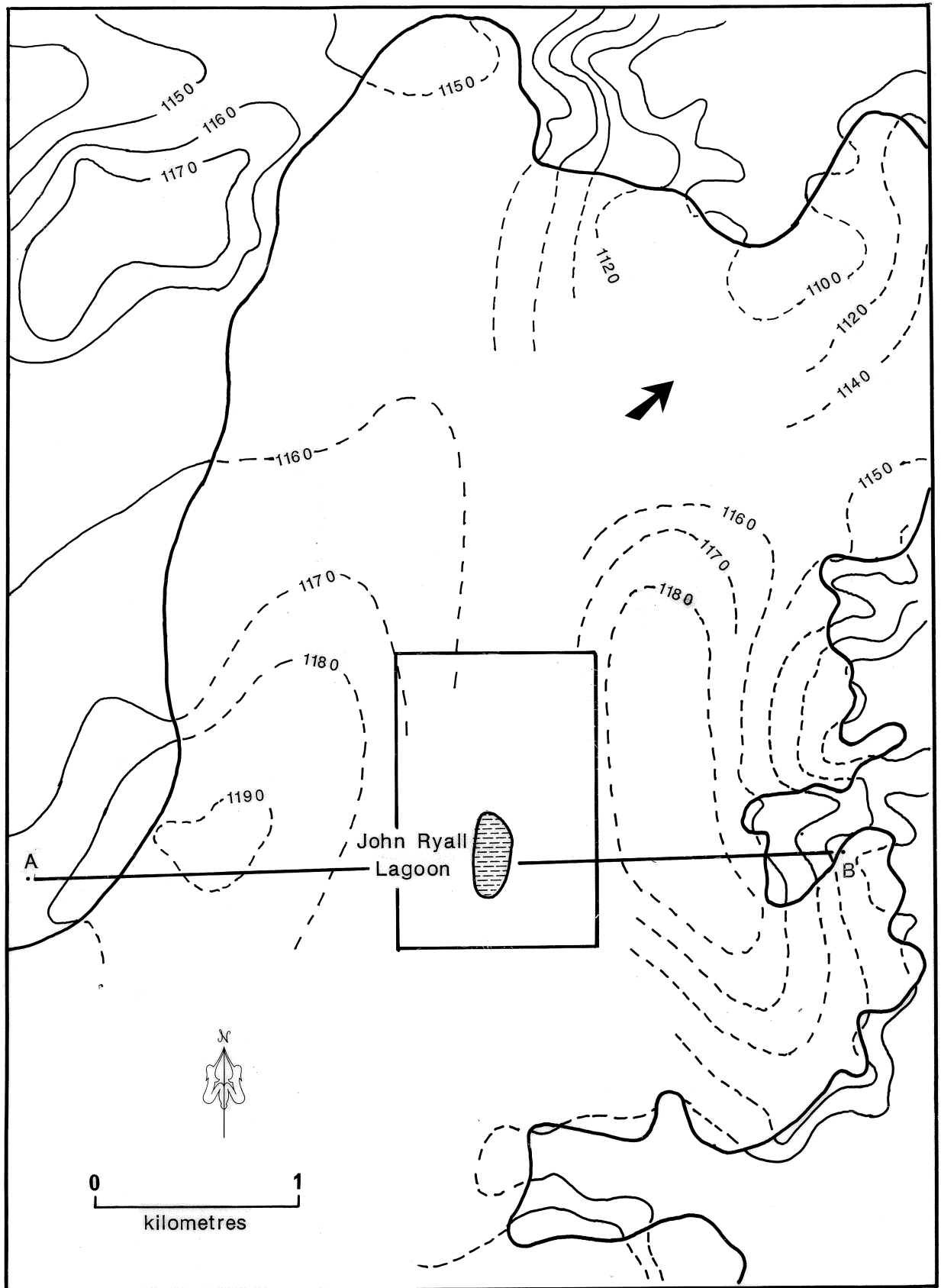


Figure 6-9. Basement topography in the vicinity of John Ryall Lagoon. Contours are in metres and shown dashed below the basalt. The edge of the basalt is shown as a solid line. The position and direction of pre-basaltic drainage is emphasized by solid arrows. The location of cross section AB and the area of the photograph, Fig. 6-5, are also shown.

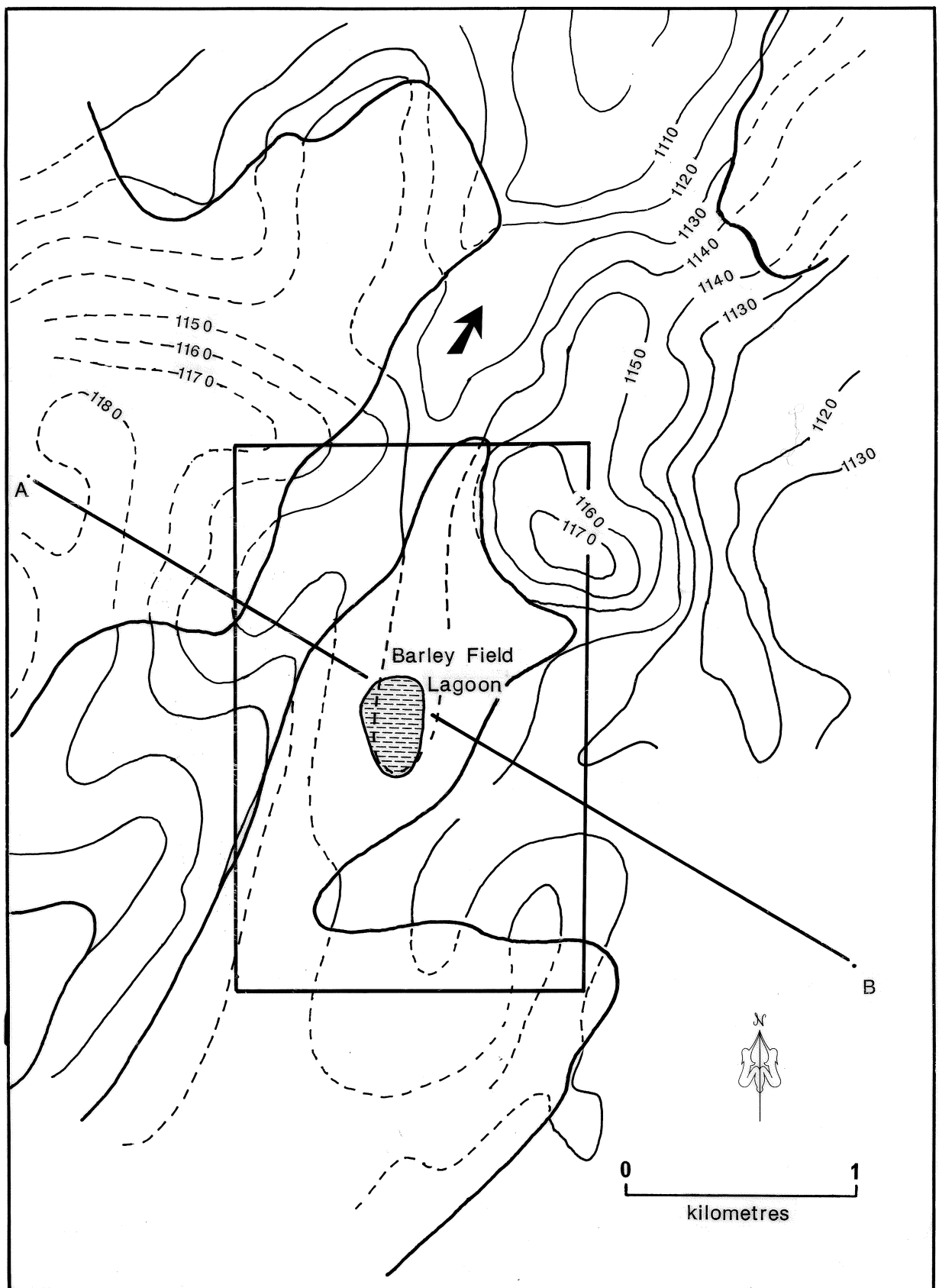


Figure 6-10. Basement topography in the vicinity of Barley Field Lagoon. Contours are in metres and shown dashed below the basalt. The edge of the basalt is shown as a solid line. The position and direction of pre-basaltic drainage is emphasized by solid arrows. The location of cross section AB and the extent of the photograph, Fig. 6-6, are also shown.

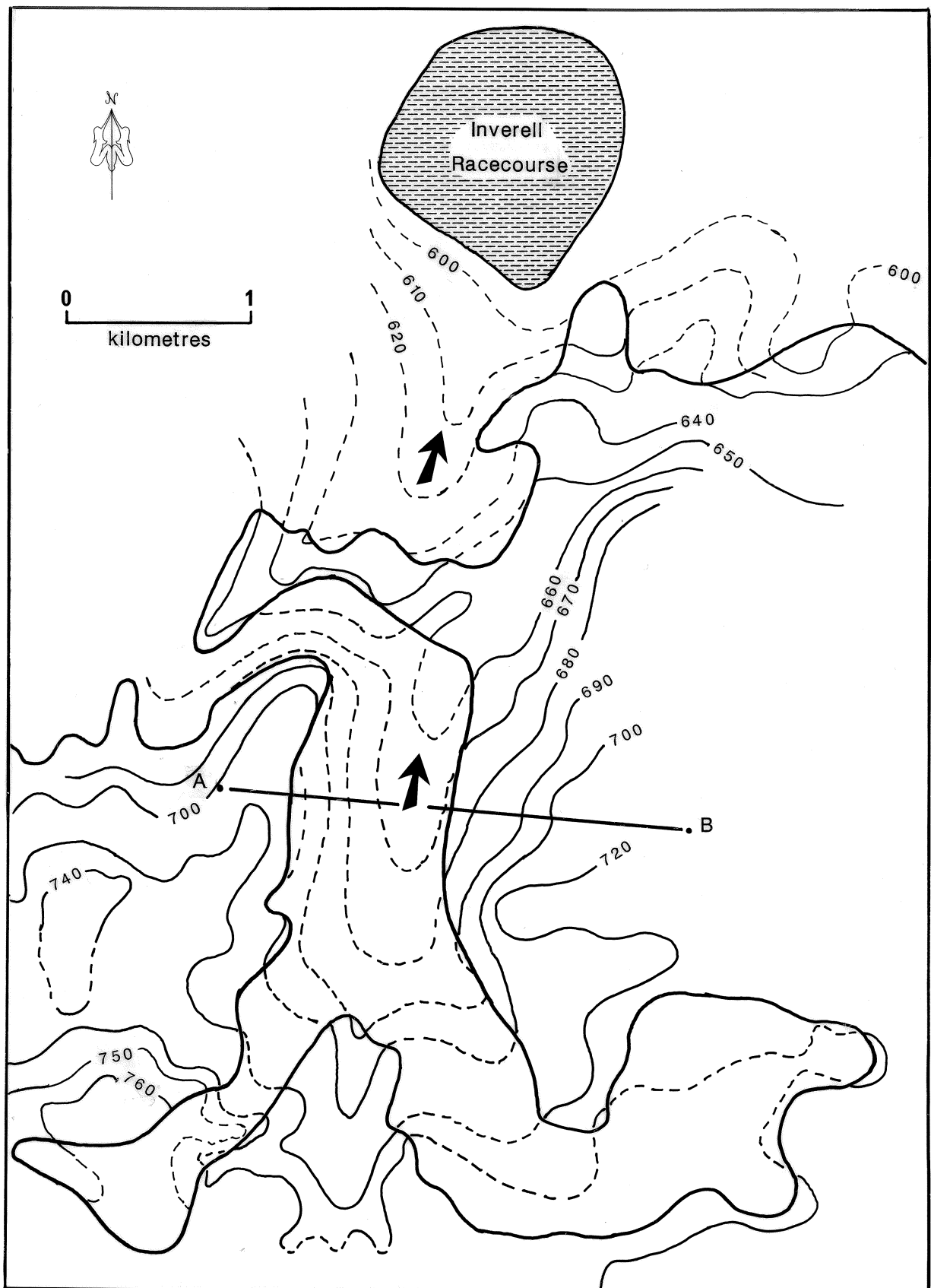


Figure 6-11. Basement topography in the vicinity of Inverell Racecourse. Contours are in metres and shown dashed below the basalt. The edge of the basalt is shown as a solid line. The position and direction of pre-basaltic drainage is emphasized by solid arrows. The location of cross section AB is also shown.

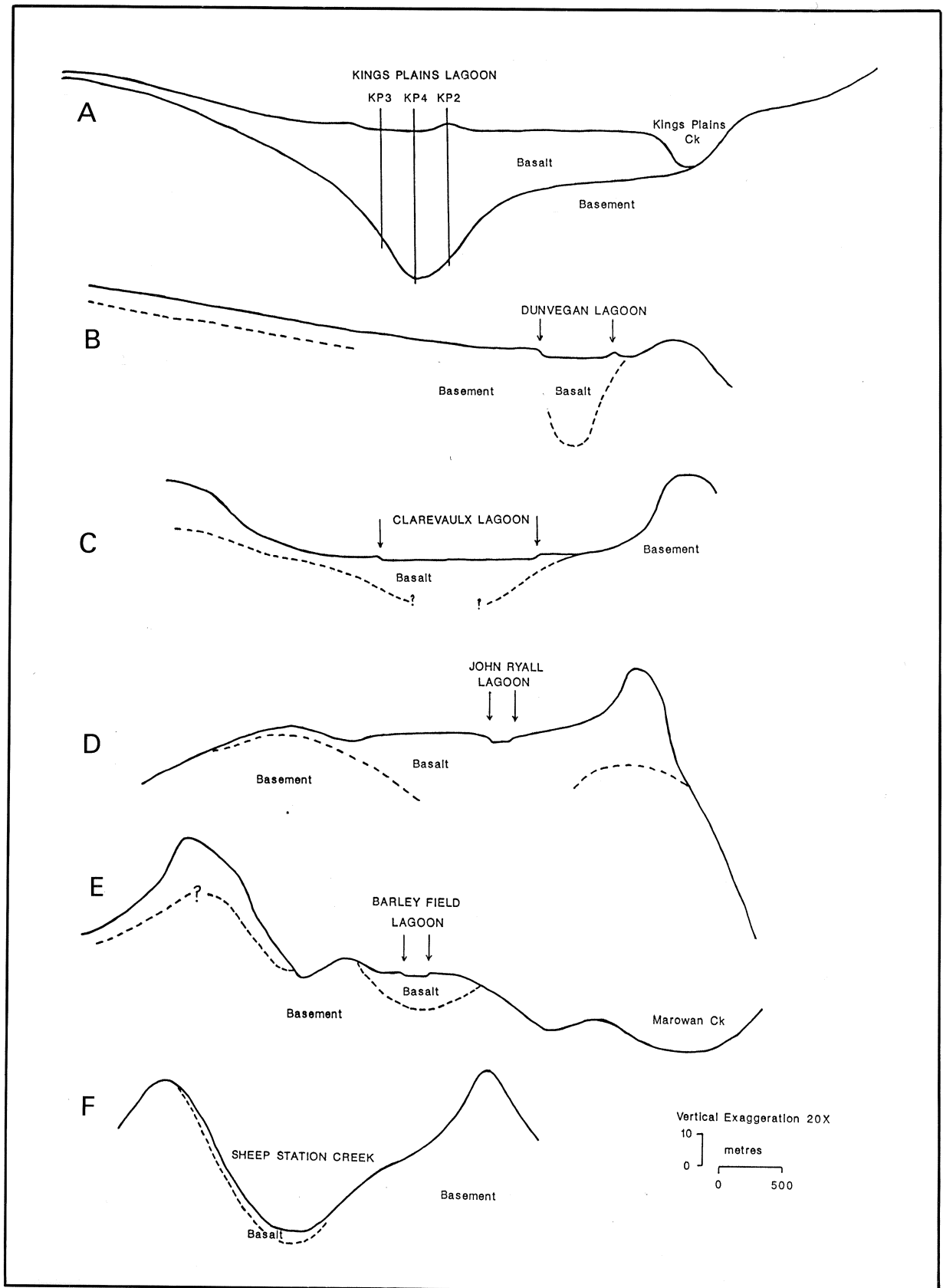
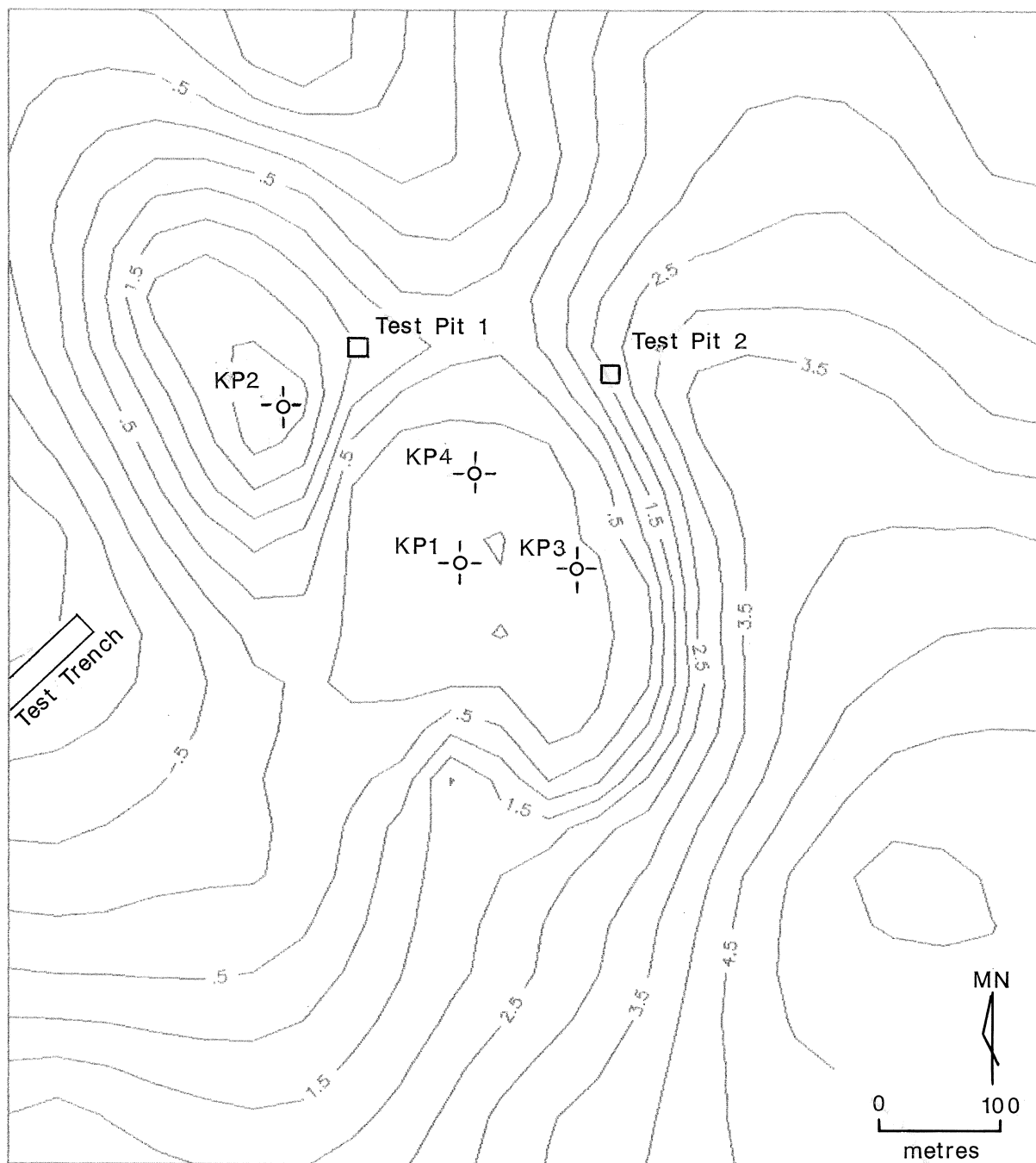


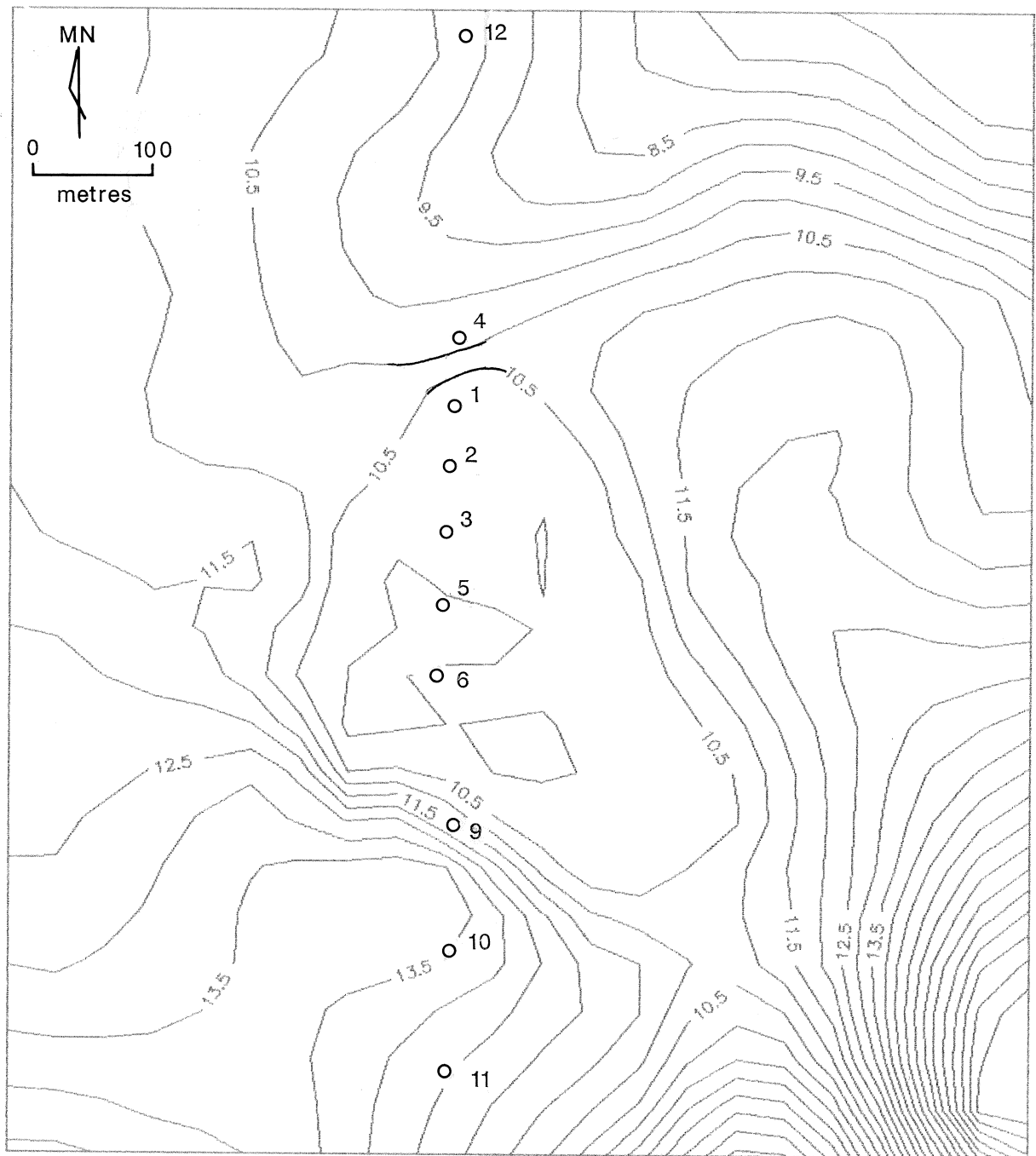
Figure 6-12. Cross sections through; A; Kings Plains Lagoon from Fig. 6-7. B; Dunvegan Lagoon from Fig. 6-8. C; Clarevaux Lagoon from Fig. 6-8. D; John Ryall Lagoon from Fig. 6-9. E; Barley Field Lagoon from Fig. 6-10. F; Sheep Station Creek in the vicinity of Inverell Racecourse from Figure. 6-11. The pre-basaltic surface is shown dashed, with the exception of that below Kings Plains which is shown as a solid line as its position is known exactly through drill holes KP1, KP2, KP3 and KP4. The dashed line below Dunvegan Lagoon, which would otherwise be terminated by question marks, is based on the geophysical data.

- 1) A test trench 180 metres long was cut to a depth of 7 metres by Jingellic Minerals N.L. to test the material on the flanks of the Kings Plains structure. The location of the trench is shown on Figure 6-13. No sapphires were found in the concentrate.
- 2) Diamond drill holes KP1 and KP2 were designed by the Department of Minerals and Energy to test if the Kings Plain feature is a maar (Lishmund, 1987). KP1 was drilled in the geometric centre of the feature and KP2 on the rim as shown on Figure 13. The holes encountered basalt flows to a depth of 44 metres overlying basement. The core is located at the Department's core library at Londonderry.
- 3) Geophysical surveys (magnetics, gravity and seismic reflection; see Appendix 3) were carried out for T.J. & P.V. Nunan Pty Ltd in order to assess the subsurface structure of the Kings Plains and Dunvegan features and provide a basis for the location of any future drill holes. The surveys covered an area of one square kilometre (the extent of Figs. 6-13 and 6-14) and models were constructed using the information from the Kings Plains drilling data. The data are held by R. Coenraads at Macquarie University.
- 4) Two test pits (numbered 1 and 2 on Fig. 6-13) were opened by Jingellic Minerals N.L. to test the economic potential of the rim material at Kings Plains. Eight cubic metres of material from the surface to a depth of 1.5 metres were removed and processed in a test plant. Only trace amounts of sapphire and zircon were found in pit 1 (0.3 grams/cubic metre) and none in pit 2. No spinel or ilmenite were recovered.
- 5) A line of 15 shallow bulk test holes (numbered on Fig. 6-14) were drilled across the Dunvegan structure by T.J. & P.V. Nunan Pty Ltd in order to test the economic potential of the near surface material. A Cauldwell rig with a bucket diameter of 1 m was used. Sapphires were found in almost all holes with some good grades. Grades of 13.0 g/m³ at 2.1-2.4 m. in hole 14, 10.7 g/m³ at 0.5-1.2 m. in hole 4 and 9.5 g/m³ at 2.4-2.7 m. in hole 13 were recorded.
- 6) Percussion holes KP3 and KP4 were drilled by Jingellic Minerals N.L. in the most likely position to encounter a vent below the Kings Plains feature based on the geophysical data (see Fig. 6-13). The drill cuttings are held by Jingellic Minerals N.L. in Inverell and the logs are described in Appendix 4, (Coenraads, 1988b). The drilling programme was designed to test the following:
 - (a) To test for the presence of any volcanoclastic material within the crater that may have undergone some secondary reworking and contain economic sapphire concentrations;
 - (b) To test for the possibility of a vent structure or breccia pipe in the eastern and northern portion of the crater based on the geophysical data (KP3 was positioned on the gravity high according to a geophysical model in which the pipe material is



KINGS PLAINS ELEVATION

Figure 6-13. Kings Plains Lagoon geophysical survey area. Elevation is in metres with a contour interval of 0.5 metres. The location of holes KP1, KP2, KP3 & KP4, test pits 1 & 2 and the test trench are shown. The shoreline of the lagoon corresponds to the zero metre contour.



DUNVEGAN ELEVATION

Figure 6-14. Dunvegan Lagoon geophysical survey area. Elevation is in metres with a contour interval of 0.5 metres. The location of shallow test holes are shown. The shoreline of the lagoon corresponds to the 10.5 metre contour

fresher than the surrounding rocks and KP4 on the gravity low according to a model in which the pipe material is highly altered);

- (c) To determine the depth to the basement rocks (Permian silicic volcanics);
- (d) To examine the nature of the contact between the Permian basement and overlying basalt flows and to determine whether any alluvial deposits encountered in this position are economically prospective for sapphires;
- (e) To take the opportunity to examine the concentrate from large quantities of crushed basalt and see whether any indication can be found of sapphires originating from this material.

6.3.1 Discussion

The lack of internal structures and unaltered rock types in the lagoon rims makes it impossible to identify these features positively by field inspection alone. Based on the observational data available at the time, (circular shape, raised rim, arcuate drainage around the features etc), the description of these features as maars, (Pecover, 1987), seemed justified.

In light of the failure to locate feeder pipes or brecciated material within the structures, using geophysical methods and a subsequent drilling programme, a new model is required. The present model proposes filling of pre-Tertiary basement channels with lava flows as illustrated in Figure 6-15 (A-D). Basalt lavas flowed down these channels (diagram A) and filled them to a uniform level (diagram B). On cooling, shrinkage occurred, tending to leave the deeper centre sections at lower levels. The creation of a broad flat river channel (diagram C) led to the development of an extremely low energy system of interconnected lagoons and swamps. Lagoons and swamps occur in lower lying areas of the broad flat-floored valley associated with the old channel axis. The geophysical modelling (Appendix 3, Figs. A3-21 and A3-22), suggests that the lagoons are located over the old drainage axis, possibly in areas where the palaeochannel was slightly wider and the basalt surface slightly lower.

During dry periods the lagoons and swamps dry out and if there is a strong prevailing wind, the floor of the lagoon may be scoured to the level of the watertable. Transported clays and fine particles form a smooth crescentic dune, or lunette on the downwind side (Fig. 6-15, diagram D), leaving a cliffed margin on the lee side. The process is similar to that described by Mabbutt (1977) for seasonally dry saline playas. This process will occur selectively within the lagoons where there is no vegetation binding the soil. Eventually, when the lunette reaches a sufficient height, the lagoon will become isolated and the throughgoing streams will be diverted around them. The similarity of the position and shape of the pisolitic lagoon rim or lunette with respect to the cliffed basaltic portion of the rim for the cases studied, as shown in Figure 6-16, suggests that a regional southwesterly palaeowind direction has been responsible for these structures in the New England region. Furthermore, the positions of the lunettes on the northeast to easterly

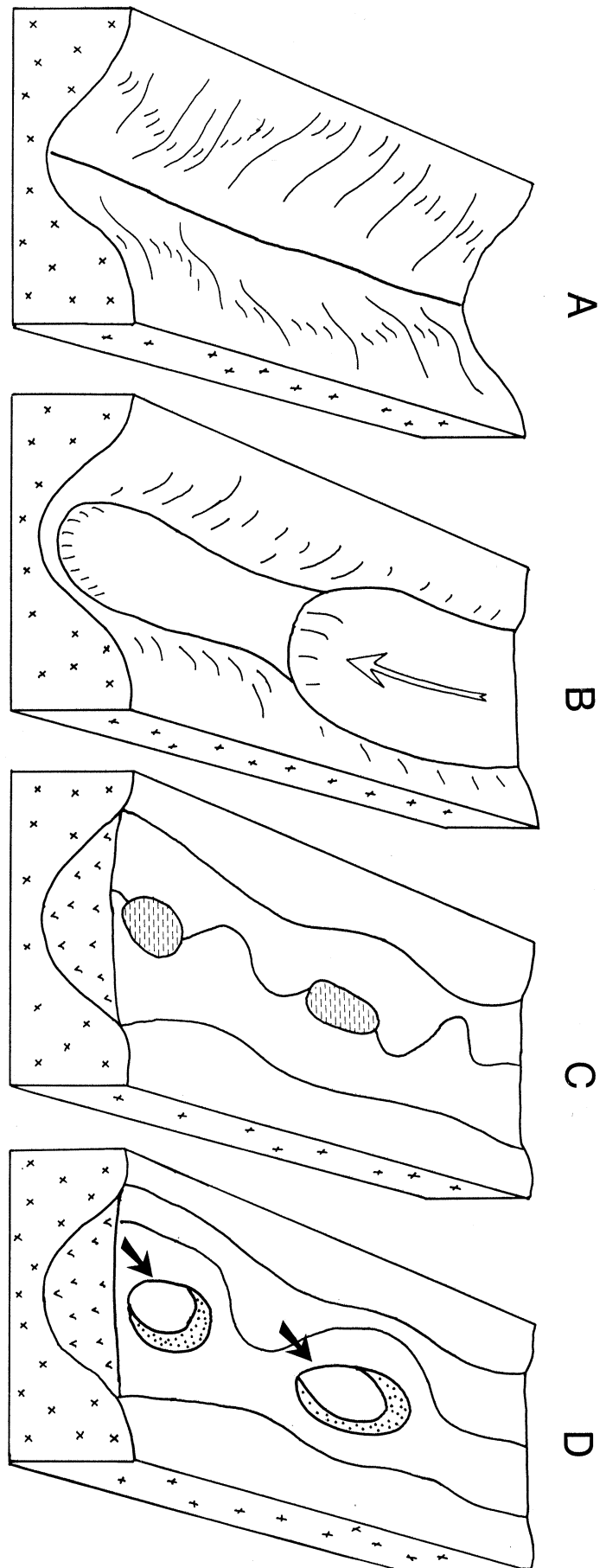


Figure 6-15. Model explaining the development of the lagoons in the Central Province. Part A; the pre-basaltic drainage channel. Part B; successive basalt flows move down the valley filling it up. Part C; a low energy system of interconnected lagoons and swamps develop in the broad, flat valley. Part D; prevailing wind direction leads to the development of lunettes during dry periods.

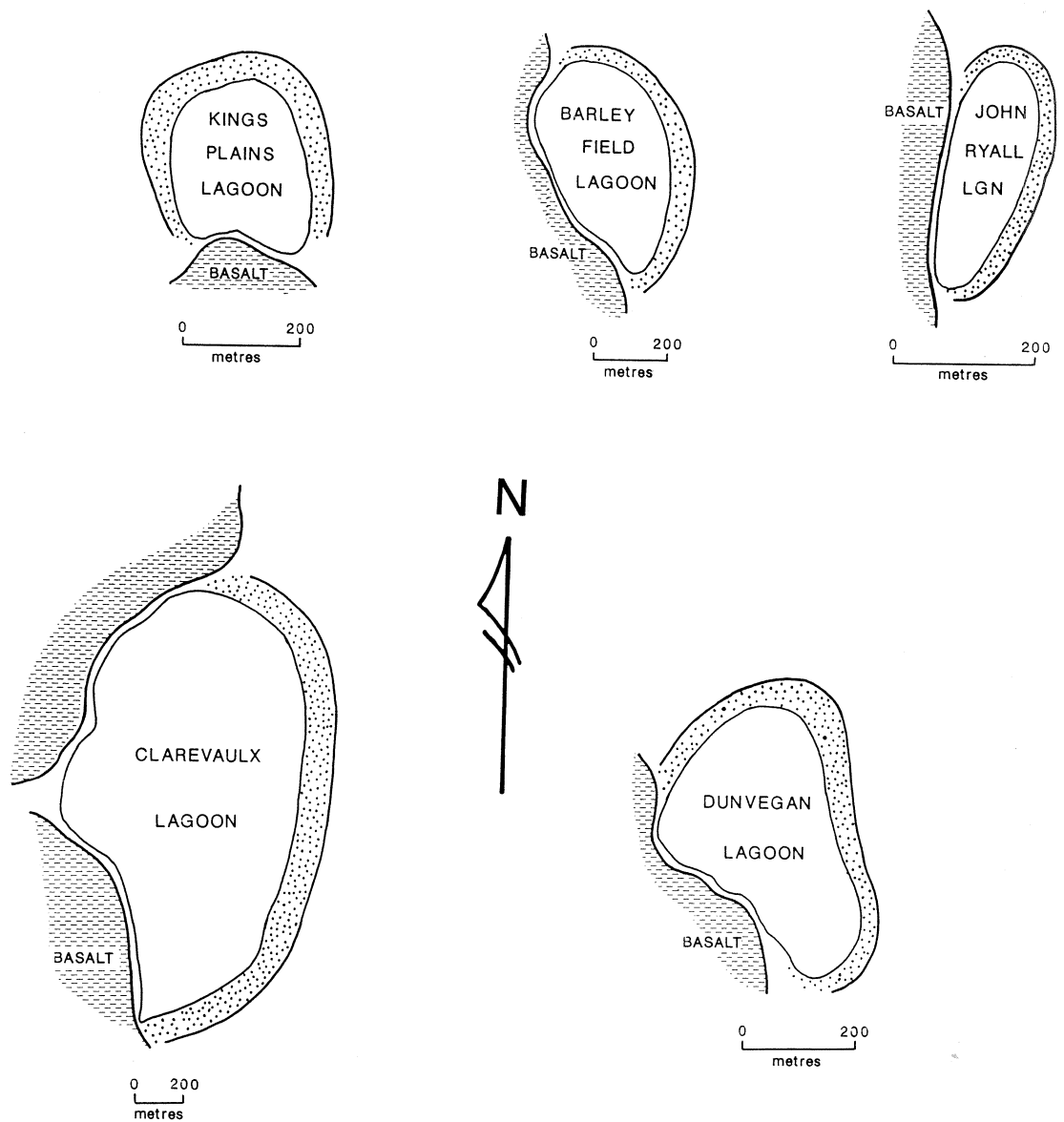


Figure 6-16. Surface configuration of Kings Plains, Dunvegan, Clarevaux, John Ryall and Barley Field Lagoons. The configuration of the pisolitic lagoon rim or lunette (stippled) is shown with respect to the steeper edges against the basalt flows (shown dashed). The similarity in position and shape of the lunette suggests a regional southwesterly palaeowind direction.

margins of the lagoons are consistent with the positions, observed by Mabbutt (1977), for the late Pleistocene and Recent clay lunettes occurring south of 29°S in Australia. The alternate filling and drying of the lagoons, with associated movement of water through the lunette material, has led to the development of pisolites and the destruction of all internal structures in the New England area.

Lagoons with downwind lunettes occur along the entire length of the Great Divide from the Cooma region to northern Queensland (Ollier, 1982; Ollier, 1976), and some are found in valleys where the floor consists of material other than basalt (Ollier, pers. comm. 1988). Ollier (1979) suggested that these lagoons are formed by tectonic activity, with uplift of the Eastern Highlands levelling formerly westerly flowing streams and thereby causing the drainage to become essentially stagnant.

The aim of the geophysical surveys and drilling was to provide data which would test the hypothesis that the observed topographic features are maars and therefore possible economic sources of sapphire. This work has provided no evidence that these lagoons are maars and a preferred explanation, consistent with the present observations, is that they are wind blown features. Sufficient work has been carried out to indicate that most, if not all, of these features do not themselves constitute an economic target.

6.4 Sapphire-source rock evaluation in the Central Volcanic Province

To find areas likely to contain sapphire-source rocks and evaluate their potential as indicators in sapphire exploration, it was necessary to:

1. Differentiate the Central Volcanic Province into water catchment areas along drainage divides or interfluves.
2. Identify individual catchments, based on those drainages from which sapphires have been recovered, as potentially economic (i.e. worthy of further exploration) or non-economic. This allows definition of exploration targets using the boundaries identified in point 1, for both alluvial deposits and their potential source rocks.
3. Evaluate potential sapphire source rocks within one of the catchments defined as being potentially economic. Major element and trace element data, together with field data, were used to test for differences between sapphire-bearing and sapphire-barren parts of the Central Province.
4. Compare lava compositions of the Central Province with those of other sapphire-bearing and sapphire barren volcanic provinces in northeastern Australia and southeastern Asia.

6.4.1 Watershed analysis of the Central Volcanic Province.

The watershed analysis was carried out over the Central Volcanic Province as outlined in Figure 6-17. Lines following the highest topographic points or water divides were drawn on the 1:100,000 scale Inverell, Glen Innes and Guyra topographic sheets to delineate the catchment areas shown in Figure 6-18. Each catchment is named after the principal creek or river flowing within it. Material cannot be moved across water divides by the normal processes of fluvial erosion; it can only move within its watershed downslope from its original location. Conversely, the source rocks for a sapphire deposit located within a particular catchment must be, or have been, located upslope within that catchment area.

In some areas source rocks may no longer exist in a catchment area. At a Public Fossicking Area, formerly a mining area, (grid reference GR:630188, Glen Innes 1:25,000 sheet), sapphires and zircons occur in alluvium trapped in cracks and crevasses in Permian granodiorite whilst former basaltic and/or volcanoclastic rocks have been completely eroded.

The watershed analysis was used to define distinct catchment areas which could then be superimposed on maps showing economic sapphire deposits (Fig. 6-18).

6.4.2 Definition of specific catchment areas for sapphire exploration.

Although sapphire is ubiquitous in almost all East Central Province drainages, only some contain mineable to very rich deposits. Using this knowledge (MacNevin, 1977; Tom Nunan and John McPhee pers. comm., 1988), drainages with significant sapphires were identified by Coenraads and Lawrence (1989). The geology and setting of the alluvial sapphire deposits, and in particular the important Kings Plains Creek and Reddestone Creek deposits currently being worked by T.J. & P.V. Nunan Pty. Ltd, were discussed by Coenraads (1990). Figure 6-18 defines the extent of the catchments of these economic deposits.

Four catchment areas within the Central Volcanic Province were identified as economic, and worthy of greater exploration for alluvial deposits and their potential source rocks, i.e. the Frazers, Kings Plains, Reddestone and Marowan catchments.

6.4.3 Source rock evaluation program

6.4.3.1 Sampling

(i) Basalts: Mt Buckley summits the water-divide between Kings Plains Creek, to the north, and Swan Brook, to the south (Figs. 6-18 & 6-19); both catchments are mined for alluvial sapphires. Mt Buckley is therefore an obvious place to sample a representative cross section of Central Province basalt types, which may contain sapphire source rocks. It also exposes the thickest vertical section.

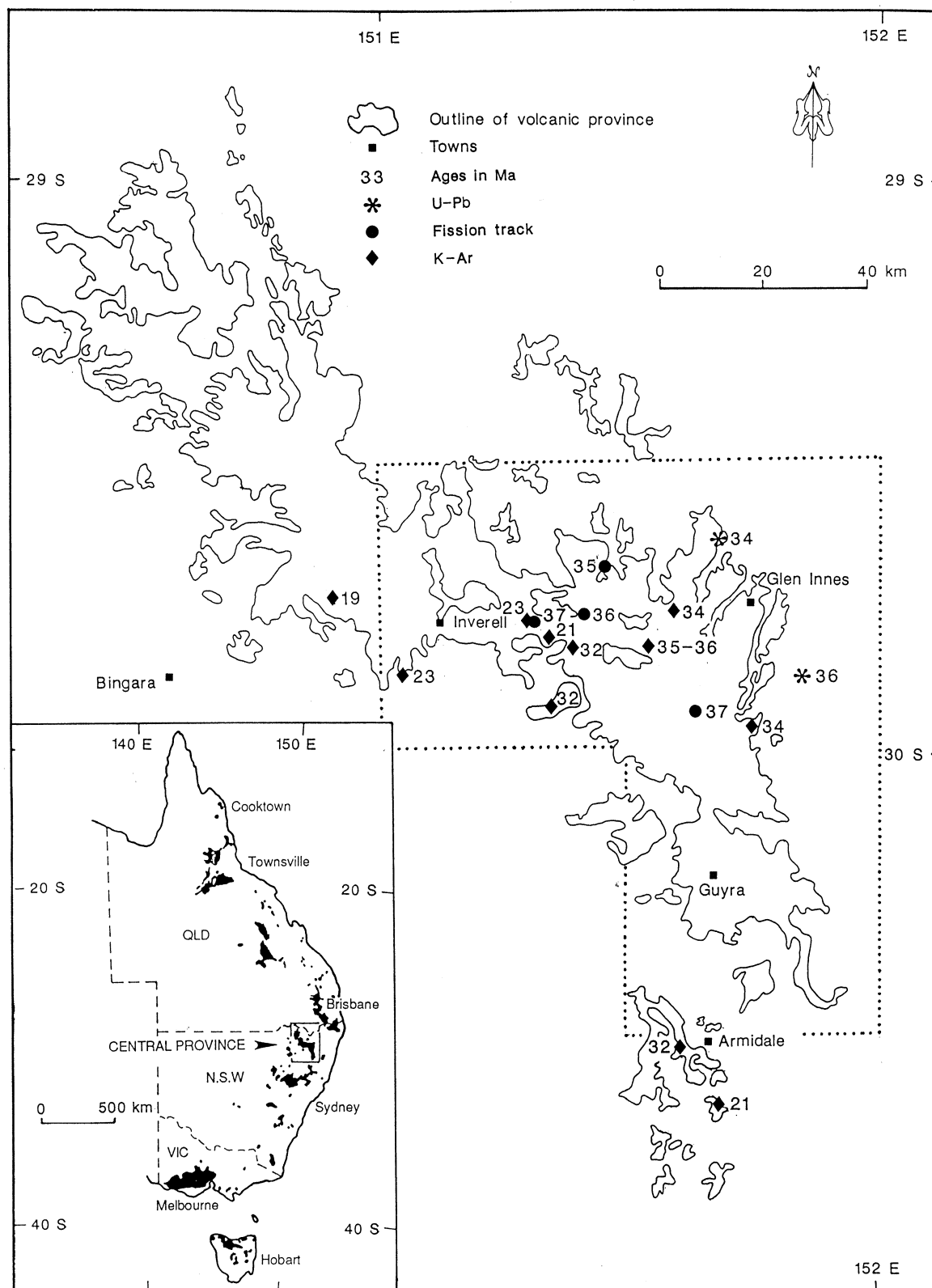


Figure 6-17. Watershed analysis for the Central Volcanic Province in northeastern New South Wales. The inset shows Mesozoic-Cenozoic volcanic provinces which form a discontinuous band within or adjacent to the Eastern Australian Highlands. The portion of the Central Province outlined over which the analysis was carried out is enlarged in Figure 6-18

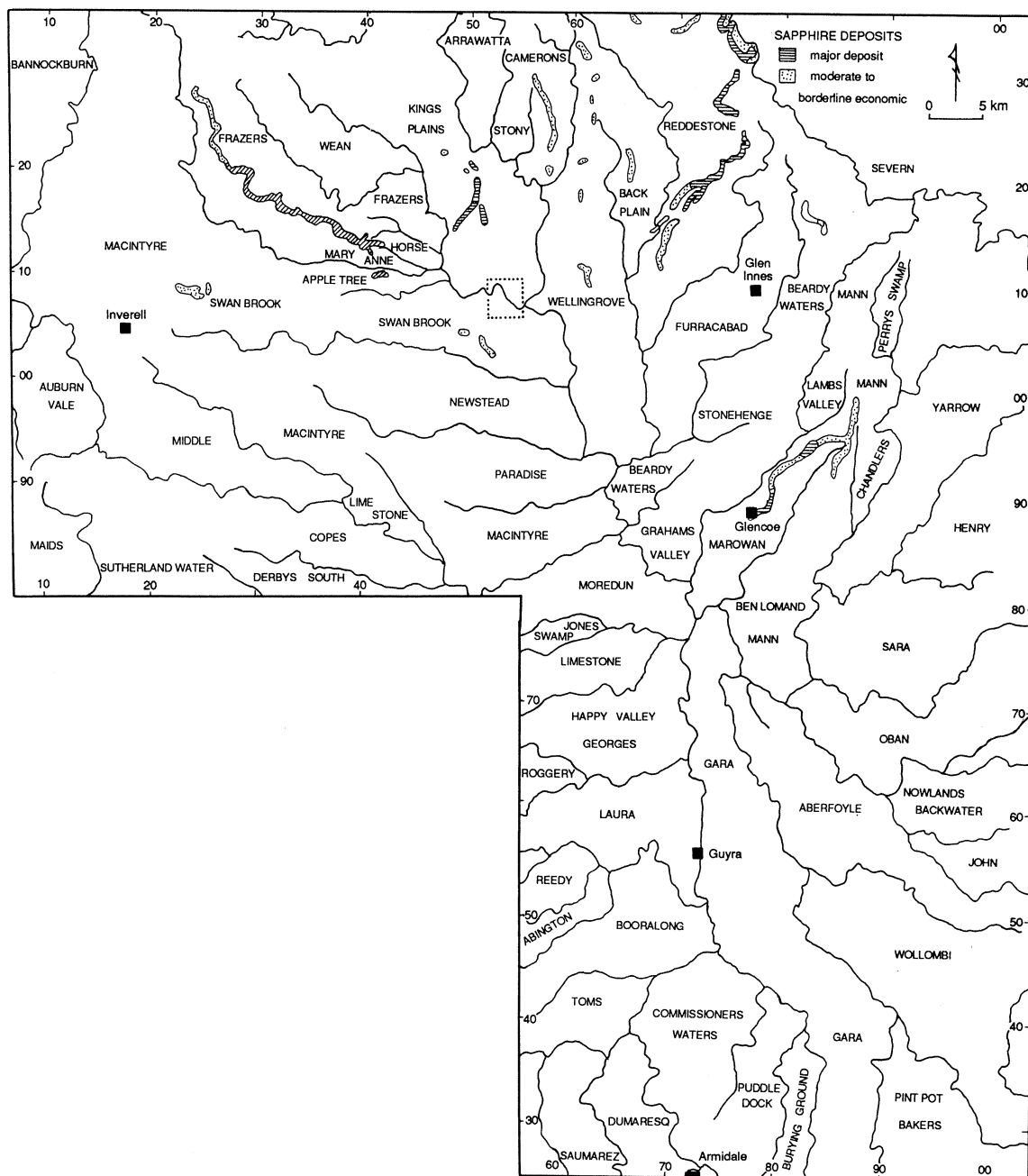


Figure 6-18. Watershed analysis for the Central Volcanic Province. Lines following the water divides separate the province into major catchment areas, each named after its principal creek or river. Economic sapphire-bearing alluvials, (MacNevin, 1977; T.J. Nunan & J. McPhee pers. comm., 1988), are shown, thus highlighting prospective watersheds in which source rocks must exist, or have previously existed. Mt Buckley is situated on the water divide between Kings Plains, Swan Brook and Wellgrove catchments. The study area outlined is enlarged in Figure 6-19.

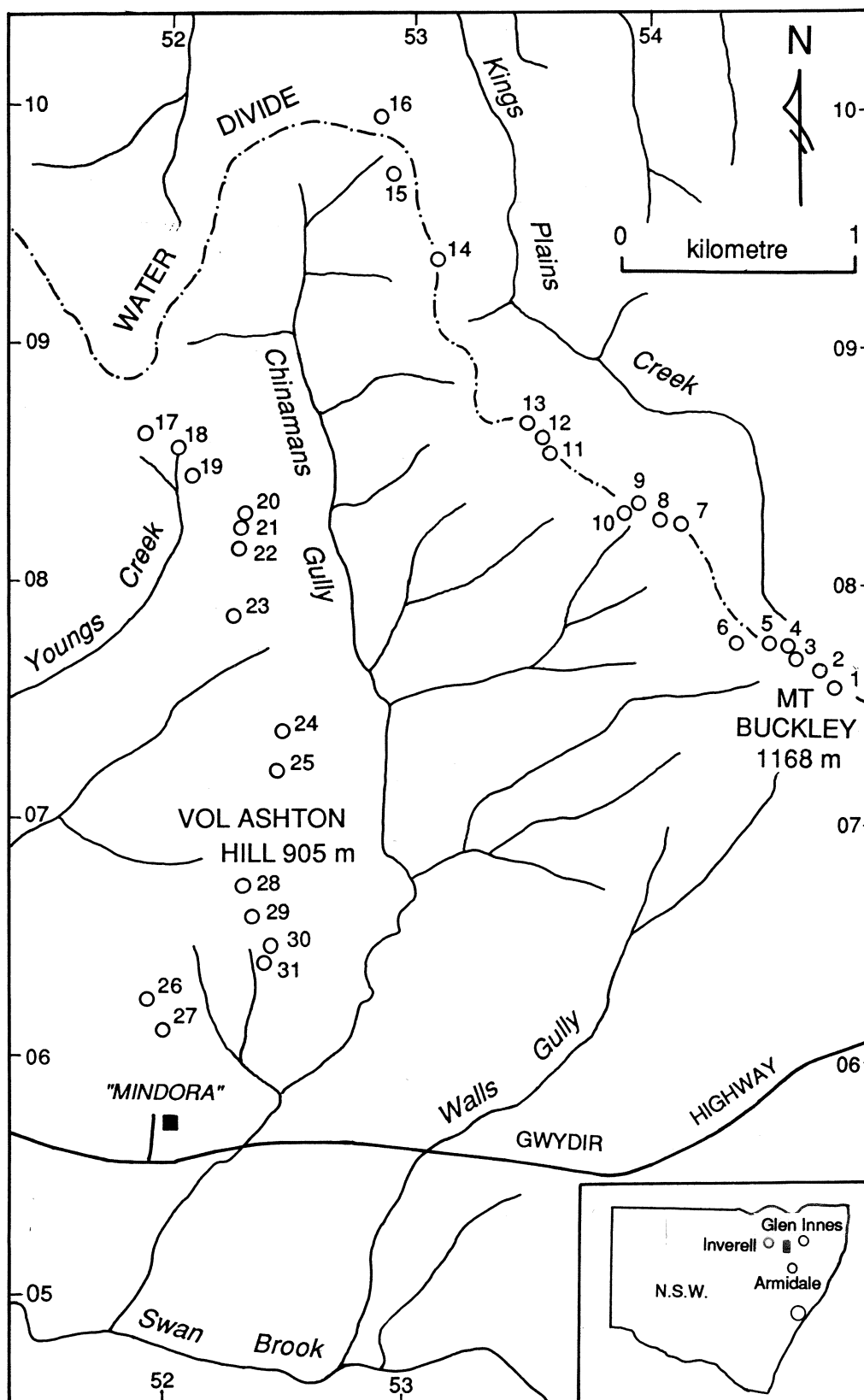


Figure 6-19. Location of basalt sample localities at Mount Buckley. Elevation and grid references on the Elsmore and Sapphire 1:25,000 topographic sheets are listed in Table 6-1.

Thirty one samples (Fig. 6-19) covering some 300 metres of vertical section were collected from locations separated by obvious breaks in slope. These breaks in slope were interpreted to separate individual flow units. From sample B1 at the top of Mt. Buckley (Matheson Trig Station elevation 1168 m GR:547077 Inverell 1:100,000), the traverse followed the ridge down to the north-west, around the head of Chinamans Gully (GR:525100) then south along a spur to Vol Ashton Hill (GR:523069), and finally down a spur to the lowermost flow, B27, resting on basement behind "Mindora" shearing sheds (840 - 860 m elevation, GR:519059). A further 4 samples B28 to B31 were collected from another spur off Vol Ashtons Hill, GR:524064, with the lowermost flow, B31, also resting on basement.

While none of the basalts have been dated, the Mt Buckley flows are most likely to be of similar age to those at Spring Mountain, 8 km to the southeast of "Mindora". The latter were dated by Cooper et al (1963) and are 35-36 Ma (Fig. 6-17). Younger ages of 21 Ma (Smith, 1988) and 23 Ma (Coenraads et al, 1990) exist 15 to 20 km to the west of "Mindora", however these are at a lower elevation and therefore it is unlikely that there are any younger flows in the Mt Buckley sequence.

(ii) Volcaniclastic Rocks: Whole-rock chemistry of the volcaniclastic rocks, as potential sapphire sources in the economic catchments, was not considered appropriate because all observed volcaniclastic rocks are entirely weathered to clays. Additional complications which would make any conclusions highly equivocal include; unknown percentage contamination by country rocks during explosive emplacement; unknown original lava type; and unknown amount of reworking.

Barron (1987) presented chemical analyses of these rocks and has attempted to unravel their origin. Observations on volcaniclastic rocks occurring at Braemar are discussed by Pecover and Coenraads (1989), and their residual heavy minerals are described by Coenraads (1990).

No volcaniclastic rocks were encountered in the Mt Buckley area.

6.4.3.2 Analytical methods:

The basalt samples were sawn to remove all weathering surfaces, cracks and fractures. Each sample was sawn into slices, from which a representative thin section was made, then broken and crushed in a tungsten carbide N.V. Tema mill. Sources of contamination, such as xenoliths, megacrysts and vugs were removed prior to crushing.

Major and trace element abundances were obtained by X-ray fluorescence spectrometry. Fused borate buttons were used for the major elements and pressed pellets were used to determine 15 trace elements. All samples were prepared in duplicate. Measurements were made on a Siemens SRS1 sequential X-ray spectrometer with a Siemens Kristallaflex 800 X-ray generator.

FeO analyses were made using the technique of hydrofluoric acid digestion and titration with ceric sulphate. The volatiles H_2O^- , H_2O^+ and CO_2 were determined by the fusion and collection method using a Leco induction furnace.

Chemical analyses of the Mt Buckley basalts are presented in Table 6-1

6.4.3.3 Treatment of the analytical data.

In order to make meaningful comparisons between rock chemistries, the raw analytical data were treated as follows.

- (a) The maximum $\text{Fe}_2\text{O}_3/\text{FeO}$ ratio was set at 0.2. If the original ratio exceeded this value it was recalculated to be 0.2. Although post eruptive alteration of the volcanic rocks may have caused some oxidation of FeO to Fe_2O_3 , this value is somewhat arbitrary, as discussed by Wass (1980), due to the uncertainty of the pre-eruptive $\text{Fe}_2\text{O}_3/\text{FeO}$ ratio.
- (b) Samples showing post-eruptive alteration were interpreted with caution. Alteration was identified in thin section (see Appendix 5), or determined to be present from the chemical analyses as high H_2O^+ ($>4\%$) or high CO_2 ($>0.5\%$) indicating presence of secondary minerals such as zeolite or calcite, and high $\text{Fe}_2\text{O}_3/\text{FeO}$ ratio (>0.75) indicating oxidation of ferrous iron. The Mt Buckley analyses interpreted with caution are B15 (approximately 20% modal zeolite, 5% H_2O); B21 (1.8% CO_2), B22 (alteration of olivine phenocrysts and along fractures, carbonate veining, 2.8% CO_2 , $\text{Fe}_2\text{O}_3/\text{FeO}=0.8$); B24 (alteration of olivine phenocrysts, alteration along fractures, $\text{Fe}_2\text{O}_3/\text{FeO}=1.0$); B27 (alteration of olivine phenocrysts, approximately 20% modal zeolite); B28 (alteration of olivine phenocrysts, presence of zeolite-filled vesicles).

6.4.3.4 Nomenclature.

The basalts are named on the basis of their chemical composition and normative components following Green & Ringwood (1967) and Coombs & Wilkinson (1969), see Table 6-1. The criteria used by Johnson (1989, p.13) to separate sub-alkaline (tholeiitic) from alkaline types requires that sub-alkaline rocks have normative quartz, or more than 10% normative hypersthene. However, this scheme classifies as sub-alkaline a number of earlier Central Volcanic Province analyses (in which the percentage SiO_2 was calculated by difference) which are clearly alkaline based on their mineralogy (McKay, 1975; McQueen, 1975). Analyses are presented on an alkalis ($\text{Na}_2\text{O} + \text{K}_2\text{O}$) versus silica plot (Fig. 6-20) with the dividing lines of MacDonald & Katsura (1964) and Saggerson & Williams (1964) provided as a reference. This diagram has limitations for those rocks which plot close to the alkalic-tholeiitic dividing line, (Wilkinson 1974).

The alkaline rocks (Fig. 6-21) have been classified using the scheme proposed by Coombs & Wilkinson (1969) based on their normative plagioclase versus differentiation index ($\text{D.I.} = \text{normative quartz} + \text{orthoclase} + \text{albite} + \text{nepheline} + \text{leucite}$). Rocks with D.I. under 75 and greater than 5% normative nepheline include basanite, or are prefixed with "nepheline" as shown in Figure 6-22.

Sample Number	B1	B2	B3	B4	B5	B6	B7	B8	B9	B10	B11	B12	B13	B14	B15	B16	B17	B18	B19
Location	B1 Buckley	B2 Buckley	B3 Buckley	B4 Buckley	B5 Buckley	B6 Buckley	B7 Buckley	B8 Buckley	B9 Buckley	B10 Buckley	B11 Buckley	B12 Buckley	B13 Buckley	B14 Buckley	B15 Buckley	B16 Buckley	B17 Buckley	B18 Buckley	B19 Buckley
1:25000 Map Sheet	Elmore	Elmore	Elmore	Elmore	Elmore	Elmore	Sapphire	Sapphire	Sapphire	Sapphire	Sapphire	Sapphire	Sapphire	Sapphire	Sapphire	Sapphire	Sapphire	Sapphire	Sapphire
Grid Reference	54800756	54730765	54630769	54500774	54500775	54380825	54040827	53950834	53890829	53500834	53470867	53390860	53090836	52890872	52850896	52500896	51890862	52020856	52090845
Elevation (metres)	1168	1160	1142	1135	1129	1115	1100	1078	1065	1056	1050	1045	1043	1035	1015	1005	1015	990	960
SiO2	43.31	43.26	45.18	44.20	44.81	44.41	43.80	45.25	44.81	43.96	44.10	44.04	45.12	46.00	45.57	46.18	46.20	45.85	45.94
Al2O3	2.42	2.41	2.08	2.43	2.57	2.57	2.53	2.73	2.46	2.86	2.71	2.89	2.39	2.23	2.39	2.68	2.71	2.67	2.62
Fe2O3	14.55	14.36	15.20	14.82	15.35	15.03	14.81	15.08	15.03	14.43	14.36	14.54	14.56	14.92	15.07	15.76	15.90	14.47	15.73
FeO	4.12	3.71	5.05	3.18	3.29	3.18	3.81	3.90	3.29	4.10	4.20	4.78	3.92	2.14	2.18	2.97	3.45	3.64	3.28
MnO	8.00	8.25	6.88	8.15	8.29	7.86	8.45	7.79	8.95	7.86	7.58	7.17	8.17	10.35	10.15	7.51	7.04	7.13	7.38
CaO	0.18	0.17	0.16	0.17	0.17	0.19	0.20	0.15	0.17	0.16	0.18	0.15	0.16	0.17	0.16	0.13	0.13	0.15	0.13
MgO	9.32	9.56	5.94	9.44	8.60	7.29	6.97	7.67	8.20	9.22	9.10	8.91	9.55	8.62	8.70	7.03	6.83	7.88	6.60
CO2	9.22	9.12	6.65	8.92	8.43	8.00	8.30	7.62	9.60	8.19	8.79	8.67	8.89	8.98	8.79	9.28	9.89	9.99	9.23
K2O	3.13	3.44	4.39	3.00	3.93	3.95	3.99	3.95	2.39	3.57	2.95	3.46	2.87	3.46	1.95	2.88	3.00	2.59	3.00
K2O	1.36	1.38	2.57	3.00	2.08	2.38	1.90	2.31	1.12	1.33	1.21	1.18	1.18	1.19	0.84	1.82	1.77	1.79	1.86
P2O5	0.62	0.56	0.96	0.66	0.65	0.82	0.82	0.75	0.48	0.62	0.52	0.62	0.44	0.49	0.23	0.49	0.52	0.47	0.50
S	0.00	0.00	0.00	0.00	0.00	0.00	0.00	0.00	0.01	0.00	0.00	0.01	0.01	0.01	0.03	0.02	0.01	0.00	0.01
H2O+	2.77	2.58	3.35	2.42	1.86	2.10	3.48	1.48	2.17	2.39	2.99	2.37	2.14	0.93	4.29	2.40	2.76	2.35	2.59
H2O-	0.77	0.74	0.91	0.59	0.47	0.57	0.52	0.56	0.53	0.56	0.67	0.67	0.55	0.40	0.73	0.59	0.61	0.49	0.50
CO2	0.17	0.22	0.10	0.19	0.11	0.12	0.13	0.08	0.10	0.08	0.07	0.06	0.03	0.06	0.09	0.01	0.06	0.09	0.08
Original Total	99.94	99.76	99.42	99.92	100.39	99.59	99.71	99.22	99.65	99.11	99.31	99.15	99.67	99.43	100.42	99.53	99.78	99.46	99.45
Total Fe as FeO	11.71	11.59	11.42	11.01	11.07	11.73	11.88	11.30	11.91	11.55	11.36	11.47	11.70	12.28	12.11	10.18	10.14	10.41	10.33
original Fe2O3/FeO	0.52	0.45	0.73	0.39	0.37	0.55	0.45	0.50	0.37	0.52	0.55	0.67	0.48	0.21	0.21	0.40	0.48	0.51	0.44
required Fe2O3/FeO	0.20	0.20	0.20	0.20	0.20	0.20	0.20	0.20	0.20	0.20	0.20	0.20	0.20	0.20	0.20	0.20	0.20	0.20	0.20
New Fe2O3	1.98	1.96	1.94	1.87	1.88	1.99	2.01	1.92	1.96	1.93	1.92	1.92	1.98	2.05	2.05	1.73	1.72	1.76	1.75
New FeO	9.92	9.82	9.68	9.33	9.38	9.94	10.07	9.58	10.09	9.79	9.63	9.72	9.91	10.40	10.26	8.63	8.60	8.82	8.76
New Total	99.73	99.59	99.11	99.79	100.27	99.36	99.53	99.02	99.52	98.90	99.08	98.87	99.48	99.42	100.41	99.41	99.61	99.27	99.30
Orthoclase	8.06	8.15	15.17	10.32	12.16	14.08	11.24	13.63	6.53	7.88	7.17	6.95	6.99	7.02	4.97	9.57	10.47	10.57	11.00
Albite	14.49	13.46	20.72	15.44	13.84	14.60	16.30	17.65	20.22	18.68	19.94	20.52	21.03	22.44	16.53	22.33	23.24	18.66	20.68
Nepheline	6.50	8.48	8.91	5.38	10.53	10.18	8.55	8.55	0.00	6.25	2.74	4.73	0.44	1.33	0.00	1.10	1.67	1.77	2.54
Anorthite	19.67	19.67	14.18	21.82	18.15	16.25	16.90	16.57	26.96	23.24	26.96	20.67	24.33	29.84	25.27	24.67	22.55	22.55	22.55
Diopside	15.44	16.61	9.77	13.68	15.17	14.15	14.84	12.89	13.78	13.53	13.64	12.99	13.21	13.88	15.64	14.22	12.33	18.55	14.76
Hypertene	0.00	0.00	0.00	0.00	0.00	0.00	0.00	0.00	1.51	0.00	0.00	0.00	0.00	0.00	0.00	0.00	0.00	0.00	0.00
Olivine	20.80	20.69	16.89	20.85	18.73	17.50	16.91	17.91	18.44	20.55	20.30	20.06	21.97	20.90	21.97	15.14	15.38	15.42	14.41
Magmrite	2.87	2.84	2.87	2.87	2.84	2.89	2.91	2.78	2.93	2.84	2.80	2.81	2.87	3.02	2.97	2.51	2.49	2.55	2.54
Ilmenite	4.60	4.57	3.95	4.62	4.89	4.88	4.80	5.19	4.87	5.43	5.14	5.48	4.55	4.24	3.12	5.09	5.15	5.07	4.98
Apatite	1.46	1.33	2.28	1.57	1.54	1.94	1.93	1.77	1.13	1.48	1.24	1.47	1.05	1.15	0.55	1.16	1.14	1.11	1.17
Calcite	0.39	0.50	0.16	0.25	0.25	0.27	0.30	0.18	0.23	0.18	0.16	0.14	0.07	0.14	0.20	0.02	0.14	0.20	0.18
Water	3.54	3.32	4.26	3.01	2.33	2.67	4.00	1.94	3.04	2.73	3.66	3.04	2.69	1.33	5.02	2.99	3.37	2.84	3.09
Total	99.78	99.62	99.17	99.83	100.32	99.41	99.57	99.06	99.54	98.90	99.13	98.86	99.50	99.44	100.38	99.40	99.64	99.29	99.30
100An/An+Ab	59.9	59.4	40.6	58.6	56.7	52.7	50.9	48.4	57.1	50.9	52.8	50.2	53.9	51.7	64.4	53.1	51.5	54.7	53.7
Differentiation Index	29.05	30.09	44.80	31.14	36.53	38.86	39.98	39.83	26.85	32.81	29.85	32.20	28.46	30.79	21.50	33.00	34.87	31.00	34.22
Rock Name	basaltic	basaltic	ne-hawaiite	basaltic	basaltic	basaltic	basaltic	ne-hawaiite	basaltic	basaltic	ACB	ACB	ACB	ACB	ACB	ACB	ACB	ACB	ACB
Trace Elements (ppm)																			
Ba	183	184	186	223	250	312	302	276	189	290	243	298	176	181	126	291	298	280	288
Rb	13	12	19	23	20	24	23	20	10	7	7	10	12	13	15	16	19	21	20
Sr	832	786	1236	856	1160	1279	1100	1145	886	885	924	1035	592	645	403	898	800	753	773
Pb	4	4	9	4	4	4	4	7	3	3	2	4	3	3	3	3	1	3	3
Th	4	6	7	4	5	5	5	7	2	5	2	6	2	4	3	5	1	4	4
U	1	0	2	2	1	2	2	0	2	2	1	1	1	2	1	2	1	1	1
Zr	217	215	377	212	261	314	318	279	143	221	222	196	162	143	87	208	221	209	208
Nb	45	45	63	49	65	76	74	68	43	57	57	51	36	34	16	56	56	52	54
Y	22	21	19	20	20	22	22	18	18	20	21	20	20	20	18	18	21	20	20
V	187	187	178	178	172	148	138	148	186	178	180	172	187	190	180	195	183	220	191
Cr	257	257	203	203	203	117	106	168	223	216	228	202	277	207	202	162	129	263	193
Ni	185	197	91	210	148	106	93	138	144	206	195	191	217	180	215	81	73	92	80
Cu	39	48	27	49	36	33	33	43	91	59	57	56	62	88	106	64	56	54	58
Zn	86	88	119	86	88	102	102	92	88	79	78	76	85	93	92	81	79	79	83
Ga	21	16	21	16	21	22	21	22	21	20	19	18	20	20	16	21	22	22	22
K/Rb	868	955	928	765	855	823	686	959	930	1577	1435	980	816	760	465	841	773	708	772

Table 6-1. Location, chemical analyses and CIPW norms for the Mt Buckley basalts.

Sample Number	B20	B21	B22	B23	B24	B25	B26	B27	B28	B29	B30	B31
Location	Mt Buckley	Mt Buckley	Mt Buckley	Mt Buckley	Mt Buckley	Mt Buckley	Mt Buckley	Mt Buckley	Mt Buckley	Mt Buckley	Mt Buckley	Mt Buckley
1:25000 Map Sheet	Sapphire	Sapphire	Sapphire	Elsmore	Elsmore	Elsmore	Elsmore	Elsmore	Elsmore	Elsmore	Elsmore	Elsmore
Grid reference	52300830	52290823	52270816	52260786	52470737	52450711	51920625	51900612	52300673	52300660	52440049	52400642
Elevation (metres)	955	948	940	945	911	892	884	855	903	892	875	865
SiO ₂	44.63	46.43	43.67	44.65	47.98	46.95	44.15	46.08	44.73	44.39	44.44	43.95
TiO ₂	2.37	2.77	2.80	1.51	1.51	1.74	2.95	1.99	2.49	2.51	3.07	2.84
Al ₂ O ₃	13.58	14.26	15.82	15.68	15.21	13.86	14.08	14.24	14.01	14.03	15.48	14.65
Fe ₂ O ₃	3.05	3.28	4.98	3.83	3.83	3.44	3.62	3.68	3.60	3.31	3.84	3.95
FeO	8.33	7.88	6.32	8.44	4.89	7.27	8.84	7.35	8.43	8.77	7.58	8.40
MnO	0.16	0.16	0.17	0.17	0.15	0.15	0.17	0.15	0.17	0.18	0.16	0.16
MgO	10.53	10.53	4.86	7.31	7.12	11.07	9.29	9.44	9.36	9.38	7.82	8.03
CaO	9.65	8.81	7.82	7.75	5.59	6.59	9.34	8.64	9.42	9.50	9.32	8.42
Na ₂ O	2.24	3.35	4.28	3.85	4.26	3.49	2.52	2.24	2.16	2.27	3.00	3.39
K ₂ O	1.68	1.53	2.17	2.38	2.37	1.80	1.79	1.27	0.98	1.04	1.49	1.64
PCO ₅	0.44	0.39	0.76	0.78	0.66	0.58	0.60	0.36	0.51	0.51	0.59	0.85
S	0.01	0.00	0.01	0.00	0.00	0.00	0.01	0.00	0.01	0.01	0.00	0.00
H ₂ O ⁺	2.49	1.08	2.43	1.66	2.65	2.07	1.71	3.35	3.24	2.87	2.35	2.25
H ₂ O ⁻	0.38	0.41	1.00	0.45	0.34	0.34	0.47	0.57	0.72	0.53	0.74	1.02
CO ₂	0.03	1.84	2.82	0.05	0.29	0.02	0.08	0.04	0.09	0.03	0.21	0.29
Original Total	99.57	99.54	99.86	99.81	98.90	99.37	99.62	99.40	99.92	99.33	100.09	99.84
Total Fe as FeO	11.07	10.84	10.80	11.89	9.45	10.37	12.10	10.66	11.67	11.75	11.04	11.95
original Fe ₂ O ₃ /FeO	0.37	0.42	0.79	0.45	1.04	0.47	0.41	0.50	0.43	0.38	0.51	0.47
required Fe ₂ O ₃ /FeO	0.20	0.20	0.20	0.20	0.20	0.20	0.20	0.20	0.20	0.20	0.20	0.20
New Fe ₂ O ₃	1.88	1.84	1.83	2.01	1.60	1.76	2.05	1.81	1.98	1.99	1.87	2.03
New FeO	9.39	9.19	9.15	10.07	8.01	8.78	10.25	9.04	9.89	9.96	9.35	10.13
New Total	99.45	99.39	99.54	99.63	98.55	99.20	99.46	99.21	99.76	99.20	99.89	99.65
Orthoclase	9.94	9.04	12.82	14.06	13.98	10.66	10.56	7.50	5.80	6.14	8.80	9.66
Albite	13.90	22.21	17.68	15.50	29.62	24.39	14.70	18.94	18.28	19.20	18.98	19.65
Nepheline	2.74	3.09	10.04	9.23	3.46	2.76	3.57	0.00	0.00	0.00	4.89	4.89
Anorthite	22.04	19.57	17.54	18.48	15.40	16.84	21.84	25.04	25.63	25.02	24.37	19.94
Dipside	18.39	17.57	13.43	11.90	5.42	9.59	16.25	12.26	13.97	15.08	13.57	11.77
Hypersthene	0.00	0.00	0.00	0.00	0.00	0.00	0.00	9.85	6.88	1.76	0.00	0.00
Olivine	21.28	16.67	12.10	18.18	20.19	25.30	20.19	14.36	16.25	19.68	17.24	19.50
Magnetite	2.73	2.67	2.65	5.31	2.86	2.55	2.97	2.62	2.87	2.89	2.71	2.94
Ilmenite	4.49	4.35	5.26	5.31	2.86	3.30	5.60	3.78	4.73	4.77	5.83	5.40
Apatite	1.05	0.92	1.80	1.85	1.56	1.38	1.43	0.86	1.21	1.21	1.39	2.01
Calcite	0.07	0.00	0.00	0.11	0.66	0.05	0.18	0.11	0.20	0.07	0.48	0.66
Water	2.87	1.49	3.43	2.11	3.10	2.41	2.18	3.92	3.96	3.40	3.09	3.27
Total	99.50	97.56	96.75	99.64	98.57	99.23	99.47	99.24	99.78	99.22	99.92	99.69
100Ar/Ar+Ab	61.3	46.8	49.8	54.4	34.2	40.8	59.8	56.9	58.4	56.6	56.2	50.4
Differentiation Index	26.58	34.34	40.54	38.79	47.06	37.81	28.83	26.44	24.08	25.34	31.24	34.20
Rock Name	ACB	hawaiite	hawaiite	basaltic	hawaiite	hawaiite	ACB	ACB	ACB	ACB	ACB	ACB
Trace Elements (ppm)												
Ba	372	337	266	268	286	255	282	293	361	373	319	305
Rb	30	27	19	20	28	21	22	21	23	22	20	21
Sr	564	565	1066	1211	924	817	914	931	730	772	937	1022
Pb	4	2	5	4	6	1	4	2	2	2	2	5
Th	3	3	8	5	7	5	5	2	4	2	3	6
U	2	3	3	3	3	2	2	2	0	2	1	2
Zr	148	127	317	357	241	173	117	117	146	149	194	272
Nb	40	27	66	66	72	56	19	18	35	44	60	69
Y	21	20	21	20	19	17	19	17	19	19	20	21
V	202	178	151	130	95	127	212	287	240	201	223	172
Cr	337	280	143	150	276	489	216	230	208	234	147	163
Ni	261	203	111	110	268	429	186	230	208	204	113	146
Cu	58	51	38	39	32	32	63	58	66	65	43	48
Zn	85	101	99	99	84	89	93	94	97	96	85	105
Ga	19	20	23	24	21	20	21	21	21	19	21	22
K/Rb	465	470	948	988	703	712	675	502	354	392	618	648

Table 6-1. Location, chemical analyses and CIPW norms for the Mt Buckley basalts.

Central Province, N.S.W.

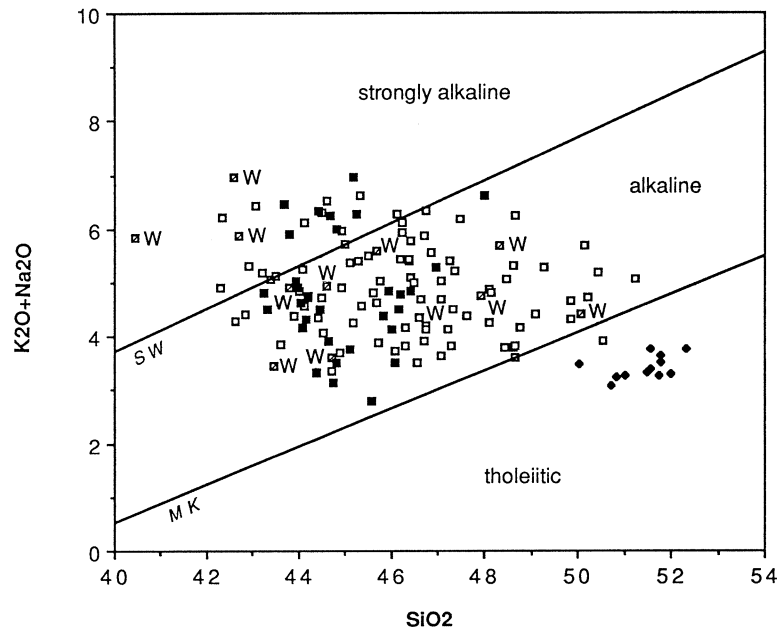


Figure 6-20. Total alkalis versus silica plot. The lines of MacDonald & Katsura (1964) (MK) and Saggerson & Williams (1964) (SW) divide the plot into sub-alkaline (tholeiitic), alkaline and strongly alkaline fields. All existing analyses of basalts of the Central Volcanic Province are shown as open squares, and the Mt Buckley analyses (this paper) as filled squares. The Mt Buckley flows are dominantly alkaline or strongly alkaline and lie within the compositional field for the Province. The tholeiites from the Inverell area (Duggan, 1972) are plotted as filled diamonds. Analyses marked with "w" are alkaline lavas from the sapphire-barren West Central Province.

Central Province N.S.W.

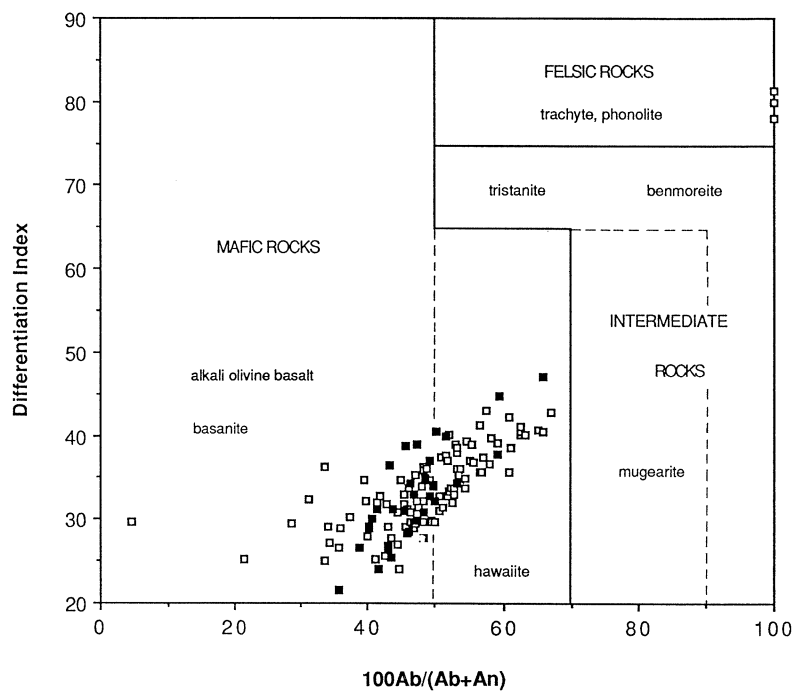


Figure 6-21. C.I.P.W. normative plagioclase versus differentiation index (D.I.= normative quartz+orthoclase+albite+nepheline+leucite). The Mt Buckley flows are shown as filled squares and the analyses in the felsic field are phonolites from the Swan Peak Plug (Stroud, Karaolis and Coenraads, unpublished data).

Central Province N.S.W.

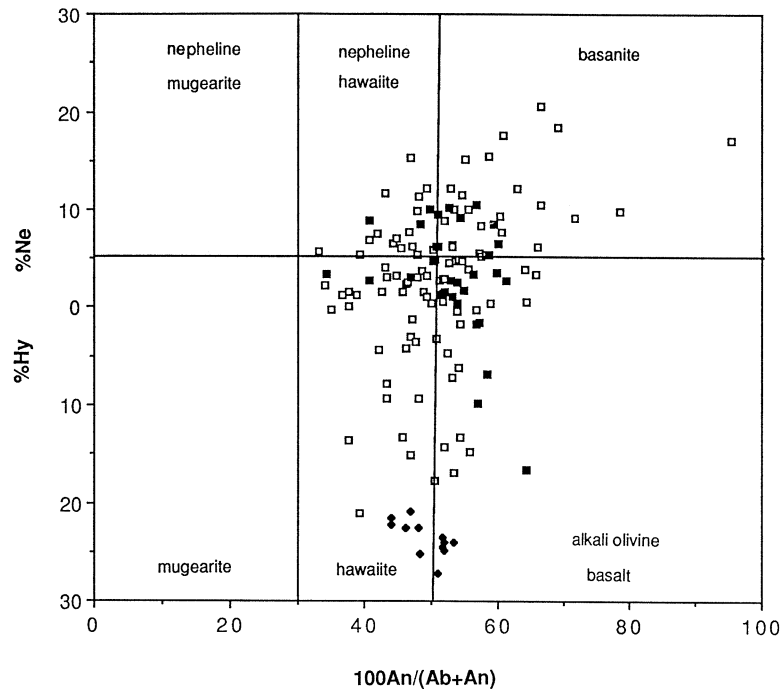


Figure 6-22. C.I.P.W. nepheline or hypersthene versus normative plagioclase. Lines of Coombs and Wilkinson (1969) subdivide the field of alkaline rocks. Rocks with greater than 5% normative nepheline include basanites, or are prefixed with "nepheline". All analyses for the Central Province are shown with the Mt Buckley basalts shown as filled squares, and the tholeiites from the Inverell area as filled diamonds.

Mt Buckley

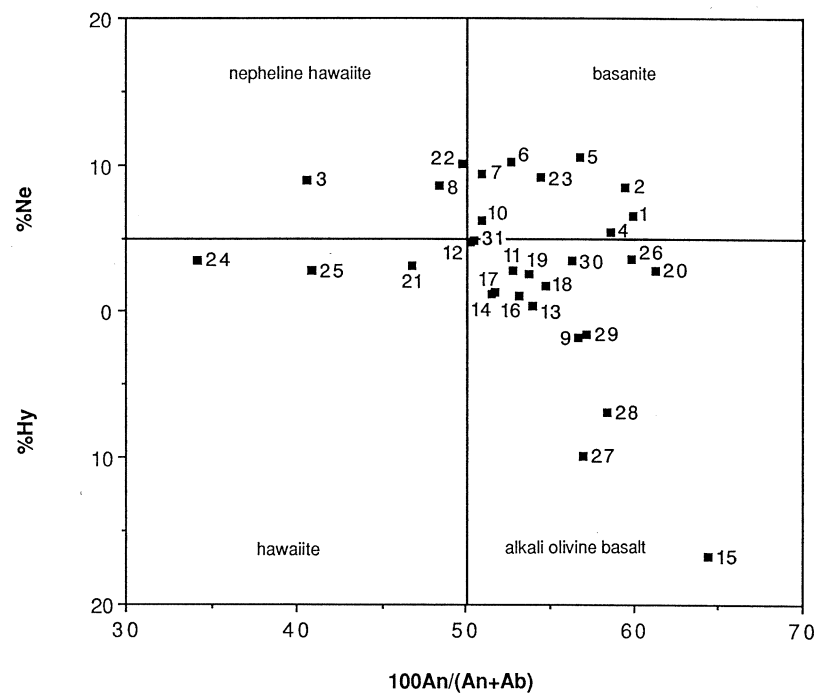


Figure 6-23. C.I.P.W. nepheline or hypersthene versus normative plagioclase for the Mt Buckley analyses. The uppermost flows (B1 to B10) largely nepheline hawaiites and basanites and the lower flows (B11 to B31) largely alkali olivine basalts and hawaiites. Flows B9, B15, B22 and B23 are exceptions to this observation.

6.4.4 Chemical features of the Mount Buckley lavas

All the Mt Buckley Series rocks are basic, with SiO₂ contents between 45 - 50% (Carmichael et al., 1974, p. 29). Plots of normative hypersthene or nepheline against normative plagioclase composition (Fig. 6-23) shows most are alkali olivine basalts and basanites. The uppermost flows are predominantly basanite and nepheline hawaiites whereas the lowermost flows are predominantly alkali olivine basalts and hawaiites.

A positive correlation can be seen on the normative plagioclase versus differentiation index plot (Fig. 6-21), but there is no systematic variation between stratigraphic occurrence and position on this plot.

In terms of the alkalis ratio, K₂O : Na₂O, the Mt Buckley flows (Fig. 6-24) are neither distinctly sodic nor potassic but tend to cluster about a line, K₂O : Na₂O = 1 : 2, between the sodic Hawaiian alkalic suite (McDonald & Katsura, 1964) and the potassic Tristan de Cunha alkalic series (Baker et al, 1964).

6.4.4.1 Chemistry versus stratigraphic position at Mount Buckley

Normative hypersthene or nepheline (Fig. 6-25), major oxides (Fig. 6-26), and trace elements (Fig. 6-27) were plotted versus flow number to discern any trends.

A trend towards increasing undersaturation with time is revealed in Figure 6-25. The uppermost flows, B1 to B10, are all moderately silica undersaturated (>5% normative nepheline) and are all basanites or nepheline hawaiites, with the exception of B9 which is an alkali olivine basalt. B3 is chemically quite distinct having the highest Zn (119 ppm), Zr (377 ppm), K₂O (2.71%), Na₂O (4.63%), P₂O₅ (1.01%) and Ga (25 ppm), high Sr (1237), low Ca (7.02%), Ni 92 (ppm), MgO (6.27%) and V (103 ppm) and the lowest Cr (94 ppm) and Cu (27 ppm). B9 is also different from its neighbours being coarse grained with distinct CaO, Zr, Nb and Cu values. Their field relations, however, are conformable. The lowermost flows, B11 to B27, are mildly undersaturated alkali olivine basalts or hawaiites with the exception of B23 which is a basanite. The additional four lower flows, B28 to B31, are also alkali olivine basalts. The only flows plotting within or close to the tholeiitic compositional field on Figure 6-25 are B15 and B27 respectively; however, their modal mineralogy is distinctly alkaline.

Figures 6-26 and 6-27 show systematic correlations between various elements, such as MgO, Ni, Cr, Al₂O₃, Na₂O, P₂O₅, CaO and V.

The following adjacent flows within the Mt Buckley sequence appear to behave as groups, with members of each group having similar chemical compositions and apparently common genesis. These include; flows B16, B17, B18 and B19 (all coarse grained alkali olivine basalts), flows B10, B11, B12 and B13 (alkali olivine basalts except B10 a fine grained basanite), and flows B5, B6, B7 and B8, (basanites except B8 a nepheline hawaiite). Some elements in these groups of flows change in a regular manner from flow to flow suggesting a probable fractionation pattern.

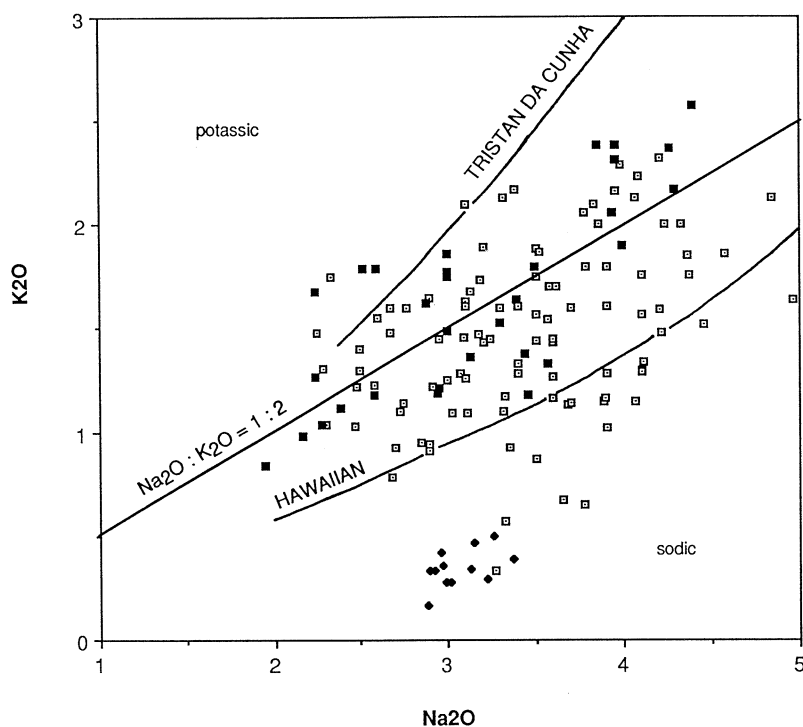


Figure 6-24. Na_2O versus K_2O plot. Basalts of the Central Volcanic Province are plotted, with the Mt Buckley analyses shown as filled squares. The field for the Central Province is centred about the line $\text{Na}_2\text{O}:\text{K}_2\text{O} = 2:1$ and lies between the sodic Hawaiian alkalic suite (McDonald & Katsura, 1964) and the potassic Tristan de Cunha series (Baker et al, 1964). The group of analyses low in K_2O (filled diamonds) are the tholeiites in the vicinity of Inverell mapped by Duggan (1972).

Central Province, N.S.W.

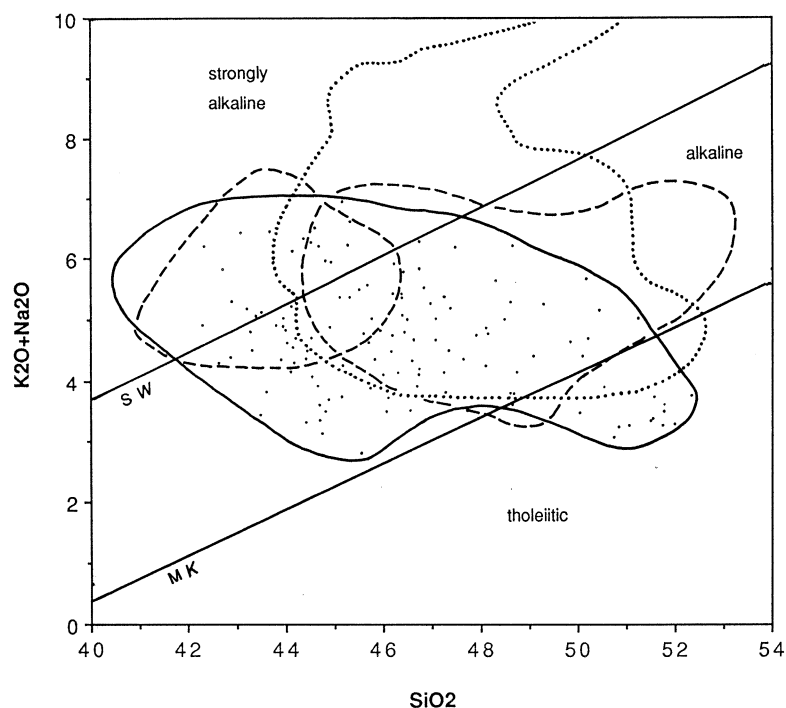


Figure 6-28. Total alkalis versus silica plot. The compositional field of the Central Volcanic Province, outlined by a solid line, and that of the northeastern Australian corundum-bearing provinces (Atherton, Chudleigh and McBride; Stephenson et al, 1980), outlined by a dotted line, are superimposed on the overlapping fields for the corundum-bearing (dashed line, right hand field) and corundum-less (dashed line, left hand field) southeast Asian volcanic provinces (Vichit et al., 1978).

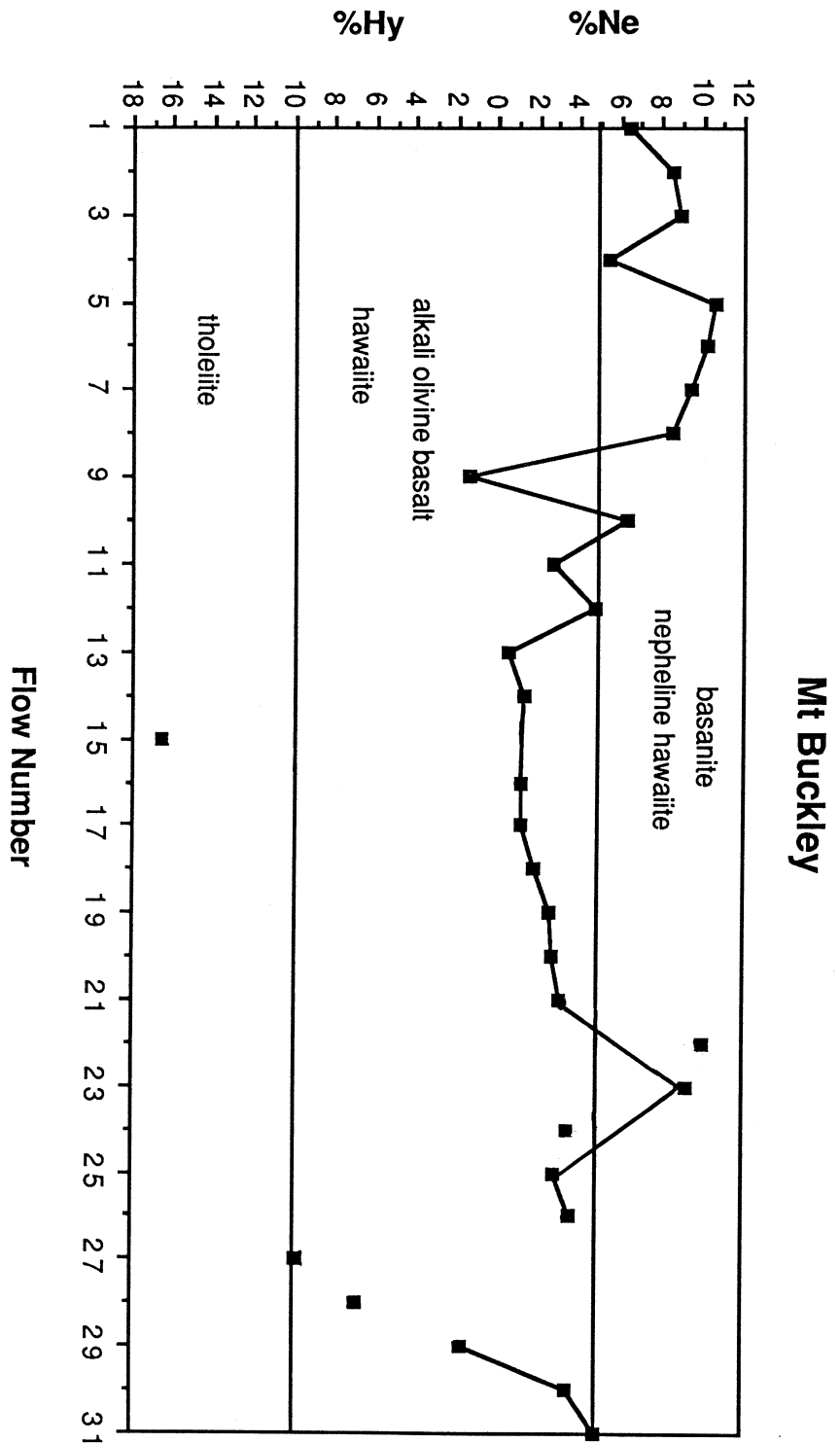


Figure 6-25. C.I.P.W. nepheline or hypersthene versus flow number. The numbers are from 1, the youngest flow at the top of Mt Buckley to the lowermost flows. The plot shows that the uppermost flows are, in general, more undersaturated than the lowermost flows. Flows with excessively altered phenocryst olivine and/or abundant modal zeolite, (B15, B22, B24, B27 and B28) are not considered suitable for comparison of normative mineralogy and are not linked to adjacent flows by the solid line.

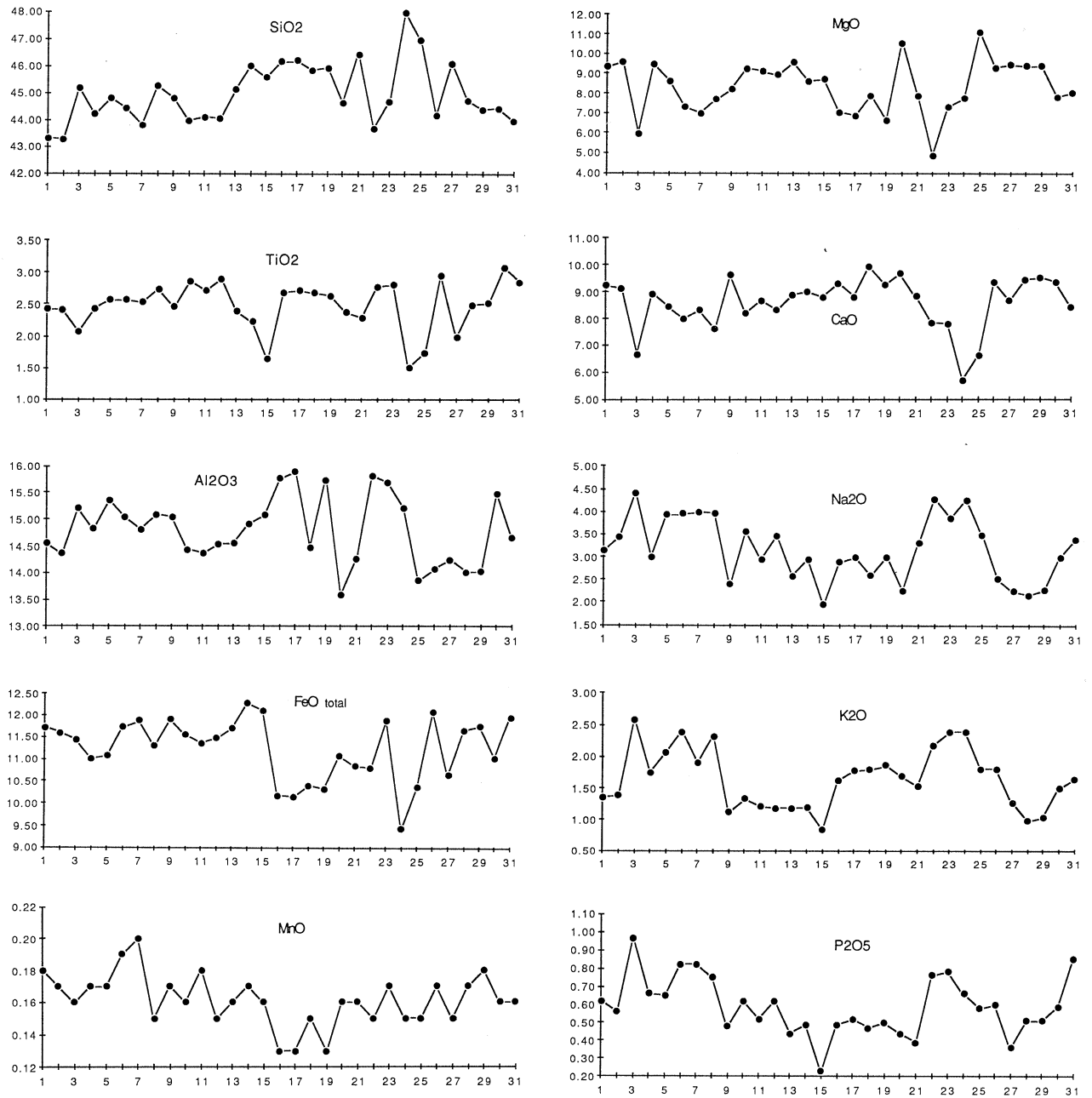


Figure 6-26. Major elements versus flow number. The plots allow comparisons to be made between successive flows. Flow number 1 is the youngest being the uppermost flow on Mt Buckley. Major elements are plotted as oxide weight percents.

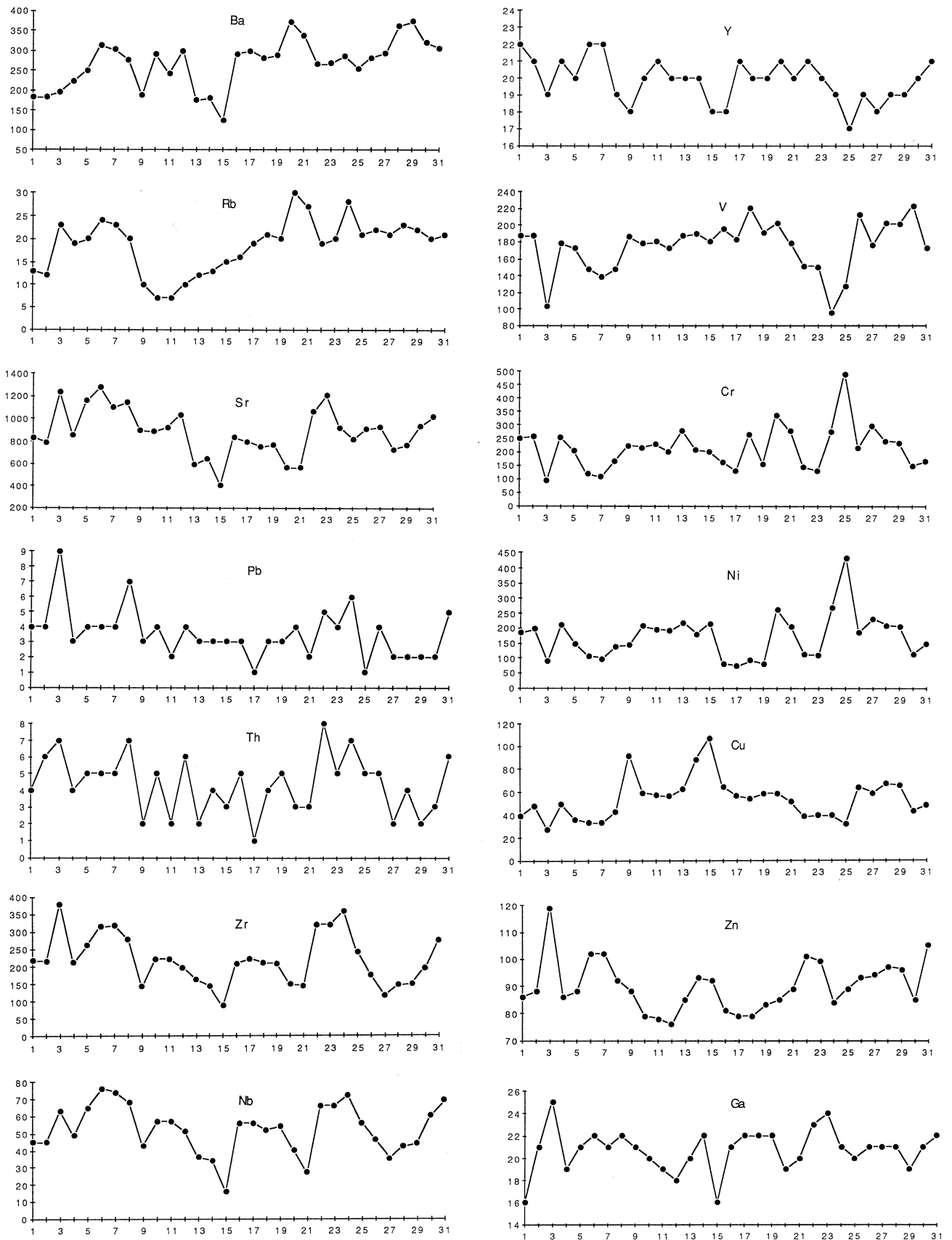


Figure 6-27. Trace elements versus flow number. The plots allow comparisons to be made between successive flows. Flow number 1 is the youngest being the uppermost flow on Mt Buckley. Trace elements are plotted as parts per million.

For the overall Mt Buckley sequence (Figs. 6-26 & 6-27), when chemically distinct flows B3 and B15 are ignored, the SiO₂ content decreases from about 48% in B19 to 45% in B1. V decreases from flows B18, B19 to a minimum in flow B7 then increases again from flow B6 to B1. CaO follows the same trend with the minimum occurring at B8. MgO also shows a minimum in B7.

6.4.4.2 Xenolith-bearing and primary lavas at Mount Buckley.

Ultramafic xenoliths occur in flows B1, B2, B4, B6, B7, B10, B12, B24 and B25. The location of the pyroxenite and lherzolite bearing flows, described by Wilkinson (1973), is in a small tributary of Youngs' Creek (GR:520075 Inverell 1:100,000, Fig. 6-19, Len Stewart, pers. comm.). The tributary incises the flows comprising Vol Aston Hill, numbered B24 and B25. Wilkinson (1973) determined the pyroxenites and peridotites to be samples of essentially unmodified, layered upper mantle. These xenoliths are characteristic of more alkaline and undersaturated flows which must have moved directly and rapidly from upper mantle levels to the surface. Such flows are therefore either primary melts or produced by crystal fractionation processes at high pressures (Irving and Green, 1976; Wass, 1980). Criteria for recognition of primary alkaline magmas include;

- a) An Mg-value ($100\text{Mg}/[\text{Mg}+\text{Fe}^{2+}]$) of 66 to 75 which represents liquids that could be in equilibrium with upper mantle residual olivine compositions (Fo89 - Fo99)
- b) high Ni values (>300 ppm)

Flow B25 satisfies these criteria with a Mg value of 69, Ni = 429 ppm and has the highest observed MgO, Cr and Ni in the entire sequence. The rest of the xenolith-bearing flows have Mg values of less than 65 and Ni less than 300 ppm, suggesting fractionation in the mantle through high pressure crystallization (Green et al, 1974) or direct derivation from more iron rich peridotite (Wilkinson and Binns, 1977). Such conditions of rapid transport to the surface are also consistent with the preservation of sapphires in their carrier magmas (Coenraads et al, 1990)

Xenoliths were notably absent in the coarse grained flows (B9, B11, B14, B15, B16, B17, B18, and B19) as was also observed by Wass (1980) for flows in the Southern Highlands. This may indicate a longer transit time to the surface, and/or residence in reservoirs, for such flows. If this is the case, they are also less likely to be sapphire carriers.

6.5 Comparison between volcanics of the sapphire-bearing East and sapphire-barren West Central Province

Chemical analyses for the Central Volcanic Province have been separated into those from the sapphire-bearing East and sapphire-barren West Central Province. Analyses for samples close to the boundary between the two (i.e. the MacIntyre River region) were included with the eastern group as these constitute the majority and will include both sapphire-bearing and sapphire-barren flows. The purpose of this comparison was to test

whether the sapphire-barren flows form a separate subset or a distinct, smaller compositional field, as was observed by Vichit et al. (1978) for the southeast Asian volcanic provinces. However, apart from more tholeiitic compositions, the rest of the sapphire-barren West Central Province analyses range over the entire compositional field, (see samples flagged with "w" in Fig. 6-20). The tholeiites found by Duggan (1972) are distinctly different from any basalts in the East Central Province. The identification of such tholeiites may be a discriminant against finding sapphire as these lavas show evidence of some low pressure fractional crystallisation (Wilkinson and Duggan, 1973), which would involve residence at higher levels.

6.6 Comparison between the Central Province and other volcanic provinces in northeastern Australia and southeast Asia

Stephenson et al (1980) compare the compositional fields for the volcanic provinces of north Queensland on a number of variation diagrams (i.e. alkalis versus silica, K_2O versus Na_2O , AFM, and normative plagioclase versus differentiation index plots). The compositional fields largely overlap one another, and those known to have associated sapphire (Atherton, Chudleigh and McBride) are not significantly different from the rest of the north Queensland provinces. Not surprisingly, the Central Volcanic Province compositional field also overlaps with those for Queensland (Fig. 6-28). The implications are that, either all the north Queensland provinces and the West Central Province are potentially sapphire-bearing, or more likely, that this type of data and its scatter are insufficient to predict likely sapphire-bearing and sapphire-barren provinces.

6.7 Conclusions

1. The basalt flows examined at Mt Buckley show a trend of increasing undersaturation with time, and range from predominantly alkali olivine basalts and hawaiites to predominantly basanites and nepheline hawaiites. They probably represent intercalated flows from several different mantle and crustal sources, particularly as many of the major and trace element values for flows, such as B3, B9 and B15, vary markedly from their neighbouring flows. The group of hawaiites B21, B22, B24 and B25 show widely varying values but consistently differ from their neighbours by having higher K_2O and Na_2O and lower CaO and V . These flows include a possible primary representative (B25). A large number of the flows carry high pressure xenoliths, implying their rapid movement from upper mantle depths.
2. There appears to be little distinction between the compositions from the sapphire-bearing East Central Province and the sapphire-barren West Central province on the variation diagrams. Tholeiites occurring to the west of Inverell appear to be an exception.

3. The compositional fields for the northeastern Australian volcanic provinces and the Central Volcanic Province overlap extensively and there is no apparent compositional distinction between fields known to contain corundum and those which do not.
4. The compositional field for the Central Volcanic Province overlaps both the corundum-bearing and corundum-barren fields for southeast Asian volcanic provinces.
5. Common compositional variations in basaltic fields do not appear to be useful indicators for predicting sapphire prospectivity in volcanic provinces.

Chapter 7

SUMMARY AND CONCLUSIONS

7.1 Origin of corundum associated with volcanic provinces

7.1.1 Aims and achievement of aims

A principal aim of this study was to shed light on the origin of corundum associated with volcanic provinces, using the Central Volcanic Province in northeastern New South Wales as a case study. The surface morphology of the corundum crystals and their inclusions were studied with a view to determine likely source rocks, the age relationship between the sapphires and the basalts, and the effects of transport in magma and fluvial environments on the corundum.

A second principal aim of this study was to investigate hydrologic and geomorphic factors which contributed to sapphire concentration to form known economic deposits and to assess prospectivity for sapphire and diamond exploration within the New England Gem Fields.

The aims of this study have been achieved. A summary of results and conclusions are presented in the sections following. Publications generated during this study are listed in Appendix 6.

7.2.1 Inclusion studies

Uranium-lead isotope dating of two zircon inclusions in sapphires from the Central Province, New South Wales gave ages of 35.9 ± 1.9 and 33.7 ± 2.1 million years (Ma). These ages fall within the range of basalt potassium-argon ages (19 to 38 Ma) and zircon fission track ages (2 to 49 Ma) for the timing of volcanism in the Central Volcanic Province (Coenraads et al, 1990). **These data, combined with the observation that corundum is found associated with many alkali basaltic provinces, indicate a genetic link between the growth of large corundum crystals and contemporaneous processes involved in alkali basaltic magma generation.**

The reported failure of experimental attempts to grow corundum from a corundum-bearing basaltic composition, (Green *et al.* 1978), and more significantly, the abundance of incompatible elements such as U, Th, Zr, Nb and Ta in inclusion minerals, indicate that the melting/crystallization process is not simple. Corundum, and other minerals (such as zircon, columbite, thorite, uranium pyrochlore, alkali feldspar etc.) found as inclusions in corundum, could not have crystallized from most basaltic compositions. A more complex process must occur in which crystallization of coarse aggregates takes place when high proportions of incompatible elements and volatiles are present in early melt fractions. These unusual crystallization products are subsequently transported to the surface by

voluminous basaltic magmas. **The extent to which this process occurs, together with the rate of transport to the surface, presumably determine whether a particular basaltic province carries sufficient corundum to be worked into economic concentrations of sapphire.**

7.1.2 Surface features

The majority of surface features observed on natural rubies and sapphires of volcanic origin reflect their trigonal crystal structure and are the result of layer dissolution or etching that occurred while the crystals were exposed to the hostile melt environment whilst en route to the surface. Such features generated by magmatic resorption include trigonal prismatic hillocks, trigonal pyramids, inverted trigonal pyramids, flat floored trigonal and hexagonal depressions (often with a central rhombohedral or pyramidal termination), and "brick-like" stacks of trigonal prisms. The style of features observed on a given surface is dependent both on the angle of the surface to the c-axis of the corundum crystal and the degree of subsequent etching. More irregular sculpture-like features appear to arise from continued dissolution, and the growth and merging of the above-mentioned features. Many of the crystal surfaces also show a superimposed surface texture consisting of fine corrosion-pits.

Fluvial transport and residence in the the alluvial environment are responsible for additional surface features. These include conchoidal fracture surfaces radiating from points of impact (particularly along exposed edges on some stones), clean fracture surfaces where pyramidal and prismatic protrusions have been broken, and exposed healed-fracture surfaces. There is often little evidence of abrasion due to fluvial transport.

It has been observed that pitting and etching on associated heavy minerals is commonly the result of surface biodegradation and this is particularly pronounced for the spinels.

The grain surface features, coupled with the spatial variability in the character the corundum, and the differences in proportions of heavy minerals in placer deposits collectively indicate minimal amount of fluvial transport, and minimal degree of downstream reworking and mixing. Such observations indicate that the corundum is derived from local multiple sources.

7.2 Division of the New England gem fields into three exploration regions

Key areas for diamond and sapphire exploration may be defined within the New England gem fields of eastern Australia through an understanding of the geologic and geomorphic processes that operated within the Tertiary Central Volcanic Province.

At least two distinct periods of volcanic activity - one at 32-38 Ma and the other at 19-23 Ma - were controlled by SSE/NNW trending fracture sets revealed by landsat data. The locus of volcanism stepped westwards with time from the Glen Innes-Ben Lomond-Guyra area (the East Central Province) to the area west of Inverell and Armidale (the West Central Province). Drainage and pre-volcanic topography indicate a radial pattern of drainage associated with East Central Province uplift and volcanism (32 - 38 Ma). This was modified by the later West Central Province volcanism (19 - 23 Ma) which established its own radial pattern. This division of the Central Volcanic Province defines broad regions suitable for sapphire and diamond exploration.

Highly prospective diamond-bearing "deep leads" associated with the palaeo-Gwydir River can be traced under the younger basalts of the West Central Province via reconstruction of the pre-volcanic topography.

In the East Central Province the post-eruptive fluvial history was vital in controlling the concentration of economic sapphire deposits from lower grade source rocks. The sapphire-bearing placer deposits occur as "shoestring" type accumulations occupying channels within broad, flat, basalt-filled valleys. The highest grades generally correspond to areas where channels are deepest.

The Central Province has been divided into three prospective target regions. These regions comprise a western region with a potential for "palaeo-Gwydir type" alluvial diamond deposits, a central belt with "Braemar type" sapphire deposits, and an eastern division with "Kings Plains- Reddestone type" alluvial sapphire deposits.

A detailed palaeotopographic reconstruction technique had not been applied previously to the search for economic deposits of diamond or sapphire in the Central Volcanic Province. This method has proven to be a valuable exploration tool for delineating palaeochannels containing the above-mentioned deposits.

7.2.1 Diamond-bearing deep leads of the West Central Volcanic Province

The Palaeo-Gwydir River system was buried by 19-23 Ma volcanism of the West Central Province. Prospectivity for diamond-bearing deep lead alluvium is considered to be favorable in two major palaeodrainage systems that extend northward from the present Gwydir River in the vicinity of Copeton Dam. These are the palaeo-Hobbs and palaeo-Gwydir systems. **The palaeotopographic reconstruction indicates at least 3 separate systems of diamond bearing alluvials and therefore, local, multiple sources for the diamonds.**

7.2.2 Holocene alluvial sapphire deposits of the East Central Volcanic Province

Two major sapphire deposits are situated in the Kings Plains and Reddestone Creeks of the East Central Province (Figs 4-3 and 4-4). These Holocene alluvial deposits are currently being worked by T.J. & P.V. Nunan Pty Ltd using mechanized mining methods. Each mine processes approximately 1000 tonnes of alluvium per day, yielding 1 tonne of heavy mineral concentrate containing about 10 kilograms of corundum (Nunan, 1989). There is a clear association between these deposits which have developed since the filling of the palaeovalleys with basalt, and the present drainage. Higher grades generally correspond to areas where channels are deepest, and sapphire grades in excess of 500 grams per cubic metre have been recorded. In this ideally balanced system the heavy minerals have moved vertically downwards, rather than downstream, and become concentrated with time.

Palaeotopographic reconstruction highlights potential abandoned channel deposits which may no longer show any obvious association with the present day drainage. Such sapphire deposits may occur along abandoned palaeovalleys which continue below the points of capture by the present drainage; they may be economic if the original drainage existed for sufficient time to allow concentration to take place.

7.2.3 Braemar-type deep lead deposits in the zone-of-overlap:

Exploration areas for deep lead sapphire deposits, such as those found at Braemar were defined via mapping of palaeochannels in which the deposits are situated. Palaeotopographic reconstruction, based on the elevation of the contact between the Tertiary volcanic rocks and the Palaeozoic basement, together with available drill hole data, were used. The potential sapphire-bearing palaeochannels have been delineated within the zone in which the 19-23 million year old volcanics forming the western portion of the Central Volcanic Province (the West Central Province) overlap onto 32-38 million year old sapphire bearing volcanics forming the eastern portion of the province (the East Central Province). In this zone, the 19-23 Ma basaltic lavas flooded a number of major palaeodrainage systems already containing 32-38 Ma basalt flows and alluvial deposits reworked from them.

Potential sapphire deposits have been delineated in the Braemar palaeochannel and its tributaries up-palaeostream from the Braemar sapphire mine where sapphires are recovered along with other heavy minerals. The highest concentration occurring at the base of the channel. "Braemar-type" deep lead deposits considered in this thesis had approximately 10 million years in which to form, and required the presence of a younger basalt capping (19-23 Ma) for their preservation.

Potential sapphire-bearing alluvials are also delineated along the topographically inverted palaeo-Swan Brook. The extent of these "deep lead"

deposits to the east of Braemar, in palaeochannels that drained the sapphire-bearing East Central Province, is related to the easternmost incursions of the lavas of the West Central Province.

7.3 Heavy mineral suites in the New England gem fields

7.3.1 Sapphire associates of the East Central Volcanic Province

Heavy minerals associated with sapphire in the alluvial gravels are pleonaste, ilmenite, chromium-spinel, titanium-magnetite, magnetite, corundum, zircon and minor chrysoberyl. Additional minerals found in nearby *in situ* basaltic soils comprise olivine, clinopyroxene, enstatite and amphibole, with zircon and sapphire being extremely rare.

Investigation of heavy mineral suites from 12 collection sites indicated significant variability in mineral species within and between particular drainage catchments. Visual characteristics of the sapphires also vary within and between catchments. This implies that sources are 'local' to the placer deposits. The similarity in composition of minerals from soil and placer sites indicates that the sapphire-bearing placers have formed through extensive reworking of the immediately surrounding alkali basaltic and volcanoclastic rocks. Concentration was largely through vertical movement, with fine or light material being winnowed downstream leaving behind a heavy gem-bearing residue, within low gradient, low energy drainage systems.

7.3.2 Ilmenite-mantled rutile crystals of the Uralla area

Ilmenite-mantled rutile crystals of enigmatic origin are found in Late Tertiary conglomeratic arkoses and Quaternary alluvium in the vicinity of Uralla, New South Wales. They comprise homogeneous, single, rutile crystal cores with ilmenite replacing the crystals and penetrating along (100) planes. The ilmenite ranges from higher TiO₂ adjacent to the rutile core to higher FeO at the outer edge. MgO decreases away from the core. This is consistent with reaction in a magma containing iron but poor in magnesium. The crystals are not associated with any obvious parent rock type. Comparisons of the chemistry of the ilmenites with a wide range of known ilmenite associations indicate that the source rock is unlikely to be mafic or ultramafic and that they are unlikely to be an indicator for diamond source rocks. The minerals may have formed as late-stage or cavity crystallizations from fractionated felsic magmas before eruption.

7.3.3 Pyrope-almandine garnets from Horse Gully

Deep red to purplish, gem quality garnets have been recovered from sapphire-bearing river gravels at Horse Gully in the New England gem fields. Seven garnets were faceted, gemmologically tested and analyzed with an electron microprobe. They are

members of the pyrope-almandine intermediate series ranging in composition from pyrope 55%-almandine 34% to pyrope 39%-almandine 49%. The stones with the highest end-member pyrope content (highest magnesium and lowest iron) display a most attractive mauve-purple to pinkish hue. They also have the lowest refractive index and specific gravity. The garnets are derived from a local, probably mafic, source situated within the catchment area of Horse Gully.

7.4 Investigation of sapphire source rocks and potential source structures in the Central Volcanic Province

Basaltic and volcanoclastic rocks in the East Central Volcanic Province are potential sources of the alluvial sapphires being mined in the New England gem fields. The associated drainage catchment areas generally contain sapphire, but only four major catchments contain rich deposits. These are the Frazers, Kings Plains, Reddestone and Marowan catchments and are the most likely targets for sapphire source rocks.

The basalt flows and intrusives comprising Mount Buckley divide Kings Plains Creek and Swan Brook, two important catchment areas for alluvial sapphire. Thirty one whole-rock analyses show mostly alkaline to strongly alkaline types and a general trend of increasing undersaturation with time. The top flows are predominantly basanite and nepheline hawaiites whilst the lowest are predominantly alkali olivine basalts and hawaiites. Ultramafic xenoliths in several flows suggest rapid movement from upper mantle levels. Marked variation in major and trace elements between groups of flows suggests that the sequence contains intercalated flows from different levels. No volcanoclastic rocks were encountered in the Mt Buckley area.

Within the Central Province, variation diagrams show no significant difference between the 32-38 Ma sapphire-associated eastern basalts and the 19-23 Ma sapphire-barren western alkali-basalts. The compositional fields also overlap the Atherton, McBride and Chudleigh provinces in north Queensland, known to contain sapphire, as well as those of the sapphire-barren northeastern Australian volcanic provinces. These Australian compositional fields also overlap the corundum-bearing and corundum-barren fields defined by Vichit et al (1978) for the southeast Asian volcanic provinces.

Major and minor element chemistry of basaltic rocks is not considered to be a useful exploration tool for discriminating sapphire-bearing from sapphire-barren volcanic provinces, nor for recognizing potentially high-grade areas within a sapphire-bearing province. This suggests that basaltic rocks are not the initial sapphire source rocks, but only one of the potential carriers.

Lagoons located in the basalts of the Central Province were investigated to determine whether they could be maars and therefore potential sources of sapphire-bearing volcanoclastic rocks. This was found not to be the case and the lagoons are interpreted to have formed within wind blown lunettes occupying the wide, flat floors of basalt filled

valleys. This interpretation was based on drilling, geophysical modelling and geological mapping which revealed the lagoons to be axial to pre-basaltic drainage channels overlying at least 10 metres of valley fill flow basalts. Drilling at Kings Plains Lagoon intersected basalt flows overlying silicic volcanic basement and failed to encounter any breccia within, or feeder vent below, the structure. **Bulk testing at Kings Plains and Dunvegan lagoons indicates that these features do not constitute economic targets.**

REFERENCES

- Atkinson, W.J., Hughes, F.E. and Smith, C.B. (1984). A review of the Kimberlitic rocks of Western Australia, in J.Kornprobst (Ed.). Kimberlites I. Kimberlites and Related Rocks, 195-224, Developments in Petrology, 11A, Elsevier, Amsterdam.
- Anderson, W. (1888). Appendix No. 8 in Report in progress for 1887 by the Geological Surveyor in Charge. Report, Department of Mines N.S.W. for 1887 155-156.
- Atkinson, D. and Kothavala, R.Z. (1983). Kashmir sapphire. *Gems and Gemmology*, **19**, 64-76.
- Australian Centre for Remote Sensing, Landsat images, 090-080F, 096-081, and 095-081: New South Wales Government Department of Lands, Remote Sensing Unit, 23-33 Bridge Street, Sydney, Australia.
- Baker, P.E., Gass, I.G., Harris, P.G., and Le Maitre, R.W. (1964). The volcanological report of the Royal Society expedition to Tristan de Cunha, 1962. *Philosophical Transactions of the Royal Society of London*, **256**, 439-578.
- Barr, S.M. and MacDonald, A.S. (1981). Geochemistry and geochronology of late Cenozoic basalts of Southeast Asia: Summary. *Geological Society of America Bulletin*, **92** (1), 508-512.
- Barron, L.M. (1987). Summary of petrology and chemistry of rocks from the sapphire project, New South Wales Geological Survey Report GS1987/050, 1-106. (Unpubl.).
- Binns, R.A. (1969). High-pressure megacrysts in basanitic lavas near Armidale, N.S.W. *American Journal of Science* **267-A**, 33-49,
- Binns, R.A., Duggan, M.B. and Wilkinson, J.F.G. (1970). High pressure megacrysts in alkaline lavas from northeastern New South Wales, *American Journal of Science* **269**, 132-168.
- Birch, W.D. (1979). Mineralogy and Geochemistry of the leucitite at Cosgrove, Victoria. *Journal of the Geological Society Of Australia*, **25**, 369-385.
- Birch, W.D., Smith, N. and Hatley, J. (1982). Andesine, augite and ilmenite in vesicles in an alkali olivine basalt from Portland, Victoria. *Australian Mineralogist*, **37**, 195-198.

- Bischoff, G.C.O. and Coenraads, R.R. (in prep). Fossil and Recent Traces of Biodegradation on Heavy Minerals.
- Broughton, P.L. (1979). Economic geology of the Anakie sapphire mining district Queensland. *Journal of Gemmology.*, **16**, (5), 318-337.
- Brown, R.E. (1987). Detailed geological mapping in the Elsmore and Kings Plains areas, New South Wales Geological Survey - Report GS1987/058, 22-24. (Unpubl.).
- Brown, R.E. and Pecover, S.R. (1986a). The geology of the Braemar sapphire deposit. New South Wales Geological Survey - Report GS1986/270. (Unpubl.).
- Brown, R.E. and Pecover, S.R. (1986b). The geology of the Kings Plains sapphire field. New South Wales Geological Survey - Report GS1986/271. (Unpubl.).
- Brownlow, A.H. and Komorowski, J.C. (1988). Geology and origin of the Yogo sapphire deposit, Montana. *Economic Geology* **83**, 875-880.
- Brownlow, J.W. (1989). Guyra 1:100,000 Geologic Sheet, Department of Minerals and Energy, Armidale Branch, State Government Office Building, cnr. Faulkner and Dumeresq streets, Armidale, N.S.W., 2350.
- Carmichael, I.S.E. (1967). The iron titanium oxides of salic volcanic rocks and their associated ferromagnesian silicates. *Contributions to Mineralogy and Petrology*, **14**, 36-64.
- Carmichael, I.S.E., Turner, F.J. and Verhoogen, J. (1974). *Igneous Petrology*, McGraw Hill Inc. New York.
- Cassidy, K.F., Groves, D.I. and Binns, R.A. (1988). Manganoan ilmenite formed during regional metamorphism of Archaean mafic and ultramafic rocks. *Canadian Mineralogist*, **26**, 999-1012.
- Cawthorne, R.G., Maske, S., de Wet, M., Groves, D.I. and Cassidy, K.F. (1988). Contrasting magma types in the Mount Ayliff (Insizwa complex), Transkei: evidence from ilmenite compositions. *Canadian Mineralogist*, **26**, 145-160.
- Clarke, D.B. and MacKay, R.M. (1990). An ilmenite-garnet-clinopyroxene nodule from Matsoku: Evidence for oxide-rich liquid immiscibility in kimberlites? *Canadian Mineralogist*, **28**, 229-239.

- Coenraads, R.R. (1988a). Kings Plains drilling project. Report for Jingellic Minerals N.L., 11th March. (Unpubl.).
- Coenraads, R.R. (1988b). Six monthly report to the Department of Mines, E.L.'s 2988 and 2989 for the period to 12 July 1988. New South Wales Geological Survey - Reports GS1988/250, GS1990/003 and GS1990/314. (Unpubl.).
- Coenraads, R.R. (1988c). Structural control and timing of volcanism in the Central Province. Implications for regional targeting of prospective areas for sapphire and diamond exploration, *in* New England Orogen Tectonics and Metallogenesis. J.D.Kleeman (Ed.). Department of Geology and Geophysics, University of New England, Armidale, Australia, pp.302-307.
- Coenraads, R.R. (1989). Evaluation of the natural lagoons of the Central Province, N.S.W. - are they sapphire producing maars? *Bulletin of the Australian Society of Exploration Geophysicists*, **20**, 347-363.
- Coenraads, R.R. (1990). Key areas for alluvial diamond and sapphire exploration in the New England gem fields, New South Wales, Australia. *Economic Geology*, **85**, 1186-1207.
- Coenraads, R.R. (in press). Palaeogeography of the Braemar sapphire deposit: Implications for deep-lead sapphire exploration in the Central Volcanic Province, New South Wales. *Journal and Proceedings Royal Society of New South Wales*,
- Coenraads, R.R. (in prep). Evaluation of potential sapphire source rocks within the catchments of Kings Plains Creek and Swan Brook, near Inverell, New South Wales. *Records of the Australian Museum*
- Coenraads, R.R. and Lawrence, D. (1989). Six monthly report to the Department of Mines, E.L.'s 2988 and 2989 for the period to 12 January 1989. New South Wales Geological Survey - Reports GS1988/250, GS1990/003 and GS1990/314. (Unpubl.).
- Coenraads, R.R. and van der Graaf, R. (1991). An occurrence of gem garnets from Horse Gully in the New England gem fields, New South Wales. *The Australian Gemmologist* , **17**(10)

- Coenraads, R.R., Paige, S.C.B. and Sutherland, F.L. (in press). Ilmenite mantled Rutile Crystals from the Uralla District, New South Wales. *Journal and Proceedings Royal Society of New South Wales*
- Coenraads, R.R., Pope, G.J. and Whittle, M.A. (1989). Six monthly report to the Department of Mines, E.L.'s 2988 and 2989 for the period 15 January, 1989 to 14 July, 1989. New South Wales Geological Survey - Reports GS1988/250, GS1990/003 and GS1990/314. (Unpubl.).
- Coenraads, R.R., Sutherland F.L. and Kinny P.D. (1990). The origin of sapphires: U-Pb dating of zircon inclusions sheds new light. *Mineralogical Magazine*, **54**, 113-122.
- Coldham, T. (1985). Sapphires from Australia, *Gems and Gemology*, **21**, 130-146.
- Compston, W., Williams, I.S. and Meyer, C. (1984). U-Pb geochronology of zircons from Lunna breccia 73217 using a sensitive high mass-resolution ion microprobe. *Journal of Geophysical Research*, **89**, 525-534.
- Coombs, D.S. and Wilkinson, J.F.G. (1969). Lineages and fractionation trends in undersaturated volcanic rocks from the East Otago volcanic province (New Zealand) and related rocks. *Journal of Petrology*, **10**(3), 440-501.
- Cooper, J.A., Richards, J.R. and Webb, A.W. (1963). Some potassium-argon ages in New England, New South Wales, *Journal of the Geological Society of Australia*, **10**, 313-316.
- Cotton, L.A. (1914). The diamond deposits of Copeton, New South Wales, *Proceedings of the Linnean Society of New South Wales*, **39**, 803-838.
- Cundari, A. (1973). Petrology of the leucite bearing lavas in New South Wales. *Journal of the Geological Society of Australia*, **20**, 465-492.
- Curran, J.M. (1897). On the occurrence of precious stones in New South Wales and the deposits in which they are found. *Journal of the Proceedings of the Royal Society of N.S.W.*, **30**, 228-237.
- Dalrymple, G.B. (1979). Critical tables for conversion of K-Ar ages from old to new constants. *Geology*, **7**, 558-560.

- David, T.W.E. (1886). Report on the geology of the Rocky River goldfields. New South Wales Department of Mines Annual Report for 1885, pp. 153-158.
- Dawson, J.B. (1980). Kimberlites and their Xenoliths (Minerals and rocks; 15). Springer-Verlag, Berlin. J.B. Dawson (Ed.).
- Deer, W.A., Howie, R.A. and Zussman, J. (1975). Rock-Forming Minerals 5. Non-Silicates, Longmans Green and Co., London. W.A. Deer, R.A. Howie and J. Zussman (Eds.).
- Duggan, N.T. (1972). Tertiary volcanics of the Inverell area, Honours Thesis (unpubl.), University of New England, Armidale, Australia.
- Dunstan, B. (1902). The sapphire fields of Anakie. *Queensland Government Mining Journal* **3**, 239-246 and 293-298.
- Gibbons, G.S. and Pogson, D.J. (1963). Diamond Deposits at Mount Ross. Rep. Geol. Surv. N.S.W., GS1963/002 (unpubl.).
- Green, D.H., Edgar, A.D., Beasley, P., Kiss, E., and Ware, N.G. (1974). Upper mantle source for some hawaiites, mugearites and benmoreites. *Contributions to Mineralogy and Petrology*, **48**, 33-43.
- Green, D.H. and Ringwood, A.E. (1967). The genesis of basaltic magmas. *Contributions to Mineralogy and Petrology*, **15**, 103-190.
- Green, T.H., Wass, S.Y. and Fergusson, J. (1978). Experimental study of corundum stability in basalts. Abstracts of the Third Australian Geological Convention, Townsville, August 28-31, Geological Society of Australia, p.34.
- Gubelin, E.J. and Koivula, J.I. (1986). Photoatlas of Inclusions in Gemstones. ABC Edition, Zurich.
- Gunawardene, M. and Chawla, S.S. (1984). Sapphires from Kanchanaburi Province, Thailand. *Journal of Gemmology*, **19** (3), 228-239.
- Gunawardene, M. and Rupasinghe, M.S. (1986). The Elahera gem field in central Sri Lanka. *Gems and Gemology*, **22**(2). 80-95

- Haggerty, S.E. (1976). Opaque mineral oxides in terrestrial igneous rocks. *in* Oxide Minerals. Reviews in Mineralogy 3, Hg-101 to Hg-300, Mineralogical Society of America, Washington. D.C. P.H. Ribbe and D. Rumble III (Eds.).
- Hänni, H.A. (1987). On corundums from Umba valley, Tanzania. *Journal of Gemmology*, **20** (5), 278-284.
- Harte, B., Winterburn, P.A. and Gurney, J.J. (1987). Metasomatic and enrichment phenomena in garnet peridotite facies mantle xenoliths from the Matsoku kimberlite pipe, Lesotho. *in* Mantle Metasomatism, pp. 145-220. Academic Press Inc., London. M.A. Menzies and C.J. Hawkesworth (Eds.).
- Hollis, J.D. and Sutherland, F.L. (1985). Occurences and origins of gem zicons in Eastern Australia, *Records of the Australian Museum*, **36**, 299-311.
- Hollis, J.D., Sutherland, F.L. and Pogson, R.E. (1983). High pressure minerals and the origin of the Tertiary breccia pipe, Ballogie Gem Mine, near Proston, Queensland. *Records of the Australian Museum*, **35**, 181-194.
- Horton, D.R., and Connah, G.E. (1981). Man and megafauna at Reddestone Creek, near Glen Innes, northern New South Wales. *Australian Archaeology* **13**, 35-52.
- Irvine, T.N. and Barager, W.R.A. (1971). A guide to chemical classification of the common volcanic rocks. *Canadian Journal of Earth Science*, **8**, 523-548.
- Irving, A.J. (1980). Petrology and geochemistry of composite ultramafic xenoliths in alkalic basalts and implications for magmatic processes within the mantle. *American Journal of Science*, **280A**, 389-426.
- Irving, A.J. (1986). Polybaric magma mixing in alkalic basalt and kimberlites: evidence from corundum, zircon and ilmenite megacrysts. Fourth International Kimberlite Conference. Extended Abstracts. Perth. *Geological Society of Australia Abstracts Series*, **16**, 262-263.
- Irving, A.J. and Green, D.H. (1976). Geochemistry and petrogenesis of the Newer Basalts of Victoria and South Australia. *Journal of the Geological Society of Australia*, **23** 45-66
- Irving, A.J. and Price, R.C. (1981). Geochemistry and evolution of Iherzolite-bearing phonolitic lavas from Nigeria, Australia, East Germany and New Zealand. *Geochimica et Cosmochimica Acta*, **45**, 1309-1320.

- Irving, A.J. and Price, R.C. (1981). Geochemistry and evolution of Iherzolite-bearing phonolitic lavas from Nigeria, Australia, East Germany and New Zealand. *Geochimica et Cosmochimica Acta*, **45**, p. 1309-1320.
- Iyer, L.A.N. (1953). The geology and gem-stones of the Mogok Stone Tract, Burma. *Memoirs of the Geological Society of India*, **82**, 1-100
- Jackson, B. (1984). Sapphire from Loch Roag, Isle of Lewis, Scotland. *Journal of Gemology*, **19** (4), 336-342.
- Jaques, A.L., Kerr, I.D., Lucas, H., Sun, S.S. and Chappell, B.W. (1989). Mineralogy and petrology of picritic monchiquites from Wandagee, Carnarvon Basin, western Australia, in Kimberlites and Related Rocks. I. J. Ross (Ed.). *Geological Society of Australia, Special Publication*, **14**, 120-139.
- Jaques, A.L. and Perkin, D.J. (1984). A mica, pyroxene, ilmenite megacryst-bearing lamprophyre from Mt Woolooma, north eastern New South Wales. *Bureau of Mineral Resources Journal of Australian Geology and Geophysics*, **9**, 33-40.
- Jobbins, E.A. and Berrange, J.P. (1981). The Pailin ruby and sapphire gemfield, Cambodia. *Journal of Gemmology*, **17** (8), 555-567.
- Johnson, R.W. (1989). Volcano distribution in and classification; distribution in eastern Australia, in Johnson, R.W. and Taylor, S.R., eds, *Intraplate Volcanism in Eastern Australia and New Zealand*: Cambridge University Press. p. 9-10.
- Jones, D.R. (1983). Difficulties associated with using indicator minerals for diamond exploration in north Queensland. M.Sc. Thesis, James Cook University of North Queensland. (Unpubl.).
- Keller, A.S. and Keller, P.C. (1986). The sapphires of Mingxi, Fujian Province, China. *Gems and Gemology*, **22** (1), 41-45.
- Keller, P.C. (1982). The Chanthaburi-Trat gem field, Thailand. *Gems and Gemology*, **18** (2), 186-196.
- Keller, P.C. and Wang, F. (1986). A survey of gemstone resources of the People's Republic of China. *Gems and Gemology*, **22** (1), 3-13.

- Keller, P.C., Koivula, J.I. and Jara, G. (1985). Sapphire from the Mercaderes-Rio Mayo area, Cauca, Colombia. *Gems and Gemology*, **21** (1), 20-25.
- Kiefert, L. and Schmetzer, K. (1987). Blue and yellow sapphire from Kaduna Province, Nigeria. *Journal of Gemmology*, **20** (7-8), 427-442.
- Kinny, P.D., Williams, I.S., Froude, D.O., Ireland, T.R. and Compston, W. (1988). Early Archaean zircon ages from orthogneisses and anorthosites at Mount Narryer, Western Australia. *Precambrian Research*, **38**, 325-341.
- Kinny, P.D., Compston, W., Bristow, J.W. and Williams, I.S. (1989). Archaean mantle xenocrysts in a Permian kimberlite: Two generations of kimberlitic zircon in Jwaneng DK2, southern Botswana. in: *Kimberlites and Related Rocks*, Geological Society of Australia Special Publication, **14**.
- Lacombe, P. (1969-1970) Le massif basaltique quaternaire a zircon-gemmes de Ratanakiri (Cambodge-oriental). *Bull. Bureau Recherches Geol. Min.* (2nd series) Sect. iv: No. 3-1969, p.31-91; No. 2-1970, p.29-57; No. 4-1970, p.33-79. Paris.
- Leitch, E.C. (1974). The geological development of the southern part of the New England Fold Belt. *Journal of the Geological Society of Australia*, **21** 133-156.
- Lishmund S.R. (1987), Regional distribution of sapphire, diamond and volcanoclastic rocks, Department of Mineral Resources, extended abstracts from a seminar on Tertiary volcanics and sapphires in the New England District, 1st May, 9-12- Report GS 1987/058.
- Lishmund, S.R. and Oakes, G.M. (1983). Diamonds, sapphires and Cretaceous/Tertiary diatremes in New South Wales. *New South Wales Geological Survey - Quarterly Notes*, **53**, 23-27.
- Lovering, J.F. (1964). The eclogite-bearing basic igneous pipe at Ruby Hill near Bingara, New South Wales. *Journal and Proceedings, Royal Society of New South Wales*, **97**, 73-79
- Mabbutt, J.A. (1977), Desert Landforms. ANU Press, Canberra.
- MacDonald, G.A. and Katsura, T. (1964). Chemical composition of Hawaiian lavas. *Journal of Petrology*, **5**, 82-133.

- MacNevin, A.A. (1972). Sapphires in the New England District, New South Wales. *Records of the Geological Survey of New South Wales*, **14**(1), 19-35.
- MacNevin, A.A. (1977). Diamonds in New South Wales. Department of Mines, Geological Survey of New South Wales, Sydney. Mineral Resources No. 52. 1-125.
- McMinn, A. (1987). Miocene palynology of DM Elsmore DDH2 and 3, near Inverell, Geological survey of N.S.W., Palynological Report 1987/005. (Unpubl.)
- McMinn, A. (1989). Tertiary palynology in the Inverell area. *New South Wales Geological Survey - Quarterly Notes*, **76**, 1-10.
- McDougall, I. and Wilkinson, J.F.G. (1967). Potassium-argon dates on some Cainozoic volcanic rocks from northeastern New South Wales, *Journal of the Geological Society of Australia*, **14**, (2), 225-233.
- McKay, G.J. (1975). Volcanic and other petrology of the Wellingrove area, New England. Honours Thesis, University of New England, Armidale, Australia. (Unpubl.).
- McQueen, L.B. (1975). Permian acid volcanic rocks and Tertiary alkaline basaltic rocks of an area northeast of Inverell, N.S.W, Honours Thesis, University of New England, Armidale, Australia. (Unpubl.).
- Mitchell, R.H. (1973). Magnesian ilmenite and its role in kimberlite petrogenesis. *Journal of Geology*, **81**, 301-311
- Mitchell, R.H. (1979). Mineralogy of the Tunraq kimberlite, Somerset Island, N.W.T. Canada. *Proceedings of the Second International Kimberlite Conference*. Volume 1: The Mantle Sample: Inclusions in Kimberlites and other Volcanics. F.R. Boyd Jr and H.O.A. Meyer (Eds.). American Geophysical Union, Washington D.C.
- Moore, A.E. (1987). A model for the origin of ilmenite in kimberlite and diamond: implications for the genesis of the discrete nodule (megacryst) suite. *Contributions to Mineralogy and Petrology*, **95**, 245-253.
- Munasinghe, T. and Dissanayake, C.B. (1986). The origin of gemstones of Sri Lanka. *Economic Geology*, **76**, 1216-1225.

- Neal, C.R. and Davidson, P. (1989). An unmetasomatized source for the Malaitan alnoite (Solomon Islands): Petrogenesis involving zone refining, megacryst fractionation and assimilation of oceanic lithosphere. *Geochemica et Cosmochimica Acta*, **53**, 1975-1990.
- New South Wales Government Department of Lands, 1:25,000 and 1:100,000 topographic sheets, Aerial Photography and Map Sales, 23-33 Bridge Street, Sydney 2000, Australia.
- New South Wales Government Department of Minerals and Energy: Dorrigo-Coffs Harbour, Grafton, Inverell and Manilla, 1:250,000 geological sheets, Publications Section, 29-57 Christie Street, St Leonards, N.S.W. 2065.
- New South Wales Government Department of Minerals and Energy. (1987). Tertiary Volcanics and Sapphires in the New England District, seminar held in Sydney, 1st May 1987. 29-57 Christie St, St. Leonards, New South Wales, 2065.
- New South Wales Government Department of Water Resources, 10 Valentine Ave, Parramatta, New South Wales, 2150.
- Nunan, T.J. (1989). The mining of sapphires. *The Australian Gemmologist*, **17**(1) 7-12.
- Ollier C.D. (1967). Maars: their characteristics, varieties and definition, *Bulletin of Volcanology*, **31**, 46-73.
- Ollier C.D. (1979). Evolutionary geomorphology of Australia and Papua- New Guinea, *Transcripts of the Institute of British Geographers*, **4**, 516-539.
- Ollier C.D. (1982). Geomorphology and tectonics of the Armidale region, Voisey Symposium 1982, New England Geology. P.G. Flood and B. Runnegar (Eds.).
- Ollier C.D. and Joyce E.B. (1976). Newer volcanic landforms, in *Geology of Victoria*. J.G. Douglas and I.A. Ferguson (Eds.). Geological Society of Australia, Special Publication 5, 341-345.
- Orlov, Y.L. (1977). *The Mineralogy of the Diamond*. John Wiley and sons, New York, Brisbane.
- Parasnis, D.S. (1975), *Methods in Geochemistry and Geophysics 3, Mining Geophysics*. 2nd edition Elsevier Scientific Publishing Company.

- Patel, A.R. and Agarwal, M.K. (1966). Unusual microstructures on some South African natural diamonds. *Industrial Diamond Review*, **26** (307), 240-244.
- Pecover S.R. (1987). Tertiary maar volcanism and the origin of sapphires in northeastern New South Wales, Department of Mineral Resources, extended abstracts from a seminar on Tertiary volcanics and sapphires in the New England District, 1st May, 13-21. New South Wales Geological Survey - Report GS 1987/058.
- Pecover, S.R. and Brown, R.E. (1986) Tertiary volcanism in northeastern New South Wales: Implications for sapphire and diamond exploration. New South Wales Geological Survey - Report GS1986/272. (Unpubl.).
- Pecover, S.R. and Coenraads, R.R. (1989). Tertiary volcanism, alluvial processes, and the origin of sapphire deposits at "Braemar" near Elsmore, northeastern New South Wales. *New South Wales Geological Survey - Quarterly Notes*, **77**, 1-23.
- Pithers, G. (1988). Final Report for E.L. 2987, Inverell-Tingha Area, Hooker Resources Pty. Ltd. Report New South Wales Geological Survey - Report GS1988/248. (Unpubl.).
- Pittman, E.F. (1897). Report on the Boggy Camp diamond fields: A Report to the Department of Mines for 1896, Geological Survey of New South Wales, Sydney, 98-99.
- Porter, H.M. (1899). Diamonds at Inverell, N.S.W. *Australian Min. Stand.*, **16**, 169-170.
- Rudnick, R.L. and Williams, I.S. (1987). Dating the lower crust by ion microprobe. *Earth and Planetary Science Letters*, **85**, 145-161.
- Rumble, D. (1976). Oxide minerals in metamorphic rocks, *in* Oxide Minerals. Reviews in Mineralogy 3, R1-R24, Mineralogical Society of America, Washington D.C. P.H. Ribbe and D.Rumble (Eds.).
- Saggerson, E.P. and Williams, L.A.S. (1964). Ngurumanite from southern Kenya and its bearing on the origin of rocks in the northern Tanganyika alkaline district. *Journal of Petrology*, **5**, 40-81.
- Scott Smith, B.H., Skinner, E.M.W. and Loney, P.E. (1989). The Kapamba lamproites of the Luangwa Valley, Eastern Zambia, *in* Kimberlites and Related Rocks I. J. Ross (Ed.). *Geological Society of Australia Special Publication*, **14**, 189-205.

- Simpson, E.S. (1951). Minerals of Western Australia 2. Government Printer, Perth, Western Australia.
- Slansky, E. (1987). X-ray examination of concentrates from sapphire-bearing rocks. New South Wales Geological Survey - Report GS1987/12, pp. 1-8. (Unpubl.).
- Smith, N.M. (1988). Reconstruction of the Tertiary drainage systems in the Inverell Region, Honours Thesis, University of Sydney, Australia. (Unpubl.).
- Spencer, L.K. (1983). Sapphires in Australia. AMAX Office, Inverell, N.S.W. 2360, report, August 1983, 83 p. (Unpubl.).
- Spencer, R. (1987). Ground geophysical surveys conducted for the sapphire project, Department of Mineral Resources, extended abstracts from a seminar on Tertiary volcanics and sapphires in the New England District, 1st May, 36-39.
- Stephenson, P.J. (1976). Sapphire and zircon in some basaltic rocks from Queensland, Australia. Abstracts, 25th International Geological Congress, Sydney, 2, 602-603.
- Stephenson, P.J., Griffin, T.J. and Sutherland, F.L. (1980). Cainozoic volcanism in eastern Australia, *in* Geology and geophysics of northeastern Australia. R.A. Henderson and P.J. Stephenson (Eds.). Geological Society of Australia, Queensland Division, Brisbane.
- Stonier, G.A. (1895). Report on the Bingarra diamond fields. A Report to the Department of Mines for 1894, Geological Survey of New South Wales, Sydney, 131-136.
- Street, G.J. (1974). An examination of the Permian granitic plutons and Tertiary alkaline basaltic rocks, east of Glencoe, northern N.S.W., Honours Thesis, University of New England, Armidale, Australia. (Unpubl.).
- Stroud, W.J. (1989). Bingara, Bukkulla, Cherry Tree Hill, Delungra, Dinoga, Elsmore, Gum Flat, Hurricane Hill, Indianna, Inverell, Mt Rodd, Nullamanna, Sapphire, Tingha, and Warialda 1:25,000 Geologic Sheets. Department of Minerals and Energy, Armidale Branch, State Government Office Building, cnr Faulkner and Dumeresq streets, Armidale, N.S.W., 2350.
- Sutherland, F.L. (1980). The Geology and Petrology of some Tertiary Volcanic Rocks in the Bowen-St.Lawrence Hinterland. PhD. Thesis, James Cook University of North Queensland, Townsville, Australia. (Unpubl.).

- Sutherland, F.L. (1985). Regional controls in eastern Australian volcanism, *in* Volcanism in Eastern Australia with case histories from New South Wales. F.L. Sutherland, B.J. Franklin and A.E. Waltho (Eds.). Geological Society of Australia, New South Wales Division Publication 1, 13-32.
- Sutherland, F.L., Kinny, P.D. and Hollis, J.D. (1991). Use of zircons to resolve origins of sapphires in east Australian gem fields - the mysterious case of the shuffling sapphire volcanoes, *in* "Exploration in a Changing Environment", The Australian Society of Exploration Geophysicists 8th Conference and Exhibition and The Geological Society of Australia Exploration Symposium, Sydney 1991, Abstracts No. 30. p. 227-228.
- Sutherland, F.L., Robertson, A.D., Hendry, D.F. and Hollis, J.D. (1990). Xenolith suites from southern Queensland: The lithosphere below volcanic regions, *in* The Eromanga-Brisbane Geoscience Transect. D.M. Finlayson (Ed.). Department of Primary Industries and Energy, Bureau of Mineral Resources, Geology and Geophysics.
- Sweeney, J.W. (1971). Rhodesian sapphire deposits. *Lapidary Journal*, November, 1076-1077.
- Temby, P.A. (1986). Exploration Licence 2285, Elsmore, Final report covering the period 24/10/85 - 24/10/86. Blue Circle Southern Cement Limited. New South Wales Geological Survey - Report GS1985/246. (Unpubl.).
- Thompson, R.N., Morrison, M.A., Dicken A.P., Gibson, I.L. and Harmon, R.S. (1986). Two contrasting styles of interaction between basic magmas and continental crust in the British Tertiary volcanic province. *Journal of Geophysical Research*, **91** B6, 5985-5997.
- Upton, B.J.G., Aspen, P. and Chapman, N.A. (1983). The upper mantle and deep crust beneath the British Isles: evidence from inclusions in volcanic rocks. *Journal of the Geological Society of London*, **140**, 105-121.
- Vichit, P. (1987). Gemstones in Thailand. *Journal of the Geological Society of Thailand*, **9** (1-2), 108-133.
- Vichit, P., Vudhichativanich, S. and Hansawek, R. (1978). The distribution and some characteristics of corundum-bearing basalts in Thailand. *Journal of the Geological Society of Thailand*, **3** (1), M4-1 to M4-38.

- Wass, S.Y. (1973). Oxides of low pressure origin from alkali basaltic rocks, Southern Highlands, N.S.W., and their bearing on the petrogenesis of alkali basalt magmas. *Journal of the Geological Society of Australia.*, **20**, 427-448.
- Wass, S.Y. (1980). Geochemistry and origin of xenolith-bearing and related alkali basaltic rocks from the Southern Highlands, New South Wales, Australia. *American Journal of Science*, **280A**, 639-666.
- Wass, S.Y., Henderson, P. and Elliot, C.J. (1980). Chemical Heterogeneity and metasomatism in the upper mantle: Evidence from Rare Earth and other Elements in Apatite-Rich Xenoliths in Basaltic Rocks from Eastern Australia. *Philosophical Transactions of the Royal Society of London, A.*, 297, 333-346.
- Webring M. (1985). SAKI: A fortran program for generalized linear inversion of gravity and magnetic profiles, Open file report 85-122, United States Department of the Interior.
- Webster, R. (1975). *Gems, Their Sources, Descriptions and Identification*. Butterworths & Co. Ltd, London, Sydney.
- Wellman, P. (1971). The age and palaeomagnetism of the Australian Cenozoic Volcanic Rocks. Ph.D. Thesis, Australian National University, Canberra, Australia. (Unpubl.)
- Wellman, P. (1988). Intrusions beneath large intraplate volcanoes. Geological Society of Australia, Abstracts No. 21. 9th Australian Geological Convention, February 1-5.
- Wellman, P. and McDougall, I. (1974). Cainozoic igneous activity in eastern Australia, *Tectonophysics*, **23**, 49-65.
- Wellman, P. and McDougall, I. (1974). Potassium- Argon ages on the Cainozoic volcanic rocks of New South Wales. *Journal of the Geological Society of Australia.*, **21**, 247-272.
- Wilkinson, J.F.G. (1962). Mineralogical, geochemical and petrogenetic aspects of an analcite-basalt from the New England district N.S.W., *Journal of Petrology*, **3** (2), 192-214.
- Wilkinson, J.F.G. (1966). Residual glasses from some alkali basaltic lavas from New South Wales, *Mineralogical Magazine*, **35**, 847.

- Wilkinson, J.F.G. (1973). Pyroxenite xenoliths from an alkali trachybasalt in the Glen Innes area, northeastern N.S.W., *Contributions to Mineralogy and Petrology*, **42**, 15-32.
- Wilkinson, J.F.G. (1974). Garnet clinopyroxenite inclusions from diatremes in the Gloucester area, New South Wales, Australia, *Contributions to Mineralogy and Petrology*, **46**, 275-299.
- Wilkinson, J.F.G. and Binns, R.A. (1977). Relatively iron rich lherzolite xenoliths of the Cr-diopside suite: a guide to the nature of anorogenic tholeiitic andesite magmas, *Contributions to Mineralogy and Petrology*, **65**, 199-212.
- Wilkinson, J.F.G. and Duggan, N.T. (1973). Some tholeiites from the Inverell area, N.S.W., and their bearing on low pressure tholeiite fractionation. *Journal of Petrology*, **14**, 339-348.
- Willis, I.L. (1989). Dundee, Glen Innes, Maybole, Mount Slow, Rangers Valley, Red Range, Shannon Vale, and Stonehenge 1:25,000 Geologic Sheets, Department of Minerals and Energy, Armidale Branch, State Government Office Building, cnr Faulkner and Dumeresq streets, Armidale, N.S.W., 2350.
- Wright, J.B. (1969). High pressure phases in Nigerian Cenozoic lavas, distribution and geotectonic setting. Paper presented at the IAVCEI symposium, "Volcanoes and Their Roots" Oxford, Sept. 1969.
- Yaemniyom, N. (1982). The petrochemical study of corundum bearing basalts at Bo Phloi district, Kanchanaburi. M.Sc. Thesis, Chulalongkorn University, Thailand. (Unpubl.).
- Zwaan P. (1982). Sri Lanka: The gem island. *Gems and Gemology*, **18**(2), 62-71.

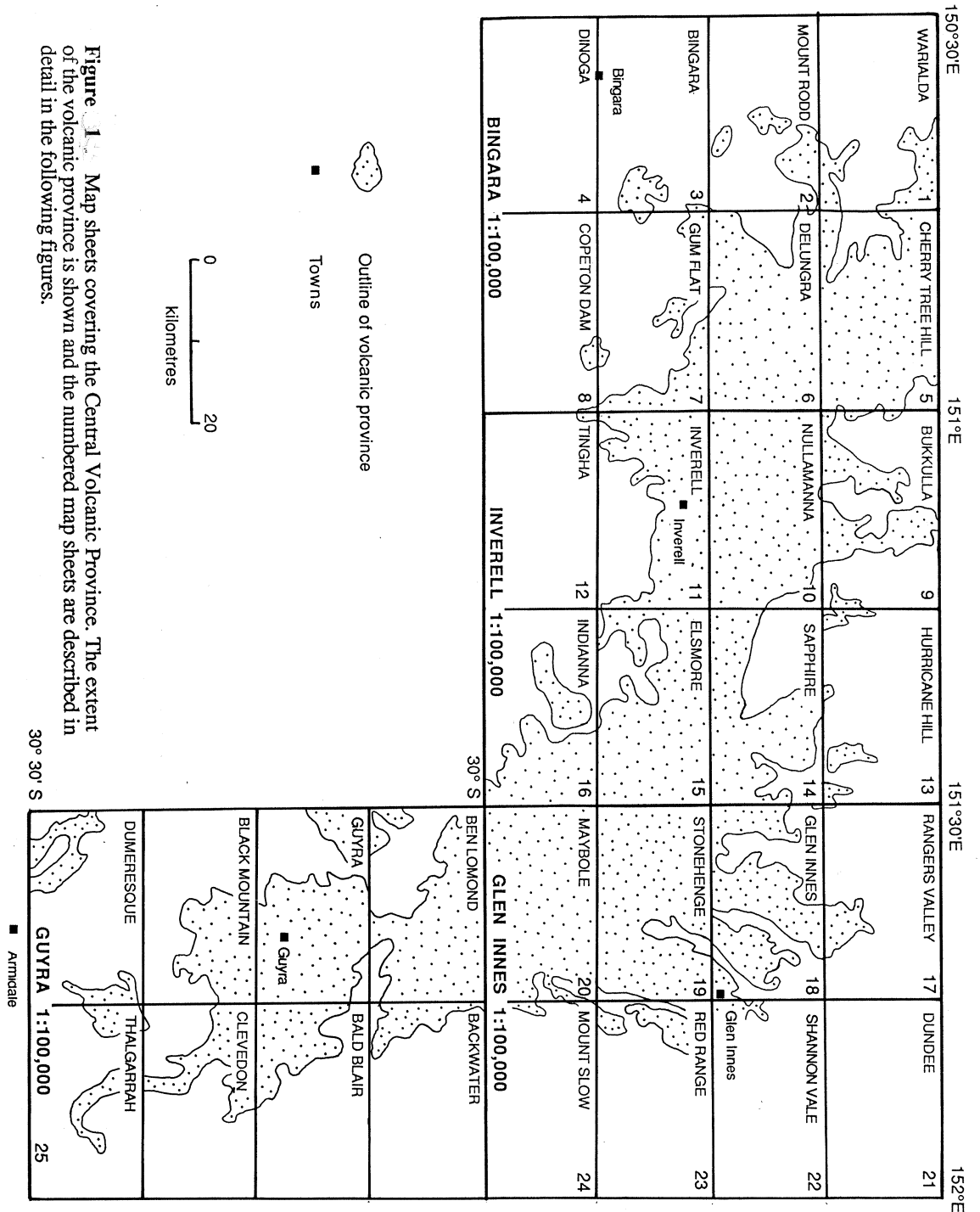
Appendix 1

PRE-VOLCANIC TERTIARY LANDSCAPE AND DRAINAGE OF THE NEW ENGLAND REGION, NEW SOUTH WALES

The accompanying catalogue of maps provides a coverage of the topography and drainage that existed prior to the Tertiary volcanic activity of the Central Province. Figure A1-1 shows the 25 map sheets used in the analysis. The interpretation of sheets 1 to 24 was carried out at the 1:25,000 scale, and sheet 25 (Guyra) at 1:100,000 scale. Geological maps, prepared by Stroud (1989), Willis (1989) and Brownlow (1989) were used as a base. Geological boundaries between Central Province volcanics and older basement rocks were overlain on the topographic sheets (New South Wales Government, Department of Lands). Elevations for each mapped boundary were plotted and then contoured. The interpretation used is conservative, that is to say, in areas of basalt cover the basement surface is interpreted to dip gently and smoothly underneath and the least amount of basalt cover was inferred in areas of poor control.

In order to improve the analysis, data from some 430 water bores (New South Wales Government, Department of Water Resources) were also plotted on the 1:25,000 and 1:100,000 sheets. The logs, tabled numerically for each map sheet, are included in Appendix 2. The logs are poorly described but serve to distinguish between basalt and basement rocks, or at least indicate a minimum depth of basalt in a given borehole. The bore data generally supported the basement topographic analysis and, in many cases, indicated that the basalt filled valleys are steeper and deeper than are given by the conservative analysis. After contouring the pre-volcanic topography for each 1:25,000 sheet, the information was reduced to 1:100,000 scale and linked to the surrounding sheets in order to interpret the pre-volcanic drainage. Palaeodrainages are shown as heavy black lines, which are dashed where the interpretation is less confident. It is important to note that the interpretation of the pre-volcanic drainage becomes more uncertain in areas of extensive basalt cover, especially where borehole information is sparse, or where different relative ground movements have occurred during and after volcanic activity. The full size plastic transparencies lodged with the New South Wales Government Department of Minerals and Energy, Armidale Branch (cnr Faulkner and Dumeresq streets, Armidale, N.S.W., 2350) should be used in conjunction with their equivalent topographic sheets (New South Wales Government, Department of Lands) and should be refined as more detailed geological boundary information and borehole data become available. The use of these maps in exploration for diamond and sapphire deposits in the New England region is discussed by Coenraads (1990).

The map sheets, as numbered in Figure A1-1, are described below:



Appendix 1

PRE-VOLCANIC TERTIARY LANDSCAPE AND DRAINAGE OF THE NEW ENGLAND REGION, NEW SOUTH WALES

The accompanying catalogue of maps provides a coverage of the topography and drainage that existed prior to the Tertiary volcanic activity of the Central Province. Figure A1-1 shows the 25 map sheets used in the analysis. The interpretation of sheets 1 to 24 was carried out at the 1:25,000 scale, and sheet 25 (Guyra) at 1:100,000 scale. Geological maps, prepared by Stroud (1989), Willis (1989) and Brownlow (1989) were used as a base. Geological boundaries between Central Province volcanics and older basement rocks were overlain on the topographic sheets (New South Wales Government, Department of Lands). Elevations for each mapped boundary were plotted and then contoured. The interpretation used is conservative, that is to say, in areas of basalt cover the basement surface is interpreted to dip gently and smoothly underneath and the least amount of basalt cover was inferred in areas of poor control.

In order to improve the analysis, data from some 430 water bores (New South Wales Government, Department of Water Resources) were also plotted on the 1:25,000 and 1:100,000 sheets. The logs, tabled numerically for each map sheet, are included in Appendix 2. The logs are poorly described but serve to distinguish between basalt and basement rocks, or at least indicate a minimum depth of basalt in a given borehole. The bore data generally supported the basement topographic analysis and, in many cases, indicated that the basalt filled valleys are steeper and deeper than are given by the conservative analysis. After contouring the pre-volcanic topography for each 1:25,000 sheet, the information was reduced to 1:100,000 scale and linked to the surrounding sheets in order to interpret the pre-volcanic drainage. Palaeodrainages are shown as heavy black lines, which are dashed where the interpretation is less confident. It is important to note that the interpretation of the pre-volcanic drainage becomes more uncertain in areas of extensive basalt cover, especially where borehole information is sparse, or where different relative ground movements have occurred during and after volcanic activity. The full size plastic transparencies lodged with the New South Wales Government Department of Minerals and Energy, Armidale Branch (cnr Faulkner and Dumeresq streets, Armidale, N.S.W., 2350) should be used in conjunction with their equivalent topographic sheets (New South Wales Government, Department of Lands) and should be refined as more detailed geological boundary information and borehole data become available. The use of these maps in exploration for diamond and sapphire deposits in the New England region is discussed by Coenraads (1990).

The map sheets, as numbered in Figure A1-1, are described below:

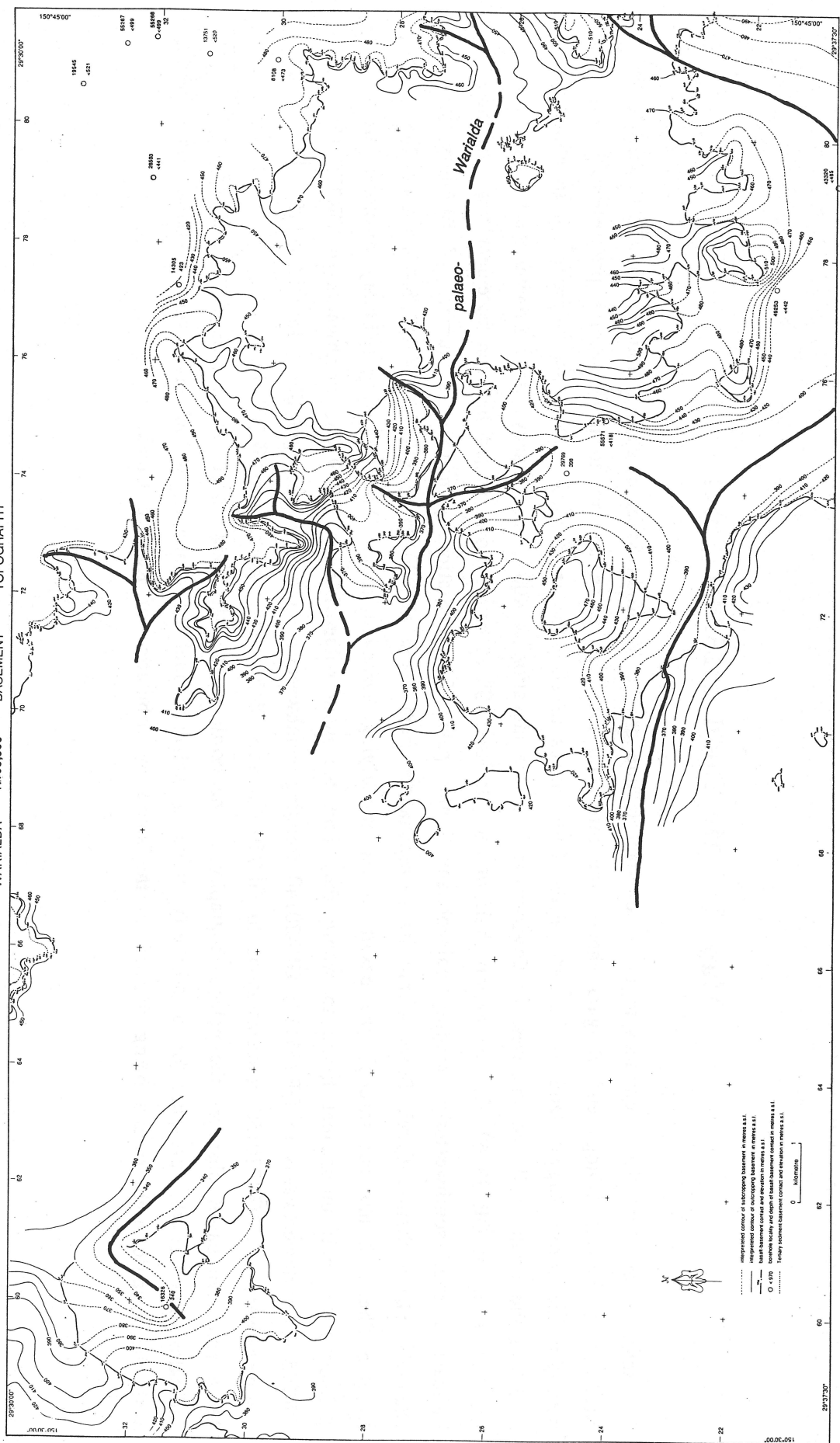
Map 1. Warialda 1:25,000 Sheet

The steep scarp of the Peel Fault, dominant on the Dinoga, Bingara and Mt Rodd Sheets, is no longer as evident. It trends north from the Mt Rodd Sheet at about GR625210 where the scarp is of the order of 100 m but this quickly reduces to zero. North of the township of Warialda the Peel Fault is no longer visible. Basalt flows on the eastern portion of the Warialda Sheet indicate the existence of two northwesterly trending palaeosystems. Only a small area of basalt is present on the western portion of the map lying in a palaeotopographic low. Water bore 16326 (GR599313) supports this interpretation.

The westerly trending palaeochannel described on the Delungra Sheet continues via the Mount Rodd sheet onto the southeastern edge of the Warialda Sheet, (GR755202), and northwest to GR700234, beyond which point it cannot be traced due to the absence of basalt. Waterbore 49253 (GR775215) supports the presence of this palaeochannel. Kellys Gully and its tributaries flow within these palaeovalleys.

The Warialda Creek palaeochannel trends westerly from the Cherry Tree Hill Sheet onto the Warialda Sheet at GR820267. It possibly continues from here to GR760270 although no basalt remains to support this suggestion. The presence of a palaeochannel is again supported by basalt from GR760270 to GR700290. Warialda Creek flows within its palaeovalley and has cut through the basalt to the underlying basement rocks along its entire length. The following tributary channels are defined from their up-channel limits to where they join the main palaeochannel; GR745250 northwestwards to GR737277; GR758280 southwestwards to GR748270; and GR740300 southwestwards to GR710285.

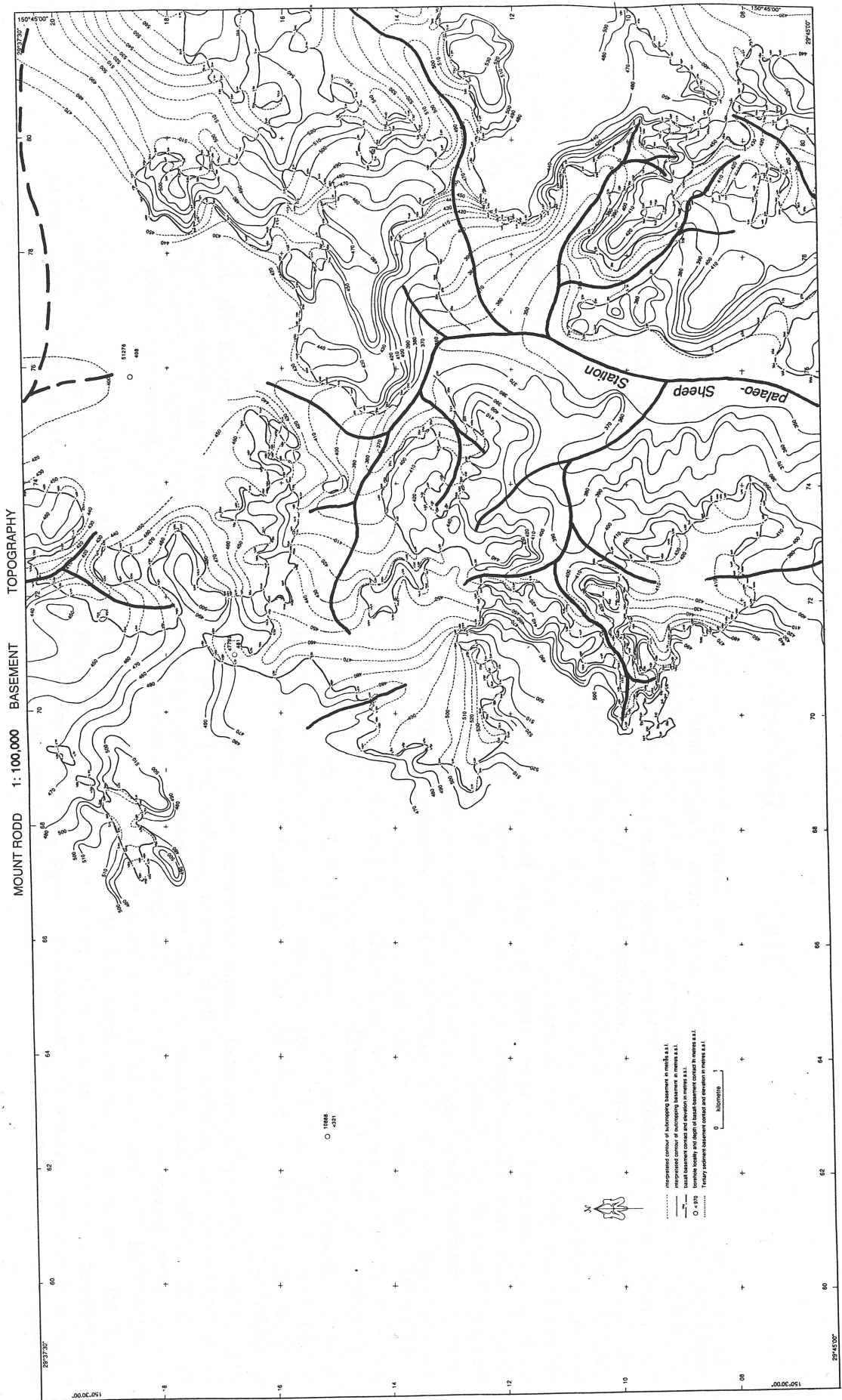
Extensive basalt cover obscures the palaeotopography to the northeast of the Warialda Sheet. Water bore 14305 (GR773317) indicates however that the basalt has filled a palaeotopographic depression.



Map 2. Mt Rodd 1:25,000 Sheet

The scarp of the Peel Fault continues to be a dominant feature on the Mt Rodd Sheet extending from GR630070 to GR630200 although, as on the Dinoga and Bingara sheets, the throw on the fault scarp appears to have become progressively less with distance north. Rugged land to the east of the fault ranges in elevation from about 600 m asl in the south to about 500 m asl in the north, while on the west or downthrown side the elevation is 400 m asl. Oakey Creek flowing west cuts across the Peel Fault at GR633162. On the eastern half of the Mt Rodd Sheet basalt flows nested between basement high ground, indicate a south-southwesterly trending palaeochannel, the palaeo-Sheep Station, joined by a number of tributary channels. Sheep Station Creek flows within its palaeochannel from about GR790105 to GR755070 and beyond onto the Bingara Sheet. It has cut through the basalt to the underlying basement rocks. The following tributary channels are defined from their up-channel limits to where they join the main palaeochannel; GR797082 northwards to GR775112; GR795095 northwestwards to GR765115; GR820140 trending southwesterly from the Delungra Sheet to GR765115; GR755160 southwestwards and GR710150 southeastwards to GR750145; and GR700100 eastwards to GR760095.

More extensive basalt obscures the palaeotopography to the north of the Mt Rodd Sheet. Water bore 51276 (GR759187) indicates however the presence of a northerly trending palaeochannel or channels. Relief inversion is taking place here with the basaltic high ground being drained to the south by tributaries of Reserve Creek.



Map 3. Bingara 1:25,000 Sheet

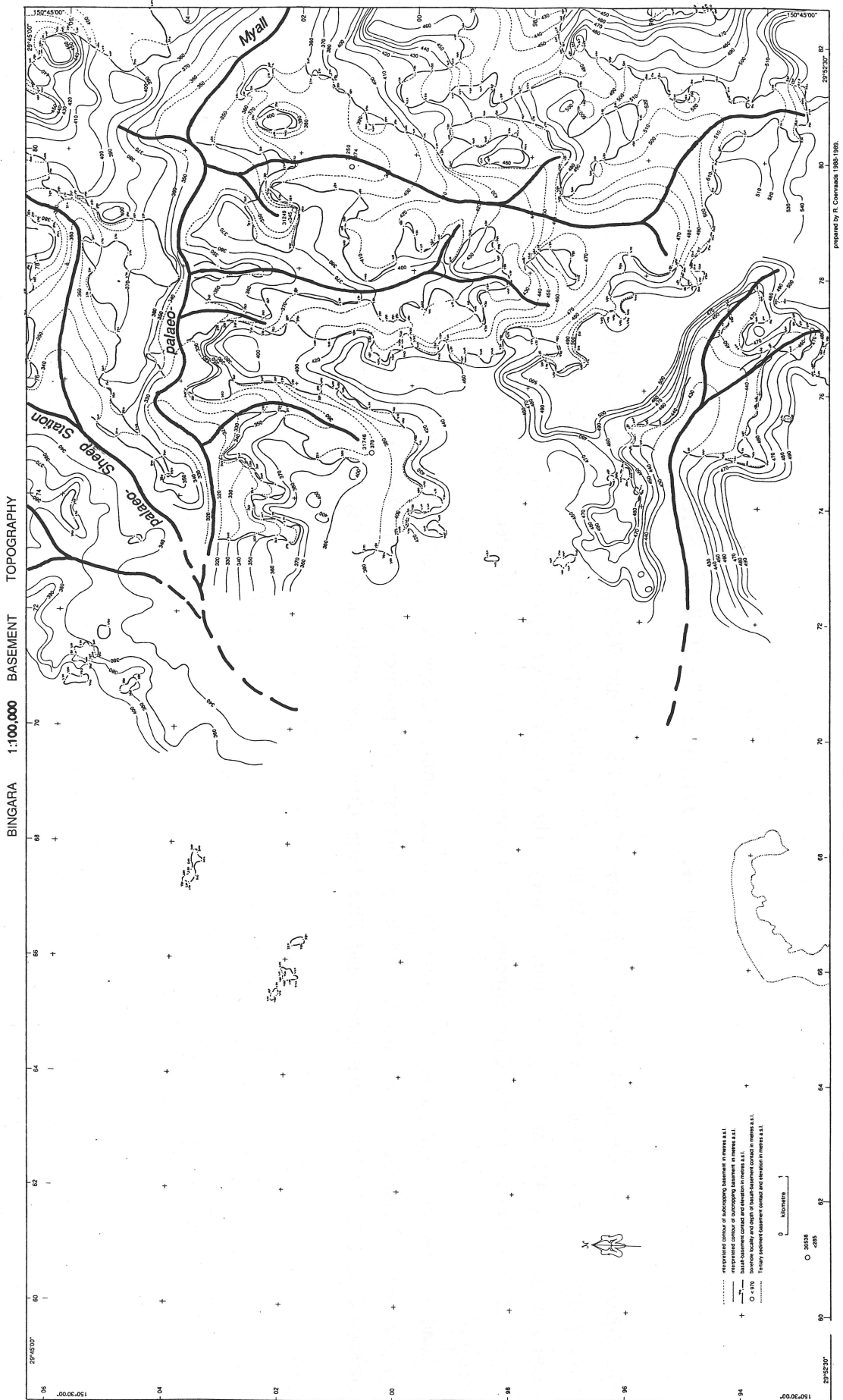
The steep scarp of the Peel Fault, as on the Dinoga Sheet, is a dominant feature on the Bingara Sheet extending from GR660930 near Bingara to GR630060 in the north. Rugged land to the east of the fault is at a general elevation of about 600 m asl, while on the west or downthrown side, the general elevation is 400m. The Gwydir River (GR660940), Whitlow Creek (GR650970), Myall Creek (GR640000) and Harts Creek (GR640023) cut across the Peel Fault and flow into the Stoddarts Valley. The Gwydir River is at a elevation of 290 m asl at this point whereas the adjacent land, Molroy Trig (GR668954), is up to 590 m asl implying some 300 m of downcutting.

On the western half of the Bingara Sheet basalt flows indicate a palaeodrainage system comprised of a westerly trending palaeochannel joined by a number of northerly trending palaeochannels and a southwesterly palaeosystem. The westerly trending palaeochannel continues from the Gum Flat Sheet (GR820025) and can be traced to about (GR730036). Myall Creek flows within this palaeochannel and has cut through the basalt into the underlying basement. The longest northerly trending basalt filled palaeochannel can be traced for about 10 kilometres from GR810935 to GR795030 where it joins the westerly trending Myall palaeochannel. The interpretation is supported by water bore 31250 (GR798011). The palaeochannel is cut by the westerly flowing Whitlow Creek (GR787962) and northwesterly flowing Horseshoe Creek (GR792990). Relief inversion has begun in places along the palaeochannel particularly noticeable at GR795995 where the basalt is at 440 m asl with the land surface falling off into the adjacent creeks. Two northerly flowing creeks, (GR792010 and GR805000), form twin laterals at this point. Another palaeochannel trends north from GR775975 to the Myall palaeochannel at GR780035, Horseshoe Creek flows within this channel and has cut through the basalt into the underlying Carboniferous meta-sedimentary basement. The third northerly trending palaeochannel is supported by water bore 31746 (GR748008) and joins the Myall palaeochannel at GR750035.

The Sheep Station palaeochannel trends southwest from the Mt Rodd sheet and probably joined the Myall palaeochannel approximately in the position of their present confluence (GR724039). A westerly trending tributary from GR791065 joins the Sheep Station palaeochannel at GR755060. Sheep Station Creek and the tributary creek flow within the palaeochannels at this point, however at GR791065 relief inversion has occurred with two southerly flowing tributaries (GR788065 and GR794065) of Rainbow Creek, forming twin laterals.

Basalt remnants in a valley at about 450 m asl (GR767945) surrounded by Late Devonian-Early Carboniferous metasediments up to 150 m higher in elevation indicates the existence of a westerly trending palaeochannel here.

Whitlow Creek cuts across the metasediment ridge at 450 m asl flowing west (GR772955) indicating that since the time westerly drainage was established downcutting of the order of 150 m has taken place.



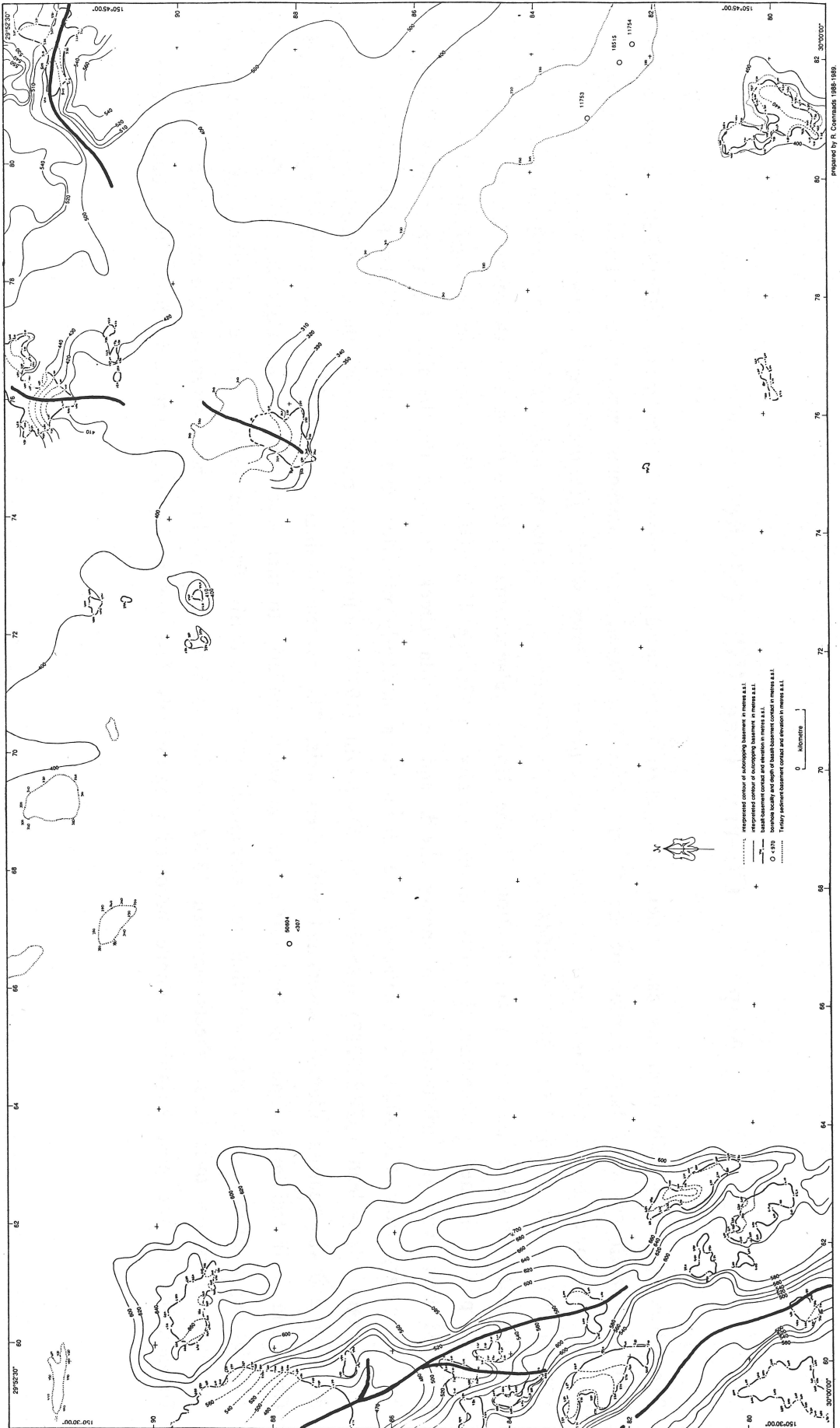
Map 4. Dinoga 1:25,000 Sheet

The Dinoga sheet is dominated by the steep scarp of the Peel Fault. Rugged land to the east of the fault ranges in elevation from 700 m asl in the south to 600 m asl in the north along Serpentine Ridge while on the west or downthrown side, the elevation is about 400 m asl in Stoddarts Valley. The Gwydir River flows northwest, crosscutting the resistant fault parallel ridges of late Devonian-early Carboniferous meta-sediments coming across the Peel Fault into Stoddarts Valley just north of Bingara.

Isolated pockets of basalt, now relief inverted, indicate former valleys at GR820920, GR760920 and GR755880.

To the west of the Peel Fault patches of basalt indicate the position of two northwesterly trending palaeochannels at GR600810 and GR600850. Pallal Creek and Five Mile Creek flow within these valleys.

DINOGA 1:100,000 BASEMENT TOPOGRAPHY



Prepared by R. Connors 1986-1988

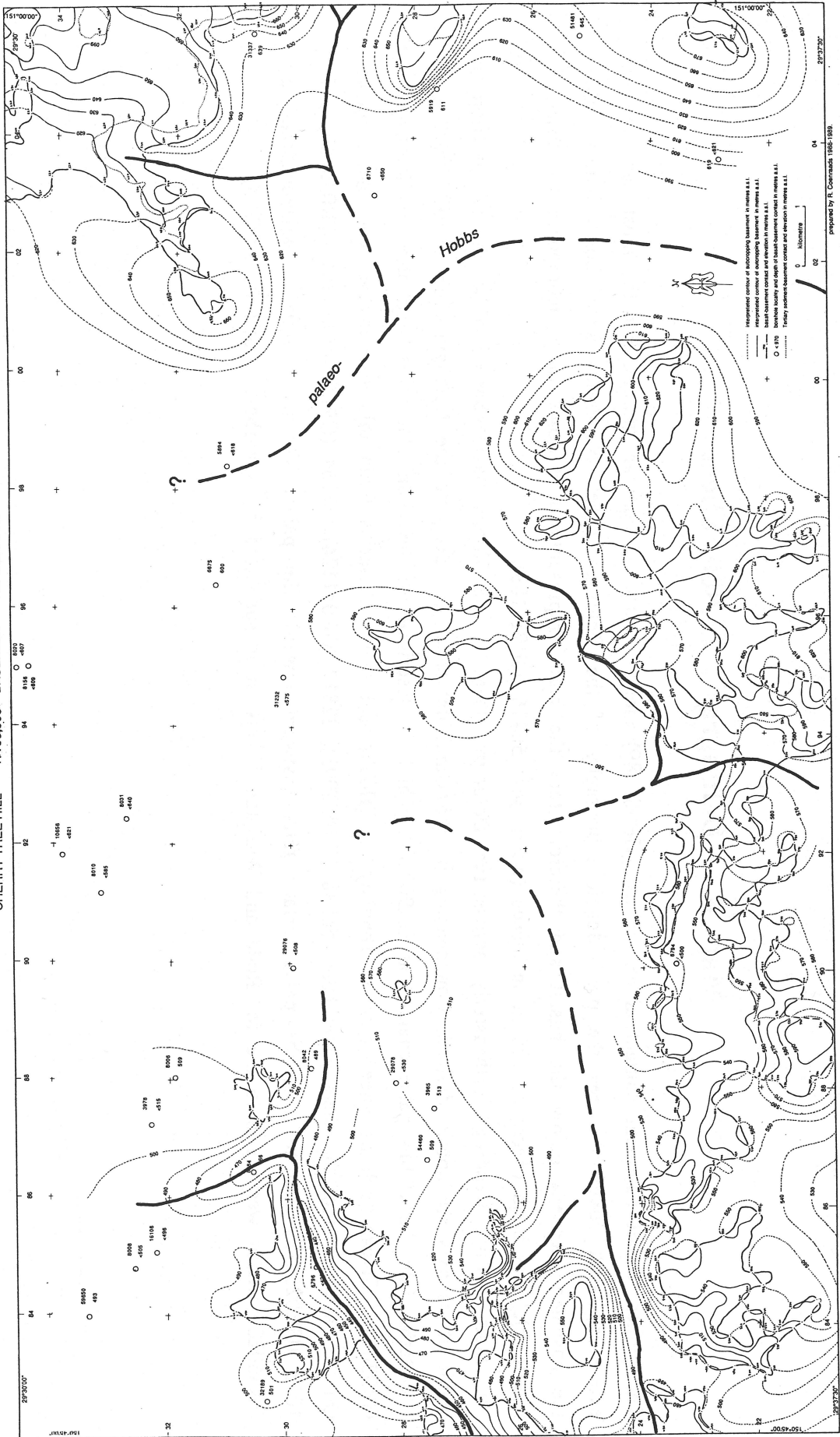
Map 5. Cherry Tree Hill 1:25,000 Sheet

The palaeotopography falls from the east, where the highest basalt basement contact is 670 m asl (GR060230), to the west. Although basalt covers a large portion of the Cherry Tree Hill Sheet, key waterbores support the interpretation that the basement is lower below the basalt and that the basalt represents flows within palaeotopographic lows. Water bores 619 (GR037229), 51481 (GR058252), 5919 (GR048276) and 6675 (GR964313) indicate the presence of a northerly trending palaeochannel which is possibly a continuation of the Hobbs palaeochannel described on the Delungra Sheet.

Another poorly defined palaeochannel exists in the vicinity of Gunnee Hill (GR923255). Some relief inversion has occurred here with the tributaries of Boundary Creek and Warialda Creek draining the basaltic topographic high. Joined by a tributary from GR930240 the palaeochannel trends in a northerly direction and possibly joins the palaeo-Hobbs.

The Gragin "deep lead" (GR820283) mentioned by MacNevin (1977) indicates the potential for these palaeochannels to have diamond and tin bearing alluvium associated with their axis. The present drainage, Black Creek, Boundary Creek, Warialda Creek and their tributaries drain the land surface to the west, similarly to that described for the Copeton Dam, Gum Flat and Delungra Sheets. It is proposed that the disruption of the northerly trending palaeodrainage and the establishment of the westerly system over these sheets occurred 18-22 Ma due to West Central Province volcanism and associated uplift. Downcutting by the post basaltic drainage becomes progressively less severe moving northwards from the Copeton area.

CHERRY TREE HILL 1:100,000 BASEMENT TOPOGRAPHY



prepared by R. Coenraads 1985-1989

Map 6. Delungra 1:25,000 Sheet

The highest basalt basement contact is 680 m asl (GR985089) along a ridge of Permian granite. For the most part however, extensive basalt cover obscures the pre volcanic topography of the Delungra Sheet. Numerous water bores indicate that the basement deepens below the basalt and therefore that the basalt represents lava flows in palaeotopographic lows. Basalt thickness is in excess of 125 m in places (water bore 56416, GR916183).

The main feature trending northeasterly across the Delungra Sheet is the Hobbs palaeochannel although the position and depth of its axis are poorly defined. Commencing on the Gum Flat sheet, it runs onto the Delungra sheet at GR850070. Tributaries join the Hobbs palaeochannel at GR900100 (which is described on the Gum Flat sheet) and also at GR950180 and GR930140. Creeks such as Sheep Station, Dumboy and Hobbs and their tributaries drain this area to the west and southwest.

On the eastern end of the sheet water bores 56938 (GR053093), 32817 (GR041124), 57764 (GR057166), 1106 (GR030169) and 1073 (GR025189) indicate that the palaeosurface falls eastward towards the palaeo-Macintyre. Another palaeochannel at GR860200 trends westerly onto the Mt Rodd and Warialda Sheets. It is supported by waterbore 10082 (GR880203)



Map 7. Gum Flat 1:25,000 Sheet

The highest observed basalt basement contact is 750 m asl at GR035980, on the eastern end of the sheet. The palaeosurface falls to the west where at GR840020 it is 370 m asl. Three major palaeorivers once traversed the Gum Flat Sheet from south to north as evidenced by ribbons of basalt lying between basement highs.

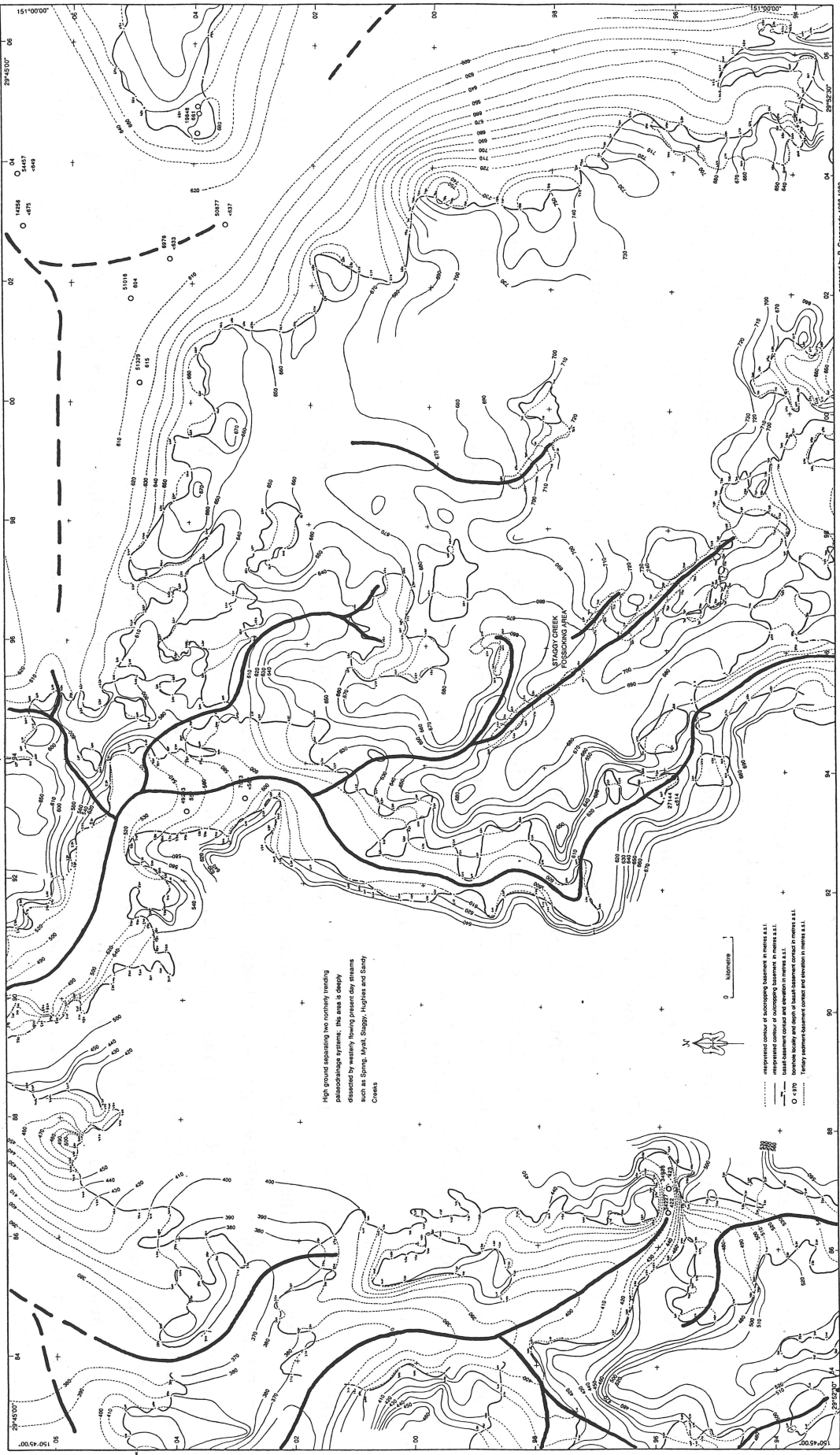
The palaeo-Gwydir (GR068960) has been described on the Inverell sheet. Extensive volcanic cover obscures the fall of the palaeotopography into this palaeovalley.

Easterly trending tributaries (GR020060) of the palaeo-Macintyre are also obscured by volcanics. Water bores 51329 (GR003048), 51016 (GR017050) and 50877 (GR030035) indicate a fall in the elevation of the palaeosurface below the volcanic blanket, although the positions of the palaeoaxes are not clear.

The next major palaeochannel to the west begins on the Copeton Dam Sheet trending north from GR960943 to GR902069 and then onto the Delungra Sheet where it joins the northeasterly trending Hobbs palaeochannel. Water bores 27144 (GR939958), 7073 (GR934030) and 49293 (GR932039) have been drilled into the basalt filling this palaeovalley. The Wonderland (GR969954) and Staggy Creek (GR955975) mining areas are located on a northwesterly trending tributary of the above-mentioned palaeochannel. The Wonderland lead consists of two isolated patches of basalt capped alluvium and the Staggy Creek lead forms part of a system marked by patches of gravel. The streams flowed from the vicinity of Emu Hills (GR970965) to the NW, then along the present course of Staggy Creek, joining the main palaeochannel approximately where Staggy Creek crosses it (GR930015). It is possible that the main palaeochannel also contains diamond and tin-bearing deep lead alluvium, although there has been no attempt to exploit these as yet and this is probably due to the fact that this palaeochannel has not been previously recognized as such. "Deep lead" alluvium has not been seen north of the Staggy Creek crossing due to the thickness of the basalt cover. This system is now entirely disrupted by a number of westerly flowing creeks. Sandy creek, Staggy Creek and Myall Creek flow west and cut the palaeochannel at GR918973, GR930015 and GR922055 respectively and then pass into its steep western valley wall composed of resistant early carboniferous volcanic lithic greywacke. Assuming that the original height of the land surface on which the westerly flowing streams were set up was at least as high as the greywacke ridge through which they are now cut, then there has been at least 90 m of downcutting (0.005 mm/year since 18 Ma). The streams have not yet cut through the basalt flows lying within the palaeovalley. The westernmost palaeosystem is comprised of two tributaries (GR830970 and GR860962) meeting at GR845985 and trending northwest to GR826023. Pockets of basalt mark its position and Kangaroo and Ironbark Creeks flow within the palaeovalley for the majority of their length. Relief inversion has occurred of the uppermost portion of the tributaries on this sheet and the Copeton Dam sheet. In the vicinity of Leaderville (GR867949), tributaries of Ironbark Creek and Daffey's Creek flank the palaeochannel, now a basalt ridge. Water bores 34227 (GR866958) and 34936 (GR870958) support this concept and indicate the presence of a palaeochannel beneath the basalt ridge at "Caroline". Tributaries of Kangaroo Creek form twin laterals to the palaeochannel (now a basalt ridge) at GR834934. On the northwestern corner of the Gum Flat sheet (GR840060) the Hobbs palaeochannel trends in a northeasterly direction onto the Delungra sheet. Hobbs Creek flows in a southwesterly (reversed) direction within this palaeovalley.

The presence of a formerly northerly trending palaeodrainage direction cross cut by a now predominantly westerly flowing network is particularly well displayed on this sheet. It is proposed that the disruption of the old system and establishment of the new, occurred 18-22 Ma due to West Central Province volcanism and/or associated uplift.

GUM FLAT 1:100,000 BASEMENT TOPOGRAPHY



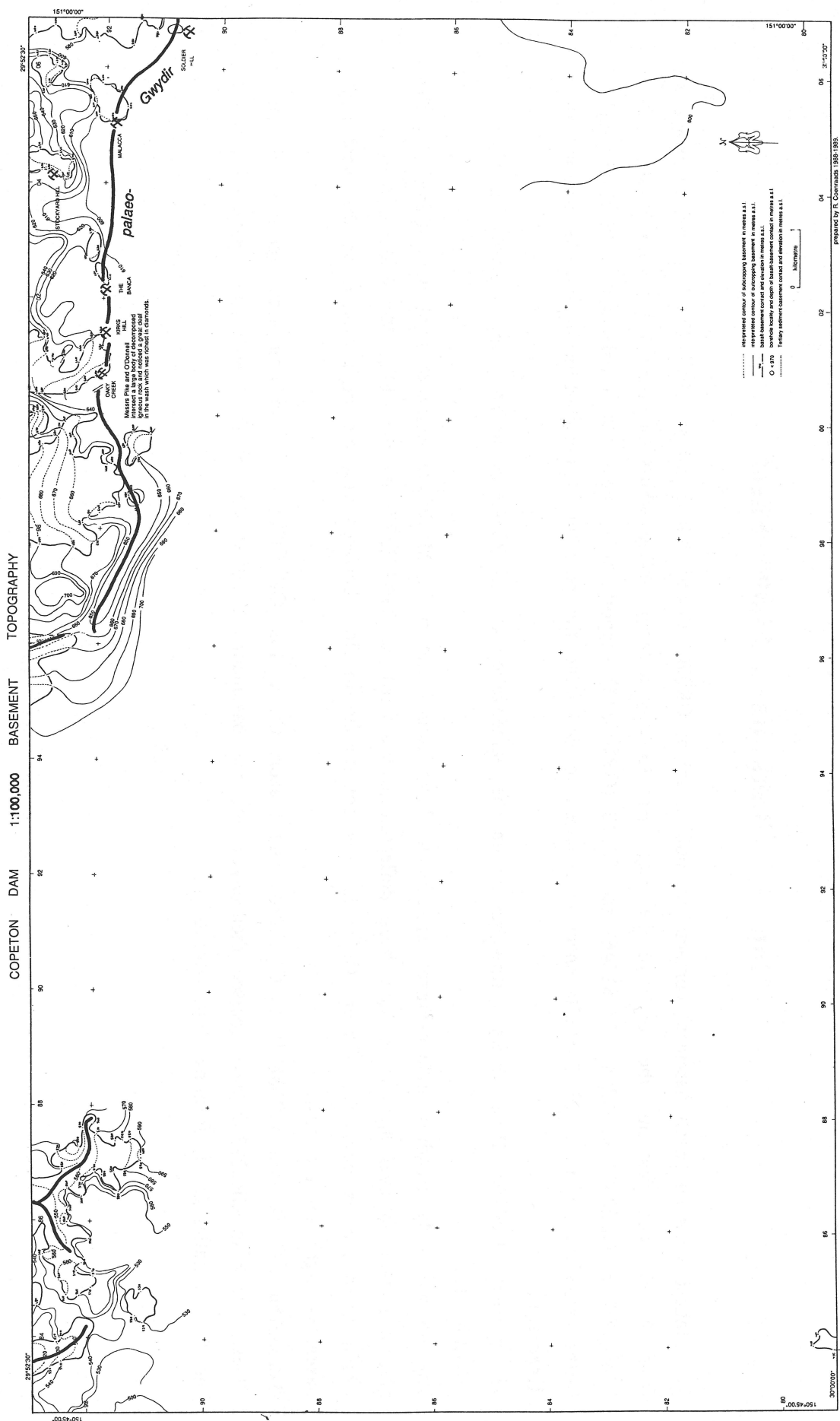
Map 8. Copeton Dam 1:25,000 Sheet

Only a few isolated areas of basalt remain on the Copeton Sheet. A palaeochannel of historic significance, the palaeo-Gwydir, has been extremely well defined by the presence of diamond bearing alluvium along the length of its palaeoaxis. Where pods of this material remain, as "deep leads" protected by basalt caps, they have been extensively mined for diamond and tin (MacNevin, 1977). The palaeo-Gwydir trends east from a divide at GR962922, 650 m asl and joins the northern flowing tributary at Crown Jewel Hill on the Tingha Sheet. Old workings indicate the exact position and elevation of the palaeoaxis; from the west Oaky Creek (GR007920), Kirks Hill (GR014920), The Banca (GR021920) and Stockyard Hill (GR041929) are at 620 m asl, Malacca (GR052918) is at 620 m asl and Soldier Hill (GR067906) is at 590 m asl.

The fall of this important palaeochannel to the east was originally verified by Cotton (1914) who made numerous aneroid elevation readings of deep leads. The Staggy Creek and Wonderland diamond bearing leads on the Gum Flat 1:25,000 sheet form part of a NNW trending tributary of the Hobbs palaeochannel and are not part of the same system as the above-mentioned leads which occur at a lower elevation in the vicinity of Copeton Dam. They must come from a separate source, as was first suggested by Stonier (1895). Another palaeochannel trends northwest onto the Gum Flat sheet from the divide at GR962922.

On the northwest corner of the Copeton Dam sheet remnant tongues of basalt, now relief inverted, indicate the presence of northerly trending palaeochannels at GR837926 and GR865927.

The present day Gwydir River flows west, having been deflected from its originally northerly trending channel (described on the Inverell Sheet) by basalt from a source west of Inverell. At the base of Copeton Dam the Gwydir River is at 471 m asl, indicating some 180 m of downcutting since the original, easterly flowing tributary through the mining areas was displaced, probably 18-22 Ma. That represents a rate of downcutting of some 0.01 mm/year. The westerly flowing Sandy, Hughies, Staggy, Myall and Spring creeks on the Gum Flat 1:25,000 sheet also show evidence of downcutting of the order of 100 m.



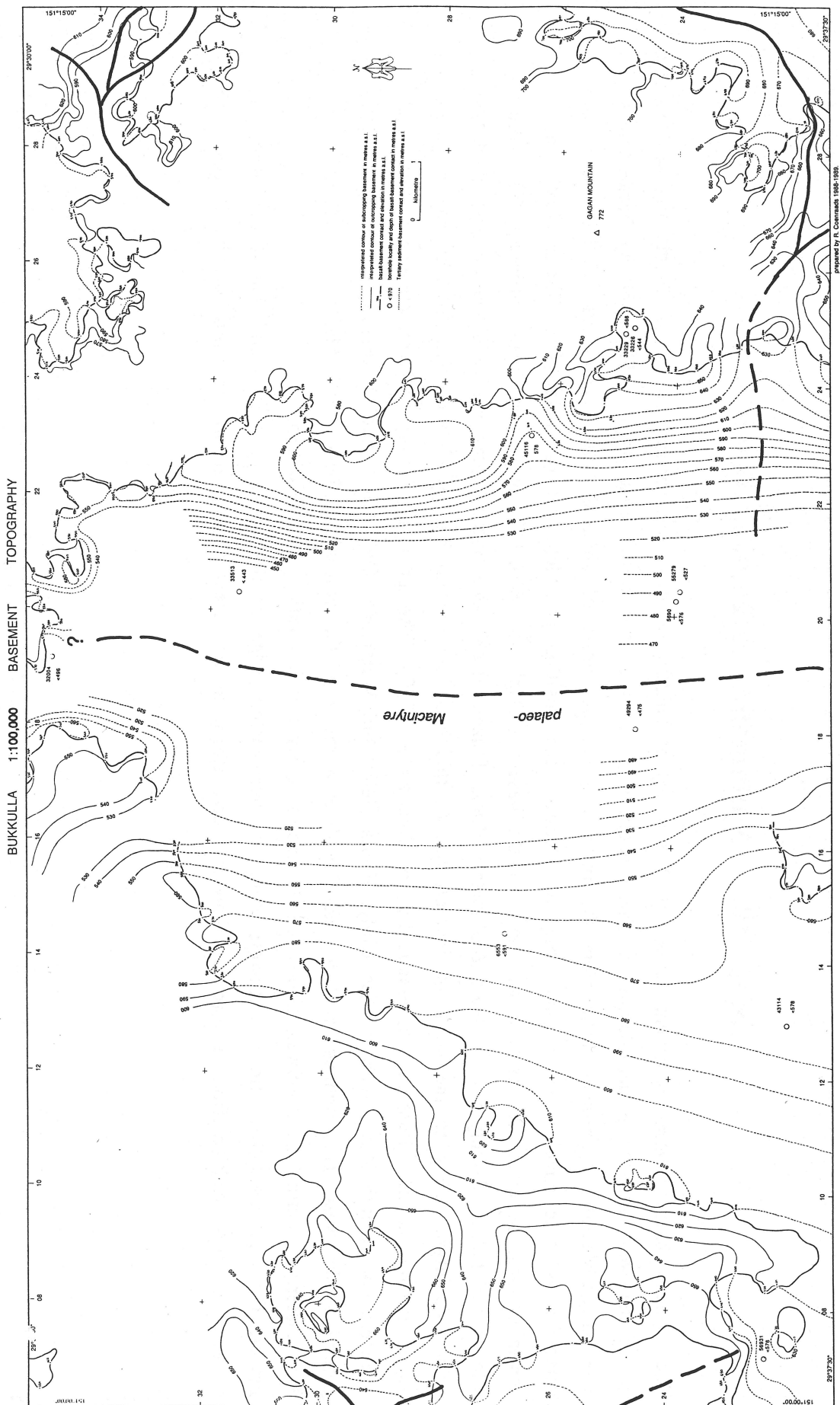
Map 9. Bukkulla 1:25,000 Sheet

The highest observed basalt basement contacts are 660 m asl at GR070270 and 700 m asl at GR293240. The palaeosurface dips from the east and west into the centre of the map sheet forming a broad valley which has been filled with basalt. Water bores 55279 (GR204249), 49294 (GR181246) and 33513 (GR203315) support the existence of a palaeovalley here, although further work to the north of Bukkulla sheet is required to determine the position of the palaeoaxis and the original flow direction.

The present Macintyre River flows northwards within the palaeovalley to GR170319 at which point it swings to the northwest.

The northwesterly trending palaeo-Frazer appears to have joined the main Macintyre palaeochannel at (GR245225), the present stream however appears to have been deflected to the north at (GR253227) by the 18-22 Ma volcanic activity which filled the palaeovalleys. Frazers Creek is now constrained to flow between volcanic high ground on the west and basement highs on the east.

Bannockburn Creek from GR088215 to GR129301 and Frazers Creek from GR253228 to its junction with Weean Creek and Weean Creek to GR222352 have incised themselves into the basement on either side of the basalt filled palaeo-Macintyre and flow parallel to it, forming twin laterals.



Map 10. Nullamanna 1:25,000 Sheet

The highest observed basalt basement contact is 720 m asl at GR303145, the palaeosurface falling off sharply (by at least 200 m) to the west into the palaeo-Macintyre. The western two thirds of the Nullamanna sheet is blanketed by basalt flows.

The palaeo-Macintyre continues north from the Inverell sheet, but north of about GR170100 the lack of deep bores and extensive volcanic cover make it impossible to determine the position and depth of the palaeoaxis. The channel may continue north on either the east or west side of the basement high at GR175140) or it may head northwest. The volcanic pile in the palaeo-Macintyre is at least 200 metres thick. Frazers Creek and Byron Creek are twin laterals and flank the palaeo-Macintyre valley to the north of Inverell but in this case the present day Macintyre still flows in the original basalt filled channel, illustrated schematically in Coenraads (1990). The present Macintyre River meanders north and Spencers Gully, Rob Roy Creek, Jessies Gully, Hunts Gully and Waterfords Gully flow into it, draining the volcanic high ground to the west. This drainage probably developed as a result of the volcanic activity 18-22 Ma.

The easterly trending palaeo-Swan Brook enters the Macintyre palaeovalley at GR205085.

Frazers Creek at GR280200 flows northwest along the northeastern edge of the basalt pile. It seems that it has been deflected to this position from a formerly more westerly trend, as has clearly occurred to the north on the Bukkulla sheet.



Map 11. Inverell 1:25,000 Sheet

The palaeosurface falls away from the south where the highest exposed basalt-basement is at 800 m asl (GR148938) and also from the west and east towards the centre and north of the sheet where, in the vicinity of Inverell water bore 2524 (GR191047) indicates basement to be deeper than 447 m asl. A network of palaeodrainage joins in the vicinity of Inverell and heads north. The palaeo-Macintyre heads west from the Elsmore Sheet marked by a low ridge of basalt hills (GR288030) & (GR260065). The presence of a valley here is supported by water bore 61426 (GR284061) and numerous bores in the vicinity of Inverell. The palaeo-Gwydir heads north from the Tingha Sheet at (GR075945) then most likely swings northeast towards Inverell. The exact position of the palaeoaxis is unclear due to the extensive volcanic blanket here which the water bores indicate to be of the order of 100 m thick. The "severing" of the northwesterly trending palaeo-Gwydir by basalt flows approximately 18-22 million years ago was first described by Cotton (1914). Observations of flow indicators in the basalts by Smith (1988) indicate that the lavas flowed from north to south in this palaeovalley. Today Cooks Creek (GR080010), Fern Creek (GR100020) and Auburn Vale Creek (GR110990) flow in a southerly (reversed) direction within the basalt filled channel towards Copes Creek and the Gwydir River.

To the north east of the present basalt water divide, Spring Creek (GR1600300) and its tributaries flow in a northeasterly direction into the Macintyre River.

The northerly trending Sheep Station palaeochannel also joins the palaeo-Macintyre and palaeo-Gwydir in the vicinity of Inverell (GR170010). It is marked by tongues of basalt and is possibly the northerly continuation of the palaeochannel at Inverell Airport described on the Tingha Sheet. Basalt flows mark two tributaries to the palaeo-Sheep Station at (GR163980) and at (GR160949). Water bores 53277 (GR160947) and 29028 (GR157944) help constrain the position and depth of the palaeoaxis of the second tributary. Sheep Station Creek flows within the palaeovalley until (GR171000) at which point it turns eastwards to Middle Creek. At Gilgai (GR180960) Gilgai Creek, flowing northeasterly, cuts through the palaeochannel and is now at a level 20 m deeper than the palaeochannel axis (which is 750 m asl at this position).

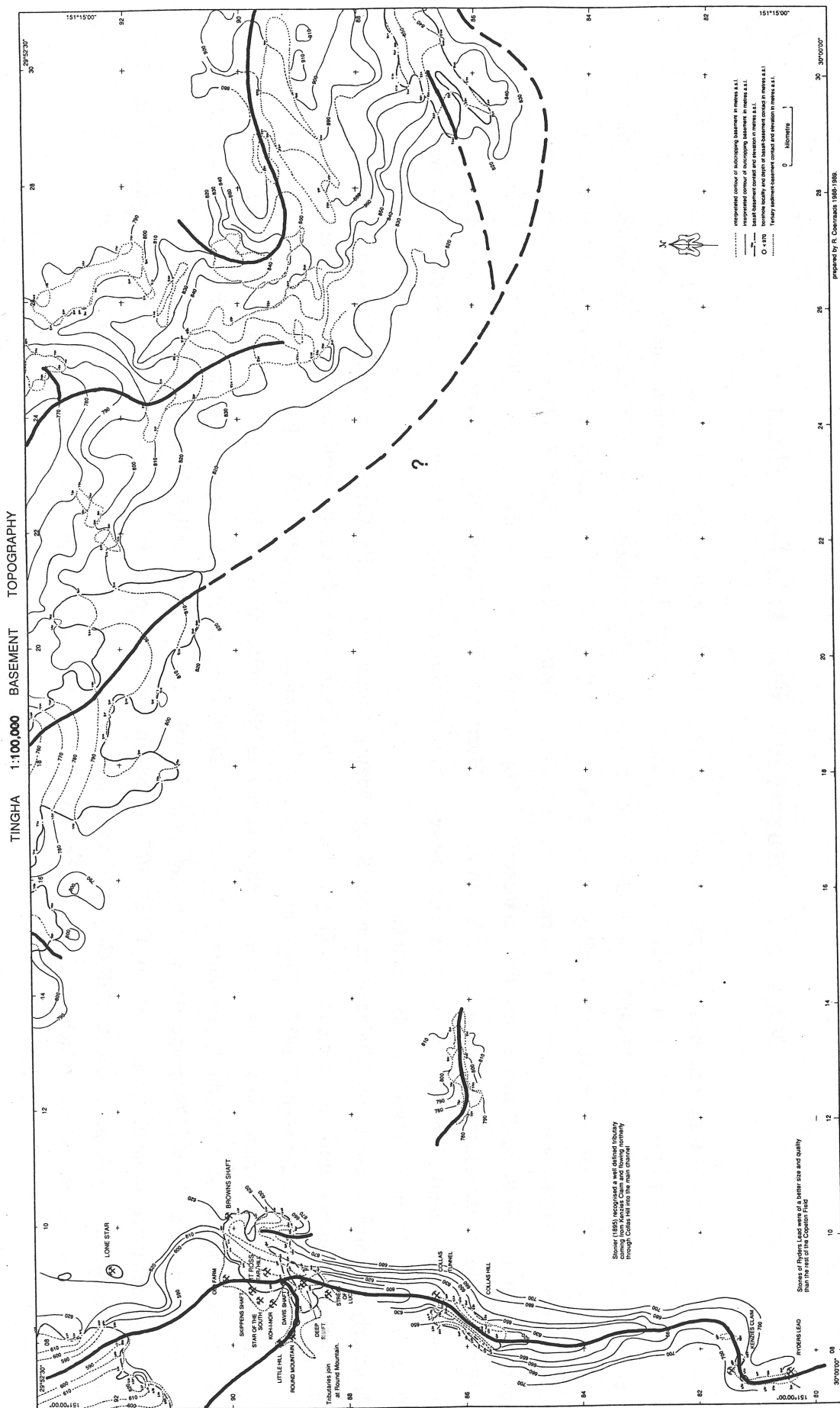


Map 12. Tingha 1:25,000 Sheet

The palaeosurface falls from the east where Tertiary alluvium is found overlying basement at 900 m asl (GR305895) to 580 m asl in the west (GR083920). The well defined northerly trending palaeochannel, the palaeo-Gwydir on the western edge of the Tingha sheet was first recognized by Stonier (1895). Remnant patches of valley flow basalt protect diamond bearing Tertiary alluvium in the palaeochannel and the old diamond mines mark the exact position of the palaeoaxis. Some of these are Ryders Lead (GR076804), Kenzies Claim (GR074813), Collas Tunnel (GR088865) and Streak of Luck (GR090884), they are described in detail by MacNevin (1977). Maids Creek flows in the palaeovalley to (GR079856) at which point it leaves and forms a lateral on the west side of Collas Hill.

Another palaeochannel from the west joins in the vicinity of Crown Jewel Hill (GR088888).

On the high ground to the northeast of the Tingha sheet, patches of basalt such as that at Inverell Airport (GR210910) and Tertiary Alluvium such as that at GR250900 and GR290890 indicate the presence of former, generally northwesterly trending channels. It is possible that the major westerly flowing palaeochannel on the Indiana Sheet which comes onto the Tingha Sheet at GR310863 and the palaeochannel at Inverell Airport (GR200920) are part of the same system. However, all evidence that may have supported this, has been removed by Copes Creek. Copes Creek and Middle Creek flank the high ground on the southwest and northeast respectively and their small tributaries drain this area. Their positions on either side of, and parallel with the palaeochannel suggest that they may be lateral streams.



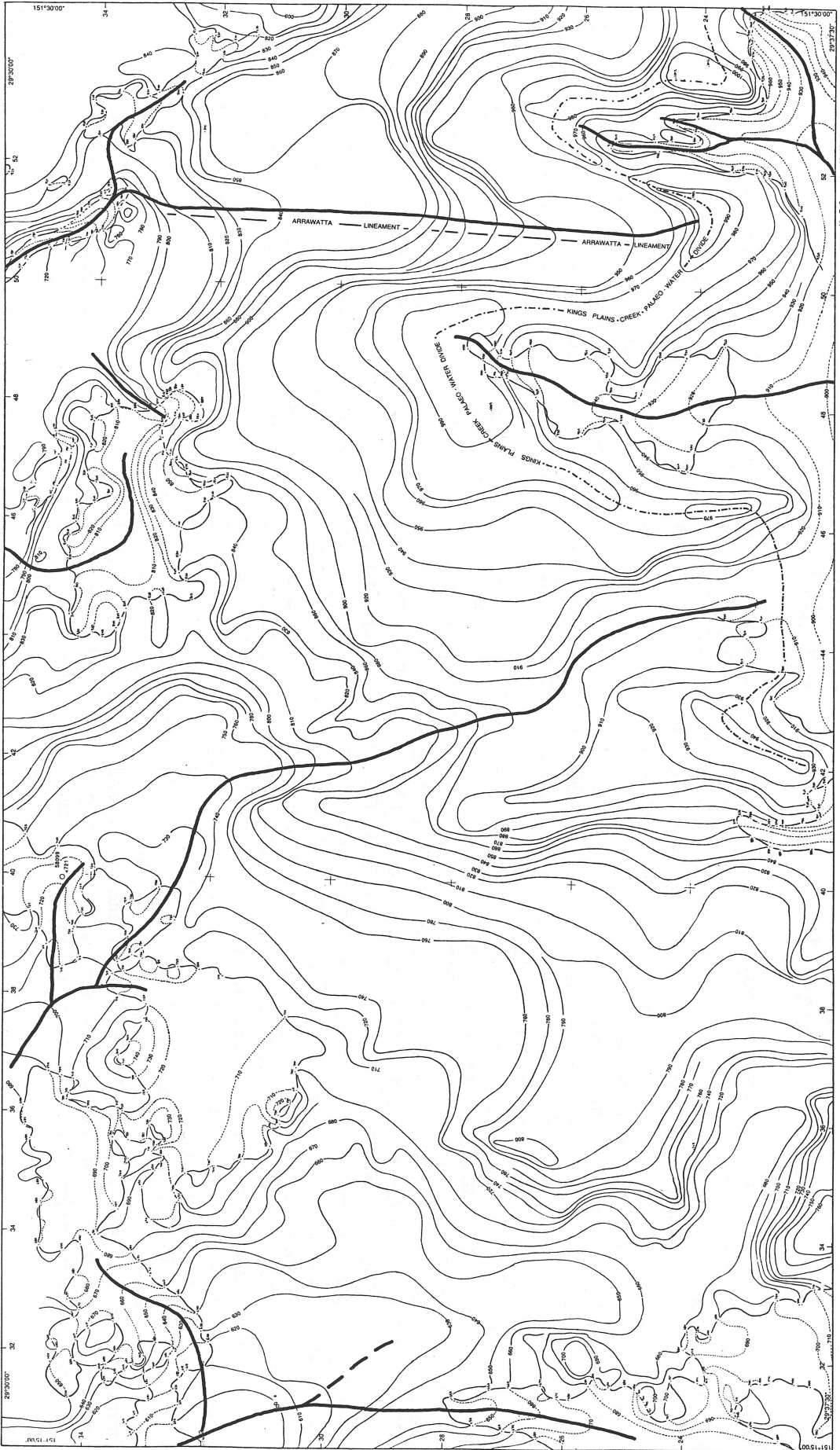
Map 13. Hurricane Hill 1:25,000 Sheet

The highest observed basalt basement contact on this sheet is seen at the very northern edge of Kings Plains (GR490279) 990 m asl. The Hurricane Hill sheet covers the northern edge of Kings Plains. Two southern trending basalt filled palaeochannels can be seen at GR480250 and GR525235 which join the westerly trending Kings Plains System on the Sapphire sheet. The westernmost palaeovalley contains a present day stream, the easternmost however is starting to show some relief inversion with Stoney Creek located on the basalt-basement contact (GR528240) and downcutting at this position. To the north of Kings Plains the palaeosurface drops rapidly to a level of about 800-850 m asl as indicated by the height of the basalt-basement contact in the vicinity of Hurricane Hill (GR474334). A northwesterly flowing palaeochannel is marked by the basalt here and the elevation of Hurricane Hill, 942 m asl, indicates that there would have been at least 130 m of basalt in this channel.

Northerly trending present day drainage such as Kings Plains Creek, Five Mile Creek, Arrawatta Creek and Stoney Creek are actively cutting into the plateau of Kings Plains by headward retreat along north-south trending lineaments or planes of weakness (Coenraads, 1988). The best example is Arrawatta Creek (GR510290). Kings Plains Creek flows within its basalt filled palaeochannel until it is captured and diverted to the north at (GR456220). At (GR310260) a tongue of basalt marks the position of a northerly trending palaeochannel. Tributaries of Weean Creek flank the basalt to the east and west at GR320270 and GR307270 respectively, forming twin laterals and creating relief inversion.

The palaeochannel probably continued to GR306325 at which point it joins with a south-westerly trending channel and heads northwest. Mordington Creek (GR330320) flanks the southwesterly trending channel for a few kilometres as a lateral; it joins Weean Creek which cuts across the main palaeochannel at GR308310.

HURRICANE HILL 1:100,000 BASEMENT TOPOGRAPHY



Map 14. Sapphire 1:25,000 Sheet

The highest observed basalt basement contact is on Kings Plains, 980 m asl at GR540192. Kings Plains is a elevated, large, relatively flat area, largely covered by volcanics occupying the eastern portion of the sapphire 1:25,000 sheet. The basement beneath Kings Plains is also elevated being all over 850 m asl with a significant proportion over 900 m asl. The highest point is Mt Buckley, 1168 m asl on the southern edge of Kings Plains (GR548078; Elsmore 1:25,000). Mt Buckley is comprised of basalt flows implying that the volcanic pile may have been in excess of 200 metres here. The palaeosurface falls sharply to the west and to the south into the palaeo-Swan Brook, that is of the order of 200 metres over a few kilometres. This observation and also the observation that the southern and western boundary of Kings Plains are relatively straight may lead one to speculate that Kings Plains is a fault bounded, raised, basement block. In any case, the presence of basalt at all elevations on the escarpment indicates that the Kings Plains was a basement topographic high prior to the finish of Central Province volcanism.

The Sapphire Sheet is dominated by the westerly flowing Kings Plains-Frazers Creek palaeosystem. The presence and location of the Kings Plains palaeovalley is quite accurately pinpointed with the aid of water bores 32244 (GR544135), 32241 (GR525134), 32239 (GR535138), 31273 (GR497177), 31272 (GR507209) and 51436 (GR486201); exploration test holes by T.J.& P.V.Nunan Pty.Ltd., NA1 (GR49951600), NA2 (GR49891600), NA3 (GR49831602) and NA4 (GR49771605); test holes by Dept of Mineral Resources (Lishmund 1987) KP1 (GR48392064) and KP2 (GR48202086) and test holes by Jingellic Minerals N.L. (Coenraads, 1989) KP3 (GR48482058) and KP4 (GR48392074). The Kings Plains Eastern and Western Feeder palaeochannels join at GR507177, the channel continues northwards, turning sharply west at GR510210 then south-westwards to join the palaeo-Frazer at GR420170. Kings Plains Creek flows within its palaeovalley, although, in places it has become localized by the basalt basement contact on the northern side of the basalt filled valley. It follows the contact as a lateral stream to the palaeovalley for approximately 4 kilometres westerly until it is captured (at GR456220) and diverted northwards into a steep narrow valley formed by headward erosion controlled by a prominent north-south lineament. Arrawatta Creek, actively eroding headwards along another north-south lineament, has not yet captured Kings Plains Creek. Economic quantities of sapphire have been recovered from the Kings Plains System.

Another palaeotributary rising at GR455125 heads west through Whites Hill (GR432121) and joins the palaeo-Frazer at GR385143. Relief inversion can be seen in the headwaters of this tributary with Horse Gully and Mary Anne Creek forming twin laterals flanking White Hill to the north and south respectively. Economic quantity of sapphires have also been recovered from these creeks downstream from the point at which their valleys widen and their gradients drop.

The palaeo-Weean heads northward from GR369207. Weean Creek flows within its palaeochannel at this point.



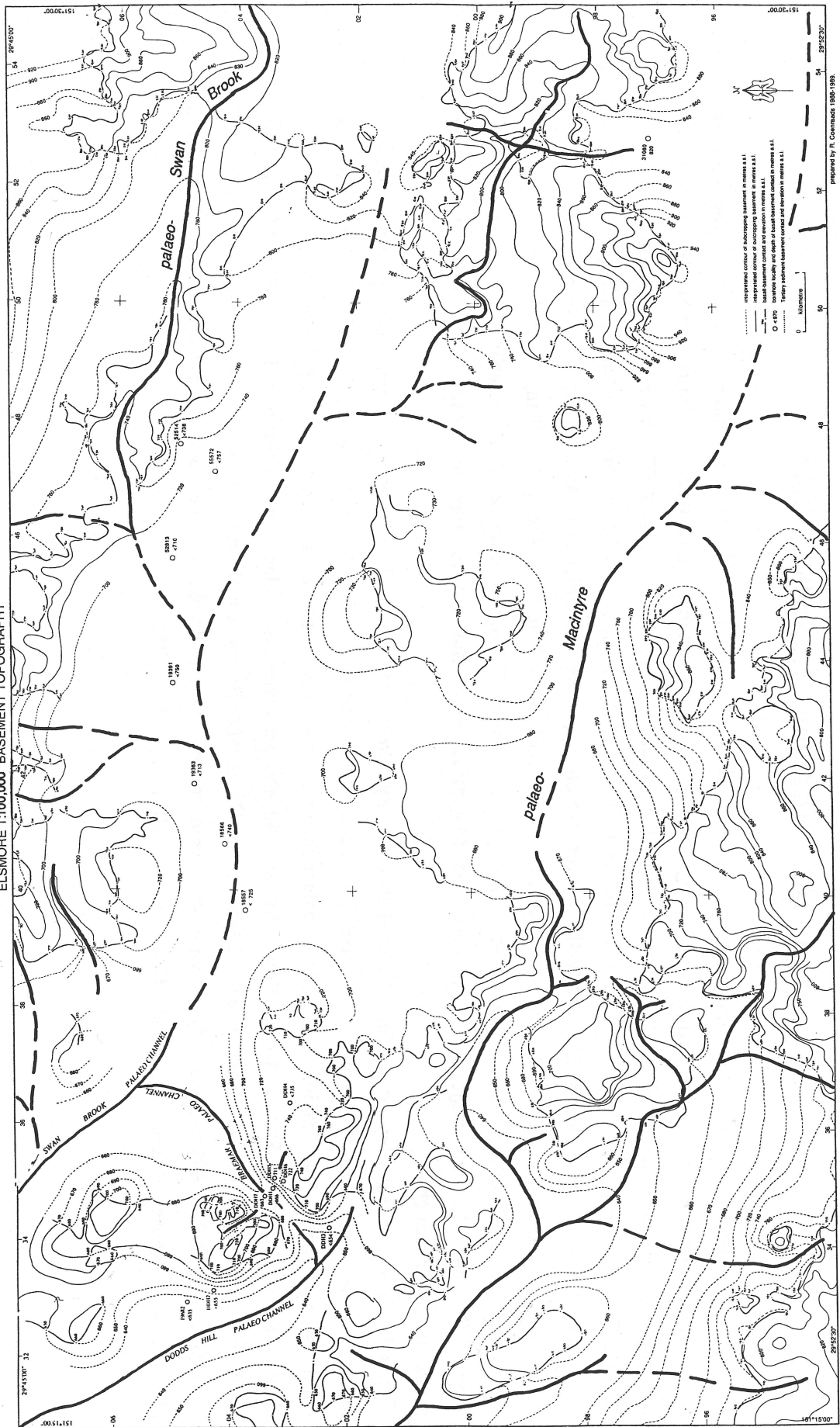
Map 15. Elsmore 1:25,000 Sheet

The maximum height of the basalt basement contact is 920 m asl at GR540967 and GR547063. The palaeotopography falls into two major channels trending west. The palaeo-Swan Brook and the palaeo-Macintyre (Kings Creek).

The palaeo-Swan rises on the Stonehenge Sheet, then heads westward onto the Elsmore Sheet at GR549040. It joins the main channel in the vicinity of Kerosene Hill (GR430040). The main channel is completely relief inverted standing out as a west northwesterly trending ridge of flat topped or slightly concave upwards hills including Table Top Hill (GR492022), Kerosene Hill and Langari Hill (GR361059). Wet Gully and Swan Brook to GR380068 and Kings Creek to about GR410010 are twin laterals, flanking the palaeo-Swan. Swan Brook downstream from GR380068 and Kings Creek from GR400986 return to their respective palaeovalleys which are no longer relief inverted.

In the vicinity of Braemar (GR348033) the basalt basement contact outcrops at a maximum of 750 m asl. The basement high ground forms a northwesterly trending ridge of height 760 m asl at GR360023, 722 m asl at GR338040 and 719 m asl at GR344062. The ridge separates the palaeo-Swan from a basalt filled tributary of the palaeo-Swan at GR320050. The fall of the palaeosurface into this tributary is supported by water bore 19682 at GR329047.

The Braemar sapphire deposit is situated in a saddle in the basement ridge marking the presence of a small basalt filled palaeochannel trending northeast into the palaeo-Swan. The palaeochannel is well defined here by Department of Minerals and Energy diamond drill holes 1, 4, 5, 6 and 7 (Brown and Pecover, 1986). The other major palaeochannel rising on the Maybole and Indiana Sheets is also marked by a prominent ridge of high ground including Carters Mountain (GR539953) and Eaglehawk Mountain (GR508950). The fall of the palaeosurface beneath this ridge is supported by waterbore 31080 (GR539971). Kings Creek to GR410010 and Paradise Creek to GR450940 are twin laterals flanking the ridge to the north and south respectively.



Map 16. Indiana 1:25,000 Sheet

The maximum height of the basalt-basement contact is 1130 m asl at GR518820 in the southeast corner of the Indiana Sheet. The height of the palaeosurface falls progressively to the northwest. Extensive volcanics cover the eastern side of the sheet (adjoining the Maybole Sheet) obscuring the palaeotopography in this area. However waterbore 31076 (GR515920) indicates that the height of the basement is lower by at least 30-90 m than the surrounding basement outcrops. The exact trend of this palaeovalley or valleys over which the volcanics are situated is not clear, however channels probably head north on either side of the basement high (GR492932) joining the palaeo-Kings Creek and the palaeo-Macintyre on the Elsmore Sheet. The palaeo-Macintyre (or Kings Creek) follows a northwesterly path and is traceable from about GR490840. For the majority of its path, the Macintyre River has cut through the basalt cover exposing basement rocks in its channel.

A basalt filled palaeovalley at GR362925 containing Oaky Creek within it, flows northward also joining the palaeo-Macintyre. A northwesterly trending palaeochannel containing tertiary sediment is found at GR335900. Lowes Creek flows within this channel. Two major basalt-filled palaeochannels run west, parallel to, and north of Copes Creek, joining at about GR370870. Sheep Station Creek flows, in part, in the southernmost palaeochannel leaving it at GR392859 to flow southwest into Copes Creek. Snake Creek, Dead Horse Creek and Boney Creek cut across the palaeochannel at GR354870, GR365870 and GR380865 respectively flowing southward to join Copes Creek. The headwaters of Copes Creek flow for a short distance in a westerly trending, basalt filled, palaeovalley at GR465835.

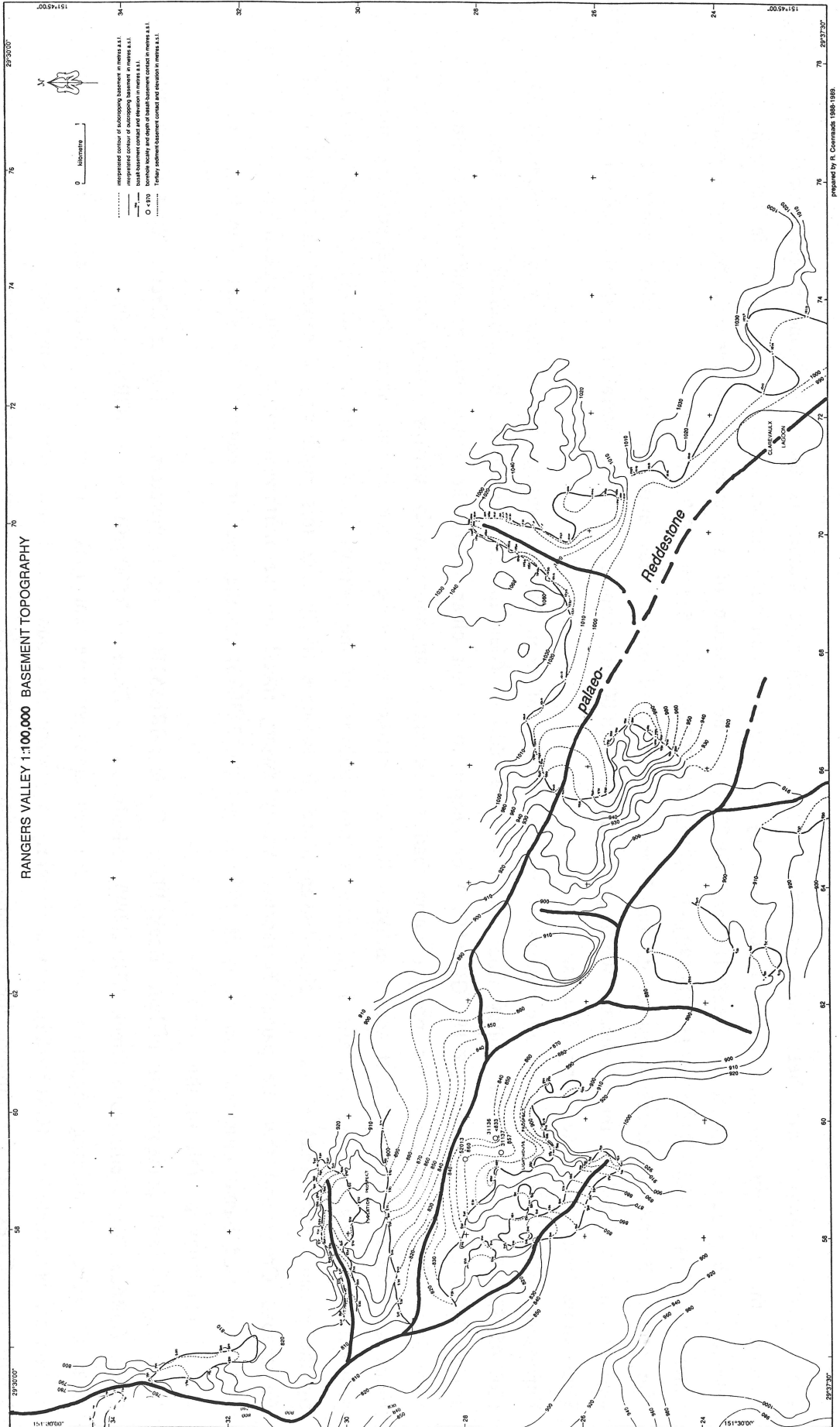


Map 17. Rangers Valley 1:25,000 Sheet

The dominant feature of this sheet is the Reddestone palaeochannel. Patches of basalt mark its former path from the vicinity of Clarevaulx Lagoon (GR720230) towards the northwest (GR550350). Insufficient data exist to say whether the major palaeochannel passed through the north or the south of the basement high ground in the vicinity of Balmoral (GR665250). To the north McCarthys Creek (GR660265) flows within the palaeochannel and to the south, a tributary of Black Plain Creek (GR670235).

The tongue of basalt at (GR698270) marks a former tributary to the palaeo-Reddestone. Here tin has been mined from deep-lead gravels below the basalt (T.J. Nunan, pers. comm.). Two more small basalt filled channels also form tributaries: they are the "Isolation Prospect" channel (GR570300) and the "Lighthouse Prospect" channel (GR580270). The northerly flowing Wellingrove Creek cuts across the palaeo-Reddestone at GR620280

The highest exposed basalt basement contact is 1040 m asl (GR695270). The height of this contact continues to fall to the northwest along the palaeo-Reddestone to 780 m asl (GR552338).



Map 18. Glen Innes 1:25,000 Sheet

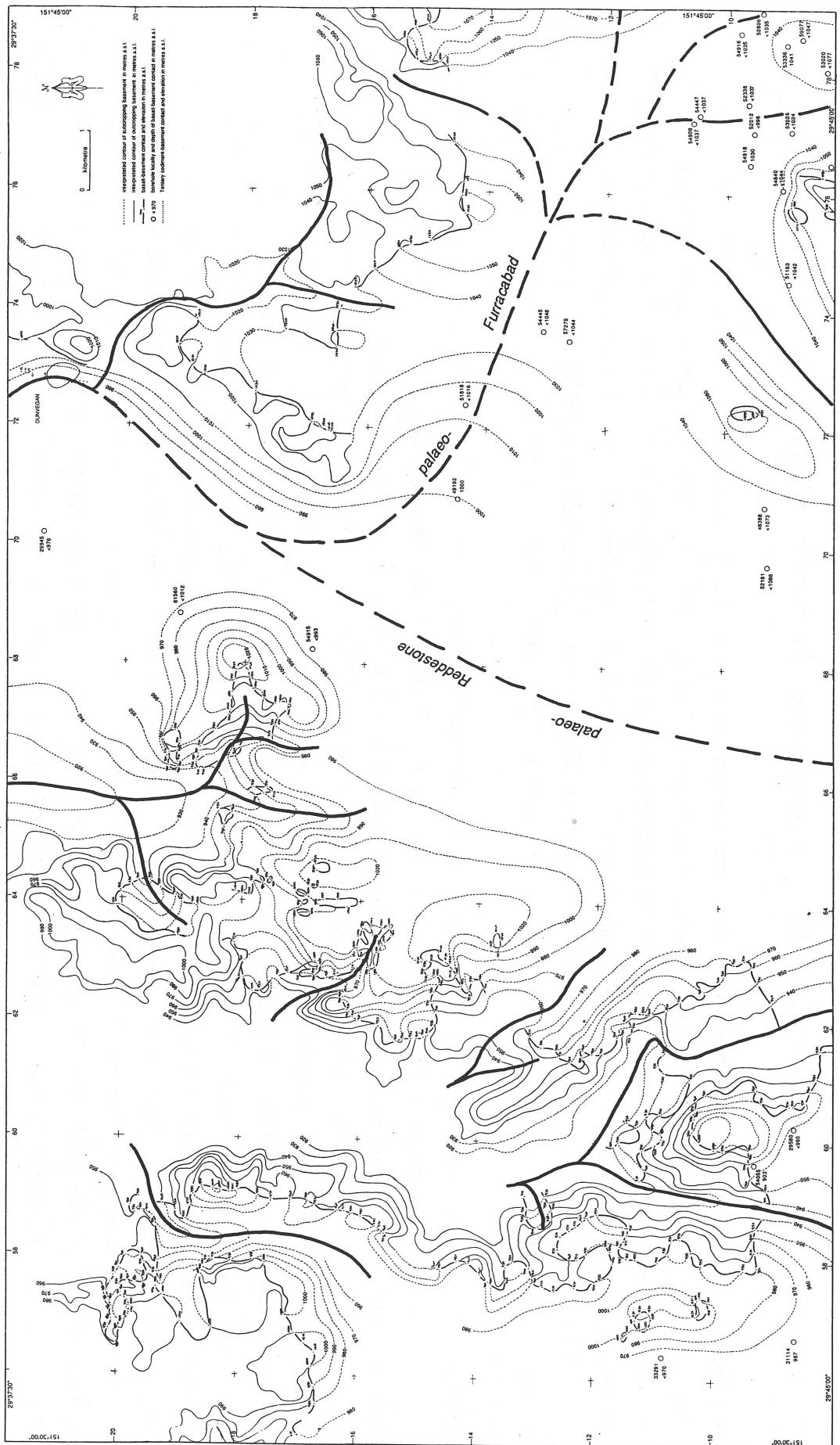
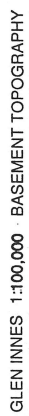
The palaeodrainage on this sheet flows essentially north. The dominant feature is the Reddestone palaeochannel and, although the exact position of its axis is obscured by an extensive volcanic blanket, it is constrained to lie between basement high ground exposed at GR680180 and GR720170. The presence of a channel below the volcanics is supported by waterbores 29945 (GR702214), 54915 (GR682169), 49192 (GR709144) and 51818 (GR724143).

The present Reddestone Creek flows in its flat-floored, basalt filled palaeovalley until GR730205 at which point it is captured and diverted to the northeast. Wellingrove Creek (GR:600200) appears to be a lateral to both the palaeo-Reddestone and the palaeo-Kings Plains.

Furracabad palaeovalley bends to the northwest in the vicinity of Glen Innes township and is supported by bore 51163 (GR745089). The height of the valley floor under the township of Glen Innes, as indicated by numerous water bores, is around 1030 m asl (Eg. bore 54918, GR765097) or deeper. It is not clear where the Furracabad palaeochannel continues from here. To the northeast, the present Furracabad Creek enters an anomalously narrow valley cut in the basement rocks at 1040 m (GR780158). It seems unlikely that this marked the trace of the original Furracabad palaeovalley unless post-volcanic block faulting has raised the area to the northeast of the potential fault line at (GR775155) and downcutting by the present Furracabad Creek has since taken place. It is more likely that this represents a capture and diversion of Furracabad Creek and that the palaeo-Furracabad valley swung round to the northwest to join the palaeo-Reddestone. The highest exposed basalt basement contact is at 1080 m asl (GR723096) on the southern edge of the sheet. The height of the contact continues to fall to the north.

Other basalt filled palaeovalleys include Back Plains Creek (GR655190), the headwaters of Punchs Creek (GR630160), Pine Creek (GR625130), Wellingrove Creek (GR620090), Maids Valley Creek (GR590090) and at (GR583180).

A small valley containing sapphires and zircon trapped amongst basement rock, but with no volcanic rocks in its catchment, is situated at (GR630188). It was formerly a mining area and now is a public fossicking area. Wellingrove Creek has cut through the volcanic pile into basement and is a lateral to the palaeo-Reddestone system to the east and the palaeo-Kings Plains system to the west.



prepared by R. Coenraads 1988-1989.

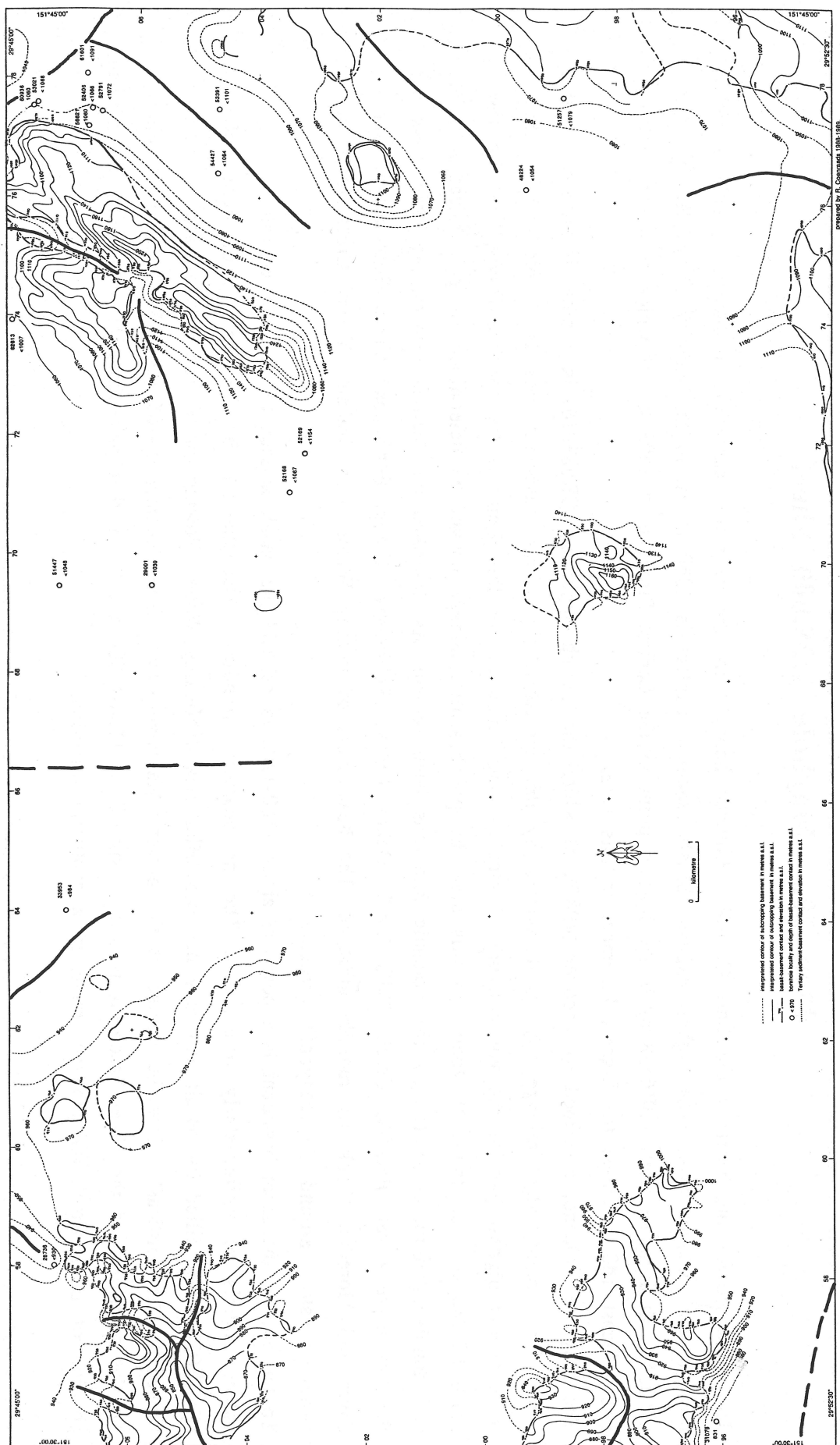
Map 19. Stonehenge 1:25,000 Sheet

Interpretation of the Stonehenge sheet poses the same problem as that of the Maybole 1:25,000 sheet to the south, with very few exposures of basement rocks showing through the volcanic cover. The highest basalt basement contact exposed is at 1240 m asl (GR735040). The elevation of the basement falls to the north, east and west. Towards the edges of the sheet where basement rocks are again exposed, basalt is seen to have flowed away from the central portion of the map into the pre existing drainage. On the northern corner of the sheet, basalt flows at GR750070 and GR764047 surrounded by basement highs indicate pre basaltic drainage to the northeast. This observation is supported by waterbore 54427 (GR764047).

Basalts fill the palaeo-Reddestone, a major pre basaltic channel trending in northerly direction on the northern end of the sheet, and at this position the present Reddestone Creek still flows within the confines of its original palaeovalley. Lying under extensive volcanic cover, the exact position of the headwaters of the palaeo-Reddestone is unclear.

To the northwest at GR558063, GR572058 and GR574048 tongues of basalt have flowed into the westerly trending palaeo-Swan Brook. At GR581072, waterbore 28736 indicates the presence of Maids Creek palaeovalley trending northward.

To the southwest at GR566983 and GR575970 tongues of basalt have flowed into the palaeo-Kings Creek. The White Rock Volcano centred on Spring Mountain volcanic plug (GR579003) is very similar in appearance to the Maybole Volcano to the south on the Maybole sheet. White Rock Mountain (GR595010), elevation 1330 m asl, and Arthurs Seat (GR616025), elevation 1244 m asl, are comprised of basalt flows putting the height of the volcanic pile at approx. 350 m above the highest observed basement in the area. Present day streams in this area, controlled by the volcanic pile flow out radially. These are the headwaters of Spring Creek, Swan Brook, Kennedys Gully, Bessies Creek and tributaries of Falls Creek and Little Oak Creek. Falls Creek from (GR608995) to its junction with Wellingrove Creek downstream to (GR630053) appear to describe and arc around the eastern side of the structure.



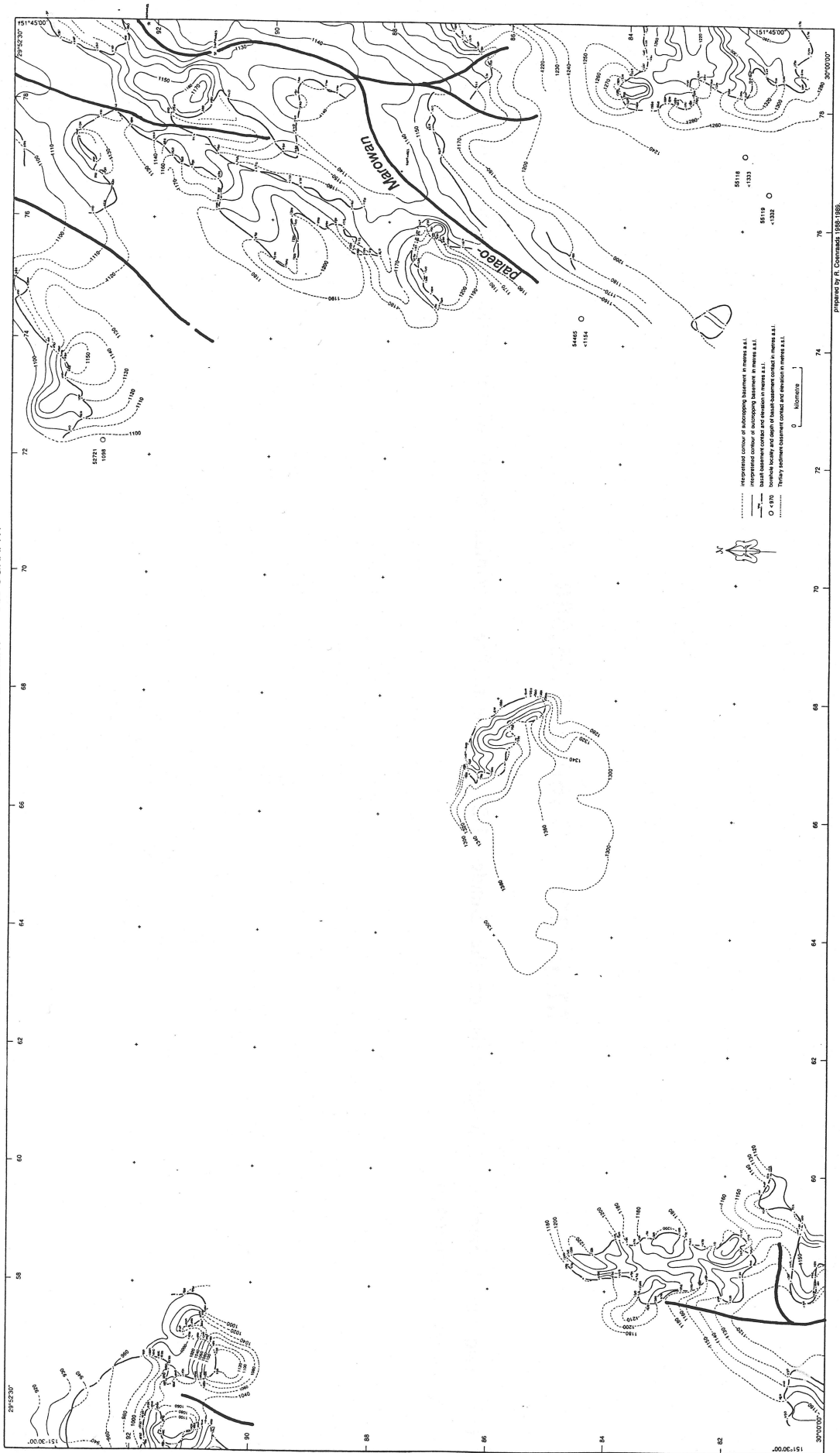
Map 20. Maybole 1:25,000 Sheet

This sheet covers the heart of the East Central Province hence there are very few exposures of basement rocks showing through the volcanic cover. The highest exposed basalt basement contact is 1360 m asl in the vicinity of Mt Rumbee (GR: 675855). Mt Rumbee itself (GR653856) is the highest point in the Central Province at 1503 m asl which puts the volcanic pile at least 140 m above the highest basement in this area. The Maybole Volcano, described by Pecover (1987), of which the Gough Sugarloaf (GR683916) is a plug, is situated on this sheet. The present day drainage appears dominated by this structure. Very little basement rock is visible through the thickest and highest part of the volcanic pile, stretching from south of the Ben Lomond area on the Guyra Sheet to the north of Maybole on the Glen Innes. In this area the pre basaltic drainage cannot be determined. A post-volcanic radial and annular pattern, controlled by the volcanic pile, has been set up. As described by Pecover (1987), the headwaters of the Macintyre River, Paradise Creek, Falls Creek, Oakey Creek, Wellingrove Creek, Furracabad Creek Stonehenge, Gara River and Moredun Creek are radially arranged. The headwaters of Beardy Waters and Grahams Valley Creek form an annular system around the Maybole Structure.

To the east of the sheet basement is exposed at about 1100-1200 m asl and the basalt is seen to have flowed into palaeochannels of northeasterly orientation. The northeasterly trending palaeochannel, in the vicinity of Fern Hill (GR736911) was filled by basalt and now has two tributaries of Beardy Waters flowing on it. The palaeo-Marowan also flowed to the northeast below the course of the present Marowan Creek. Bore Number 54465 (GR743847) supports this.

To the southwest of the sheet basement is again exposed at 1100-1200 m asl. Another palaeochannel marked by the present position of Back Creek (GR575810) trends in a southerly direction.

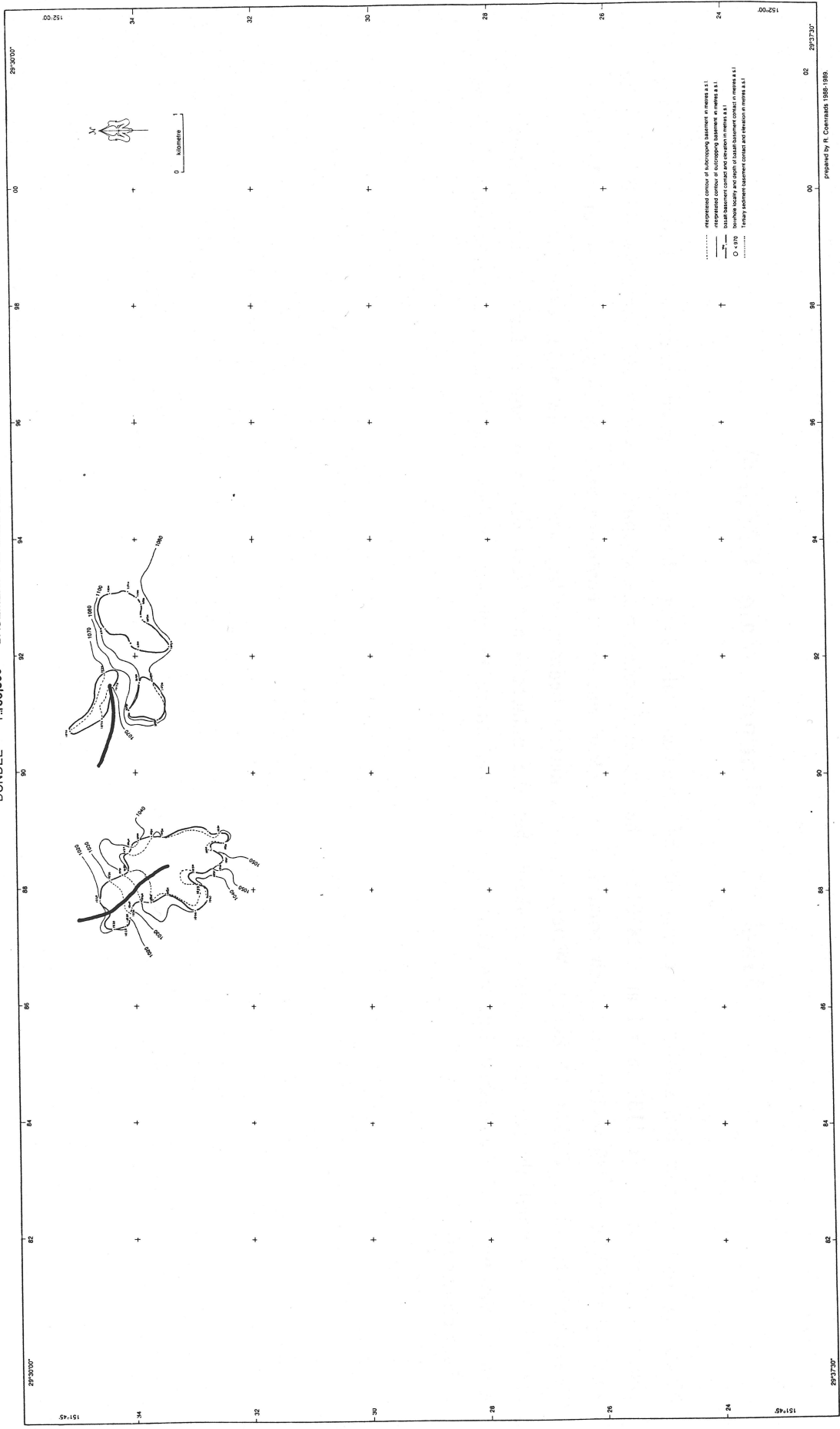
MAYBOLE 1:100,000 BASEMENT TOPOGRAPHY



Map 21. Dundee 1:25,000 Sheet

Only two small patches of basalt exist on the Dundee 1:25,000 sheet. The maximum height of the basalt basement contact is 1100 m asl at GR930340.

DUNDEE 1:100,000 BASEMENT TOPOGRAPHY

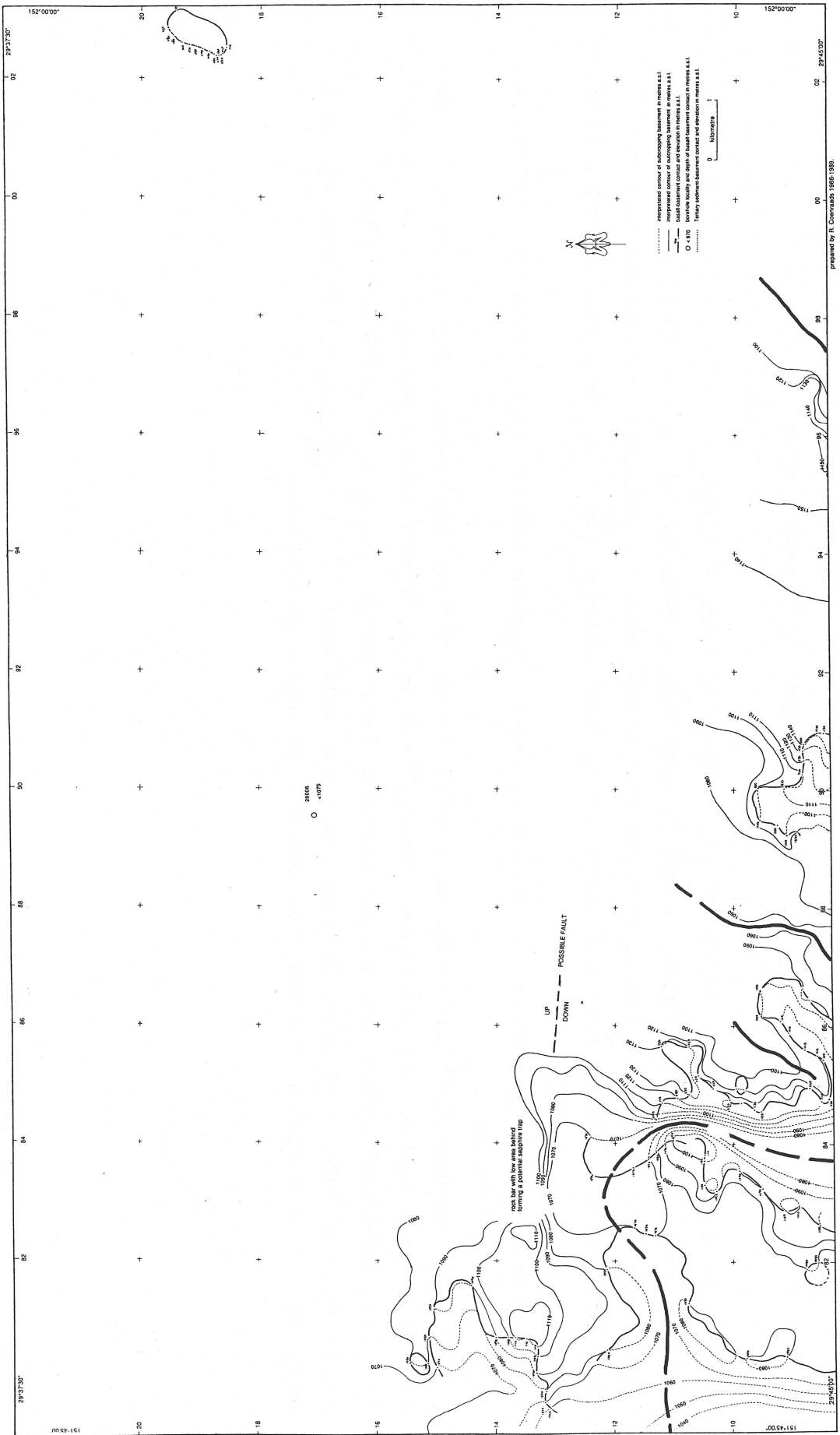


prepared by R. Connors 1985-1989.

Map 22. Shannon Vale 1:25,000

Volcanics only occupy the south west corner of the Shannon Vale Sheet, the highest point where the basalt basement contact is exposed is at 1130 m asl at GR850110. The relief inverted palaeochannel at GR840090 continues north from the Red Range Sheet to GR843110 at which point it is not clear whether it continues north or swings west to join the palaeo-Furracabad. North of GR831132 Beady Waters enters a narrow bedrock valley and no more basalt exists in the vicinity of the channel beyond this point. It seems unlikely that the palaeochannel went this way unless faulting has uplifted the area to the north of the dashed line on the map and downcutting by modern streams has affected the appearance of the palaeochannel.

SHANNON VALE 1:100,000 BASEMENT TOPOGRAPHY



Map 23. Red Range 1:25,000 Sheet

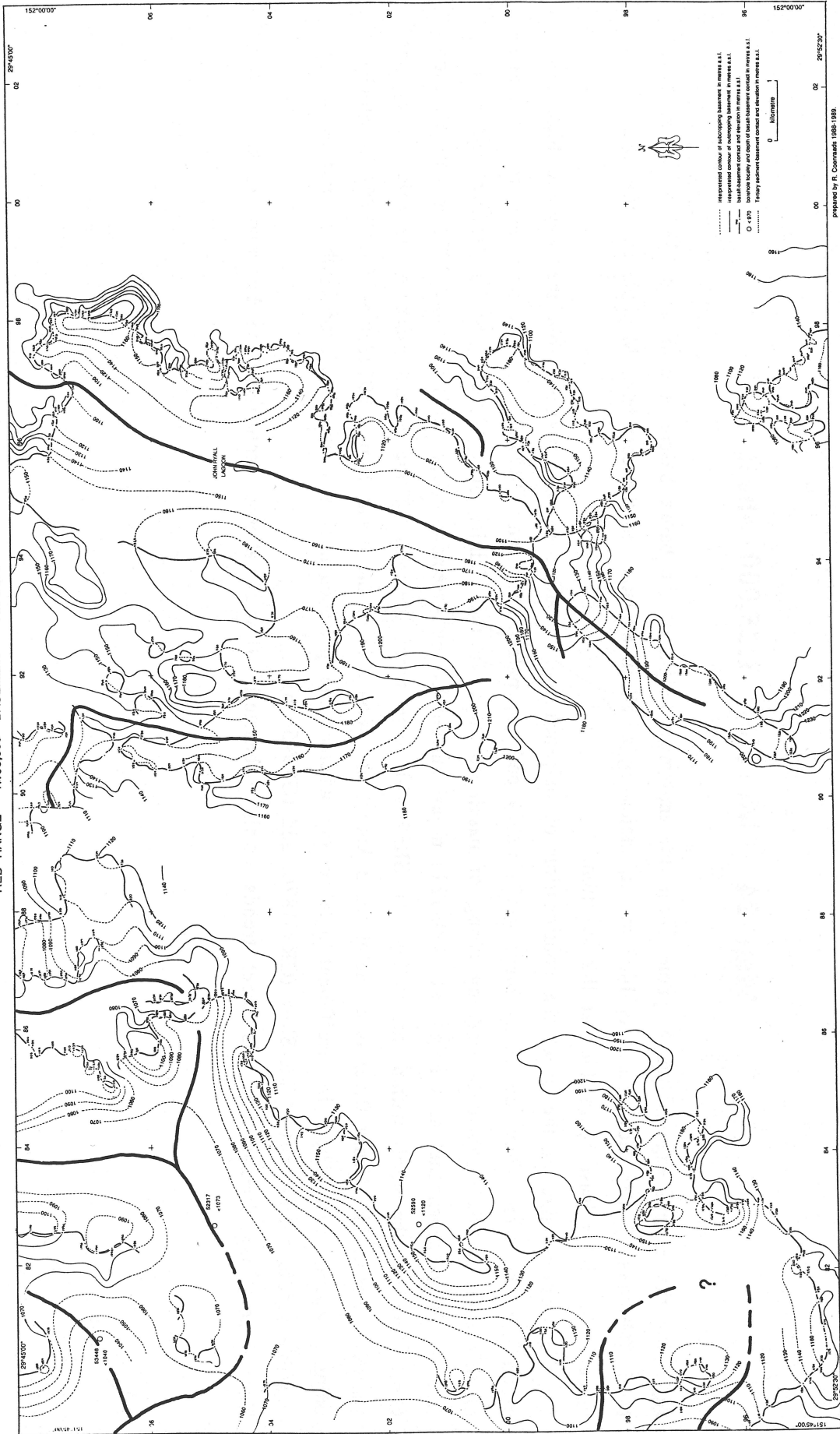
The basalt basement contact falls to the north across the Red Range Sheet, the highest point 1230 m asl is at GR908952. From this point a prominent palaeochannel marked by basalt flow remnants proceeds north to GR970070. John Ryall Lagoon (GR955045) and the headwaters of Oaky Creek are situated within the palaeovalley at its northern end. The palaeochannel is severed by the more northeasterly flowing present drainage. That is by Sheep Station Creek at GR940994 and Concertina Creek at GR950023.

Another northerly trending palaeochannel is indicated by basalt in between basement highs at GR909045. Middle Creek flows in this palaeochannel.

At GR828050, waterbore 52317 supports the interpretation that the northerly trending basalt ridge, or extension to the Great Divide is a relief inverted palaeochannel. Beady Waters and the Mann River are twin laterals to this palaeochannel. Bore 53448 (GR808069) indicates that the palaeosurface is falling into the palaeo-Furzacabad below Glen Innes.

A palaeovalley, or valleys exist below the volcanic pile upon which Blair Hill Lagoon is situated (GR818960) although it is ambiguous as to their direction. They may have flowed to the west or to the north.

RED RANGE 1:100,000 BASEMENT TOPOGRAPHY



prepared by R. Conradt 1985-1986

Map 24. Mt Slow 1:25,000 Sheet

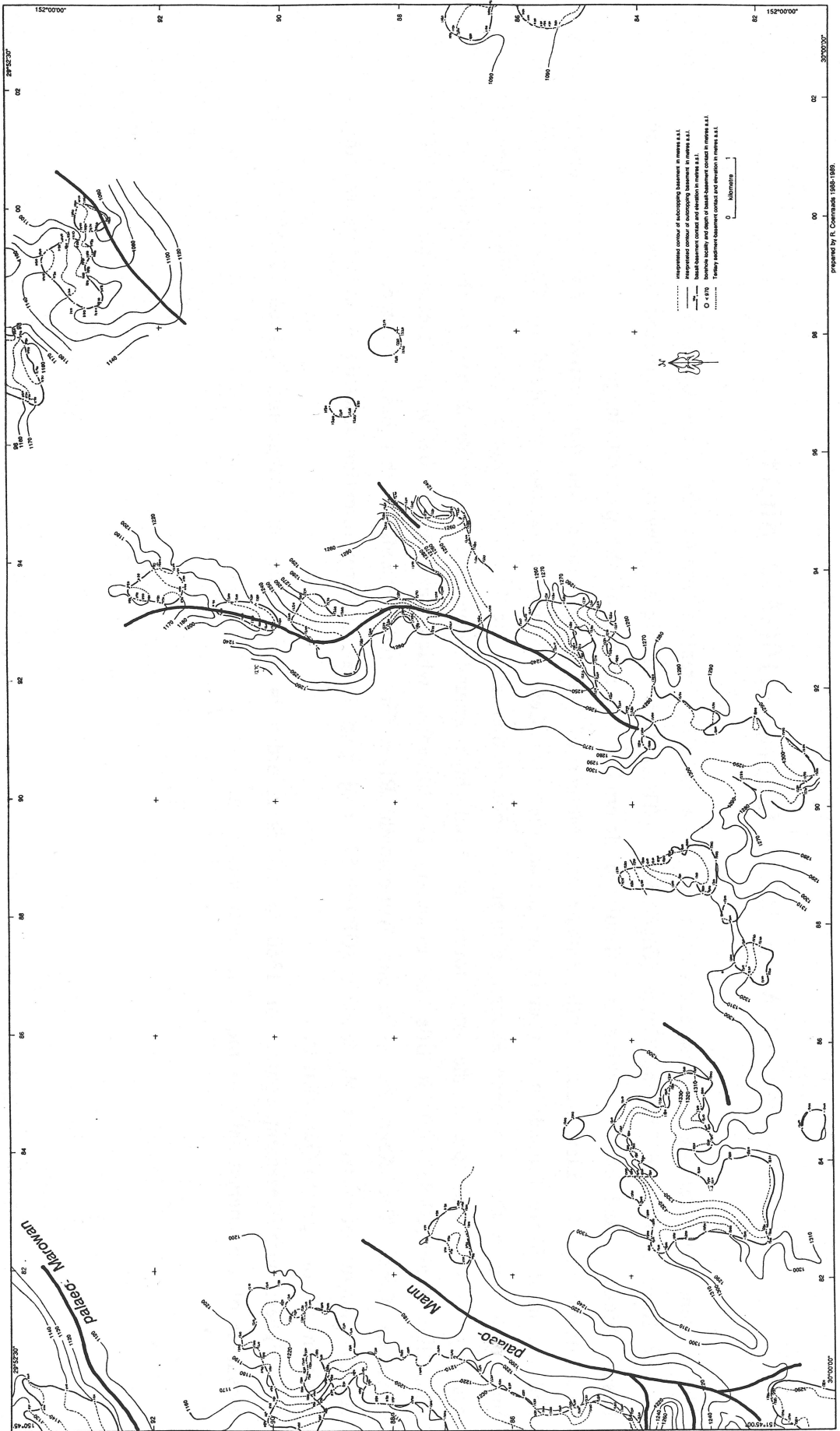
Adjoining the eastern edge of the Maybole Sheet, the maximum height of the basalt basement contact is 1330 m asl at Ben Nevis (GR843837). Ben Nevis itself is 1409 m asl, indicating a fall in elevation to the east from Maybole and that the volcanic pile is at least 80 m thick at this position.

On the western edge of the sheet the continuation of palaeochannels heading to to northeast from the Maybole high ground can be seen. They are palaeo-Mann (GR800830) and the palaeo-Marowan (GR796923). Most prominent in the middle of this sheet is the north-south trending string of basalt outcrops. In the vicinity of GR930900 the basalt flow remnants exist in the palaeochannel at a height of 1180-1240 m asl surrounded by basement valley walls to about 1270 m asl. Mt Slow Creek flows to the north within this valley. At GR920840 some relief inversion of the basalts marking the palaeovalley has started to occur. The Henry River is a lateral for 3 km on the west side of the basalt from GR912836 to GR928862 at which point it swings east. There is insufficient data to say whether the palaeochannel also went east or north or northwest. Possible saddle points exist at Mt Slow (GR931876) and (GR945876).

The present day drainage on this sheet trends north-northeasterly flowing almost exclusively on basement rocks.

MOUNT SLOW BASEMENT TOPOGRAPHY

1:100,000



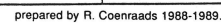
Map 25. Guyra 1:100,000 Sheet.

The present day drainage and palaeodrainage are both radially arranged around the areas of high ground in the vicinity of The Brothers (GR716778) and Guyra (GR720560). These areas of highest elevation also represent areas of maximum basalt thickness and cover, making it difficult to determine the nature of the palaeodrainage.

The natural lagoons, Llangothlin, Little Balbair and Mother of Ducks are situated on the relatively flat basalt covered areas and are most likely formed in a manner similar to the other Central Province lagoons described by Coenraads (1989). The bore data, where they are deep enough, support the observation that the basalt has flowed into, and filled, earlier drainage. A clear example is the large tongue of basalt high ground projecting to the south east in the vicinity of Chandlers Peak (GR853530). It fills the Boundary palaeochannel which lies roughly below the present position of Boundary Creek. The Aberfoyle River and Wollomombi River form twin laterals to this basalt tongue.

Another tongue of basalt at Mt Killalee (GR795351) projecting in a southerly direction towards Armidale marks the position of the palaeo-Gara River.

The highest basalt/basement contact of 1360 m asl. is recorded in the vicinity of Llangothlin Lagoon (GR805770). The elevation of the contact falls to the south, east and west.



Appendix 2

DESCRIPTION OF WATER BORES DRILLED IN THE NEW ENGLAND REGION, NEW SOUTH WALES

The accompanying table provides a summary of the water bores drilled into the Tertiary volcanic rocks of the Central Province in the area covered by the 25 map sheets shown in Figure A1-1. All bores drilled for water are catalogued by the New South Wales Government, Department of Water Resources. Their offices are located at 10 Valentine Ave, Parramatta, New South Wales, 2150.

Some 430 water bore logs are tabled numerically for each of the 1:25,000 and 1:100,000 sheets described in Appendix 1. The logs are poorly described but serve to distinguish between basalt and basement rocks, or at least indicate a minimum depth of basalt in a given borehole.

Other exploration drilling and testing carried out in the New England region by T.J. & P.V. Nunan Pty. Ltd and Jingellic Minerals N.L. are described in Appendix 4.

BORE NUMBER	GRID REFERENCE	DEPTH (metres)	BORE DESCRIPTION	ELEVATION COLLAR	DEPTH BASEMENT	MAP SHEET 1:25,000
51956	GR:814768	30.5	basalt to 30.5	1368	<1338	Backwater
59093	GR:812757	45.7	clay & soil to 5.5, basalt to 45.7	1359	<1313	Backwater
30812	GR:894541	46	basalt to 46.0	1323	<1277	Bald Blair
52643	GR:851557	35.1	basalt to 35.1	1290	<1255	Bald Blair
57182	GR:822635	37.7	clay to 4.8, ironstone to 37.7	1295	<1257	Bald Blair
62641	GR:812588	42.7	soil to 1.0, basalt to 42.7	1311	<1268	Bald Blair
31218	GR:556712	30.5	15.2 -17.1 basalt	1098		Ben Lomond
55273	GR:727745	36.8	basalt to 36.6	1378	<1341	Ben Lomond
30538	GR:611929	39.6	basalt to 39.6	325	<285	Bingara
31249	GR:791021	38.1	shale to 14.3, basalt to 38.1	383	<345	Bingara
31250	GR:798012	26.8	basalt to 26.8	403	<374	Bingara
31748	GR:749007	30.4	clay over shale at 10.1	380	370	Bingara
56929	GR:770038		topsoil to 16.5 over porphyry	383	345	Bingara
33370	GR:728503	14.9	basalt to 14.9	1358	<1343	Black Mountain
48037	GR:777442		gravel to 15.0 over granite	1310		Black Mountain
51763	GR:713446	42.6	basalt to 40.1 over gravel	1335	<1295	Black Mountain
52720	GR:675494	35.1	basalt to 35.1	1300	<1265	Black Mountain
54250	GR:745439	22.9	basalt to 21.6 over clay	1328	<1308	Black Mountain
55190	GR:739454	21.4	bslt to 12.4, gravel to 18.6 over qtz & hd rk	1330	1311	Black Mountain
57268	GR:711513	49.4	basalt to 45.4 over grey clay	1342	<1297	Black Mountain
60664	GR:692509	32.6	clay to 6.7, basalt to 32.6	1323	<1290	Black Mountain
60913	GR:677440	30.5	clay to 14.2, basalt to 30.5	1320	<1290	Black Mountain
6553	GR:145269	24.4	basalt to 24.4	615	<591	Bukkulla
32004	GR:191348	83.8	basalt to 83.8	580	<496	Bukkulla
33226	GR:250248	106.1	basalt to 106.1	650	<544	Bukkulla
33229	GR:250248	83.82	basalt to 83.82	650	<566	Bukkulla
33513	GR:203315	121.9	basalt to 121.9	565	443	Bukkulla
43114	GR:130220	47.2	basalt to 47.2	625	<578	Bukkulla
45116	GR:231265	121.9	basalt to 36.6 over rock	615	578	Bukkulla
49294	GR:181247	63.4	basalt to 63.4	538	<475	Bukkulla
55279	GR:204239	95.1	21.3-21.6 coal, 21.6-38.1 cong, bslt to 95.1	622	<527	Bukkulla
56931	GR:072223	61	31-32m bedrock, clay, basalt to 61.0	637	<576	Bukkulla
619	GR:038229	39	basalt to 39.0	660	<621	Cherry Tree Hill
3965	GR:876276	62.7	basalt to 48.8 over yellow clay	562	613	Cherry Tree Hill
3978	GR:872323	29.8	basalt to 29.8	545	<515	Cherry Tree Hill
5894	GR:984311	52.1	basalt to 52.1	670	<618	Cherry Tree Hill
5919	GR:049277	53	bluemetal to 48.8 over rock	670	611	Cherry Tree Hill
6675	GR:964313	46.3	basalt to 46.3	646	600	Cherry Tree Hill
6710	GR:030287	47.6	basalt to 47.6	698	<650	Cherry Tree Hill
6794	GR:901235	55.3	basalt to 55.3	555	<500	Cherry Tree Hill
6796	GR:849295	39.6	basalt to 39.6	460	<420	Cherry Tree Hill
8006	GR:880319	43.8	basalt to 29.0 over granite	538	509	Cherry Tree Hill
8008	GR:848326	30.4	basalt to 30.4	535	<505	Cherry Tree Hill
8010	GR:911331	24.9	basalt to 24.9	610	<585	Cherry Tree Hill
8020	GR:950346	20.7	basalt to 20.7	628	<607	Cherry Tree Hill
8031	GR:924328	29.9	basalt to 29.9	670	<640	Cherry Tree Hill
8042	GR:882297	46	basalt to 45.4 over hard, brown rock	534	489	Cherry Tree Hill
8084	GR:868309	65.2	basalt to 43.6 over blue clay to 47.5 over cqlm &	510	466	Cherry Tree Hill
8156	GR:950344	20.7	basalt to 20.7	630	<609	Cherry Tree Hill
10656	GR:919339	39	basalt to 39.0	660	<621	Cherry Tree Hill
11303	GR:880342	55.7	basalt to 55.7	650	<594	Cherry Tree Hill
16106	GR:851322	44.2	basalt to 44.2	540	<496	Cherry Tree Hill
29076	GR:900300	62.4	basalt to 62.4	570	<508	Cherry Tree Hill
29078	GR:8890281	32	basalt to 32.0	562	<530	Cherry Tree Hill
31232	GR:949301	30.5	basalt to 30.5	605	<575	Cherry Tree Hill
31337	GR:057307	22.86	basalt to 21.3 over granite	660	639	Cherry Tree Hill
32189	GR:826303	47.7	basalt to 29.3, cqlm, snd bsl, clay 43.3 over sst	530	501	Cherry Tree Hill
51481	GR:058252	45.7	baux-clay to 32.9 over granite	678	645	Cherry Tree Hill
54460	GR:867277	101.2	clay to 41.15 over cong	550	509	Cherry Tree Hill
59650	GR:840334	82.3	blue rock to 67.0 over unknown	560	493	Cherry Tree Hill
43602	GR:904469	39.9	basalt to 35.4, basalt & gravel 39.6 over clay	1315	<1275	Cleodon
43625	GR:913448	10.7	basalt to 10.7	1128	<1117	Cleodon
45509	GR:897487	19.2	basalt to 19.2	1314	<1295	Cleodon
1026	GR:928202	32.3	basalt to 32.3	590	<558	Delungra
1032	GR:922175	72.57	basalt to 72.6	595	<522	Delungra
1073	GR:025189	54.9	basalt to 54.6 over hard blue rock	670	615	Delungra
1086	GR:029102	90.8	basalt to 90.8	720	<630	Delungra
1106	GR:030169	61	basalt to 61.0	680	<619	Delungra
1149	GR:975164	77.7	basalt & rock to 58.5 over rock	705	<646	Delungra
1181	GR:000181	53.3	basalt to 53.3	690	<637	Delungra
8904	GR:014073	80.77	blue metal to 80.77	681	<600	Delungra
10082	GR:880203	83.8	hard blk claystone to 52.7 over shale	575	522	Delungra
10681	GR:013080	28.4	basalt to 28.4	693	<665	Delungra
12654	GR:061140	28.04	basalt to 28.0	656	<628	Delungra
14256	GR:029068	22.6	basalt to 22.6	668	<675	Delungra
17991	GR:996077	25.6	basalt to 25.6	660	<634	Delungra
27852	GR:944095	38.1	basalt to 37.8 over black clay	645	<607	Delungra
29182	GR:057133	32.3	basalt to 32.3	660	<628	Delungra
29835	GR:041124	88.4	basalt to 88.4	698	<610	Delungra
31911	GR:965158	55.5	basalt to 55.5	678	<622	Delungra
32817	GR:0411247	104.2	bauxite & basalt to 104.2	700	<596	Delungra
34814	GR:942123	92.7	basalt to 92.7	663	<570	Delungra
35014	GR:864069	29.9	basalt to 29.9	425	<395	Delungra
38179	GR:965164	51.8	basalt to 51.8	700	<648	Delungra
43436	GR:063092	64	basalt to 64.0	680	<616	Delungra
45400	GR:017092	68.6	basalt to 68.6	699	<630	Delungra
47746	GR:004091	45.7	basalt to 45.7	668	<622	Delungra
51278	GR:973123		basalt to 27.43, greywacke to 70.1	653	<626	Delungra
51663	GR:003103		basalt to 45.72	665	<620	Delungra
52007	GR:962182		basalt to 32.0	660	<528	Delungra
53193	GR:873193		stone clay on sandstone at 25.6	575	550	Delungra
53832	GR:040131		basalt to 127.41	691	<564	Delungra
54218	GR:002100		bauxite to 36.58, basalt to 45.72	665	<620	Delungra
55266	GR:879114		basalt to 94.48	525	<430	Delungra
56411	GR:909141		basalt to 42.1	585	<543	Delungra
56416	GR:916183		basalt to 125.58	632	<507	Delungra
56440	GR:915116		basalt to 11.6	590	<578	Delungra
56938	GR:053093		basalt to 50.9, bauxite to 160.0	730	<570	Delungra
57764	GR:057166		bauxite 26.5 - 36.8, basalt to 76.2	640	<564	Delungra
60724	GR:035088		basalt to 109.73	736	<626	Delungra
11753	GR:810830	19.5	sand and gravel to 19.5	315	<295	Dinoga
11754	GR:823823	43.3	sand, gravel & clay to 38.7 over conglomerate	315	<272	Dinoga
18515	GR:819825	34.7	sand, gravel & clay to 34.7	315	<280	Dinoga
50604	GR:669879	4.0	dolerite to 40.0	347	<307	Dinoga

BORE NUMBER	GRID	DEPTH	BORE DESCRIPTION	ELEVATION	DEPTH	MAP SHEET
	REFERENCE	(metres)		COLLAR	BASEMENT	1:25,000
34603	GR:655279	77.7	topsoil & boulders to 8.2, basalt to 77.7	1100	<1023	Dumaresq
35877	GR:788307	35	basalt to 34.7 over gravel & wash	1063	1028	Dumaresq
42759	GR:656243	28.9	loam to 10.9, basalt to 24.6 over volcanic rock	1079	<1050	Dumaresq
45700	GR:655263	41.5	clay to 5.5, basalt to 40.0 over clay	1085	<1045	Dumaresq
46733	GR:623258	61	clay to 15.3, basalt to 61.0	1049	<988	Dumaresq
47539	GR:655252	29	basalt to 29.0 over sandy clay	1082	<1053	Dumaresq
47830	GR:647263	18.2	clay to 12.1, basalt to 18.2	1075	<1053	Dumaresq
48457	GR:658251	20	clay to 9.0, basalt to 18.0	1079	<1059	Dumaresq
48504	GR:631270	52.4	loam to 8.8 over blue shale	1054	<1002	Dumaresq
48759	GR:632276	26.2	basalt to 26.2	1054	<1028	Dumaresq
49362	GR:640300	15.8	clay to 2.7, basalt to 14.0	1255	<1241	Dumaresq
52119	GR:702311	72.9	basalt to 47.4, clay to 60.2 over granite	1080	1033	Dumaresq
52298	GR:785277	38.1	basalt to 38.1	998	<960	Dumaresq
52463	GR:744258	72.9	basalt to 2.4, clay to 11.5 over shale	1045	1043	Dumaresq
53094	GR:774287	48.6	basalt to 10.7, shale to 45.6 over granite	1000	954	Dumaresq
53749	GR:676258	50	basalt to 50.0	999	<949	Dumaresq
54024	GR:709272	60	basalt to 60.0	1040	<980	Dumaresq
55150	GR:592263	52.7	basalt to 31.7 over gravel	1078	1046	Dumaresq
55599	GR:616251	15.2	basalt to 15.2	1063	<1048	Dumaresq
57318	GR:719277	22.8	basalt to 22.8	1015	<992	Dumaresq
57665	GR:722287	22	basalt to 22.0	995	<973	Dumaresq
58253	GR:634264	28	basalt to 18.0 over clay	1051	<1033	Dumaresq
58770	GR:666263	73.2	basalt to 73.2	1050	<977	Dumaresq
60708	GR:645263	38	basalt to 35.0 over sediment	1075	1040	Dumaresq
48759	GR:640272	26.2	basalt to 26.2	1068	<1042	Dumaresq
18557	GR:397038	40.23	dolerite to 40.23	765	<725	Elsmore
18566	GR:408041	28.7	basalt to 28.7	769	<740	Elsmore
19363	GR:418047	34.7	basalt to 34.7	748	<713	Elsmore
19391	GR:435051	25	Basalt to 25.0	775	<750	Elsmore
19682	GR:330048	54.9	slippery back to 54.9	690	<635	Elsmore
31080	GR:530970	53.4	basalt to 51.2 over gneiss	850-900	800-850	Elsmore
52514	GR:475049	51.5	basalt to 51.5	790	<738	Elsmore
52813	GR:456051	30.5	basalt to 30.5	740	<710	Elsmore
55572	GR:471044	22.8	basalt to 22.8	780	<757	Elsmore
29580	GR:603087	30.5	dolerite to 30.5	990	<960	Glen Innes
29945	GR:702214	45.7	basalt to 45.7	1022	<976	Glen Innes
31114	GR:568086	38.1	basalt to 38.1	1005	<967	Glen Innes
33291	GR:564108	45.7	basalt to 45.7	1015	<970	Glen Innes
48388	GR:708093	36.9	basalt to 36.9	1110	<1073	Glen Innes
49192	GR:709144	48.8	basalt & conglomerite to 43.9 over conglomerite	1044	1000	Glen Innes
51163	GR:745090	45.7	basalt to 11.9 over clay	1054	<1042	Glen Innes
51818	GR:724144	39.4	ironstone to 21.2, basalt to 39.4	1055	<1016	Glen Innes
52012		70	basalt to 70.0	1068	<998	Glen Innes
52181	GR:697092	32	basalt to 32.0	1120	<1088	Glen Innes
52338		21.3	basalt to 21.3	1058	<1037	Glen Innes
52806		75.3	basalt to 75.3	1110	<1035	Glen Innes
53020		25.2	basalt to 12.5 over clay and sandstone	1090	<1077	Glen Innes
53216		44.2	basalt to 44.2	1068	<1024	Glen Innes
53336	GR:786090	66.8	basalt to 41.3 over granite	1082	1041	Glen Innes
54055	GR:597093	67.1	basalt to 66.74 over hard blk rock	970	903	Glen Innes
54445	GR:737131	17.3	basalt to 17.3	1065	<1048	Glen Innes
54447		19.7	basalt to 12.5 over clay	1051	<1038	Glen Innes
54840		19.8	basalt to 19.8	1064	<1044	Glen Innes
54909		20.1	basalt to 13.7 over sand and clay	1051	<1037	Glen Innes
54915	GR:683169	54.7	loam and clay to 18.2, basalt to 54.7	1048	<993	Glen Innes
54916		44.5	basalt to 44.5	1080	<1035	Glen Innes
54918		39.6	basalt to 34.7 over rock	1065	1030	Glen Innes
54925		16.8	basalt to 16.8	1078	<1061	Glen Innes
57275	GR:735162	36.6	basalt to 36.6	1081	<1044	Glen Innes
59077		43	basalt to 43.0	1090	<1047	Glen Innes
61560	GR:688191	25.9	basalt to 25.9	1038	<1012	Glen Innes
6976	GR:023043	24.9	basalt to 24.9	658	<633	Gum Flat
7073	GR:934030	26	basalt to 26.0	613	<587	Gum Flat
19848	GR:048039	24.3	clay to 19.2 over granite	680	661	Gum Flat
27041	GR:045038	32.3	granite	683		Gum Flat
27144	GR:939959	15.6	gravel to 13.1 over basalt	629	<614	Gum Flat
34227	GR:866958	103.6	black rock to 80.7 over shale	502	422	Gum Flat
34936	GR:870958	51.8	basalt to 50.29 over shale	473	423	Gum Flat
44471	GR:045039	54.9	clay to 37.49 over rock & clay	683		Gum Flat
49293	GR:932039	143.3	basalt to 42.6 over clay -rock	600	557	Gum Flat
50877	GR:030035	36.3	basalt to 36.3	673	<637	Gum Flat
51016	GR:017050	67.1	basalt to 60.96 over hard coarse blk-gry rk	665	604	Gum Flat
51329	GR:003048	59.4	basalt to 57.91 over granite	673	615	Gum Flat
54457	GR:038069	61	basalt to 61.0	710	<649	Gum Flat
61174	GR:049039	45	clay to 15.0 over granite	680	665	Gum Flat
54031	GR:735648	32.6	clay to 6.1 over granite	1280		Guyra
55931	GR:732661	21.3	basalt to 7.62 over siltst to 13.72 over granite	1268	1262	Guyra
57269	GR:716542	55.5	silt to 15.5 basalt to 55.5	1318	<1262	Guyra
58099	GR:398345	15.2	Basalt to 13.7 over clay	735	<721	Hurricane Hill
31076	GR:505920	45.7	basalt to 45.7	900	<854	Indiana
43850	GR:469858	36.58	basalt to 34.1 over red shale	1005	970	Indiana
1889	GR:172045	11.7	basalt to 113.1 over slate	590	477	Inverell
2524	GR:191048	153	basalt to 153.0	600	<447	Inverell
2646	GR:125054	78	basalt to 78.0	735	<657	Inverell
2995	GR:158037	45.7	basalt to 37.5 over rock	615	578	Inverell
4799	GR:168015	53.3	basalt to 53.3	640	<587	Inverell
5127	GR:167062	46.3	basalt to 46.3	600	<554	Inverell
6936	GR:107058	69.5	basalt to 69.5	772	<702	Inverell
6991	GR:083062	68.6	basalt to 68.6	770	<701	Inverell
7654	GR:143060	67.1	basalt to 67.1	650	<583	Inverell
19233	GR:120049	99.4	basalt to 87.2 over shale, rock & clay	130	643	Inverell
24091	GR:082941	35.7	basalt to 35.2	640	605	Inverell
24701	GR:161038	52.7	basalt to 52.7	600	<547	Inverell
25113	GR:172953	19.8	basalt to 19.8	748	<728	Inverell
29004	GR:105085	57.3	basalt to 56.7 over clay	766	<711	Inverell
29028	GR:158944	35.05	basalt to 22.25 over clay	785	763	Inverell
29551	GR:148050	62.5	basalt to 55.2 over blue rock	650	595	Inverell
29598	GR:163016	105.2	basalt to 105.2	650	<545	Inverell
29723	GR:085989	57.9	basalt to 57.9	673	<615	Inverell
31289	GR:159006	85.3	basalt to 85.3	675	<590	Inverell
31483	GR:167028	91.4	basalt to 91.4	605	<514	Inverell
31628	GR:143044	76.2	basalt to 76.2	673	<597	Inverell
32419	GR:221050	153.9	basalt to 142.0 over clay	700	558	Inverell
33098	GR:099954	61	basalt to 61.0	650	<589	Inverell

BORE NUMBER	GRID REFERENCE	DEPTH (metres)	BORE DESCRIPTION	ELEVATION COLLAR	DEPTH BASEMENT	MAP SHEET 1:25,000
35627	GR:156.36	81.7	basalt to 81.68 over clay	610	528	Inverell
35962	GR:156008	53.3	basalt to 53.3	620	<587	Inverell
37809	GR:096069	61	basalt to 52.1 over shale & clay	730	680	Inverell
38097	GR:104068	99.97	basalt to 99.97	771	<671	Inverell
38268	GR:131054	102.4	basalt to 102.4	695	<593	Inverell
38489	GR:097069	56.2	basalt to 51.8 over granite	730	678	Inverell
38830	GR:099065	60.96	basalt to 60.96	770	<709	Inverell
42911	GR:091030	77.7	basalt to 77.7	720	<642	Inverell
43928	GR:159090	82.3	basalt to 82.3	608	<526	Inverell
44668	GR:127052	137.2	basalt to 137.2	737	<600	Inverell
44702	GR:192066	101.2	basalt to 101.2	600	<499	Inverell
45377	GR:191048	126.5	basalt to 126.5	600	474	Inverell
47244	GR:157033	57	basalt to 52.7 over sand & wood	605	552	Inverell
47389	GR:160948	55.8	topsoil & clay on granite at 7.61	775	769	Inverell
47537	GR:193040	117	basalt to 101.19 over clay & sand	621	<620	Inverell
47547	GR:089047	115.8	basalt to 115.8	803	<687	Inverell
47637	GR:104068	146.7	basalt to 146.7	771	<624	Inverell
47660	GR:155033	58.8	basalt to 50.9 over sandstone	605	554	Inverell
47791	GR:097043	146.3	basalt to 146.3	786	<640	Inverell
47984	GR:188027	29.9	basalt to 29.9	603	<573	Inverell
50135	GR:111060	76.2	basalt to 76.2	770	<694	Inverell
50211	GR:115067	73.2	basalt to 73.2	730	657	Inverell
50360	GR:124003	45.7	basalt to 45.7	660	<614	Inverell
50905	GR:129022	76.19	basalt to 76.2	665	<590	Inverell
51162	GR:105973	41.1	basalt to 41.1	642	<601	Inverell
51224	GR:166019	128	basalt to 112.2 over lime- & sandstone	642	530	Inverell
51570	GR:188065	82.3	basalt to 80.8 over clay	595	<515	Inverell
51711	GR:241043	81.7	basalt to 32.0, coal & soil to 51.8 on granite	682	630	Inverell
52017	GR:193057	74.7	basalt to 68.6 over clay	593	524	Inverell
52240	GR:163024		basalt to 77.42 over clay	619	<542	Inverell
52361	GR:127007	45.7	basalt to 45.7	669	<623	Inverell
52784	GR:168024	77.7	basalt to 74.7 over rock	610	<635	Inverell
52873	GR:219055	121.9	basalt to 121.9	692	<570	Inverell
53077	GR:156029	57.9	basalt to 53.9 over cgl, firm clay and sand	610	556	Inverell
53108	GR:224037	167.6	basalt to 163.1 over clay	691	528	Inverell
53228	GR:182039	30.5	basalt to 30.5	590	<560	Inverell
53234	GR:211040	62.8	basalt to 62.8	650	<587	Inverell
53277	GR:160947	24.7	basalt to 21.3 over granite	779	758	Inverell
53333	GR:251941	34.9	weathered basalt to 15 over granite	785	770	Inverell
53370	GR:180040	65.2	basalt to 65.2	590	<525	Inverell
53731	GR:165028	90.8	basalt to 90.5 over clay	600	510	Inverell
54220	GR:123062	132.6	basalt to 132.6	697	<564	Inverell
54424	GR:202049	73.1	basalt to 73.1	635	<562	Inverell
54425	GR:193041	189	basalt to 148.0 over sandstone & rock	618	470	Inverell
54436	GR:162041	45.7	basalt to 45.7	606	<560	Inverell
54442	GR:148025	71.2	topsoil to 16.5, basalt to 71.2	655	584	Inverell
54443	GR:144026	76.8	basalt to 76.2 over clay	650	574	Inverell
54450	GR:222044	173.4	basalt to 173.1 over clay	692	519	Inverell
54717	GR:102074	62	blue rock to 62.0	782	<720	Inverell
54912	GR:184046	22.2	basalt to 22.2	585	<563	Inverell
54922	GR:159038	45.7	basalt to 45.7	608	<562	Inverell
54928	GR:157046	61	basalt to 61.0	642	<581	Inverell
54929	GR:172050	65.5	basalt to 65.5	608	<542	Inverell
54935	GR:109046	152.4	basalt to 152.4	765	<613	Inverell
55011	GR:156047	56.4	basalt to 56.4	639	<583	Inverell
55223	GR:189043	36.2	basalt to 36.2	600	<564	Inverell
55228	GR:202042	64	basalt to 59.1 over clay	630	571	Inverell
55234	GR:193027	78.6	basalt to 78.6	603	<524	Inverell
55269	GR:100969	30.5	basalt to 30.5	615	<585	Inverell
55270	GR:120072	121.9	basalt to 121.9	690	<578	Inverell
55573	GR:112062	111.3	topsoil to 53.3, basalt to 111.3	770	<659	Inverell
55662	GR:125012	79.2	basalt to 79.2	672	<593	Inverell
56405	GR:240042	56.4	basalt to 56.4	682	<626	Inverell
56422	GR:077020	111.3	basalt to 111.3	730	<619	Inverell
56425	GR:083024	82.3	basalt to 82.3	715	<633	Inverell
56427	GR:142048	71.6	basalt to 71.6	668	<596	Inverell
56915	GR:205053	79.2	basalt to 79.2	645	<566	Inverell
56918	GR:145028	54.9	basalt to 54.9	645	<590	Inverell
56942	GR:169019	99.1	basalt to 99.1	630	<531	Inverell
56982	GR:164024	45.7	basalt to 45.7	620	<574	Inverell
57206	GR:165027	50.3	basalt to 50.3	613	<563	Inverell
57930	GR:161049	131	basalt to 131.0	622	<491	Inverell
58923	GR:206041	138.1	basalt to 135.64 over sand	640	504	Inverell
58935	GR:107072	143.3	basalt to 147	770	<623	Inverell
59842	GR:197030	134.1	basalt from 5.49 over granite to 79.3 over coal	609	530	Inverell
60993	GR:125008	20.1	basalt to 20.1	665	<645	Inverell
61426	GR:283061	50	basalt to 50	652	<602	Inverell
61565	GR:159018	53.3	basalt to 53.34	630	<577	Inverell
61566	GR:122996	26	basalt to 26.0	662	<636	Inverell
62540	GR:139049	76.2	basalt to 76.2	682	<606	Inverell
62694	GR:121991	60.3	basalt to 60.3	652	<592	Inverell
62835	GR:139052	860.6	basalt to 73.1 over blue-black porous rock	672	599	Inverell
62963	GR:239051	50.3	basalt to 50.3	670	<620	Inverell
62721	GR:722927	44.2	clay to 22.8 over granite	1120	1098	Maybole
64465	GR:745847	24.4	basalt to 24.4	1178	<1154	Maybole
65118	GR:772820	16.5	basalt to 16.5	1350	<1333	Maybole
65119	GR:766816	9.8	basalt to 9.8	1342	<1332	Maybole
10888	GR:626152	49.1	basalt to 49.1	370	<321	Mt Rodd
43320	GR:793207	38.1	basalt to 38.1	523	<485	Mt Rodd
47792	GR:710188	121.9	basalt to 18.6 over sandstone/coal	480	461	Mt Rodd
51276	GR:759187	75	basalt to 74.68 over clay	483	408	Mt Rodd
2967	GR:145120	61.87	basalt to 54.9 over rock	565	530	Nullamanna
4935	GR:223092	35.7	basalt to 35.7	583	<547	Nullamanna
4936	GR:255142	47.2	basalt to 47.2	700	<653	Nullamanna
5690	GR	44.2	basalt to 44.2	620	<576	Nullamanna
6689	GR:078074	96	basalt to 96.0	735	<640	Nullamanna
7023	GR:118171	42.7	basalt to 42.7	620	<577	Nullamanna
7394	GR:129101	42.1	basalt to 42.1	630	<568	Nullamanna
7483	GR:114109	71.3	basalt to 71.3	706	<L 5	Nullamanna
8579	GR:165086	52.1	basalt to 46.0 over aquifer	600	<554	Nullamanna
15383	GR:200110	38.7	basalt to 38.7	580	<541	Nullamanna
20140	GR:072087	30.8	basalt to 30.8	680	<650	Nullamanna
20770	GR:105185	26.5	basalt to 26.5	625	<598	Nullamanna
23981	GR:209083	71.6	basalt to 71.6	592	<520	Nullamanna

BORE NUMBER	GRID	DEPTH	BORE DESCRIPTION	ELEVATION	DEPTH	MAP SHEET
	REFERENCE	(metres)		COLLAR	BASEMENT	
25960	GR:140103	51.8	basalt to 51.8			Nullamanna
29156	GR:136129	76.2	basalt to 76.2	578	502	Nullamanna
29552	GR:232182	24.38	basalt to 23.5 over marl	660	635	Nullamanna
31094	GR:212134	53.3	basalt to 53.3	670	<617	Nullamanna
31395	GR:224125	68.6	basalt to 68.6	670	<602	Nullamanna
34044	GR:1971007	32	basalt to 32.0	588	<556	Nullamanna
37460	GR:132119	60.96	basalt to 60.96	585	<524	Nullamanna
43784	GR:163016	94.5	basalt to 94.5	645	<550	Nullamanna
44595	GR:207108	52.4	basalt to 52.4	600	548	Nullamanna
45861	GR:118169	50.3	basalt to 30.5 over rock & conglomerate	620	590	Nullamanna
47034	GR:205100	52.5	basalt to 23.8 over sand, clay & coal	595	<543	Nullamanna
47725	GR:081084	70.1	basalt to 70.1	680	<610	Nullamanna
48123	GR:073148	84.7	basalt to 84.7	641	<558	Nullamanna
48243	GR:171078	35.4	basalt to 35.4	592	<557	Nullamanna
49690	GR:140103	74.1	basalt to 74.1	615	<541	Nullamanna
50124	GR:197103	91.4	basalt to 45.7 over conglomerate	592	546	Nullamanna
50183	GR:159082	42.7	basalt to 42.7	621	<578	Nullamanna
51018	GR:138103	62.5	basalt to 60.9 over clay	625	<564	Nullamanna
51125	GR:105076	140.2	basalt to 140.2	784	<624	Nullamanna
51161	GR:079078	79.9	basalt to 97.5 on clay	722	620	Nullamanna
51816	GR:129084	47.3	basalt to 47.3	648	<589	Nullamanna
51942	GR:119188	64.3	basalt to 61.6 on clay	590	528	Nullamanna
52006	GR:271160	40	Basalt to 35.0 over clay	705	<670	Nullamanna
52011	GR:168169	44.2	basalt to 44.2	585	<541	Nullamanna
52719	GR:078117	45.7	basalt to 45.7	680	<634	Nullamanna
52769	GR:134105	67	basalt to 67.0	619	<522	Nullamanna
53140	GR:128203	25.9	basalt to 25.9	596	<570	Nullamanna
54462	GR:121199	36.6	basalt to 23.7 over bauxite	598	<574	Nullamanna
55039	GR:129209	39.6	basalt to 39.6	610	<570	Nullamanna
55217	GR:210151	152.4	basalt to 152.4	665	<513	Nullamanna
55265	GR:081127	71.6	basalt to 71.6	695	<623	Nullamanna
55982	GR:148088	61.6	basalt to 61.6	620	<558	Nullamanna
56327	GR:167092	42.1	basalt to 42.1	602	<560	Nullamanna
56408	GR:067120	48.8	basalt to 48.8	665	<616	Nullamanna
56410	GR:108178	13.7	basalt to 13.7	618	<604	Nullamanna
56441	GR:171079	41.8	basalt to 41.8	604	<562	Nullamanna
56939	GR:159079	53.3	basalt to 53.3	620	<567	Nullamanna
57810	GR:166079	55.8	basalt to 55.8	612	<566	Nullamanna
58098	GR:067164	76.2	basalt to 76.2	646	<570	Nullamanna
58317	GR:164095	54.9	basalt to 31.4 over clay and coal	602	<570	Nullamanna
58915	GR:091074	15.3	basalt to 15.3	700	<685	Nullamanna
62655	GR:214107	61	basalt to 45.7 over pipeclay	652	606	Nullamanna
31136	GR:596275	68.6	basalt to 68.6	902	<833	Rangers valley
31137	GR:594274	68.6	basalt to 30.8 over gry grn granite	888	857	Rangers valley
51437	GR:611287	19.8	clay and gravel to 7.0 over rock	878	<871	Rangers Valley
52013	GR:593281	44.2	clay to 17.98 over granite	878	860	Rangers Valley
52317	GR:828050	67.05	basalt to 67.05	1140	<1073	Red Range
52590	GR:826015	19.8	basalt to 19.8	1140	<1120	Red Range
53448	GR:808069	30.5	basalt to 30.5	1070	<1040	Red Range
61067	GR:932057		Granite	1158		Red Range
15850	GR:478125	10.7	basalt to 10.7	965	<954	Sapphire
19665	GR:440092	36.3	basalt to 36.3	835	<800	Sapphire
19914	GR:521117	30.5	basalt to 30.5	976	<945	Sapphire
27851	GR:454097	36.6	basalt to 36.0 over clay	840	804	Sapphire
31272	GR:505209	76.2	clay to 17.4 over granite	918	901	Sapphire
32239	GR:534138	48	basalt to 30.48 over granite	958	928	Sapphire
32240	GR:528135	12.2	basalt to 12.2 over granite	948	936	Sapphire
32241	GR:526137	15.2	basalt to 8.5 over porphy	948	940	Sapphire
32244	GR:544135	91.4	basalt to 27.7 grey clay 36.9 over granite	975	948	Sapphire
33273	GR:497177	61	clay to 31.4 over granite	945	914	Sapphire
33900	GR:544104	45.7	basalt to 45.7	1020	<974	Sapphire
38637	GR:423146	64	basalt to 64.0	813	<749	Sapphire
43585	GR:459089	89	basalt to 88.7 over rock	800	711	Sapphire
61436	GR:486201	61	basalt to 61.0, clay to 48.0	928	<867	Sapphire
54435	GR:527116	24.1	basalt to 24.1	670	<946	Sapphire
56413	GR:418157	64	basalt to 64.0	830	<766	Sapphire
56420	GR:417161	137.2	und traprock to 9.75 over porphy	827	817	Sapphire
28006	GR:895171	30.5	basalt to 30.5	1105	<1075	Shannon Vale
28736	GR:580072	30.5	basalt to 30.5	960	<930	Stonehenge
29001	GR:895057	45.7	basalt to 45.7	1075	<1030	Stonehenge
31079	GR:558961	68.58	basalt to 65.5 over grey clay	900	831	Stonehenge
33953	GR:641071	21.3	basalt to 21.3	1005	<984	Stonehenge
48224	GR:762994	80.1	basalt to 39.0 over hard rock to 43.6 over congl	1094	<1054	Stonehenge
51257	GR:778988	15.8	basalt to 15.8	1095	<1079	Stonehenge
51447	GR:695072	31.4	basalt to 31.4	1079	<1048	Stonehenge
52168	GR:711035	62.5	basalt to 62.5	1130	<1067	Stonehenge
52169	GR:718032	80.8	basalt to 80.8	1235	<1154	Stonehenge
52406	GR:777077	11.9	basalt to 11.9	1080	<1068	Stonehenge
52791	GR:774066	42.6	basalt to 42.6	1115	<1072	Stonehenge
53021	GR:775068	42.4	basalt to 42.1 over clay	1110	1068	Stonehenge
53391	GR:775047	21.3	basalt to 21.3	1122	<1101	Stonehenge
54427	GR:764047		basalt to 60.95	1125	<1064	Stonehenge
56621	GR:772069	39.6	basalt to 39.6	1100	<1060	Stonehenge
60936	GR:775078	24.4	basalt & conglom to 19.8 over conglom	1080	1060	Stonehenge
61601	GR:781069	24	weathered basalt to 24.0	1115	<1091	Stonehenge
62613	GR:740081	54.9	basalt to 54.86	1062	<1007	Stonehenge
8108	GR:812301	27.4	basalt to 27.4	500	<473	Warialda
13751	GR:812312	37.8	basalt to 35.4 over pipeclay	555	<520	Warialda
14305	GR:773317	121.9	basalt to 42.7 over andstine to 76.2 over granite	465	423	Warialda
16326	GR:599314	113.1	basalt to 45.7 over limestone	386	340	Warialda
19545	GR:807333	27.4	basalt to 27.4	548	<521	Warialda
28503	GR:79132	44.19	basalt to 44.2	485	<441	Warialda
29769	GR:742250	91.7	clay to 22.3 over siltstone to 43.3 over granite	420	398	Warialda
49253	GR:775215	47.6	basalt to 47.6	490	<442	Warialda
55267	GR:814326	61	basalt to 61.0	560	<499	Warialda
55268	GR:814321	74.9	basalt to 74.9	574	<499	Warialda
55571	GR:752244	10	basalt	428	<418	Warialda

Appendix 3

GEOPHYSICAL ASSESSMENT; KINGS PLAINS AND DUNVEGAN LAGOONS

A3.1 Fieldwork

The natural lagoons chosen for the investigation are listed with their grid references below and aerial photographs are shown in Chapter 6:

Lagoon	Grid Reference & Map Sheet			
-Kings Plains Lagoon	GR:484206	Inverell	1 : 100,000	(Fig. 6-2)
-Dunvegan Lagoon	GR:728210	Glen Innes	1 : 100,000	(Figs 6-3 & 6-4)
-Clarevaulx Lagoon	GR:720225	Glen Innes	1 : 100,000	(Fig. 6-4)
-John Ryall Lagoon	GR:955045	Glen Innes	1 : 100,000	(Fig. 6-5)
-Barley Field Lagoon	GR:774905	Glen Innes	1 : 100,000	(Fig. 6-6)
-Inverell Racecourse	GR:180030	Inverell	1 : 100,000	

The geophysical surveys were designed to assess the hypothesis proposed by Pecover (1987) that the lagoonal features of the Central Province are maars and to determine optimum locations for the testing of their economic viability.

Initial computer modelling was carried out at Macquarie University based on the assumption that any feeder vents could be represented as vertical pipes or dykes. The purpose of the modelling was to determine the minimum size and physical property contrasts necessary for such a feature to be detectable and to determine optimum station spacing. It was determined that a pipe of diameter 100 m would be just within the limits of detection giving a $2 \mu\text{ms}^{-2}$ (0.2 mGal) anomaly with a density contrast of 100 kgm^{-3} . Adequate anomaly definition required a 50 m sample interval. Near surface noise problems were anticipated for the magnetics as indicated by Spencer (1987) and therefore a finer sample spacing deemed necessary.

During the period 15-26 July 1987 a field party consisting of 4 persons carried out geophysical surveys over the Kings Plains and Dunvegan structures in the Glen Innes-Inverell area.

A3.1.1 Gridding

A grid covering an area of approximately one square kilometre (about 150 stations) was erected at each locality. A 100 m. grid interval was chosen with a 50 m grid within the lagoon area to ensure adequate definition of any geophysical anomaly within this area.

A3.1.2 Levelling

The grids were levelled, using a levelling telescope and 4 metre staff, to an accuracy of 2 cm for the purpose of applying elevation corrections to the gravity data. Levelling was completed for the Kings Plains grid. Owing to shortage of time, however, levelling for the Dunvegan grid was carried out by David Morris of J.I. Noad & Co., Inverell.

A3.1.3 Gravity

Gravity was measured at each grid locality using a Canadian CG-2 gravimeter (provided by the New South Wales Department of Minerals and Energy). The aim of the survey is to define any gravity anomaly that may exist due to a density contrast between the materials below the lagoon area.

A3.1.4 Magnetism

The earth's total magnetic field was measured at 10 m spacings within the inner portion of the grid (covering the lagoon floor and flanks) and at a 20 m spacing for the outer portion of the grid. A Geometrics proton precession magnetometer was used (provided by the New South Wales Department of Minerals and Energy). The aim of the survey was to define any magnetic anomaly that may exist due to differing magnetic susceptibilities between the materials below the lagoon area.

A3.1.5 Seismic

Seven reversed seismic refraction lines were carried out using a Geometrics Nimbus single channel, signal enhancement seismograph with a hammer source (provided by Geo-Instruments Ltd.). They were carried out both on the lagoon floor and rim in order to ascertain the seismic nature of the near surface materials and to define any near surface sub-horizontal layering. Knowledge of these factors assisted in the gravity and magnetic modelling studies.

A3.2 Data Reduction

Standard reduction procedures were used on the gravity data. Data were adjusted for their elevation (free air and Bouguer corrections) with respect to the base station and their distance north or south of the base station (latitude correction) in accordance with the formula (Parasnis, 1975).

$$\Delta g = \Delta g_{\text{obs}} + \Delta g_{\Phi} + (3.086 - 4.191 \times 10^{-4} \rho)h \quad \mu\text{ms}^{-2}$$

where Δg_{obs} is the observed gravity
 $\Delta g_{\Phi} = 0.081 \sin 2\Phi \quad \mu\text{ms}^{-2}$ per 10 m distance north
 Φ is the latitude of the base station
 h is the elevation difference in metres
 ρ is the density of the slab of material in kgm^{-3}

Note, gravity values are given in micrometres per second squared ($10 \mu\text{ms}^{-2} = 1 \text{ mGal}$)

A terrain correction was not applied because topographic variation across the survey area was only in the order of a few metres.

Bouguer correction densities between $2,100 \text{ kgm}^{-3}$ and $3,000 \text{ kgm}^{-3}$ were applied in 100 kgm^{-3} steps to examine the effect on the gravity data. If the density chosen is too high, the gravity surface moves in a direction opposite to topography and if too low the gravity moves in accordance with the topography. Within the lagoon area, where there is no topographic variation, the Bouguer correction density has no effect. The rim consists of clays and ironstone pisoles as well as pebbles, cobbles, boulders and flows of basalt. A suitable average density will be somewhat higher than that of $1950\text{-}2050 \text{ kgm}^{-3}$ for normal sediments (Parasnis, 1975) and lower than that of $2700\text{-}3300 \text{ kgm}^{-3}$ for basalt (Parasnis, 1975). A Bouguer correction density of 2300 kgm^{-3} was chosen as a compromise and supported by the above analysis.

The data were plotted on 1:1,000 scale and both hand and computer contoured. Three-dimensional perspectives were generated to assist interpretation.

A3.3 Comparison of the Data Sets

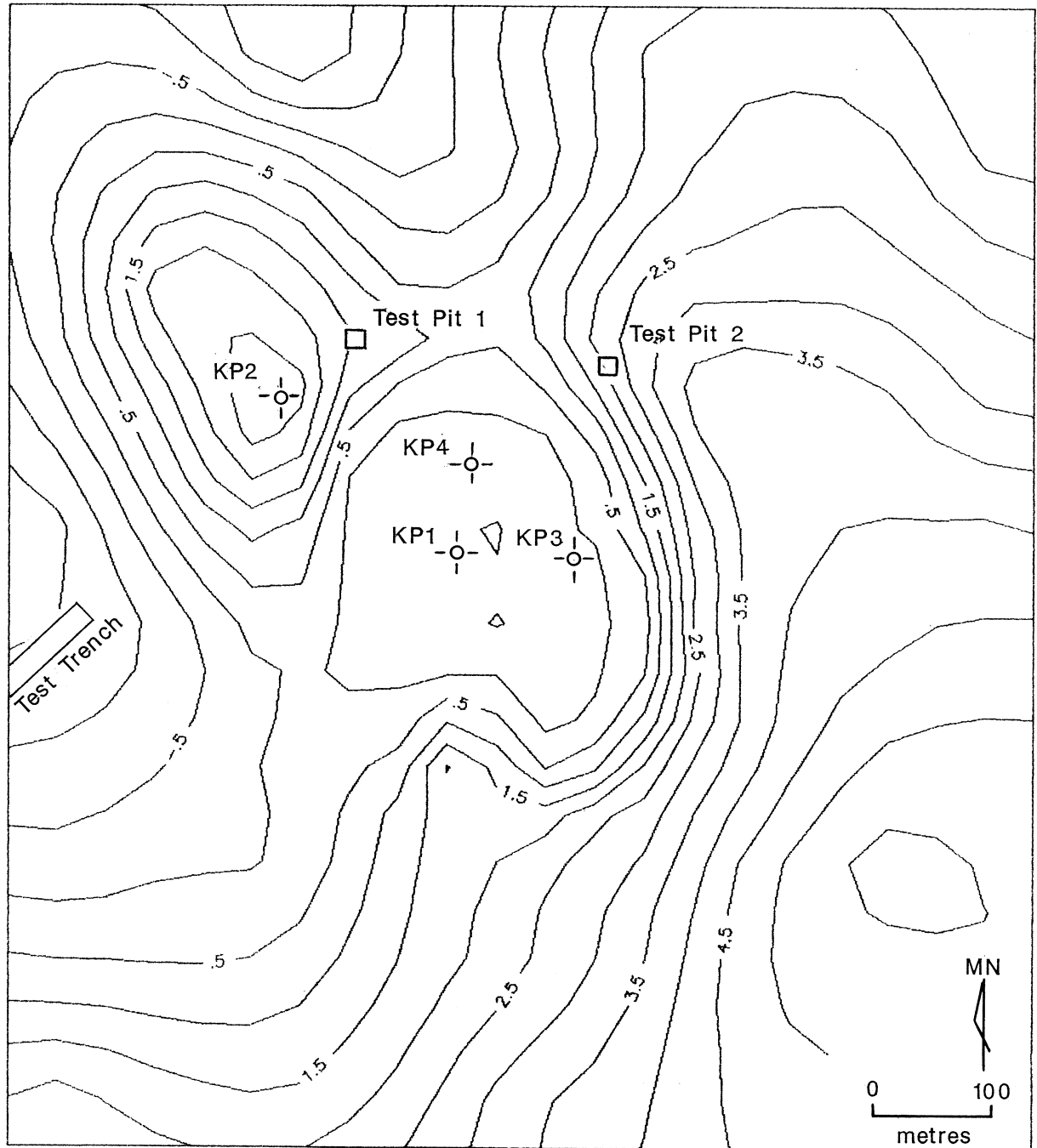
The contoured data sets in this study are shown in the following Figures;

Kings Plains Lagoon

Fig. A3-1	elevation,	contour interval 0.5 metres
Fig. A3-2	gravity,	contour interval $0.5 \mu\text{ms}^{-2}$
Fig. A3-3	magnetics,	contour interval 50 nanoteslas (nT)
Fig. A3-7	elevation,	a 3-D perspective
Fig. A3-8	gravity,	a 3-D perspective
Fig. A3-9	magnetics	a 3-D perspective

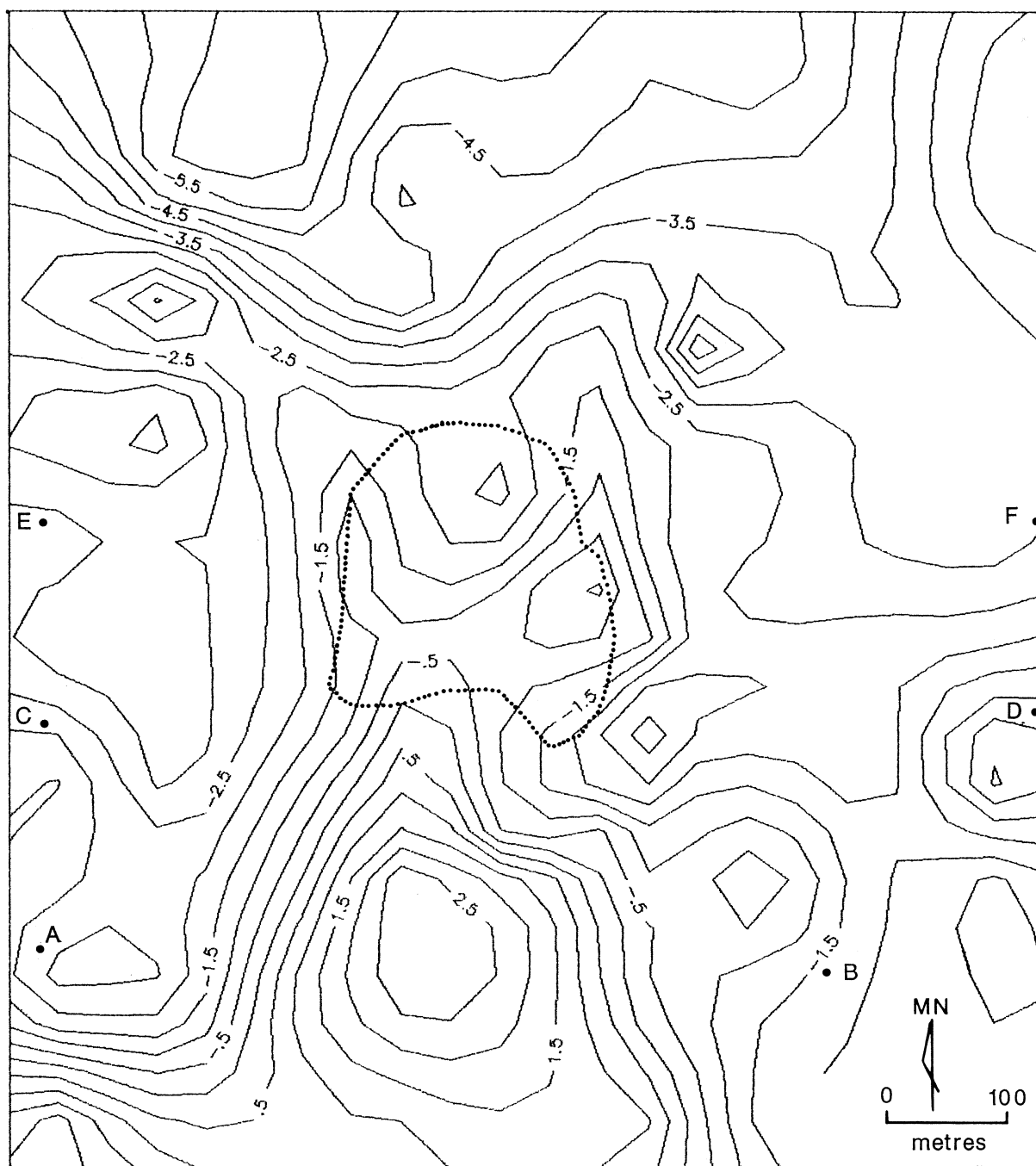
Dunvegan Lagoon

Fig. A3-4	elevation,	contour interval 0.5 metres
Fig. A3-5	gravity,	contour interval $0.5 \mu\text{ms}^{-2}$
Fig. A3-6	magnetics,	contour interval 200 nT



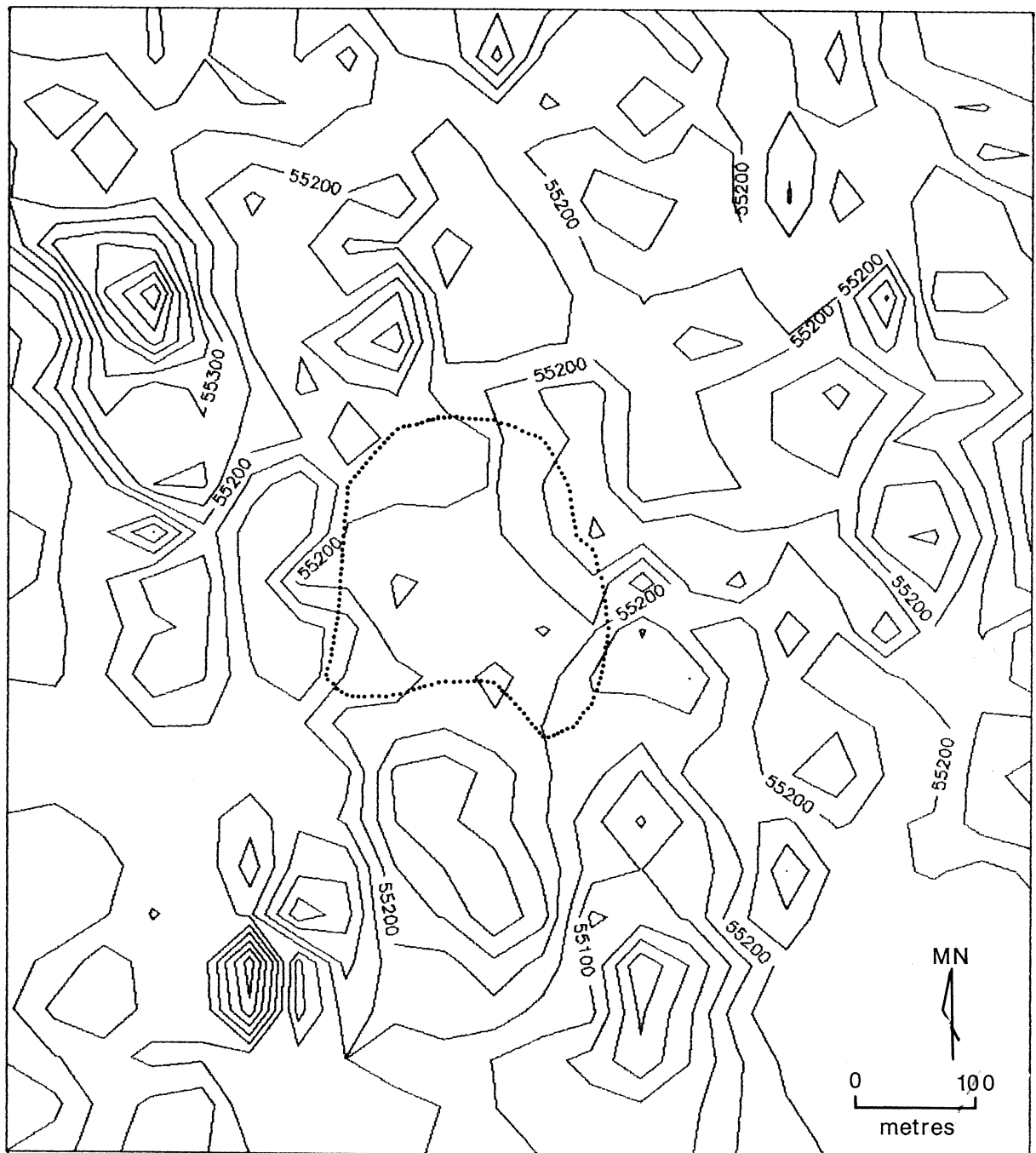
KINGS PLAINS ELEVATION

Figure A3-1. Kings Plains Lagoon geophysical survey area. Elevation is in metres with a contour interval of 0.5 metres. The location of holes KP1, KP2, KP3 & KP4, test pits 1 & 2 and the test trench are shown. The shoreline of the lagoon corresponds to the zero metre contour.



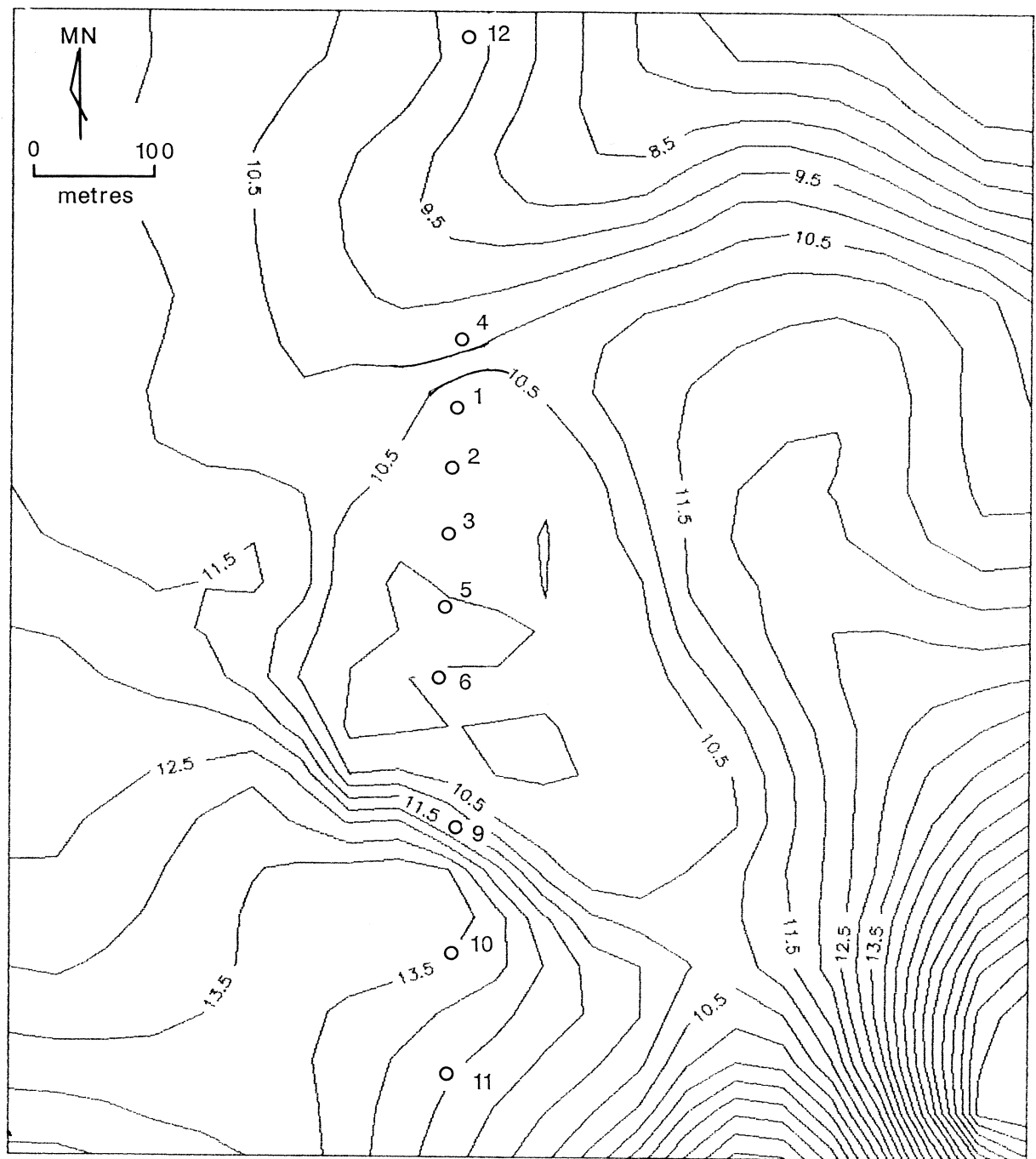
KINGS PLAINS GRAVITY 2300

Figure A3-2. Kings Plains Lagoon geophysical survey area. Gravity is in μms^{-2} with a contour interval of $0.5 \mu\text{ms}^{-2}$ (note, $1 \mu\text{ms}^{-2} = 0.1 \text{ mGal}$). Location of gravity profile lines AB CD & EF used for modelling are shown. The lagoon outline is shown dotted.



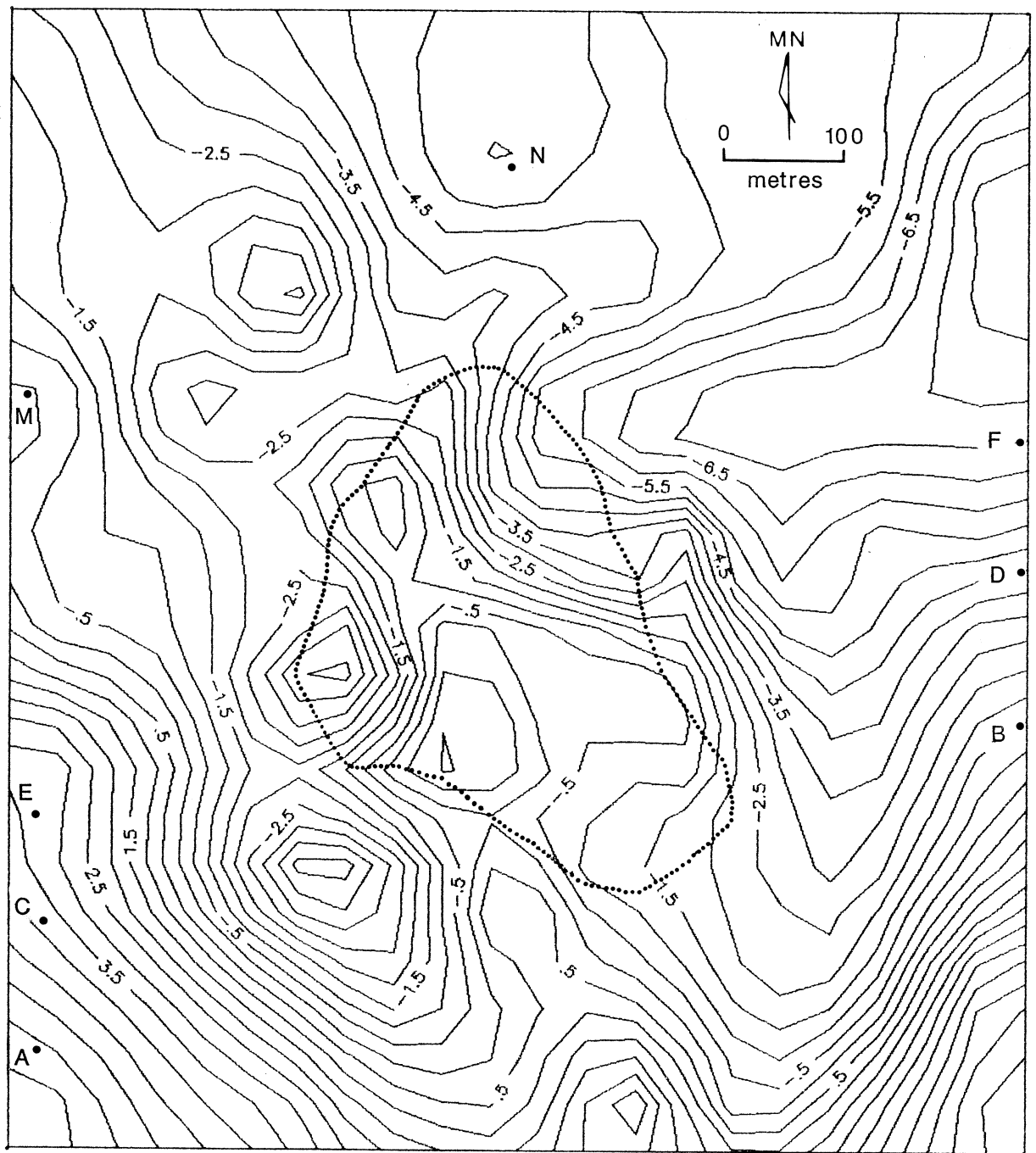
KINGS PLAINS MAGNETICS

Figure A3-3. Kings Plains Lagoon geophysical survey area. Magnetic intensity is in nanoteslas with a contour interval of 50 nT. The lagoon outline is shown dotted.



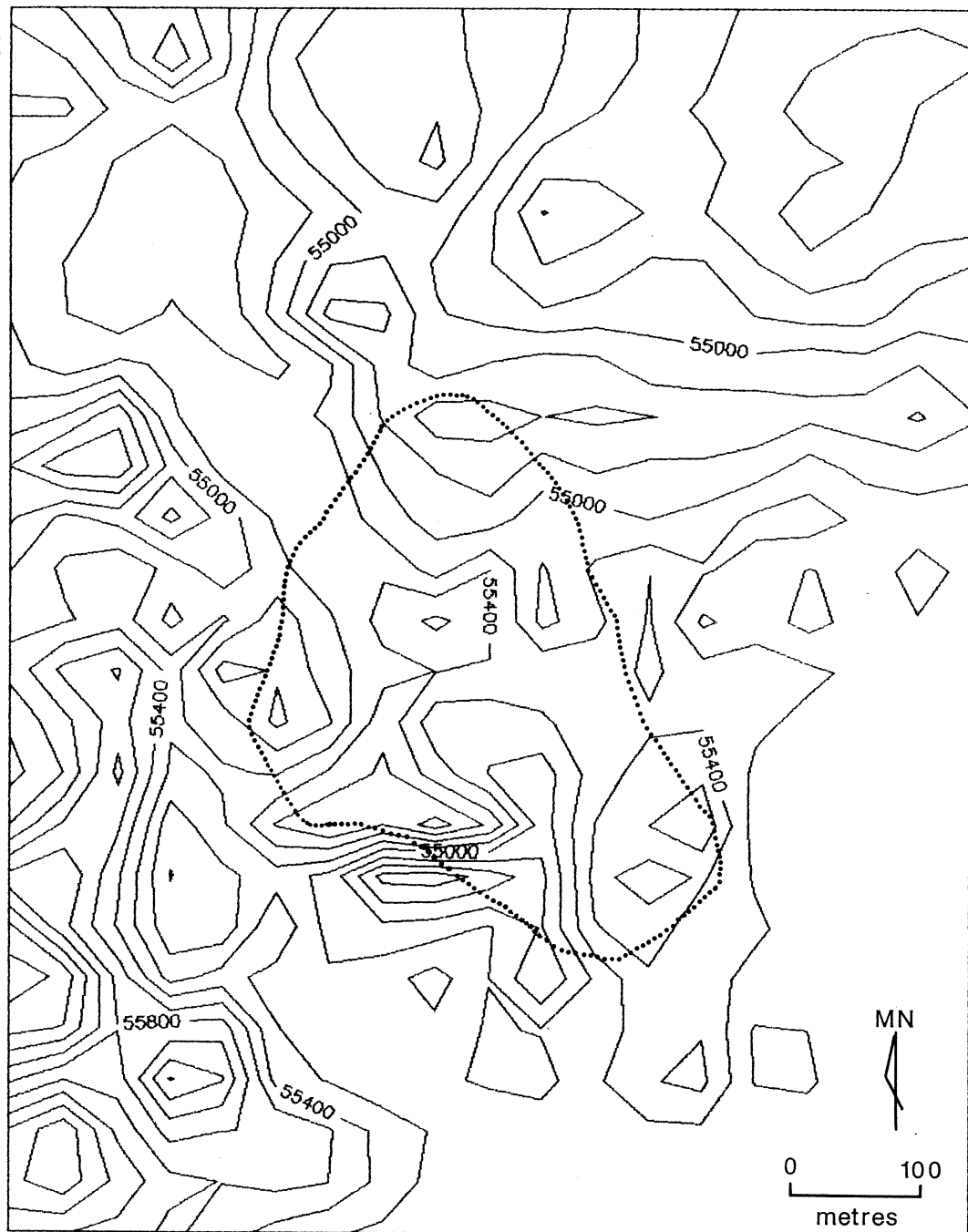
DUNVEGAN ELEVATION

Figure A3-4. Dunvegan Lagoon geophysical survey area. Elevation is in metres with a contour interval of 0.5 metres. The location of shallow test holes are shown. The shoreline of the lagoon corresponds to the 10.5 metre contour



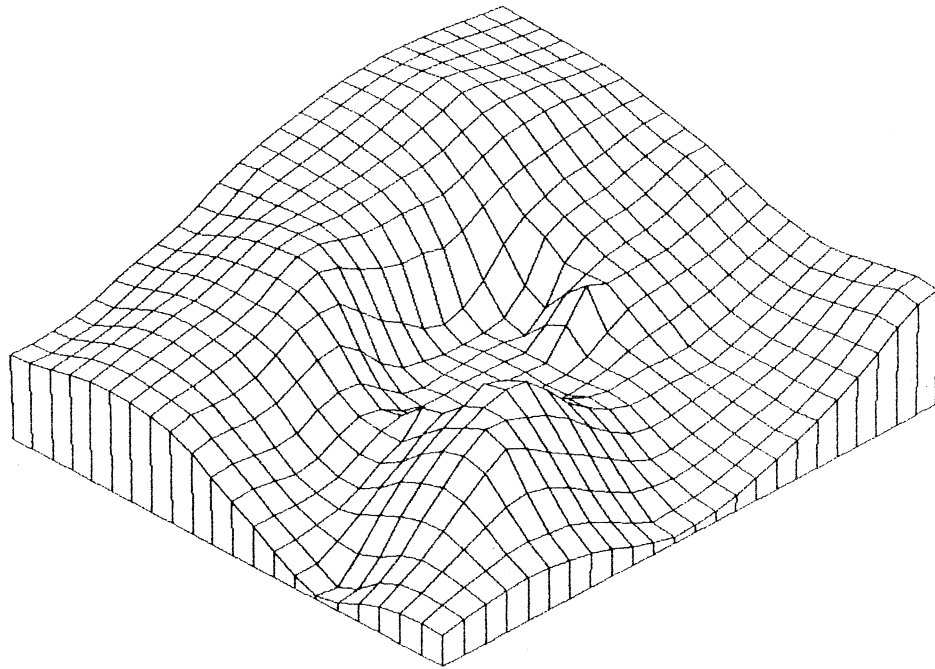
DUNVEGAN GRAVITY 2300

Figure A3-5. Dunvegan Lagoon geophysical survey area. Gravity is in μms^{-2} with a contour interval of $0.5 \mu\text{ms}^{-2}$ (note, $1 \mu\text{ms}^{-2} = 0.1 \text{ mGal}$). Location of gravity profile lines AB, CD, EF & MN used for modelling are shown. The lagoon outline is shown dotted.

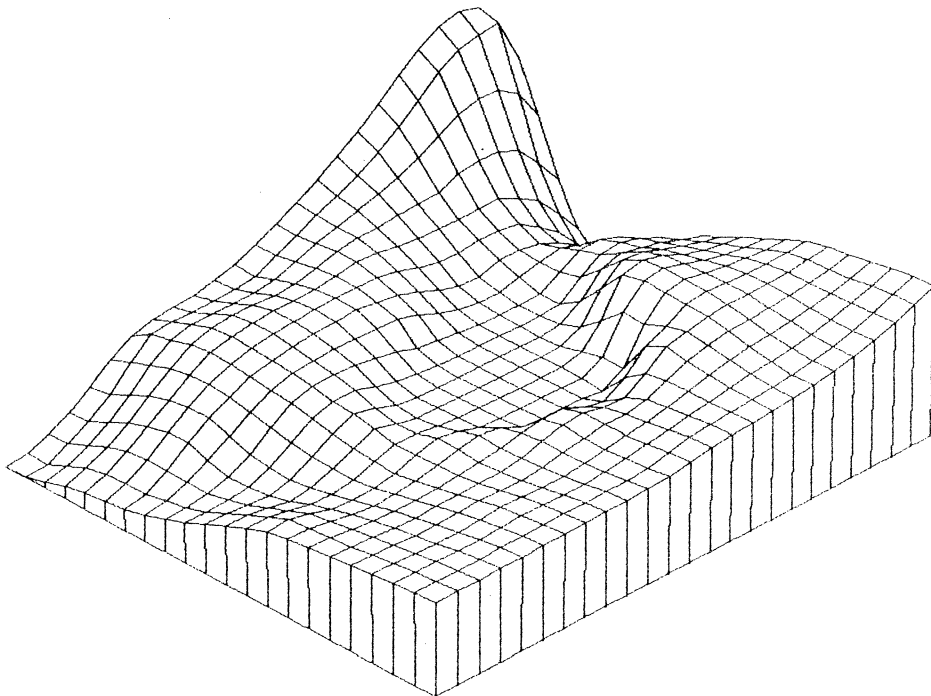


DUNVEGAN MAGNETICS

Figure A3-6. Dunvegan Lagoon geophysical survey area. Magnetic intensity is in nanoteslas with a contour interval of 200 nT. The lagoon outline is shown dotted.

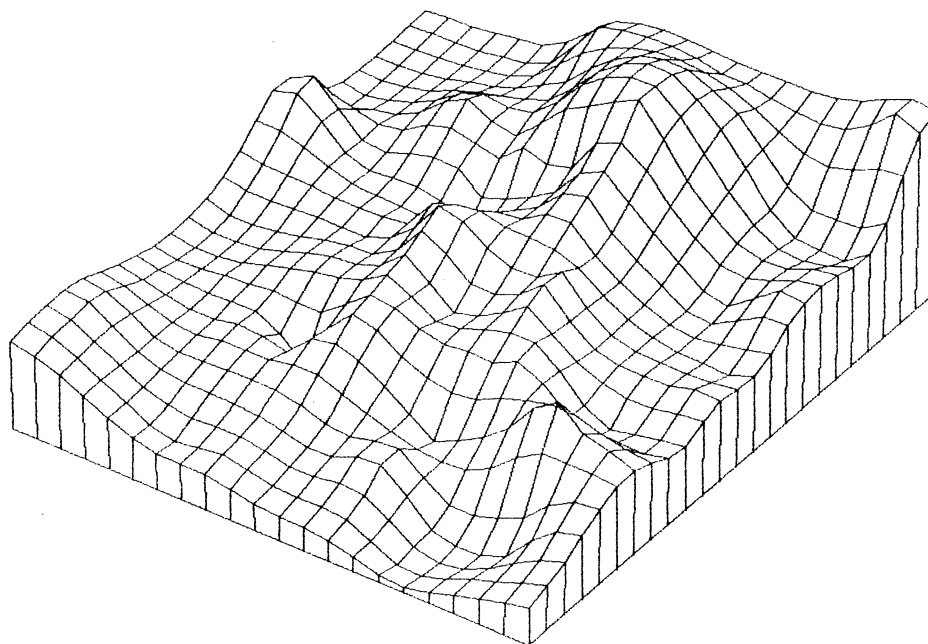


KINGS PLAINS ELEVATION

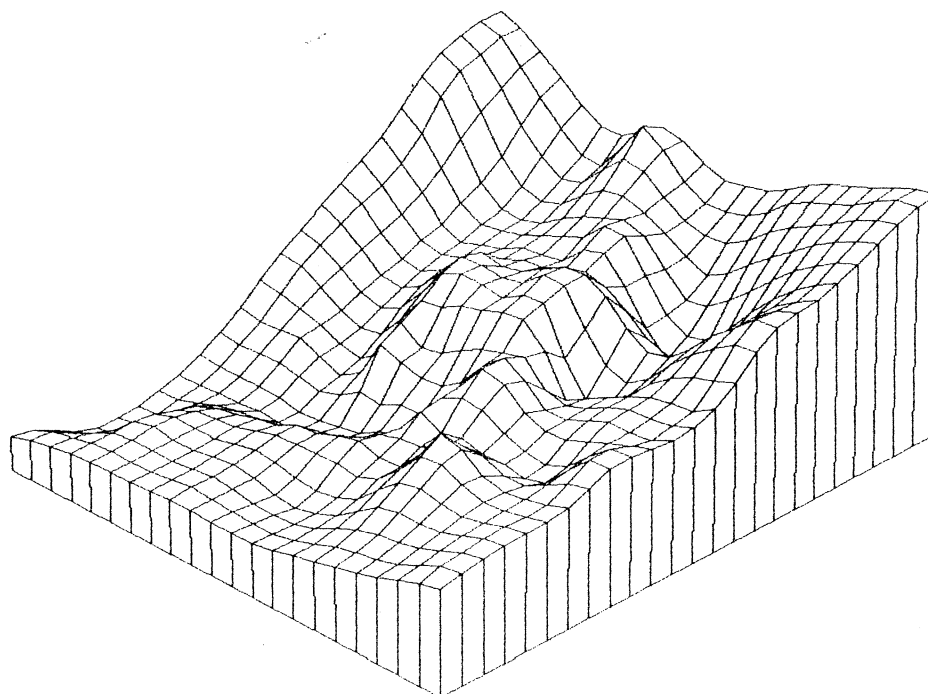


DUNVEGAN ELEVATION

Figure A3-7. Three dimensional representation of the elevation data for Kings Plains and Dunvegan lagoons presented as an aerial view from N45°W.

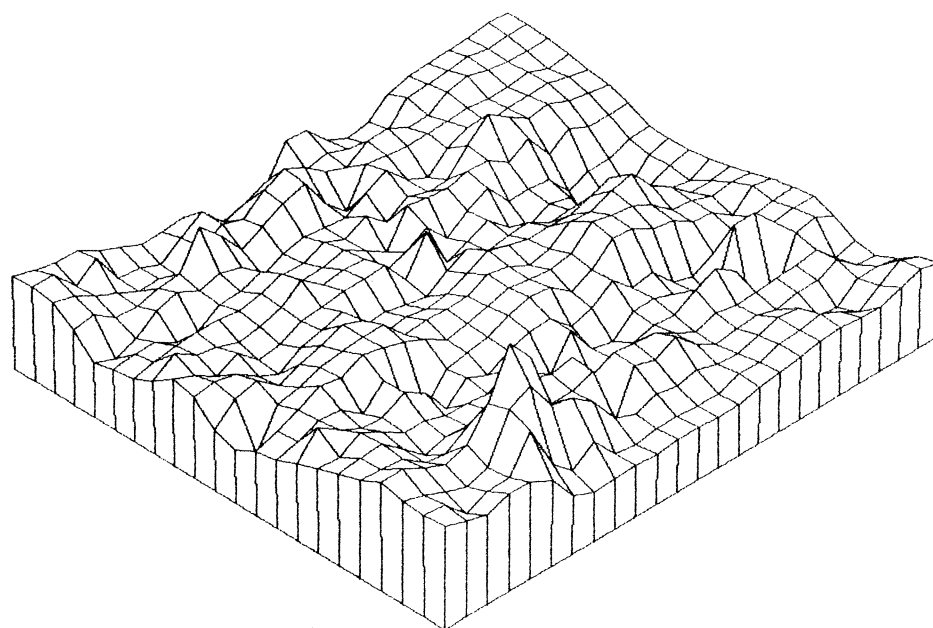


KINGS PLAINS GRAVITY

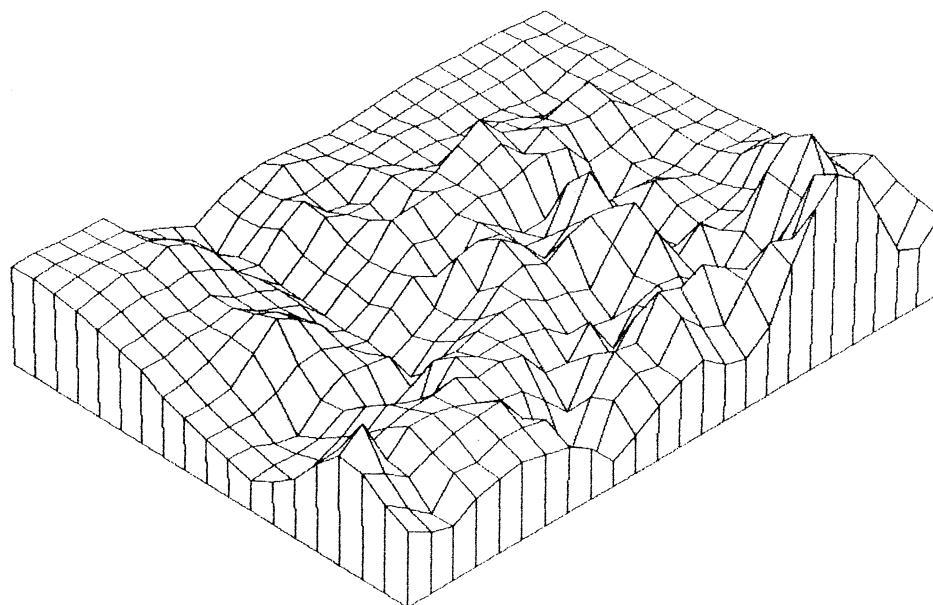


DUNVEGAN GRAVITY

Figure A3-8. Three dimensional representation of the gravity data for Kings Plains and Dunvegan lagoons presented as an aerial view from N45°W.



KINGS PLAINS MAGNETICS



DUNVEGAN MAGNETICS

Figure A3-9. Three dimensional representation of the magnetic field data for Kings Plains and Dunvegan lagoons presented as an aerial view from N45°W.

Fig. A3-7	elevation,	a 3-D perspective
Fig. A3-8	gravity,	a 3-D perspective
Fig. A3-9	magnetics	a 3-D perspective

The advantages of a comparison of data sets over two similar structures are that subtle, almost unnoticeable, features on one may be better visible on the other. Figures A3-1, A3-4 & A3-7 show that Kings Plains and Dunvegan Lagoons are remarkably similar in appearance. Dunvegan Lagoon is approximately twice the area of Kings Plains and elongated in a NNW/SSE direction. Both gravity data sets (Fig. A3-8), show a gravity high over the lagoon area nested in a broader regional gravity low, particularly well demonstrated by the Dunvegan data. The anomaly associated with Dunvegan Lagoon is approximately twice as large in amplitude, that is $8 \mu\text{ms}^{-2}$ as compared with the $4 \mu\text{ms}^{-2}$ at Kings Plains (Figs. A3-2 & A3-5). The gravity high appears to be part of a throughgoing gravity ridge, particularly prominent on the Dunvegan data. At Dunvegan, the gravity ridge trends about N20°W, which corresponds to the long axis of the topographic feature and is in direct line with Clarevaux Lagoon, 2 kilometres to the NNW.

A prominent gravity low or "dimple" in the central and northern portion of the Kings Plains Lagoon area is superimposed on the broad gravity high (Fig. A3-2 & A3-8) and appears to reflect the presence of the lower density lacustrine clays in the lagoon, as will be discussed later. A "dimple" is also present in the Dunvegan gravity data towards the northern portion of the lagoon area, but is less obvious.

The magnetics data (Figs. A3-3 & A3-6), although more variable and erratic owing to near surface noise, appear to correspond to the gravity features. At Dunvegan a magnetic high (Fig. A3-6) supports the linear trends observed in the gravity data. The magnetic anomalies at Dunvegan are some 3 to 4 times as large as those at Kings Plains. The Kings Plains magnetics have a large amount of near surface interference, probably due to the ironstone. The gravity and magnetic highs immediately to the south of Kings Plains Lagoon (Figs. A3-2 & A3-3) reflect the presence of a surface basalt flow here.

The seismic refraction data indicate that the areas have between 1 to 2 m of unconsolidated sediments, (velocity 250 to 500 ms⁻¹). Below these soils, more consolidated material, (velocity 750 to 1150 ms⁻¹), extends to a depth of about 5 to 9 m, which in turn sits on weathered basalt (velocity 2000 to 4200 ms⁻¹). Although it is not a good idea to generalize from only 7 refraction spreads, the layer 3 velocities seem to be higher at Dunvegan Lagoon, 2800-4200 ms⁻¹, as compared with 1900-3000 ms⁻¹ at Kings Plains. This suggests that the shallow basalts are less weathered at Dunvegan Lagoon than at Kings Plains.

A3.4 Geophysical Modelling

Profiles at locations shown on Figures A3-2 and A3-5 were selected for modelling using a Fortran program for generalized linear inversions of gravity and magnetic profiles (Webring, 1985).

Three profiles were chosen at Kings Plains and four at Dunvegan. They were selected to be at right angles to the observed geophysical strike.

A smooth regional gravity field, also cross-smoothed between profile lines, was subtracted from each profile in order to remove wavelengths broader than the topographic feature. An attempt was also made to model this regional field.

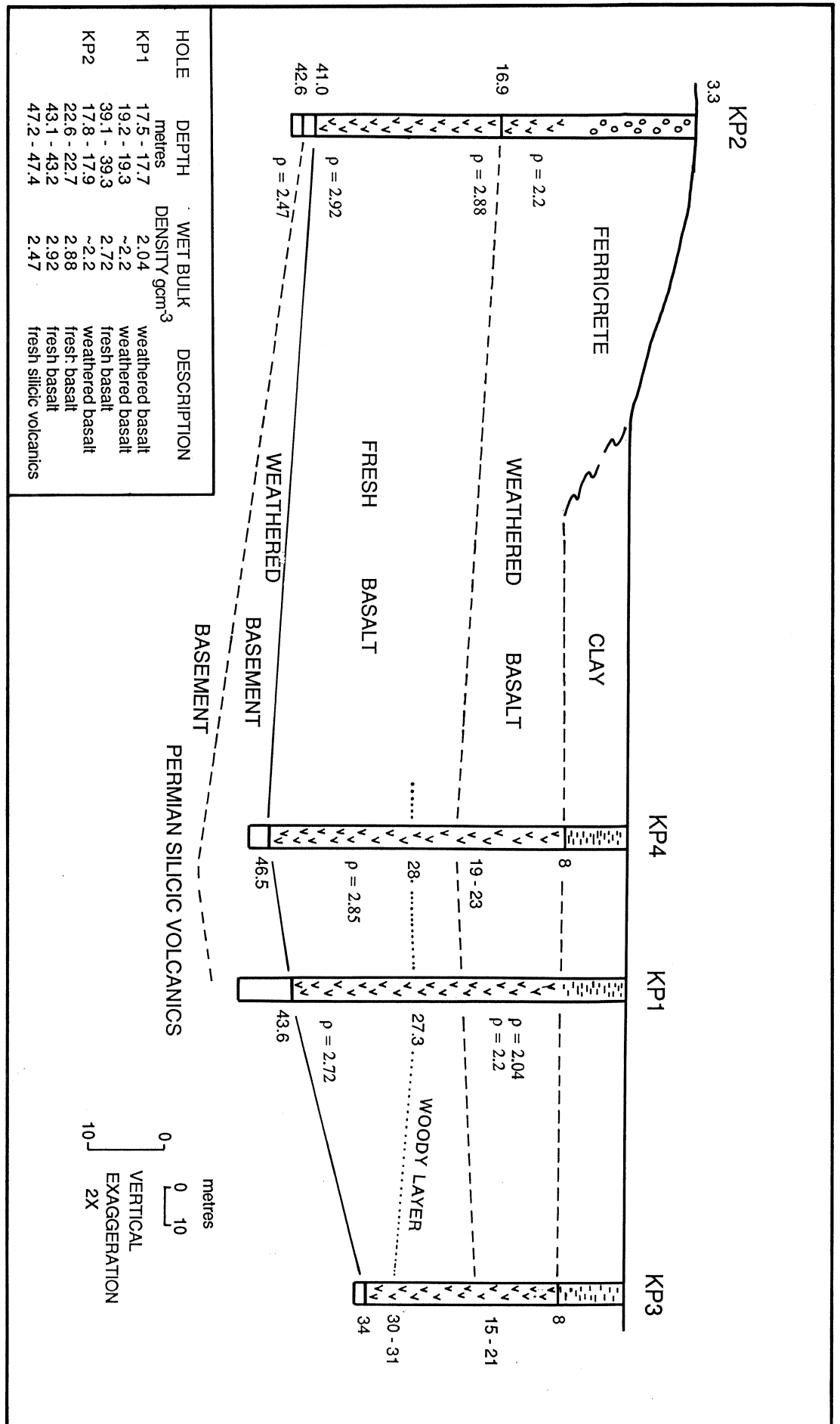
A3.4.1 Setting up the Model

A model consisting of 3 layers; weathered basalt, fresh basalt and Permian basement was designed, based on the data from diamond drill holes KP1 and KP2 at Kings Plains. Densities for each layer were determined from dry bulk density and apparent porosity measurements of representative samples from the drill core (courtesy D. Emerson of Sydney University). The data are included in Figure A3-10.

One of the aims of the geophysical surveying was to assess the existence of a feeder pipe or pipes below the topographic feature, thus the gravity anomalies were modelled as simple dykes penetrating the plane layered model. A dyke of uniform density penetrating a stack of layers of different density may be modelled as a stack of blocks of different density contrast as shown in Figure A3-11, part A. For example, a basalt dyke of density 2810 kgm^{-3} penetrating soil of density 2200 kgm^{-3} is modelled as a block of 610 kgm^{-3} positive density contrast. Basalt penetrating basalt has a contrast of zero. Figure A3-12 is an example of a final model that satisfies the observed field data for profile EF.

The drilling of holes KP3 and KP4 showed this simple model to be invalid. KP3 intersected basement 10 m shallower than expected, KP4 intersected basement 4 m deeper and both failed to encounter any pipes or brecciated material.

A new, more complex model had to be developed for Kings Plains based on variations in layer thicknesses and densities and using the data from all four drill holes. The drill hole data is summarized in Figure A3-10. The depth of weathering of the basalt and the depth to the Permian basement were allowed to vary. An extra surface layer representing the lower density lacustrine claypan and surrounding sediments was introduced to partially account for the dimple in the top of the gravity high. The model is shown in Figure A3-11 part B. For simplicity of modelling, the density of the weathered basalt was set equal to that of the Permian silicic volcanics, thus enabling the fresh basalt to be modelled as a single body of positive density contrast to its surroundings. The lacustrine clay in the lagoon was modelled as a body of negative density contrast with respect to the sediments around it. The densities of the different materials were held constant from profile to profile within each survey area during the modelling exercise.



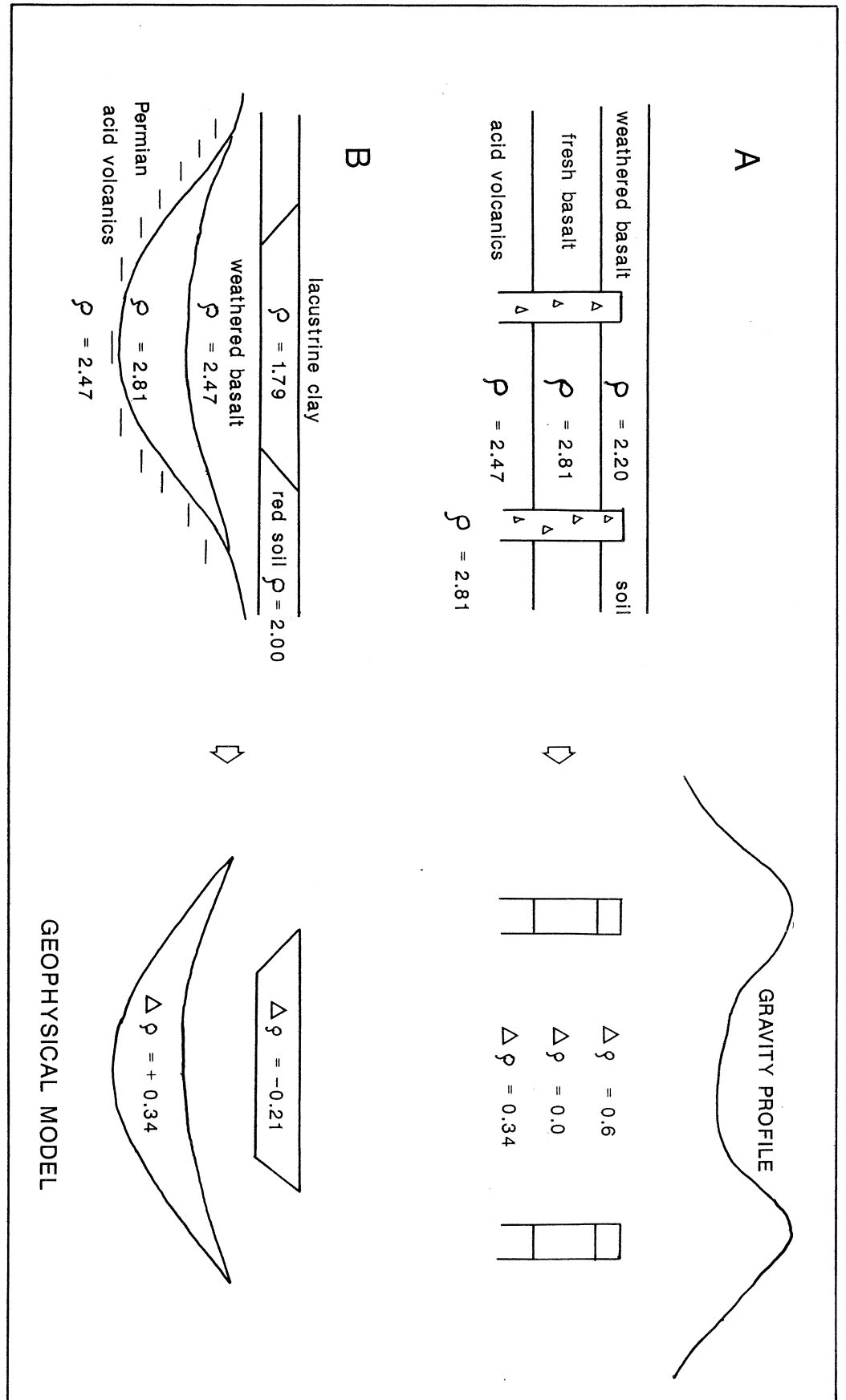


Figure A3-11. Initial gravity models designed to satisfy profile EF at Kings Plains. Model A is 2 dykes intruding a layered medium. Model B is channel flow basalt. Density contrasts are used for geophysical modelling as shown on the right hand side of the diagram. In case A, the density contrasts are given relative to the fresh basalt of density 2470 kgm^{-3} . In case B, the contrasts are relative to the silicic volcanics ($\rho = 2470 \text{ kgm}^{-3}$) in the lower part of the model and with respect to the red soil ($\rho = 2000 \text{ kgm}^{-3}$) in the upper part of the model.

KINGS PLAINS GRAVITY PROFILE EF

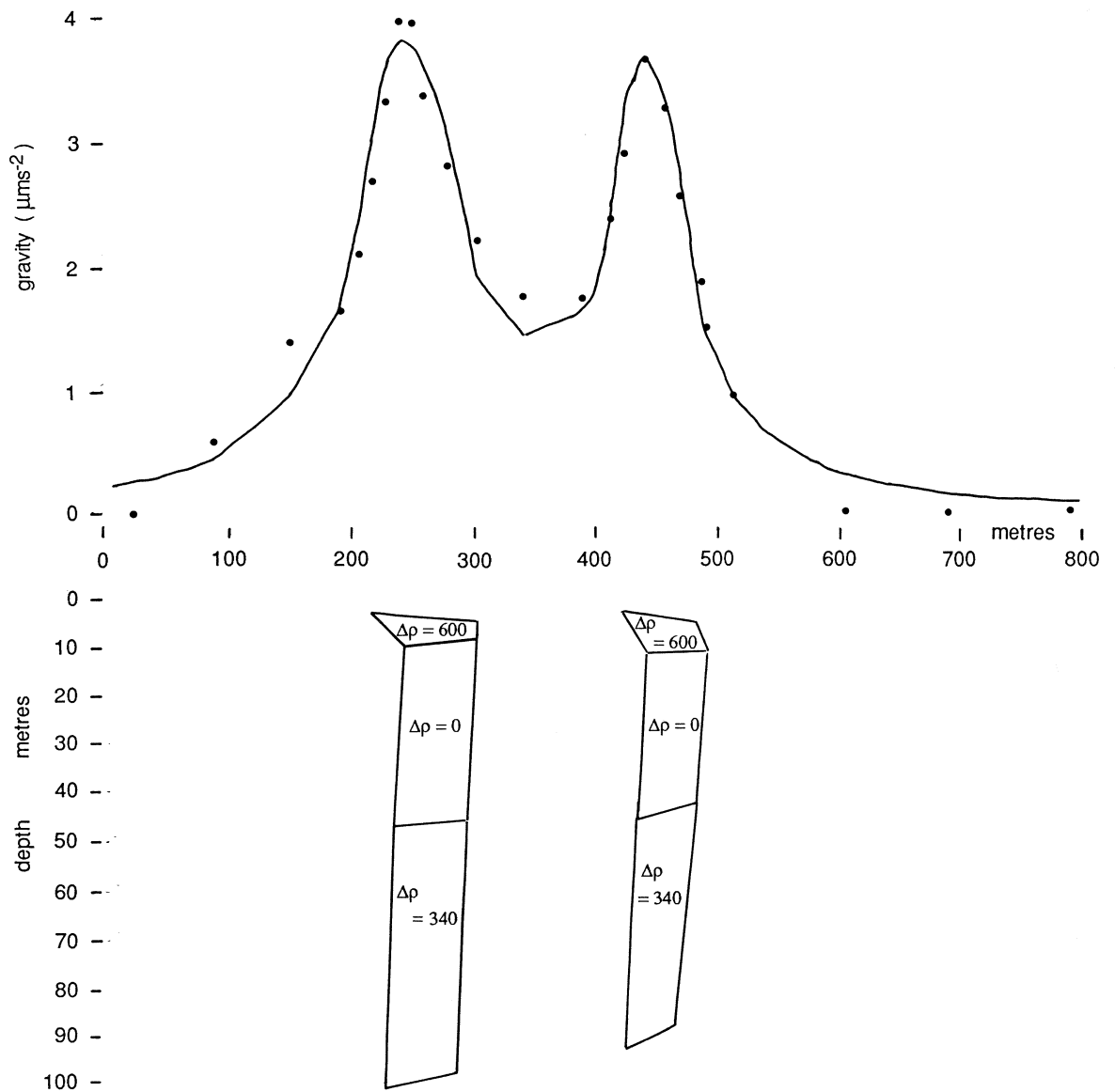


Figure A3-12. Example of a final model satisfying the observed gravity data for profile EF at Kings Plains. The model represents 2 dykes penetrating a layered medium as shown in Fig. A3-11 part A. Observed gravity values are shown as dots and the solid line is the model field. Drilling proved this model to be invalid.

A3.4.2 The Modelling Results

Figures A3-13, A3-14 and A3-15 show final models that satisfy the observed gravity data for the Kings Plains profiles AB, CD and EF and support the hypothesis that a depression in the basement, filled with fresh basalt, is responsible for the broad gravity high. The gravity high is flat-topped, as can be seen in profile EF, owing to a deepening in the level of weathering of the top of the basalt coincident with the axis of the basement channel. The dimple in the top of the gravity high is due to the slightly lower density lacustrine clays filling the lagoon.

The gravity high to the south of Kings Plains Lagoon is coincident with fresh basalt observed on the surface. Profiles AB and CD are affected by this basalt flow and may be modelled with a similar configuration as used in EF, except with a thin surface sheet of fresh basalt creating the extra gravity high.

A similar model was used for the Dunvegan gravity data. Figures A3-16, A3-17, A3-18 & A3-19 show models which fit the observed data for Dunvegan profiles AB, CD, EF and MN. The larger positive gravity anomaly at Dunvegan Lagoon requires, firstly, that the fresh basalts have a slightly higher density contrast (440 kgm^{-3} as opposed to 340 kgm^{-3}), secondly, a deeper Permian basement beneath the topographic structure (60 m as opposed to 46 m) and thirdly, a shallower depth of weathering. The less pronounced dimple on the top of the gravity high requires that the lacustrine sediments are not as thick here.

An attempt was made to explain the longer wavelength regional gravity field which was removed from the data. Kings Plains profile CD was used for this purpose and the model shown in Figure A3-20. The regional field is satisfied by decreasing the basement density by 10 kgm^{-3} in a series of steps, to a minimum under the deepest point. A geological explanation for this is based on the observation that Permian basement channels are localized or controlled by planes of structural weakness. Fracturing and deeper weathering would be expected along these zones which would lower the bulk rock density of the basement.

A3.5 Conclusion

a/ The presence of feeder pipes below the topographic structures is not required by the geophysical data and furthermore, such pipes have not been found by the drilling programme at Kings Plains designed to encounter them. In fact, drilling at Kings Plains did not encounter any material that could be described as brecciated (Coenraads, 1988a).

b/ The geophysical anomalies do not require any unusual aberrations in the channel floor morphology. This is illustrated in the block diagrams (Figs. A3-21 & A3-22) showing sections of the basalt filled channels modelled across the geophysical survey areas. Differences between the gravity profiles were accommodated by minor changes in

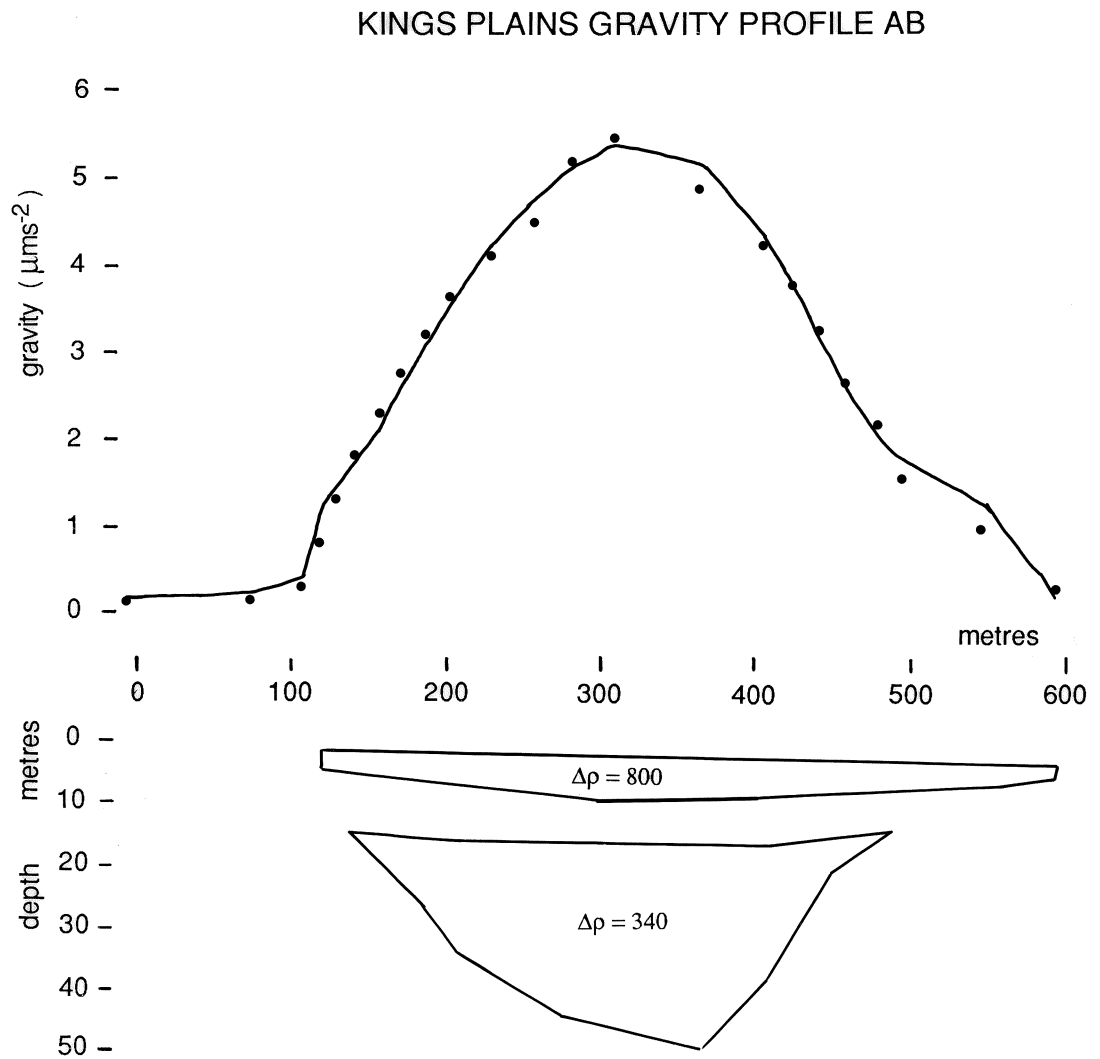


Figure A3-13. A final model satisfying the observed gravity data for profile AB at Kings Plains. The lower polygon represents a basalt flow ($\rho = 2810 \text{ kgm}^{-3}$) in a Permian basement channel ($\rho = 2000 \text{ kgm}^{-3}$) giving a positive density contrast of 340 kgm^{-3} . The upper polygon represents a surface basalt sheet ($\rho = 2800 \text{ kgm}^{-3}$) that has flowed over sediments giving a positive contrast of 800 kgm^{-3} . Observed gravity values are shown as dots and the solid line is the model field.

KINGS PLAINS GRAVITY PROFILE CD

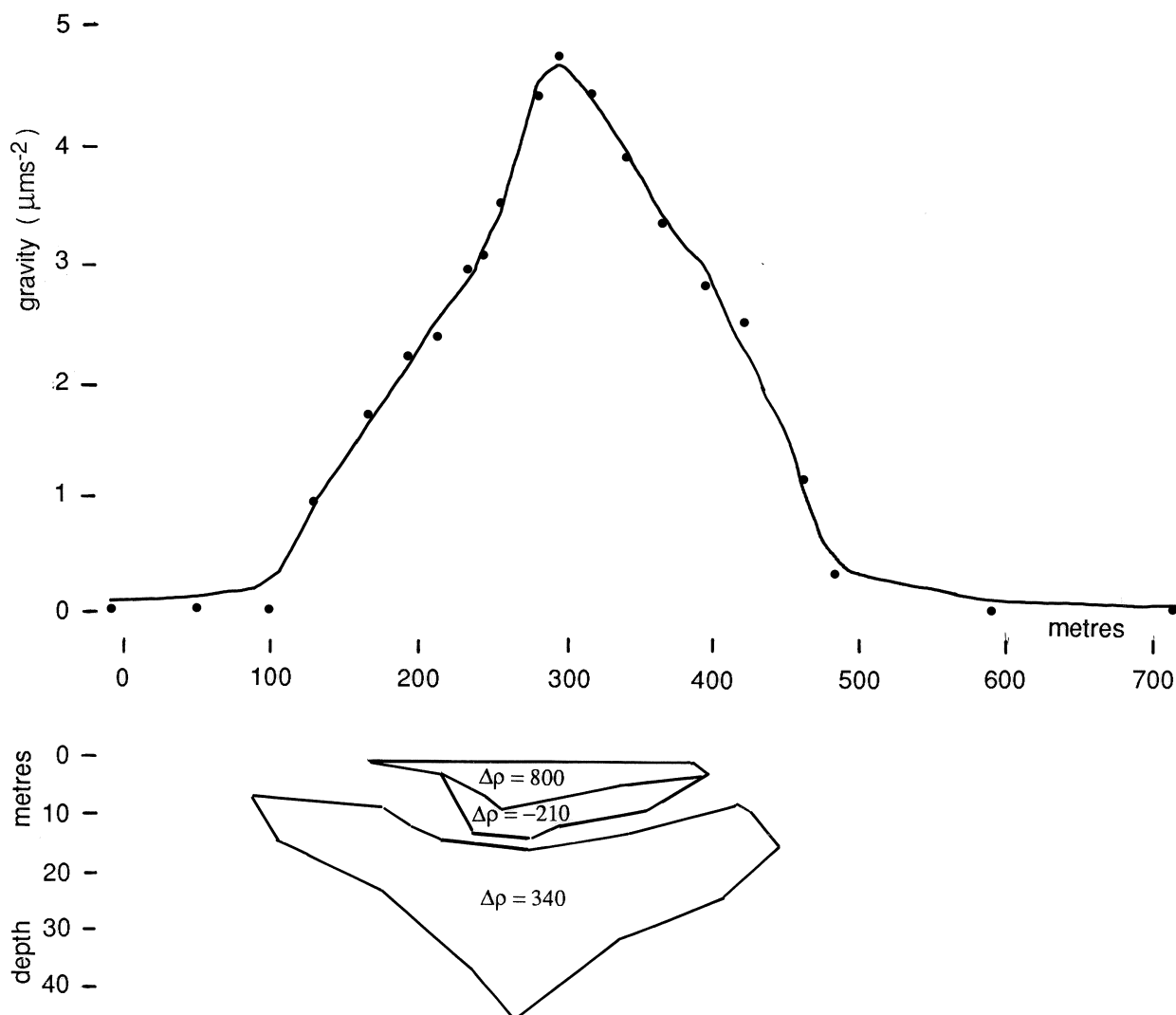


Figure A3-14. A final model satisfying the observed gravity data for profile CD at Kings Plains. The lower polygon represents a basalt flow ($\rho = 2810 \text{ kgm}^{-3}$) in a Permian basement channel ($\rho = 2000 \text{ kgm}^{-3}$) giving a positive density contrast of 340 kgm^{-3} . The upper polygon represents a surface basalt sheet ($\rho = 2800 \text{ kgm}^{-3}$) that has flowed over sediments giving a positive contrast of 800 kgm^{-3} . In this profile the flows also cover the lagoon clays ($\rho = 1790 \text{ kgm}^{-3}$) which is represented by the middle polygon with a negative density contrast of 210 kgm^{-3} . Observed gravity values are shown as dots and the solid line is the model field.

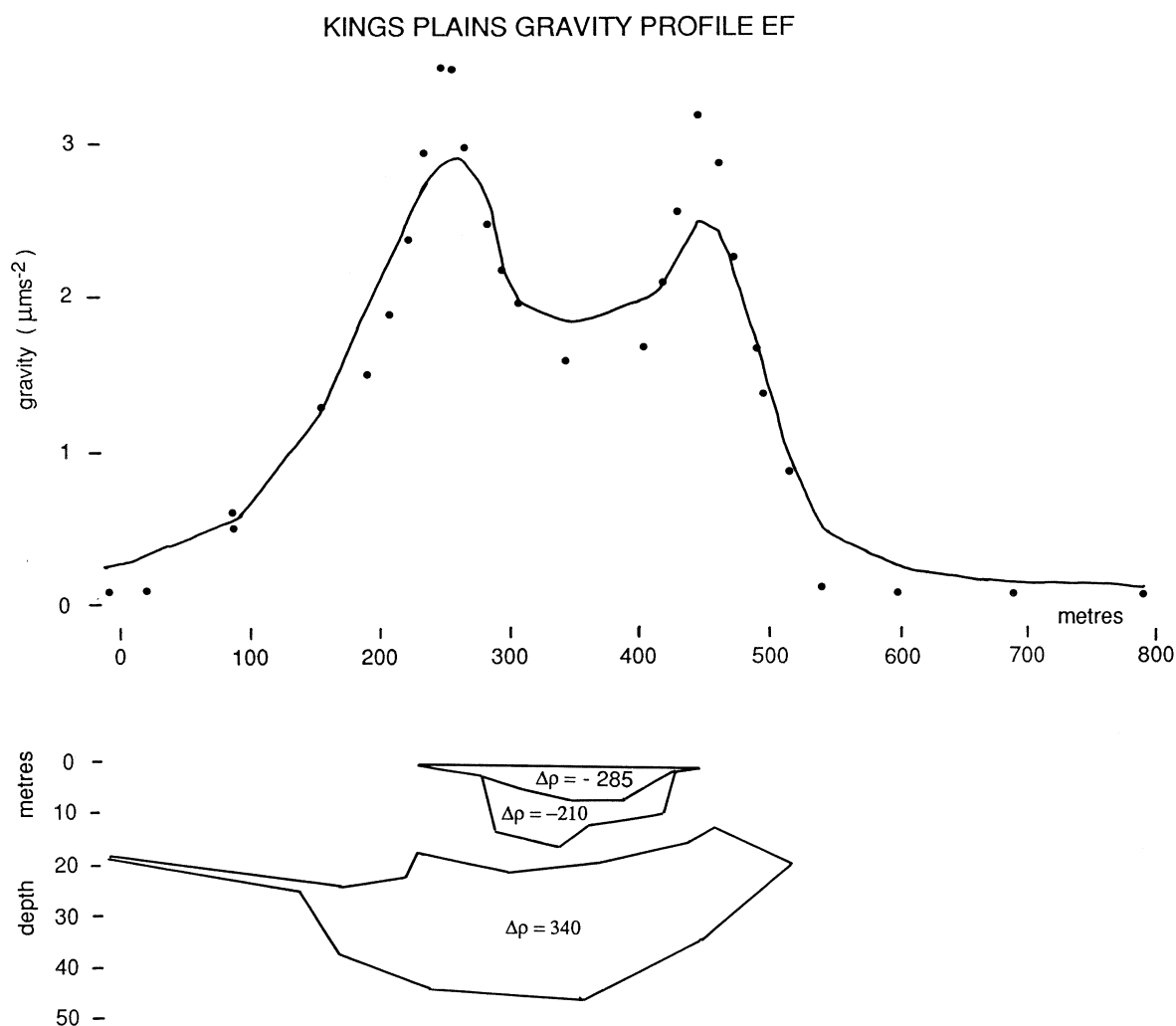


Figure A3-15. A final model satisfying the observed gravity data for profile EF at Kings Plains. The lower polygon represents a basalt flow ($\rho = 2810 \text{ kgm}^{-3}$) in a Permian basement channel ($\rho = 2000 \text{ kgm}^{-3}$) giving a positive density contrast of 340 kgm^{-3} . The upper polygons represent the lagoon sediments ($\rho = 1790 \text{ kgm}^{-3}$ below and 1715 kgm^{-3} above the water table) which have negative density contrasts of 210 kgm^{-3} and 285 kgm^{-3} with respect to the surrounding sediments. The depths and density values used in this model have been constrained by core logging and measurements made on the material recovered. Observed gravity values are shown as dots and the solid line is the model field.

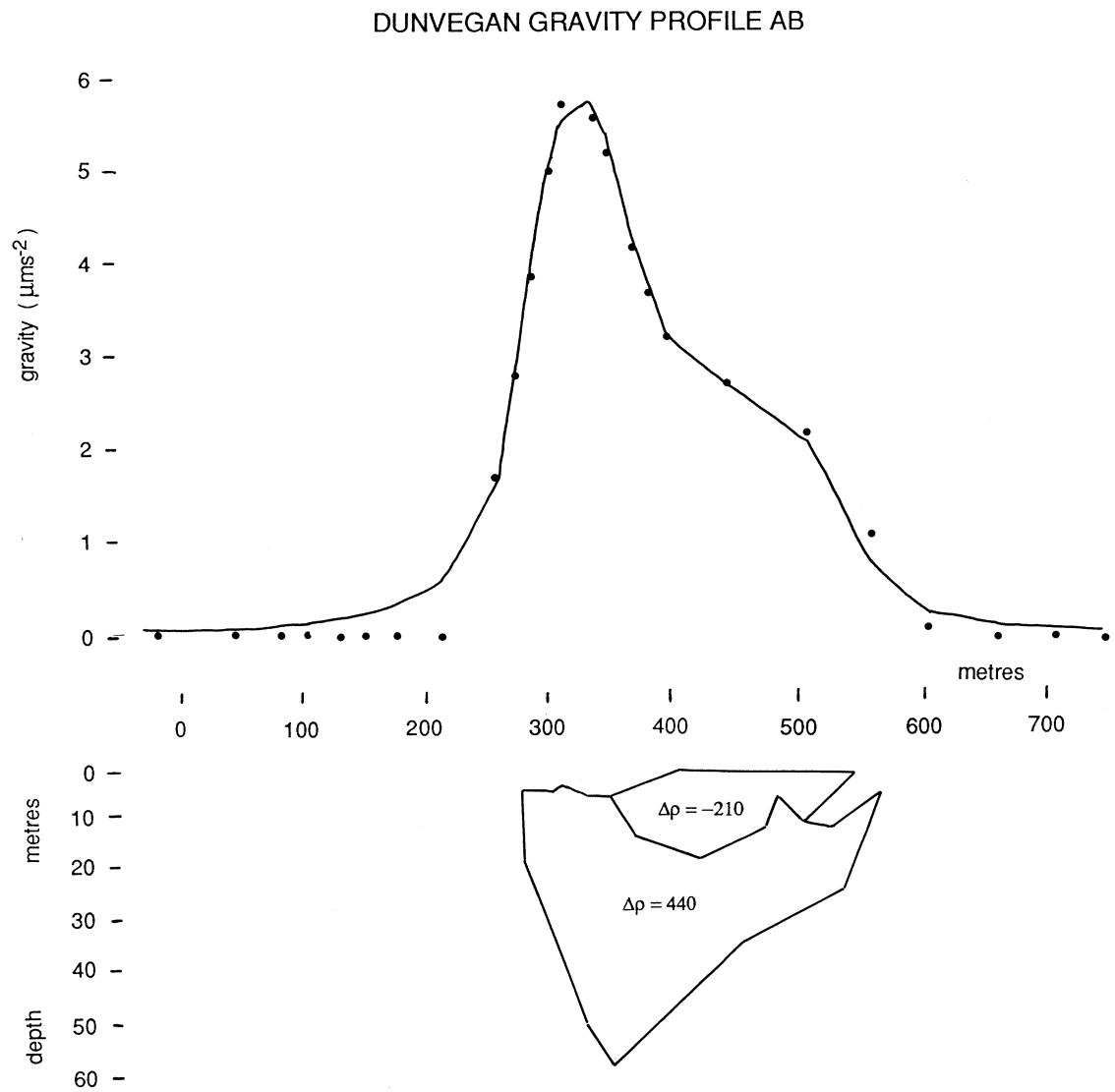


Figure A3-16. A final model satisfying the observed gravity data for profile AB at Dunvegan Lagoon. The lower polygon represents a basalt flow in a Permian basement channel. A density contrast of 440 kgm^{-3} is required between the basalts and the basement in this model. The upper block represents the lagoon sediments which are modelled with a negative contrast of 210 kgm^{-3} with respect to the surrounding sediments. Observed gravity values are shown as dots and the solid line is the model field.

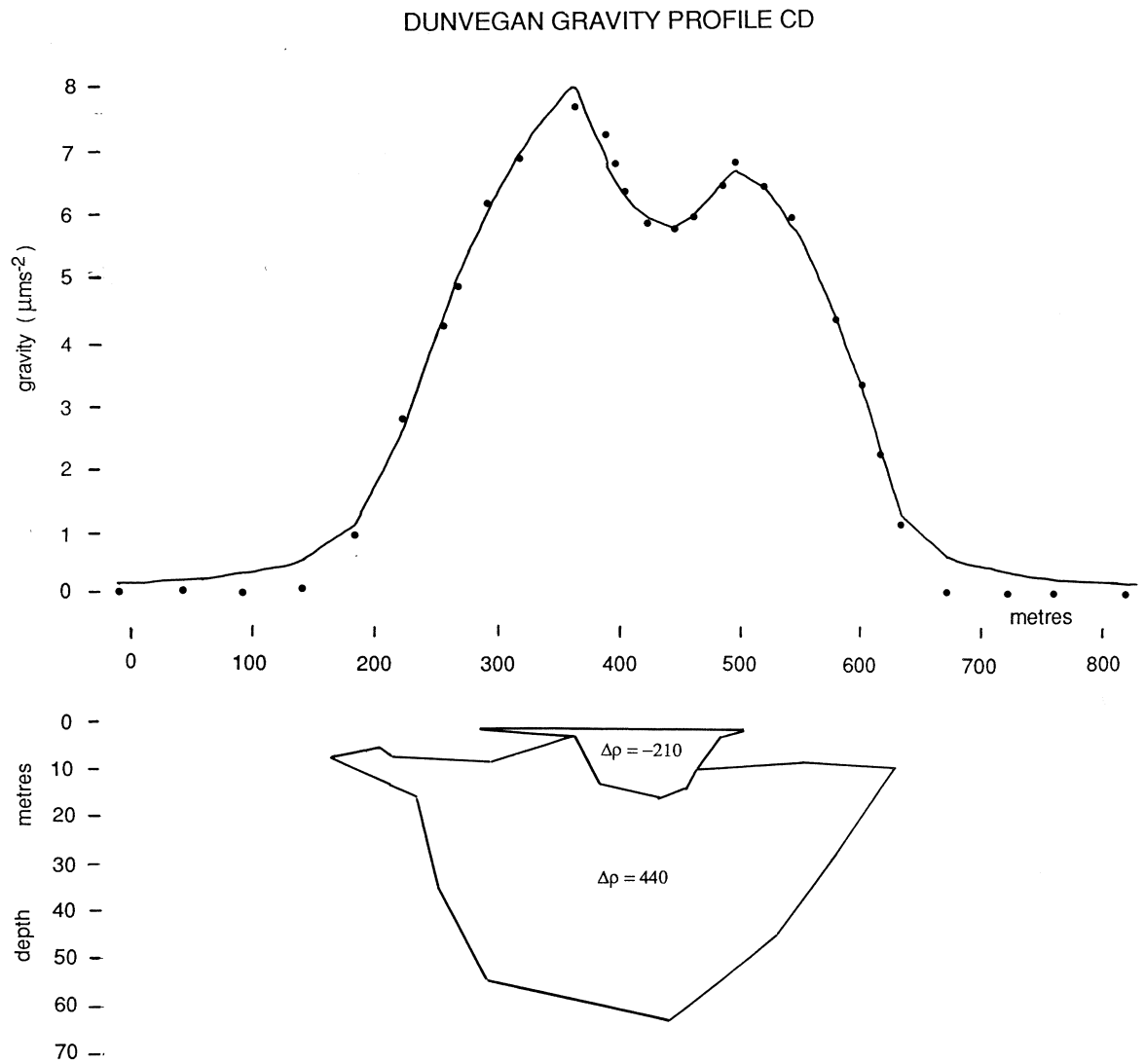


Figure A3-17. A final model satisfying the observed gravity data for profile CD at Dunvegan Lagoon. The lower polygon represents a basalt flow in a Permian basement channel. A density contrast of 440 kgm^{-3} is required between the basalts and the basement in this model. The upper block represents the lagoon sediments which are modelled with a negative contrast of 210 kgm^{-3} with respect to the surrounding sediments. Observed gravity values are shown as dots and the solid line is the model field.

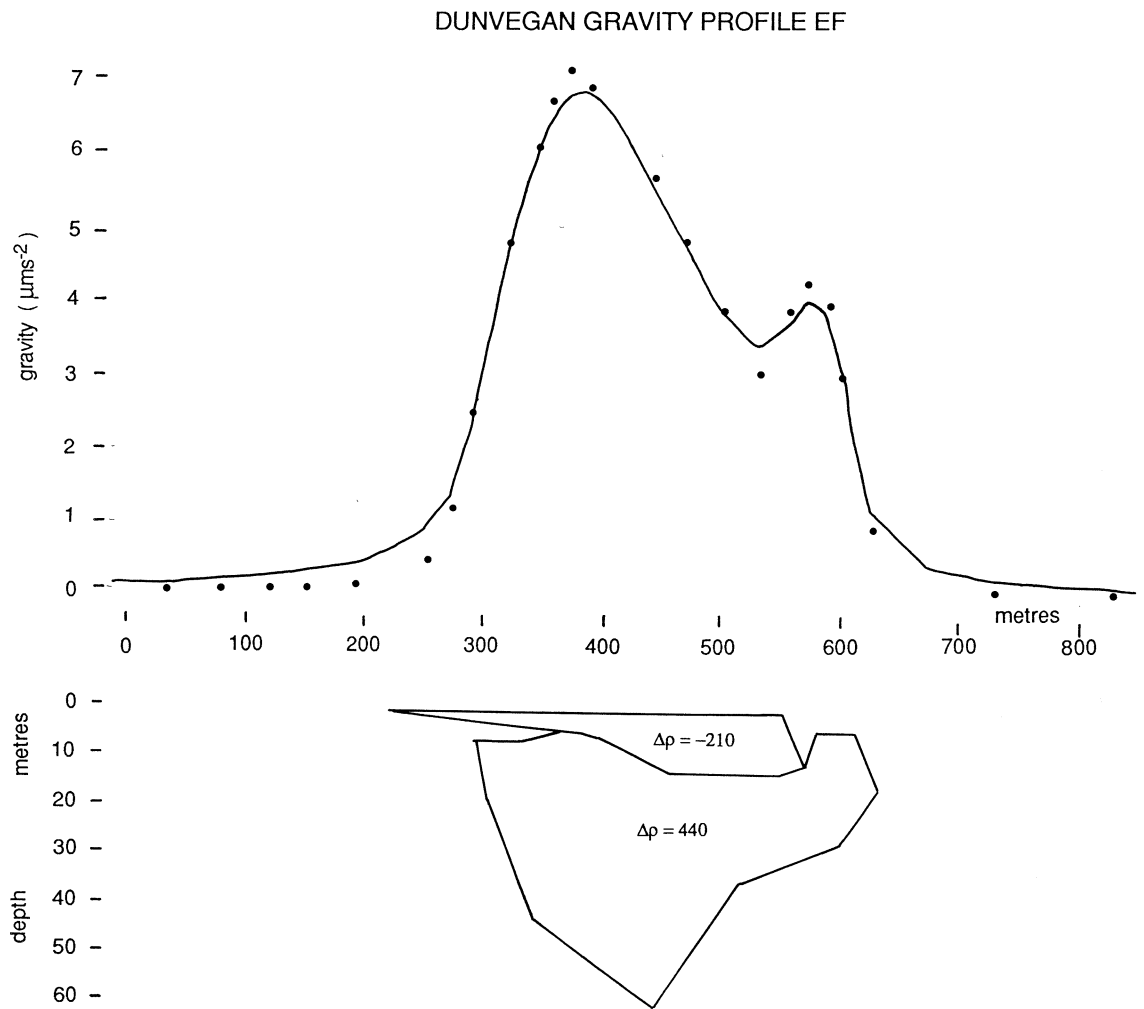


Figure A3-18. A final model satisfying the observed gravity data for profile EF at Dunvegan Lagoon. The lower polygon represents a basalt flow in a Permian basement channel. A density contrast of 440 kgm^{-3} is required between the basalts and the basement in this model. The upper block represents the lagoon sediments which are modelled with a negative contrast of 210 kgm^{-3} with respect to the surrounding sediments. Observed gravity values are shown as dots and the solid line is the model field.

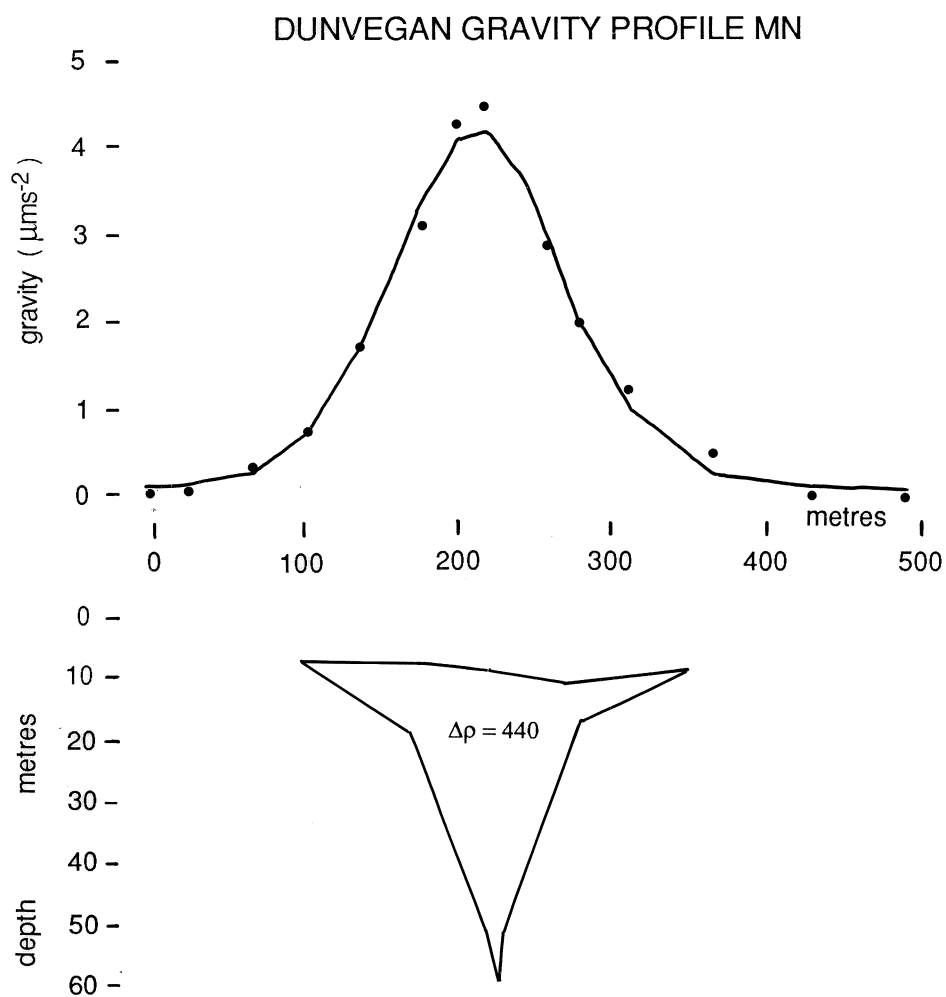


Figure A3-19. A final model satisfying the observed gravity data for profile MN at Dunvegan Lagoon. The polygon represents a basalt flow in a Permian basement channel. A density contrast of 440 kgm^{-3} is required between the basalts and the basement in this model. Observed gravity values are shown as dots and the solid line is the model field.

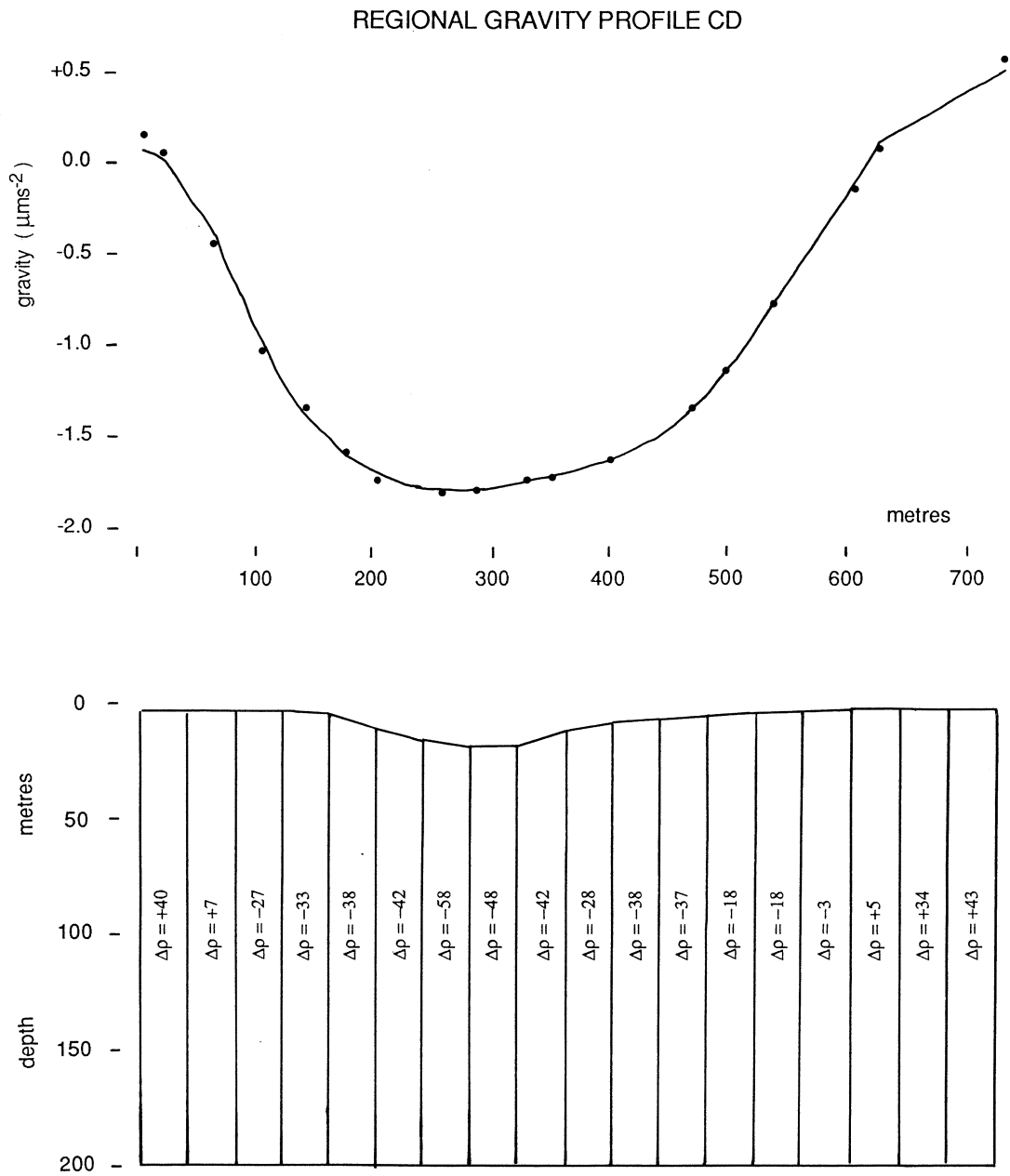


Figure A3-20. Model satisfying the observed regional gravity data. The basement density ($\rho = 2470 \text{ kgm}^{-3}$) is decreased by 100 kgm^{-3} in a series of steps to a minimum ($\rho = 2370 \text{ kgm}^{-3}$) under the deepest point. Geologically this represents a basement fracture or plane of weakness along which a palaeochannel has located itself. Observed gravity values are shown as dots and the solid line is the model field.

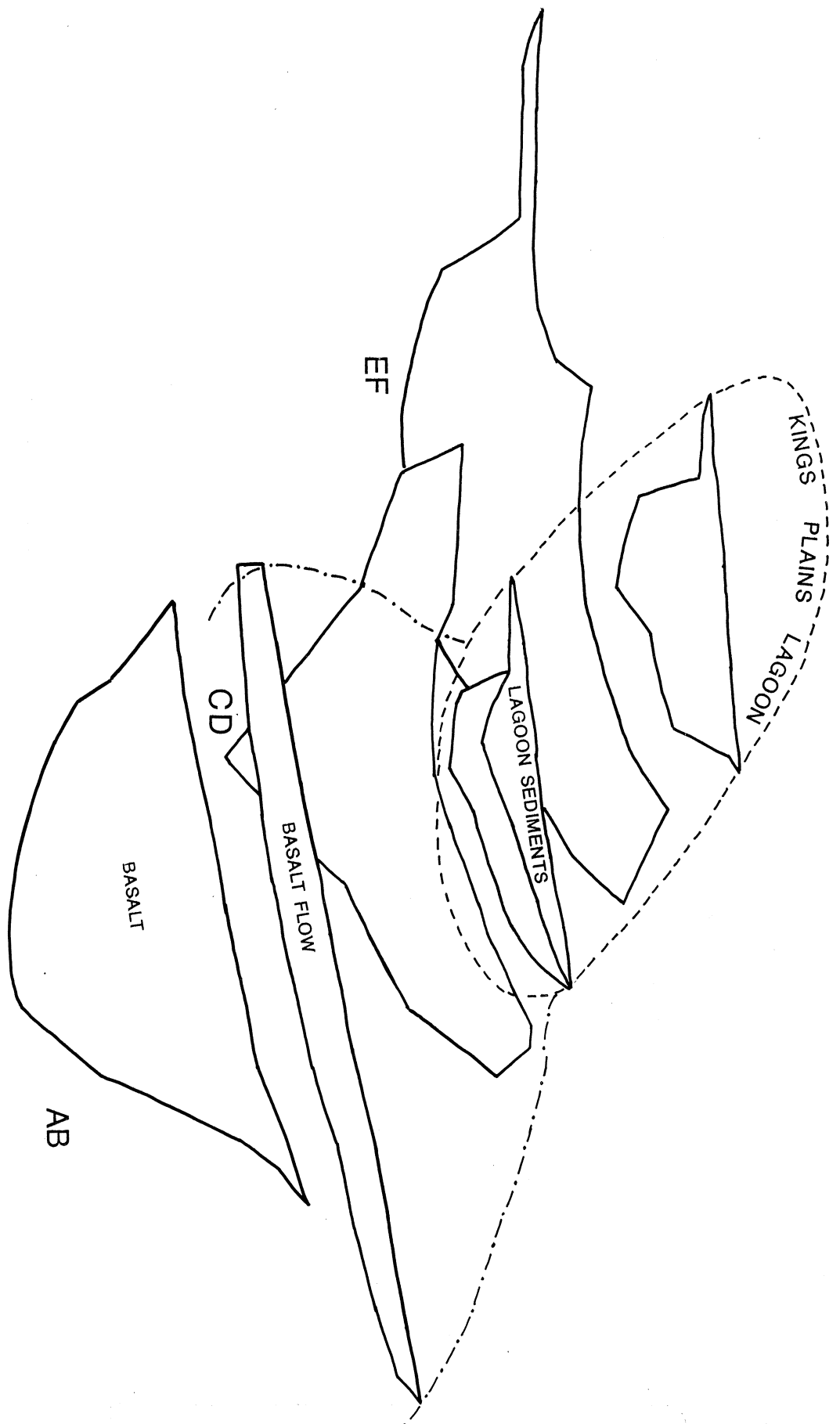


Figure A3-21. Kings Plains Lagoon Geophysical Model. Stacked geophysical models AB, CD and EF show the position and shape of the basalt filled channel below Kings Plains Lagoon. The extent of the lagoon is shown as a dashed line. The position of the surface basalt flow is shown as a dot-dashed line.

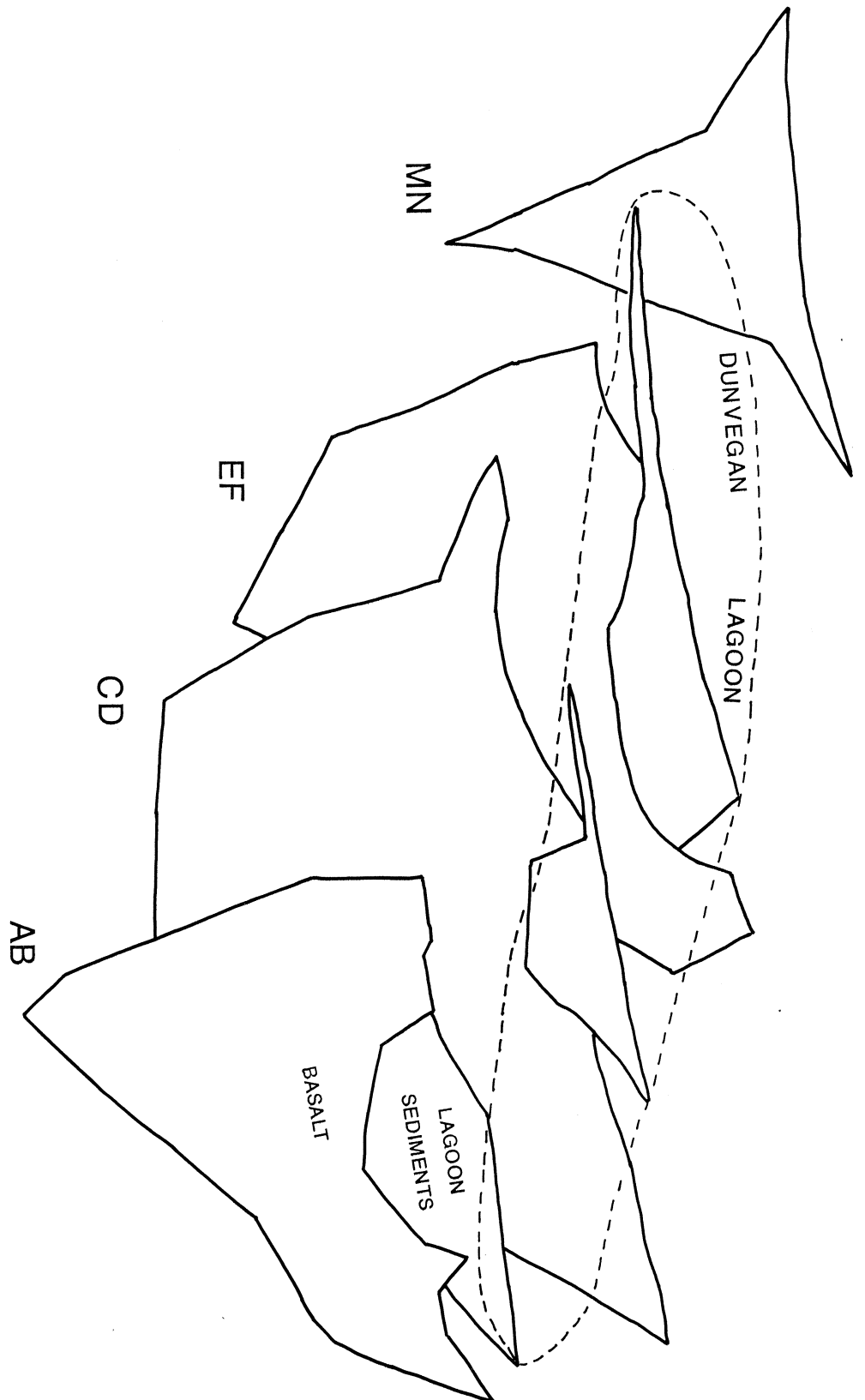


Figure A3-22. Dunvegan Lagoon Geophysical Model. Stacked geophysical models AB, CD, EF and MN show the position and shape of the basalt filled channel below Dunvegan Lagoon. The extent of the lagoon is shown as a dashed line.

the depth of weathering of the basalts, width of pre basaltic channel and presence or absence of claypan sediments or surface basalt sheets as determined by surface mapping.

c/ The association of these features with older drainage systems that are basalt filled has been clearly demonstrated and the existence of fresh basalts on a portion of the rim is probably significant. Figure A3-23 highlights this relationship, the steeper portions of the rim are edged against basalt shown dashed and the clayey pisolitic portion is shown stippled.

d/ The fact that sapphires and spinels are found at Dunvegan Lagoon may be coincidental because they were not seen at any of the other lagoons visited.

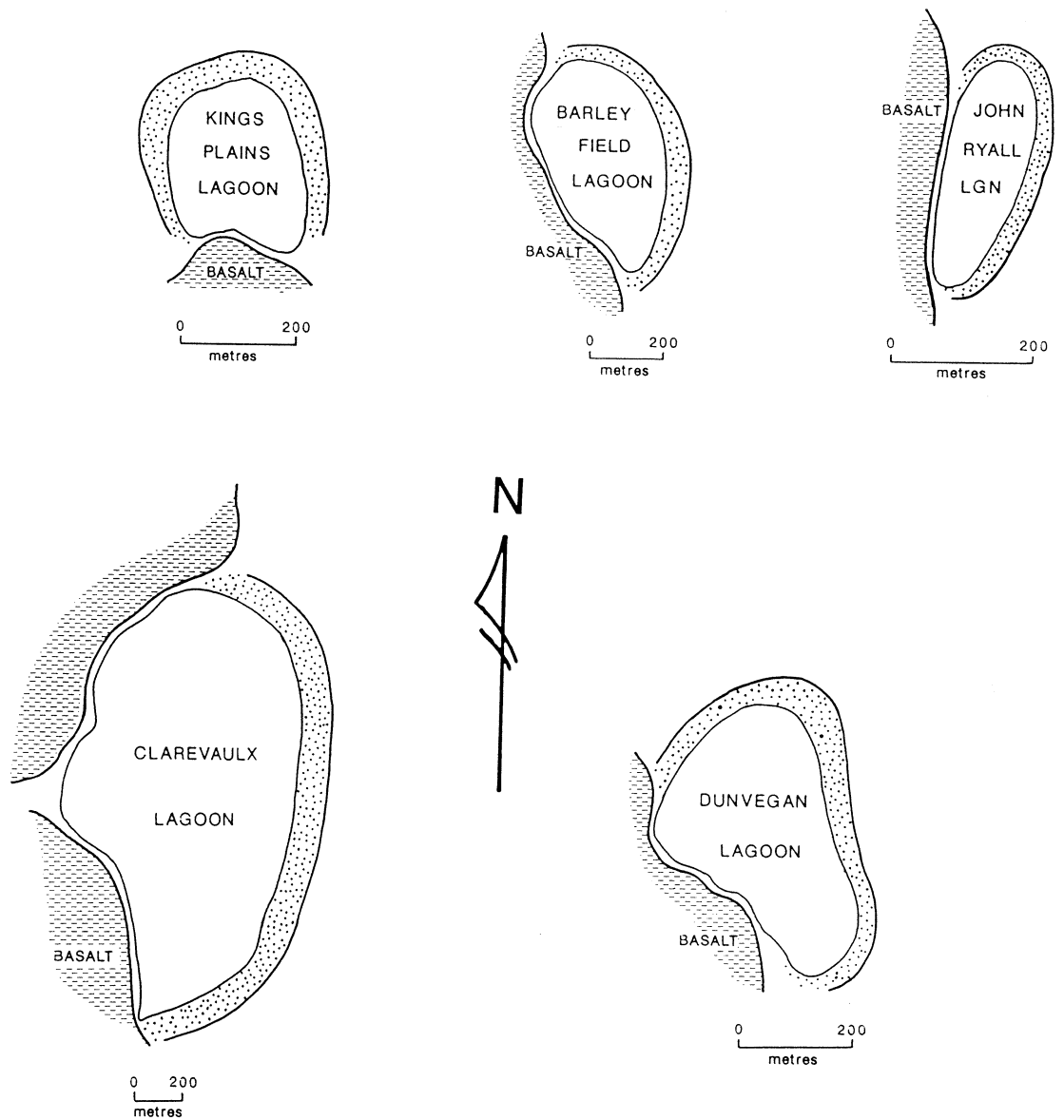


Figure A3-23. Surface configuration of Kings Plains, Dunvegan, Clarevaux, John Ryall and Barley Field Lagoons. The configuration of the pisolitic lagoon rim or lunette (stippled) is shown with respect to the steeper edges against the basalt flows (shown dashed). The similarity in position and shape of the lunette suggests a regional southwesterly palaeowind direction.

Appendix 4

DRILLING PROGRAMME; KINGS PLAINS & DUNVEGAN LAGOONS, AND KINGS PLAINS VALLEY

A4.1 Drillhole Locations

This appendix contains detailed descriptions of the exploration drilling and testing carried out at Kings Plains and Dunvegan Lagoons, and in the Kings Plains Valley by T.J. & P.V. Nunan Pty. Ltd and Jingellic Minerals N.L.

Exploration Hole	1:25,000 Map Sheet	Grid Reference	Elevation (metres)	Total Depth (metres)
KP3	Sapphire 9138-1-S	48482058	921	35.0
KP4	Sapphire 9138-1-S	48392074	921	35.0
TEST PIT#1	Sapphire 9138-1-S	48482090	923	1.5
Dunvegan 1	Glen Innes 9138-4-S	72772134	1007	7.6
Dunvegan 2	Glen Innes 9138-4-S	72762128	1007	7.9
Dunvegan 3	Glen Innes 9138-4-S	72752122	1007	3.7
Dunvegan 4	Glen Innes 9138-4-S	72782140	1007.5	1.8
Dunvegan 5	Glen Innes 9138-4-S	72752116	1007	3.0
Dunvegan 6	Glen Innes 9138-4-S	72742111	1007	2.1
Dunvegan 7	Glen Innes 9138-4-S	72732104	1007	2.4
Dunvegan 8	Glen Innes 9138-4-S	72722096	1010	2.4
Dunvegan 9	Glen Innes 9138-4-S	72712090	1011	3.7
Dunvegan 10	Glen Innes 9138-4-S	72702084	1010	
4.1				
Dunvegan 11	Glen Innes 9138-4-S	72692077	1009.5	
2.1				
Dunvegan 12	Glen Innes 9138-4-S	72812163	1006	
2.1				
Dunvegan 13	Glen Innes 9138-4-S	72822169	1005	
3.0				
Dunvegan 14	Glen Innes 9138-4-S	72832175	1005	
2.7				
Dunvegan 15	Glen Innes 9138-4-S	72842180	1005	
3.0				
NA1	Sapphire 9138-1-S	49791603	935	18.0
NA2	Sapphire 9138-1-S	49851601	935	27.0
NA3	Sapphire 9138-1-S	49921600	935	21.0
NA4	Sapphire 9138-1-S	49981599	935	10.0
NA5	Sapphire 9138-1-S	51291581	935	27.0
NB1	Sapphire 9138-1-S	51191581	935	36.0
NB2	Sapphire 9138-1-S	51141598	935	36.6
NB3	Sapphire 9138-1-S	49921645	931	14.3
NB4	Sapphire 9138-1-S	48501493	938	18.9
NB5	Sapphire 9138-1-S	50121639	931	7.3

A4.2 Kings Plains Lagoon Drilling Programme

Five inch holes were drilled using an Ingersoll Rand T4 Drillmaster high percussion drill. The material, which varied in size from fine powder to rock chips up to 3 cm, was collected each metre. Sieves were used to separate the coarse material for geological description and the fine material was panned to obtain the heavy mineral concentrate.

A4.2.1 Results

KP3 encountered dark lacustrine clay and lighter clay overlying, and probably derived from, weathered basalt at about 8 m. The basalt becomes increasingly fresh in the interval from 15 to 21 m. and in the interval from 19 to 20 m. the muddy slurry from the drill hole changed from a yellow-tan to a blue-grey colour, indicating that the material becomes predominantly fresh at this depth. Above this depth, an extremely fine grained, black, magnetic concentrate can be panned from the material and probably represents magnetite/ilmenite remaining after the decomposition of the basalt. In the interval 30-31m some coaly fragments were encountered indicating a clear break between two lava flows. This break can be correlated to similar breaks found in KP1 and KP4. The upper flow is more altered in places, the basalt is vesicular with open, partially filled and filled vesicles, whereas in the flow below the woody horizon the basalt is compact, non vesicular and fresh. Weathered Permian basement, consisting of crystalline quartz in a white clay matrix, was encountered under fresh basalt at 34 metres.

KP4 encountered similar clay to KP3 overlying weathered basalt at 8 metres which becomes increasingly fresh in the interval from 19-23m. The woody horizon between the two distinctive basalt flows was found at 28 metres. Weathered Permian basement was encountered under fresh basalt at 46.5 metres.

No traces of sapphire were found in either hole.

Test Pit # 1 & 2 were dug into the rim of Kings Plains Lagoon to a depth of 1.5 m. The material was ironstone pisoles 1 - 2 mm in red clay becoming increasingly cemented with depth. Eleven cubic yard of material were removed and tested. Only trace amounts of sapphire and zircon were found in pit #1 (0.2 g/cu.yd) and none in pit #2.

The drilling and outcrop data suggest the presence of a pre basaltic valley some 2.5 kilometres wide and 60 metres deep along which successive basaltic lavas have flowed forming a broad flat plain. Kings Plains Creek has been displaced from its original position to a more northerly position on the edge of the basalt- basement contact.

KP3 and KP4 were completed as water bores flowing 1000 and 2000 gallons per hour respectively.

Detailed logs for KP3 and KP4 are included and the information summarized on cross section, Fig. A3-10.

Drill Hole KP3

Depth Interval (metres)	Description
0 - 1	Fine olive- grey lacustrine clay
1 - 2	Clay material becoming a little coarser and lighter
2 - 3	Yellow- brown clay
3 - 4	Yellow- brown clay
4 - 5	Yellow- brown clay
5 - 6	Yellow- brown clay with some decomposed rock frags
6 - 7	Yellow- brown wet clay with some larger tan coloured rock fragments (decomposed basalt)
7 - 8	Yellow- brown wet clay with some larger tan coloured rock fragments (basalt ?)
8 - 9	Yellow- brown wet clay with tan coloured altered basalt. Fine black magnetic concentrate panned from this material.
9 - 10	As above
10 - 11	Clay as above with larger weathered fragments, easily broken, black oxide along fractures in rock.
11 - 12	Mostly clay with completely altered buff to red- brown basalt fragments, easily broken.
12 - 13	Very light grey to buff amygdaloidal basalt (texture obvious with altered plagioclase laths visible), altered, easily broken. Rare blue- grey basalt fragments more difficult to break.
13 - 14	Altered basalt as above
14 - 15	Altered basalt as above
15 - 16	Altered basalt as above with green, soapy, spherical grains derived from vesicles in the basalt. Approx 10% blue- grey basalt fragments.
16 - 17	Altered basalt as above with green, soapy, spherical grains derived from vesicles in the basalt. Approx 10% blue- grey basalt fragments.
17 - 18	As per 12 - 13 but with approx 10% blue- grey basalt.
18 - 19	Altered basalt as above but with blue- grey basalt with zeolite, calcite? filled vesicles becoming more abundant (80%), moderately altered, more difficult to break
19 - 20	Mud changes colour at this depth from an oxidized red- brown colour to a blue colour. Blue- grey vesicular basalt with white (zeolite, calcite) cavities, mod. altered (80%)
20 - 21	Blue- grey vesicular basalt with white (zeolite, calcite) cavities, mod. altered (100%).
21 - 22	Basalt as above
22 - 23	Basalt as above
23 - 24	Light grey basalt, hard but altered, veins & vesicles (up to 4mm) filled with green black soapy material which in some cases shows signs of alteration to a white material.
24 - 25	Basalt as above but with vesicles up to 12mm.
25 - 26	Basalt as above but vesicles to 5mm, some empty, some lined with botryoidal blue zeolite.
26 - 27	Basalt as per 25 - 26.
27 - 28	Basalt as above but with blue zeolite lined vesicles to 15mm.
28 - 29	Basalt as per 25 - 26.
29 - 30	Basalt as per 25 - 26 but with abundant small (< 1mm) vesicles filled with white needlelike zeolite.
30 - 31	Appearance of coaly fragments and first appearance of a fresh, hard, dark grey, non- vesicular basalt, apparently another flow unit.
31 - 32	Fresh basalt as above.
32 - 33	Basalt as above, only moderately altered, softer, cut by fine veinlets and containing some vesicles filled with white material, probably due to flowing over basement.
33 - 34	Weathered basement (Permian acid volcanics), crystalline quartz (approx 1-3mm often bipyramidal) in a white clay matrix.
34 - 35	Weathered basement.

Depth Interval (metres)	Drill Hole KP4 Description
0 - 1	Olive grey lacustrine clay with vegetation.
1 - 2	Olive grey clay.
2 - 3	Olive grey clay.
3 - 4	Medium grey clay.
4 - 5	Med. grey clay with some altered tan rock (basalt?) frags.
5 - 6	Med. grey clay with some altered tan rock (basalt?) frags.
6 - 7	Yellow- brown clay becoming wetter (water table).
7 - 8	Completely altered greenish- grey basalt with red- brown to tan vesicles in tan clay (similar to KP3 12-13)
8 - 9	Altered basalt and clay as above.
9 - 10	Greenish- light grey completely altered basalt, soft.
10 - 11	Altered basalt as above.
11 - 12	Altered basalt as above.
12 - 13	Altered basalt as above.
13 - 14	Altered basalt as above.
14 - 15	Altered basalt as above with vesicles up to 4mm partially filled with green and tan secondary minerals.
15 - 16	Altered basalt as per 14 - 15
16 - 17	Altered basalt as per 14 - 15
17 - 18	Altered basalt as per 14 - 15
18 - 19	Altered basalt as per 14 - 15 with the appearance of some harder, non- vesicular, blue- grey, altered basalt chips (<5%). Corresponds to KP3 15-16m
19 - 20	Altered basalt as per 18 - 19
20 - 21	As per 18 - 19 but with approx 10% blue- grey basalt.
21 - 22	As per 18 - 19 but with approx 80% blue- grey basalt.
22 - 23	Harder blue- grey, altered basalt (100%) with vesicles, some containing soft, fine, greenish- black secondary mineral.
23 - 24	Basalt as per 22-23, vesicles increase in size to 6mm.
24 - 25	Basalt as above, some large vesicles coated with transparent secondary mineral.
25 - 26	Basalt becoming fresher, dark grey, cut by veins and fractures filled with white mineral, vesicles as above.
27 - 28	Basalt as above, evidence of vesicles or veins to 20mm partially filled with yellow- green translucent botryoidal chalcedony.
28 - 29	Coaly wood fragments at 28m. Fresh, fine grained, dark grey basalt, fresh pyroxene and plagioclase phenocrysts visible. Some white veinlets and vesicles filled/ partially filled with transparent secondary mineral. Apparently another flow unit below woody layer.
29 - 30	Basalt as above.
30 - 31	Basalt as above, minor vesicles.
31 - 32	Fresh, fine grained, dark grey basalt, fresh pyroxene and plagioclase phenocrysts visible, no vesicles.
32 - 33	Basalt as above.
33 - 34	Basalt as above.
34 - 35	Basalt as above.
35 - 36	Basalt as above.
36 - 37	Basalt as above but with some olivine phenocrysts and plagioclase rich patches with a stockwork appearance.
37 - 38	Basalt as above.
39 - 40	Basalt as for 36-37.
40 - 41	Basalt as above.
41 - 42	Basalt as above but with some green soapy secondary mineral liberated from fractures.
42 - 43	Basalt as above.
43 - 44	Basalt as above.
44 - 45	Basalt as above, with some small soft red crystals (probably altered olivine).
45 - 46	Basalt as above, with some small soft red crystals and green soapy veins.
46 - 47	Basalt as per 45-46, some vesicles partially filled with botryoidal blue zeolite. Drill break at 46.5m.
47 - 48	Weathered basement (Permian acid volcanics), crystalline quartz, approx 1-3mm often bipyramidal, in a white clay matrix.
48 - 49	Weathered basement.

A4.3 Dunvegan Lagoon Drilling and Testing Programme

A line of fifteen holes were drilled accross Dunvegan Lagoon using a Cauldweld large diameter bucket drill. Bulk samples were processsed and grades are given in grams per loose cubic yard and are for minerals in the size range 1/16" - 7/8".

A4.2.1 Results

Depth Interval (metres)	Description	Grade Sapphire g/cu.yd	Grade Spinel g/cu.yd
Dunvegan 1 0.0 - 2.0 m 2.0 - 2.4 m 2.4 - 4.5 m 4.5 - 7.6 m	stiff grey clay (lagoon sediments) transition from clay to extremely weathered basalt weathered basalt weathered basalt and basalt boulders becoming quite hard at 7.6 m		
Dunvegan 2 0.0 - 1.5 m 1.5 - 7.9 m	stiff grey clay soft weathered basalt & basalt boulders becoming harder with depth		
Dunvegan 3 0.0 - 1.5 m 1.5 - 1.8 m 1.8 - 3.7 m	stiff grey clay wash with basalt pebbles weathered basalt	0.8 1.0	42.8 42.3
Dunvegan 4 0.0 - 0.5 m 0.5 - 1.2 m 1.3 - 1.8 m	ironstone pisoles in red clay orange wash grey wash with large basalt boulders	1.5 8.2 0.6	36.2 55.6 20.9
Dunvegan 5 0.0 - 1.5 m 1.5 - 1.8 m 1.8 - 3.7 m	stiff grey clay grey wash weathered basalt	- 0.5	17.0 4.8
Dunvegan 6 0.0 - 1.1 m 1.1 - 1.6 m 1.6 - 2.1 m	stiff grey clay clay with basalt pebbles, possibly wash weathered basalt with basalt cobbles	4.5	61.3
Dunvegan 7 0.0 - 1.2 m 1.2 - 1.6 m 1.6 - 2.4 m	stiff grey clay brown grey weathered basalt brown grey weathered basalt	2.5	13.5
Dunvegan 8 0 - 1.2 m 1.2 - 2.4 m	basalt topsoil brown grey weathered basalt		

Depth Interval (metres)	Description	Grade Sapphire g/cu.yd	Grade Spinel g/cu.yd
Dunvegan 9			
0.0 - 0.6 m	iron stone pisoles in red clay	0.6	24.6
0.6 - 3.5 m	weathered basalt		
3.5 - 3.7 m	weathered basalt with basalt boulders	-	24.0
Dunvegan 10			
0.0 - 0.3 m	topsoil	3.3	31.8
0.3 - 0.9 m	ironstone	0.4	19.8
0.9 - 1.7 m	grey clay		
1.7 - 2.0 m	transition grey clay to weathered basalt	0.5	10.3
2.0 - 4.1 m	weathered basalt becoming hard at 4m		
Dunvegan 11			
0.0 - 0.3 m	topsoil		
0.3 - 0.6 m	ironstone	2	11.3
0.6 - 1.5 m	orange grey	0.3	5.0
1.5 - 1.8 m	orange clay & weathered basalt	-	6.8
1.8 - 2.0 m	weathered basalt	-	6.8
2.0 - 2.1 m	weathered basalt becoming harder	2.5	47.0
Dunvegan 12			
0.0 - 1.8 m	topsoil		
1.8 - 2.1 m	clayey orange brown alluvium with	-	32.3
2.1 - 2.4 m	weathered basalt		
Dunvegan 13			
0.0 - 2.4 m	topsoil		
2.4 - 2.7 m	clayey orange brown alluvium	7.25	-
Dunvegan 14			
0.0 - 2.1 m	topsoil		
2.1 - 2.4 m	clayey orange brown alluvium with some larger basalt pebbles	10.0	132.3
2.4 - 2.7 m	weathered basalt		
Dunvegan 15			
0.0 - 2.4 m	topsoil grading into clay		
2.4 - 2.7 m	clayey orange brown alluvium	2.0	57.8
2.7 - 3.0 m	weathered basalt		

A4.4 Kings Plains Valley Deep Drilling Program

The Kings Plains Valley Deep Drilling Program was designed to test for the possibility of intra-basaltic and sub-basaltic sapphire deposits. The concept of the program was developed as a result of the Braemar sapphire deposit being recognized as intra-basaltic, sandwiched between older basalt flows and capped by younger flows; coupled with the observation of weathered basalts covering portions of some of the alluvial deposits mined on Kings Plains (T. Nunan pers. comm. 1988)

An initial series of five, one metre diameter holes (the Nunan A series) were drilled; NA1 on the eastern feeder, and NA2, NA3, NA4 and NA5 on the western feeder, of Kings Plains Creek (see Figure A4-1). The locations of the exploration holes were based on the palaeo-topographic analysis and they were designed to pinpoint the exact position of the palaeo channel axes and to test the nature of any material existing in them. At the same time, the holes would test for the presence of intra-basaltic deep leads.

Sampling was done at 2 metre intervals, commencing from the top of the basalt. A half cubic yard sample was washed from each 2 m section and the concentrate examined. Each hole is described in detail in the results section and a cross section is shown in Figure A4-2.

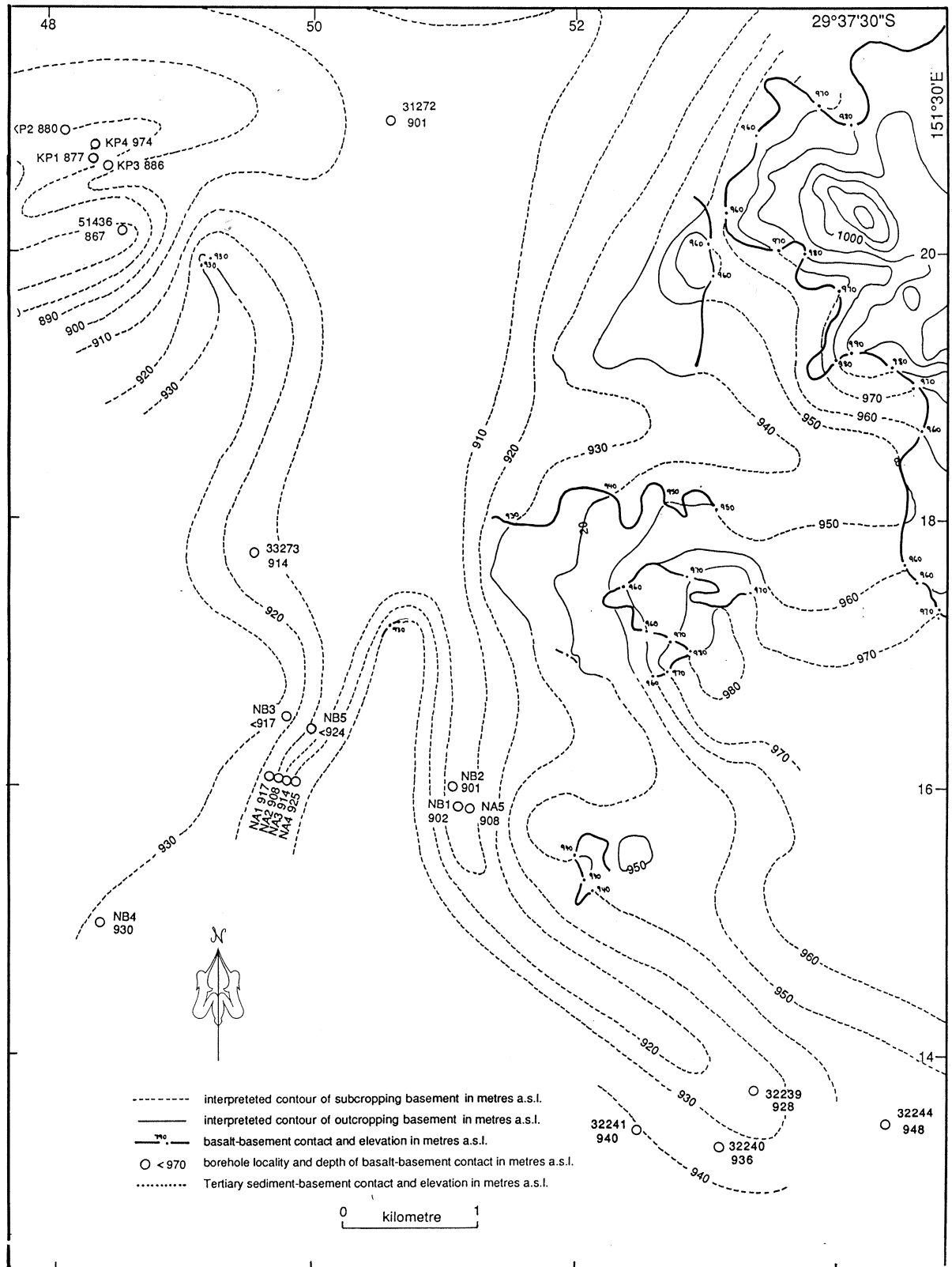
Hole NA1 encountered a layer of red clay, between 9 and 12 metres below the surface, containing bipyramidal quartz sandwiched between two weathered basalt flows. A horizon of similar description was encountered between 33 and 35 m, directly overlying silicic volcanic basement.

It is unclear if these horizons represent weathered red volcanoclastic rocks with basement contamination, such as observed at Braemar, or whether they have been reworked by fluvial processes.

Trace amounts of sapphire were recovered from these horizons. However, as this first series of holes were uncased, there remains some doubt as to whether the sapphires were derived from the horizons of interest or are contamination from the overlying sapphire bearing alluvium.

A second series of 5 cased holes (the Nunan B series) were drilled to repeat the experiment under more rigorous conditions (see Figure A4-1). Hole NB1 drilled adjacent to NA1 experienced recovery problems in the zone of interest and the other holes (NB2 to NB5) essentially encountered basalt overlying weathered basement. The intra-basaltic material was not seen in any of these holes although it may have been too thin to be noticed.

No further sapphires were recovered during the second phase of exploration drilling.



prepared by R. Coenraads 1988-1989.

Figure A4-1. Location of the Nunan A and B series of large diameter drill holes on Kings Plains.

KINGS PLAINS PROFILE

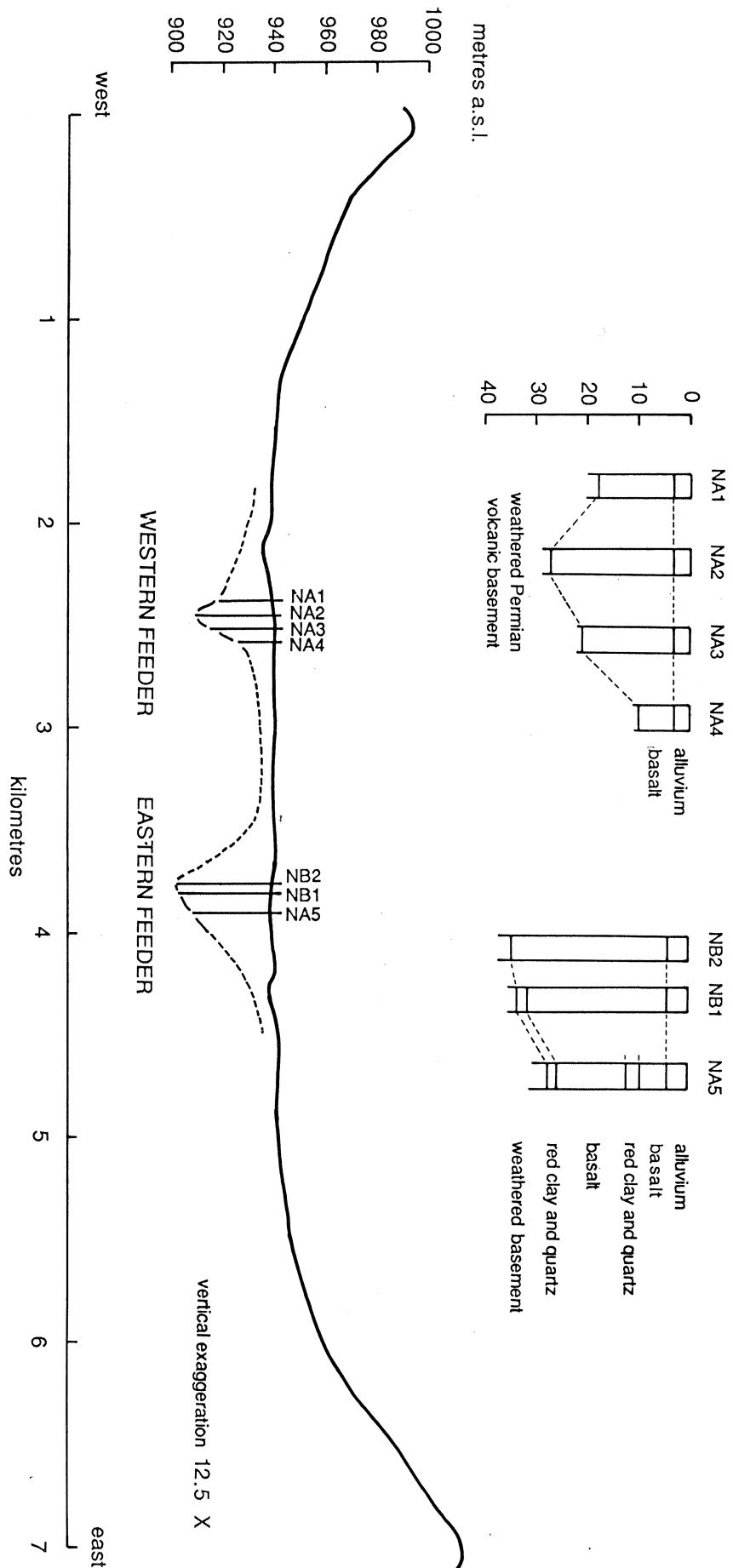


Figure A4-2. Cross section through Nunan A and B series large diameter drill holes at Kings Plains.

A4.4.1 Results

The deep drilling program consisting of 10 holes to date supports the presence of at least one time break between the lava flows that filled the Kings Plains palaeo-valley. Intra-basaltic and possibly sub-basaltic material was encountered only in hole NA1 and this material at best contained trace amounts of sapphire.

Although rich, sub-basaltic and intra-basaltic deep leads have not been found during this program, the possibility of their presence cannot be discounted. If present however, they will be thin and extremely difficult to find

Grades are given in grams per loose cubic yard and are for minerals in the size range 1/16" - 7/8"

Depth Interval (metres)	Description	Grade Sapphire g/cu.yd	Grade Spinel g/cu.yd
NA1			
0 - 4 m	brown clayey soil (alluvial sediments)	-	-
4 - 18 m	grey weathered basalt overlying weathered Permian basement	-	-
NA2			
0 - 4 m	brown clayey soil (alluvial sediments)	-	-
4 - 27 m	soft grey weathered basalt overlying weathered Permian silicic volcanics	-	-
NA3			
0 - 4 m	brown clayey soil (alluvial sediments)	-	-
4 - 21 m	soft grey weathered basalt overlying weathered Permian silicic volcanics	-	-
NA4			
0 - 4 m	brown clayey soil (alluvial sediments)	-	-
4 - 10 m	soft grey weathered basalt overlying weathered Permian silicic volcanics	-	-
NA5			
0 - 4 m	brown clayey soil (alluvial sediments)	-	-
4 - 5 m	transition from soil to extremely weathered basalt	-	-
5 - 9 m	weathered basalt	-	-
9 - 12 m	red clay with abundant bipyramidal quartz up to several cm in size	trace	trace
12 - 25 m	weathered basalt	-	-
25 - 27 m	red clay with bipyramidal quartz, this may represent weathered Permian silicic volcanics	-	-
27 - 30 m	Permian silicic volcanics		

Depth Interval (metres)	Description	Grade Sapphire g/cu.yd	Grade Spinel g/cu.yd
NB1			
0.0 - 4.0 m	dark brown soil (alluvium)	-	-
4.0 - 7.0 m	transition from soil to extremely weathered basalt		
7.0 - 21.0 m	weathered basalt no recovery		
21.0 - 23.0 m	greenish grey to grey weathered basalt, some vesicular with vesicles filled with olive green soapy material.- some black heavy mineral, either spinel or ilmenite and some water clear grains showing distinct cleavages and striations on flat faces, probably feldspar, generally 2-3mm although frag up to 10mm found as for 21.0 - 23.0	-	trace
23.0 - 25.0 m	weathered basalt, fine grained, some vesicular as above. Some cream to tan concretions and fragments of concretions derived from the basalt spinel and clear quartz		
25.0 - 27.0 m	fragments approx 1mm.	-	trace
27.0 - 29.0 m	weathered basalt, ironstone concretionary fragments becoming more abundant, some spinel & occasional translucent green striated pyroxene, occasional clear quartz.	-	trace
29.0 - 31.0 m	ironstone fragments & concretions abundant, some heavy minerals	-	trace
31.0 - 33.0 m	weathered Permian silicic volcanics, abundant bipyramidal clear to smokey quartz in red clay, some basalt fragments & ironstone concretions.	-	-
33.0 - 35.0 m	weathered Permian silicic volcanics, bipyramidal quartz, approx 2mm, grains often showing fresh crystal faces and edges.	-	-
NB2			
0.0 - 3.7 m	dark brown topsoil (alluvium)		
3.7 - 34.1 m	grey weathered basalt	-	-
34.1 - 36.6 m	clay with abundant bipyramidal quartz (weathered Permian acid volcanics)		
NB3			
0.0 - 5.2 m	dark brown topsoil (alluvium)	-	-
5.2 - 14.3 m	grey weathered basalt becoming harder with depth. Hole bottomed at 14.3m as rock became too hard to proceed	-	-
NB4			
0.0 - 4.3 m	dark brown topsoil (alluvium)	-	-
4.3 - 7.9 m	grey weathered basalt		
7.9 - 18.9 m	clay with abundant bipyramidal quartz (weathered Permian acid volcanics)		
NB5			
0.0 - 4.6 m	dark brown topsoil (alluvium)	-	-
4.6 - 7.3 m	grey weathered basalt, bore caved in below steel casing at 7.3 m.		

Appendix 5

MOUNT BUCKLEY BASALT FLOWS: THIN SECTION DESCRIPTIONS

Thin sections made from the thirty one basalt samples collected from Mt Buckley are described in this appendix. The locations of the sample sites are shown in Fig. 6-19 and grid references provided in Table 6-1.

B1

Very fine grained holocrystalline rock, porphyritic, showing evidence of flow banding. Subhedral to anhedral equant phenocrysts or megacrysts of olivine give the rock a porphyritic texture in a groundmass of euhedral plagioclase laths, stubby euhedral augite prisms and interstitial nepheline.

B2

Same as B1.

B3

Very fine grained rock with euhedral altered olivine and ragged anhedral nepheline crystals in a groundmass of euhedral plagioclase laths, opaque minerals and glass.

B4

Medium to fine euhedral to subhedral olivine phenocrysts in groundmass of euhedral to subhedral elongate plagioclase laths, equant euhedral to subhedral opaques and augite. Some alteration of the olivine is evident.

B5

Same as B4 with some interstitial glass.

B6

Very fine grained hypohaline rock with a porphyritic texture similar to B3. Subhedral to euhedral olivine, ragged low relief inclusions consisting of equigranular anhedral grains in a groundmass of smaller plagioclase laths and brown glass.

B7

Euhedral olivine phenocrysts or megacrysts in a groundmass of short euhedral plagioclase laths and brown glass.

B8

Similar to B6.

B9

Medium-grained holocrystalline rock. Glomoporphyritic texture with medium-sized, zoned, single euhedral crystals or clots of subhedral crystals of pink augite and medium euhedral plagioclase laths. Groundmass comprises of equant subhedral to euhedral finer plagioclase, olivine, pyroxene and opaques with minor brown glass.

B10

Phenocrysts or megacrysts of equigranular euhedral olivine. Description as per B7 except groundmass is mostly granular with only minimal glass.

B11

Euhedral equant and elongate olivine (with some minor alteration along cracks and around the rims), euhedral elongate plagioclase and some pink augite aggregates in a fine holocrystalline groundmass of plagioclase laths and euhedral augite and opaques.

B12

Subhedral equant olivine in a fine holocrystalline groundmass of euhedral subparallel plagioclase laths which give the rock a trachytic texture, euhedral equant augite and opaques.

B13

Medium to fine subhedral equant to elongate olivine phenocrysts in a holocrystalline groundmass of finer subhedral to anhedral olivine, plagioclase laths, very fine equant euhedral augite prisms and opaques.

B14

Medium sized subhedral to euhedral equant to elongate phenocrysts of olivine and zoned pink augites with plagioclase displaying subophitic texture in a fine to medium grained groundmass of elongate euhedral plagioclase equant subhedral olivine, augite and opaques. Rock is essentially equigranular holocrystalline.

B15

Phenocrysts of subhedral to euhedral olivine, pink augites displaying a subophitic relationship with the included plagioclase, equant euhedral opaque minerals. The rock is essentially holocrystalline with interstitial areas filled with a equant anhedral low relief, low birefringence zeolite. The presence of approximately 20% modal zeolite renders B15 unsuitable for normative mineralogy comparisons.

B16

Medium to coarse grained glomerophritic aggregates of subhedral pink augite and medium to coarse grained elongate subhedral to euhedral plagioclase which are crudely aligned imparting a trachytic texture to the rock. Some altered clots of euhedral crystals probably were olivine phenocrysts or megacrysts. The groundmass consists of fine euhedral augite and isotropic brown glass with some euhedral, equant and acicular opaque minerals. Zoning of augite from light centres to pink rims indicates titanium enrichment.

B17

Same as B16 but contains some ragged edged euhedral zeolite with strange curved, less distinct zoning.

B18

Same as B16, but with more aggregates of ophitic pink augite.

B19

Same as B18.

B20

Fine-medium grain size, euhedral single augite (zoned with a darker pink rim) and olivine crystals in a finer granular groundmass comprising euhedral augite, subhedral opaques and feldspar laths with some minor anhedral granular aggregates of ?alkali feldspars.

B21

Equant to elongate subhedral olivine megacrysts in a holocrystalline groundmass of plagioclase, pink augite and opaques.

B22

This sample appears to be quite altered, phenocrysts of olivine have all altered to orange iddingsite?, and carbonate veins are present. The groundmass consists of subhedral plagioclase laths, opaque and glass. The extensive alteration renders B22 unsuitable for normative mineralogy comparisons.

B23

Subhedral equant to elongate olivine phenocrysts, otherwise like B22.

B24

Euhedral, equant olivine phenocrysts in a granular groundmass of finer olivine (considerably altered red-brown around edges of grains and within fractures, euhedral plagioclase laths, small euhedral brownish augite and opaques. The extensive olivine alteration renders B24 unsuitable for normative mineralogy comparisons.

B25

Same as B24 but with much less alteration of the groundmass olivine.

B26

Abundant medium to fine euhedral olivine phenocrysts in a trachytic textured granular groundmass of fine elongate euhedral plagioclase laths, fine equat augite and opaques.

B27

Similar to B26 but with fewer olivine phenocrysts and fewer opaques in the groundmass. The phenocrystal olivine shows some alteration and there is approximately 20% zeolite thus rendering B27 unsuitable for normative mineralogy comparisons.

B28

Euhedral elongate to equant olivine phenocrysts in a groundmass of plagioclase, augite and dark brown isotopic glass. Many zeolite-filled vesicles are also present thus rendering B27 unsuitable for normative mineralogy comparisons.

B30

Similar to B28.

B31

Similar to B28 but groundmass is almost entirely glass with some plagioclase laths.

Appendix 6

MATERIAL PUBLISHED DURING THE PERIOD OF DOCTOR OF PHILOSOPHY CANDIDATURE

- Coenraads, R.R. (1988), Structural control and timing of volcanism in the central province. Implications for regional targeting of prospective areas for sapphire and diamond exploration; New England Tectonics and Metallogenesis, Kleeman J.D. (ed). Proceedings of a symposium held at the University Of New England, Armidale New South Wales 14-18 November 1988, 302-307.
- Coenraads, R.R. (1989), Evaluation of the natural lagoons of the Central Province, N.S.W. - Are they sapphire producing maars? *Bulletin of the Australian Society of Exploration Geophysicists*, **20**, 347-363.
- Pecover, S.R. & Coenraads, R.R. (1989). Tertiary volcanism, alluvial processes, and the origin of sapphire deposits at "Braemar" near Elsmore, northeastern New South Wales. *New South Wales Geological Survey - Quarterly Notes* **77**, 1-23.
- Coenraads, R.R., Sutherland, F.L. and Kinny, P.D. (1990), The Origin of Sapphires: U-Pb dating of zircon inclusions sheds new light. *Mineralogical Magazine* , **54**, 113-122.
- Coenraads, R.R. (1990). Key areas for alluvial diamond and sapphire exploration in the New England gem fields, NSW, Australia. *Economic Geology*, **85**, 1186-1207.
- Coenraads, R.R. & van der Graaf, R. (1991). An occurrence of gem garnets from Horse Gully in the New England gem fields, NSW. *Australian Gemmologist*, **17**(10) 412-415.
- Coenraads, R.R. (1990). Palaeogeography of the Braemar sapphire deposit: Implications for deep-lead sapphire exploration in the Central Volcanic Province, New South Wales. *Royal Society of New South Wales*, **123**, 75-84
- Bischoff, G.C.O., Coenraads, R.R. and Lusk, J. (in press). Microbial gold; an example from Venezuela. *N.Jb.Geol.Paläont.Abh.*,
- Bischoff, G.C.O., Coenraads, R.R. and Lusk, J. (in press). Microbial gold; an example from Venezuela. *N.Jb.Geol.Paläont.Abh.*,
- Coenraads, R.R., Paige, S.C.B. and Sutherland, F.L. (1991). Ilmenite mantled rutile crystals from the Uralla District, New South Wales. *Royal Society of New South Wales*, **124**, 23-34.
- Coenraads, R.R. (under review). Evaluation of potential sapphire source rocks within the catchments of Kings Plains Creek and Swan Brook, near Inverell, New South Wales. *Records of the Australian Museum*,
- Coenraads, R.R. (under review). Depositos Diamantíferos del Río Guaniamo del Estado Bolívar, Venezuela. *Boletín de la Sociedad de Geólogos Venezolanos*,

Coenraads, R.R. (under review). Surface Features of Natural Rubies and Sapphires associated with Volcanic Provinces. *Journal of Gemmology*,

Bischoff, G.C.O. and Coenraads, R.R. (in prep). Fossil and recent traces of biodegradation on heavy minerals.

A6-1 Reports:

Coenraads, R.R. (1988). T.J.& P.V. Nunan Pty. Ltd. Six monthly report to the Department of Mines, E.L.'s 2988 and 2989 for the period to 12 July 1988, (unpubl.).

Coenraads, R.R. (1988). Jingellic Minerals N.L. Final Report for the Kings Plains Drilling Project, New England, New South Wales. (unpubl.).

Coenraads, R.R. and Lawrence, D. (1989). T.J.& P.V. Nunan Pty. Ltd. Six monthly report to the Department of Mines, E.L.'s 2988 and 2989 for the period to 12 January 1989, (unpubl.).

Coenraads, R.R., Pope, G.J. and Whittle, M.A. (1989). T.J.& P.V. Nunan Pty. Ltd. Six monthly report to the Department of Mines, E.L.'s 2988 and 2989 for the period 15 January, 1989 to 14 July, 1989. (unpubl.).

Coenraads, R.R., Pope, G.J. and Whittle, M.A. (1989). T.J.& P.V. Nunan Pty. Ltd. Six monthly report to the Department of Mines, E.L.'s 2988 and 2989 for the period 15 July, 1989 to 14 January, 1990. (unpubl.).

A6-2 Symposium abstracts:

Coenraads, R.R. (1991). Sapphires and rubies associated with volcanic provinces: Inclusions and surface features shed light on their origin. Gemmological Association of Australia 45th Federal Conference and Seminar, Canberra, May 3-5, 1991, p. 2-14.